Durham E-Theses

Carbon Storage and Distribution in a Temperate Saltmarsh – A case study of the Ribble Estuary, UK

JARDINE, ALEXANDER,PAUL

How to cite:

JARDINE, ALEXANDER,PAUL (2020) *Carbon Storage and Distribution in a Temperate Saltmarsh – A case study of the Ribble Estuary, UK* , Durham theses, Durham University. Available at Durham E-Theses Online: http://etheses.dur.ac.uk/13575/

Use policy

This work is licensed under a Creative Commons Public Domain Dedication 1.0 (CC0)

Academic Support Office, Durham University, University Office, Old Elvet, Durham DH1 3HP
e-mail: e-theses.admin@dur.ac.uk Tel: +44 0191 334 6107
http://etheses.dur.ac.uk

Carbon Storage and Distribution in a Temperate Saltmarsh – A case study of the Ribble Estuary, UK


Source: Lytham Wildfowlers, 2018

Alexander Jardine

Department of Geography

Durham University

2020

Thesis submitted for the degree of Master of Science

Abstract

Temperate saltmarshes serve as important stores of blue carbon and climatic regulators, however little is currently known about the contemporary carbon storage capacities of UK saltmarshes. This study quantifies the carbon storage capacity of the saltmarshes in the Ribble estuary and analyses the influence of elevation, gradient and watercourse proximity on carbon distribution. The study specifically focusses on carbon stored within the 'active section' which is comprised of the above-ground biomass and surface organic layer, defined as the 'active layer' in this research. Overall, the findings indicate that 1.26×10^7 kg and 12.9×10^7 kg (3.s.f) of carbon is stored within the above-ground biomass and active layer sediment respectively, although carbon is unevenly distributed between the sub-environments that comprise the saltmarshes of the Ribble. Whilst elevation, gradient and watercourse proximity are recognised to exert an interconnected influence on sub-environment and carbon distribution, only gradient and watercourse proximity were found to be statistically significant. In all sub-environments watercourse proximity exhibits a standardised influence between 50.1% and 72.0% greater than gradient. The overall distribution findings rebuke the simple elevation ramp model of distribution and support the theory that saltmarsh sub-environment and carbon distribution is controlled by a multitude of interconnected ecogeomorphological factors. The study also highlights the overall active section carbon storage capacity of the Ribble saltmarshes could decrease by 23.8%, 30.7% or 30.9% of the 2012 capacity by 2100 under the respective RCP 2.6, 4.5 and 8.5 (50^{th} percentile) sea level rise scenarios. There is also the potential for greater degradation and carbon loss to occur as result of sea level rise driven headward expansion of creeks given the significant influences of watercourse proximity and gradient on sub-environment distribution. Therefore, it is important future shoreline management policies are adapted to limit future degradation in order to allow the saltmarshes of the Ribble to continue to act as an important store of blue carbon.

Keywords

Blue carbon, saltmarsh, elevation, gradient, watercourse proximity, sea level rise.

Acknowledgements

Firstly, I would like to thank my supervisors Dr Matthew Brain, Dr Sarah Woodroffe and Dr Mark Kincey for their time, guidance and enthusiasm. I would also like to thank Frank Davies and Chris Dale who provided technical assistance before fieldwork periods and during the laboratory analysis. My thanks are also due to my fieldwork assistants Timothy Shackles and Emmanuel Bustamante Fernandez who made the fieldwork possible. Likewise, I also owe thanks to Peter, Andrew and Sarah Smith who could not have been better hosts during my time in Lytham.

Last but not least, I'd like to thanks to my friends and family, who have provided invaluable support and motivation throughout this project.

Thank you all.

Contents

Abstract ..... *i*
Acknowledgements ..... *ii*
Contents ..... *iii*
List of Figures ..... *vi*
List of Tables ..... *xi*
Abbreviations ..... *xiv*
Statement of Copyright ..... *xv*
Chapter 1 – Introduction **1**
1.1 - Background and Motivation **1**
1.2 - Approach and Focus **2**
1.3 - Aims and Objectives **3**
Chapter 2 – Location **4**
2.1 – Setting and Background **4**
2.2 - Geomorphological and Ecological Characteristics **5**
2.3 - Carbon Storage **7**
2.4 - Future Change **7**
Chapter 3 – Research Rationale and Literature Review **10**
3.1 - The Value and Characteristics of Saltmarshes **10**
3.1.1 - The Importance of Saltmarshes 10
3.1.2 - Saltmarsh Characteristics and Dynamics 10
3.1.3 - Carbon Storage in UK Saltmarshes 11
3.2 – Saltmarsh Species Distribution and Surface Dynamics **12**
3.2.1 – Controls of Species Distribution 12
3.2.2 - Internal Influences on Ecology and Geomorphology 13
3.2.3 - External Influences on Ecology and Geomorphology 15
3.3 – Sub-Surface Dynamics **18**
3.3.1 - Storage Potential 18
3.3.2 - The Active and Fossil Layers 19
3.3.3 - Sequestration Potential 21
3.4 - Sea Level Rise and Marsh Evolution **21**
3.4.1 - Predicting Geomorphological and Ecological Response 21

3.4.2 - Submergence 22
3.4.3 - Equilibrium and Accretion 23
3.4.4 - Influence of Relative Sea Level Change 24
3.5 - Summary 25
Chapter 4 - Methodology 26
4.1 Introduction 26
4.2 Spatial Analysis 26
4.2.1 - Elevation Analysis 26
4.2.2 - Landcover Classification 28
4.2.3 - Variables Influencing Sub-environment Distribution 32
4.3 - Field and Laboratory Analysis 34
4.3.1 - Field Assessments 35
4.3.2 - Laboratory Carbon and Biomass Assessment 41
4.4 - Determining Overall Carbon Storage 43
4.5 – The Influence of Sea Level Rise on Marsh Evolution 45
Chapter 5 – Results 46
5.1 – Spatial Analysis of Land Cover 47
5.1.1 – Areal Quantification 47
5.1.2 - Influence of Elevation on Sub-environment Distribution 58
5.1.3 - Influence of Gradient on Sub-environment Distribution 69
5.1.4 - Influence of Watercourses on Sub-environment Distribution 80
5.1.5 – Key Controls on Sub-environment Area – Multiple Regression Analysis 90
5.2 – Geomorphological Analysis and Carbon Quantification 94
5.2.1 Introduction 94
5.2.2.1 - Above-ground Biomass 94
5.2.2.2 - Sub-Surface 95
5.2.2.3 - Active Layer Characteristics 97
5.2.2.4 – Above-ground Biomass and Active Layer Carbon 100
5.3 – Overall Carbon Content of Sub-environments 101
5.3.1 – Introduction 101
5.3.2 – Variability in Carbon Content 101
5.3.3 – Spatial Distribution of Carbon Content 121
5.3.4 – Key Controls on Carbon Distribution 147
5.4 – Summary 152
6 – Discussion 153
6.1 – Introduction 153

6.2 – The Spatial Distribution of Sub-environments and Influence of Elevation, Gradient and Watercourse Proximity 153
6.3 - The Distribution of Carbon within the Ribble Estuary 165
6.3.1 – Above-ground Carbon Storage 165
6.3.2 – Active Layer Carbon Content 168
6.4 - Sea level rise and Marsh Evolution 174
6.4.1 - Potential Scenarios and Consequences 174
6.4.2 – Implications for Coastal Management and Further Research 183
7 – Conclusions 188
References 191
Appendices 221
Appendix A – Sea Level Rise and Carbon Projections 221
Appendix B –Spatial Analysis of Land Cover 236
Appendix C - Marsh Specific Geomorphological Findings 273

List of Figures

Chapter 2 – Page Nº

Figure 2.1 - Location of the saltmarshes of the Ribble estuary as defined in this study. 4

Figure 2.2 - Geomorphological evolution of Ribble estuary from 1737 to 1967. 6

Figure 2.3 - Annual mean high-water values at the Port of Liverpool from 1768 to 1999. The curve shown is a linear trend which highlights the nodal variation in tidal cycles and the progressive SLR. 8

Chapter 3 –

Figure 3.1 - Theoretical variation of species distribution on a typical temperate saltmarsh on the 'tidal ramp'. 12

Figure 3.2 - Spatial variation of saltmarsh species in the Venice lagoon. 13

Figure 3.3 - Reduction in saltmarsh area in the Humber Estuary between 3-2 cal. ka BP (a) and present (b). Although both lower and mature saltmarsh are present in parts of the landward fringes of the intertidal zone they are too small to be detailed at this scale. 17

Figure 3.4 - Conceptual model of the active section and fossil layers within a theoretical saltmarsh environment (a) and their response to SLR (b). The difference indicated by the arrow is the lateral distance of active layer theoretically lost as a result of SLR. 20

Figure 3.5 - The interaction of sea-level rise, hydroperiod, depositional processes and vegetation on saltmarsh accretional response to SLR (Reed *et al.* 1995). 22

Chapter 4 –

Figure 4.1 - Summary of the overall methodology and the relationships between differing methods. Methods are categorised as follows: field based (dark green), remote sensing (dark blue), laboratory (dark yellow), combined field and laboratory (red) and all methods combined (turquoise). 27

Figure 4.2 - The different stages of supervised and unsupervised classification processes. 29

Figure 4.3 - Diagrammatic representation of the flow direction model and the resultant flow accumulation raster. 33

Figure 4.4 - 'N Site A' on Marsh D after above-ground and subsurface sediment sampling. 36

Figure 4.5 - Sediment consistency component of thee Troels-Smith classification sediment procedure. 37

Figure 4.6 - Test stratigraphy from Marsh B. The active layer (light blue) is clearly distinguishable due to its higher organic content, light brown colour and clear connection to the above-ground vegetation. Alternatively, the fossil layers (red) show no clear connection to the above-ground vegetation, have a lower organic content and are darker in colour. The distinctions between the active layer and all fossil layers were made with aid of the Troels-Smith (1955) sediment classification scheme. 39

Figure 4.7 - Summary of field protocol and key equipment used. 40

Figure 4.8 - Acronyms for laboratory carbon and biomass assessment methodology. 41

Figure 4.9 - Acronyms for overall carbon storage assessment. 43

Chapter 5 –

Figure 5.1 - Sub-environment distribution throughout the saltmarshes of the Ribble estuary. 48

Figure 5.2 - Variability in remote sub-environment remote accuracy classification on the four different marshes and overall (mean value). 51

Figure 5.3 - Summary of the overall land cover area assessments, highlighting variability in projected areas according to the original ML classification and the remote uncertainty assessment over all marshes. 56

Figure 5.4 - Summary of the overall land cover area assessments, highlighting variability in projected areas according to the original ML classification and the manual uncertainty assessment over all marshes. 56

Figure 5.5 - Comparative kernel density plot highlighting the variability in elevation of all sub-environments over all marshes. 60

Figure 5.6 - Variability in elevation between all sub-environments over all marshes. 61-62

Figure 5.7 - Variability of sub-environment areal coverage with elevation. Error bars indicate the RMSE of 15 cm associated with the Lidar data. 64

Figure 5.8 - Variability in the elevation across the overall saltmarsh environment (%). 65

Figure 5.9 - Variability of sub-environment areal coverage with elevation. 65

Figure 5.10 - Spatial variability in elevation above ordnance datum over all marshes 67

Figure 5.11 - Sub-environment distribution throughout the saltmarshes of the Ribble estuary. 68

Figure 5.12 - Variability in the density of distribution of gradient over all marshes. 71

Figure 5.13 - Variability in gradient distribution between all sub-environments over all marshes. 72 - 73

Figure 5.14 - Variability of sub-environment areal coverage with gradient. 75

Figure 5.15 - Variability in the gradient across the overall saltmarsh environment (%). 76

Figure 5.16 - Variability of sub-environment areal coverage with gradient. 76

Figure 5.17 - Spatial variability in gradient over all marshes. 78

Figure 5.18 - Sub-environment distribution throughout the saltmarshes of the Ribble estuary. 79

Figure 5.19 - Comparative kernel density plot exhibiting the variability in the distance of each sub-environment zone from watercourses over all marshes. 81

Figure 5.20 - Variability in distance from watercourse between all sub-environments over all marshes. 82-83

Figure 5.21 - Variability of sub-environment areal coverage with watercourse proximity. 85

Figure 5.22 - Variability in watercourse proximity across the overall saltmarsh environment (%). 86

Figure 5.23 - Variability of sub-environment areal coverage with watercourse proximity. 86

Figure 5.24 - Raster model exhibiting the proximity of differing areas of all marshes to watercourses. 88

Figure 5.25 - Sub-environment distribution throughout the saltmarshes of the Ribble estuary. 89

Figure 5.26 - Correspondance between the depth, organic carbon density and bulk density throughout all sub-surface horizons. 96

Figure 5.27 - Correspondance between the depth, organic carbon density and bulk density in all active layer horizons. 98-99

Figure 5.28 - Correspondance between the mean carbon mass per unit area in both the above-ground biomass and active layer in each sub-environment. 100

Figure 5.29(a-d) - Disparity in overall above-ground biomass carbon projections assuming mean OCD. 103-105

Figure 5.30(a-d) - Variability in projected overall volume for the sub-environments. 109-111

Figure 5.31(a-e) - Variability in projected overall active layer carbon storage for the sub-environments. 114-116

Figure 5.32(a-h) - Above-ground biomass carbon variability with elevation within the sub-environments. 123-124

Figure 5.33 - Average above-ground biomass carbon variability with elevation across all sub-environments. 125

Figure 5.34(a-h) - Sub-surface active section carbon variability with elevation within the sub-environments. 127-128

Figure 5.35 - Average sub-surface active section carbon variability with elevation across all sub-environments. 129

Figure 5.36(a-h) - Above-ground biomass carbon variability with gradient within the sub-environments. 131-132

Figure 5.37 - Average above-ground biomass carbon variability with gradient across all sub-environments. 133

Figure 5.38(a-h) - Sub-surface active section carbon variability with gradient within the sub-environments. 135-136

Figure 5.39 - Average sub-surface carbon variability with gradient across all sub-environments. 137

Figure 5.40(a-h) - Above-ground biomass carbon variability with watercourse proximity within the sub-environments. 140-141

Figure 5.41 - Average above-ground biomass carbon variability with watercourse proximity across all sub-environments. 142

Figure 5.42(a-h) - Sub-surface active section carbon variability with gradient within sub-environments. 144-145

Figure 5.43 - Average sub-surface carbon variability with watercourse proximity across all sub-environments. 146

Chapter 6 –

Figure 6.1 - Tidal height projections relative to land cover on Marsh C. 155

Figure 6.2 (a-b) - A comparison of sub-environment distribution and elevation around a major creek in Marsh B. 159

Figure 6.3 - Elevation distribution of saltmarsh species in Morecambe Bay. The IQR is indicated by the dark boxes, whilst the overall range is shown by maximal extent of the arrows. 160

Figure 6.4 - A comparison of standardised and unstandardised beta values for the two significant influences on sub-environment and above-ground carbon spatial distribution. 166

Figure 6.5 - Correspondance between the findings of this research and SCSP carbon stock projections (kg m^{-3}) where *Atriplex portulacoides (a), Juncus gerardii (b) and Puccinelia Martima (c)* was the predominant, 2nd or 3rd most numerous species. 170

Figure 6.6 - Carbon variation with depth comparison highlighting the change in carbon content with depth in this study (a) and in the Yellow River Delta (b) (Bai *et al.* 2016). This figure is only an illustration of the rapid change in carbon between the surface/active and fossil layers. 173

Figure 6.7 - Projected heights of MHWS at present in 2050 (a) and 2100 (b) under different sea level rise prediction scenarios assuming no topographic change. The UKCP 18 RCP 50th percentile projections shown are specific to a 25km^2 area encompassing the Ribble estuary, whilst the Low 2 scenario represents Pfeffer et al's (2008) median global sea level rise projection. 174-175

Figure 6.8 - Projected change in overall carbon storage during the 21st century under the three differing RCP scenarios featured in the UKCP 2018 report. 177

Figure 6.9 - Predicted change in overall carbon stocks in accordance with the level of sea level rise (SLR). 178

Figure 6.10 - Projected change in overall active layer (a) and above-ground biomass (b) carbon storage during the 21st century under the three differing RCP scenarios featured in the UKCP 2018 report. 179

Figure 6.11 - Shoreline management plan for the Ribble Estuary from 2010 to 2100. 187

List of Tables

Chapter 4

Table 4.1 - Comprising species of the six predominately vegetated sub-environments. 31

Chapter 5

Table 5.1 - Overall area and % composition of each sub-environment determined following the original land cover classification. 48

Table 5.2 - Summary of the remote uncertainty analysis over all marshes (by sub-environment type). 49

Table 5.3 - Confusion matrix exhibiting the accuracy of the ML classification indicated by the remote uncertainty analysis. The average correspondence value (A) indicates the overall accuracy of the procedure whilst the Kappa coefficient (k) likewise represents the overall accuracy but also takes into account the possibility of the agreement occurring by chance. 50

Table 5.4 - Summary of the remote uncertainty analysis for each marsh. 50

Table 5.5 - Summary of the manual, field-based uncertainty analysis for all species over all marshes. Species Zone F is absent as it wasn't recognised before the analysis. 52

Table 5.6 - Confusion matrix exhibiting the accuracy of the ML classification indicated by the manual uncertainty analysis. The average correspondence value (A) indicates the overall accuracy of the procedure whilst the Kappa coefficient (k) likewise represents the overall accuracy but also takes into account the possibility of the agreement occurring by chance. 53

Table 5.7 - Summary of the manual, field-based uncertainty analysis for all marshes and overall. 53

Table 5.8 - Comparison of the overall accuracy of both analyses. 54

Table 5.9 - Summary of the land cover area assessments. Both remote and manual uncertainty figures represent the minimal area covered by each sub-environment and utilise overall accuracy figures for all marshes. 57

Table 5.10 - Elevation (OD to tidal datum conversion table for three nearest tidal gauges. (Source = Admiralty Chart Tables, 2018) 58

Table 5.11 - Variability in the elevation distribution between all sub-environments over all marshes. 63

Table 5.12 - F values produced during the ANOVA analyses for all land cover types. The values indicate the variance of the mean elevation values for two respective land cover types divided by the mean of the variances within each respective land cover type. 66

Table 5.13 - Probability (p) values accompanying each of the respective F values. The values indicate the probability of producing the respective F value result, given that the null hypothesis (F≈1) is true. Statistically insignificant values (alpha level= 0.05) are indicated in green. 66

Table 5.14 - Variability in the gradient distribution between all sub-environments over all marshes. 74

Table 5.15 - F values produced during the ANOVA analyses for all land cover types. The values indicate the variance of the mean elevation values for two respective land cover types divided by the mean of the variances within each respective land cover type. 77

Table 5.16 - Probability (p) values accompanying each of the respective F values. The values indicate the probability of producing the respective F value result, given that the null hypothesis (F≈1) is true. Statistically insignificant values (alpha level= 0.05) are indicated in green. 77

Table 5.17 - Variability in the proximity of all sub-environment zones from watercourses over all marshes. 84

Table 5.18 - F values produced during the ANOVA analyses for all land cover types. The values indicate the variance of the mean elevation values for two respective land cover types divided by the mean of the variances within each respective land cover type. 87

Table 5.19 - Probability (p) values accompanying each of the respective F values. The values indicate the probability of producing the respective F value result, given that the null hypothesis (F≈1) is true. Statistically insignificant values (alpha level= 0.05) are indicated in green. 87

Table 5.20 - Multiple regression parameters and the significance of predictor variables concerning elevation and sub-environment area (km^2). 91

Table 5.21 - Multiple regression parameters and the significance of predictor variables concerning gradient and sub-environment area. 92

Table 5.22 - Multiple regression parameters and the significance of predictor variables concerning watercourse proximity and sub-environment area. 92

Table 5.23 - Statistical summary of carbon mass (kg/m^2) stored within the above-ground biomass in the differing sub-environments incorporating data from all sampling sites. 94

Table 5.24 - Statistical summary of carbon mass ($kg\ m^{-3}$) stored within the sub-surface sediments in the differing sub-environments. 96

Table 5.25 - Statistical summary of carbon density ($kg\ m^{-3}$) of active layer sediments in the differing sub-environments. 99

Table 5.26 - Disparity in overall above-ground biomass carbon projections for all sub-environments considering the different sub-environment areal uncertainties (1.d.p). 106

Table 5.27 - Above-ground biomass carbon (kg x 10^{-3}) statistics for all sub-environments considering the variability in OCD assuming the sub-environment coverage projected in the original areal remote classification (1.d.p). 106

Table 5.28 - Above-ground biomass carbon (kg x 10^{-3}) projections assuming the minimal and maximal possible areal and OCD projections (1.d.p). 106

Table 5.29 - Key for volume projection uncertainty analysis. 107

Table 5.30 - Volume projections for all sub-environments (1.d.p). 112

Table 5.31 - Volume projections for all sub-environments (1.d.p). 112

Table 5.32 - Active layer overall carbon mass projections for all sub-environments (1.d.p). 117

Table 5.33 - Uncertainty (standard deviation) surrounding sub-surface active section overall carbon mass projections for all sub-environments (1.d.p). 118

Table 5.34 - Uncertainty (minimal bounds) surrounding sub-surface active section overall carbon mass projections for all sub-environments (1.d.p). 119

Table 5.35 - Uncertainty (maximal bounds) surrounding sub-surface active section overall carbon mass projections for all sub-environments. 120

Table 5.36 - Multiple regression parameters and the significance of predictor variables concerning elevation and sub-environment above-ground biomass carbon storage (kg). 147

Table 5.37 - Multiple regression parameters and the significance of predictor variables concerning elevation and sub-environment active layer carbon storage (kg). 148

Table 5.38 - Multiple regression parameters and the significance of predictor variables concerning gradient and sub-environment above-ground biomass carbon storage (kg). 149

Table 5.39 - Multiple regression parameters and the significance of predictor variables concerning gradient and sub-environment active layer carbon storage (kg). 149

Table 5.40 - Multiple regression parameters and the significance of predictor variables concerning watercourse proximity and sub-environment above-ground biomass carbon storage (kg). 150

Table 5.41 - Multiple regression parameters and the significance of predictor variables concerning watercourse proximity and sub-environment active layer carbon storage (kg). 151

Abbreviations

General

MR – Managed realignment

SLR – Sea level rise

OCD – Organic carbon density

RCP – Representative concentration pathway

Methodology Specific

AGDM – Above-ground dry mass (g)

AGCM – Above-ground carbon mass (g)

AGWM – Above-ground wet mass (g)

AGWMT – Above-ground wet mass and tray (g)

AM – Ashed mass (g)

ASMF – Above surface multiplication factor

ASTCS – Above surface total carbon store (kg)

BGDM – Below-ground dry mass (g)

DEM – Digital elevation model

DM – Dry mass (g)

Lidar - Light detection and ranging

LOI – Loss on ignition

ML Area – Maximum likelihood classification area (m^2)

OCC – Organic carbon content (g)

OCD – Organic carbon density (g m^3 or kg m^3)

OCCS – Organic carbon content per stratum (g)

OMC – Organic matter content (%)

SSCS – Sub-surface carbon storage (g)

SSTCS - Sub-surface total carbon stored (kg)

SSVMF – Sub-surface volume multiplication factor

TCS – Total carbon stored in an individual sub-environment (kg)

TESSA – Toolkit for Ecosystem Service Site-based Assessment

TM – Tray mass (g)

Statement of Copyright

“The copyright of this thesis rests with the author. No quotation from it should be published without the author's prior written consent and information derived from it should be acknowledged.”

Chapter 1 – Introduction

1.1 - Background and Motivation

Saltmarshes are key environments for carbon storage and play an important role in carbon cycling and climatic regulation (McLeod *et al*. 2011; Beaumont *et al.* 2014). However, the distribution and quantity of carbon throughout a saltmarsh environment is highly dependent on site-specific geomorphological and ecological characteristics which are spatially and temporally variable (Cacador *et al*. 2004; D'Alpaos, 2011; Kelleway *et al*. 2016).

Accelerated sea level rise (SLR) during the 21st century is predicted to substantially influence saltmarsh evolution, resulting in spatial migration and adjustment (Allen and Pye, 1992; Morris *et al.* 2002; Horton *et al.* 2018). Although the consequences of this adjustment are marsh specific, it is widely thought that SLR could result in progressive submergence and loss of saltmarshes and the ecosystem services they provide (e.g. Reed, 1995; Horton *et al.* 2018) if they do not vertically accrete at the same rate as sea level rises (Craft *et al.* 2009; Spencer *et al.* 2010). The consequences of SLR driven loss and degradation on saltmarsh carbon storage go beyond the regional setting however, as the loss of efficient saltmarsh carbon sinks would influence atmospheric carbon concentrations and consequently global climatic change (Craft *et al.* 2009; Pendleton *et al.* 2012).

To improve the understanding of the role that saltmarshes play in the global carbon cycle, it is important that current saltmarsh carbon stores are accurately quantified. With a greater understanding of the current storage, it is subsequently possible to calculate potential SLR catalysed saltmarsh carbon loss. Despite this importance, little attention has previously been directed towards accurately quantifying the carbon storage potential of UK saltmarshes (e.g. Andrews *et al.* 2008). This study seeks to address this issue by assessing the carbon stored within the saltmarshes of the Ribble Estuary, UK. The findings could be used to accurately predict the influence of SLR on the carbon storage capacity of the saltmarshes of the Ribble and therefore aid the assessment of their contribution to future atmospheric carbon levels and climatic change.

1.2 - Approach and Focus

This study seeks to determine the carbon storage of the saltmarshes of the Ribble Estuary and assess carbon spatial distribution using a combination of remote sensing and fieldwork techniques. Central to the analysis is the remote assessment and determination of different geomorphological and ecological sub-environments which collectively comprise the saltmarshes of the Ribble Estuary. Following the assessment of the areal coverage the study also seeks to analyse the influence of elevation, gradient and watercourse proximity on the spatial distribution of the individual sub-environments with the view to determining the key controls on sub-environment zonation. As the ecological and geomorphological characteristics of each sub-environment determine carbon storage capacity (Garcia *et al.* 1993; Cacador *et al.* 2004; Zhou *et al.* 2007), the respective influences of elevation, gradient and watercourse proximity on the spatial distribution of carbon storage is subsequently assessed.

Due to the different geomorphological and ecological characteristics of sub-environments, the study employs standardised laboratory and fieldwork techniques to assess carbon storage (see Section 4.3). The purpose of this assessment is to quantify the carbon stored within the 'active section' of sub-environments, which is defined as the section of the sub-environment that is directly connected to surface processes and is most likely to be influenced by external change in the form of SLR (see section 3.3.2).

The study subsequently seeks to combine the findings of the remote spatial analysis and active section carbon assessment to quantify active section carbon storage of different sub-environments and determine the spatial distribution of carbon throughout the saltmarshes of the Ribble Estuary. The influence of SLR on active section carbon storage under different future SLR scenarios is also assessed.

1.3 - Aims and Objectives

Aim:

- To quantify and determine the spatial distribution of carbon stored within the active sections of the sub-environments that comprise the saltmarshes of the Ribble estuary.

This aim will be achieved through the following objectives:

- To determine the spatial distribution of the sub-environments that comprise the saltmarshes of the Ribble estuary through a remote and field assessment of sub-environment distribution – Sections 5.1 and 6.2.
- To determine the influence of elevation, gradient and watercourse proximity on the spatial distribution of the sub-environments that comprise the saltmarshes of the Ribble estuary – Sections 5.1 and 6.2
- To determine the active sections of the saltmarsh sub-environments following an assessment of ecological and geomorphological characteristics – Sections 5.2 and 6.3.
- To quantify the total carbon stored within the active sections of all saltmarsh sub-environments in order to assess the spatial and temporal variability of carbon storage at present and under different future sea level rise scenarios – Sections 5.3, 6.3 and 6.4.

Chapter 2 – Location

2.1 – Setting and Background

The Ribble estuary is a macrotidal tidal estuary in North West England that divides the counties of Merseyside to the south and Lancashire to the north. The estuary is approximately 16 km in length from its head 7 km west of Preston to the mouth in Liverpool Bay, where the width of the estuary reaches a maximum of 6.1 km. Extensive mudflats and saltmarshes currently characterise the basin, rendering it a suitable habit for an array of wildlife and the wetland environment also provides key ecosystem services (See Section 3.1) such as storm surge defence for the town of Lytham St. Annes (Halcrow, 2013).

The temperate saltmarshes of the estuary also serve as a climatic regulator, acting as a significant sink for key greenhouse gases (Olsen *et al.* 2011; Ford *et al*. 2012). However, no attempts to assess the spatial distribution and overall carbon storage capacity of the saltmarsh environments have been published at present. For the purposes of this study, the saltmarshes of the Ribble were divided into the four individual marshes (A-D) shown in Figure 2.1. This division was made purely to prevent any confusion with regards to the spatial focus of the study during the field and remote sensing analyses.

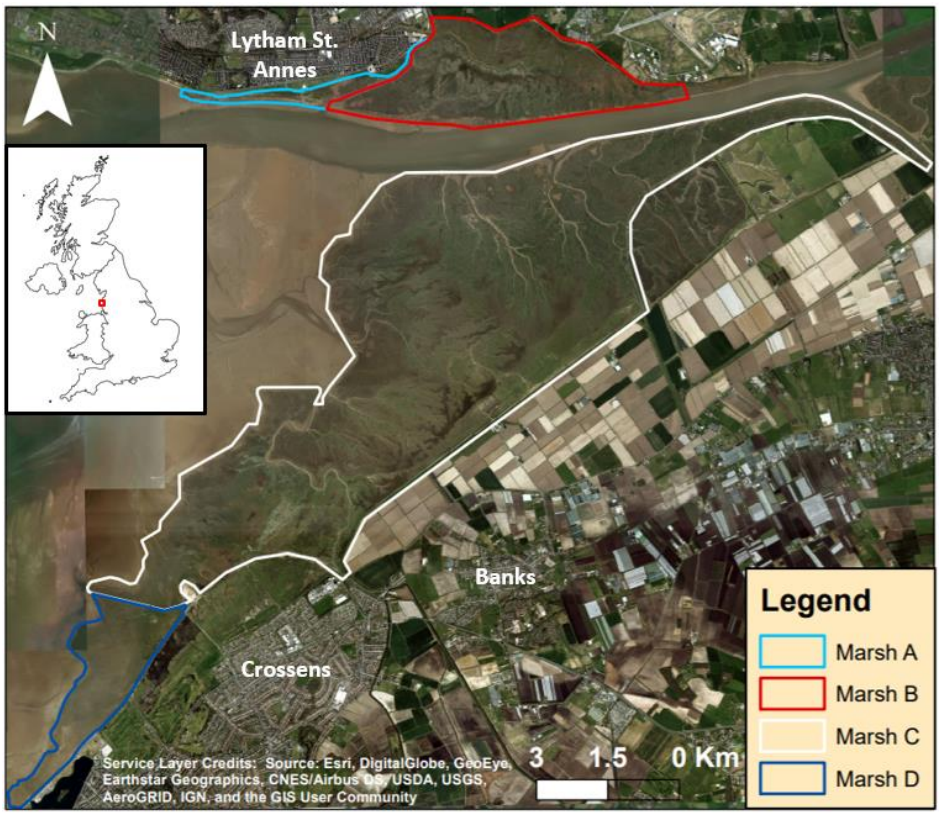

Figure 2.1. Location of the saltmarshes of the Ribble estuary as defined in this study.

2.2 - Geomorphological and Ecological Characteristics

The geology of the Ribble estuary is characterised by Pleistocene glacial drift and Holocene sediments which are underlain by Triassic Mercia Mudstone (Van der Wal and Pye, 2002). The Ribble is largely characteristic of the estuaries in North West England which have progressively evolved since their formation after glacial retreat approximately 17,000 ka BP (Clark *et al*. 2012). The influence of a flood-dominated tidal regime currently results in a net import of sediment into the estuary which when combined with fluvial deposition creates suitable conditions for estuarine saltmarshes, which cover approximately 20 km^2 of the 120 km^2 intertidal hectares of the estuary (Ford *et al*. 2012; Halcrow, 2013). The key species found in the environment are characteristic of those found within UK saltmarshes including: *Elymus Repens* and *Festuca Rubra* in the higher marsh, while *Spartina Anglica* and *Salicornia Spp.* are more prominent in the lower marsh (Ford *et al.* 2012).

The Ribble has experienced significant human modification over the past few hundred years which has influenced ecogeomorphological evolution (see Figure 2.2). Most prominently, channelisation of the lower course and dredging of the main channel for navigational purposes have served to confine channel flow largely to the North bank creating greater flood-dominant conditions on either side (Johnson, 1985; Van der Wal and Pye, 2003). Combined with embanking and reclamation on both North and South banks, the consequence of the anthropogenic modifications has been to enhance the natural tendency for the estuary to import sediment from the adjoining nearshore and coastal areas (Halcrow, 2013). This enhanced net accumulation has led to progressive saltmarsh expansion on the South bank at Crossens in particular, resulting in considerable variability in saltmarsh age and ecogeomorphological characteristics (Van der Wal *et al.* 2002).

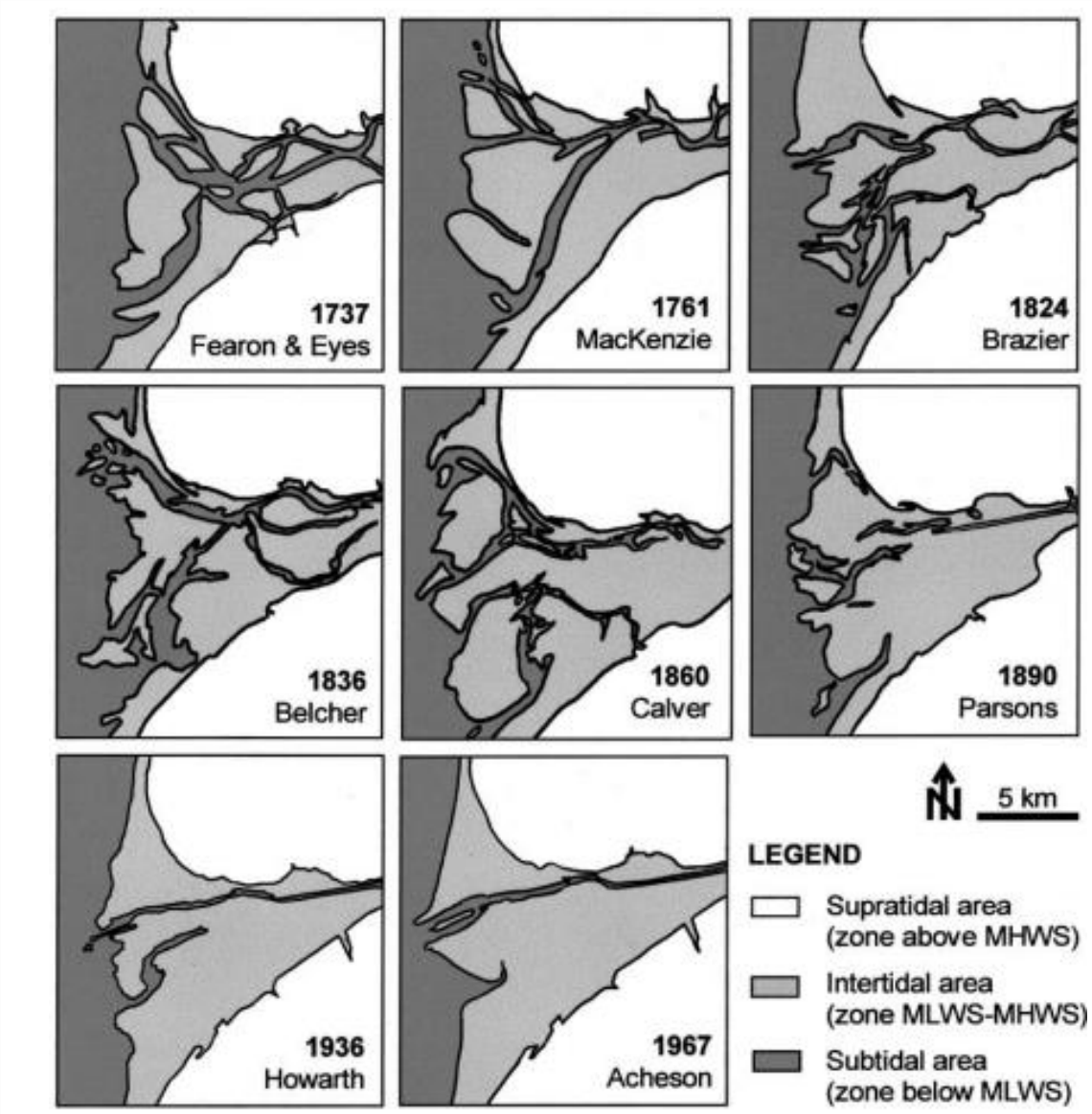

Figure 2.2. Geomorphological evolution of Ribble estuary from 1737 to 1967.

(Williams and Webb, 1848; Port of Preston Authority, 1904; UK Hydrographic Office 1951 and 1994 in Van der Wal and Pye, 2002)

2.3 - Carbon Storage

At present there are two published examples of research that concerns the influence of human saltmarsh modification and the subsequent effects on carbon stocks and cycling in the estuary. The study of Olsen *et al.* (2011) demonstrated that long-term grazing by cattle in the Ribble had led to changes in the: structure and composition of the saltmarsh plant community, abiotic conditions of the sediment as well as soil microbial biomass and respiration. This was found to have subsequently increased microbial immobilisation of carbon and slowed carbon cycling, ultimately affecting the duration of carbon storage within the marsh sediment.

The research of Ford *et al.* (2012) also highlighted links between grazing intensity, vegetation characteristics and carbon storage throughout the Ribble saltmarshes. The overall conclusion was that grazing resulted in lower above-ground carbon storage in the living biomass but contrastingly corresponded with higher sub-surface organic sediment carbon stocks. Whilst the inverse relationship between above-ground biomass carbon storage and grazing intensity was attributed purely to livestock biomass consumption, Ford *et al.* (2012) reasoned the increased sub-surface carbon was a product of cattle trampling and compaction that resulted in the creation of an anoxic environment in grazed areas. Consequently, decomposition rates were reduced in grazed areas resulting in comparatively greater sub-surface carbon stocks, compared to the well-aerated, free-draining sediment of the un-grazed marsh.

Whilst these findings are not of direct use to this study, they do indicate variability in carbon storage within the above-ground living biomass and sub-surface organic sediments. Ford *et al.* (2012) also highlighted the localised variability in the spatial distribution of species such as *Elymus repens* and *Juncus gerardii* which characterise different marsh sub-environments with variable carbon storage capacities, exhibiting the heterogeneity of the saltmarsh environment as a whole. Overall, both studies indicated that a multitude of factors including environmental change could potentially influence the sustainability of the substantial carbon stocks of the Ribble saltmarshes.

2.4 - Future Change

According to current projections, the Ribble estuary is likely to evolve geomorphologically and ecologically as a result of the influence of climatic change in the 21st century (Halcrow, 2010a, 2010b & 2013). The influence of progressive SLR as well as the changing nature of Irish Sea storm surges are described by the Halcrow Consultancy (2013) as the most likely factors to catalyse this evolution,

although the long-term impacts on saltmarsh characteristics of these influences are surrounded by considerable uncertainty.

Due to the constrictions on marsh migration imposed by man-made structures, there is the potential that SLR driven saltmarsh loss and degradation will occur in the Ribble, should the current coastal management policy remain unchanged (Holden, 2008; Halcrow, 2013). The most recent projections named the 2018 United Kingdom Climate Projections (UKCP 18) which take into account localised (25 km^2) variability in glacial isostatic adjustment and include a regional thermosteric model, highlight that a relative SLR of between 0.31 m (representative concentration pathway (RCP) 2.6 – 50th percentile) and 0.63 m (RCP 8.5 – 50th percentile) could occur by 2100 (Church *et al.* 2013; Palmer *et al.* 2018). There is also the potential for a sea level rise of 2.01 m by 2100 (H++ high scenario 1 - Pfeffer *et al.* 2008), although unlike the UKCP 18 estimates, these projections are not specific to the Ribble estuary (Pfeffer *et al.* 2008) (see Appendix Section A for all projections). However, even under the lowest UKCP 18 scenario, the predicted rate of SLR in the region will most likely be greater than between 1900-2000 (see Figure 2.3). Therefore, predicting how the saltmarshes of the Ribble will respond to this enhanced SLR can only be achieved through a modelling-based approach which encompasses the temporal and spatial uncertainties of SLR projections (e.g. Horton *et al*. 2018).

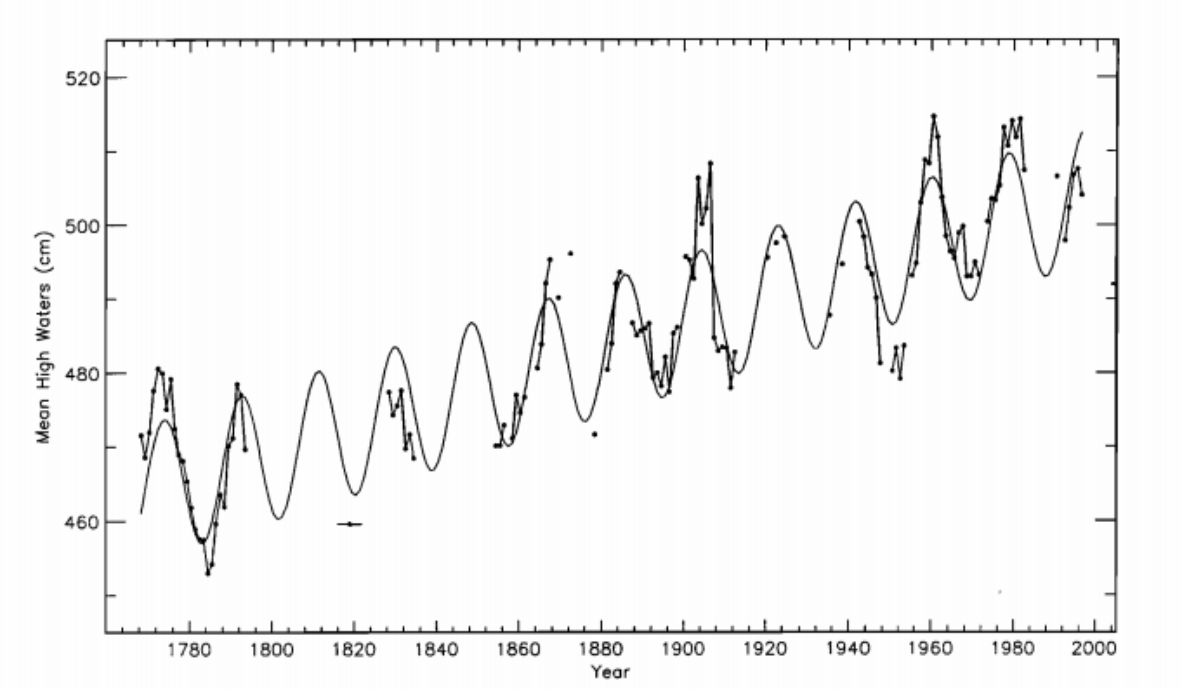

Figure 2.3. Annual mean high-water values at the Port of Liverpool from 1768 to 1999. The curve shown is a linear trend which highlights the nodal variation in tidal cycles and the progressive SLR (Woodworth, 1999).

Although uncertainty surrounds future marsh response modelling, even under the lowest plausible scenario SLR could result in a reduction in saltmarsh area by 2100 (Halcrow, 2013) (see Section 3.4). The most recent research concerning SLR in the Ribble conducted by Halcrow Consultancy (2010a), considers how SLR will influence the balance between sediment supply and relative SLR (Reed *et al.* 1995). The findings highlighted that there is no evidence that sediment supply will significantly increase or diminish over the next 100 years, and so the quantity of available sediment should remain relatively consistent in the estuary. Moreover, subsequent modelling of the impacts of SLR within the coastal cell indicates that there is a potential for increased flood dominance and sediment transport into the estuary (Halcrow, 2013). However, it is acknowledged that the influence of this potential increase in sediment delivery on accretion will depend on localised hydrological and geomorphological processes, and therefore it cannot be assumed that sediment delivery will universally increase as sea level rises (see Section 3.4) (Halcrow, 2013)

The ecological and geomorphological impact of future SLR is further complicated by the influence of relative SLR on tidal dynamics and range in the Ribble which could lead to a comparative 20% increase in mean sea level in the inner Ribble should the regional sea level rise by 0.5m (Halcrow 2010b). Whilst this could increase the potential for submergence and possible carbon loss, the influence of relative SLR could increase flood dominance in the estuary resulting in net accretion (Halcrow, 2013). In summary, there is evidence to suggest the saltmarshes of the Ribble could either: accrete, submerge or remain in equilibrium as a result of relative SLR, although contemporary research published by Horton *et al.* (2018) suggests there is >80% positive tendency of marsh submergence, degradation and retreat in Liverpool Bay by as early as 2020 under the RCP 8.5 scenario. Given this range of tenable scenarios and the likelihood of saltmarsh submergence and degradation in the region, it is important to predict the potential carbon losses under different submergence scenarios.

Chapter 3 – Research Rationale and Literature Review

3.1 - The Value and Characteristics of Saltmarshes

3.1.1 - The Importance of Saltmarshes

Saltmarshes are highly diverse environments that provide a range of benefits from coastal flood defence to 'blue carbon' storage which are collectively termed ecosystem services (Constanza *et al.* 1997; Barbier *et al.* 2011; D'Alpaos *et al.* 2019). Whilst ecosystem services such as flood defence and wetland habitat provision are clear regional benefits, saltmarshes are also globally significant as they are highly efficient long-term carbon stores that play a key role in climatic regulation (Chmura *et al.* 2003; Mcleod *et al.* 2011; Johnson *et al.* 2016). Unlike other environments which serve as efficient carbon stores, the abundance of sulphate in saltmarsh sediments also hinders the production of CH_4 making them negligible sources of methane and potential carbon sinks (Magenheimer *et al.* 1996; Beaumont *et al.* 2014; Otani and Endo, 2019).

However, there is a strong potential that temperate saltmarshes and their carbon stores will become increasingly vulnerable to submergence resulting from SLR in the 21st century (e.g. Cahoon *et al.* 2006; Craft *et al.* 2009; Horton *et al.* 2018). This could lead to saltmarshes transforming into carbon sinks and contributing towards an increase in global atmospheric carbon concentrations and therefore the exacerbation of global warming (e.g. DeLaune and White 2012; Hopkinson *et al.* 2012; Crosby *et al.* 2016). Therefore, it is essential to improve the understanding of carbon storage dynamics within saltmarsh environments so well-informed predictions concerning the contribution of saltmarsh carbon to future climate change can be made.

3.1.2 - Saltmarsh Characteristics and Dynamics

The temperate maritime climate of North West Europe creates conditions that are highly suitable for saltmarsh development which has resulted in saltmarshes becoming prominent geomorphological coastal features (Maddock, 2008; Foster *et al.* 2013). These marshes have two key geomorphological characteristics:

1) A convex, planar, or concave vegetated platform high in the tidal frame that is regularly flooded by the tide (Allen, 2000). This surface typically rises progressively with distance from the marsh edge and hosts a range of halophytes with differing salinity tolerances (Suchrow and Jensen, 2010; Belliard *et al.* 2017).
2) A dendritic network of tidal channels that dissect the marsh surface which are generally unconnected and diminish as they progress inland toward the interior of the marsh from the

seaward edge (Townend *et al*. 2011; Kim *et al.* 2013). However, it is also possible that these creek networks may connect with fluvial inflows creating brackish channels that transport sediment and nutrients from both tidal and fluvial environments (Alber, 2002; Colon-Rivera *et al.* 2012).

As a result of their geomorphological characteristics, vegetation colonisation patterns are dictated by a combination of salinity induced stress and species competition which results in spatial variability in species land cover and carbon storage (Cacador *et al*. 2004; Silvestri *et al*. 2005 Owers *et al*. 2018) (see Section 3.2).

In estuarine saltmarshes the sediment is often comprised of coarser silts and sands than is found in back-barrier and fringing saltmarshes as the majority of sediment is sourced from marine deposits in areas of high energy around the estuary mouth (Dalyrymple and Choi, 2007; De Groot *et al.* 2011). Moreover, distinctive coarse-grained horizons marking previous storm surges are often present within the saltmarsh stratigraphy (e.g. Tsompanoglou *et al.* 2011; Swindles *et al.* 2018). The extent of deposition from either fluvial or tidal sources is often substantially influenced by the geological setting and human modification of the estuarine environment (e.g. Allen and Pye, 1992; Adam, 2002; Gedan *et al.* 2009). The effect of such geological or manmade structures on accretional and erosional trends can dictate ecogeomorphological evolution and transform the morphology of an estuary (Pethick, 1992; French, 2006; Freiss *et al.* 2012)

3.1.3 - Carbon Storage in UK Saltmarshes

Active saltmarshes are widely distributed throughout the UK covering an estimated 656 km^2 (Boorman *et al*. 2003). Therefore UK saltmarshes are significant contributors to global carbon storage and their evolution has the potential to impact upon future climatic change (Beaumont *et al*. 2014).

Although SLR remains a key influence on saltmarsh evolution in UK marshes, their ecogeomorphological characteristics have been fundamentally altered due to previous human estuarine modification (Allen, 1997; Allen and Pye, 2002; Gedan *et al.* 2009). This combined human and ecogeomorphological variability contributes to spatial and temporal variability in carbon storage within and between UK saltmarshes (Boorman *et al*. 2003; Olsen *et al*. 2011). To understand why this variability exists it is important to consider the factors that influence the ecogeomorphological characteristics of a saltmarsh.

3.2 – Saltmarsh Species Distribution and Surface Dynamics

3.2.1 – Controls of Species Distribution

UK saltmarshes are highly diverse environments that contain multiple sub-environments or zones that are defined by the presence of specific species with different salinity tolerances (Boorman *et al.* 2003; Foster *et al.* 2013). This species zonation has been hypothesised to be controlled by salinity exposure which is determined by the variability of elevation and hydroperiod throughout the marsh (e.g. Williams *et al.* 1994; Plater and Rahman, 2014). According to this 'ramp' theory of zonation, a distinct halophyte species zonation is produced in accordance with the relative elevation of different tidal levels (see Figure 3.1) (Flowers and Colmer, 2008).

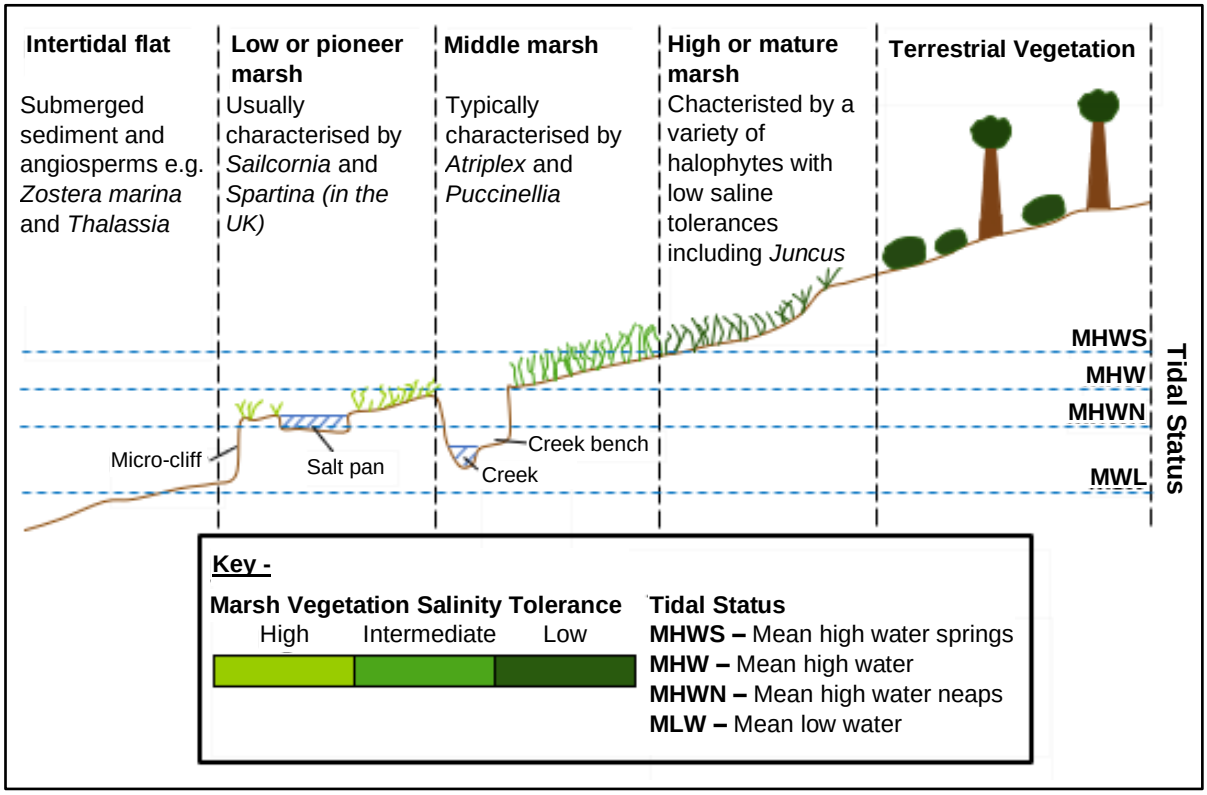

Figure 3.1 Theoretical variation of species distribution on a typical temperate saltmarsh on the 'tidal ramp'. Modified from Williams *et al.* 1994.

Figure 3.1. illustrates that the lower marsh sub-environment is usually characterised by inter-tidal species with high salinity tolerances such as *Spartina Anglica* which can withstand the physical stress imposed by frequent saline inundation (Silvestri *et al.* 2005). In contrast, the less frequently inundated higher marsh, is colonised by less tolerant halophytes such as *Festuca Rubra* which are able to outcompete lower and middle marsh species such as *Atriplex Portulacoides* as salinity stress no longer dictates species variability (Pennings *et al.* 2005; Colmer and Flowers, 2008).

The result of this stress and competition-induced species zonation is a theoretical spatial variability in the carbon capacity of differing saltmarsh sub-environments (e.g. Cacador *et al.* 2004; Zhou *et al.*

2007). This is controlled by the organic production of the zone-specific species and the rate and nature of sediment deposition (Teal, 1962; Bai *et al.* 2016). As living biomass carbon stock is estimated to be 47% of total dry biomass (Peh *et al.* 2017), species type and abundance has a direct effect on the carbon storage content of a marsh (Garcia *et al.* 1993; Cacador *et al.* 2004). The variability of species type also has a significant impact on sub-surface carbon storage potential which is discussed in section 3.4.

3.2.2 - Internal Influences on Ecology and Geomorphology

Although differences in saltmarsh vegetation between the lower and high marsh are commonly observed in estuarine saltmarshes, creek structures and inflow streams also produce spatial ecogeomorphological variability (Pennings & Callaway 1992; Brewer *et al.* 1997; Kim *et al.* 2012). The result is highly variable species diversity and distribution which is specific to the individual marsh creating a unique 'mosaic' pattern (Adam *et al*. 1990; Boorman *et al*. 2003) (See Figure 3.2).

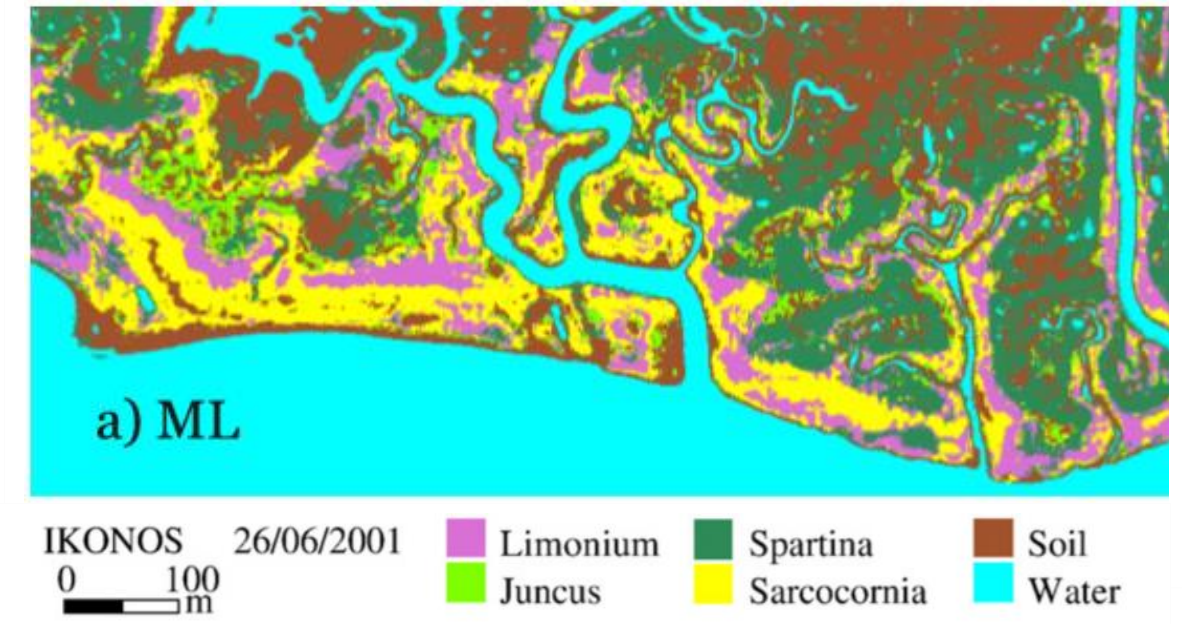

Figure 3.2. Spatial variation of saltmarsh species in the Venice lagoon (Belluco *et al.* 2006).

The ability of both creeks and inflow streams to act as internal sediment transport channels also means the watercourses act as veins of nutrient supply, leading to the establishment of specific species types on both creek benches and levees (French, 1993; Kearney and Fagherazzi, 2016). The influence of creek inflows significantly affects the 'mosaic' species distribution as creeks permit saline tidal water and thus tolerant halophytes to penetrate the upper marsh zones, creating specific sub-environment patterns around dendritic creek systems (Reed *et al.* 1985; Kim *et al.* 2013). This colonisation pattern alters both the accretional and erosional trends throughout the saltmarsh (e.g.

van Eerdt, 1985; Boorman *et al.* 1998; Moller, 2006). Halophytes within the creek system and on the seaward edge of the marsh stabilise sediment and reduce erosion by dissipating wind-blown waves and reducing flow velocity (Van der Wal and Pye, 2004). This creates a lower energy environment favourable to deposition of both halophyte seeds and nutrients allowing distinctive creek communities to become established (Boorman *et al*. 2003; Moffett *et al.* 2012). Consequently, the rate of sediment interception increases due to the frictional effect of vegetation which results in enhanced levels of deposition, raising creek banks and forming characteristic creek benches and levees (Moller, 2006; Kim *et al.* 2016).

This relationship between vegetation, energy dissipation and sediment interception is dependent on the unique environment and the exact species present however. Although an increase in the Manning's coefficient of roughness 'n' of a surface increases energy dissipation and thus deposition rates, the rigidity of plant stems is also a key control on wave energy dissipation (Boorman *et al.* 1998; Moller *et al.* 2014). This cumulative effect of vegetation interception on accretion rates over annual tidal cycles can result in a large variability in sediment organic and carbon content of different sub-environments (Pethick, 1981; Turner *et al.* 2002).

Whilst creek benches enable landward encroachment of highly tolerant halophytes such as *Suaeda maritima* which favours the silt-sand sediment typical of creek margins (Cooper, 1982; Adam, 1990), seldom inundated, fertile creek levees permit seaward encroachment of higher marsh species (Kim *et al.* 2016). This creates distinct sub-habitats that are distinguishable in high-resolution satellite images (Hladik and Alber, 2014; Collin *et al.* 2018). The outcome is a high spatial variability in carbon stored within the predominant surface species throughout the marsh, whilst biomass abundance and carbon storage also varies spatially and temporally with meteorological change and tidal variability (Pennings and Callaway, 1992; Santilan *et al.* 2013).

Salt pans are also key features of saltmarsh landscapes that influence and are influenced by vegetation distribution (Pennings *et al*. 2005; Escapa *et al.* 2015). These features can be characterised into two categories: primary pans which are roughly circular, flat bottomed pools; and channel pans, which are longer sinuous, sometimes branching pools (Pethick *et al.* 1974; Goudie, 2013). Pans often develop irregularly in depressions throughout the marsh where ground saturation in the depression often results in exposed sediment becoming surrounded by vegetation creating an ill-defined embryo pan (Pestrong, 1965; Escapa *et al.* 2015). As a marsh matures and creek/inflow levees rise progressively as a result of net accretion, these waterbodies cease to receive a regular supply of water resulting in stagnation. Consequently, the waterbodies are only replenished during spring tides and during periods of high fluvial inflow so transform into isolated waterlogged brackish pans, creating poor conditions for plant growth. In periods of high evaporation during neap tides in

the summer the water becomes highly saline creating conditions that can only be withstood by the most tolerant of halophytes (Bertness *et al.* 1992; Shen *et al.* 2018). The presence of salt pans further contributes to the irregularity of the saltmarsh mosaic (Griffin *et al*. 2011; Kulawardhana *et al*. 2014) of vegetation and carbon distribution throughout a marsh.

3.2.3 - External Influences on Ecology and Geomorphology

It is acknowledged that a range of influences from livestock to channelisation can impact upon saltmarsh vegetation distribution and carbon storage (e.g. Olsen, 2011; Needles *et al.* 2015). Grazing wildfowl have been found to influence the mosaic pattern of species in saltmarshes, especially where farming or hunting is restricted or forbidden (Ankney, 1996; Pimental *et al*. 2014). A combination of the grubbing of roots and rhizomes of salt-marsh species leads to species loss creating spatial variability of biomass within a sub-environment (McLaren and Jefferies, 2004; Yu and Chmura, 2009). The use of the highly productive upper marsh over centuries for livestock grazing has also substantially influenced saltmarsh geomorphology and species composition (Allen and Pye, 1992; Davidson *et al.* 2017). According to Bos *et al.* (2002) the ecological and geomorphological response to livestock grazing is largely species-specific as their study on Wadden Sea marshes found whilst grazing negatively influenced *Atriplex portulacoides* and *Elymus athericus* in contrast *Puccinellia maritima* and *Festuca rubra* became more abundant. However, the influence of grazing livestock is environment specific as they are restricted by creek location and slope, whilst the highly tolerant halophytes found of the less accessible lower marsh are often not directly affected (Nolte, 2014).

Grazing also influences the carbon storage potential of the surface sediment changes due the influence on microbial biomass and soil respiration rates (Olsen *et al.* 2011). However, the influence of grazing on carbon storage and sequestration is not uniform. The study of Ford *et al.* (2012) on the Ribble saltmarshes found carbon dioxide efflux was on average 87 mg m^{-2} h^{-1} greater in un-grazed marsh than the grazed marsh (mean of 333 mg m^{-2} h^{-1}) throughout the year. Over a 100-year period the Global Warming Potential (GWP), calculated from mean yearly chamber fluxes for CH_4 and CO_2, did not differ significantly with grazing treatment and carbon efflux was instead positively correlated with the water table depth, sediment temperature and species type. Moreover, the research of Elschot *et al.* (2015) also suggested that compaction as a result of livestock grazing on mature marshes resulted in the creation of anoxic conditions in the marsh surface strata which reduced microbial organic decomposition and consequently minimised saltmarsh carbon loss rates.

Direct human environmental modification has also been shown to play a key part in determining ecogeomorphological evolution, substantially altering saltmarsh ecological and geomorphological processes (Allen and Pye, 2002; Atkins *et al.* 2016). Attempts to control and contain saltmarsh environments through diking and dredging of the lower course and main estuarine channels have been exhibited to significantly alter tidal symmetry which consequently affects erosional and accretional trends (e.g. Browne, 2017; Schepers *et al.* 2018). Channelisation and land reclamation considerably influence the tidal cycle and with consequent effects on the distribution of nutrients and species colonisation patterns (Moore *et al.* 2009; Muller-Navarra *et al.* 2016). According to Andrews *et al.* (2000) land reclamation was responsible for a >99% reduction in saltmarsh area and carbon storage capacity in the Humber Estuary when compared to the paleo-estuary 3-2 cal. ka BP (see Figure 3.3). On a larger scale Connor *et al.* (2001) stated that if all previously reclaimed areas in Canada were to revert to saltmarsh, the 2.4 - 3.6 x 10^{11} g C yr^{-1} likely to be sequestered would be equivalent to 4-6% of Canada's targeted reduction of 1990-level emissions under the Kyoto Protocol.

In summary, a combination of external influences have substantially influenced the ecology and geomorphology of UK saltmarshes, serving to alter the current and past carbon storage potential of living biomass and sub-surface sediments. Therefore, it is important to consider these influences when analysing spatial and temporal change in carbon storage in a unique saltmarsh environment.

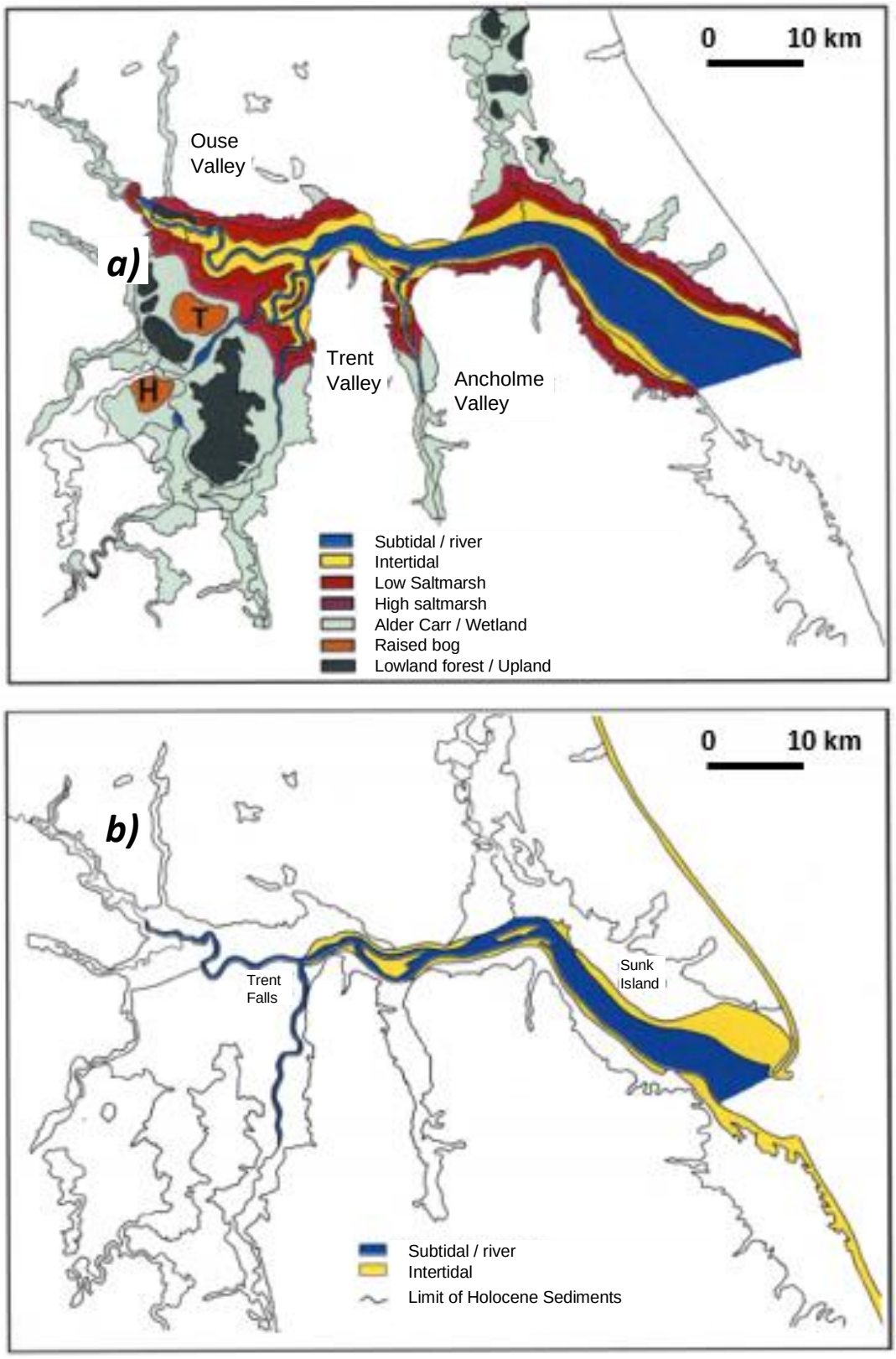

Figure 3.3. Reduction in saltmarsh area in the Humber Estuary between 3-2 cal. ka BP (a) and present (b). Although low and high saltmarsh areas were present in 2000 at the landward fringes of the intertidal zone they are too small to be identified at this scale (Andrews *et al.* 2000).

3.3 – Sub-Surface Dynamics

3.3.1 - Storage Potential

Although the living biomass acts as a significant store and influences the rate of carbon burial and removal, the carbon stored within the living vegetation often represents a low proportion of the total carbon stored within the environment (Rabbenhorst *et al.* 1995; Livesley and Andrusiak, 2012). Whilst the disparity been carbon density stored within the sediments and above-ground living biomass is dependent on the geomorphological history of a saltmarsh (Bridgham *et al.* 2006), in many saltmarshes significant accretion of organic-rich sediments over time results in sub-surface carbon totals exceeding carbon stored in the living biomass (Zedler, 2000; Adam, 2002; Baustian *et al.* 2012). However, it is also possible underlying minerogenic layers perhaps representing previous sand-dominated beach/estuarine environments, can possess lower carbon storage capacities than the living above-ground vegetation (Adam, 1990; Wigand *et al.* 2015).

The periodic sediment and mineral deposition that stimulates a high rate of organic productivity at the surface (Kelleway *et al.* 2016) results in the formation of organic and carbon-rich sediment strata compared to the majority of terrestrial environments (Chmura, 2013). Sediment oxygenation is also generally far lower than in terrestrial environments as sediments remain semi-saturated, primarily because their topography is rarely conducive to rapid drainage but also due to the low sediment hydraulic conductivity (Adam, 1990; Xin *et al.* 2017). The retention of saline water from the flood tide and fresh water from fluvial courses results in the saturation of the surface organic-rich sediments which serves to inhibit oxygen delivery creating an anoxic environment (Colmer *et al*. 2013). Therefore, decomposition rates are reduced and carbon is retained and gradually integrated into successive layers, rendering saltmarsh environments highly efficient carbon stores (Kelleway *et al.* 2016).

However, the overall carbon storage and density throughout the marsh is highly variable (e.g. Cacador *et al.* 2004; Zhou *et al.* 2007). Whilst the lower marshes and creek bench areas are inundated most frequently, the middle and high marsh environments are also significant carbon sinks as the majority of the transported sediment and organic matter is retained after flooding compared to the lower marsh (Dankers *et al.* 1984; Bouchard et al. 2003; Li *et al.* 2010). As a consequence of this, limited nutrient loss and periodic replenishment, the middle-higher marsh is often the most productive and most densely vegetated (Nixon, 1980; Roner *et al.* 2016). However, the presence of creeks and other waterbodies results in the extension of more tolerant halophytes into the higher-middle marsh as the hydroperiod increases around the low-lying areas within the dendritic networks defined as ‘creek benches’ (see Figure 3.1) (French and Stoddart, 1992). The

result of this is a highly localised spatial variability in both species distribution and carbon storage around creek environments that form the saltmarsh 'mosaic' (Mudd *et al.* 2009; Couto *et al.* 2013).

3.3.2 - The Active and Fossil Layers

To accurately assess the carbon stores which could be potentially affected by external influences it is key that a consistent distinction is drawn between the sections of the marsh that directly respond to external processes and those which are not influenced or affected to a lesser extent. When an external influence such as SLR or anthropogenic modification prompts geomorphological evolution, the directly connected 'active' section may regress or transgresses over the 'fossil' layer depending on the geomorphological response (Allen, 1990) (see Figure 3.4). This has clear implications on saltmarsh carbon storage capacity as carbon storage change should largely result from active section response, whereas the carbon stored within the fossil layer should theoretically remain largely undisturbed (Fagherazzi *et al.* 2012; Theurkauf *et al.* 2015). In the context of this study the 'active section' is defined as the section of the marsh most likely to respond to the forcings of external processes which drive geomorphological and ecological evolution. It is comprised of the above-ground living biomass and the active surface layer. The depth of the active layer varies between saltmarsh sub-environments as it is defined by sediment OCD. Specifically, the maximal depth is marked by the depth at which an exponential decrease in sediment OCD occurs which usually coincides with the depth at which undecomposed organic material is found in the sediment. This indicates the depth that a clear ecogeomorphological connection between the above-ground biomass and sediment persists to (Mishra *et al.* 2009; Bai *et al.* 2016). In this study the mean active layer depth ranges between 6 – 39 cm between the different sub-environments (see Sections 4.3.1.2 and 4.3.2.2 for methodology).

In contrast, the fossil layers represent a previous environment which may have had different sedimentological and organic characteristics. This layer is not directly ecogeomorphologically connected to the surface environment so is therefore not as likely to immediately respond to the forcings of external processes (Rahman and Plater, 2014). Whilst it is acknowledged that processes as broad as marine transgression or as localised as bioturbation have the potential to alter the ecogeomorphological characteristics and therefore carbon storage capacity of sub-surface horizons (Allen, 1990; Kostka *et al.* 2002; Hughes *et al.* 2009), taking the approach that the active section only comprises the above-ground living biomass and the directly connected active surface layer ensures that study does not assume any unproven ecogeomorphological connections between sub-surface horizons.

Although it is likely carbon content and density would commonly be higher within surface strata (Cacador *et al.* 2004; Bai *et al.* 2016), in an environment that has rapidly transformed from an intertidal beach to a saltmarsh, discontinuities in the stratigraphy can occur in the form of narrow coarse-grained sediment deposits which are potentially indicative of past high energy events (Roman and Daiber, 1989; Elhers *et al.* 1993; Leonardi *et al.* 2017). Therefore, it is key that the correspondence between sediment carbon content and sediment consistency is assessed throughout the entire core to distinguish between the active section and fossil layers (Leatherman, 1985; Beeftink and Rozema, 1993; Goman *et al.* 2008) (see Figure 3.4).

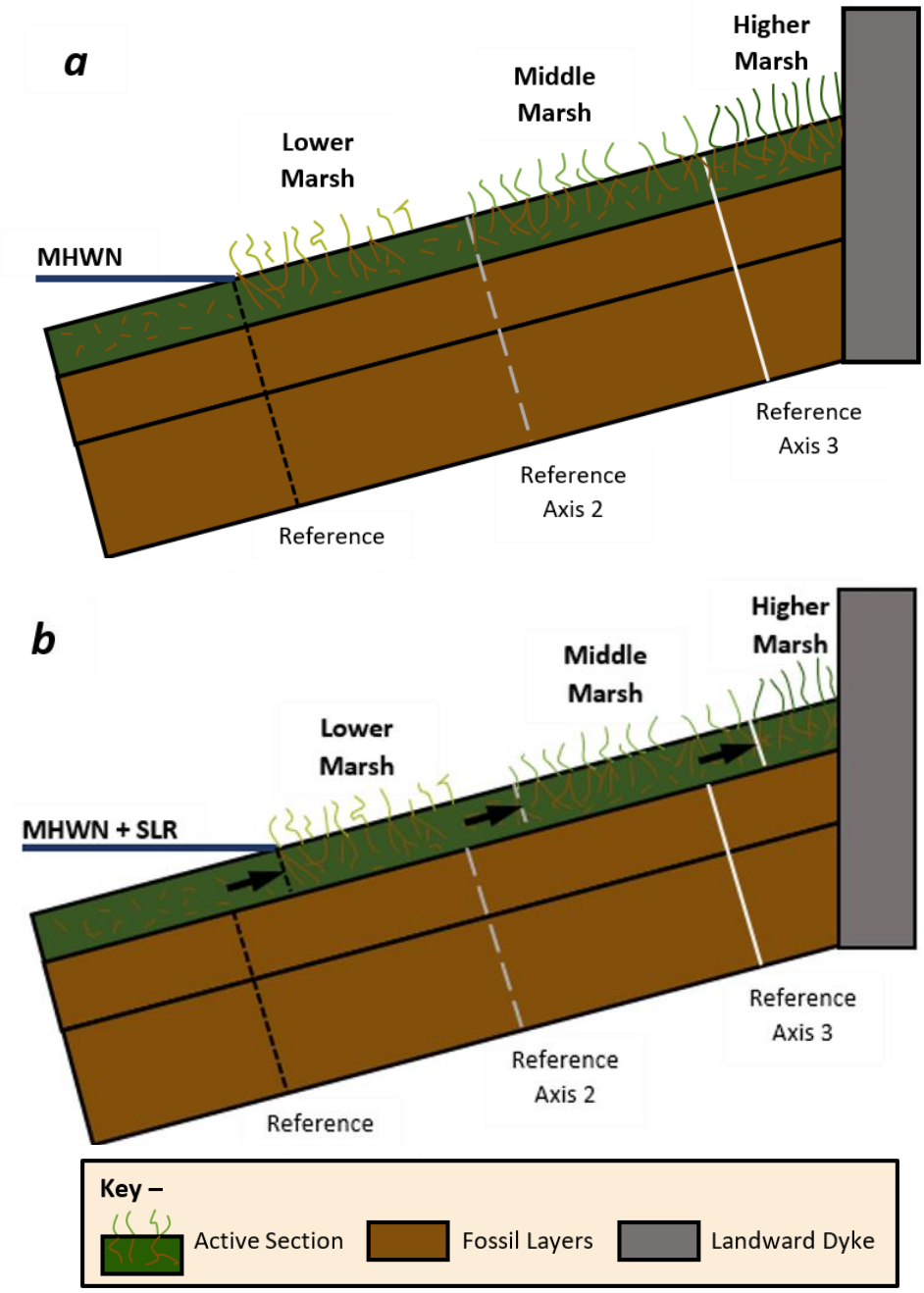

Figure 3.4. Conceptual model of the active section and fossil layers within a theoretical saltmarsh environment (a) and their response to SLR (b). The difference indicated by the arrow is the lateral distance of active layer theoretically lost as a result of SLR.

3.3.3 - Sequestration Potential

Whilst the active section has significant carbon storage potential (Siikmaki *et al.* 2013; Beaumont *et al.* 2014), saltmarshes are also recognised as key environments of carbon sequestration (Callaway, 2012; Burden *et al.* 2013). The high rate of atmospheric carbon uptake is a result of their high biological productivity and their partially anoxic nature, rendering many saltmarshes carbon sinks (McLeod *et al.* 2011). However, the uncertainties surrounding the calculation of carbon sequestration throughout an entire marsh are greater than the uncertainties concerning current carbon storage (Howe *et al.* 2009). Such uncertainties are further exacerbated when predicting future change in sequestration rates as the ecological responses of different species to regional meteorological change must also be additionally factored into calculations along with other climatically dependent variables (Scavia *et al.* 2002; Craft *et al.* 2009). Therefore, research assessing how carbon storage may change under different SLR scenarios is subject to considerably less uncertainty than a study that incorporates both storage and sequestration (e.g. Cacador *et al.* 2004; Zhou *et al.* 2007; Burden *et al.* 2013), hence the emphasis on carbon storage in this research.

3.4 - Sea Level Rise and Marsh Evolution

The influence of SLR on temperate saltmarshes is a topic that has been extensively analysed over the past 30 years, however, there are varying predictions of saltmarsh response to SLR ranging from submergence to equilibrium and expansion (e.g. Park *et al.* 1989; Allen, 1995; Cahoon *et al.* 2006). This highlights how saltmarsh response is both environment and scenario dependent (Reed, 1995; Donnelly and Bertness, 2001; Temmerman *et al.* 2016). As is exhibited in the following section, the evidence which suggests saltmarshes will accrete as a response to SLR is heavily outweighed by the volume of research pointing to the increasing vulnerability of saltmarshes to submergence and degradation as sea level continues to rise (e.g. Morris *et al.* 2002; Horton *et al.* 2018).

3.4.1 - Predicting Geomorphological and Ecological Response

The response of a saltmarsh to SLR is ultimately determined by the balance between sedimentation and SLR which dictates whether a coastal marsh accretes, remains in equilibrium or submerges (Reed *et al.* 1995; Morris *et al.* 2002). However, the mechanisms controlling sedimentation in marsh environments are dictated by the relationships between the key controlling factors: hydroperiod, sediment deposition and vegetative growth (see Figure 3.5). There is also variability in response within the marsh itself as different sub-environments, comprised of various halophytes, respond in a non-uniform manner which can lead to localised responses and vulnerability to SLR (Van Wijnen and Bakker, 2001; Feagin *et al.* 2010).

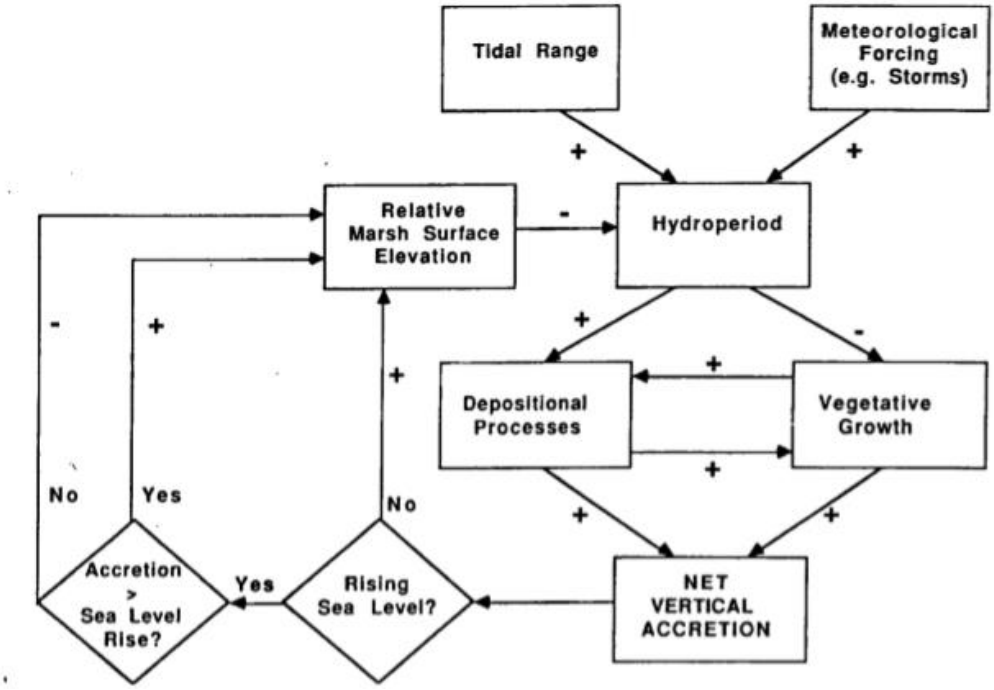

Figure 3.5. The interaction of sea-level rise, hydroperiod, depositional processes and vegetation on saltmarsh accretional response to SLR (Reed *et al.* 1995).

3.4.2 - Submergence

According to key conceptual models, when sea level rises at a greater rate than a marsh vertically accretes, the hydroperiod will increase, leading to an increase in the elevation that certain tidal heights reach (Fitzgerald *et al.* 2008; Day *et al.* 2011). This results in the inundation of previously submerged areas to a greater depth depending on the individual marsh gradient, topography and the rate of localised SLR (Fagherazzi *et al.* 2012; Cahoon, 2015).

As a consequence of the increased height and duration of inundation, halophytes at certain elevation intervals on the saltmarsh experience a progressive increase in exposure to sodium chloride (Donnelly and Bertness, 2001; Morris *et al.* 2002). Moreover, prolonged periods of saturation of the top surface strata may prevent adequate nitrogen uptake by plants and induce sulphide toxicity in *Spartina* species which often dominate the lower section of UK marshes such as the Ribble (Gray *et al.* 1991; Boorman *et al.* 2003; Halcrow *et al.* 2013). Consequently, formerly colonised areas at low elevations gradually submerge and become uninhabitable for even highly tolerant halophytes such as *Spartina anglica* and S*alicornia europaea* (French, 1993; Cahoon et al. 2006). However, there would theoretically be no net marsh or carbon storage loss if the entire saltmarsh was able to progressively migrate landward and re-establish itself at higher elevations. In reality however, either geological structures or dikes often prevent uniform migration leading to the process of 'coastal squeeze' and a rate of saltmarsh loss which is approximately proportional to the

rate of relative SLR (Doody, 2004). This occurs as the most biologically-productive species of the middle-higher marsh such as *Festuca Rubra* and *Phragmites Australis* are unable to migrate to areas of higher elevation and are therefore lost along with the ecosystem services they provide (Warren and Niering, 1993; Boorman, 2003; Feagin *et al.* 2010).

Submergence can also prompt internal dissection and headward extension of the creeks instigating widespread degradation particularly in the middle-upper marsh where saltmarsh adjustment is often constrained by geological or man-made structures (Van der Wal and Pye, 2004; Hughes *et al.* 2009). This initial decolonisation and degradation leaves the formerly protected anoxic active organic layers vulnerable to erosion leading to a carbon storage loss in the former lower marsh and creek sediments as the marsh regresses (Theuerkauf *et al.* 2015). As a result of this, a strong positive feedback cycle is formed (Long *et al.* 2006), where the marsh continues to degrade as local RSL rises (Delaune *et al.* 1994; Watson *et al.* 2017). Consequently, saltmarsh plant communities may be irreversibly damaged, leading to a potential transition to a mudflat environment as the area is gradually submerged and becomes unsuitable for halophyte colonisation (French, 1993; Roman, 2012; Crosby *et al.* 2016).

Although marsh vulnerability to submergence is scenario and locality dependent (Simas *et al.* 2001; Cahoon *et al.* 2006), the coupling of estimated probabilities of marsh retreat with projections of future relative SLR suggests that UK tidal marshes are highly vulnerable to degradation in the 21st century (Nicholls *et al.* 2007; Spencer *et al.* 2016). If the highest plausible SLR predicted in the IPCC RCP 8.5 scenario occurs, by 2100 it is estimated that there will be a >80% probability of saltmarsh retreat in Britain (Horton *et al.* 2018), which would substantially impact on the national saltmarsh carbon storage.

3.4.3 - Equilibrium and Accretion

In contrast to the submergence theory, select conceptual models and predictions suggest vertical accretion on temperate saltmarshes will match or even exceed SLR (e.g. Stralberg *et al.* 2011; Rodgers *et al.* 2012). Kirwan *et al.* (2016) argue that catastrophic predictions of marsh loss in response to future SLR are difficult to defend on the basis of observed marsh responses to historical SLR. According to Kirwan *et al.* (2016), saltmarshes across Europe and North America kept pace with a progressively increasing rate of SLR of >2m over the past 4,000 years ago, highlighting high saltmarsh resilience and adaptability (Kemp *et al.* 2013). It has also been reasoned that incidents of marsh loss within the past 500 years have been largely a result of anthropogenic alteration of tidal estuaries which has severely restricted sediment supply and vertical accretion, as opposed to the sole effect of SLR (Mudd, 2011; Schuerch *et al.* 2018).

Morris *et al.* (2002) and Kirwan and Gutenspergen (2012) also highlighted that the productivity of several marsh plant species tends to increase with relative SLR due to the enhanced level of nutrient deposition which fertilises the environment. The secondary effects of this increased organic production theoretically include the further enhancement of soil structure and the formation of a denser vegetational canopy which encourages deposition and reduces erosion leading to potential marsh growth and expansion (Langely *et al.* 2009; Temmerman, 2012).

3.4.4 - Influence of Relative Sea Level Change

In areas where isostatic uplift exceeds SLR, accretion is likely to reduce as the hydroperiod decreases in correspondence with the rate of relative SLR fall (Ward *et al.* 2016). The result is that sodium chloride exposure reduces along with tidal nutrient deposition and delivery to saltmarsh species. Consequently, there is a gradual replacement of tolerant halophytes such as *Puccinellia maritima* and *Sailicornia europea* with higher-mid marsh types such as *Agrostis stolonifera*, *Festuca rubra* and dicotyledonous plants as the species distribution becomes gradually less dictated by saline stress (Pennings *et al.* 2005; Barnett *et al.* 2015).

However, as the North-west of England is estimated to be subsiding at a constant rate of c. 0.21 mm yr^{-1} (Dawson *et al.* 2001; Shennan and Horton, 2002; Shennan *et al.* 2018) and local sea level is projected to rise by approx. 3.5 mm yr^{-1}, even under the low RCP 2.6 SLR scenario it is highly unlikely that local RSL fall would occur (Palmer *et al.* 2018). Therefore, as the expansion of saltmarshes over tidal flats is unlikely except when relative sea level is falling or gradually rising, the majority of contemporary geomorphological observations suggest that marsh retreat in North West England will be more likely than marsh expansion (e.g. Wolters *et al.* 2005; Nicholls *et al.* 2007; Horton *et al.* 2018).

3.5 - Summary

This review highlights the global importance of saltmarshes as carbon stores and climatic regulators as well as the issues surrounding their future sustainability. The influence of a combination of intrinsic and extrinsic variables has been exhibited to result in unique ecogeomorphological development of estuarine saltmarsh environments, producing variability in the carbon distribution and storage capacity both between and within saltmarsh environments. Most prominently, the impact of SLR will instigate geomorphological change and potentially the degradation of UK saltmarshes. This will most likely lead to degradation and reduce their ability to act as carbon stores.

In order to model and quantify this potential loss it is firstly key to independently assess the variability in carbon storage within the active section of a saltmarsh. In order to address this, an accurate analysis of carbon storage variability within an individual saltmarsh is required. Suitable methods to achieve this are discussed in Chapter 4 (Methodology).

Chapter 4 - Methodology

4.1 Introduction

This study combines a series of methods to quantify and assess the distribution of the carbon stored within the saltmarshes of the Ribble estuary. The approach combines remote sensing analysis with a field and laboratory assessment drawing upon a range of techniques which are described and explained in this chapter. The relationships between the processes and their connection to the overall project aims are summarised in Figure 4.1.

4.2 Spatial Analysis

4.2.1 - Elevation Analysis

To determine the spatial variability in elevation over the saltmarshes of the Ribble estuary a digital elevation model (DEM) for the area was rendered utilising Lidar (light detection and ranging) point cloud data. This is a surveying method that measures the distance to a target by illuminating the target with pulsed laser light and measuring the reflected pulses with a sensor (ESRI, 2018a). Measurements of the differences in laser return times are used to produce 3D point cloud data which can subsequently be converted into 2.5D digital elevation models of the surface (Pack *et al.* 2012).

The Lidar data used in this study was sourced from an Environment Agency 2012 survey from EDINA Digimap which was the highest resolution (0.25 m) survey with the most extensive spatial coverage. However, two separate distorted areas on marshes C and D collectively comprising 4.1% of the total marsh area were identified and excluded from the analysis. Whilst, the topography of the Ribble will have evolved over the 8 years since the Lidar survey and the commencement of this study, recent assessments of the Ribble suggest that significant geomorphological and ecological evolution during this period has not been observed and is highly unlikely (Halcrow *et al.* 2013). Therefore, the DEM utilised is likely to most accurately represent the current spatial variability in elevation over the saltmarshes of the Ribble, enabling the determination of subtle changes in elevation and gradient. Moreover, although data of this quality and resolution has been available in select UK locations, relevant published studies in the locality have only utilised manual levelling techniques to identify variability in elevation (Gray *et al.* 1979; Marks and Truscott, 1985). Whilst levelling is accurate, it does not provide a comprehensive assessment of the spatial variability in elevation across an entire saltmarsh, hence the use of Lidar makes this study the most comprehensive assessment of the influence of: elevation, gradient and creek distance on the spatial distribution of vegetation in the marsh environment to date.

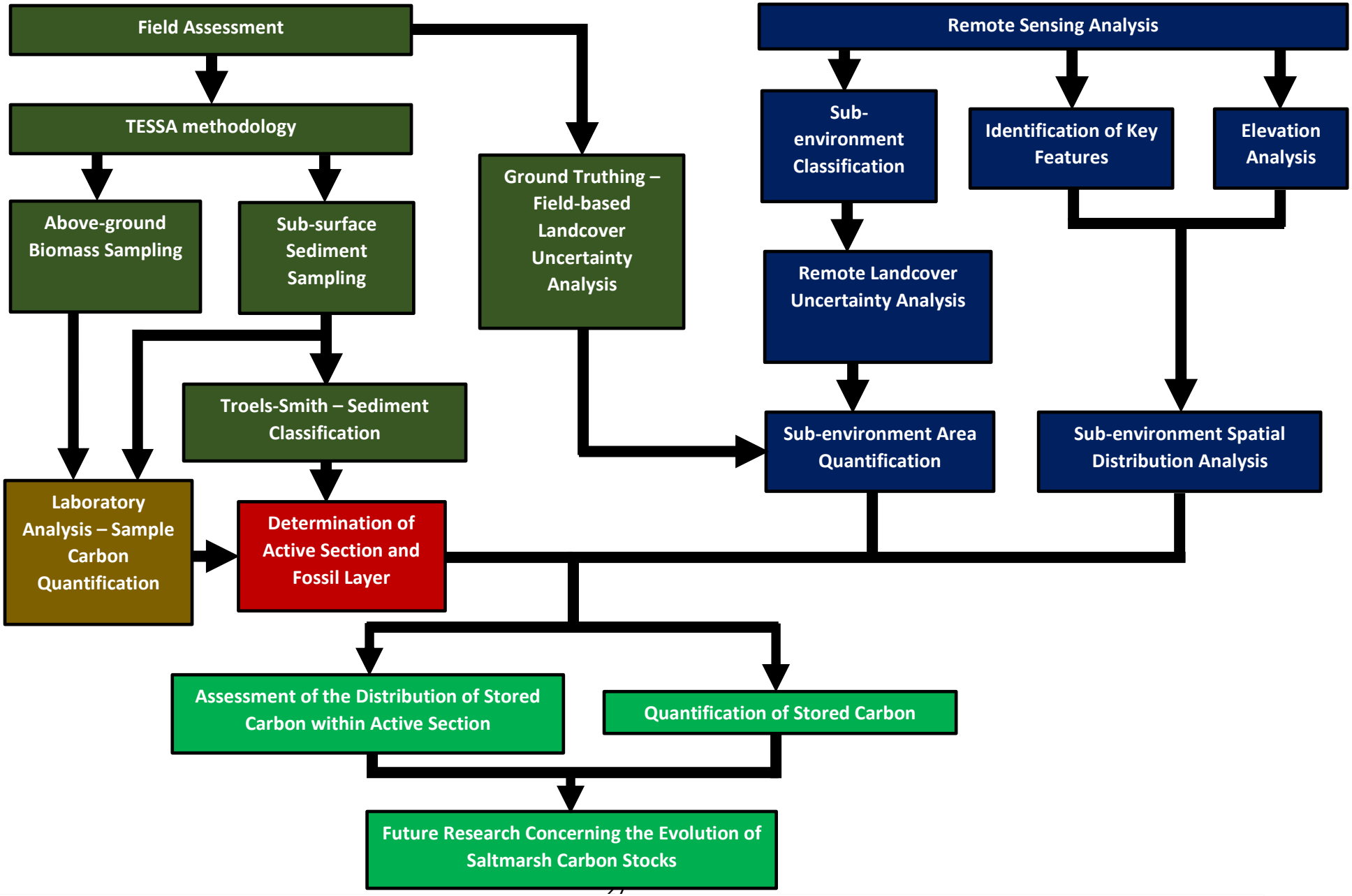

Figure 4.1. Summary of the overall methodology and the relationships between differing methods. Methods are categorised as follows: field based (dark green), remote sensing (dark blue), laboratory (dark yellow), combined field and laboratory (red) and all methods combined (turquoise).

In order to produce the DEMs of the Ribble estuary the point cloud data had to be firstly converted from the compressed LAZ format into uncompressed LAS format using the program laszip.exe so that it was compatible with the GIS software ArcMap (Isenburg, 2018). The LAS dataset was then converted into a DEM in a raster format with a cell size of 0.25 m using the 'LAS Dataset to Raster' tool to interpolate the data. Although the spatial variance in elevation could be observed due to the high resolution of the data, a slope model of an identical resolution was also created on ArcMap to exhibit spatial variability in gradient.

4.2.2 - Landcover Classification

The decision was taken to use high spatial resolution imagery (0.25 m) with three spectral bands (R-G-B) over imagery with a lower spatial resolution (e.g. 10 m) but more spectral bands (e.g. Sentinel-2 satellite imagery) (Digimap, 2018; ESA, 2018). This was because the high spatial resolution of the aerial imagery allowed differentiation between details on small scales (0.25 m). This was essential to the study, despite the reduced ability to differentiate between very subtle differences in reflectance values (colour) (Rocchini, 2007). Individual 1 km^2 tiles were amalgamated using the 'Mosaic' tool on ArcMap allowing a uniform landcover classification to be carried out so the areal extent of the different species/landcover types that comprised the saltmarsh could be identified.

The image classification process involved the classification of multi-band raster imagery into a single-band raster with categories that indicated different types of land cover. Due to the use of 3-band aerial imagery and the high similarity in reflectance values among saltmarsh landcover types, it was decided after experimentation that a 'supervised' maximum likelihood (ML) classification was more appropriate than the alternative 'unsupervised' classification as a means to identify spatial variability in landcover. The 'supervised' classification method required the mosaiced image to be classified using spectral signatures representing reflectance values that were obtained from training samples. The training samples consisted of manually digitised polygons comprised of pixels with a range of reflectance values (ESRI, 2018). Overall eight different landcover types were classified using this technique as this enabled the ecologically and geomorphologically distinct sub-environments to be determined. The 'supervised' classification of each sub-environment was automatically determined by the best fit of the spectral distribution to the values of each class.

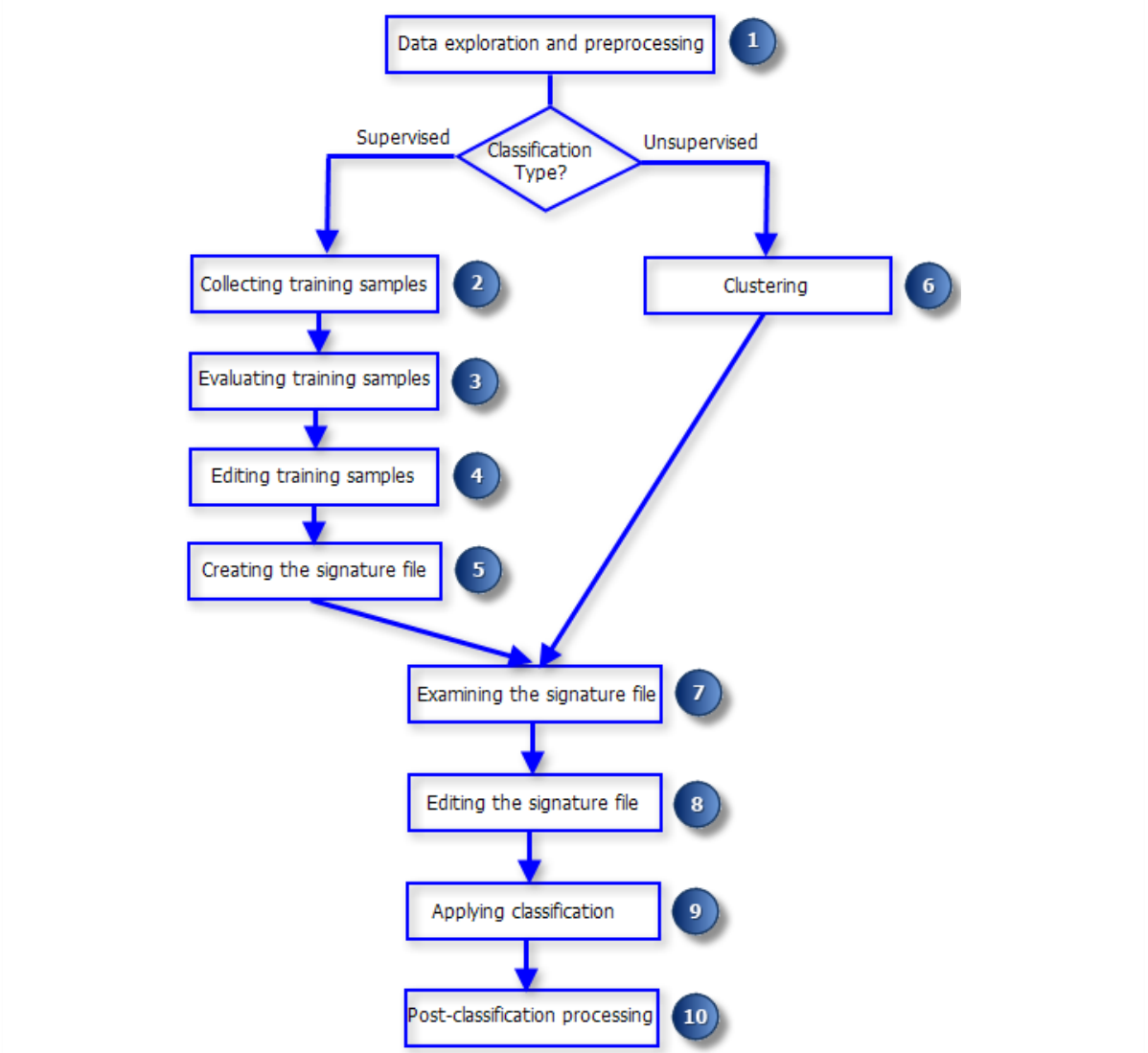

Figure 4.2. The different stages of supervised and unsupervised classification processes (ESRI, 2018b).

Although Goodwin *et al.* (2018) demonstrated an unsupervised classification using Topographical Identification Platforms (TIPs) could potentially be used to distinguish between saltmarsh sub-environments at different elevations, a supervised classification was selected because the majority of the researched published during the time of the remote analysis highlighted supervised analyses were more accurate in wetland environments (Thomson *et al.* 1998; Shalaby & Tateishi, 2007; Martin *et al.* 2014). On the completion of the ML classification a landcover raster was produced with discrete categories and specific identification values for each determined landcover types. These landcover categories were initially given non-species-specific names such as 'Light green creek terrace vegetation' as the exact species that comprised various sub-environments, termed 'zones', would be later determined after ground-truthing. The area of each landcover type within the marsh was then initially determined by multiplying the number of pixels representing areal cover by their area of 0.0625 m^2 (0.25 x 0.25 m).

4.2.2.1 - Uncertainty Analyses

Although previous research exhibited that supervised ML classifications in wetlands environments have a high accuracy (>80%), the accuracy of classifications can vary between different environments (Ozesmi and Bauer, 2002; Zhang *et al.* 2011; Gosselin *et al.* 2014). Therefore, it was important to undertake an assessment of the accuracy/uncertainty of the ML classifications for each sub-environment and Ribble saltmarshes as a whole. Consequently, two uncertainty analyses were undertaken both remotely and in the field to verify the accuracy of the supervised classification and assess the uncertainty surrounding the landcover areal assessment.

4.2.2.1.1 - Remote Uncertainty Analysis

The remote uncertainty analysis was performed using ArcGIS using 2003 reference points which were randomly distributed throughout each sub-environment and the Ribble marshes as a whole. Each reference point was given an identification value for the sub-environment they represented and a stratified sampling method was employed so the number of points was approximately proportional to area covered by the sub-environment in each saltmarsh with a sampling point representing an area of 0.0145 km^2. Reference points were then converted to a raster TIF format (format of the aerial imagery) before the 'Combine' tool was used to identify the correspondence between the identification values of reference pixels and the identification values of the discrete categories for each classified landcover type.

Subsequently a quantitative assessment of the ML performance was undertaken using a confusion matrix. This enabled the determination of the classification accuracy for each landcover type and the overall accuracy, A:

$$A = \frac{\Sigma\ Correctly\ classified\ values}{\Sigma\ All\ values} \quad (1)$$

A confusion matrix was produced to enable the classes erroneous reference points had fallen into to be identified and establish trends in errors between discrete classes. It also enabled the calculation of the Kappa coefficient (k) which describes the proportion of correctly classified validation sites after random agreements are removed (Rosenfield & Fitzpatrick-Lins, 1986) (see section 5.1.1 – Areal Quantification). This analysis was undertaken over the entire saltmarsh and on each of the four pre-defined marshes in order to establish whether any differences in landcover accuracy classification existed at different spatial scales.

k was determined as follows:

$$k = \frac{Pr(a) - (Pr(e)}{1 - Pr(e)} \quad (2)$$

Where –

$$\Pr(a) = \text{Observed agreement rate} = \frac{\Sigma\ Correctly\ classified\ values}{\Sigma\ All\ values} \quad (3)$$

$$\Pr(e) = \text{Hypothetical probability of chance agreement} = \frac{1}{N^2}\sum_k nk_1 nk_2 \ldots \quad (4)$$

Where –

$N = \text{Number of land cover classifications}$

$nk_i = \text{Number of times i predicted category k}$

4.2.2.1.2 - Field Uncertainty Analysis

The second uncertainty analysis was the ground-truthing process where the variability in landcover was analysed in the field at pre-determined points evenly distributed throughout each marsh. Each site was determined to a vertical and lateral position of ~5 m due to uncertainties surrounding the handheld GPS measurements. As with the remote analysis the number of reference points were proportional to the area of the sub-environment, although due to practical constraints there were 51 manual observations compared to 2003 remote observations. Once the reference sites were reached using GPS, photos and physical samples of each site were taken before the Stace (1997) vegetation classification was used to identify the species. This also enabled the species present in certain sub-environments to be classified (see Table 4.1).

Table 4.1. Comprising species of the six predominately vegetated sub-environments.

Pre-Fieldwork Classification	Post-Fieldwork Classification - Species Zone	Present Species
Dark Green Higher Marsh Vegetation	A	*Agrostis stolonifera, Atriplex portulacoides, Juncus gerardii, Armeria maritima*
Very light green vegetation	B	*Festuca rubra, Elymus repens, Triglochin maritima, Tripolium pannonicum*
Mid-Green Lower Terrace Vegetation	C	*Atriplex portulacoides, Puccinellia maritima, Cochlearia officinalis, Sueda martima*
Light Green Higher Terrace Vegetation	D	*Puccinellia maritima, Agropyron pungens, Elymus repens*
Orange-Brown Vegetation	E	*Spartina Anglica, Salicornia spp, Sagina maritima*
Unrecognised	F	*Eleocharis uniglumis, Juncus gerardii*

Subsequently the correspondence between the ML classification and ground observations was determined by comparing the consistency of the appearance of certain species throughout all saltmarsh environments. The overall accuracy of ML classification following ground-truthing was

then calculated and erroneous trends between certain sub-environment/landcover types were identified (see Section 5.1 – Spatial Analysis of Landcover). A comparison between both remote and ground-based uncertainty analyses was then undertaken as exhibited in Section 5.1.

4.2.3 - Variables Influencing Sub-environment Distribution

As a high-resolution DEM had been produced and an accurate landcover classification had been undertaken it was possible to undertake a quantitative analysis of the key factors that influenced the spatial distribution of sub-environments and therefore carbon storage in the Ribble (see Section 4.2).

4.2.3.1 - Elevation and Gradient

Using the 'Extract by Mask' function in ArcMap it was first possible to determine how elevation and gradient affected species spatial variability and distribution. This enabled the collection of data regarding both elevation and gradient for every pixel categorised by the ML classification to be in a certain sub-environment/landcover category. This data was subsequently exported into .txt format so that it could be read by R-studio. Utilising the C++ programming language, the elevation, gradient and watercourse proximity of the different sub-environments was quantitatively assessed and compared. Specifically, this involved the comparison and assessment of histograms and associated kernel density distributions concerning the elevation and gradient distributions of each species. This enabled a quantitative assessment of the elevation and gradient of each certain sub-environment throughout each marsh and the environment as a whole (see Section 5.2 – Influence of Elevation and 5.3 – Influence of Gradient).

Although the kernel density and violin plots highlighted the different influences of the three key controls on the different marsh sub-environments these results did not reveal the relative influence of each key influence on sub-environment and consequently carbon distribution. Therefore, a multiple regression analysis was undertaken using SPSS primarily to produce beta coefficients (standardised and unstandardised) which are measures of how strongly each of the key controls (independent) influence sub-environment distribution (dependent). Specifically, this analysis enabled the determination of the t statistic and p value as well as unstandardised beta coefficient produced by regression analysis which represented the amount of change in a dependent variable due to a change of X units of the independent variable. This gave a quantitative indicator of the influence when compared with the raw data (i.e. elevation (mOD) or gradient (°)). Alternatively, the standardised beta values produced by the analysis were presented as units of standard deviation

(i.e. a beta value of 5 means indicates a change of one standard deviation in the independent variable will produce a change of 5 standard deviations in the dependent variable) permitting a direct quantitative comparison of the influence of the three key controls on the spatial distribution of the different sub-environments.

4.2.3.2 - Watercourses

To identify the influence of creek systems the 'Hydrology' toolkit in ArcMap was used. This firstly involved using the 'Fill' function to ensure that all erroneous artificial sinks and peaks in the 0.25 m resolution DEM were removed. A raster dataset indicating flow direction at 45° intervals (D8 flow direction) was then produced to determine the location of cells of water accumulation (see Figure 4.3). This enabled the location of fluvial inflows and creeks to be identified.

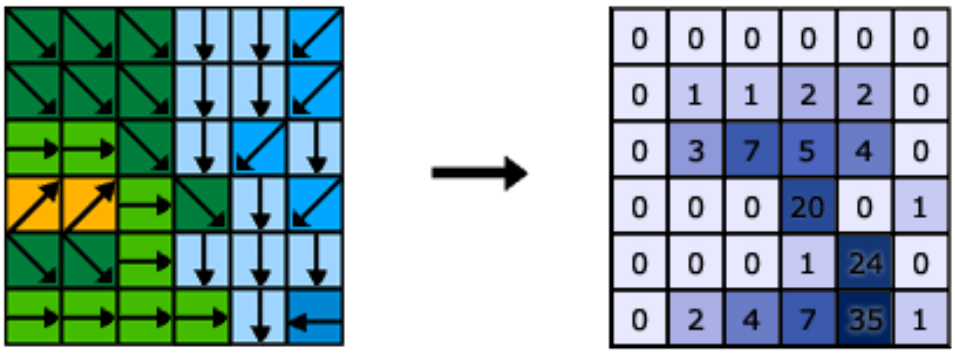

Figure 4.3. Diagramatical representation of the flow direction model and the resultant flow accumulation raster (ArcGIS, 2018).

The subsequent flow accumulation raster was then modified from a 'stretched' ramp display view to a 'classified' format to enable one to distinguish between discrete arbitrary values of flow accumulation. After experimenting with the arbitrary flow accumulation value, it was decided that the value of 3500 was to be universally used as this value enabled all major creek systems and fluvial inflows visible in the digital imagery to be distinguished throughout the saltmarshes. This meant that all cells defined as watercourses had a minimal catchment area of 219 m^2 (i.e. a minimum of 3500 cells with an individual area of 0.625 m^2). Using the 'reclassify' and 'raster to polyline' functions it was then possible to create shapefiles identifying the cells of water accumulation representing the watercourses. Following this an identical process using the 'Euclidean Distance' and 'Extract by Mask' functions was performed along with a statistical analysis in R-studio which was identical to those performed for elevation and gradient. This allowed a quantitative assessment of the control of watercourses on species distribution (see Section 5.4 – Influence of watercourses). The multiple regression analysis mentioned in 4.2.3.1 was repeated for watercourse proximity.

4.2.3.3 - Summary

In summary, the GIS, R and SPSS-based analyses enabled a comprehensive assessment of the spatial variability of sub-environments based on their landcover type, whilst also permitting a quantitative assessment of the influence of: elevation, gradient and watercourse proximity on the spatial distribution of sub-environments. However, as the overall total carbon stored in a sub-environment and throughout the saltmarsh was a product of the areal coverage, active layer depth and active layer organic carbon density (OCD) it was important that the latter was accurately quantified and the uncertainty around OCD was determined (see Section 4.3). The OCD calculations were subsequently incorporated with the uncertainty assessments concerning area, depth and volume to determine projections for total carbon storage at present (Section 4.4) and under different future sea level rise scenarios (Section 4.5).

4.3 - Field and Laboratory Analysis

The field assessment undertaken on the saltmarshes of the Ribble was performed with the primary aim of accurately quantifying the carbon storage of the above-ground biomass and active layer sediment in the different sub-environments. This enabled the spatial assessment of both the contemporary distribution of carbon and organic production in the form of the above-ground biomass, but also the sampling of carbon in the active layer sediments enabled an assessment of how carbon storage had changed in the sediment record in differing sub-environments. By combining the two assessments the aim was to determine the overall carbon storage of the active section.

As the principal purpose of the study was to assess the spatial distribution of sub-environments and carbon throughout the Ribble estuary, the primary requirement was to select an approved technique that would enable a standardised assessment of carbon stock in wetland and saltmarsh environments. Following a review of the potentially applicable methodologies it was decided the standardised procedures outlined in the Toolkit for Ecosystem Service Site-based Assessment (TESSA) (Peh *et al.* 2017) were most appropriate for the analysis. This was because the TESSA details methods for site-based sampling of both above-ground living biomass as well as sub-surface biomass and sediments which comprise the active section and fossil layer(s) in marsh/wetland environments (see Figure 3.4 for conceptual model). Unlike the majority of toolkits such as the Coastal and marine ecosystem services valuation system devised by Luisetti *et al* (2011) or the Saltmarsh Carbon Stock Predictor (Skov *et al.* 2016) the TESSA methodology had been adapted for use at a localised, in-field levels. It also enabled a quantifiable, replicable, credible and affordable assessment to be

undertaken, which is essential for any ecosystem service assessment (Bagstad *et al.* 2013). Overall the TESSA field methodology enabled the analysis to be undertaken most efficiently without the requirement for specialist ecosystem services assessment training which was not possible given temporal and financial restraints. Moreover, the TESSA also featured a specific laboratory methodology designed to ensure an accurate standardised assessment of the organic carbon density of the above-ground biomass and sub-surface sediments.

Sampling was undertaken in all sub-environments identified in the previous ML classification to determine how biomass/carbon mass varied both within and between differing sub-environments. Overall sampling was undertaken at 39 different sites and the number of sites in each sub-environment approximately represented the proportion of the area it covered on each marsh (ML area) although access and time restrictions meant that this was not possible on every marsh (see Appendix Section C for locations). The rationale behind this sampling strategy was a product of fact that the geomorphological, ecological and carbon characteristics of sub-environments that covered larger areas were more likely to exhibit greater inter-site variability than those which covered comparably small areas such as Species Zone F (e.g. Zhou *et al*. 2007; Tong *et al.* 2010).

All field sampling was conducted over two 5-day periods between 5th February and March 10th 2018 in order to minimise any temporal disparity in biological production, and therefore variability in carbon content (particularly above-ground biomass) throughout the saltmarsh. Sampling at this time also gave an insight into the annual temporal variability of sediment organic carbon and the influence of organic production over the summer of 2017. Sampling later in the year was not only impractical due to the temporal constraints of the project, but the low rates of productivity and decomposition over the winter months meant that in theory there would have been very little difference in the organic carbon density of active layer between the chosen period and the early summer (Zhao *et al.* 2016).

4.3.1 - Field Assessments

4.3.1.1 - Above Ground

In order to ensure all samples were taken as close as possible to the locations which had been pre-specified following the remote classification, a handheld GPS with a positional accuracy of ~5 m was utilised. At each site the predominant species within a 0.5 x 0.5 m quadrat (see Figure 4.4) were identified according to a universal classification developed by Stace (1997). Following this, care was

taken to remove all vegetation that was rooted within the 0.25 m^2 quadrat, ensuring vegetation was removed from as close to the stem base as possible. This material was then placed within a sealable plastic bag(s) and then placed in a domestic fridge at a temperature of 4-5°C to limit the decay of organic matter.

Figure 4.4. 'N Site A' on Marsh D after above-ground and subsurface sediment sampling.

4.3.1.2 - Sub-surface

The sub-surface assessment consisted of the extraction of sediment and underground biomass from each sampling site. This was achieved using a manually operated gouge corer with a cavity diameter of 2.4 cm used to take samples in the centre of each sampling quadrat as this was deemed to best represent the geomorphology of the specific sub-environment. Sediment samples were taken until it was no longer physically possible to core any deeper which was commonly a result of an inability to penetrate sediment layers that were comprised of either fine-medium grained sediment. For this reason, the gouge was selected over the Russian corer, as the high level of saturation of the saltmarsh sediment made penetration with only manual force very difficult or impossible. Due to the locations of certain sites in sites of special scientific interest (SSSI) only manually operated cores were used to ensure sampling was as standardised as possible.

Following the extraction of sediment from the marsh, the stratigraphy of each core was logged enabling differing horizons to be distinguished based on their observed physical properties. For this

stage a comprehensive classification for sediments from organic-rich temperate lakes and wetlands designed by Troels-Smith (1955) was undertaken at every site (see Figure 4.5). This enabled the assessment of the: composition, degree of humification and physical properties of sediment which varied with depth (see Figure 4.6). This formed a part of the identification of the organic active section from the fossil layer (see Section 3.3.2).

Lithology Key

As = Clay (<0.002mm)
Ag = Silt (0.002 – 0.06mm)
Ga = Coarse sand (0.6 – 2mm)
Ca = Calcareous shell
Sh = Humified organics beyond identification
Th = Roots, stems and rhizomes of herbaceous plants
Dh = Fragments of stems and leaves of herbaceous plants >2mm
Lf = Mineral and/or organic iron oxide

Approximate Composition –
4 = 100% 3 = 75% 2 = 50% 1 = 25% + = 12.5% (Trace)

Figure 4.5. Sediment consistency component of thee Troels-Smith classification sediment procedure.

Subsequently, 5 samples with a volume ≥1 cm^3 were taken at evenly distributed intervals throughout all cores which varied in length from 0.29 m to 1.98 m. Samples were taken following the removal of Exposed Sediment from the surface of the sediment core to avoid sampling contaminated sediment. The purpose of this was so that the carbon change with depth within horizons could be later analysed under laboratory conditions (4.3.2.2). This process was an important part of the identification of the base of the active layer as organic carbon density (OCD) is a key indicator of sediment characteristics (e.g. Bradley and Morris, 1990; Cao *et al.* 2015) and therefore the division between the base of the active and fossil layers. Due to the heterogeneous nature of sub-environments the depth of division both between and within sub-environments was unique. Using the guidance of recent research (*Bai et al. 2016*; *Skov et al.* 2016) concerning the exponential decrease in OCD with depth below the active layer and the sedimentological findings it was decided the active layer sediment was classified as that having a mean OCD (see Section 4.3.2.2) >15% than the overall sub-surface sediment and possess undecomposed organic material. The boundary of 15% was set in order to distinguish between active and fossil layers in the more homogenous sediment in sub-environments defined as Brackish Waterbodies, however the mean active layer content was on average 43.4% greater than that of all the sub-surface sediment due to the exponential decrease in OCD between sub-surface fossil layers and clearly distinguishable organic-rich surface layers. This criterion produced a mean active layer depth ranging between 12.6 cm

(Species Zone A) and 23.3 cm (Exposed Sediment), a depth similar (10 cm) to that used in recent research assessing contemporary saltmarsh carbon stocks (Ford *et al.* 2019).

Five samples with a volume ≥1 cm^3 were also taken at equal depth intervals throughout the active layer, although for short active layers (<5 cm^3 in volume) the maximum volume was sampled. The purpose of this was to determine the variability of OCD content throughout the active layer in order to later assess if there was any link between sub-environment type and OCD variability (see section 5.2.2.3).

Figure 4.6. Test stratigraphy from Marsh B. The active layer (light blue) is clearly distinguishable due to its higher organic content, light brown colour and clear connection to the above-ground vegetation. Alternatively, the fossil layers (red) show no clear connection to the above-ground vegetation and have a lower organic content.

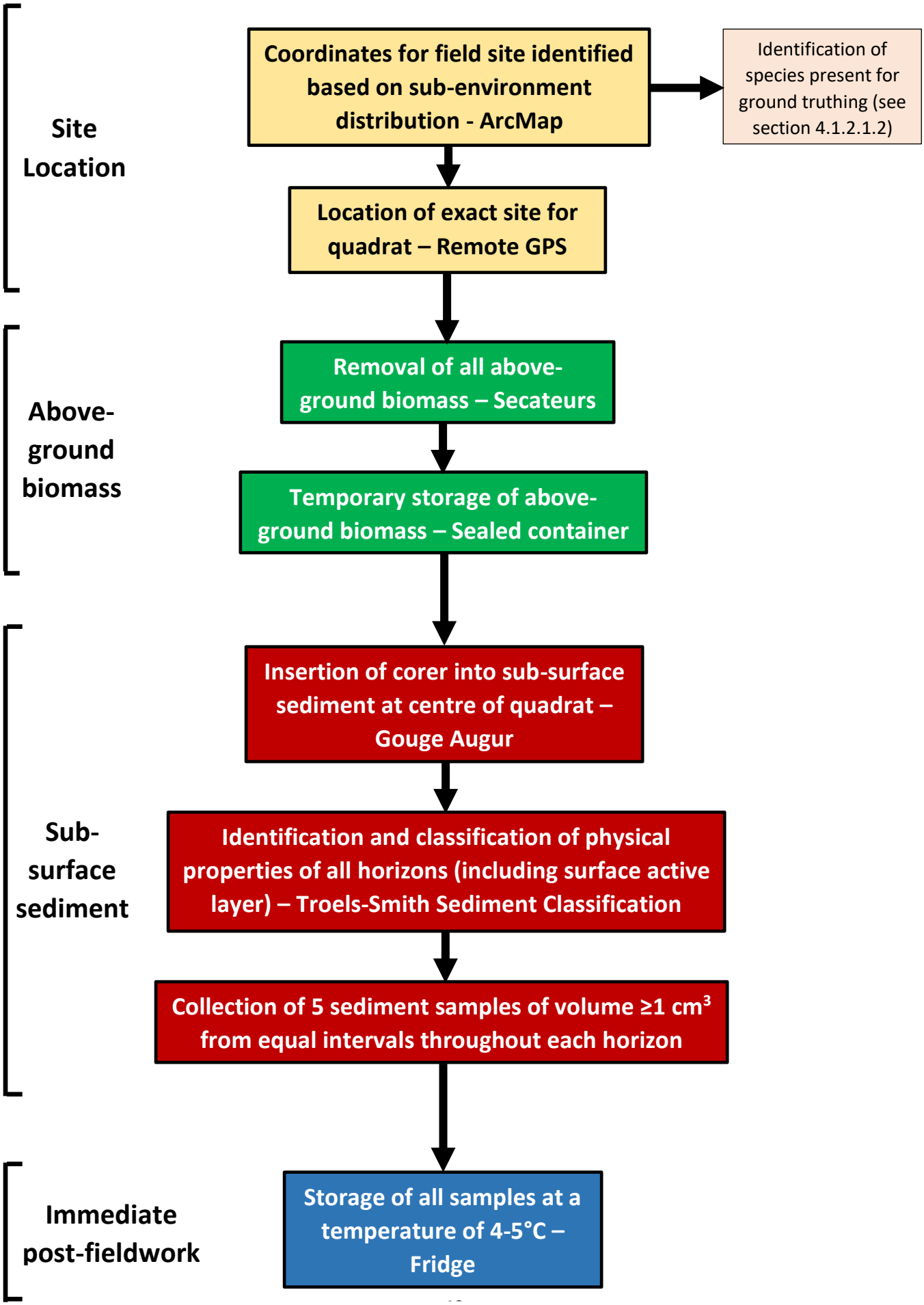

Figure 4.7. Summary of field protocol and key equipment used.

4.3.2 - Laboratory Carbon and Biomass Assessment

The following section outlines the methods used in the laboratory carbon and biomass assessment. A legend for the acronyms used in all equations is shown in Figure 4.8.

Laboratory Acronyms

AGWM – Above-ground wet mass (g)

AGWMT – Above-ground wet mass and tray (g)

AM – Ashed mass (g)

AGDM – Above-ground dry mass (g)

AGCM – Above-ground carbon mass (g)

BD – Bulk density (g cm^{-3})

BGDM – Below-ground dry mass (g)

DM – Dry mass (g)

OCC – Organic carbon content (%)

OCD – Organic carbon density (g m^{-3})

OCCS – Organic carbon content per stratum (g)

OMC – Organic matter content (%)

TM – Tray mass (g)

WV – Wet volume (cm^3)

Figure 4.8. Acronyms for laboratory carbon and biomass assessment methodology.

4.3.2.1 - Above Ground

The first part of the analysis concerning the above-ground biomass which employed TESSA methods involved washing the samples in warm (c. 40°C) deionised water to remove all sediment that could considerably influence the sample mass (Truss, 2011).

A steel sample tray(s) was then weighed to a precision of ±5 x 10^{-5} g using standard laboratory protocol (National Lacustrine Core Facility, 2013). The above-ground wet mass (AGWM) was obtained by subtracting the combined mass of the above-ground wet mass and tray by the tray mass (TM):

$$AGWM = AGWMT - TM \quad (5)$$

The sample and tray was then placed in a laboratory oven at a temperature of 105°C for 48 hours and the sample was periodically rearranged to permit aeration. The sample was then left to cool until it reached room temperature (20°C) before the mass of the dry sample and tray was obtained.

Once the above-ground dry mass (AGDM) had been obtained this value was multiplied by 0.47 in accordance with TESSA and IPCC guidance to obtain the total sample above ground carbon mass (AGCM) (Peh *et al.* 2017). The dry mass was multiplied by this value because it is estimated by the IPCC Guidelines for National Greenhouse Gas Inventories that approximately 47% of the above-ground biomass of temperate coastal wetland vegetation is comprised of carbon (Eggleston *et al.* 2006).

(6) $$AGCM = AGDM \times 0.47$$

4.3.2.2 - Sub-surface

The first stage of the sub-surface laboratory analysis required weighing individual crucibles on a calibrated balance in order to determine the mass of each to a precision of ±5 x 10^{-5} g. Subsequently, the samples with a wet volume (WV) of 1 cm^3 were added to each crucible before the difference between the two was determined. All samples and crucibles were then placed in a laboratory oven at a temperature of 105°C for 48 hours (Peh *et al.* 2017).

After this period the samples were removed from the oven and left to cool in a desiccator in accordance with standard laboratory protocol (National Lacustrine Core Facility, 2013) until they reached room temperature (~20°C). Following this, the dry mass (BGDM) of the sample and crucible was obtained before dry mass of the sample was determined by subtracting the combined mass by that of the specific crucible.

Following this the bulk density (BD) was calculated:

(7) $$BD = \frac{BGDM}{WV}$$

After the dry mass had been determined the samples were placed in a laboratory oven at 440°C for 24 hours to determine their organic matter content as according to TESSA guidelines (Peh *et al.* 2017). Subsequently, the ashed mass (AM) of the sample was determined using the identical procedure for determining below-ground dry mass (BGDM). The mass (g) of the organic matter content (OMC) of the sample was then determined:

(8) $$OMC = BGDM - AM$$

(9) $$OMC = ((BGDM-AM)/DM) \times 100$$

The organic carbon content (OCC) was then calculated using the TESSA estimate that carbon comprises 57.1% of all sediment organic matter:

(10) $$OCC = OMC / 1.75$$

The organic carbon density (OCD) for each strata was subsequently calculated:

$$OCD = BD \; x \; OCC \tag{11}$$

The results of the 5 OCD samples taken from each stratum were then averaged (mean) to give an overall mean OCD for each layer and the mean organic carbon content for each strata (OCCS) was then determined:

$$Sampled\ horizon\ volume = Observed\ horizon\ depth \; x\ corer\ area \tag{12}$$

$$OCCS\ (g) = Sampled\ horizon\ volume \; x \; OCD \tag{13}$$

4.4 - Determining Overall Carbon Storage

The total sub-surface and above-ground carbon storage for a sub-environment was then determined by combining the field and laboratory results concerning depth and carbon content with the area assessment results from the maximum likelihood classification (*ML Area*).

Overall Carbon Storage Acronyms

ASMF – Above surface multiplication factor

ASTCS – Above surface total carbon store (kg)

AGCM – Above-ground carbon mass (g)

ML Area – Maximum likelihood classification area (m^2)

SSCS – Sub-surface carbon storage (g)

SSVMF – Sub-surface volume multiplication factor

OCCS – Organic carbon content per stratum (g)

SSTCS – Sub-surface total carbon stored (kg)

TCS – Total carbon stored in an individual sub-environment (kg)

Figure 4.9. Acronyms for overall carbon storage assessment.

The above surface carbon stock (ASTCS) was determined as so:

$$Above\ Surface\ Multiplication\ Factor\ (ASMF) = \frac{ML\ Area}{Quadrat\ Area} \tag{14}$$

$$ASTCS = \frac{ASMF \; x \; AGCM}{1000} \tag{15}$$

Subsequently the sub-surface carbon storage (SSCS) of an individual horizon was calculated as follows:

(16) $$\text{Total sub-environment horizon volume} = \text{Observed Horizon depth} \times \text{ML Area}$$

(17) $$\text{Sub-surface Volume Multiplication Factor (SSVMF)} = \frac{\text{Total sub-environment horizon volume}}{\text{Sampled horizon volume}}$$

(18) $$SSCS = OCCS \times SSVMF$$

This value was subsequently summed with the SSCS values of other horizons to give an estimate of the sub-surface total carbon stored (SSTCS) within a specific sub-environment:

(19) $$\boldsymbol{SSTCS} = \frac{Sum\ of\ SSCS}{1000}$$

The total carbon stored in individual sub-environments (TCS) could then be calculated:

(20) $$\boldsymbol{TCS} = ASTCS + SSTCS$$

The values were presented as kg x 10^{-3} (1.d.p) to accurately exhibit carbon storage within results tables. In-text references to carbon are presented to 3.s.f as this level of significance was sufficient to compare the variability in carbon storage. The estimated overall carbon storage for each saltmarsh could then be determined by summing TCS values for the 8 differing sub-environments. Likewise, the spatial distribution of carbon stocks throughout the saltmarsh and the influences of key landscape features on distribution were also subsequently assessed by combining the sub-environment spatial distribution analyses with the appropriate carbon storage assessments (see Section 5.3). Specifically, the distribution analysis involved determining the controls of elevation, gradient and watercourse proximity on carbon content. This enabled an assessment of both the precision and comparative influence of each of the three variables on carbon distribution throughout each of the four defined marshes and the sub-environment as a whole. As is exhibited in Section 5.3 the uncertainties surrounding carbon stock assessments for each of the eight sub-environments and Ribble saltmarshes as a whole are accounted for. The uncertainties consider the areal coverage and depth of sub-environments as well as those surrounding organic carbon density. For each sub-environment the variability in area coverage according to the remote and manual areal uncertainty assessments was taken into account and the depth uncertainty of the active layer is calculated so to determine a range of plausible volume projections. The uncertainty surrounding organic carbon density in the active layer of each sub-environment which was determined following LOI tests is subsequently incorporated with the potential volume predictions to produce a range of potential carbon projections for each sub-environment.

4.5 – The Influence of Sea Level Rise on Marsh Evolution

The process of estimating the change in the area, volume and active section carbon content of the different sub-environments that comprise the saltmarshes featured in Section 6.3 applied the primary model of coastal squeeze (Doody, 2004; Wolters *et al.* 2005) (see Section 3.4.1). This model assumed saltmarsh submergence and degradation will occur as a result of sea level rise due to the key control of elevation on sub-environment distribution and the restrictions on landward regression which are present in the Ribble (see Figure 6.11). The research of Horton *et al.* (2018) supports this theory as it is predicted saltmarsh loss is likely to occur as there is >80% positive tendency of marsh retreat in Liverpool Bay by as early as 2020 under the most extreme RCP 8.5 scenario. Therefore, the assumption that the saltmarsh sub-environments and their carbon content is highly vulnerable to submergence and loss as a result of future SLR is supported by current research.

The calculations of saltmarsh sub-environment and carbon loss accounted for the present gradient of the Ribble saltmarshes and different plausible sea level rise scenarios at decadal intervals. Whilst the calculations would have ideally taken into account the evolution in accretion, as only very limited and spatially constrained Environment Agency data concerning accretion is currently available and future predictions of accretional change with sea level rise are highly generalised (Halcrow 2010b; Halcrow, 2013), it was not possible to estimate how accretion would change on a localised scale. The calculations assume the interdependent higher marsh sub-environments with the least tolerant halophytes found at the highest mean elevations: Species Zones A, B, D and F will be collectively converted to Exposed Sediment first. Then it is assumed the middle-lower sub-environments comprised of the most tolerant halophytes: Species Zone C, Species Zone E and Brackish Waterbodies are subsequently converted in progressive order. As explained in Section 2.4 the SLR projections incorporated into the predictions were sourced from UKCP 18 models which take into account localised (25 km^2) variability in SLR in the Ribble estuary and the north-east of Liverpool Bay. Saltmarsh and carbon storage loss under the extreme SLR scenarios predicted by Pfeffer *et al* (2008) were also considered.

Chapter 5 – Results

The results presented in this section concern the overall spatial distribution of sub-environments and carbon storage in the Ribble estuary. The contributing research concerning the spatial assessment of landcover and the carbon storage analysis for each of the four separate saltmarshes can be found in Sections B and C of the appendices respectively.

Section 5.1 presents how the spatial distributions of the eight sub-environments varied throughout the saltmarshes of the Ribble and there is a specific focus on the influences of Elevation (5.1.2), Gradient (5.1.3) and Watercourse proximity (5.1.4) on sub-environment distribution. Section 5.1.5 addresses the key controls on sub-environment distribution in a multiple regression analysis.

Section 5.2 exhibits the results sourced from the fieldwork and laboratory assessments highlighting how carbon density varied throughout the above-ground biomass, sub-surface sediment and active organic surface layers of the different sub-environments.

Section 5.3 combines the findings of 5.1 and 5.2 in order to highlight the spatial variability and distribution of active section carbon content (above-ground biomass and active layer) throughout the saltmarshes of the Ribble. Each of the eight sub-environments are individually analysed and uncertainties surrounding both the spatial and geomorphological analyses are considered in order to exhibit the plausible variability in active section carbon distribution.

5.1 – Spatial Analysis of Land Cover

Introduction

The following section exhibits the results concerning the spatial distribution and areal coverage of the eight sub-environments which comprise the saltmarshes of the Ribble (see Appendix B for individual marsh analysis).

5.1.1 – Areal Quantification

Although the spatial distribution of species is unique on each individual marsh, an initial overview highlights consistent trends in sub-environment distribution which shape the saltmarsh mosaic. The less saline tolerant Species Zones A and B which comprise 25.2% of the overall area, are predominantly found in the higher marsh environment, although the more saline tolerant species of Zone A can be found at the landward end of tidal creek systems represented by dendritic branches of exposed sediment (see Fiugre 5.1). Alternatively, the less tolerant *Festuca rubra* and *Triglochin maritima* species of Species Zone B are often clustered near fluvial inflows and almost exclusively found in the higher marsh. The distribution of Species Zone C and D appears to correspond with the location of the main creeks, although the relationship between such species and creek distance is quantitatively assessed in Section 5.1.3. Areas of the highly tolerant halophytes that comprise Species Zone E also appear to be found at close proximity to the major estuarine channel and low elevation (see Section 5.1.2) which is particularly prominent on Marshes A and B. In contrast the 20755 m^2 area of wetland reed plants which define Species Zone F are exclusively concentrated in a highly sheltered high marsh area in the south-west of Marsh C away from all major creek systems.

The spatial distribution of brackish waterbodies over 8.1% of the total area is not as clearly defined as for the majority of the predominantly vegetated environments, although there is correspondence with the location of Species Zone A and Brackish areas in the higher marsh. Exposed Sediment, which comprises 9.36 km^2 of the total area, is found throughout the marsh in creeks and partially channel saltpans, although the majority of the area classified as exposed sediment is found at low elevations (see Section 5.1.2) near the main tidal channels in areas unsuitable for colonisation.

Table 5.1. Overall area and percentage composition of each sub-environment determined following the original land cover classification (see Figure 5.1).

Land cover Type	Area (km²)	% of Overall Area
Brackish waterbodies	1.77	8.1
Exposed sediment	9.36	42.6
Shadows	0.11	0.5
Species Zone A	2.11	9.6
Species Zone B	3.42	15.6
Species Zone C	3.81	17.3
Species Zone D	0.92	4.2
Species Zone E	0.46	2.1
Species Zone F	0.02	0.1
Overall	21.99	

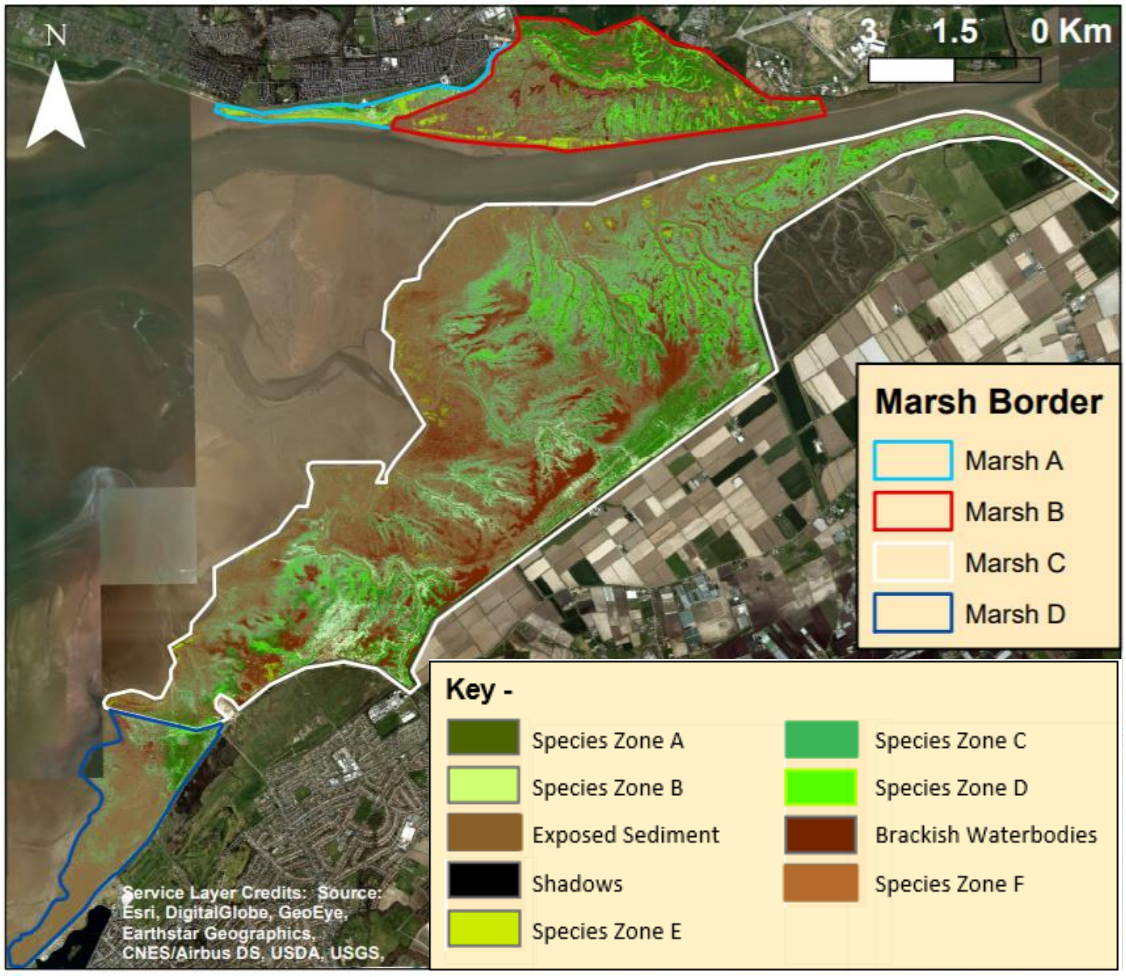

Figure 5.1. Sub-environment distribution throughout the saltmarshes of the Ribble estuary.

Remote Uncertainty Analysis

The remote landcover uncertainty analyses had an overall accuracy of 89.4% (uncertainty 10.6%) and a kappa value of 86.7%. Regarding classification accuracy, Species Zones D and Exposed Sediment are surrounded by the least uncertainty of the respective vegetated and non-vegetated environments (see Table 5.2). There are also consistent trends in confusion between land cover classification anomalies between specific sub-environments which are exhibited in Table 5.3. The most notable confusion exists between: Species Zone A and C, Species Zones B and D as well as Species Zone E and Exposed Sediment. Confusion also exists between Brackish Waterbodies and Exposed Sediment which constitutes 68.4% of anomalous classifications for the latter, although when reversed Brackish Waterbodies only contributes 40% of anomalous results for Exposed Sediment due to the influence of Species Zone E.

There is <0.15% deviation in overall accuracy classification between Marshes B, C and D, although the accuracy classification of Marsh A is notably lower at 87.4% (see Table 5.4) primarily due to the influence of Brackish Waterbodies (83.3%), Species Zone E (85%) and Species Zone A (85.2%) (see Figure 5.2 and Appendix Section B1). Figure 5.2 illustrates deviations in accuracy between marshes are dependent on the exact sub-environment type. For example, the accuracy value of Brackish Waterbodies on Marsh C is 7.1% higher than the accuracy value for the sub-environment on Marsh B, whilst the accuracy value for shadows on Marsh D is 5% below the overall mean for the sub-environment. Alternatively, values for Exposed Sediment and Species Zone B are more precisely grouped with a maximal inter-marsh range of 3.2% and 2.9% respectively.

The kappa coefficient (k) for the overall environment indicates 2.7% of the accurately classified results could have occurred by chance. Whilst a 2.7% chance in sub-environment land cover would considerably alter carbon storage in the 'active section' over an area of 0.59 km^2, overall the classification was of a similarly high accuracy to other saltmarsh and wetland supervised landcover classifications (Singh *et al.* 2014; Pande-Chhetri *et al.* 2018).

Table 5.2. Summary of the remote uncertainty analysis over all marshes (by sub-environment type).

Land Cover Type	N° Reference Points	Correctly Classified	Accuracy (%)	Uncertainty (%)
Brackish Waterbodies	151	132	87.4	12.6
Exposed Sediment	560	504	90.0	10.0
Shadows	122	118	96.7	3.4
Species Zone A	229	204	89.1	10.9
Species Zone B	260	233	89.6	10.4
Species Zone C	254	219	86.2	13.8
Species Zone D	232	212	91.4	8.6
Species Zone E	165	143	86.7	13.3
Species Zone F	30	26	86.7	13.3
Sum	2003	1791	89.4	10.6
Kappa Coefficient			86.7	13.3

Table 5.3. Confusion matrix exhibiting the accuracy of the ML classification indicated by the remote uncertainty analysis. The average correspondence value (A) indicates the overall accuracy of the procedure whilst the Kappa coefficent (k) likewise represents the overall accuracy but also takes into account the possibility of the agreement occurring by chance. Accuractely classified results in this ML assessment appear in the corresponding row and column for each sub-environment (i.e. individually outlined values), whilst anomalous values appear in columns which represent differing species to that of the row.

Land cover Type	Brackish Waterbodies	Exposed Sediment	Shadows	Species Zone A	Species Zone B	Species Zone C	Species Zone D	Species Zone E	Species Zone F	Column Total	% of Overall
Brackish Waterbodies	132	13	0	0	0	0	0	3	3	151	8.2
Exposed Sediment	16	504	0	0	0	0	5	35	0	560	27.1
Shadows	4	0	118	0	0	0	0	0	0	122	6.2
Species Zone A	1	0	0	204	0	24	0	0	0	229	10.8
Species Zone B	0	0	0	3	233	7	17	0	0	260	13.0
Species Zone C	0	5	1	29	0	219	0	0	0	254	12.2
Species Zone D	0	0	4	0	16	0	212	0	0	232	12.5
Species Zone E	4	16	0	0	0	0	2	143	0	165	8.4
Species Zone F	4	0	0	0	0	0	0	0	26	30	1.5
Row Total	157	538	123	236	249	250	236	181	29	Overall Sum	2003
% of Overall Sum	8.6	26.0	6.2	10.9	12.7	12.2	12.6	9.4	1.5	A	89.4
										k	87.6

Table 5.4. Summary of the remote uncertainty analysis for each marsh.

	Marsh A	Marsh B	Marsh C	Marsh D	Overall
Area (km^2)	0.35	3.28	16.79	1.58	21.99
N° Test samples	230	365	1092	316	2003
N° corresponding samples	201	327	980	283	1791
N° of contradicting samples	29	38	112	33	212
Average Correspondence Value	87.4	89.6	89.7	89.6	89.4
Kappa Value	85.3	87.7	87.8	87.4	87.6

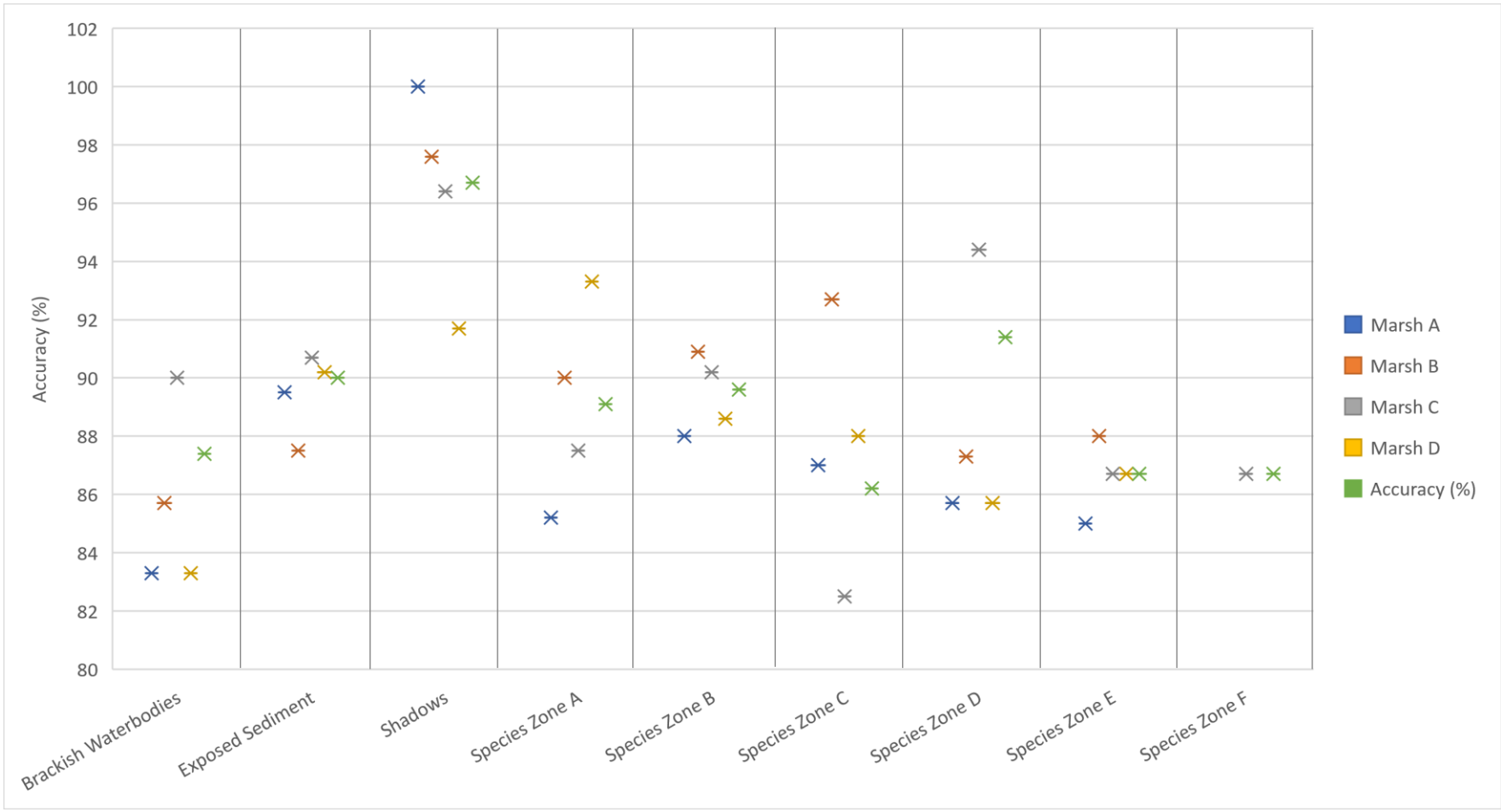

Figure 5.2. Variability in remote sub-environment remote accuracy classification on the four different marshes and overall (mean value).

Manual Uncertainty Analysis

The manual uncertainty classification had an overall accuracy of 92.2% all four marshes. The field-based uncertainty analyses highlighted the greatest uncertainties surround Species Zone B which was the only sub-environment to have an uncertainty >15% (see Table 5.5). With regards to anomalies, confusion existed between Species Zone B and D as well as Brackish Waterbodies and Species Zone F (see Table 5.6). Four of seven sampled sub-environments had an accuracy classification of 100%, although Species Zone F (areal coverage <0.1%) was not classified as it was not recognised before the analysis. On a marsh specific level, the classification accuracy on Marsh B was the closest to the overall accuracy value (92.2%) at 91.7%. The Marsh A classification was 100% accurate, whilst the lowest accuracy classification occurred on Marsh D (85.7%).

Table 5.5. Summary of the manual, field-based uncertainty analysis for all species over all marshes. Species Zone F is absent as it was not identified before the analysis.

Land cover Type	N^{o} Reference Points	Correctly Classified	Accuracy (%)	Uncertainty (%)
Brackish Waterbodies	7	6	85.7	14.3
Exposed Sediment	11	11	100.0	0
Species Zone A	8	7	87.5	12.5
Species Zone B	5	4	80.0	20
Species Zone C	10	10	100.0	0
Species Zone D	5	5	100.0	0
Species Zone E	5	5	100.0	0
Overall	51	47	92.2	7.8

Table 5.6. Confusion matrix exhibiting the accuracy of the ML classification indicated by the manual uncertainty analysis. The average correspondence value (A) indicates the overall accuracy of the procedure whilst the Kappa coefficent (k) likewise represents the overall accuracy but also takes into account the possibility of the agreement occurring by chance. Accuractely classified results in this appear in the corresponding row and column for each sub-environment (i.e. individually outlined values), whilst anomalous values appear in columns which represent differing species to that of the row.

Land cover Type	Brackish Waterbodies	Exposed Sediment	Species Zone A	Species Zone B	Species Zone C	Species Zone D	Species Zone E	Species Zone F	Column Total	% of Overall
Brackish Waterbodies	6	0	0	0	0	0	0	1	7	14.9
Exposed Sediment	0	11	0	0	0	0	0	0	11	23.4
Dark Green Higher Marsh Vegetation	0	0	7	1	0	0	0	0	8	17
Very light green vegetation	0	0	0	4	0	1	0	0	5	8.5
Mid-Green Lower Terrace Vegetation	0	0	0	0	10	0	0	0	10	21.3
Light Green Higher Terrace Vegetation	0	0	0	0	0	5	0	0	5	12.8
Orange-Brown Vegetation	0	0	0	0	0	0	5	0	5	10.6
Dark Brown Vegetation	0	0	0	0	0	0	0	0	0	0
Row Total	6	11	7	5	10	6	5	2	Overall Sum	51
% of Overall Sum	10.6	23.4	17.0	10.6	21.3	10.6	10.6	4.3	A	0.92
									k	0.90

Table 5.7. Summary of the manual, field-based uncertainty analysis for all marshes and overall.

	Marsh A	Marsh B	Marsh C	Marsh D	Overall
N° Ground Truthing Sites	13	12	19	7	51
N° corresponding sites	13	11	17	6	47
N° of contradicting Sites	0	1	2	1	4
Correspondence Rate	100.0	91.7	89.5	85.7	92.2

Comparison of Uncertainty Analyses

Overall the remote land cover classification was 2.8% less than the manual classification. The sub-environments Brackish Waterbodies and Species Zone A exhibited the lowest disparity in accuracy between classifications at 1.0% and 1.3% respectively, whilst the greatest disparity concerns Species Zone C (13.8%). The remote accuracy was higher than the manual for the Brackish Waterbodies, Species Zone A and Species Zone B, whilst the manual classification was higher in the four other comparable sub-environments (see Table 5.8).

Table 5.8. Comparison of the overall accuracy of both analyses.

Land cover Type	Remote ML Accuracy (%)	Manual Accuracy (%)	Δ
Brackish Waterbodies	87.4	85.7	1.7
Exposed Sediment	90.0	100	-10.0
Shadows	96.7	N/A	N/A
Species Zone A	89.1	87.5	1.6
Species Zone B	89.6	80	9.6
Species Zone C	86.2	100	-13.8
Species Zone D	91.4	100.0	-8.6
Species Zone E	86.7	100	-13.3
Species Zone F	86.7	N/A	N/A
Overall	89.4	92.2	-2.8
		Average Disparity	-5.1

Summary -

Overall the range in sub-environment classification accuracy of the remote ML classification of 5.2% (excluding shadows) is comparably low compared to the range of manual assessment of 20%. The remote assessment indicated that the greatest uncertainty (13.3%) surrounded Species Zones E and F which would could theoretically differ in areal cover by 61180 m^2 and 2763 m^2. However, as the remote confusion matrix indicated that 35/46 of these anomalies for Exposed Sediment were classified as Species Zone E, so in theory, the area of Species Zone E could increase by 13.3% of the original areal projection, replacing previous unvegetated areas and increasing biomass coverage throughout the lower marsh with geomorphological implications (see Section 3.2.2). The remote assessment indicated that 13/19 anomalies for Brackish Waterbodies (uncertainty = 12.6%) were classified as Exposed Sediment, so it is also plausible 1.1% of the total area of Brackish Waterbodies could alternatively be covered by the latter. However as the differences above-ground biomass density (see Section 5.2.2.1) between Brackish Waterbodies and Exposed Sediment are comparably minor in contrast to Exposed Sediment and Species Zone E, the ecogeomorhological effects of this sub-environment change are reduced.

Of the predominantly vegetated environments, Species Zone C exhibits the greatest areal disparity between original and ML remote land cover of 0.55 km^2. Whilst this would change the vegetation and biomass dynamics of the lower-middle marsh and creeks in particular, 82.9% of the anomalous remote values for Species Zone C are classified as Species Zone A which also contains *Atriplex portulacoides*. Likewise, 96% of the anomalous classifications for Species Zone A are classified as Species Zone C by the remote assessment (See Table 5.3) which is likely to be due to similar spectral values (see Section 6.2).

Whilst a similar confusion relationship also connects Species Zones B and D, the high remote accuracy classification (90.6%) of Species Zone D combined with a small original area coverage (4.2% of the overall marsh) means the overall area covered by Species Zone B would only change by 0.4%. However, despite a similar classification accuracy (89.4%), as Species Zone B covers 15.6% (3.42 km^2) of the marsh the total area covered by the sub-environment could differ by up to 1.7% of the original areal projection.

Of the sub-environments which are not indicated by the manual assessment to have 100% accuracy, the largest disparities between the original land cover area concern Species Zones A and B which could potentially change in areal cover by 1.2% and 3.5% respectively. However, whilst the anomalous relationship between Species Zone B and D confers with the remote findings, the most frequent anomalous class for Dark Green Higher Marsh Vegetation (Species Zone A) was Species Zone B as oppose to Species Zone C in the manual assessment. The accuracy of the manual classification (85.7%) for Brackish Waterbodies was similar to the remote analysis (86.7%) so the greatest possible change in areal cover only differs by 0.1% of the original areal projection between the two classifications. However, the sole anomaly surrounding the manual assessment of Brackish Waterbodies could indicate that Species Zone F covers a greater area, and therefore offers a more substantial contribution to saltmarsh carbon storage.

In summary both the ML remote and manual analyses highlight that the original classification was ≥80% accurate for all sub-environments. Despite this level of accuracy, there is the potential that a different spatial distribution of sub-environments exists throughout the Ribble saltmarshes. This could directly change the above-ground biomass and also considerably alter ecological and geomorphological processes which influence sub-surface carbon storage. The result of areal uncertainty surrounding carbon storage is examined in Section 5.3 and the impacts are considered in the discussion (Section 6.3).

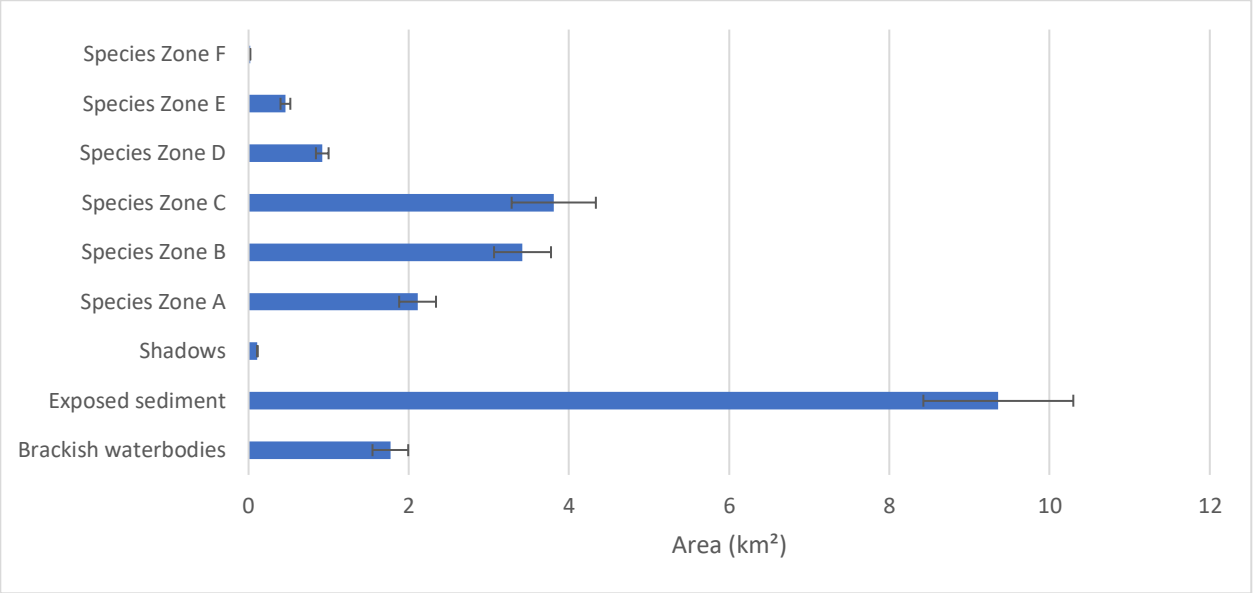

Figure 5.3. Summary of the overall land cover area assessments, highlighting variability in projected areas according to the original ML classification and the remote uncertainty assessment over all marshes.

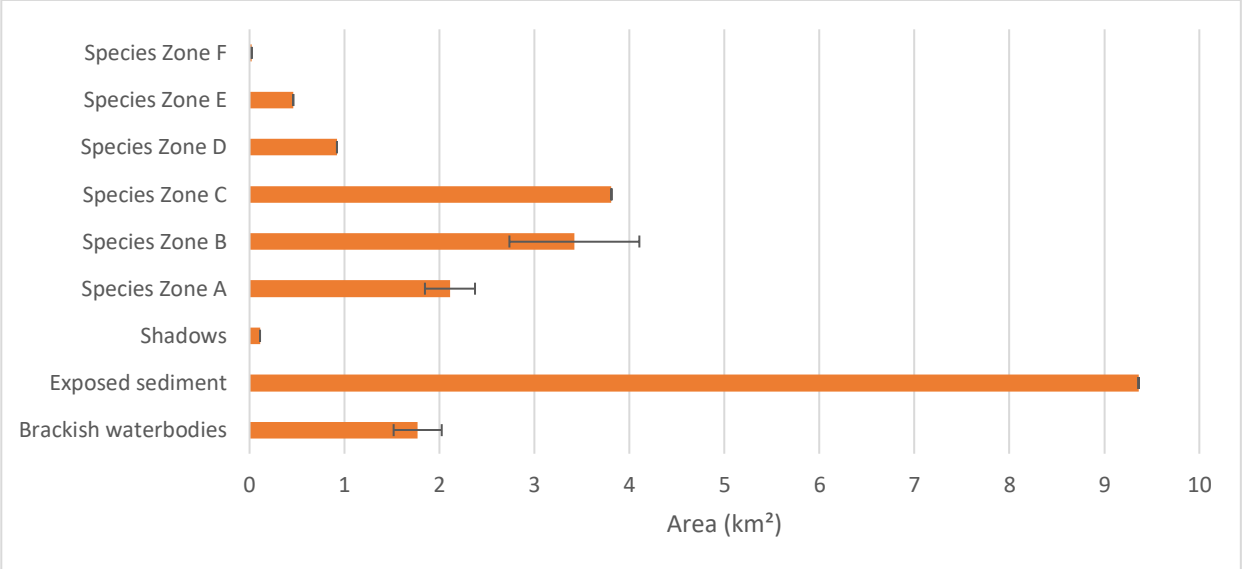

Figure 5.4. Summary of the overall land cover area assessments, highlighting variability in projected areas according to the original ML classification and the manual uncertainty assessment over all marshes.

Table 5.9. Summary of the land cover area assessments. Both remote and manual uncertainty figures represent the minimal area covered by each sub-environment and utilise overall accuracy figures for all marshes.

Land cover Type	Area (km²)	% of Overall Area	Overall Remote Accuracy (%)	Area - Remote Accuracy (km²)	% of Overall Area	Overall Manual Accuracy (%)	Area - Manual Accuracy (km^2)	% of Overall Area
Brackish Waterbodies	1.77	8.1	86.7	1.54	7.0	85.7	1.52	6.9
Exposed Sediment	9.36	42.6	89.0	8.33	37.9	100.0	9.36	42.6
Shadows	0.11	0.5	96.6	0.11	0.5	N/A	0.11	0.5
Species Zone A	2.11	9.6	86.2	1.81	8.3	87.5	1.84	8.4
Species Zone B	3.42	15.6	89.4	3.06	13.9	80.0	2.74	12.5
Species Zone C	3.81	17.3	85.6	3.26	14.8	100.0	3.81	17.3
Species Zone D	0.92	4.2	90.6	0.83	3.8	100.0	0.92	4.2
Species Zone E	0.46	2.1	86.7	0.40	1.8	100.0	0.46	2.1
Species Zone F	0.02	0.1	86.7	0.02	0.1	N/A	0.02	0.1

5.1.2 - Influence of Elevation on Sub-environment Distribution

Introduction

The following results concern the elevation distribution of the sub-environments that comprise the saltmarshes of the Ribble estuary. The findings of this analysis are later combined with the sub-environment carbon assessment in Section 5.2 to highlight how carbon stocks vary with elevation (see section 5.3.3.2). All elevations in metres concern height in metres above ordnance datum (mOD). For reference, an elevation (mOD) to tidal datum conversion table for the three nearest gauges is displayed in Table 5.10.

Table 5.10. Elevation (mOD to tidal datum conversion table for three nearest tidal gauges. (Source = Halcrow et al. 2013)

	Tidal Datum Elevation (mOD)					
Gauge Location	MLWS	MLWN	MSL	MHWN	MHWS	HAT
Formby	-3.93	-2.03	0.22	2.37	4.07	4.97
Southport	nd	nd	nd	2.2	4.1	5.1
Preston	-0.8	-0.8	nd	2.4	4.4	5.4

Overall Sub-Environment Elevation Variability

Overall the majority (63.1%) of the area covered by the eight sub-environments is found between 4.2 - 4.6 m with a mean elevation of 4.23 m, however when non-vegetated sub-environments are removed the overall mean elevation increases by 0.17 m. Most vegetated sub-environments are concentrated within an elevation range of 4.4 – 4.6 m whilst only 6% of are found below 4 m and 0.2% above 5 m. Of the four marshes, Marsh C exhibits the largest elevation range, with areas in close proximity to creeks being the main areas of localised elevation and species variability (see Appendix B3). Whilst the creek channels are largely defined as either Exposed Sediment or Brackish Waterbodies, the raised terraces either side of the creek are predominantly occupied by Species Zone D.

Species Zone A was consistently found in the higher to middle marsh almost exclusively (98.2%) between 4.2 – 4.8 m, exhibiting the 2nd highest degree of spatial clustering behind Species Zone C (see Figure 5.5). The disparity in maximal peak elevation value between Species Zone A and Brackish Waterbodies on Figure 5.5 is also exhibited in Figure 5.7 which highlights the inverse relationship concerning proportional landcover between Exposed Sediment and all predominantly vegetated sub-environments. The ANOVA analysis also indicates the high degree of variance between Exposed Sediment compared to all other sub-environments (see Table 5.13).

The less saline tolerant species such as *Festuca rubra* that comprise Species Zone B have a mean elevation value 0.25 m higher than all sub-environments. This sub-environment largely occupies the back marsh but is predominantly absent from the raised terraces of creeks, except in the south-west of Marsh C where it is found on the banks of the northward-flowing fluvial inflow where salinity is likely to be low (see Figure 5.10). The areal distribution of this sub-environment in the higher marsh is also shown by Figures 5.7 and 5.9 which exhibit that Species Zone B covers 21.2% of the saltmarsh area between 4.6-4.8 m which rises to a maximum of 39.4% at 6.4-6.6m. However the total proportion of the saltmarsh area found at the aforementioned elevation intervals is only 9.1% and 0.0026%.

The influence of salinity and halophyte composition perhaps explains why the mean values for Species Zone A and C, which are comprised of more tolerant halophytes (both contain *Atriplex portulacoides*), are 0.08 m and 0.04 m lower than the overall average. However, the significant T-value of 78.8 highlights a high degree of variance between each sub-environment when compared to the elevation variation within Species Zone A and C.

The major exception to the overall trend of clustering of the different sub-environments between 4.2 – 4.8 m is exhibited by Species Zone E as 47.2% of this sub-environment is found at elevations below 4.2 m. This is largely to be expected given the high saline tolerances of *Spartina Anglica* and *Salicornia spp,* which would explain why the sub-environment reaches the maximal overall land cover % value of 4.3% between 4.0-4.2 m. Alternatively, Species Zone F was confined to high elevations and a comparatively narrow elevation range as 98% of the area covered between by this species is between 4.4 m – 5.0 m.

The near-symmetrical rising and falling limbs of Exposed Sediment on Figure 5.5 exhibit an approximately even elevation distribution around the mode. The sub-environment also had the largest overall range spanning 7.02 m. Exposed Sediment becomes increasingly abundant as sub-environment diversity rapidly decreases below 3.8 m and above 5.0 m as shown in Figure 5.6 and 5.7 as the area occupied by common saltmarsh halophytes rapidly decreases outside the elevation range of MHWS and HAT. Although this partially conforms with the ramp theory of elevation, hydroperiod and zonation (e.g. Williams *et al.* 1994; Bao-Shan *et al.* 2011), the fact that a disproportionally high (95.6%) of predominantly vegetated sub-environments are found between MHWS (4.1 mOD) and HAT (5.1 mOD) is the first initial suggestion that vegetation distribution is not solely determined by elevation.

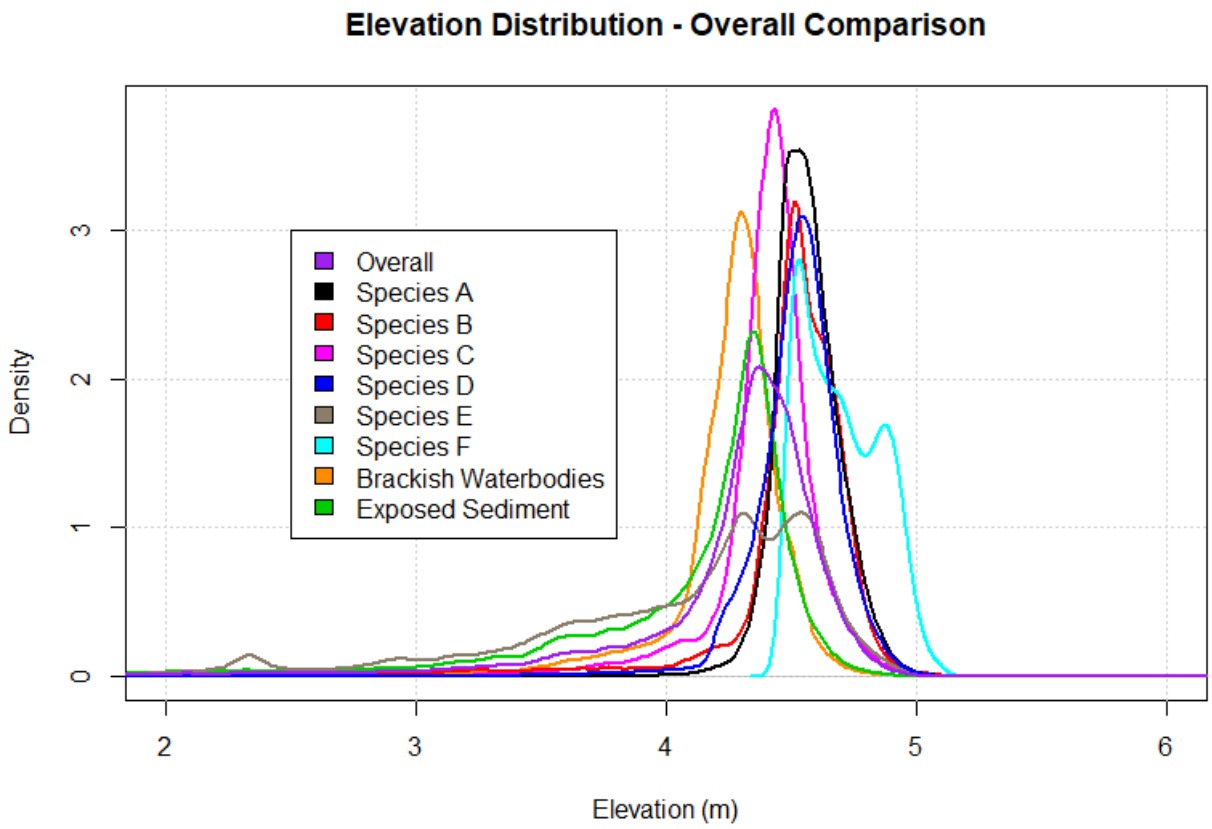

Figure 5.5. Comparative kernel density plot highlighting the variation in elevation of all sub-environments over all marshes.

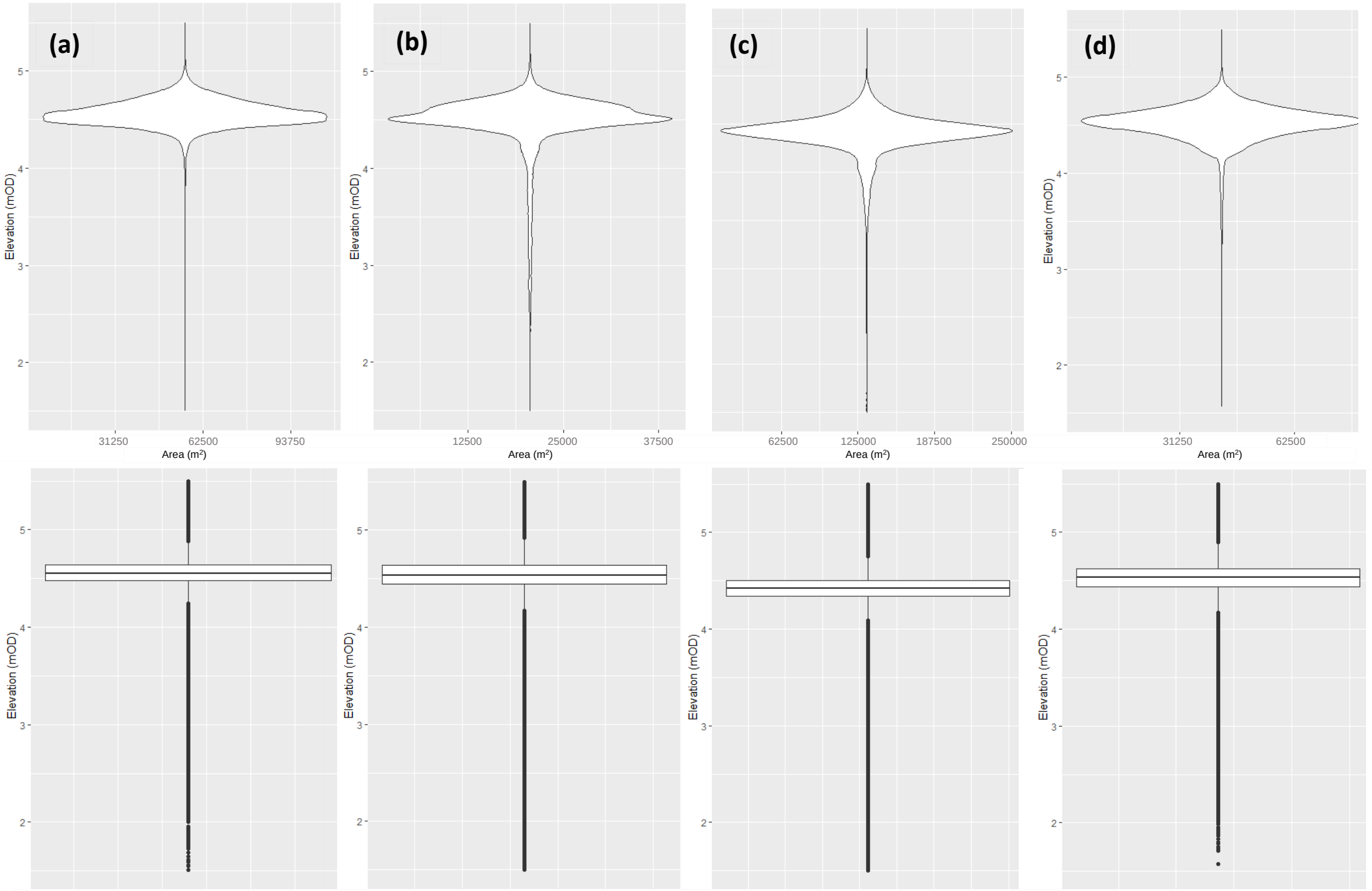

Figure 5.6. Variability in elevation distribution between all sub-environments over all marshes. The violin and box plots for the respective sub-environments are as follows: Species Zone A (a), Species Zone B (b), Species Zone C (c), Species Zone D (d), Species Zone E (e), Species Zone F (f), Brackish Waterbodies (g) and Exposed Sediment (h).

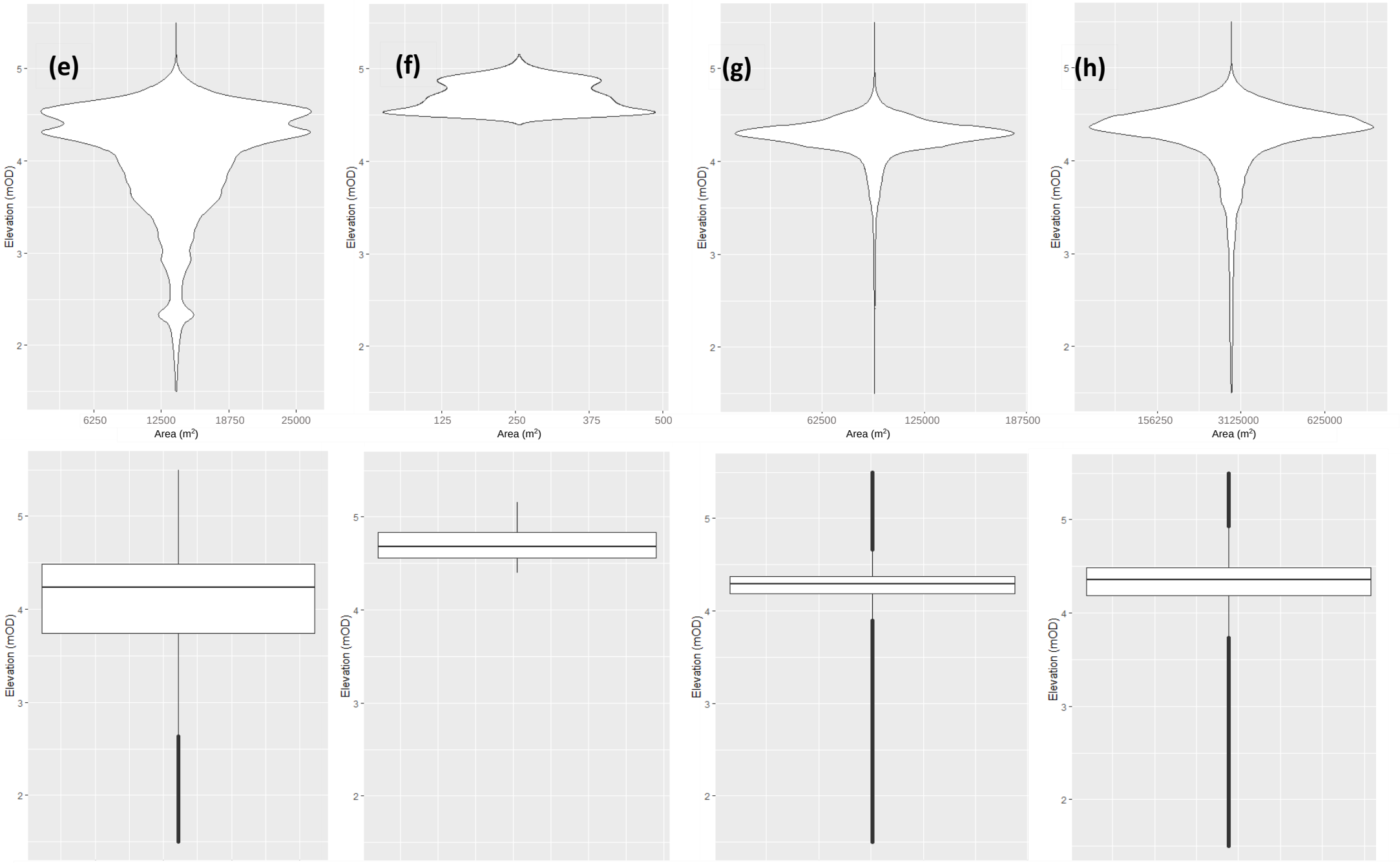

Figure 5.6. Variability in elevation distribution between all sub-environments over all marshes. The violin and box plots for the respective sub-environments are as follows: Species Zone A (a), Species Zone B (b), Species Zone C (c), Species Zone D (d), Species Zone E (e), Species Zone F (f), Brackish Waterbodies (g) and Exposed Sediment (h).

Table 5.11. Variability in elevation (mOD) distribution between all sub-environments over all marshes.

Land cover Type	Min	Mode	Mean	Max	St Dev.
Species Zone A	-0.44	4.55	4.56	6.24	0.15
Species Zone B	-0.10	4.52	4.48	6.48	0.34
Species Zone C	-0.53	4.42	4.38	6.45	0.35
Species Zone D	-0.31	4.55	4.52	5.96	0.20
Species Zone E	0.31	4.56	4.03	6.41	0.63
Species Zone F	4.40	4.52	4.70	5.15	0.16
Brackish Waterbodies	0.24	4.31	4.24	6.19	0.28
Exposed Sediment	-0.55	4.37	4.05	6.47	0.59
All Environments	-0.55	4.39	4.23	6.48	0.50

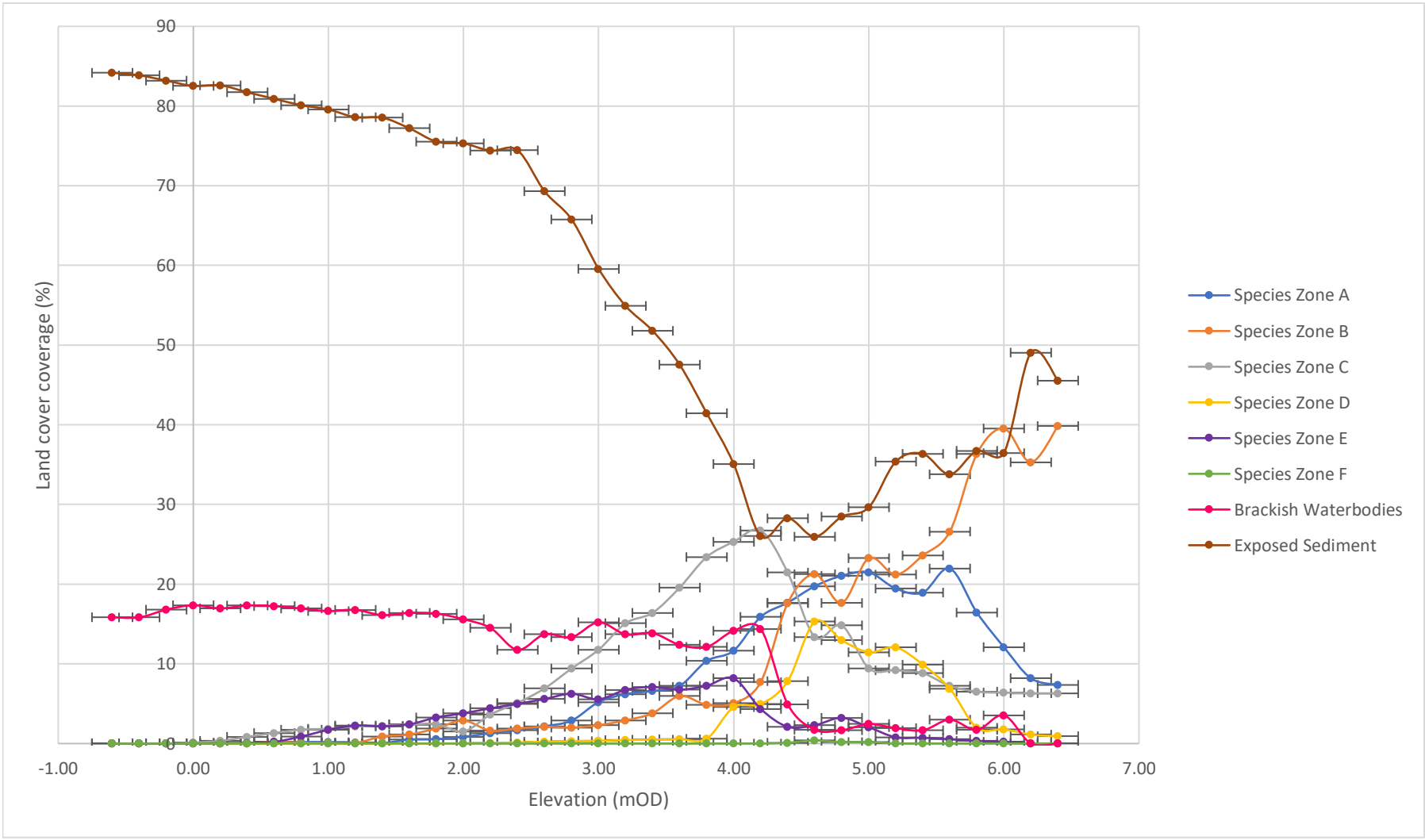

Figure 5.7. Variability of sub-environment areal coverage with elevation. Error bars indicate the RMSE of 15 cm associated with the Lidar data. See Figure 5.8 for further detail.

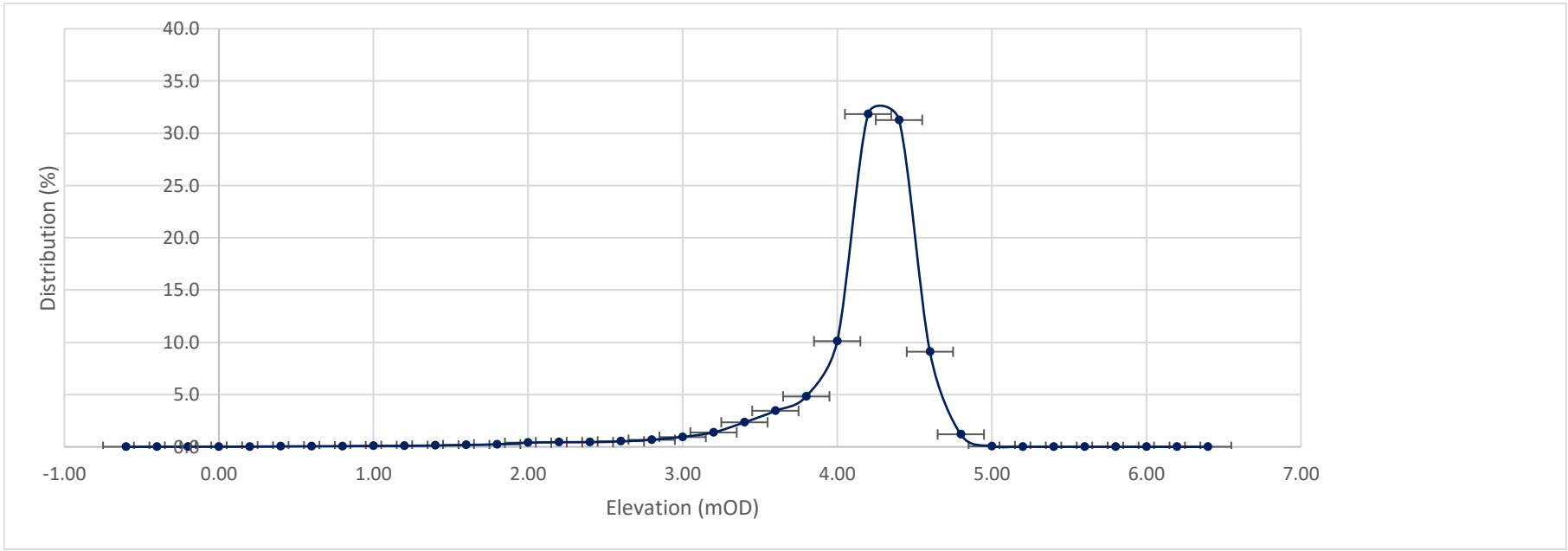

Figure 5.8. Variability in the elevation across the overall saltmarsh environment (%). Error bars indicate the RMSE of 15 cm associated with the Lidar data.

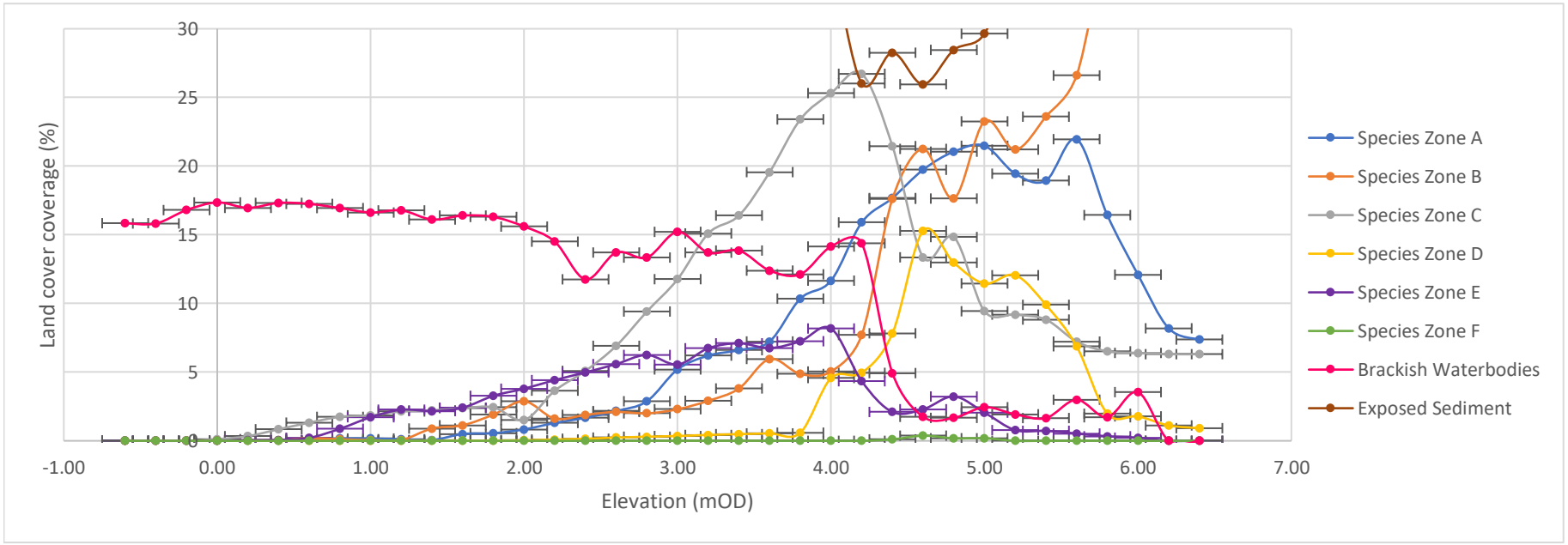

Figure 5.9. Variability of sub-environment areal coverage with elevation. Error bars indicate the RMSE of 15 cm associated with the Lidar data.

Table 5.12. F values produced during the ANOVA analyses for all land cover types. The values indicate the variance of the mean elevation values for two respective land cover types divided by mean of the variances within each respective land cover type. Significant values are highlighted in bold.

	Species Zone A	Species Zone B	Species Zone C	Species Zone D	Species Zone E	Species Zone F	Brackish Waterbodies	Exposed Sediment
Species Zone A		**383.6**	**78.8**	**1458.0**	**101.8**	3.6	**463.3**	**470.8**
Species Zone B	**383.6**		0.3	**22.4**	**44.4**	0.5	**109.3**	**13.5**
Species Zone C	**78.8**	0.3		**3802.0**	**315.1**	**278.1**	**349.8**	**15.1**
Species Zone D	**1458.0**	**22.4**	**3802.0**		**154.5**	**386.7**	**1577.0**	**477.9**
Species Zone E	**101.8**	**44.4**	**315.1**	**154.5**		**197.4**	**948.6**	**1152.0**
Species Zone F	3.6	0.5	**278.1**	**386.7**	**197.4**		**632.3**	**5.0**
Brackish Waterbodies	**463.3**	**109.3**	**349.8**	**1577.0**	**948.6**	**632.3**		**28.4**
Exposed Sediment	**470.8**	**13.5**	**15.1**	**477.9**	**1152.0**	**5.0**	**28.4**	

Table 5.13. Probability (p) values accompanying each of the respective F values. The values indicate the probability of producing the respective F value result, given that the null hypothesis (F≈1) is true. Statistically insignificant values with an alpha level ≥0.05 (hence reporting to 2.d.p) are indicated in red.

	Species Zone A	Species Zone B	Species Zone C	Species Zone D	Species Zone E	Species Zone F	Brackish Waterbodies	Exposed Sediment
Species Zone A		<2e-16	<2e-16	<2e-16	<2e-16	0.06	<2e-16	<2e-16
Species Zone B	<2e-16		0.58	2.25e-6	2.66e-11	0.50	<2e-16	2.35e-4
Species Zone C	<2e-16	0.58		<2e-16	<2e-16	<2e-16	<2e-16	1.01e-4
Species Zone D	<2e-16	2.25e-6	<2e-16		<2e-16	<2e-16	<2e-16	<2e-16
Species Zone E	<2e-16	2.66e-11	<2e-16	<2e-16		<2e-16	<2e-16	<2e-16
Species Zone F	0.06	0.50	<2e-16	<2e-16	<2e-16		<2e-16	0.03
Brackish Waterbodies	<2e-16	<2e-16	<2e-16	<2e-16	<2e-16	<2e-16		9.83e-08
Exposed Sediment	<2e-16	2.35e-4	0.01	<2e-16	<2e-16	0.03	9.83e-8	

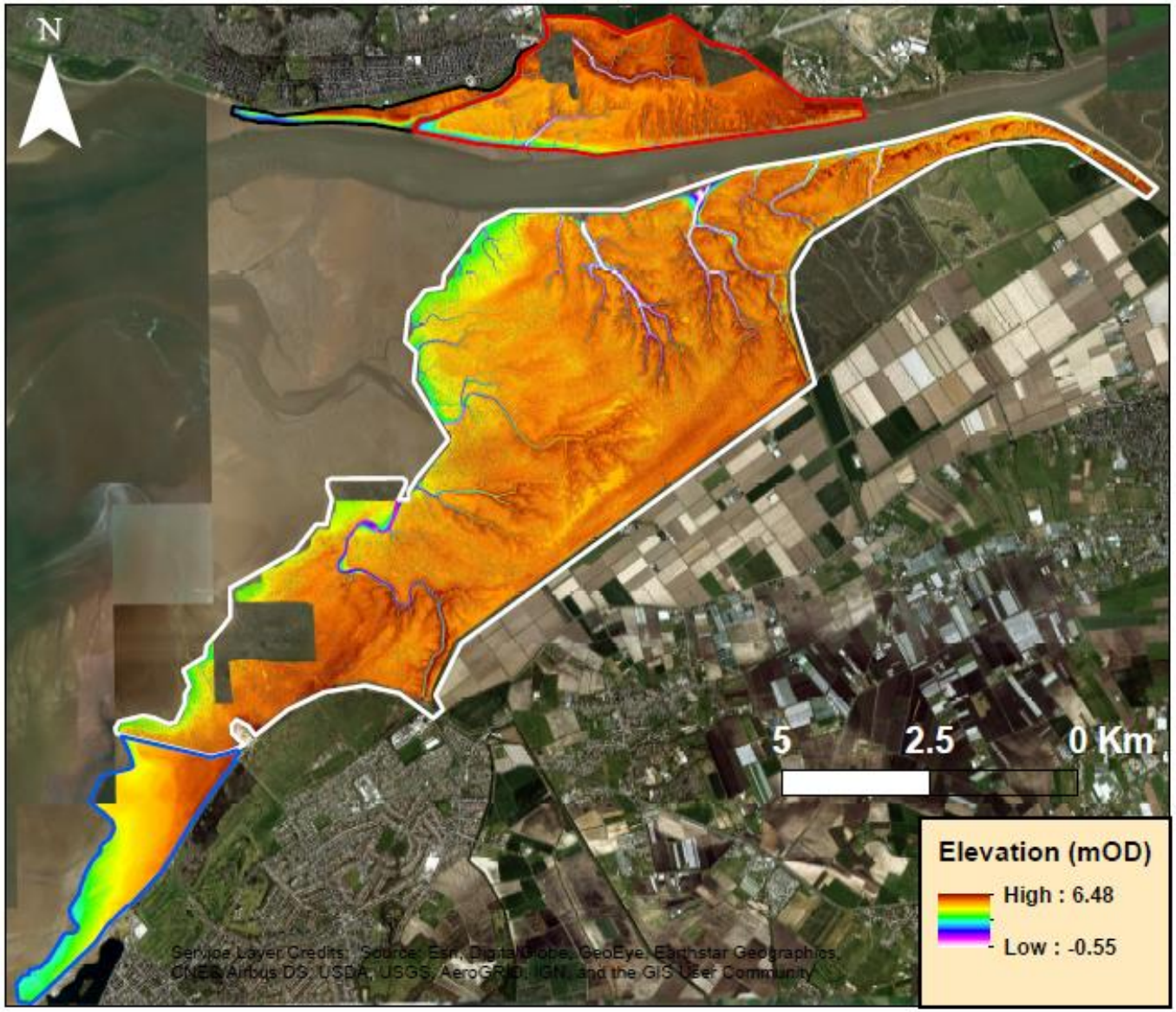

Figure 5.10. Spatial variability in elevation above ordnance datum over all marshes (see Figure 5.6. for land cover distribution).

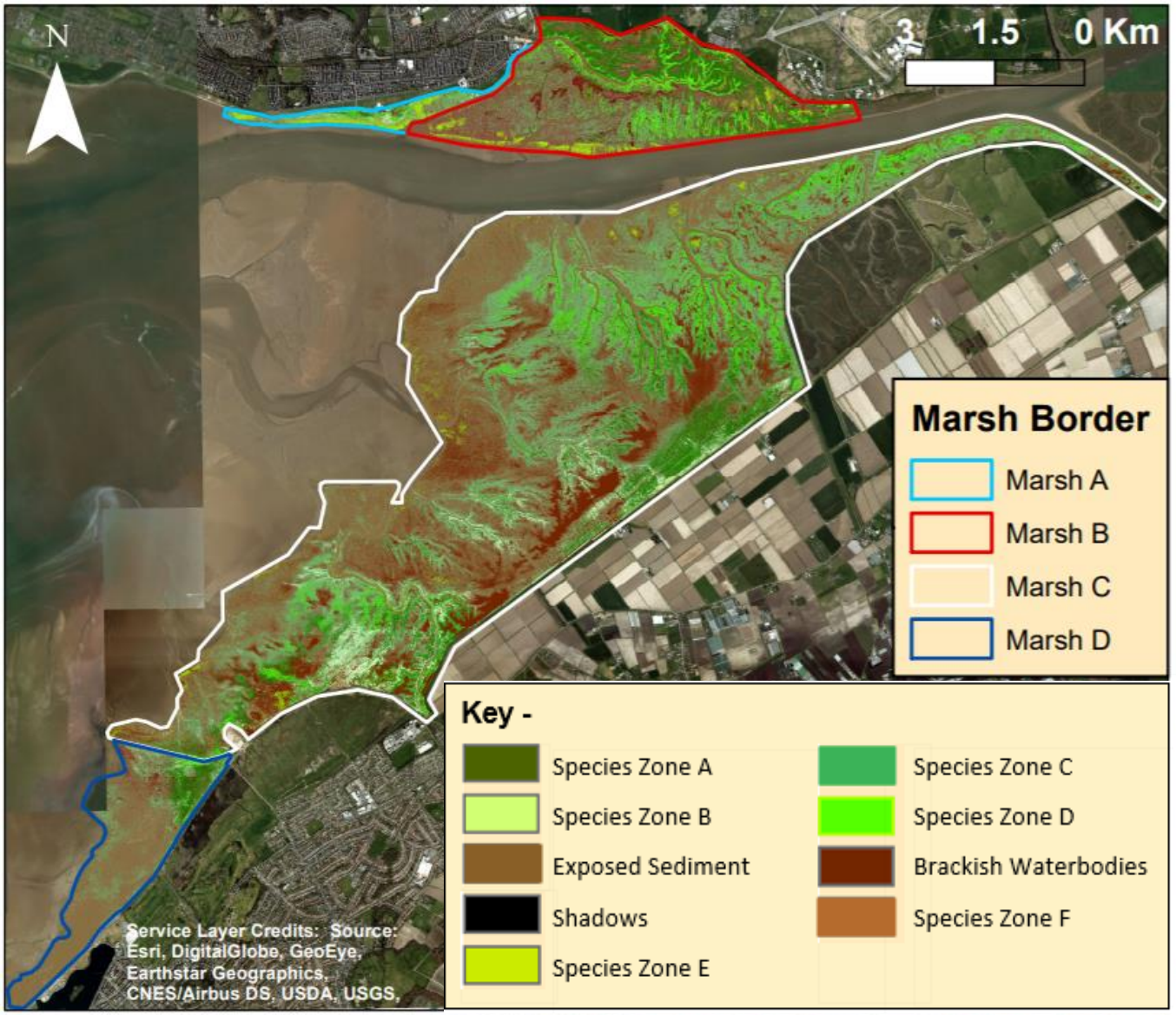

Figure 5.11. Sub-environment distribution throughout the saltmarshes of the Ribble estuary.

5.1.3 - Influence of Gradient on Sub-environment Distribution

Introduction

The variability of gradient throughout a saltmarsh is a key factor that influences environmental evolution (Huckle et al. 2000; Goodwin *et al.* 2018). Gradient determines the extent of waterlogging and marsh drainage efficiency, whilst it also dictates the rate of submergence with SLR (Byers and Chmura, 2014; *Passeri et al.* 2015).

The purpose of the analysis is to determine the variability of gradient throughout the marsh producing findings that can be combined with the carbon stock assessment to determine the extent to which gradient influences active section carbon stock distribution (see Section 5.3.3). The analysis begins with a review of the variability of gradient throughout the Ribble before the gradient distributions of individual sub-environments are assessed.

Overall Sub-environment Gradient Variability

The majority (76%) of the Ribble saltmarshes occupy areas with a gradient of <2° despite an overall range of 56.7°. Although the kernel density plots indicates differences in distribution (Figure 5.12), all sub-environments are predominantly found on areas of marsh with a gradient between 0.3 and 0.7° as would be expected in a saltmarsh environment (e.g. Jones *et al.* 2008; Hladik *et al.* 2014).

Overall, Species Zone A had the most dissimilar distribution compared to the saltmarsh as a whole, with an average gradient 0.8° lower than the overall mean. Species Zone A also had the most precise gradient density distribution (max= 0.72), whilst Species Zone E exhibited the lowest distribution density (max= 0.33) and greatest IQR indicating a wide gradient distribution (see Figure 5.13(e)). This is also apparent from Figure 5.14 and 5.16 which highlights that Species Zone E occupies a consistent portion of the total surface area when compared to other sub-environments.

Species Zones B and C exhibited highly similar gradient density distributions with near-symmetrical rising and falling limbs (see Figure 5.12) indicating a similar incline and decline in the proportion of the area of each sub-environment occupied either side of the modal values. The proportion of the total area covered by Species Zone B and C is 17.0% and 16.1% at 2°, however areal coverage at gradients greater than 36° differ markedly as the creek terrace Species Zone C covers 37.2% of the marsh at 52° whilst Species Zone B becomes increasingly less prominent at gradients greater than 26° (21.0%) (Figure 5.14). Regarding significant elevation variation with other sub-environments Species Zone B, exhibits statistically significant relationships with all sub-environments expect Species Zone F. Of the two statistically significant relationships exhibited by Species Zone F, the sub-environment exhibits the least variance with Species Zone E (T-value = 4.9) and Species Zone A (T-

value = 18.9), the latter of which also contains *Atriplex portulacoides*. Alternatively, Species Zone D was on average found in areas with a mean gradient 0.3° steeper than that of B and C with 70.5% of Species Zone D being found on land below a gradient 2°. In comparison 74.8% and 75.3% of the area respectively occupied by Species Zones B and C was found below 2°. Moreover, unlike Species Zones B and C the overall areal coverage of Species Zone D remained relatively constant between 0-30° (Figure 5.14 and 5.16) ranging between 5.3% to 4.7%.

Despite covering only 20775 m² (0.1%) of the overall environment, Species Zone F exhibited the 2nd least precise density distribution, reaching a maximal gradient density of 0.42 at 0.7°. The isolated sub-environment exhibited the smallest gradient range of 10.7° and the lowest SD of 1.4° (Table 5.14). In contrast to Species Zone F areas classified as Exposed Sediment possessed the largest overall range of 55.8° and comprised 47.9% of the area with a gradient of ≥10°. This gravitation of areas of Exposed Sediment to areas of steep gradient predominantly surrounding creeks is visually exhibited on marshes B and C (see Figures 5.17 and 5.18), and by Figure 5.14 which shows Exposed Sediment constitutes more than its overall area coverage value (42.6%) when the gradient is >4°.

Brackish Waterbodies had a distinct gradient density distribution when compared to other sub-environments as it was the only sub-environment to decrease in area between 0.1° to 0.3°. Of the significant gradient relationships between Brackish Waterbodies and other sub-environments, the lowest variance was displayed between Species Zone C (9.5), a sub-environment associated with creeks. The proportional area covered by Brackish Waterbodies is greatest at 40° (10.1% overall coverage), although the areal coverage of 8.9% at 0° potentially reflects the fact that the sub-environment is a relatively broad class which encompasses both creeks and salt pans.

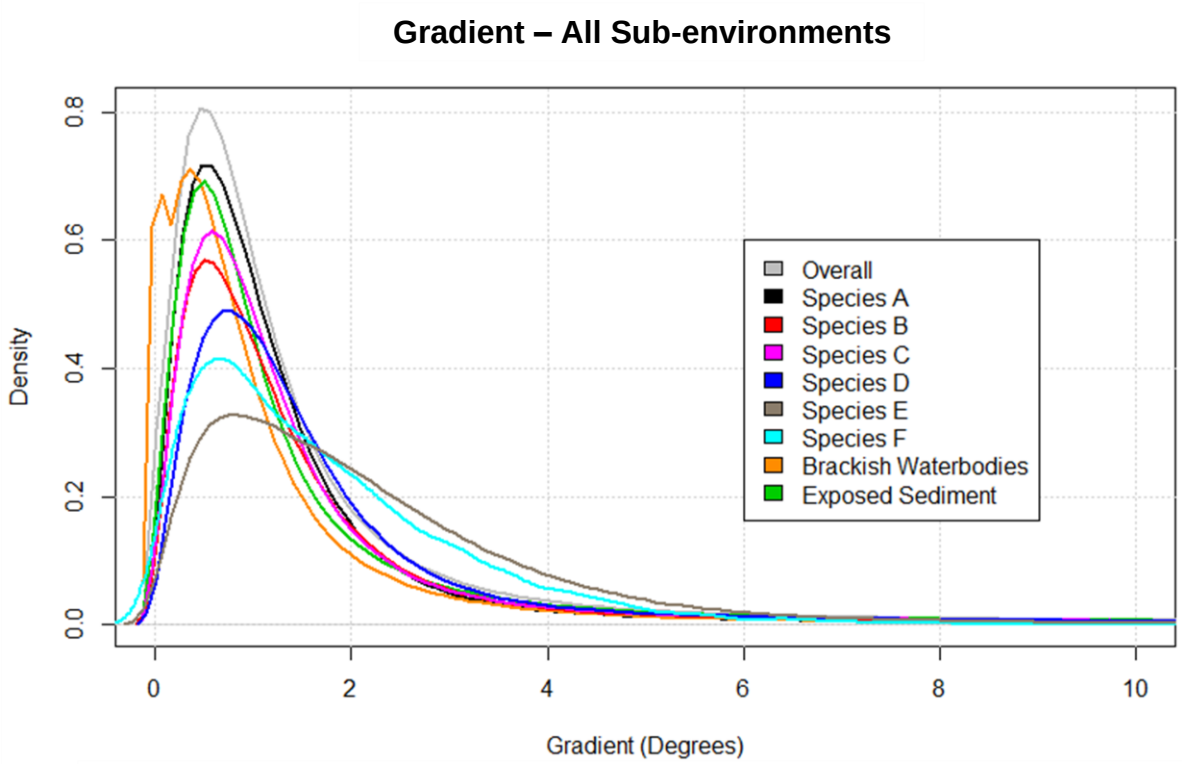

Figure 5.12. Variability in the density of distribution of gradient over all marshes.

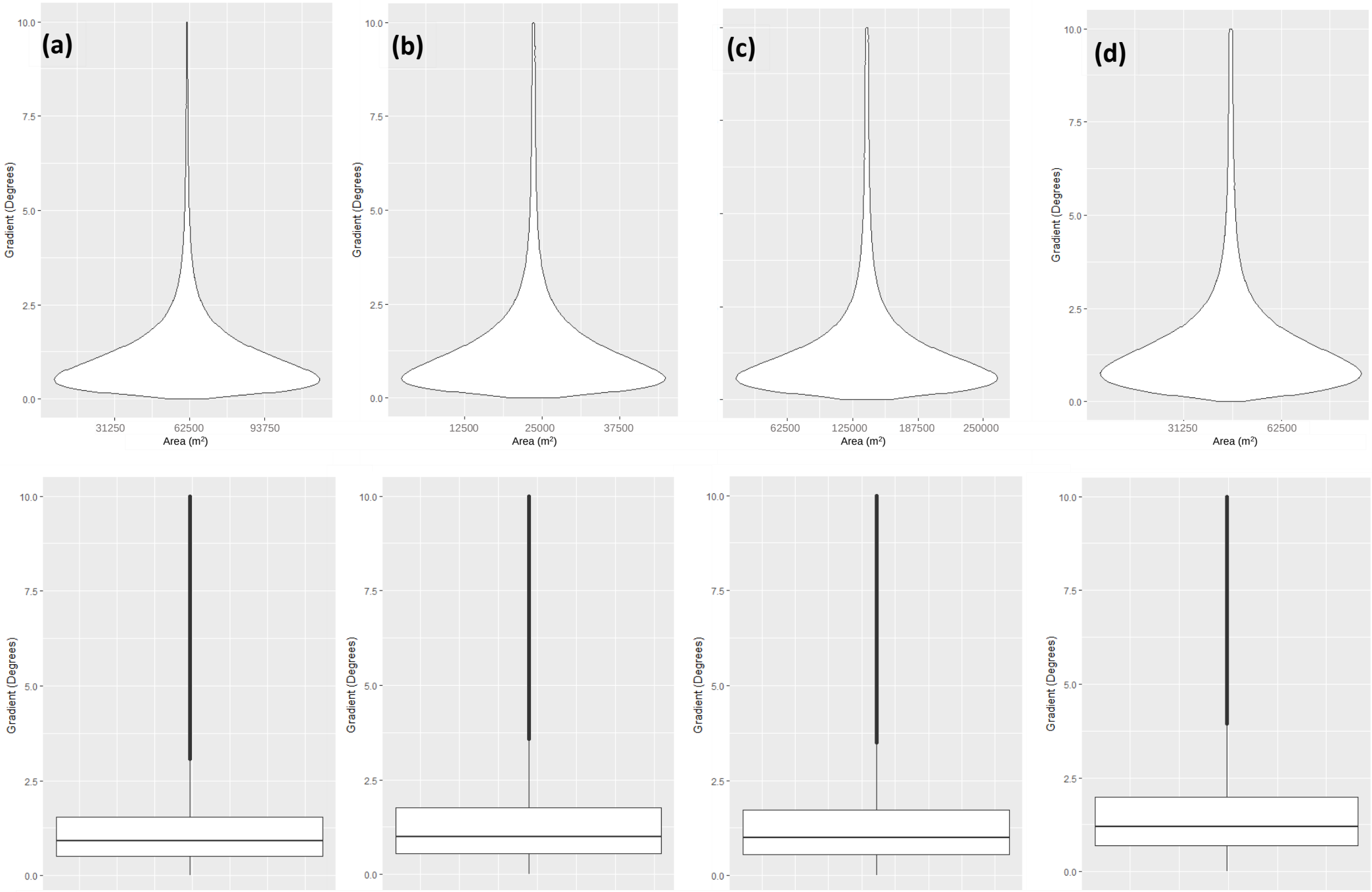

Figure 5.13. Variability in gradient distribution between all sub-environments over all marshes. The violin and box plots for the respective sub-environments are as follows: Species Zone A (a), Species Zone B (b), Species Zone C (c), Species Zone D (d), Species Zone E (e), Species Zone F (f), Brackish Waterbodies (g) and Exposed Sediment (h).

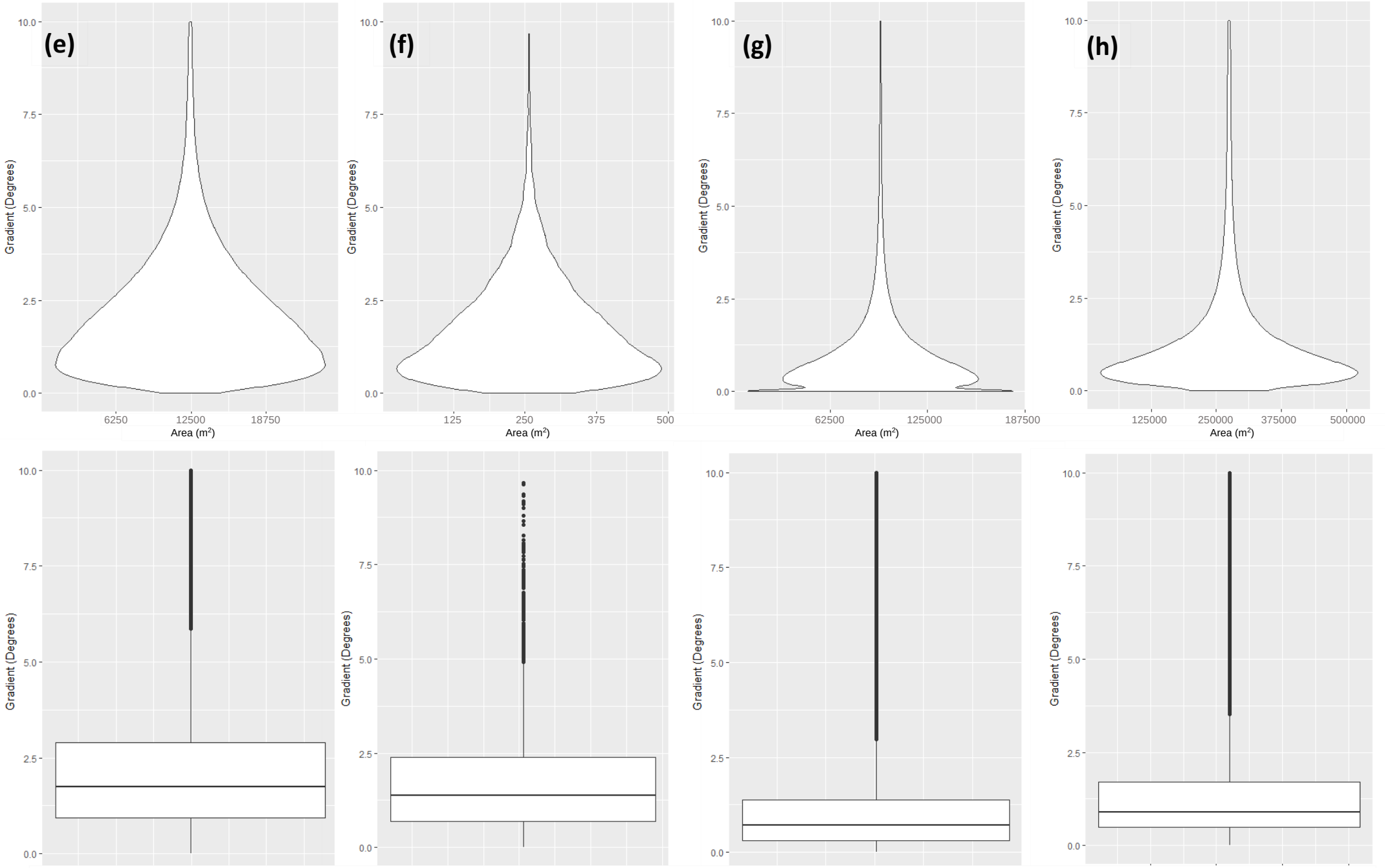

Figure 5.13. Variability in gradient distribution between all sub-environments over all marshes. The violin and box plots for the respective sub-environments are as follows: Species Zone A (a), Species Zone B (b), Species Zone C (c), Species Zone D (d), Species Zone E (e), Species Zone F (f), Brackish Waterbodies (g) and Exposed Sediment (h).

Table 5.14. The variability in gradient distribution between all sub-environments over all marshes.

Sub-Environment	Min	Mode	Mean	Max	St Dev.
Species Zone A	0.0	0.5	1.5	50.7	2.5
Species Zone B	0.0	0.5	2.4	44.1	4.4
Species Zone C	0.0	0.6	2.4	52.2	4.2
Species Zone D	0.0	0.7	2.7	49.2	4.4
Species Zone E	0.0	0.8	2.5	48.7	3.0
Species Zone F	0.0	0.7	1.7	40.7	1.4
Brackish Waterbodies	0.0	0.4	1.9	48.8	4.0
Exposed Sediment	0.0	0.5	2.4	52.8	4.2
All Environments	0.0	0.5	2.3	52.8	4.3

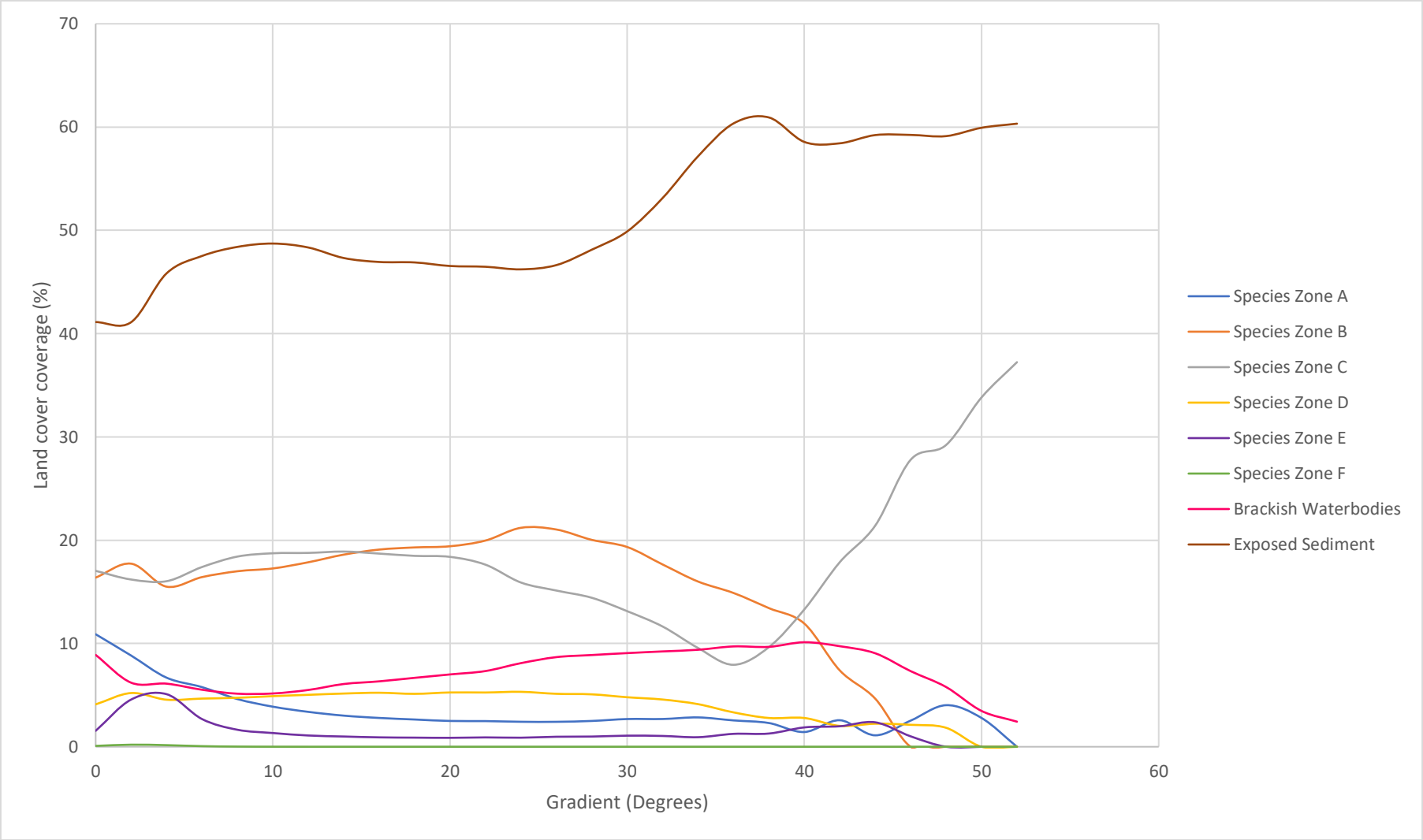

Figure 5.14. Variability of sub-environment areal coverage with gradient. See Figure 5.15 for further details.

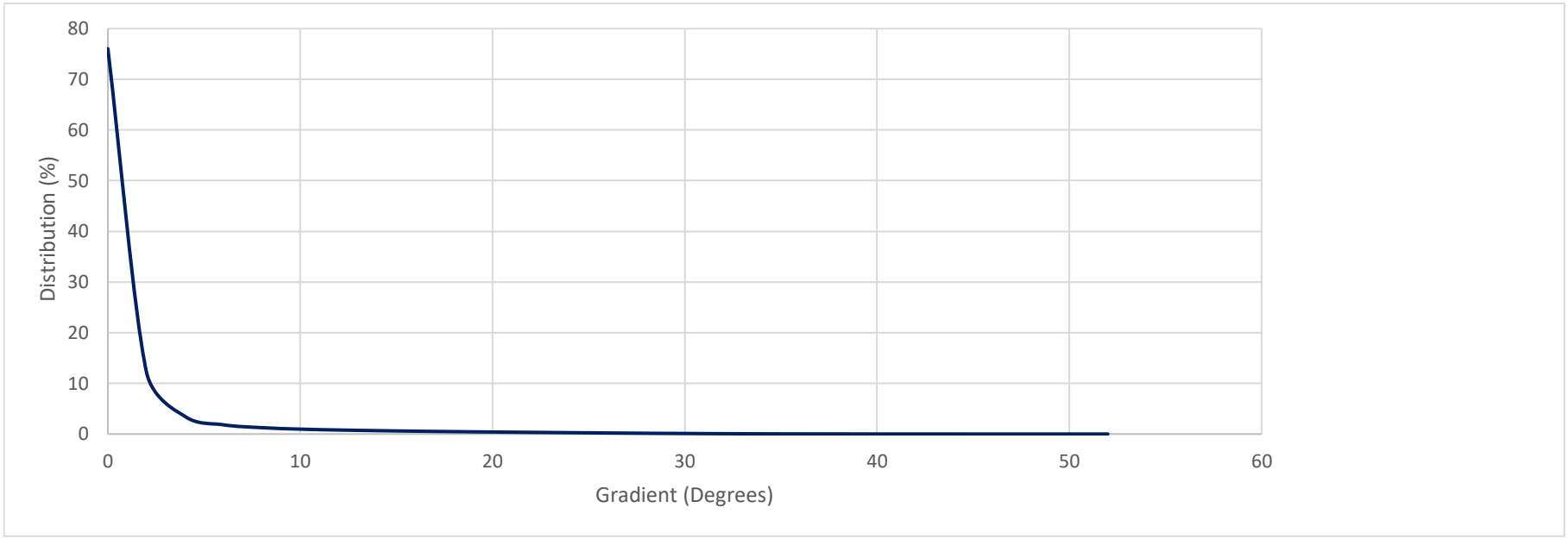

Figure 5.15. Variability in the gradient across the overall saltmarsh environment (%).

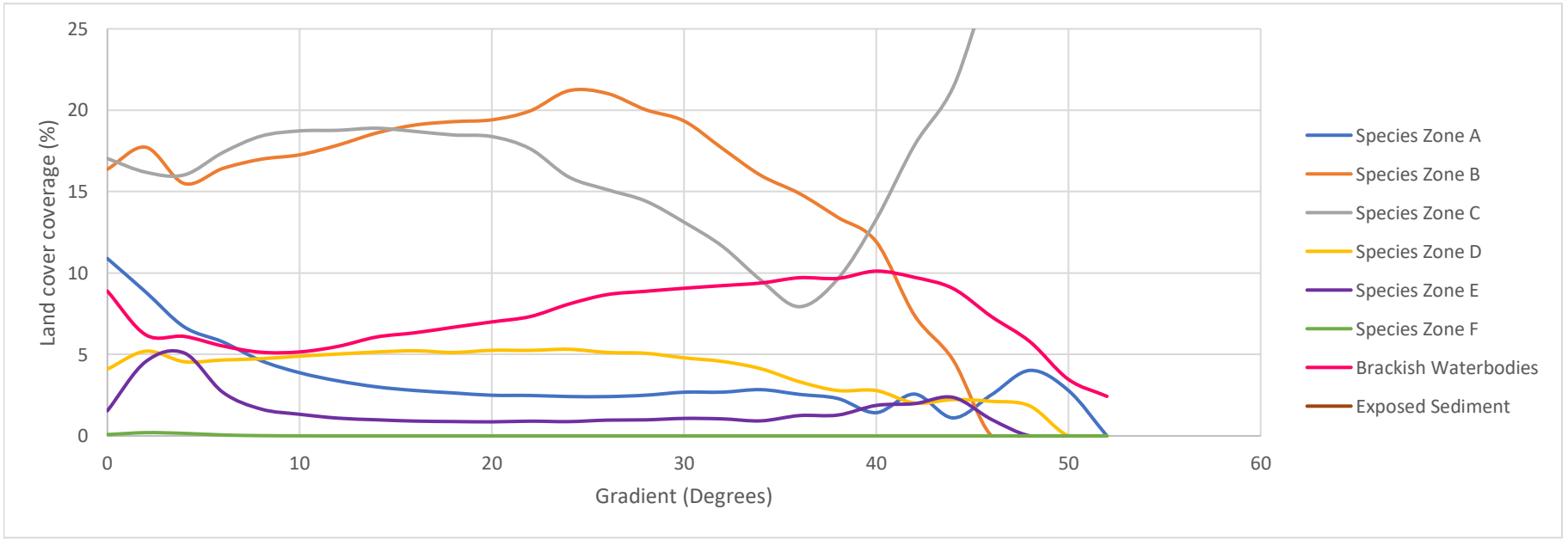

Figure 5.16. Variability of sub-environment areal coverage with gradient.

Table 5.15. F values produced during the ANOVA analyses for all land cover types. The values indicate the variance of the mean gradient values for two respective land cover types divided by mean of the variances within each respective land cover type. Significant values are highlighted in bold.

	Species Zone A	Species Zone B	Species Zone C	Species Zone D	Species Zone E	Species Zone F	Brackish Waterbodies	Exposed Sediment
Species Zone A		**586.7**	**4.9**	**89.1**	**114.6**	**18.4**	1.0	**70.5**
Species Zone B	**586.7**		**378.0**	**783.3**	**2147.0**	2.8	**103.6**	**125.5**
Species Zone C	**4.9**	**378.0**		**291.0**	0.3	3.2	**9.5**	2.4
Species Zone D	**89.1**	**783.3**	**291.0**		**100.3**	0.8	**447.3**	0.2
Species Zone E	**114.6**	**2147.0**	0.3	**100.3**		**4.9**	**733.8**	**49.3**
Species Zone F	**18.4**	2.8	3.2	0.8	**4.9**		1.8	2.5
Brackish Waterbodies	1.0	**103.6**	**9.5**	**447.3**	**733.8**	1.8		**75.7**
Exposed Sediment	**70.5**	**125.5**	2.4	0.2	**49.3**	2.5	**75.7**	

Table 5.16. Probability (p) values accompanying each of the respective F values. The values indicate the probability of producing the respective F value result, given that the null hypothesis (F≈1) is true. Statistically insignificant values with an alpha level ≥0.05 (hence display to 2.d.p) are indicated in red.

	Species Zone A	Species Zone B	Species Zone C	Species Zone D	Species Zone E	Species Zone F	Brackish Waterbodies	Exposed Sediment
Species Zone A		<2e-16	0.03	<2e-16	<2e-16	1.78E-5	0.31	<2e-16
Species Zone B	<2e-16		<2e-16	<2e-16	<2e-16	0.09	<2e-16	<2e-16
Species Zone C	0.03	<2e-16		<2e-16	0.57	0.07	2.09e-3	0.12
Species Zone D	<2e-16	<2e-16	<2e-16		<2e-16	0.38	<2e-16	0.62
Species Zone E	<2e-16	<2e-16	0.57	<2e-16		0.03	<2e-16	2.17e-12
Species Zone F	1.78E-05	0.09	0.07	0.38	0.03		0.18	0.11
Brackish Waterbodies	0.31	<2e-16	2.09e-3	<2e-16	<2e-16	0.18		<2e-16
Exposed Sediment	<2e-16	<2e-16	0.12	0.62	2.17e-12	0.11	<2e-16	

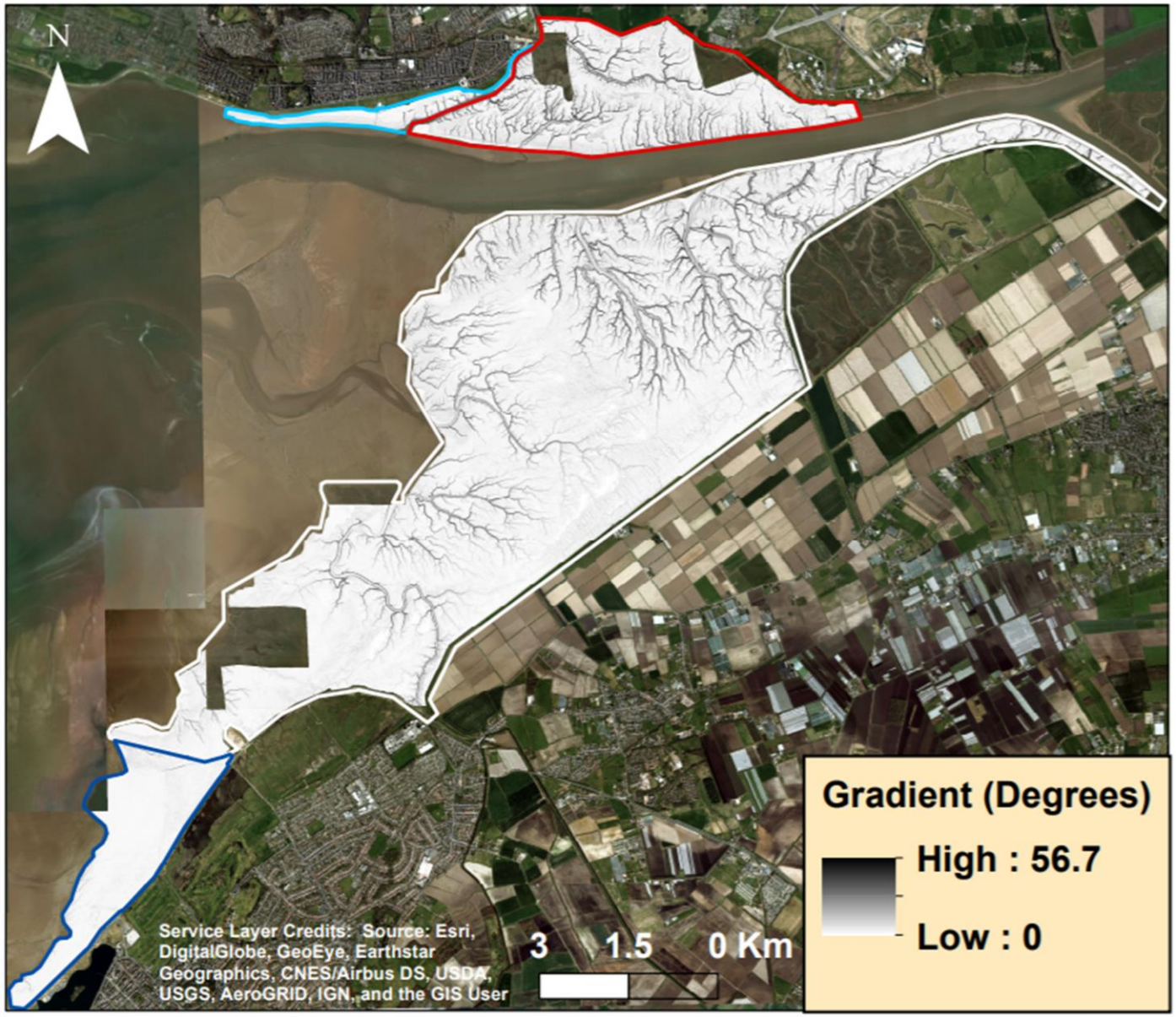

Figure 5.17. Spatial variability in gradient over all marshes.

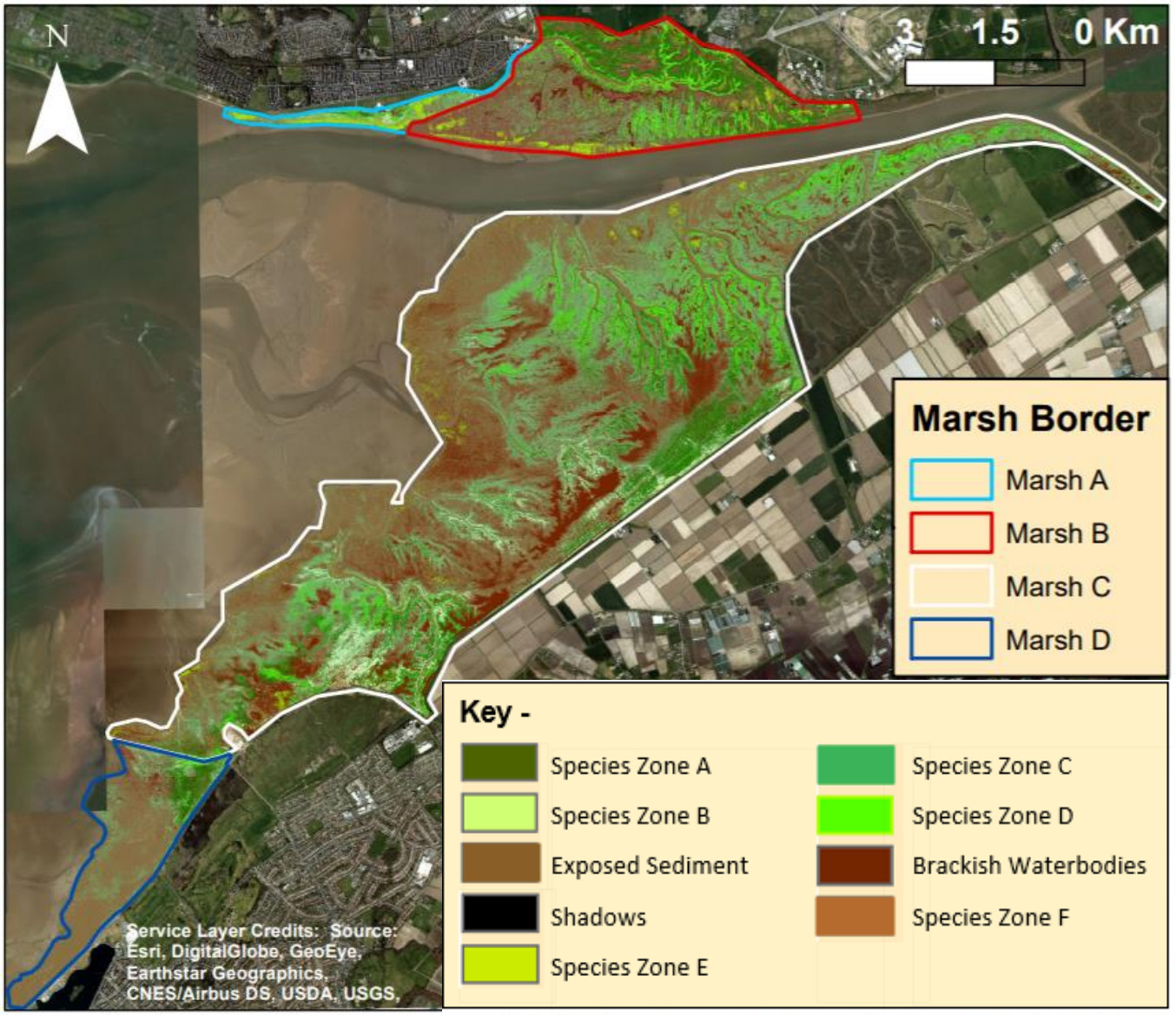

Figure 5.18. Sub-environment distribution throughout the saltmarshes of the Ribble estuary.

5.1.4 - Influence of Watercourses on Sub-environment Distribution

Introduction

This section independently assesses the influence of watercourses on the spatial distribution of sub-environments throughout the Ribble saltmarshes. The analyses review the spatial distribution of sub-environments relative to watercourses defined as fluvial inflows and tidal creeks. As Brackish Waterbodies predominantly comprise areas designated at watercourses they are largely excluded from the written analysis.

Overall Variability Between Sub-environments

Overall 54.4% of predominantly vegetated environments (i.e. Species Zones A – F) are found <20 m from a watercourse whilst 84.3% of predominantly vegetated environments are within <40 m of a watercourse. Of the predominantly vegetated environments, Species Zone D is on found at the closest mean proximity to a watercourse at a distance of 20.4 m. However, the total area of Species Zone C < 10 m from a watercourse covers an area 1.00 km^2 greater than Species Zone D. Species Zone C also exhibits the most precise distribution of any vegetated sub-environment around the modal value of 4.7 m (see Figure 5.19) and is most prominent in terms of the proportion of marsh area occupied (17.9%) at a distance of 11 m from watercourses (Figure 5.21). Although the ANOVA analysis indicates the majority of the sub-environments exhibit statistically significant watercourse proximity relationships the fact the smallest significant T-values equal 8.7 (Species Zone A and F) and 34.0 (Species Zone A and Brackish Waterbodies) indicates the uniqueness of the watercourse proximity distribution of each sub-environment.

This distribution of Species Zone F contrasts with Species Zone C as the maximal kernel distribution density is lowest of all sub-environments at 0.016 (see Figure 5.19). The distributional trend of Species Zone F is notably different from all other sub-environments (see Figure 5.19) with a mean distance value 2x greater than all other sub-environments except Species Zone E, which possess the 2nd least precise distribution. Although the IQR of Species Zone E is 2nd largest totalling 27.8 m (Figure 5.20(e)), the sub-environment possess the joint lowest standard deviation from the mean (equal with Species Zone A).

Exposed Sediment exhibited the most precise distribution of 0.043 of all sub-environments and the low mode value of 2.3 m indicated a predominance at close proximity to creeks. Despite possessing the 2nd lowest modal value the sub-environment has a mean watercourse proximity value of 24.2 m which is largely a result of the disproportionally high predominance (i.e. a greater value than the overall percentage cover of 42.6%) in areas more than 94 m from a watercourse (Figure 5.21).

Brackish Waterbodies has the lowest mode (1.7 m) and mean (19.3 m) of any sub-environment. However the in terms of overall saltmarsh areal coverage the sub-environment is most prominent 118 m from watercourses covering 9.21% of the marsh which perhaps indicates the presence of isolated saltpans. The sub-environment possesses a statistically significant watercourse proximity relationship with all sub-environments and the variation in distribution is most similar to Species Zone A (T-value = 34.0) and Exposed Sediment (T-value = 38.8).

The distribution of Species Zone A and B at close proximity to watercourses in terms of proportion is comparable with 33.5% and 33.0% of each respective sub-environment being found within 10 m of a watercourse, although the mean of Species Zone B is 3.0 m greater. The area covered in terms of the overall proportion of the saltmarsh increases to a maximum of 14.3% at 92 m (Species Zone A) and 25.1% at 78 m (Species Zone B). The ANOVA analysis highlights the ecological diverse sub-environments Species Zone B exhibits a statistically insignificant relationship with Species Zone A, whilst Species Zone A also exhibits an insignificant relationship with Exposed Sediment. Of the significant relationships, the variation of Species Zone A and F is most similar although the T-value of 8.7 highlights the distributions are unique.

As indicated in previous research, watercourse proximity had a significant influence on the distribution of all sub-environments and the extent of this influence is quantitatively assessed in Section 5.1.5. Plausible explanations for any similarities and/or discrepancies concerning the influence of watercourse proximity as well as elevation and gradient on sub-environment spatial distribution are subsequently discussed in Section 6.2.

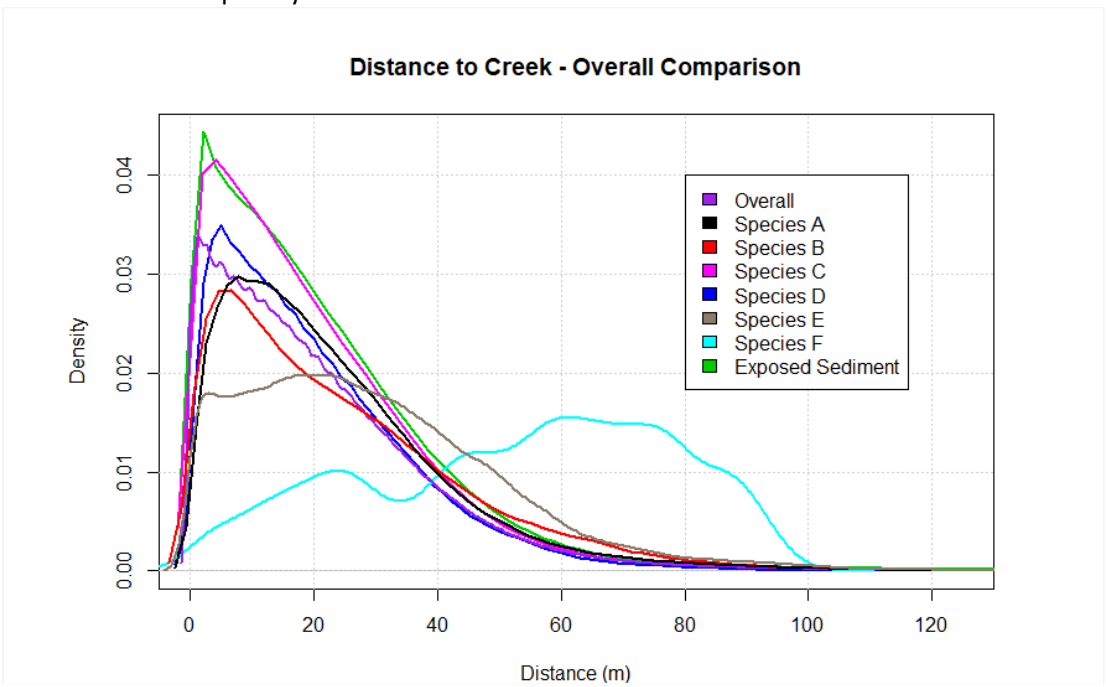

Figure 5.19. Comparitive kernel density plot exhibiting the variability in the distance of each sub-environment zone from watercourses over all marshes. Any negative values shown are a function of the kernel density distirbution smoothing display on R and do not indicate negative distances.

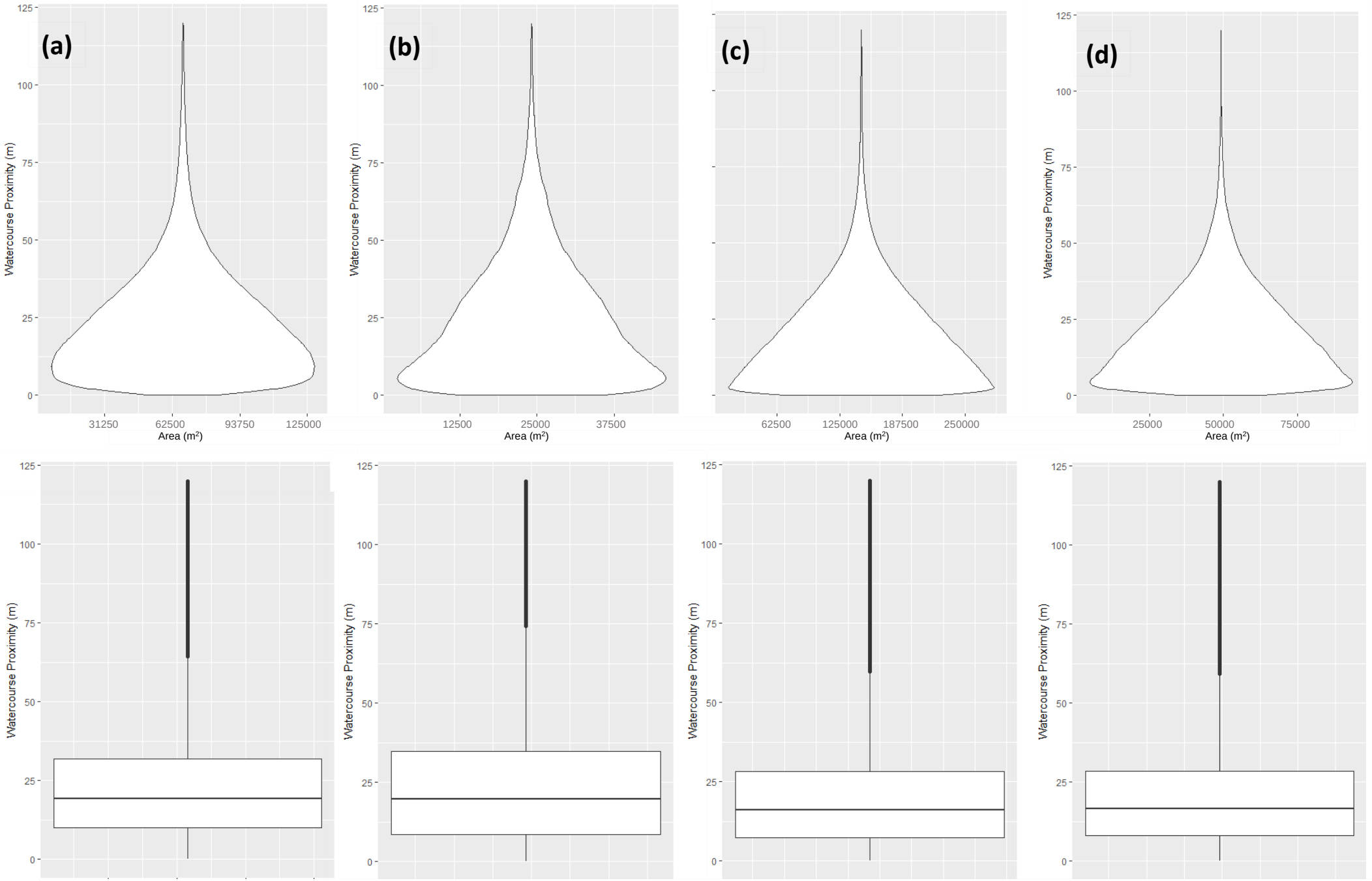

Figure 5.20. Variability in distance from watercourse between all sub-environments over all marshes. The violin and box plots for the respective sub-environments are as follows: Species Zone A (a), Species Zone B (b), Species Zone C (c), Species Zone D (d), Species Zone E (e), Species Zone F (f), Brackish Waterbodies (g) and Exposed Sediment (h).

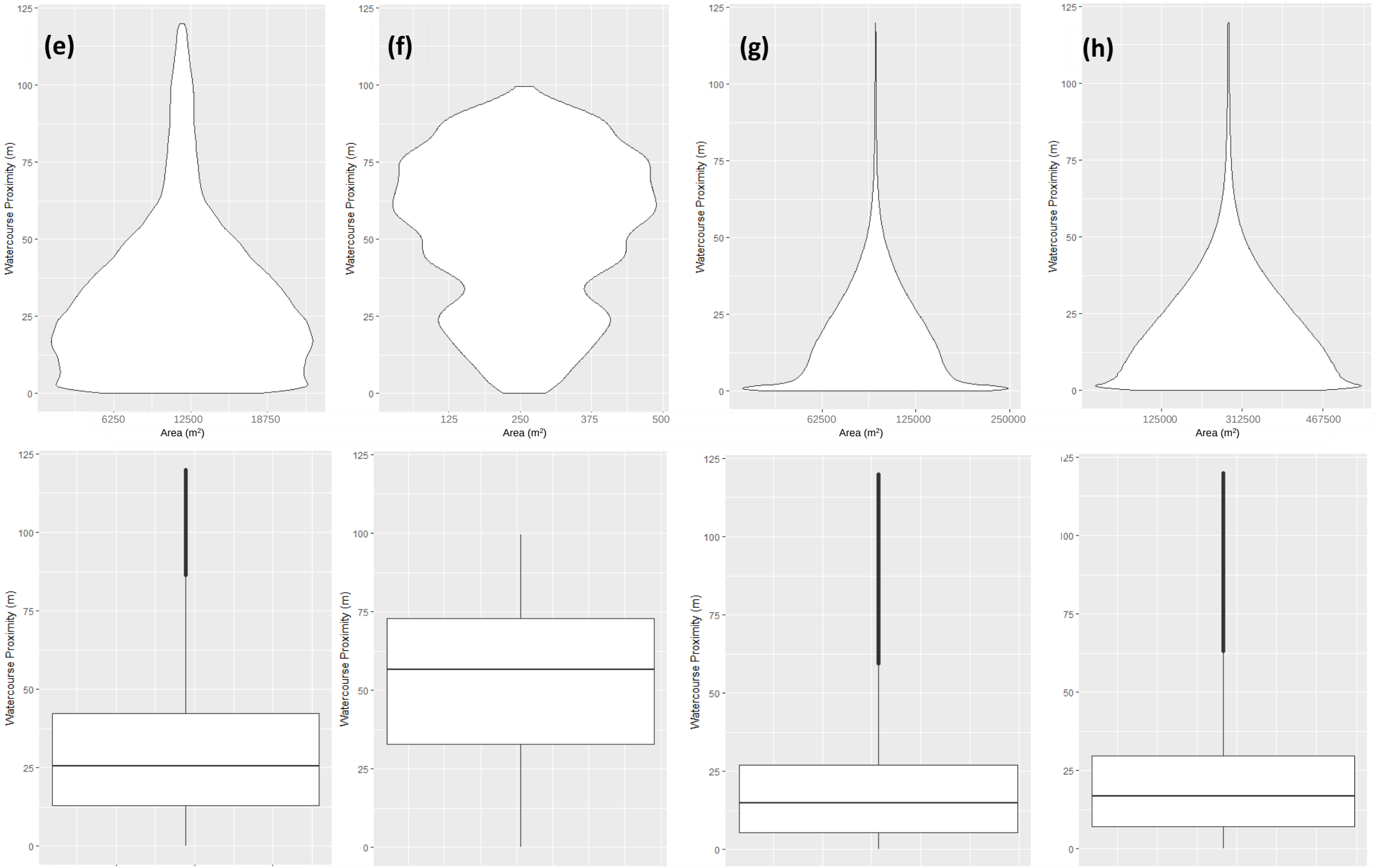

Figure 5.20. Variability in distance from watercourse between all sub-environments over all marshes. The violin and box plots for the respective sub-environments are as follows: Species Zone A (a), Species Zone B (b), Species Zone C (c), Species Zone D (d), Species Zone E (e), Species Zone F (f), Brackish Waterbodies (g) and Exposed Sediment (h).

Table 5.17. Variability in the proximity of all sub-environment zones from watercourses over all marshes.

Sub-Environment	Min	Mode	Mean	Max	St Dev.
Species Zone A	0.0	7.9	23.3	230.9	19.2
Species Zone B	0.0	5.0	26.3	247.1	21.6
Species Zone C	0.0	4.7	21.8	265.8	23.2
Species Zone D	0.0	5.2	20.4	213.3	20.1
Species Zone E	0.0	22.7	29.5	236.5	19.2
Species Zone F	0.0	61.0	52.8	99.6	24.7
Brackish Waterbodies	0.0	1.7	19.3	263.8	20.3
Exposed Sediment	0.0	2.3	24.2	267.4	21.2
All Environments	0.0	2.4	21.4	267.4	20.5

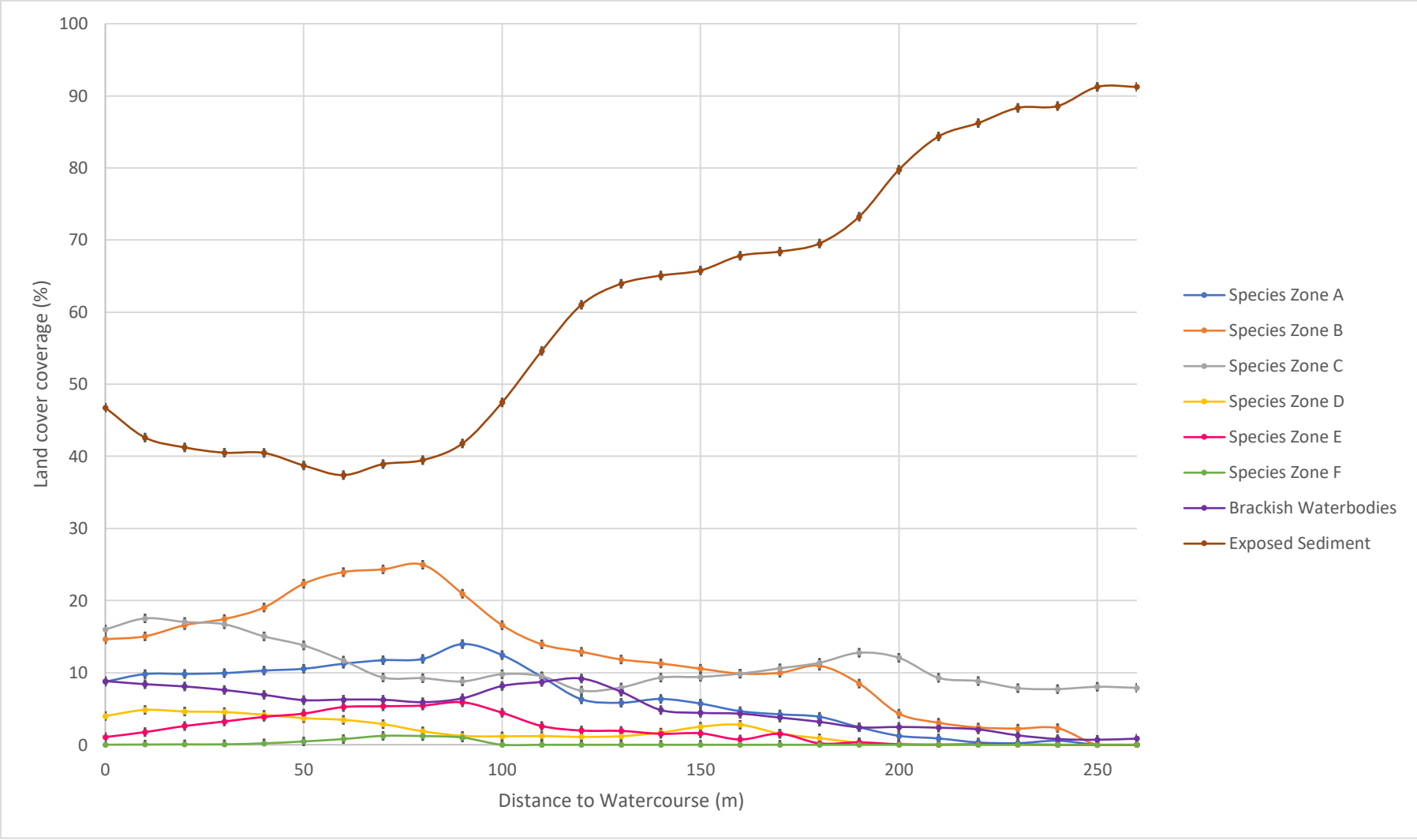

Figure 5.21. Variability of sub-environment areal coverage with watercourse proximity. Error bars indicate the RMSE of 15 cm associated with the Lidar data. See Figure 5.22 for further detail..

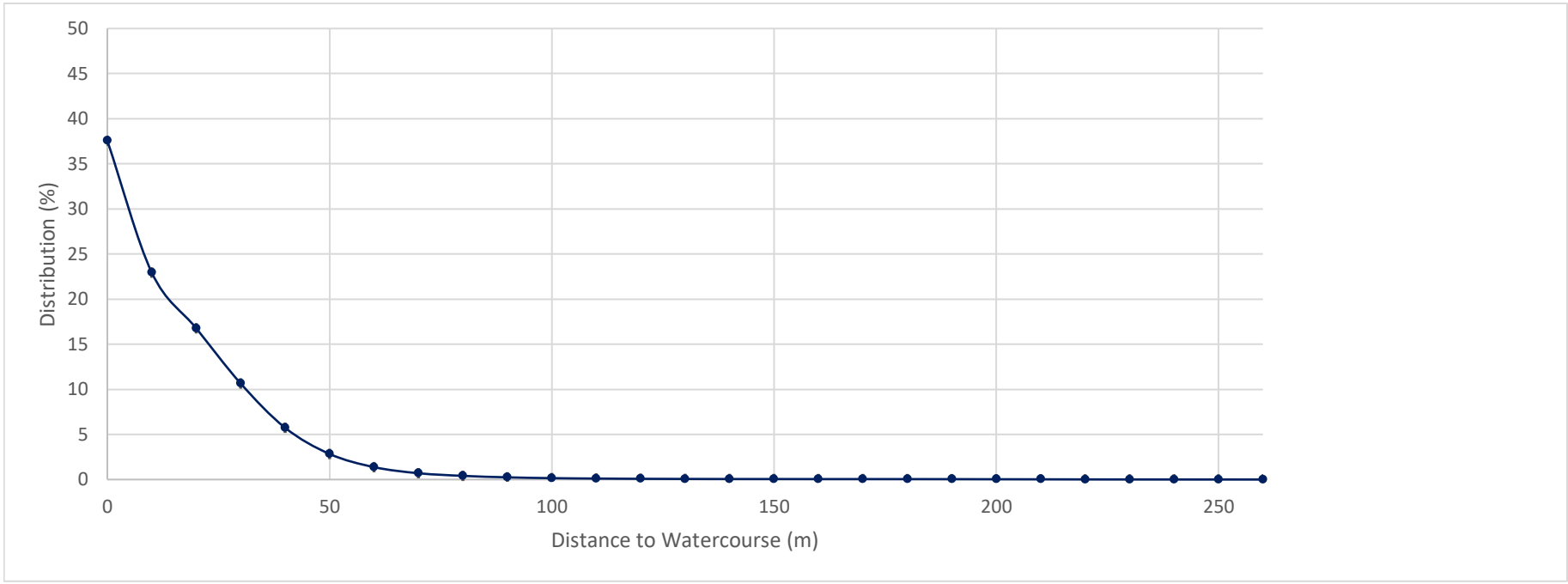

Figure 5.22. Variability in watercourse proxmity across the overall saltmarsh environment (%).

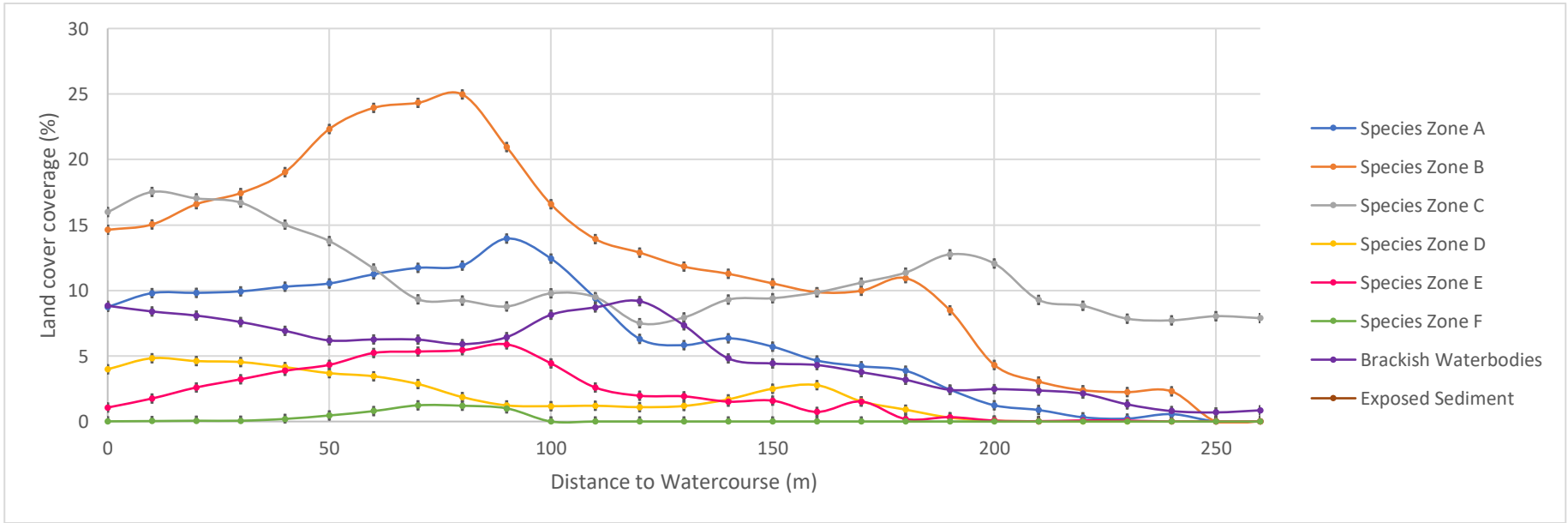

Figure 5.23. Variability of sub-environment areal coverage with watercourse proximity. Error bars indicate the RMSE of 15 cm associated with the Lidar data.

Table 5.18. F values produced during the ANOVA analyses for all land cover types. The values indicate the variance of the mean elevation values for two respective land cover types divided by mean of the variances within each respective land cover type. Significant values are highlighted in bold.

	Species Zone A	Species Zone B	Species Zone C	Species Zone D	Species Zone E	Species Zone F	Brackish Waterbodies	Exposed Sediment
Species Zone A		2.1	**34.1**	**1562.0**	**85.7**	**8.7**	**34.0**	0.1
Species Zone B	2.1		**887.8**	**133.3**	**332.1**	**25.2**	**118.8**	**512.0**
Species Zone C	**34.1**	**887.8**		**972.4**	**1228.0**	**107.8**	**291.6**	**3397.0**
Species Zone D	**1562.0**	**133.3**	**972.4**		**1768.0**	**68.9**	**89.7**	**104.8**
Species Zone E	**85.7**	**332.1**	**1228.0**	**1768.0**		**69.2**	**180.6**	**124.3**
Species Zone F	**8.7**	**25.2**	**107.8**	**68.9**	**69.2**		**255.2**	**281.2**
Brackish Waterbodies	**34.0**	**118.8**	**291.6**	**89.7**	**180.6**	**255.2**		**38.8**
Exposed Sediment	0.1	**512.0**	**3397.0**	**104.8**	**124.3**	**281.2**	**38.8**	

Table 5.19. Probability (p) values accompanying each of the respective F values. The values indicate the probability of producing the respective F value result, given that the null hypothesis (F≈1) is true. Statistically insignificant values with an alpha level ≥0.05 (hence reporting to 2.d.p) are indicated in red.

	Species Zone A	Species Zone B	Species Zone C	Species Zone D	Species Zone E	Species Zone F	Brackish Waterbodies	Exposed Sediment
Species Zone A		0.15	5.29e-9	<2e-16	<2e-16	3.27e-3	5.64e-9	0.8
Species Zone B	0.15		<2e-16	<2e-16	<2e-16	5.23e-7	<2e-16	<2e-16
Species Zone C	5.2e-9	<2e-16		<2e-16	<2e-16	<2e-16	<2e-16	<2e-16
Species Zone D	<2e-16	<2e-16	<2e-16		<2e-16	<2e-16	<2e-16	<2e-16
Species Zone E	<2e-16	<2e-16	<2e-16	<2e-16		<2e-16	<2e-16	<2e-16
Species Zone F	3.3e-3	5.2e-07	<2e-16	<2e-16	<2e-16		<2e-16	<2e-16
Brackish Waterbodies	5.64e-9	<2e-16	<2e-16	<2e-16	<2e-16	<2e-16		4.83e-10
Exposed Sediment	0.8	<2e-16	<2e-16	<2e-16	<2e-16	<2e-16	4.8e-10	

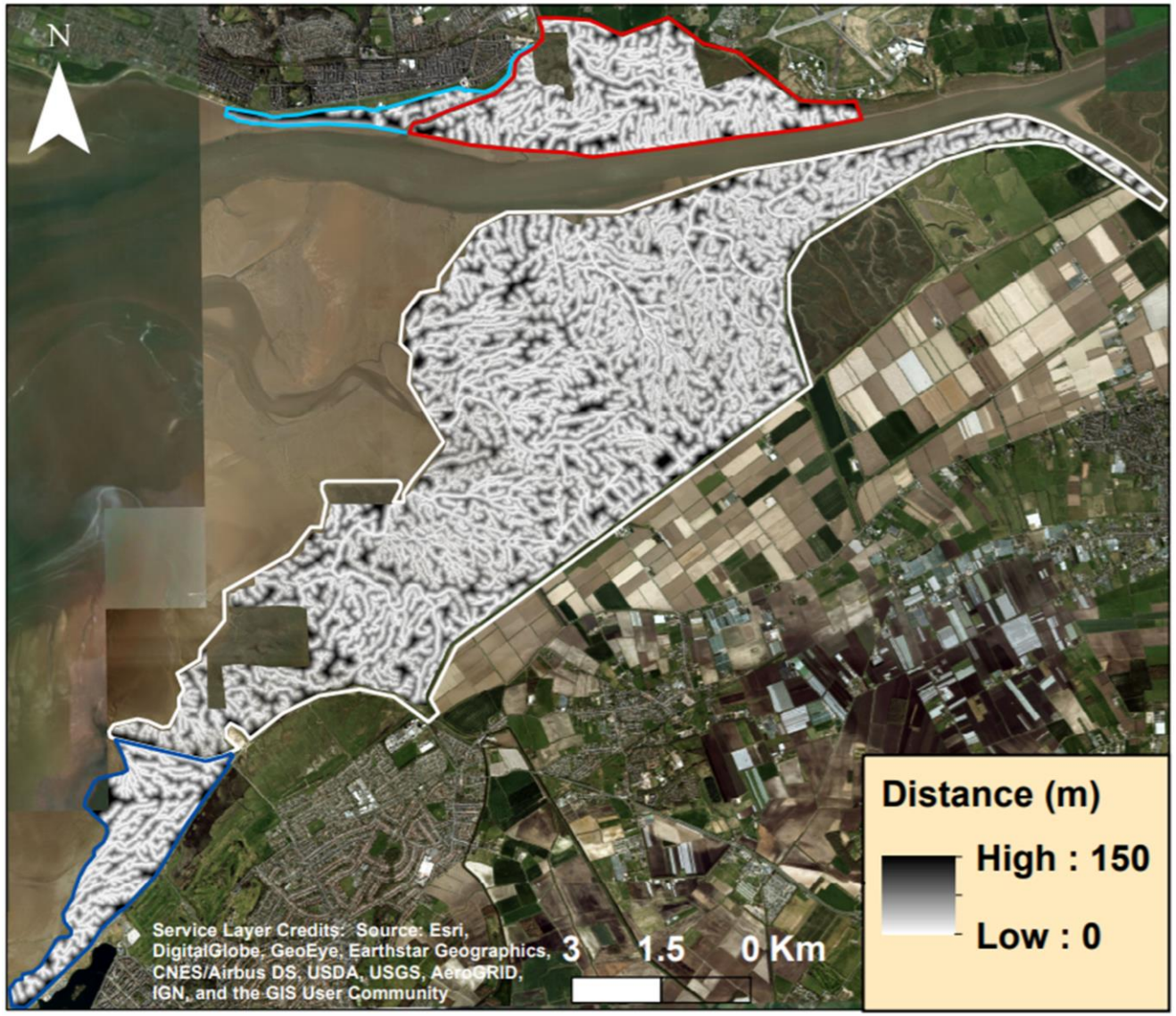

Figure 5.24. Raster model exhibiting the proximity of differing areas of all marshes to watercourses.

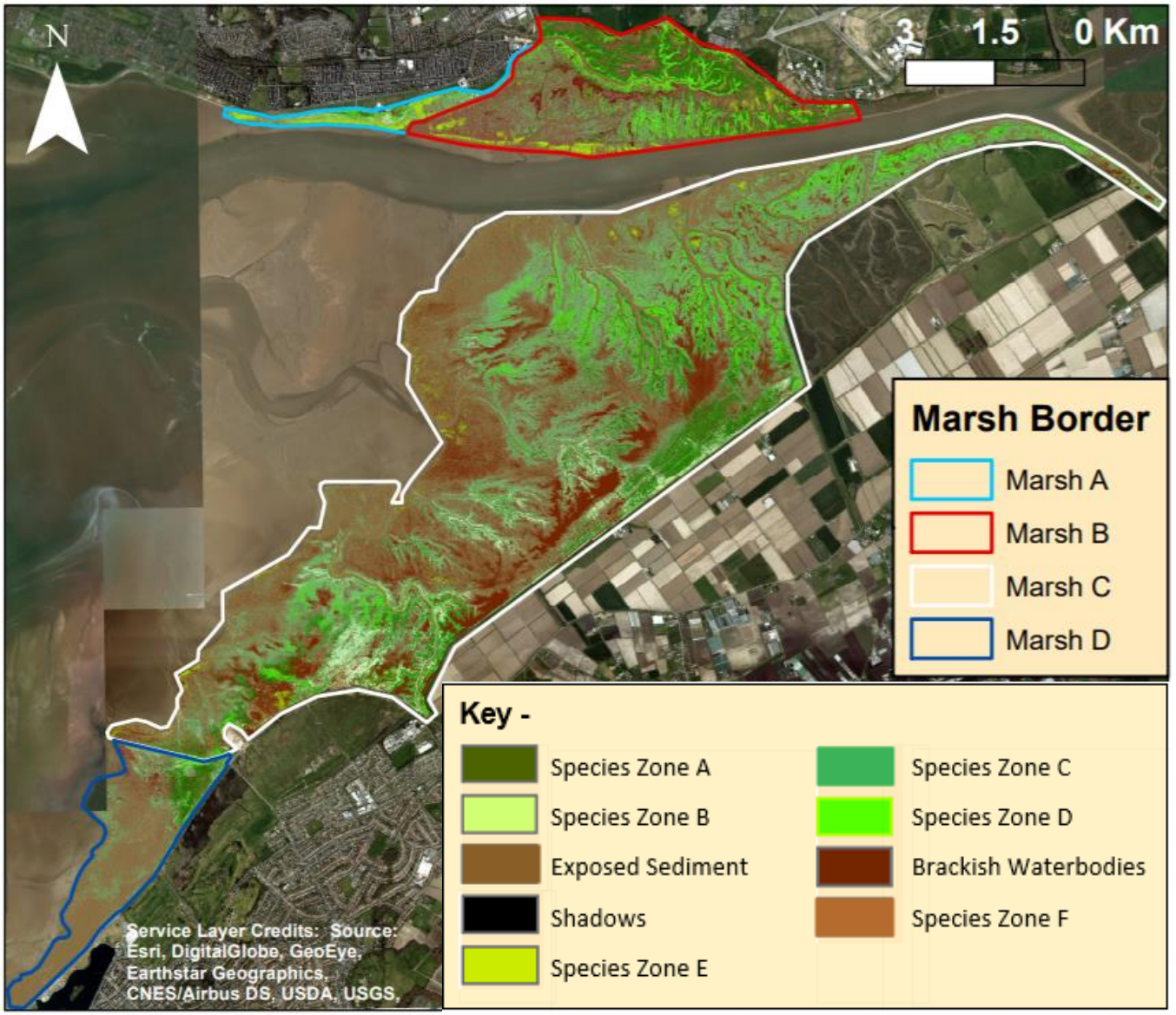

Figure 5.25. Sub-environment distribution throughout the saltmarshes of the Ribble estuary.

5.1.5 – Key Controls on Sub-environment Area – Multiple Regression Analysis

Introduction

Whilst the analyses undertaken in Section 5.1.2 – 5.1.4 highlight clear differences in sub-environment coverage and the respective influences of elevation, gradient and watercourse proximity, the observations and statistics do not fully reveal the contribution of each influence on sub-environment areal distribution.

Therefore, a multiple regression analysis was undertaken primarily to produce beta predictor coefficients (standardised and unstandardised) which are measures of how strongly each of the key controls (independent) influence sub-environment areal cover and distribution (dependent). Specifically, this analysis enabled the determination of the T statistic and p value, as well as unstandardised beta coefficient produced by regression analysis. The unstandardised beta value represented the amount of change in a dependent variable due to a change of one unit of the independent variable, which gave an idea of influence in terms of raw data. Alternatively, the standardised beta values produced by the analysis were as units of standard deviation (i.e. a beta value of 5 indicates that a change of one standard deviation in the independent variable will produce a change of 5 standard deviations in the dependent variable). This allowed for direct comparison of the influence of key controls on the spatial distribution on the different sub-environments.

Elevation

The predictor standardised beta values in Table 5.20 highlighted that Species Zone E and Species Zone F areal cover was the most proportionally influenced by the changes in elevation as the values of 0.263 and 0.25 were the greatest recorded in any sub-environment. Brackish Waterbodies (0.178) and Species Zone A (0.197) were alternatively predicted to be least influenced by elevation, whilst the sub-environment T statistic exhibited an expected strong positive correlation ($R^2 = 0.99$) with standardised beta. The unstandardised beta findings indicated that Exposed Sediment exhibited the greatest overall change in areal coverage per metre of elevation (0.072 km^2) with Species Zone C having the 2nd highest value (0.034 km^2) which was a product of surface area cover as both sub-environments possessed standardised beta values of 0.215 and 0.197 respectively. Species Zone E and F possessed the lowest unstandardised beta values despite the high standardised values which was a result of the respective areal coverage of 2.1% and 0.1% (original projection) of the overall saltmarsh area.

However, the p values for elevation are universally above the alpha value of 0.05 indicating there is a reasonable likelihood this relationship could have occurred by chance. Therefore, although the beta values show elevation influences sub-environment areal coverage, the relationships are statistically insignificant.

Table 5.20. Multiple regression parameters and the significance of predictor variables concerning elevation and sub-environment area (km^2).

Sub-environment	Unstandardised Beta (km^2)	Standardised Beta	T	p
Species Zone A	0.021	0.197	1.174	0.249
Species Zone B	0.032	0.211	1.257	0.217
Species Zone C	0.034	0.197	1.173	0.249
Species Zone D	0.009	0.212	1.267	0.214
Species Zone E	0.003	0.263	1.592	0.121
Species Zone F	1.298E-04	0.25	1.506	0.141
Brackish Waterbodies	0.014	0.178	1.056	0.298
Exposed Sediment	0.072	0.215	1.284	0.208

Gradient

The regression analysis for gradient exhibited the influence of gradient was predicted to have the greatest standardised negative influence on the area of Species Zone E and F with respective standardised beta values of -0.496 and -0.448. The areal coverage of Species Zone A and Brackish Waterbodies was predicted to be the least influenced by gradient change with a beta value of -0.384. The T statistics highlighted Species Zone E and F both exhibited the greatest difference in negative variation between gradient and area compared to variation within them, whilst Species Zone A (-2.078) and Brackish Waterbodies (-2.082) exhibited the least. The areal coverage of Species Zone C and Exposed Sediment was modelled to be equally influenced by gradient change (standardised beta = -0.409), although the negative variation differed with respective T values of -2.239 and -2.243. The unstandardised results indicated the sub-environments Species Zone B and Exposed Sediment decreased by the greatest net area per increase in degree of gradient whilst the predicted beta values indicated gradient had a very similar standardised influence of areal coverage of Exposed Sediment Species Zones B and C (0.001 disparity). In all sub-environments the p values were below the alpha value of 0.05 indicated that the relationships are statistically significant.

Table 5.21. Multiple regression parameters and the significance of predictor variables concerning gradient and sub-environment area.

Sub-environment	Unstandardised Beta (km^2)	Standardised Beta	T	p
Species Zone A	-0.008	-0.384	-2.078	0.048
Species Zone B	-0.014	-0.41	-2.247	0.034
Species Zone C	-0.013	-0.409	-2.239	0.034
Species Zone D	-0.003	-0.429	-2.37	0.026
Species Zone E	-0.002	-0.496	-2.856	0.009
Species Zone F	-7.979E-05	-0.448	-2.5	0.019
Brackish Waterbodies	-0.007	-0.384	-2.082	0.048
Exposed Sediment	-0.035	-0.409	-2.243	0.034

Watercourse Proximity

The standardised beta values for watercourse proximity exhibited that watercourse proximity had the greatest negative influence on the area covered by Species Zones E and F areal cover. The respective values of -0.757 (Species Zone E) and -0.729 (Species Zone F) indicated the two sub-environments exhibited the greatest standardised decrease in area per metre increase in distance from a watercourse. The model exhibited Exposed Sediment (-0.614) and Brackish Waterbodies (-0.627) areal cover was alternatively the least influenced by watercourse proximity. The T-value varied accordingly with standardised beta ($R^2 = 0.99$) with Species Zone E and F showing the greatest degree of variance between watercourse proximity and area compared to variation within each variable. The unstandardised values exhibited the sub-environments associated with creek sediment and terrace vegetation Exposed Sediment (-0.0065) and Species Zone C (-0.0025) showed the greatest degree in area per m from a watercourse. The p values ≤0.001 indicated that there was a very low probability that any of the relationships between watercourse proximity and areal coverage occurred by chance.

Table 5.22. Multiple regression parameters and the significance of predictor variables concerning watercourse proximity and sub-environment area.

Sub-environment	Unstandardised Beta (km^2)	Standardised Beta	T	p
Species Zone A	-0.0014	-0.661	-4.404	<0.001
Species Zone B	-0.0025	-0.679	-4.628	<0.001
Species Zone C	-0.0025	-0.635	-4.108	<0.001
Species Zone D	-0.0006	-0.649	-4.266	<0.001
Species Zone E	-0.0003	-0.757	-5.792	<0.001
Species Zone F	-1.04E-5	-0.729	-5.325	<0.001
Brackish Waterbodies	-0.0013	-0.627	-3.923	0.001
Exposed Sediment	-0.0065	-0.614	-3.889	0.001

Overview

The multiple regression analysis indicated that whilst it plausible all three factors influence sub-environment distribution, gradient and watercourse proximity are the only statistically significant influences (alpha level = 0.05). The influence of elevation cannot be deemed significant due to the p value range of 0.121 - 0.298 and the standardised beta values also indicate that elevation universally has the smallest influence on the distribution of each of the eight sub-environments. Of the significant influences, watercourse proximity had the largest standardised influence on sub-environment distribution for all eight sub-environments, with Species Zones E and F being most proportionally influenced as the areal coverage decreased by the greatest standardised values. The standardised areal coverage of Species Zones E and F were also most influenced by gradient although this influence was reduced by 0.261 and 0.281 standard deviations respectively when compared to the influence of watercourse proximity. The influence of watercourse proximity and gradient on specific sub-environments did not follow the same order as Exposed Sediment had the lowest standardised value (-0.614) for watercourse proximity whilst Species Zone A and Brackish Watebodies (-0.384) were the least influenced by gradient. This suggests there is not a direct correspondence between the influence of watercourse proximity and gradient on the distribution and areal coverage specific sub-environments. This highlights that the influence of the two significant factors on sub-environments is highly complex, especially when one considers the relationship between creek banks and increased gradient. The ensuing discussion (see Section 6.2) will consider the significant influences of both gradient and watercourse proximity on sub-environment distribution.

5.2 – Geomorphological Analysis and Carbon Quantification

5.2.1 Introduction

The following section exhibits the results concerning the observed carbon content the saltmarshes of the Ribble estuary. The results concerning the carbon density of above-ground biomass and sub-surface sediments are considered independently, whilst the relationship between depth, bulk density (BD) and organic carbon density (OCD) of active layer sediment (sub-surface part of the active section) is also reviewed. Results of the independent assessments of all four marshes can be found in Appendix C.

5.2.2.1 - Above-ground Biomass

Over the four saltmarshes, the two predominantly non-vegetated environments possessed the lowest above-ground carbon mass with averages values of 0.33 kg/m^2 (Brackish Waterbodies) and 0.12 kg/m^2 (Exposed Sediment). Alternatively, Species Zones B and C on average had the highest respective overall above-ground biomass carbon content with 1.19 kg/m^2 and 0.97 kg/m^2. Species Zone C also had the highest degree of standard deviation in kg/m^2 from the mean, whilst Exposed Sediment exhibited the highest standard deviation as a percentage of the mean. Excluding Species Zone F (one sample), the other predominantly non-vegetated sites Brackish Waterbodies has the lowest degree of standard deviation as well as the lowest range of 0.04 kg/m^2 over the three sites. Species Zone D had the 2nd lowest standard deviation in terms of percentage of the mean although the overall range was 0.03 kg/m^2 higher than that of Exposed Sediment (2nd lowest).

Table 5.23. Statistical summary of carbon mass (kg/m^2) stored within the above-ground biomass in the different sub-environments incorporating data from all sampling sites. Although above-ground biomass and carbon mass was determined to ±5 x 10^{-5} g, values are reported to 2.d.p of a kg/m^2 for ease of interpretation and to differences in carbon storage to be easily discerned.

Sub-environment Type	Minimum	Median	Mean	Max	St. Dev	St. Dev (%)
Species Zone A	0.46	1.00	0.94	1.30	0.33	35.0
Species Zone B	0.78	1.27	1.19	1.51	0.30	25.0
Species Zone C	0.18	1.02	0.97	1.40	0.43	44.7
Species Zone D	0.69	0.73	0.79	1.02	0.13	17.0
Species Zone E	0.35	0.72	0.78	1.32	0.40	52.1
Species Zone F	0.60	0.60	0.60	0.60	0.00	0.0
Brackish Waterbodies	0.31	0.32	0.33	0.35	0.02	6.9
Exposed Sediment	0.00	0.10	0.12	0.30	0.13	108.3
All Sample Sites	0.00	0.78	0.74	1.51	0.46	61.3

5.2.2.2 - Sub-Surface

The overall findings indicate a general correspondence between core consistency, OCD and BD. Although, an exception does exist on Marsh A at 'E Site A', on a site-specific level (see Appendix Section C1), the proportion of organic matter within a horizon decreases with depth, whilst OCD and BD respectively exponentially decrease and increase with depth (Figure 5.26(a & b)). Although the overall range for both OCD and BD within a core depends on the site, on average the basal horizons possess an OCD 43.4% lower than the active layer whilst mean basal BD values are 22.3% greater. The probability of the relationship between OCD and BD in all active horizons over the whole marsh is statistically significant (p= <0.001), however when viewed as a whole only 64% of the variation between OCD and BD can be explained by a linear model which highlights the site-specific nature of the correspondence.

Samples from sub-environments classed as Exposed Sediment exhibited the lowest OCDs and highest BDs, although Brackish Waterbodies had the highest mean sub-surface OCD of 3.27 kg m^{-3}. The OCD and BD of the sub-surface horizons of predominantly vegetated sub-environment is largely site-specific (see Table 5.24), with the sub-environments Species Zones B and E containing the highest mean OCD of 2.82 kg m^{-3} and 2.68 kg m^{-3}, whilst Species Zones F and C contained the lowest mean OCD of 2.44 kg m^{-3} and 2.63 kg m^{-3}. Standard deviation (%) did not appear to correspond with OCD as Species Zone B and Exposed Sediment exhibited the 1st and 2nd highest OCD standard deviation of 27.2% and 17.2%.

OCD exhibited an exponential decrease with depth (Figure 5.26(a)) which is commonly exhibited in saltmarsh sediments due to the substantial decrease in organic productivity with depth below the active surface layer (Mishra *et al.* 2009; Bai *et al.* 2016). The negative linear correlation between OCD and BD (Figure 5.26(c)) also complied with prior research indicating high carbon contents in the surface organic silts compared with the reduced OCD at greater depths in coarser silts and fine-medium grained sands with a higher BD (Elgin, 2012; Santini *et al.* 2019). BD exhibited an exponential increase with depth (Figure 5.26(b)) suggesting a coarsening of grain size in the fossil layers with a lower OCD.

Table 5.24. Statistical summary of carbon mass (kg m^{-3}) stored within the sub-surface sediments in the different sub-environments. Although sub-surface carbon mass was determined to ±5 x 10^{-5} g, values are reported to 2.d.p of a kg m^{-3} for ease of interpretation and to allow one to easily discern differences in carbon storage.

Sub-environment Type	Minimum	Median	Mean	Max	St. Dev	St. Dev (%)
Species Zone A	1.99	2.70	2.66	3.04	0.34	12.66
Species Zone B	2.27	2.48	2.82	3.69	0.77	27.2
Species Zone C	2.42	2.53	2.63	3.03	0.23	8.7
Species Zone D	2.19	2.74	2.66	2.96	0.28	10.4
Species Zone E	2.43	2.68	2.68	2.92	0.20	7.5
Species Zone F	2.44	2.44	2.44	2.44	0.00	0.0
Brackish Waterbodies	3.19	3.29	3.27	3.33	0.07	2.2
Exposed Sediment	1.65	2.19	2.16	2.61	0.37	17.2
All Sample Sites	1.65	2.60	2.62	3.69	0.42	15.9

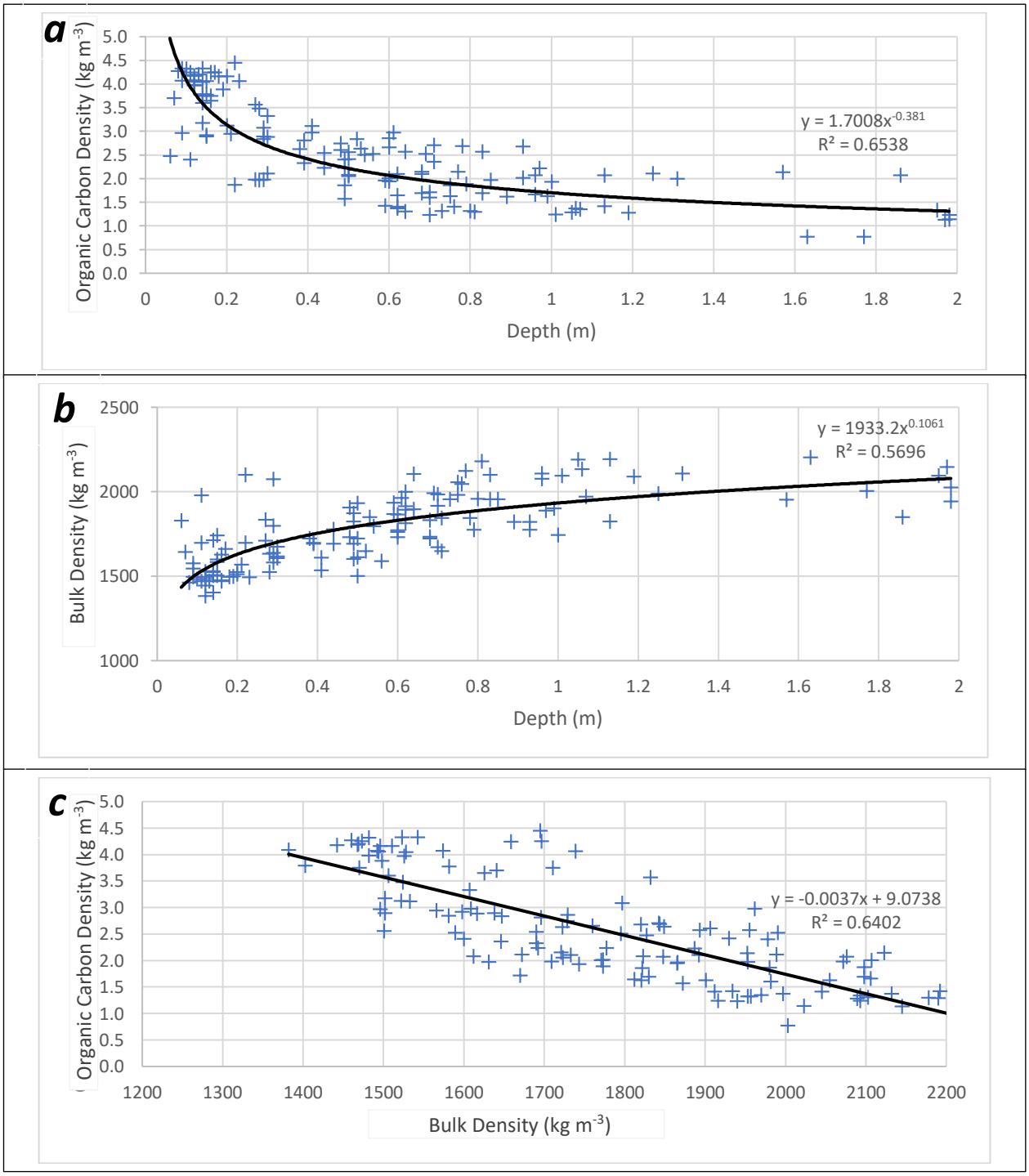

Figure 5.26. Correspondance between the depth, organic carbon density and bulk density throughout all sub-surface horizons.

5.2.2.3 - Active Layer Characteristics

In order to determine the active layer OCD and BD samples from all sub-environments were collectively analysed along with the assistance of field observations to identify the variability in active layer depth in each layer. The criteria that an active layer must have an OCD >15% than the overall sub-surface sediment and contain undecomposed organic matter produced a mean active layer depth ranging between 12.6 cm (Species Zone A) and 23.3 cm (Exposed Sediment). However, the exponential decrease in OCD which is observed between active and fossil layers (Mishra *et al.* 2009; Bai *et al.* 2016) resulted in a mean active layer content which was on average 43.4% greater than that of all the sub-surface sediment.

When OCD and BD values for all active layers are considered, the SD from the overall mean was 18% and 9.8% for OCD (average = 3.8 kg m^{-3}) and BD (average = 1578 kg m^{-3}) respectively, which highlights the variability in active layer sediment characteristics. However, the probability of a relationship between OCD and BD across all active horizons occurring by chance is negligible ($p = \leq 0.001$) which suggests OCD and BD variation is mainly site-specific. The carbon density was on average highest in Species Zone E (4.26 kg m^{-3}) and Species Zone C (4.12 kg m^{-3}) and lowest in sub-environments classified as Exposed Sediment (3.09 kg m^{-3}). Although Species Zone A has the greatest overall range of 1.84 kg m^{-3} the standard deviation as a percentage of the mean was greatest in Species Zones F (23.9%) and D (19.3%). Alternatively, Brackish Waterbodies exhibits the lowest standard deviation both in terms kg m^{-3} and percentage, suggesting little variability in active layer carbon density in the sub-environment.

OCD decreased with depth within the active layer itself but only 12.6% of the variation could be explained by an exponential model (Figure 5.27(a)), whilst only 13.4% of the increase in BD with depth could be explained (Figure 5.27(b)). Variability between the OCD and BD of active layer samples was also high as indicated by the R^2 value of 0.191 (Figure 5.27(c)). The contrast in the OCD, BD and depth relationship between all sub-surface samples (Figure 5.26) and the active layer samples plausibly suggests the depth boundary between active and fossil layers accurately divide the two layers as no exponential decrease in OCD with depth was exhibited in the active layer. Moreover, the BD of the active layer samples was consistently lower than the BD of sediments at lower depths (see Figure 5.26(b)). This highlights the active layer samples are indicative of uncompacted organic-rich silts which commonly comprise the active surface layers and are directly influenced by ecogeomorphological processes (Bartholdy, 2012; Bai *et al.* 2016)

Table 5.25. Statistical summary of carbon density (kg m^{-3}) of active layer sediments in the differing sub-environments. Although active layer carbon mass was determined to ±5 x 10^{-5} g, values are reported to 2.d.p of a kg m^{-3} for ease of interpretation and to allow one to easily discern differences in carbon storage.

Sub-environment Type	Mean Depth (m)	> Sub-surface (%)	Min	Median	Mean	Max	St. Dev	St. Dev (%)
Species Zone A	0.126	47.3	2.48	4.19	3.91	4.32	0.65	16.6
Species Zone B	0.127	39.7	3.17	4.11	3.93	4.24	0.40	10.3
Species Zone C	0.136	56.8	3.77	4.17	4.12	4.33	0.22	5.4
Species Zone D	0.14	34.1	2.41	3.65	3.56	4.16	0.69	19.3
Species Zone E	0.163	58.9	4.07	4.25	4.26	4.45	0.19	4.5
Species Zone F	0.15	42.9	2.89	3.48	3.48	4.07	0.83	23.9
Brackish Waterbodies	0.15	17.7	3.75	3.75	3.85	4.06	0.18	4.7
Exposed Sediment	0.233	43.3	2.24	3.12	3.09	3.70	0.48	15.5
All Sample Sites	0.153	43.5	2.24	3.98	3.75	4.45	0.59	15.6

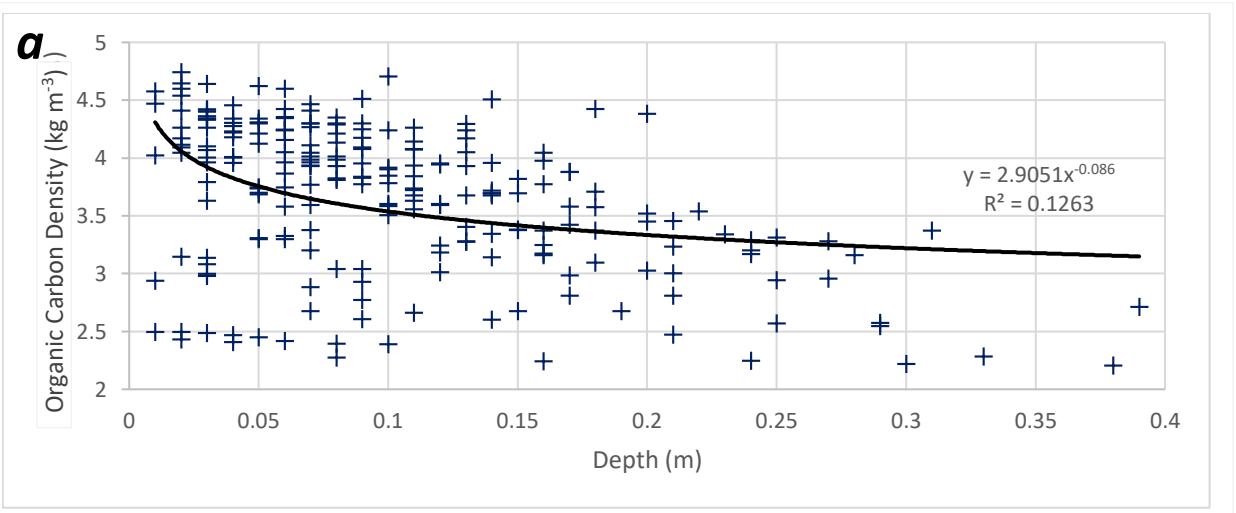

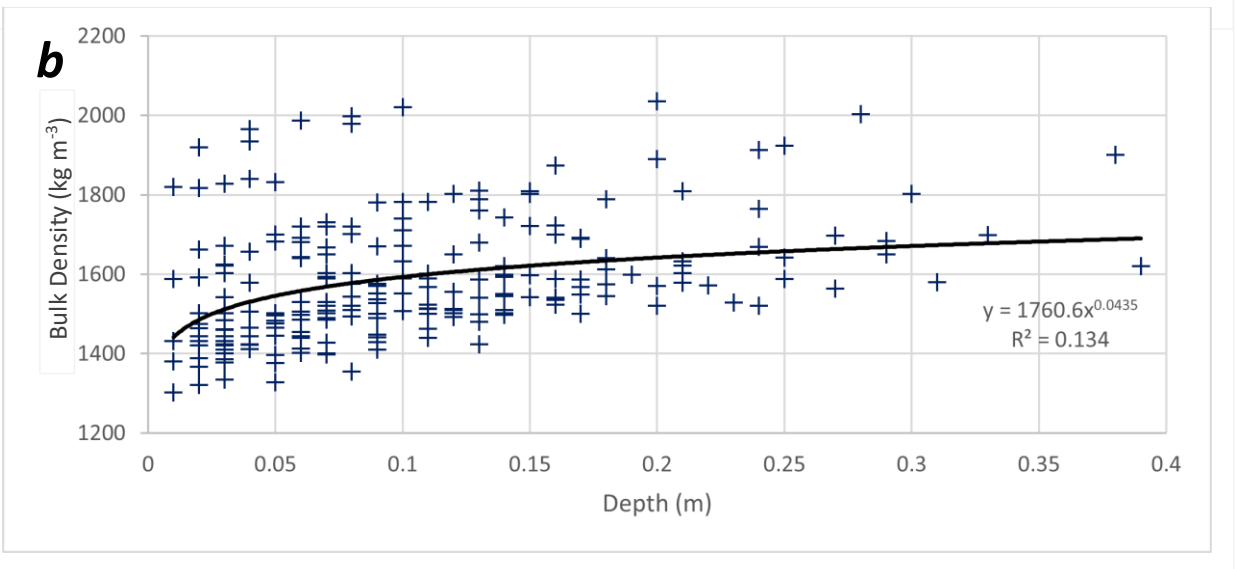

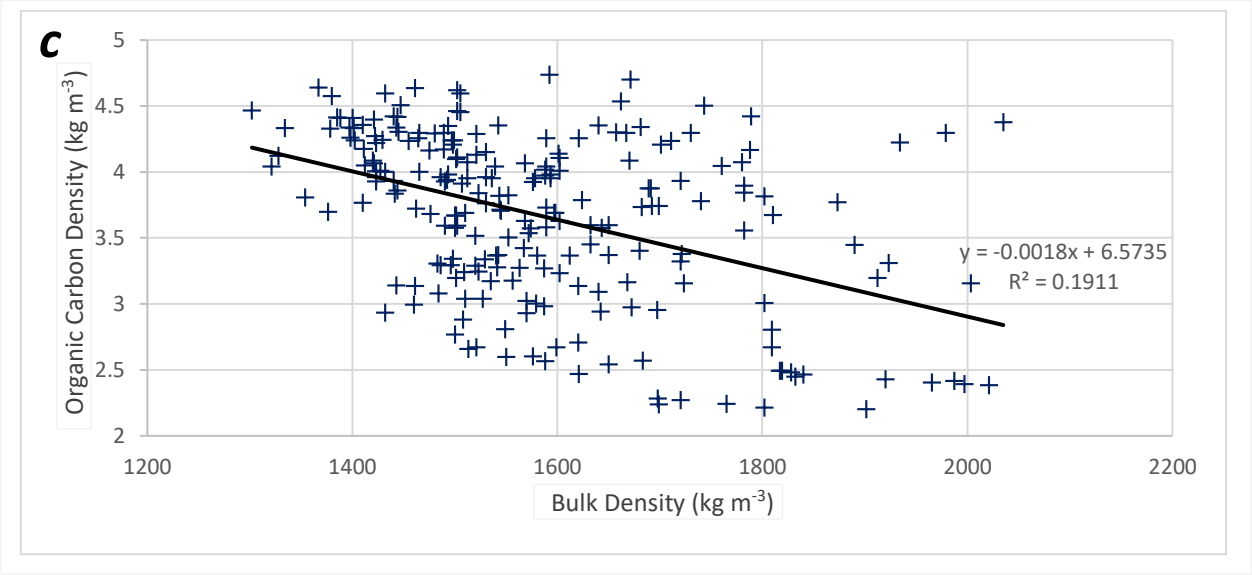

Figure 5.27. Correspondance between the depth, organic carbon density and bulk density in all active layer horizons.

5.2.2.4 – Above-ground Biomass and Active Layer Carbon

The findings concerning the correspondence between carbon stored within the above-ground biomass and active layer highlighted a degree of correlation between both variables across the entire saltmarsh (see Figure 5.28). When sub-environments are considered on an individual basis Species Zone E exhibited the largest discrepancy from this trend of positive correlation with the highest average active layer carbon density of 4.26 kg/m^2 despite an average above-surface carbon mass of 0.78 kg/m^2. Alternatively, Exposed Sediment possessed the lowest carbon density in both cases, whilst Brackish Waterbodies exhibited the greatest degree of deviation from the linear trend.

Overall 44% of the variation between the two variables can be explained by a statistically significant (T-test p value = <0.001) linear model which suggests a positive correlation between above-ground vegetation and active layer carbon content. This suggests that the above-ground carbon storage and biomass influence the mean active layer carbon storage potential, although the low R^2 value and uncertainty in organic carbon density (see Figure 5.28) indicate other factors have a more prominent influence on carbon storage (see Section 6.2).

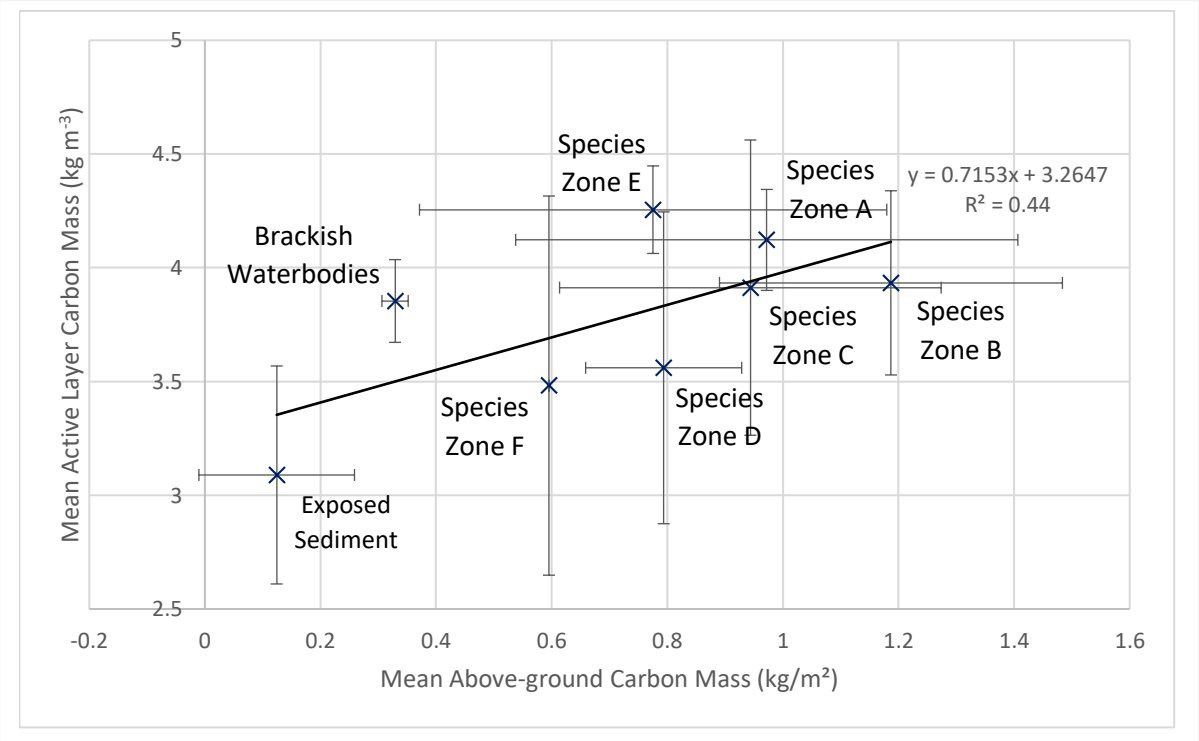

Figure 5.28. Correspondance between the mean carbon mass per unit area in both the above-ground biomass and active layer in each sub-environment. Error bars indicate the standard deviation surrounding each respective mean value.

5.3 – Overall Carbon Content of Sub-environments

5.3.1 – Introduction

This section combines the results from sections 5.1 and 5.2 in order to determine the overall carbon contents of the above-ground biomass and active layer which comprise the active section. The distribution of carbon within both the above-ground biomass and active layer sediments of all sub-environments and the uncertainty surrounding these calculations is also exhibited.

5.3.2 – Variability in Carbon Content

5.3.2.1 - Above-ground Biomass

The carbon stored within the above-ground biomass in different saltmarsh sub-environments and the uncertainty surrounding the projections according to the remote (blue) and manual (orange) landcover analyses is highlighted in Figure 5.29(a-d) and Table 5.26. The projections indicate the highest total above-ground carbon mass is held within Species Zone B which is primarily a result of the sub-environment having the highest average carbon density (1.19 kg/m^2) whilst covering the 3rd greatest area (3.06 km^2) according to the original assessment. Although Species Zone C covers 0.2 km^2 more than Species Zone B, the lower mean carbon mass (0.97 kg) means the sub-environment a carbon mass 3.57 x 10^5 kg lower than that of Species Zone B according to the original projection. However, the areal uncertainty projections suggest it is plausible that Species Zone B and C could have a total above-ground carbon mass of 3.63 x 10^5 kg and 4.24 x 10^5 kg if the lowest (Species Zone B) and highest (Species Zone C) remote land cover uncertainty projections were assumed for the respective sub-environments. Moreover, as the OCD standard deviation for Species Zone C (44.7%) was greater than in Species Zone B (25%), it is plausible that the carbon mass of the former could be higher than that of Species Zone B even assuming the original areal projections.

Of all predominantly vegetated environments the highest degree of standard deviation relative to the mean of 52.1% is observed in Species Zone E (Table 5.27), which according to the minimal and maximal carbon projection assuming the remote area could have a projected overall carbon mass as high as 6.93 x 10^5 kg or as low as 1.41 x 10^5 kg. However, when only areal projections are considered (mean OCD) Species Zone E has a standard deviation of 10.8% from the mean (Table 5.26).

The net disparity between projections is lowest (2520 kg) for Species Zone F due to the low overall projection of carbon mass and the lack of standard deviation in OCD (Table 5.28). In contrast, the carbon mass of Species Zone A could differ by 2280 kg and the maximal projection for Species Zone A (3110 kg) is 56.7% greater than the projection which assumes mean OCD and the original remote

area coverage. Therefore if the OCD or areal coverage of Species Zone A was at the upper limit of uncertainty and Species Zone C at the lower, it is plausible that Species Zone A could contain a greater mass of carbon (see Tables 5.27 and 5.28).

As the manual areal classification of Species Zone D was 100% accurate and the remote assessment had an accuracy of 90%, the standard deviation surrounding the areal projections is comparably low at 6.6% or 4.82 x 10^4 kg. Moreover the low uncertainty in OCD projection results in a low standard deviation surrounding the projections that assume original areal cover and consider OCD variability of 1.24 x 10^5 kg or 17.0%,

Brackish Waterbodies had the lowest standard deviation concerning carbon mass both in terms of mass and as percentage of the average of 0.33 kg/m^2 producing the lowest standard deviation of 6.9% when OCD variability was considered (excluding Species Zone F) (Table 5.27). Alternatively, Exposed Sediment had the largest standard deviation of carbon mass which produced a standard deviation of 108.3% when OCD variability was considered. Despite the coverage of Exposed Sediment over 42.6% of the overall marsh area the original projection indicates that Exposed Sediment will account for 9.2% of the total above-ground carbon due to the low mean OCD of 3.09 kg m^{-3}. However, the remote uncertainty analysis highlighted the overall carbon mass of the sub-environment could hypothetically vary between 0 and 3.11x 10^6 kg.

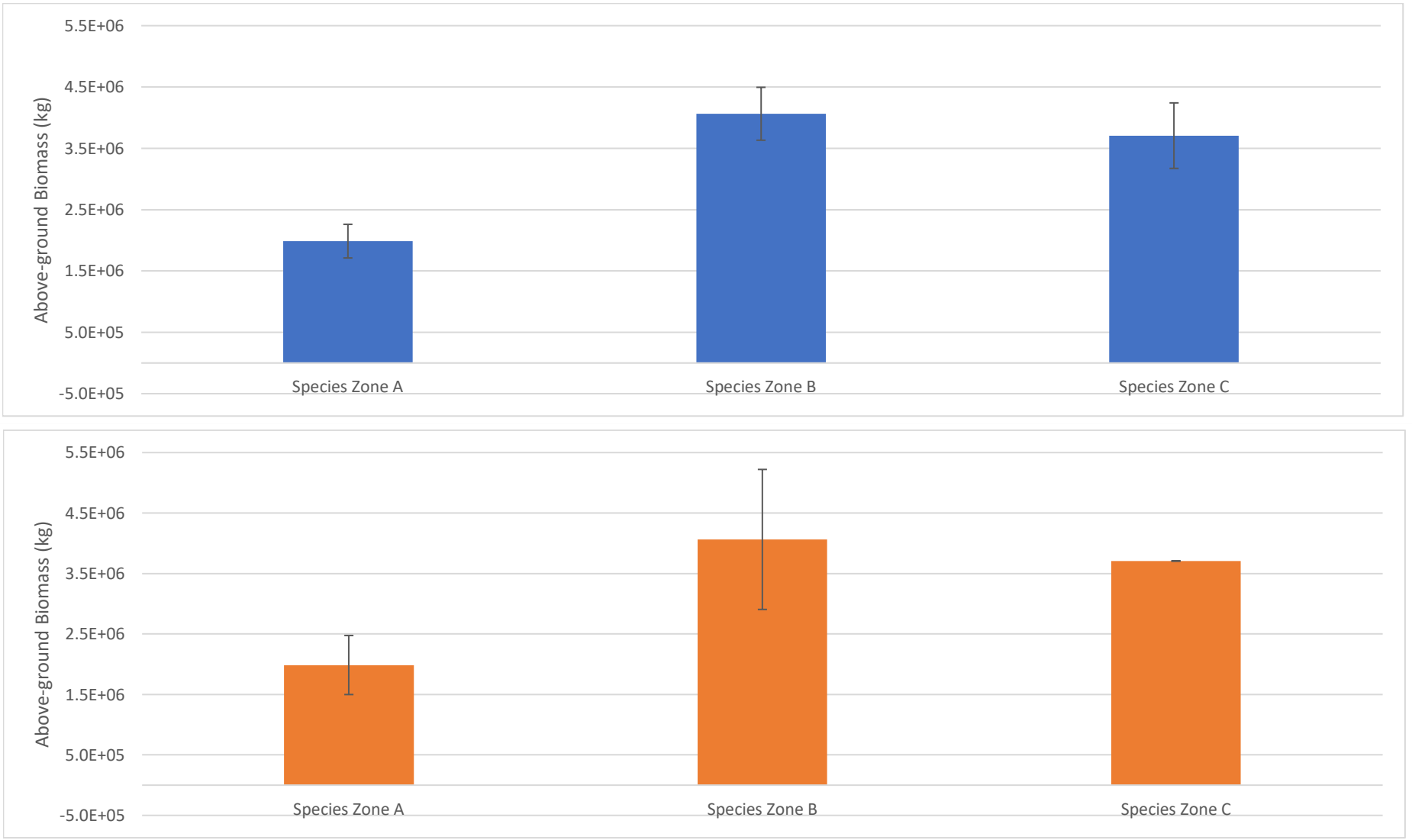

Figure 5.29(a). Disparity in overall above-ground biomass carbon projections for sub-environments: Species Zone A, B and C assuming mean OCD. Error bars represent the maximal uncertainty surrounding the remote (blue) and manual (orange) analyses.

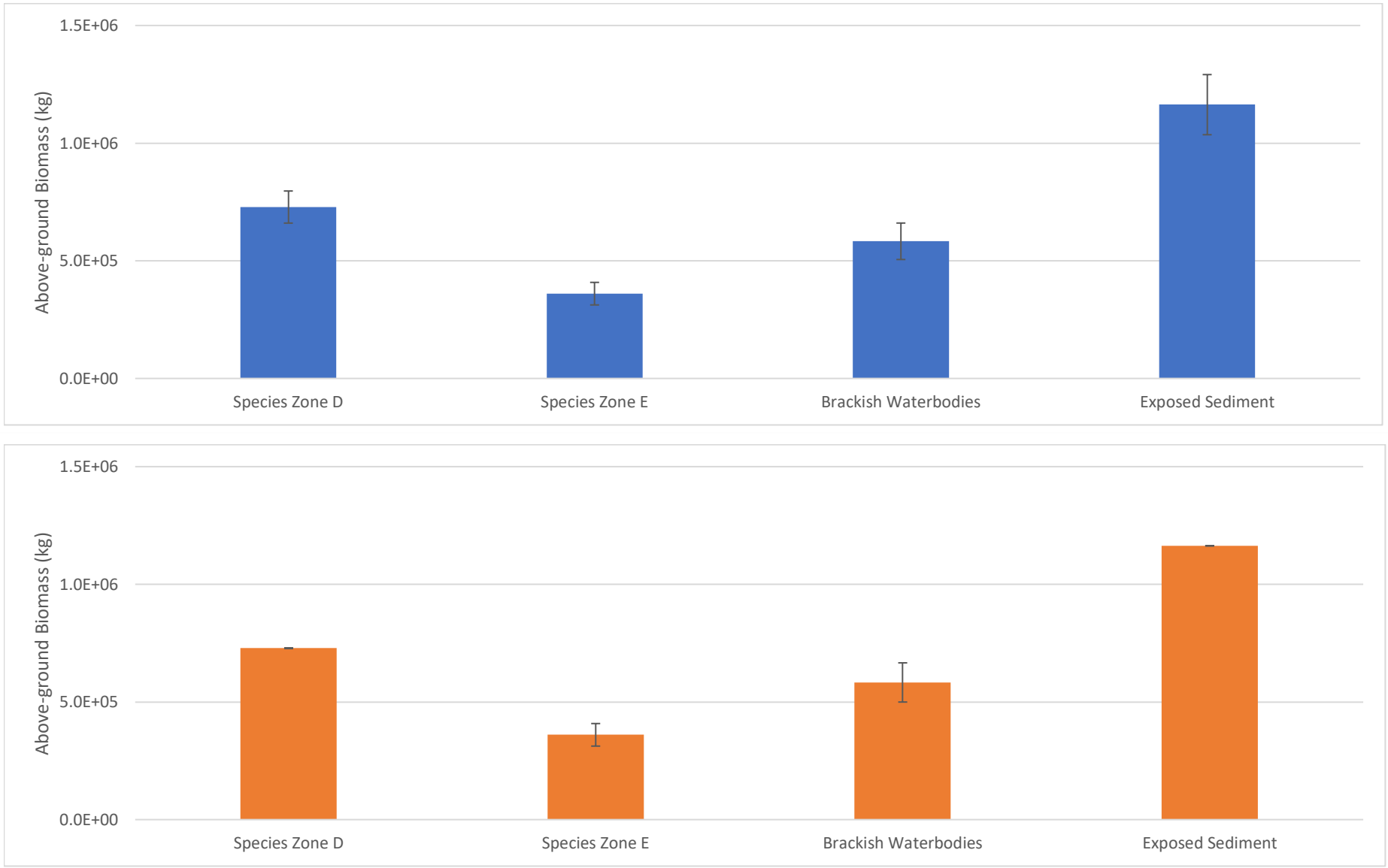

Figure 5.29(b). Disparity in overall above-ground biomass carbon projections for sub-environments: Species Zones D and E as well Brackish Waterbodies and Exposed Sediment assuming mean OCD. Error bars represent the maximal uncertainty surrounding the remote (blue) and manual

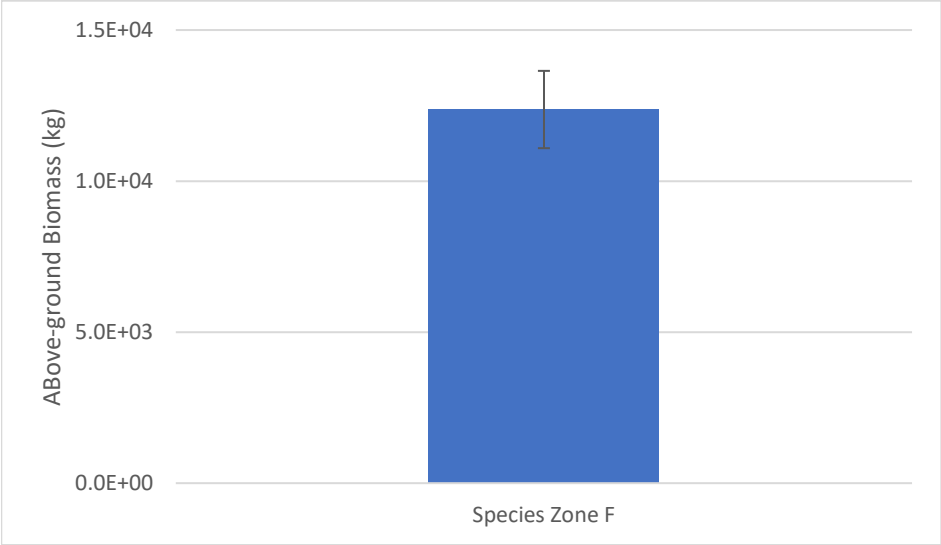

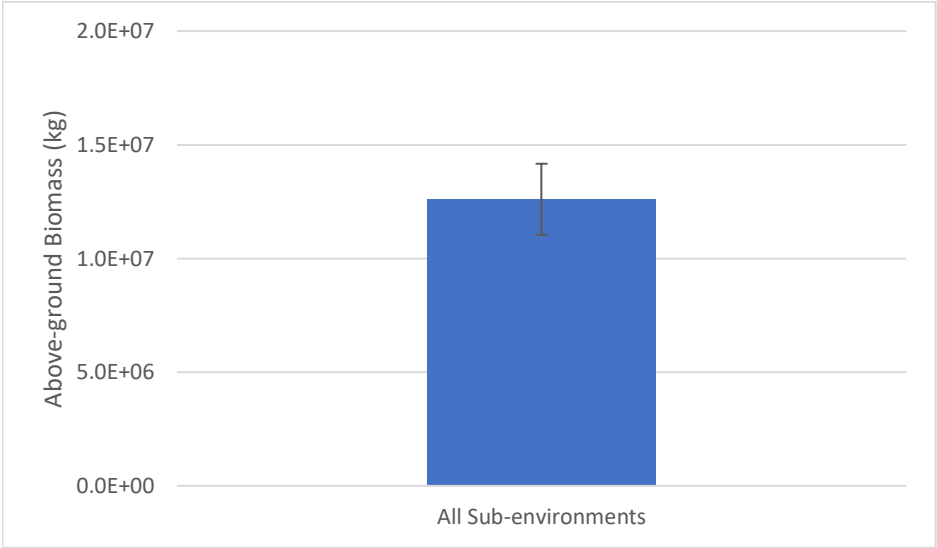

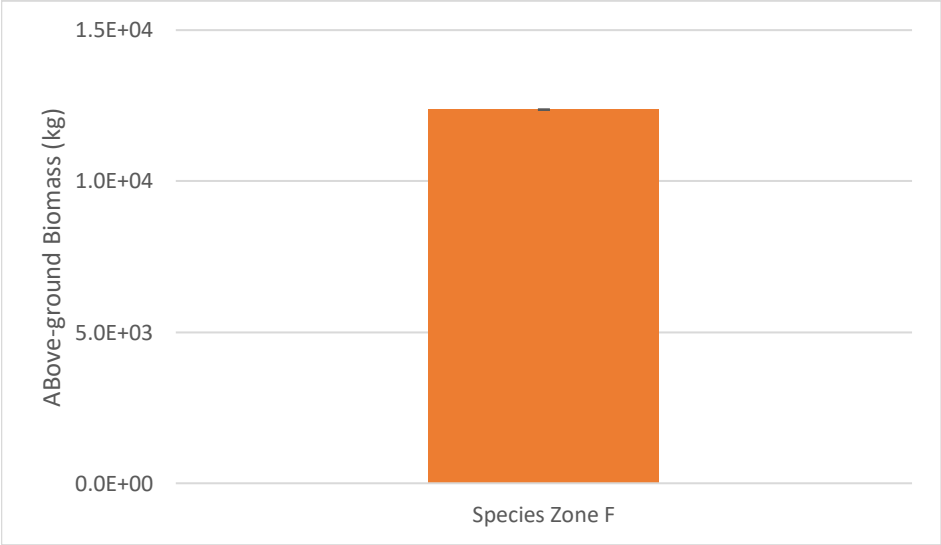

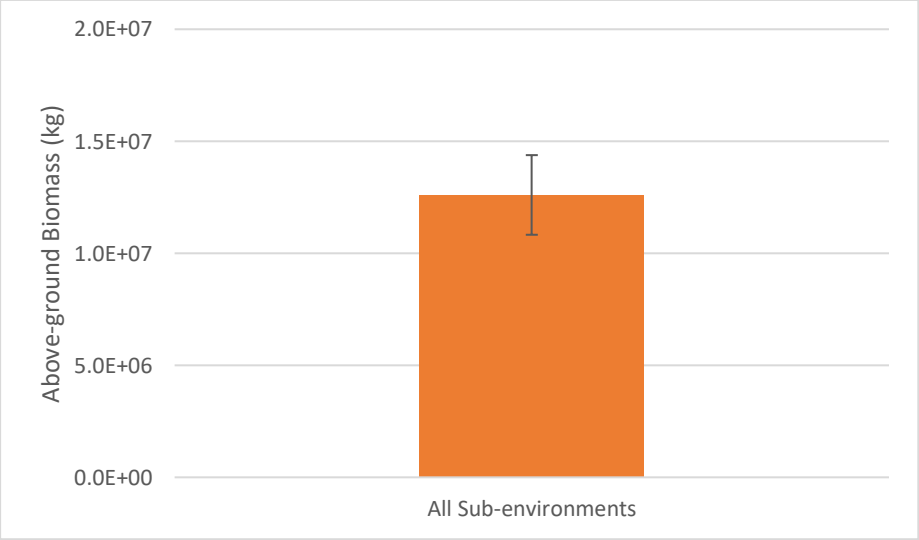

Figure 5.29(c). Disparity in overall above-ground biomass carbon projections assuming mean OCD for the sub-environments Species Zone

Figure 5.29(d). Disparity in overall above-ground biomass carbon projections assuming mean OCD for all sub-environments.

Table 5.26. Disparity in overall above-ground biomass carbon projections for all sub-environments considering the different sub-environment areal uncertainities (1.d.p).

		Overall Mass (kg x 10^{-3})							
Sub-environment Type	Mean (kg)	Original Remote	Remote Lower Bound Area	Remote Upper Bound Area	Manual Lower Bound Area	Manual Upper Bound Area	Mean	St. Dev	St. Dev (%)
Species Zone A	0.94	1986.7	1712.7	2260.7	1738.4	2474.8	2034.7	331.1	16.3
Species Zone B	1.19	4063.4	3632.2	4494.6	3250.7	5221.1	4132.4	766.3	18.5
Species Zone C	0.97	3706.9	3172.7	4241.1	3706.9	3706.9	3706.9	377.7	10.2
Species Zone D	0.79	728.4	660.2	796.6	728.4	728.4	728.4	48.2	6.6
Species Zone E	0.78	360.4	312.5	408.3	360.4	408.3	370.0	40.1	10.8
Species Zone F	0.60	12.4	11.1	13.6	12.4	12.4	12.4	0.9	7.1
Brackish Waterbodies	0.33	582.9	505.4	660.4	499.6	666.2	582.9	80.5	13.8
Exposed Sediment	0.12	1163.6	1035.8	1291.3	1163.6	1163.6	1163.6	90.3	7.8
All Environments		12604.7	11042.6	14166.7	11460.4	14381.6	12731.2	1522.1	12.0

Table 5.27. Above-ground biomass carbon (kg x 10^{-3}) statistics for all sub-environments considering the variability in OCD assuming the sub-environment coverage projected in the original areal remote classification (1.d.p).

	Projected Carbon Storage (kg x 10^{-3})					
Sub-environment Type	Min	Median	Mean	Max	St. Dev	St. Dev (%)
Species Zone A	966.8	2102.9	1986.7	2735.4	694.9	35.0
Species Zone B	2669.2	4362.8	4063.4	5165.2	1015.5	25.0
Species Zone C	681.8	3882.5	3706.9	5342.4	1656.7	44.7
Species Zone D	635.3	673.6	728.4	936.6	123.9	17.0
Species Zone E	162.3	333.9	360.4	611.4	187.8	52.1
Species Zone F	12.4	12.4	12.4	12.4	0.0	0.0
Brackish Waterbodies	553.4	566.6	582.9	628.7	40.2	6.9
Exposed Sediment	0.0	969.3	1163.6	2799.0	1260.4	108.3
All Environments	5681.2	12904.0	12604.7	18231.1	4979.3	39.5

Table 5.28. Above-ground biomass carbon (kg x 10^{-3}) projections assuming the minimal and maximal possible areal and OCD projections (1.d.p).

	Projected Carbon Storage (kg x10^{-3})	
Sub-environment Type	Minimum	Max
Species Zone A	833.4	3112.7
Species Zone B	2135.3	6198.3
Species Zone C	583.5	6112.2
Species Zone D	575.9	1024.3
Species Zone E	140.7	692.7
Species Zone F	11.1	13.6
Brackish Waterbodies	474.4	718.6
Exposed Sediment	0.0	3106.4
All Environments	4754.3	20978.7

5.3.2.2 - Active Layer Sediment

Volume

In order to determine the overall carbon content of the sediment within the active layer the volume of each active layer and the uncertainty surrounding these calculations was determined and uncertainties influencing these projections were accounted for (see Table 5.29). The original, remote and manual areal projections (see Table 5.8 for uncertainty) for each sub-environment are incorporated as well as the mean, lower and higher bounds (standard deviation) for depth so the potential variability in volume is considered.

Table 5.29. Key for volume projection uncertainty analysis.

Key	Description
OA x AD	Original Average x Average Depth
OA x UBD	Original Area x Upper Bound Depth
OA x LBD	Original Area x Lower Bound Depth
RLBA x AD	Remote Area Lower Bound x Average Depth
RUBA x AD	Remote Area Upper Bound x Average Depth
MLBA x AD	Manual Area Lower Bound x Average Depth
MUBA x AD	Manual Area Lower Bound x Average Depth
RLBA x UBD	Remote Area Lower Bound x Upper Bound Depth
RLBA x LBD	Remote Area Lower Bound x Lower Bound Depth
RUBA x UBD	Remote Area Upper Bound x Upper Bound Depth
RUBA x LBD	Remote Area Upper Bound x Lower Bound Depth
MLBA x UBD	Manual Area Lower Bound x Upper Bound Depth
MLBA x LBD	Manual Area Lower Bound x Lower Bound Depth
MUBA x UBD	Manual Area Upper Bound x Upper Bound Depth
MUBA x LBD	Manual Area Upper Bound x Lower Bound Depth

Exposed Sediment has the greatest variability in volume both in terms of the overall value and proportion which was principally a result of the larger areal coverage and variability in depth (see Table 5.30 and Figure 5.30(e)). Likewise, Species Zone E (Figure 5.30(c) exhibited a high overall range between projections with maximal and minimal values of 1.11×10^5 m^3 and 3.41×10^4 m^3 between RUBA x UBD and RLBA x LBD projections, whilst the overall degree of standard deviation (%) of volume between all sub-environments was the 2nd highest 37.2% of OA x AD.

Although the difference in volume occupied by Species Zones B and C is as low as 4.09×10^4 m^3 for the RLBA x LBD projection, this increases to 2.00×10^5 m^3 in the MLBA x UBD projection. This similarity between RLBA x LBD is a result of the similar average depths (0.13 m – Species Zone B, 0.14 m – Species Zone C) of active layers and standard deviation of depth which is 0.027 m (Species Zone B) and 0.028 m (Species Zone C) combined with only a 3.4% difference in remote areal

uncertainty. However, the 20% areal uncertainty difference in the manual analysis consequently results in a comparatively large disparity in volume between Species Zones B and C indicated by the MLBA x UBD assessment.

The volume occupied by Species Zone A and Brackish Waterbodies is also similar according to several projections with the closest projection being MLBA x AD with a disparity of 1.77×10^4 m^3 (see Figure 5.30(a)). Whilst the volume covered by Brackish Waterbodies is predicted to higher than that covered by Species Zone A in 10 of the 15 projections, the projections: OA x UBD, RLBA X UBD, RUBA x UBD, MLBA x UBD and MUBA x UBD, predict a greater volume of the marsh will be occupied by Species Zone A. This is primarily a result of standard deviation of depth for Species Zone A is 0.042 m compared to 0.12 m for Brackish Waterbodies which offsets the similarity in area coverage.

The volume of Species Zone D ranges from 8.27×10^4 m^3 (RLBA x LBD) to 1.81×10^5 m^3 (RUBA x UBD), whilst the standard deviation between all results is 25.3% of OA x AD. As there was no disparity between the OA and manual readings as the manual land cover accuracy was 100%, RLBA x LBD was lowest volume projection despite high remote accuracy of 90.6%. The standard deviation in depth of 0.041 m (29% of the mean) was therefore the most influential variable when determining volume for Species Zone D complying with the trend found in all sub-environments with the exception of Brackish Waterbodies. Overall, the volume analysis highlights that the volume of all sub-environments varies considerably according to the areal and depth uncertainty assessments and this influence on carbon storage variability is the focus of the next sub-section.

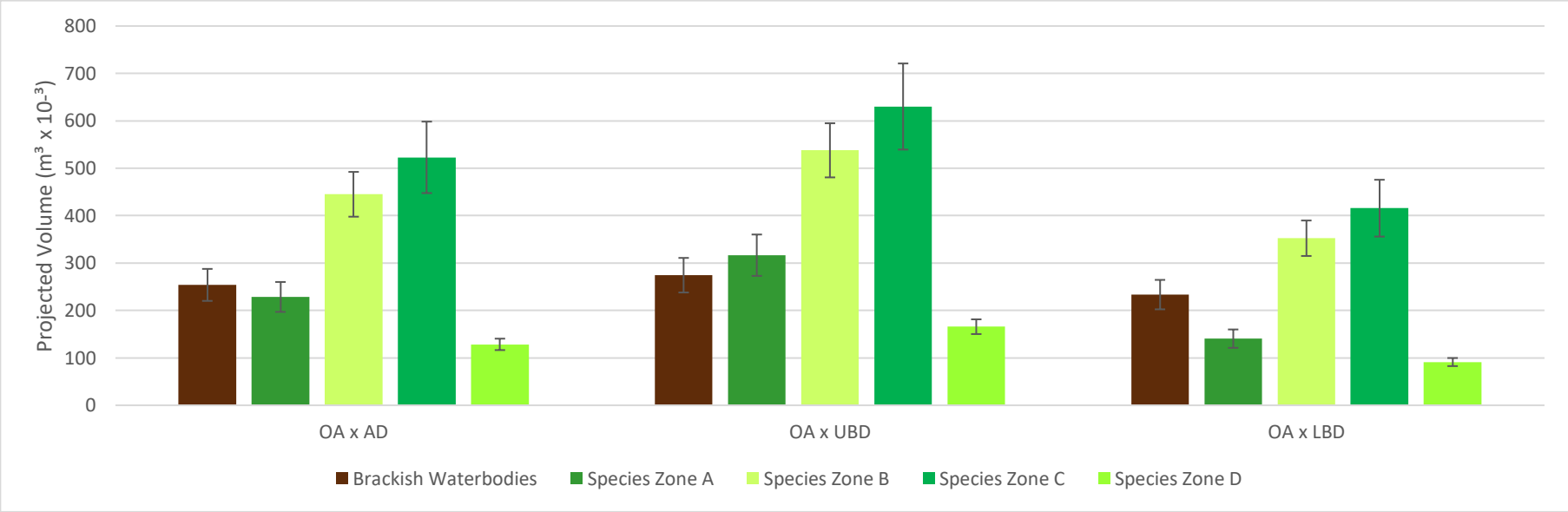

Figure 5.30(a). Variability in projected overall volume for the sub-environments: Species Zone A, B, C, D and Brackish Waterbodies. The error bars represent uncertainty in the remote areal assessment (i.e. RLBA x AD, RUBA x AD, RLBA x UBD, RUBA x UBD, RLBA x LBD and RUBA x LBD).

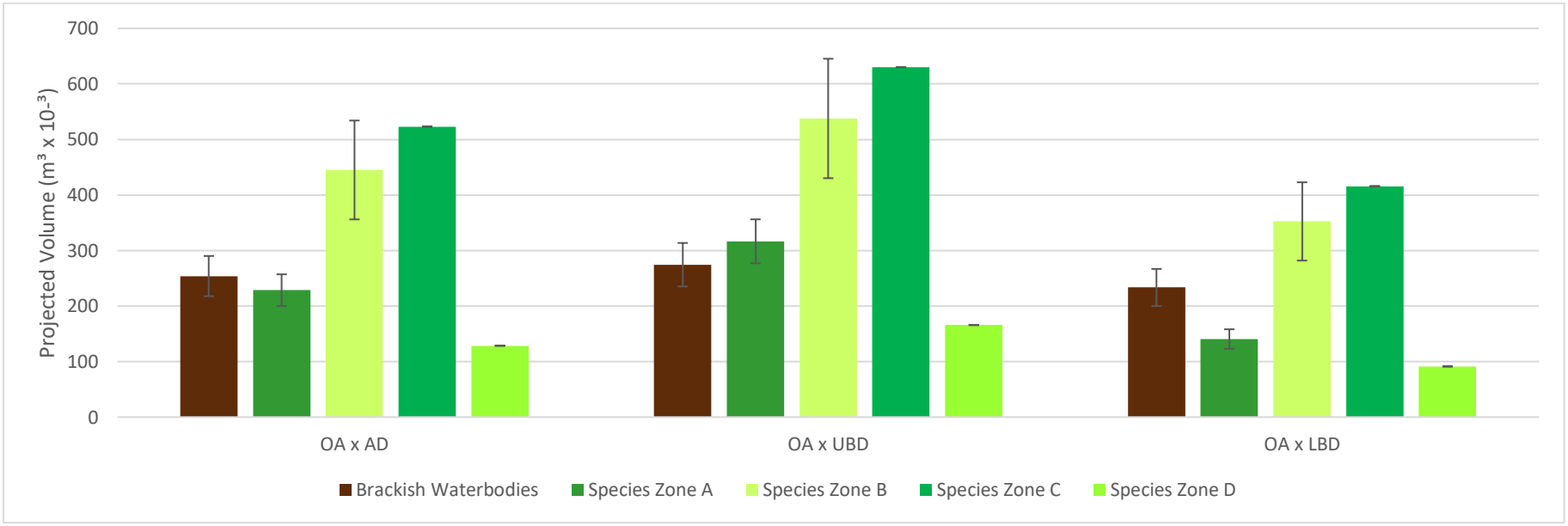

Figure 5.30(b). Variability in projected overall volume for the sub-environments: Species Zone A, B, C, D and Brackish Waterbodies. The error bars represent uncertainty in the manual areal assessment (i.e. MLBA x AD, MUBA x AD, MLBA x UBD, MUBA x UBD, MLBA x LBD and MUBA x LBD).

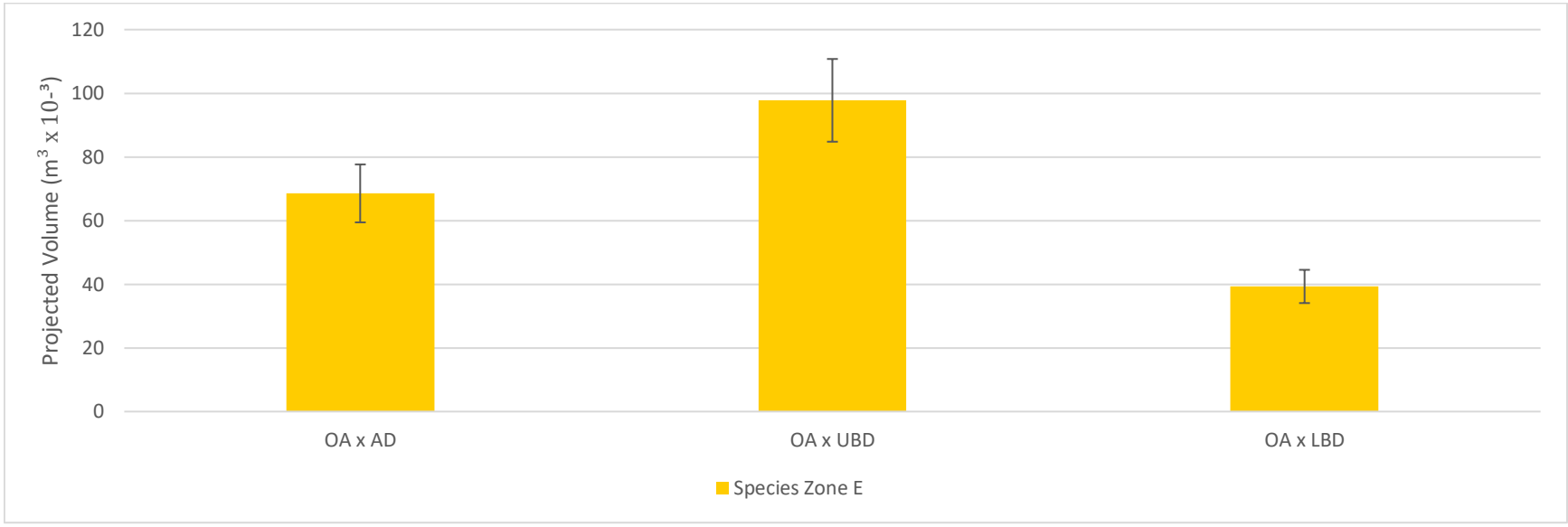

Figure 5.30(c). Variability in projected overall volume for Species Zone E. The error bars represent uncertainty in the remote areal assessment. The manual areal assessment uncertainty is not displayed as the accuracy was 100%.

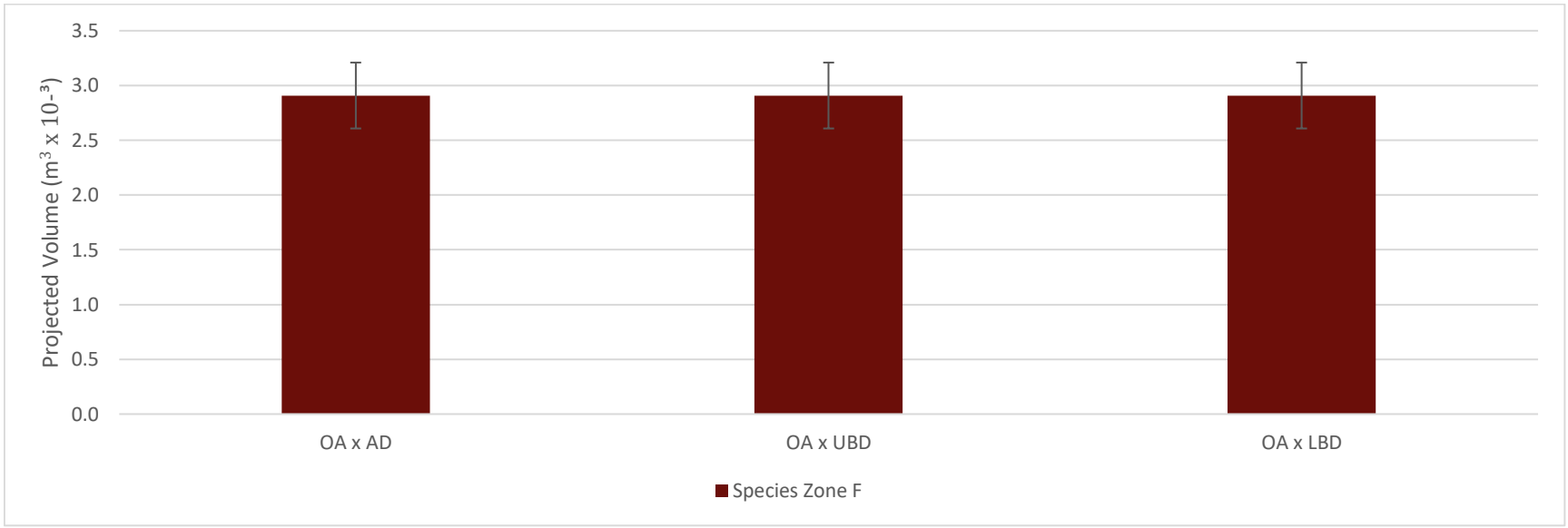

Figure 5.30(d). Variability in projected overall volume for Species Zone F. The error bars represent uncertainty in the remote areal assessment. The manual areal assessment uncertainty is not displayed as the accuracy was 100%.

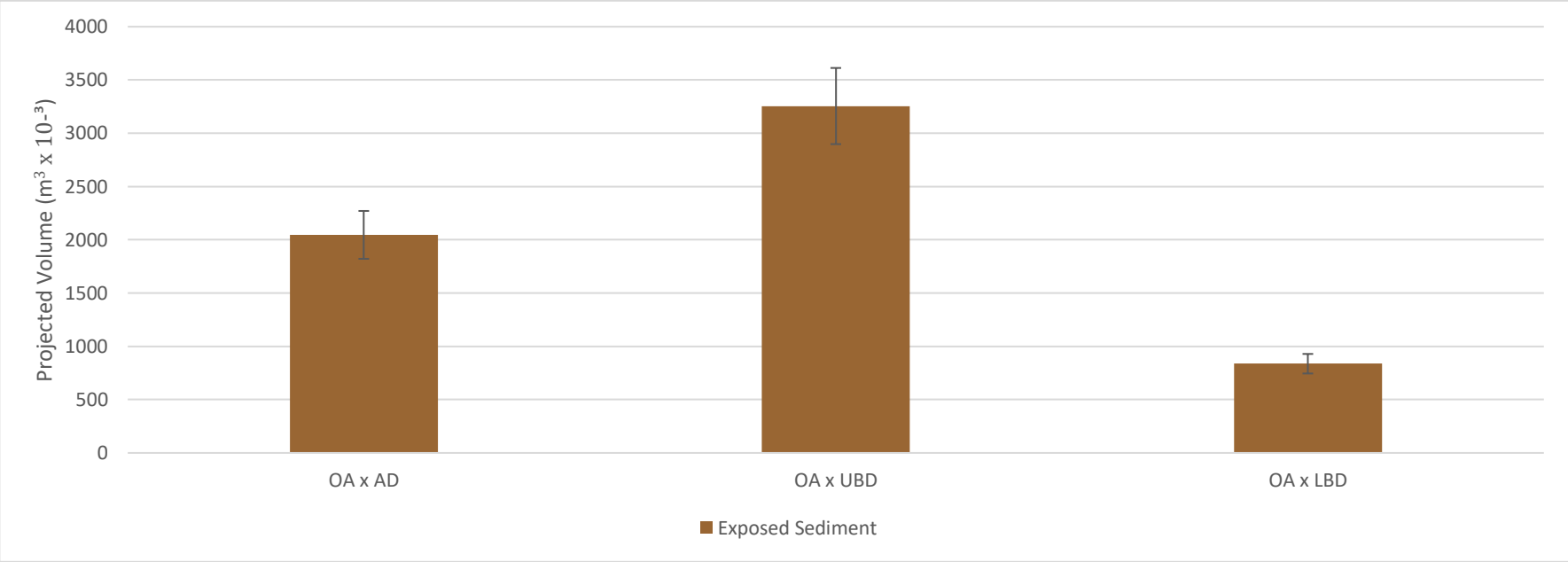

Figure 5.30(e). Variability in projected overall volume for Exposed Sediment. The error bars represent uncertainty in the remote areal assessment. The manual areal assessment uncertainty is not displayed as the accuracy was 100%.

Table 5.30. Volume projections for all volume projections for all sub-environments (1.d.p).

	Volume ($m^3 \times 10^{-3}$)										
Sub-environment Type	OA x AD	OA x UBD	OA x LBD	RLBA x AD	RUBA x AD	MLBA x AD	MUBA x AD	RLBA x UBD	RLBA x LBD	Standard Deviation	Standard Deviation (% of OA x AD)
Brackish Waterbodies	253.9	274.4	233.5	220.2	287.7	217.6	290.2	237.9	202.4	36.8	14.5
Species Zone A	228.6	316.6	140.6	197.0	260.1	200.0	257.1	272.9	121.2	79.9	35.0
Species Zone B	445.0	537.7	352.3	397.8	492.3	356.0	534.0	480.7	314.9	103.0	23.2
Species Zone C	523.0	630.2	415.7	447.6	598.3	523.0	523.0	539.4	355.8	103.5	19.8
Species Zone D	128.5	165.8	91.2	116.5	140.5	128.5	128.5	150.2	82.7	32.5	25.3
Species Zone E	68.5	97.8	39.3	59.4	77.7	68.5	68.5	84.8	34.1	25.5	37.2
Species Zone F	2.9	2.9	2.9	2.6	3.2	2.9	2.9	2.6	2.6	0.2	6.8
Exposed Sediment	2046.3	3255.4	837.1	1821.6	2271.0	2046.3	2046.3	2898.0	745.2	1034.9	50.6
Sum of All Sub-environments	3696.7	5280.7	2112.6	3262.7	4130.7	3542.8	3850.5	4666.5	1858.9		

Table 5.31. Volume projections for all volume projections for all sub-environments (1.d.p).

	Volume ($m^3 \times 10^{-3}$)							
Sub-environment Type	RUBA x UBD	RUBA x LBD	MLBA x UBD	MLBA x LBD	MUBA x UBD	MUBA x LBD	Standard Deviation	Standard Deviation (% of OA x AD)
Brackish Waterbodies	310.8	264.5	235.2	200.1	313.6	266.8	36.8	14.5
Species Zone A	360.2	159.9	277.0	123.0	356.1	158.1	79.9	35.0
Species Zone B	594.8	389.7	430.2	281.9	645.3	422.8	103.0	23.2
Species Zone C	721.0	475.7	630.2	415.7	630.2	415.7	103.5	19.8
Species Zone D	181.3	99.7	165.8	91.2	165.8	91.2	32.5	25.3
Species Zone E	110.8	44.5	97.8	39.3	97.8	39.3	25.5	37.2
Species Zone F	3.2	3.2	2.9	2.9	2.9	2.9	0.2	6.8
Exposed Sediment	3612.9	929.0	3255.4	837.1	3255.4	837.1	1034.9	50.6
Sum of All Sub-environments	5895.0	2366.3	5094.4	1991.3	5467.1	2234.0		

5.3.2.3 – Active Layer Carbon Variability

Exposed Sediment had the highest overall active layer sub-surface carbon content for each projection due to the expansive volume of the sub-environment, despite the fact it has the lowest mean carbon OCD of 3.09 kg m^{-3} (See Table 5.32). The standard deviation between overall carbon projections was also the largest for Exposed Sediment both in terms of overall carbon mass of 9.42 x 10^6 kg and percentage of 47.9% of OA x AD (see Table 5.33 and Figure 5.31(e)). Therefore, when the full range of OCD and volume uncertainties are considered (see Table 5.33 and 5.34) the active layer of the Exposed Sediment sub-environment could theoretically hold between 1.67 x 10^6 kg to 1.34 x 10^6 kg. The 15 projections for Species Zones A and E indicated the sub-environments had the highest proportional SD (%) equalling 35.0% and 37.2% respectively (see Table 5.32). The similar OCDs of Species Zone A (3.93 kg) and Brackish Waterbodies (3.85 kg) combined with the volume means that neither sub-environment can be stated to definitively contain more carbon than the other due to the variability in areal and carbon uncertainty projections. This variability in projections had a reduced influence on Brackish Waterbodies (Figure 5.31(a)) which had the lowest degree of OCD standard deviation of 0.18 kg m^{-3} (4.7%) and smallest volume standard deviation (%) (excluding Species Zone F) which consequently resulted in the low standard deviation between mean total carbon projections of 142 kg (14.5% of OA x AD). The 2nd greatest mass of carbon is stored within Species Zone C, although as a proportion, this does not exceed 66.3% of the mass within Exposed Sediment (OA x LBD projection). However, Species Zone B could theoretically store a carbon mass similar to Species Zone C according to the MUBA x AD, MUBA x UBD and MUBA x LBD with respective differences of 5.51 x 10^4 kg, 5.95 x 10^4 kg and 5.07 x 10^4 kg between projections, although Species Zone C remains the greater carbon store. This was because of the 20% areal uncertainty surrounds the manual Species Zone B predictions, whilst Species Zone C projections were 100% accurate.

Although Species Zones A and B have similar OCDs (0.02 kg m^{-3}), the projections using average OCD values (Table 5.32) highlight it is plausible that Species Zone A could contain only 39.7% (OA x LBD) of the carbon mass of Species Zone B, and when the minimal OCD values (Table 5.34) are considered this decreases to 29.3% (MUBA x LBD). This is a result of greater uncertainty surrounding OCD (SD difference = 6.3%) and the uncertainty surrounding the active layer depth of Species Zone A is also greater than Species Zone B by 17.7%. The 25.3% standard deviation between all carbon storage projections using mean OCD values of Species Zone D was primarily a result of the active layer depth uncertainty of 29.0% and the high (SD=19.3) uncertainty surrounding the mean OCD values of the sub-environment. Regardless of the projections used, the projected carbon storage value for Species Zone D did not exceed or fall below the storage of any other sub-environment indicating the areas occupied by the sub-environment had a unique carbon storage potential.

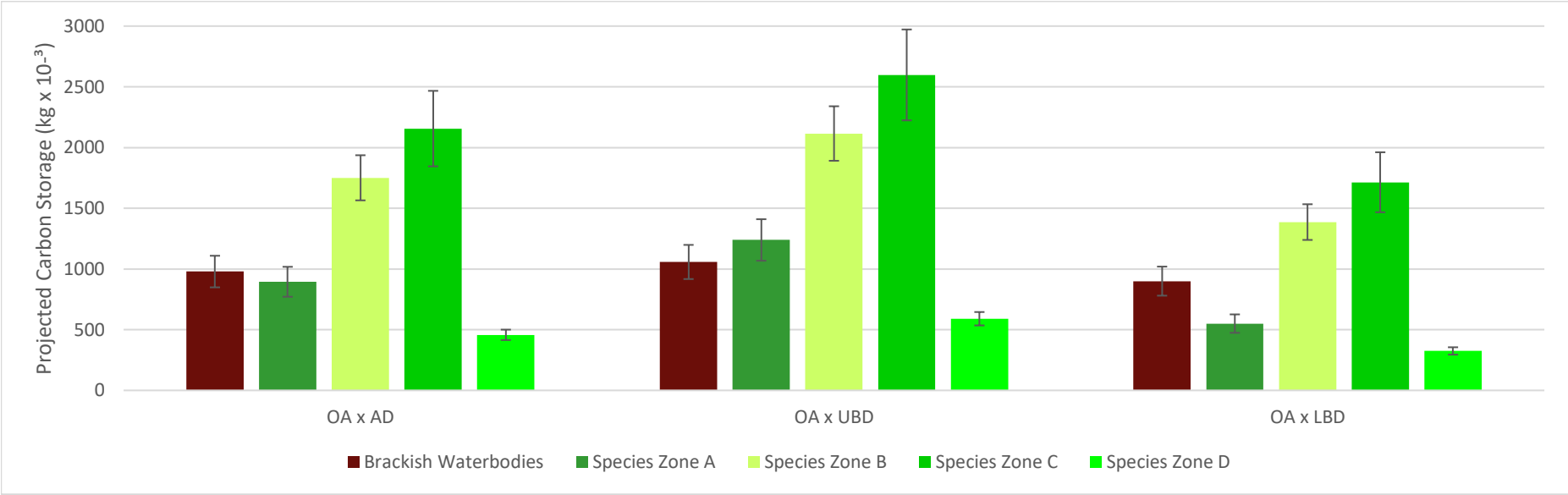

Figure 5.31(a). Variability in projected overall active layer carbon storage for the sub-environments: Species Zones A, B, C, D and Brackish Waterbodies. The error bars represent uncertainty in the remote areal assessment (i.e. RLBA x AD, RUBA x AD, RLBA x UBD, RUBA x UBD, RLBA x LBD and RUBA x

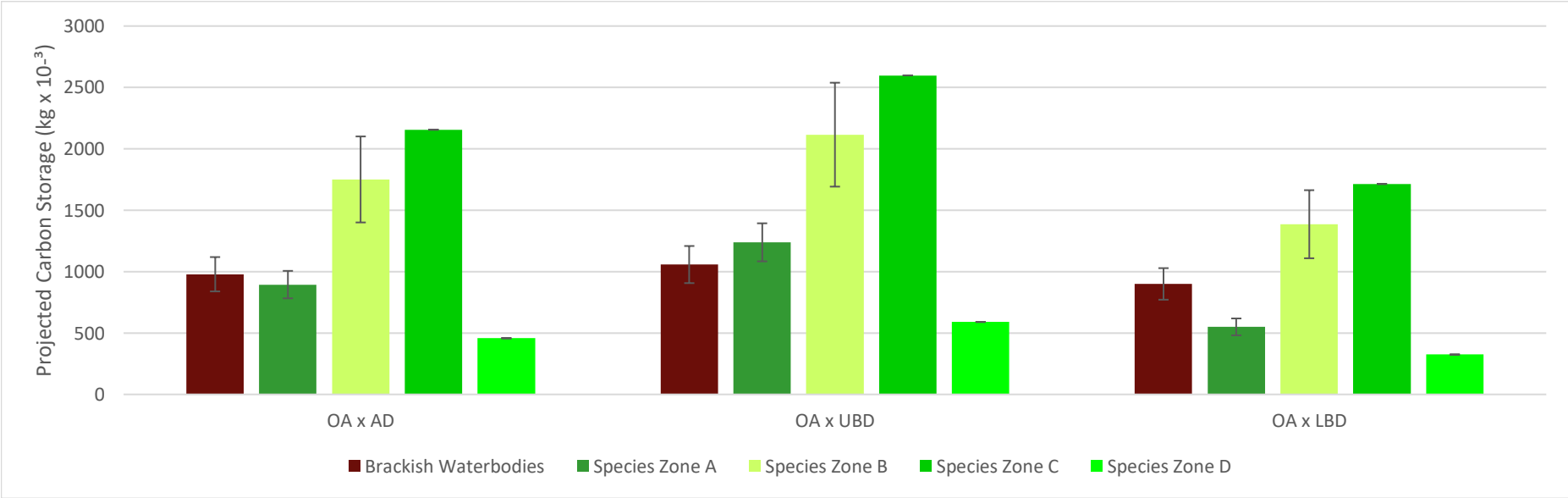

Figure 5.31(b). Variability in projected overall active layer carbon storage for the sub-environments: Species Zones A, B, C, D and Brackish Waterbodies. The error bars represent uncertainty in the manual areal assessment(i.e. MLBA x AD, MUBA x AD, MLBA x UBD, MUBA x UBD, MLBA x LBD and MUBA x LBD)..

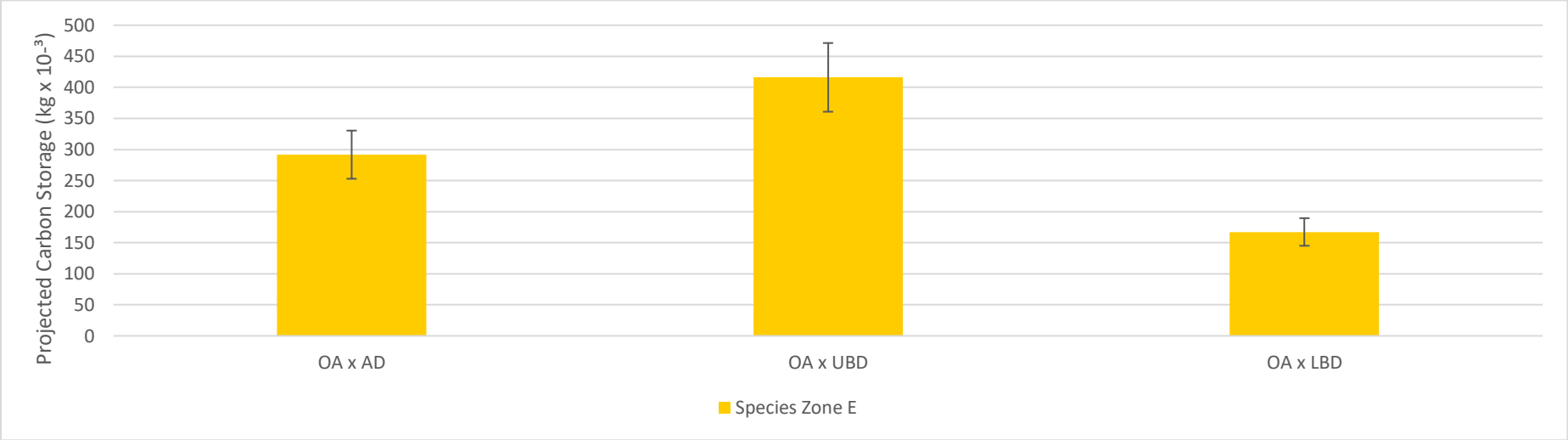

Figure 5.31(c). Variability in projected overall active layer carbon storage for the sub-environment Species F. The error bars represent uncertainty in the remote areal assessment. The manual areal assessment uncertainty is not displayed as the accuracy was 100%.

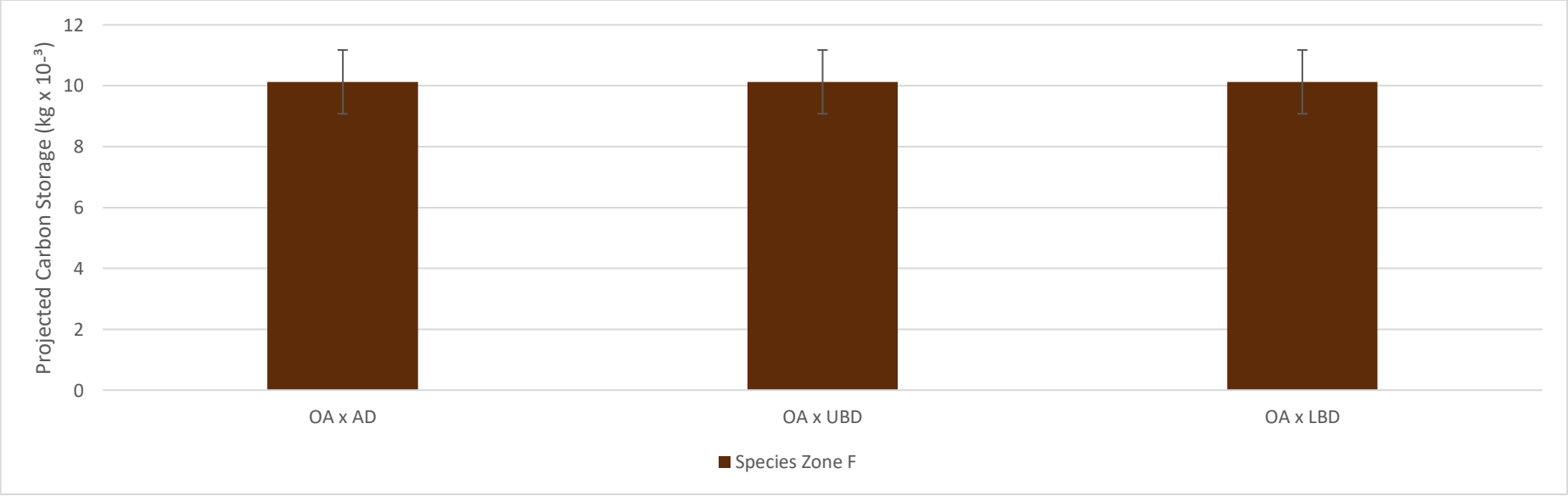

Figure 5.31(d). Variability in projected overall active layer carbon storage for Species Zone F. The error bars represent uncertainty in the remote areal assessment. The manual areal assessment uncertainty is not displayed as the accuracy was 100%.

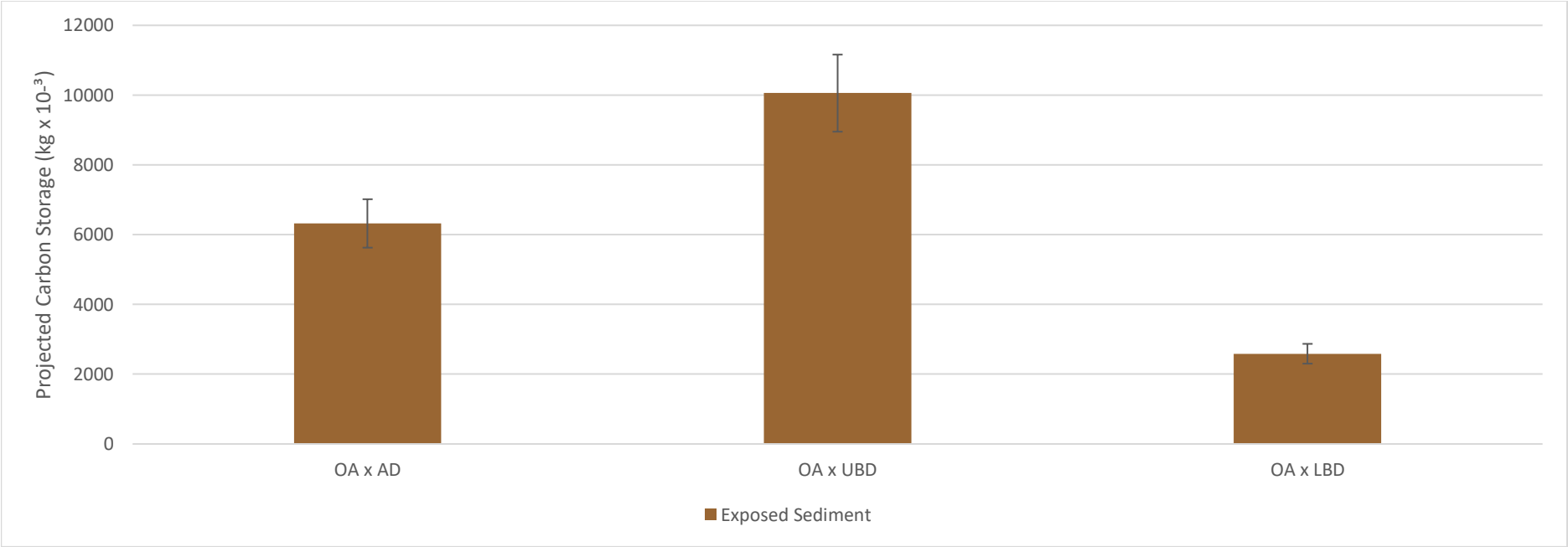

Figure 5.31(e). Variability in projected overall active layer carbon storage for Exposed Sediment. The error bars represent uncertainty in the remote areal assessment. The manual areal assessment uncertainty is not displayed as the accuracy was 100%.

Table 5.32. Active layer overall carbon mass projections for all sub-environments (1.d.p).

		Projected Carbon Mass (kg x 10^{-3})								
Sub-environment Type	Mean Organic Carbon Density	OA x AD	OA x UBD	OA x LBD	RLBA x AD	RUBA x AD	MLBA x AD	MUBA x AD	RLBA x UBD	RLBA x LBD
Species Zone A	3.91	894.3	1238.6	550.0	770.9	1017.6	782.5	1006.1	1067.8	474.1
Species Zone B	3.93	1750.6	2115.3	1386.0	1564.9	1936.4	1400.5	2100.8	1890.8	1238.9
Species Zone C	4.12	2155.9	2597.8	1713.9	1845.2	2466.5	2155.9	2155.9	2223.5	1466.9
Species Zone D	3.56	457.4	590.1	324.7	414.6	500.2	457.4	457.4	534.9	294.3
Species Zone E	4.26	291.7	416.1	167.3	252.9	330.4	291.7	291.7	360.8	145.0
Species Zone F	3.48	10.1	10.1	10.1	9.1	11.2	10.1	10.1	9.1	9.1
Brackish Waterbodies	3.85	978.6	1057.5	899.8	848.6	1108.7	838.8	1118.4	916.9	780.2
Exposed Sediment	3.09	6321.5	10056.8	2586.1	5627.3	7015.6	6321.5	6321.5	8952.5	2302.1
Sum of All Sub-environments		12860.1	18082.4	7637.8	11333.5	14386.7	12258.4	13461.8	15956.3	6710.6

Table 5.32. Active layer overall carbon mass projections for all sub-environments (1.d.p).

		Projected Carbon Mass (kg x 10^{-3})							
Sub-environment Type	Mean Organic Carbon Density	RUBA x UBD	RUBA x LBD	MLBA x UBD	MLBA x LBD	MUBA x UBD	MUBA x LBD	Projection Standard Deviation (kg)	Projection Standard Deviation (% of OA x AD)
Species Zone A	3.91	1409.5	625.8	1083.8	481.2	1393.5	618.7	312.6	35.0
Species Zone B	3.93	2339.8	1533.0	1692.2	1108.8	2538.4	1663.2	405.3	23.2
Species Zone C	4.12	2972.2	1960.9	2597.8	1713.9	2597.8	1713.9	426.7	19.8
Species Zone D	3.56	645.4	355.1	590.1	324.7	590.1	324.7	115.8	25.3
Species Zone E	4.26	471.4	189.5	416.1	167.3	416.1	167.3	108.5	37.2
Species Zone F	3.48	11.2	11.2	10.1	10.1	10.1	10.1	0.7	6.8
Brackish Waterbodies	3.85	1198.0	1019.4	906.4	771.2	1208.5	1028.3	141.9	14.5
Exposed Sediment	3.09	11161.1	2870.0	10056.8	2586.1	10056.8	2586.1	3197.0	50.6
Sum of All Sub-environments		20208.5	8564.9	17353.4	7163.3	18811.4	8112.2	4708.5	36.6

Table 5.33. Uncertainty (standard deviation) surrounding sub-surface active section overall carbon mass projections for all sub-environments (1.d.p).

				Standard Deviation in Projected Carbon Mass (kg x 10^{-3})						
Sub-environment Type	Average Organic Carbon Density (kg)	OCD Standard Deviation	OCD Standard Deviation (%)	OA x AD	OA x UBD	OA x LBD	RLBA x AD	RUBA x AD	MLBA x AD	MUBA x AD
Species Zone A	3.91	0.65	16.6	148.6	205.8	91.4	128.1	169.1	130.0	167.1
Species Zone B	3.93	0.40	10.3	178.0	215.1	140.9	159.1	196.9	142.4	213.6
Species Zone C	4.12	0.22	5.4	115.1	138.6	91.5	98.5	131.6	115.1	115.1
Species Zone D	3.56	0.69	19.3	88.7	114.4	62.9	80.4	97.0	88.7	88.7
Species Zone E	4.26	0.19	4.5	13.0	18.6	7.5	11.3	14.8	13.0	13.0
Species Zone F	3.48	0.83	23.9	2.4	2.4	2.4	2.2	2.7	2.4	2.4
Brackish Waterbodies	3.85	0.18	4.7	45.7	49.4	42.0	39.6	51.8	39.2	52.2
Exposed Sediment	3.09	0.48	15.5	982.2	1562.6	401.8	874.4	1090.1	982.2	982.2
Sum of All Sub-environments				1573.6	2306.9	840.4	1393.5	1753.8	1512.9	1634.3

Table 5.33. Uncertainty (standard deviation) surrounding sub-surface active section overall carbon mass projections for all sub-environments (1.d.p).

	Standard Deviation in Projected Carbon Mass (kg x 10^{-3})							
Sub-environment Type	RLBA x UBD	RLBA x LBD	RUBA x UBD	RUBA x LBD	MLBA x UBD	MLBA x LBD	MUBA x UBD	MUBA x LBD
Species Zone A	177.4	78.8	234.1	104.0	180.0	79.9	231.5	102.8
Species Zone B	192.3	126.0	237.9	155.9	172.1	112.7	258.1	169.1
Species Zone C	118.7	78.3	158.6	104.6	138.6	91.5	138.6	91.5
Species Zone D	103.7	57.0	125.1	68.8	114.4	62.9	114.4	62.9
Species Zone E	16.1	6.5	21.0	8.5	18.6	7.5	18.6	7.5
Species Zone F	2.2	2.2	2.7	2.7	2.4	2.4	2.4	2.4
Brackish Waterbodies	42.8	36.4	56.0	47.6	42.3	36.0	56.4	48.0
Exposed Sediment	1391.0	357.7	1734.2	445.9	1562.6	401.8	1562.6	401.8
Sum of All Sub-environments	2044.1	742.8	2569.6	938.0	2231.1	794.8	2382.7	886.0

Table 5.34. Uncertainty (minimal bounds) surrounding sub-surface active section overall carbon mass projections for all sub-environments (1.d.p).

		Projected Carbon Mass (kg x 10^{-3})						
Sub-environment Type	Min OCD (kg)	OA x AD	OA x UBD	OA x LBD	RLBA x AD	RUBA x AD	MLBA x AD	MUBA x AD
Species Zone A	2.48	566.8	785.1	348.6	488.6	645.0	496.0	637.7
Species Zone B	3.17	1410.8	1704.6	1116.9	1261.1	1560.5	1128.6	1692.9
Species Zone C	3.77	1971.6	2375.7	1567.4	1687.4	2255.7	1971.6	1971.6
Species Zone D	2.41	309.6	399.5	219.8	280.6	338.6	309.6	309.6
Species Zone E	4.07	279.0	398.0	160.0	241.9	316.0	279.0	279.0
Species Zone F	2.89	8.4	8.4	8.4	7.5	9.3	8.4	8.4
Brackish Waterbodies	3.75	952.2	1028.9	875.5	825.7	1078.8	816.2	1088.2
Exposed Sediment	2.24	4583.7	7292.2	1875.2	4080.4	5087.0	4583.7	4583.7
Sum of All Sub-environments		10082.0	13992.4	6171.7	8873.2	11290.8	9593.0	10571.1

Table 5.34. Uncertainty (minimal bounds) surrounding sub-surface active section overall carbon mass projections for all sub-environments (1.d.p).

		Projected Carbon Mass (kg x 10^{-3})					
Sub-environment Type	Min OCD (kg)	RUBA x UBD	RUBA x LBD	MLBA x UBD	MLBA x LBD	MUBA x UBD	MUBA x LBD
Species Zone A	2.48	893.4	396.7	686.9	305.0	883.2	392.1
Species Zone B	3.17	1885.5	1235.4	1363.7	893.5	2045.6	1340.3
Species Zone C	3.77	2718.1	1793.2	2375.7	1567.4	2375.7	1567.4
Species Zone D	2.41	436.9	240.4	399.5	219.8	399.5	219.8
Species Zone E	4.07	450.8	181.2	398.0	160.0	398.0	160.0
Species Zone F	2.89	9.3	9.3	8.4	8.4	8.4	8.4
Brackish Waterbodies	0	1165.7	991.9	881.9	750.4	1175.9	1000.6
Exposed Sediment	0	8092.9	2081.1	7292.2	1875.2	7292.2	1875.2
Sum of All Sub-environments		15652.6	6929.1	13406.3	5779.7	14578.5	6563.7

Table 5.35. Uncertainty (maximal bounds) surrounding sub-surface active section overall carbon mass projections for all sub-environments.

		Projected Carbon Mass (kg x 10^{-3})								
Sub-environment Type	Max OCD (kg)	OA x AD	OA x UBD	OA x LBD	RLBA x AD	RUBA x AD	MLBA x AD	MUBA x AD	RLBA x UBD	RLBA x LBD
Species Zone A	4.32	987.4	1367.5	607.2	851.2	1123.6	863.9	1110.8	1178.9	523.4
Species Zone B	4.24	1887.0	2280.0	1493.9	1686.7	2087.2	1509.6	2264.4	2038.1	1335.4
Species Zone C	4.33	2264.4	2728.6	1800.2	1938.1	2590.7	2264.4	2264.4	2335.4	1540.8
Species Zone D	4.16	534.5	689.6	379.4	484.4	584.5	534.5	534.5	625.0	343.9
Species Zone E	4.45	305.0	435.1	174.9	264.5	345.5	305.0	305.0	377.3	151.7
Species Zone F	4.07	11.8	11.8	11.8	10.6	13.1	11.8	11.8	10.6	10.6
Brackish Waterbodies	4.06	1030.9	1114.0	947.9	893.9	1168.0	883.7	1178.2	965.9	821.9
Exposed Sediment	3.70	7571.2	12045.1	3097.4	6739.9	8402.6	7571.2	7571.2	10722.5	2757.3
Sum of All Sub-environments		14592.2	20671.8	8512.7	12869.3	16315.2	13944.1	15240.3	18253.7	7484.9

Table 5.35. Uncertainty (maximal bounds) surrounding sub-surface active section overall carbon mass projections for all sub-environments

		Projected Carbon Mass (kg x 10-3)					
Sub-environment Type	Max OCD (kg)	RUBA x UBD	RUBA x LBD	MLBA x UBD	MLBA x LBD	MUBA x UBD	MUBA x LBD
Species Zone A	4.32	1556.2	690.9	1196.6	531.3	1538.5	683.1
Species Zone B	4.24	2522.0	1652.4	1824.0	1195.1	2736.0	1792.7
Species Zone C	4.33	3121.8	2059.6	2728.6	1800.2	2728.6	1800.2
Species Zone D	4.16	754.1	414.9	689.6	379.4	689.6	379.4
Species Zone E	4.45	492.9	198.2	435.1	174.9	435.1	174.9
Species Zone F	4.07	13.1	13.1	11.8	11.8	11.8	11.8
Brackish Waterbodies	4.06	1262.0	1073.9	954.8	812.5	1273.1	1083.3
Exposed Sediment	3.70	13367.7	3437.5	12045.1	3097.4	12045.1	3097.4
Sum of All Sub-environments		23089.9	9540.4	19885.7	8002.6	21457.9	9022.8

5.3.3 – Spatial Distribution of Carbon Content

5.3.3.1 – Introduction

The following results exhibit how the carbon stored within the active section of each sub-environment varies in accordance with elevation, gradient and watercourse proximity. The variability in above-ground biomass and active layer carbon is considered independently in order to determine how each of three factors influences each sub-environment.

The results concerning carbon distribution across all sub-environments for OA x AD carbon projections are combined with the findings concerning the influence of elevation, gradient or watercourse proximity of sub-environment distribution in order to indicate overall carbon distribution throughout the saltmarshes of the Ribble. The OA x AD projections are plotted in the figures of this sub-section as they are most frequently closest to the mean carbon projections across all sub-environments for both above-ground biomass and active layer sub-surface sediment. The error bars represent the maximal uncertainty surrounding the areal projections (i.e. remote or manual depending on the sub-environment), depth (active layer only) and OCD in each sub-environment.

5.3.3.2 – Elevation

Above-ground Biomass

The carbon stored within above-ground biomass was concentrated between 4.2 – 4.8 mOD as 85.7% or 1.08 x 10^6 kg is stored within this elevation range according to the original remote area assessment with 46.3% of the mass being held between 4.4 - 4.6 mOD (see Figure 5.33). Alternatively, only 8.9% of the carbon is stored below MHWS (4.10 mOD) at Southport and 0.3% was found above HAT (5.10 mOD). Of the carbon between 4.2 – 4.8 mOD the sub-environments Species Zones C and D contributed the largest proportions at 32.8% and 30.3%, whilst Species Zones E and F contributed the least at 1.7% and <0.1%. Regarding the precision of the distribution (excluding Species Zone F) Brackish Waterbodies exhibited the most precise distribution with 52.2% of carbon within the sub-environment being found in the modal class of 4.2 – 4.4 mOD, whilst Species Zone E exhibited the least precise distribution with 20.0% of the carbon being found at this interval. Species Zone F was also unique as it the only sub-environment in which the modal class is 4.6 – 4.8 mOD owing to the unique isolated distribution in Marsh C.

When uncertainty is considered Species Zone E (Figure 5.32(e)) was the most proportionally influenced of all predominantly sub-environments as it was plausible the carbon stored within the

sub-environment could differ by 65.4% when the maximal possible uncertainties concerning area and OCD are considered. As Species Zone E was most prominent between 4.0 – 4.2 mOD covering 8.1% of the area at that elevation interval this increased overall uncertainty although the influence of this sub-environment was minor compared to the influence of Exposed Sediment which covers 34.9% of the area and was surrounded by a maximal uncertainty of 118.3%. In contrast the maximal upper uncertainties surrounding Species Zone F and Brackish Waterbodies were the lowest at 13.3% and 21.2%. Regarding total uncertainty (kg) the maximal possible uncertainty influenced Species Zone C which hypothetically could contain 2.17 x 10^6 kg more or less carbon due to the large overall carbon storage capacity (3.71 x 10^6 kg – original remote area projections) of the sub-environment. When Species Zone F is excluded the smallest overall upper-bound maximal uncertainty influenced Brackish Waterbodies (1.24 x 10^5 kg of 5.83 x 10^5 kg), whilst Species Zone D has the 2nd lowest value (1.86 x 10^5 kg of 7.28 x 10^5 kg). Regarding elevation the overall uncertainties had the largest influence on the modal elevation bracket of 4.4 - 4.6 mOD which could contain 1.03 x 10^6 kg more or less carbon with Species Zone A and B being the largest uncertainty contributors with maximal uncertainties of 3.70 x 10^5 kg and 9.07 x 10^5 kg over the 0.2 m interval. The consequence of this elevational clustering of sites was that the areal above MHWS could theoretically contain 6.09 x 10^6 kg increasing above-ground carbon by 53.4% between 4.10 – 7.0 mOD.

There was correspondence between Species Zones A, B and D, in which 34.9%, 31.3 % and 30.7% of the above-ground carbon is found at elevations ≥ 4.6 m. However, for Species Zones C and E, which are comprised are more tolerant halophytes, there was a comparative shift in elevation distribution towards lower elevations as only 9.9% and 11.8% of the above-ground total carbon was found above 4.6 m. Brackish Waterbodies and Exposed Sediment possess comparable distributions (see Figure 5.32 g&h) as the modal interval in both cases was 4.2 – 4.4 m. However, the decline in carbon mass either side of this interval is more consistent for Brackish Waterbodies as there is only 855 kg (< 0.1%) disparity between the carbon stored between 4.0 – 4.2 m and 4.4 – 4.6 m, whilst the disparity between the two intervals for Exposed Sediment is 2.27 x 10^5 kg (19.5%). The carbon mass stored within Brackish Waterbodies becomes negligible (<0.5%) below elevations of 3 m, whilst 4.40 x 10^4 kg (3.8%) of above-ground biomass within Exposed Sediment is found below this elevation.

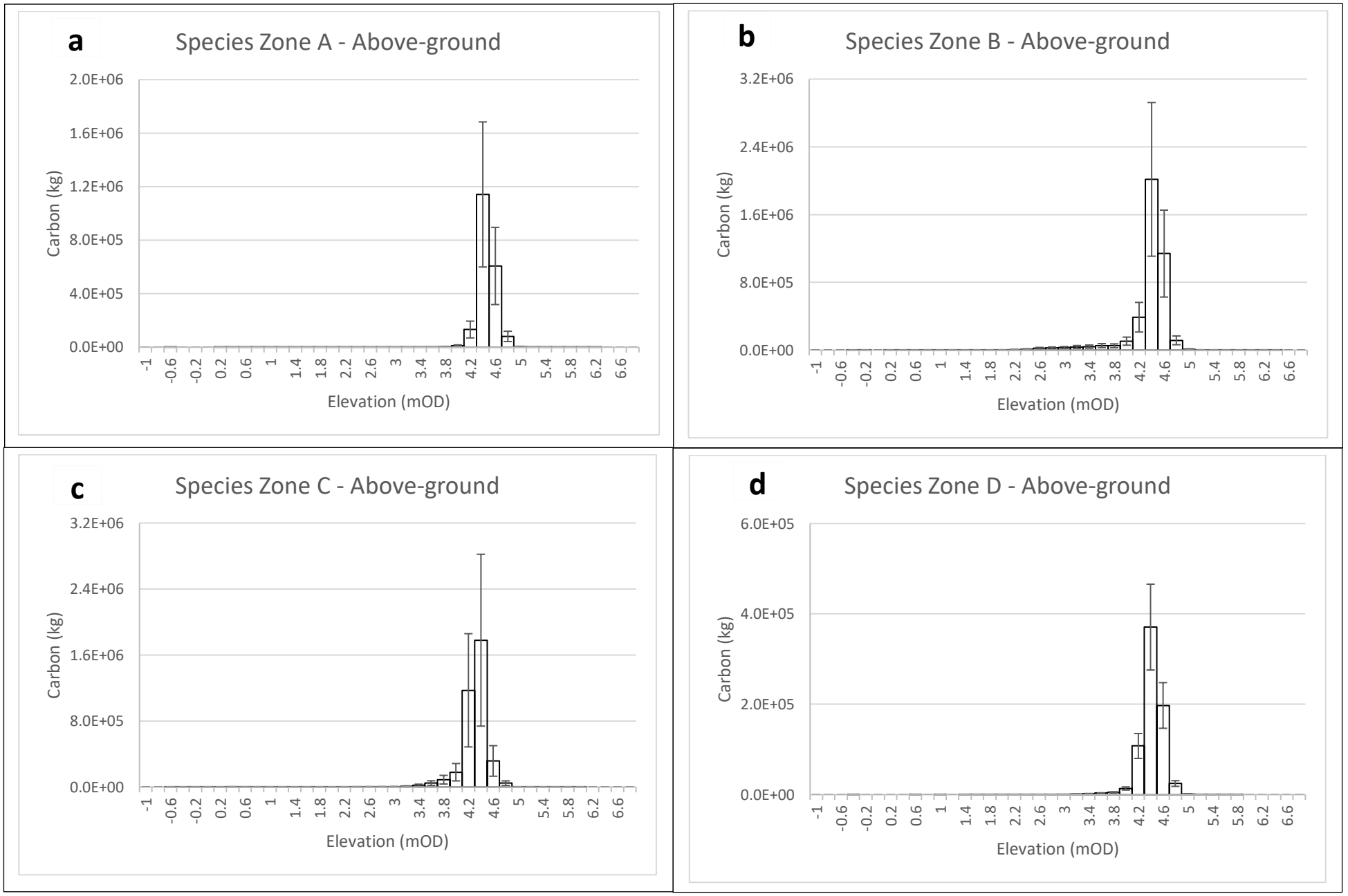

Figure 5.32(a-d). Above-ground biomass carbon variability with elevation within the sub-environments classified as Species Zone A (a), Species Zone B (b), Species Zone C (c) and Species Zone D (d). The error bars represent the maximal error including uncertainities concerning OCD and area.

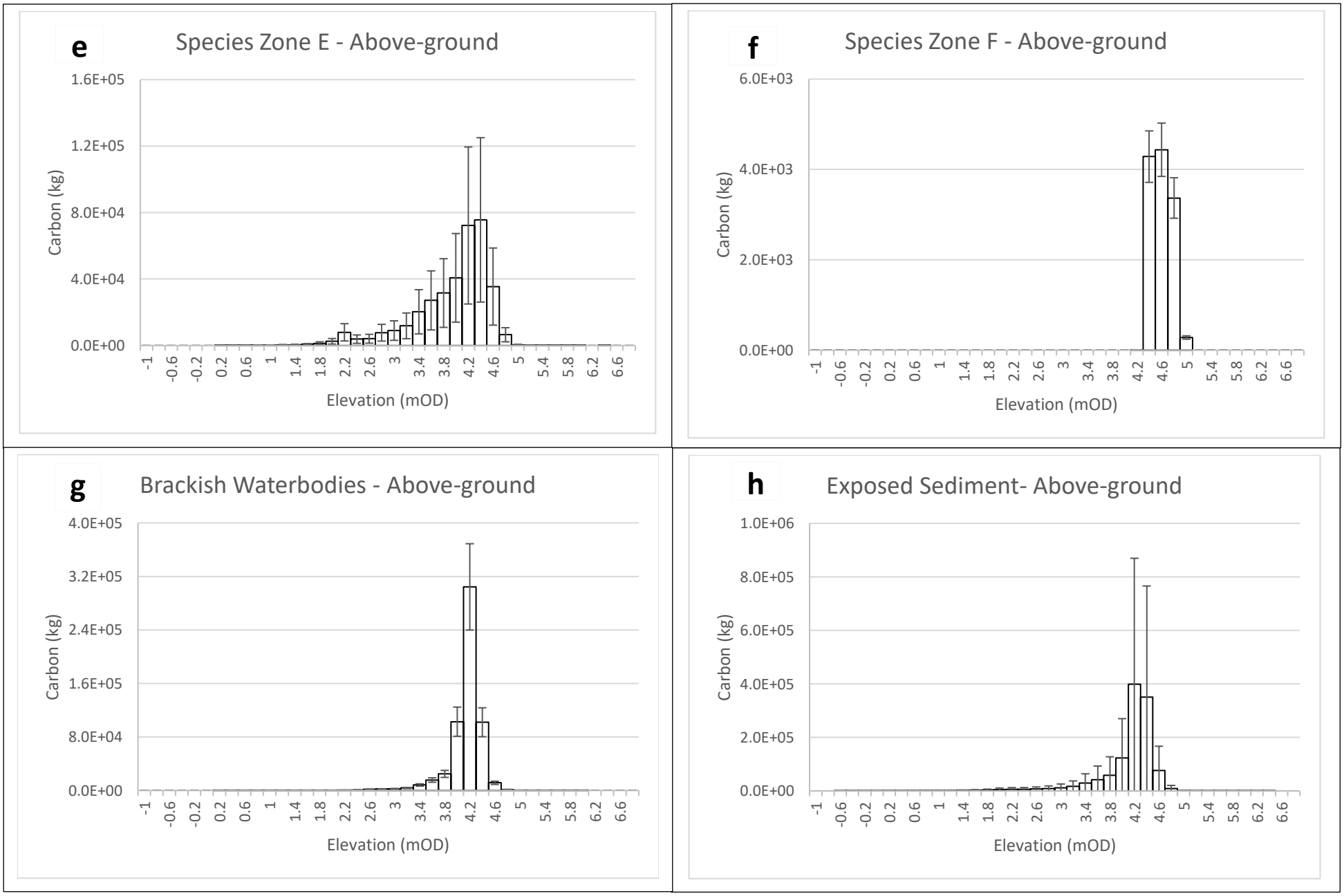

Figure 5.32(e-h). Above-ground biomass carbon variability with elevation within the sub-environments classified as Species Zone E (e), Species Zone F (f), Brackish Waterbodies (g) and Exposed Sediment (h).

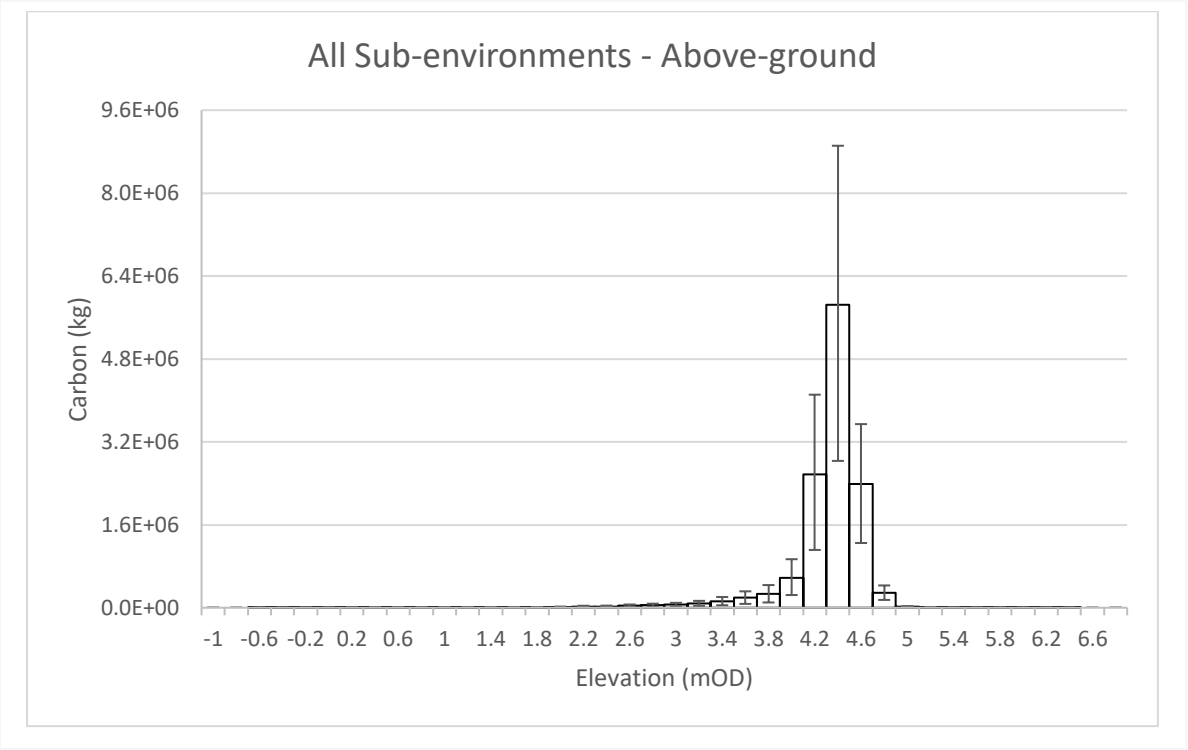

Figure 5.33. Average above-ground biomass carbon variability with elevation across all sub-environments

Active Layer

Whilst the distribution of active layer carbon partially corresponds with the above-ground biomass, disparities exist between the two concerning the total mass and the uncertainty surrounding projections in each sub-environment (see section 5.2.2.4). The most notable change in terms of overall mass contribution results from the influence of Exposed Sediment (see Figure 5.34(h)), which was the largest contributor to overall active section sub-surface carbon, contributing 49.4% of overall carbon mass as opposed to 9.2% of above-surface mass according to OA x AD projections. However, when the maximal uncertainty projections incorporating volume and OCD are considered it is plausible that the total carbon stored throughout the Ribble saltmarshes could vary by 8.37 x 10^6 kg. Exposed Sediment contributed 63.9 % of this uncertainty which was principally a result of the high uncertainty surrounding OCD in the sub-environment and the large overall volume. Regarding elevation, the uncertainty is greatest between 4.2 – 4.4 mOD which was a result of the lower mean elevation of Exposed Sediment and the reduced proportional contribution of Species Zone A, B and D commonly found in the higher marsh. As a result the maximal uncertainty totalled 2.41 x 10^6 kg or 66.3 % of the total carbon mass of the OA x AD projections between 4.2 – 4.4 mOD. In contrast, this uncertainty reduced to 9.73 x 10^6 kg or 62.1% of the OA x AD projections between 4.6 – 4.8 mOD.

When the OA x AD projections are considered, the enhanced contribution of Exposed Sediment can largely explain why 28.9% and 37.2% of active layer carbon is found between 4.2 – 4.4 m and 4.4 – 4.6 m as opposed to 20.4% and 46.3% for above-ground biomass. Similarly <0.1% of active layer carbon was found above HAT (5.10 mOD) and 16.1% is found below MHWS (4.10 mOD) which is partially due to the skewing effect of Exposed Sediment. Species Zones A, B and D, which are comprised of less tolerant halophytes and found at higher elevations (see Section 5.1.2) have a reduced contribution as they only comprise 24.6% of active layer carbon mass as opposed to 53.8% of the above-ground biomass.

The very low carbon mass of Species Zone F of 1.12×10^4 kg (OA x AD projection) means the sub-environment makes a negligible contribution to the overall carbon distribution (see Figure 5.34 (f)). The reduced contribution of Species Zone E to sub-surface carbon stores compared to above-ground biomass theoretically serves to increase the mean elevation in which sub-surface carbon is found, as the sub-environment comprises only 2.2% of the total surface carbon (OA x AD projections) as opposed to 3.0% of the above-surface store. However, this influence of Species Zone E is negligible compared to the influence of Exposed Sediment as the former only holds 3.8% of the sub-surface carbon stored in Exposed Sediment.

The net result of the low carbon mass of the sub-environments found at higher elevations is a steep rate of decline in carbon mass as elevation exceeds 4.6 m. Therefore the total active layer carbon stored between 4.6 – 4.8 m (1.57×10^6 kg) is 8.1 times higher than that stored between 4.8 – 5.0 m (1.93×10^5 kg) according to the OA x AD projections (see Figure 5.35).

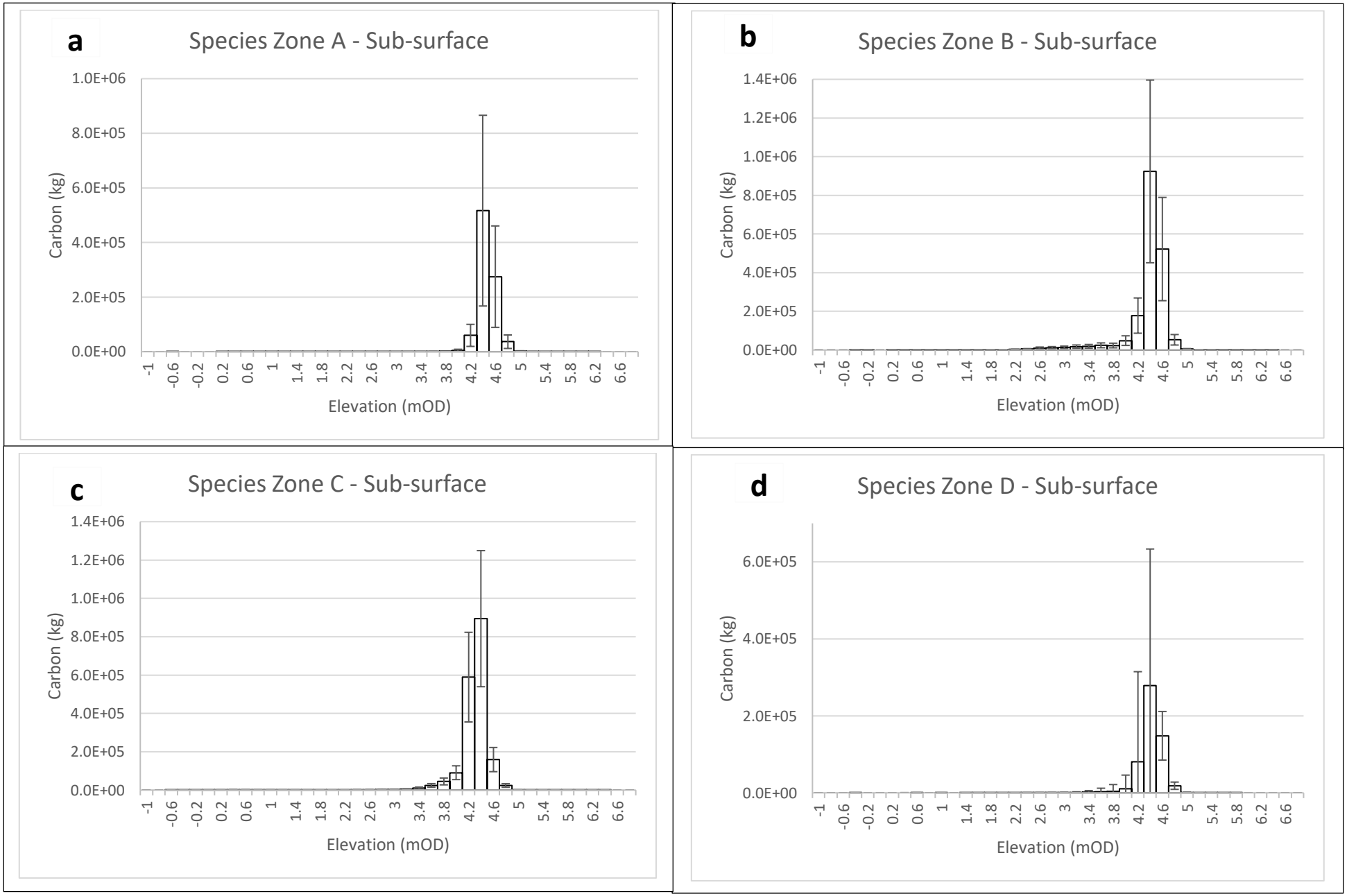

Figure 5.34(a-d). Sub-surface active section carbon variability with elevation within the sub-environments classified as Species Zone A (a), Species Zone B (b), Species Zone C (c) and Species Zone D (d). The error bars represent the maximal error including uncertainities concerning OCD and volume.

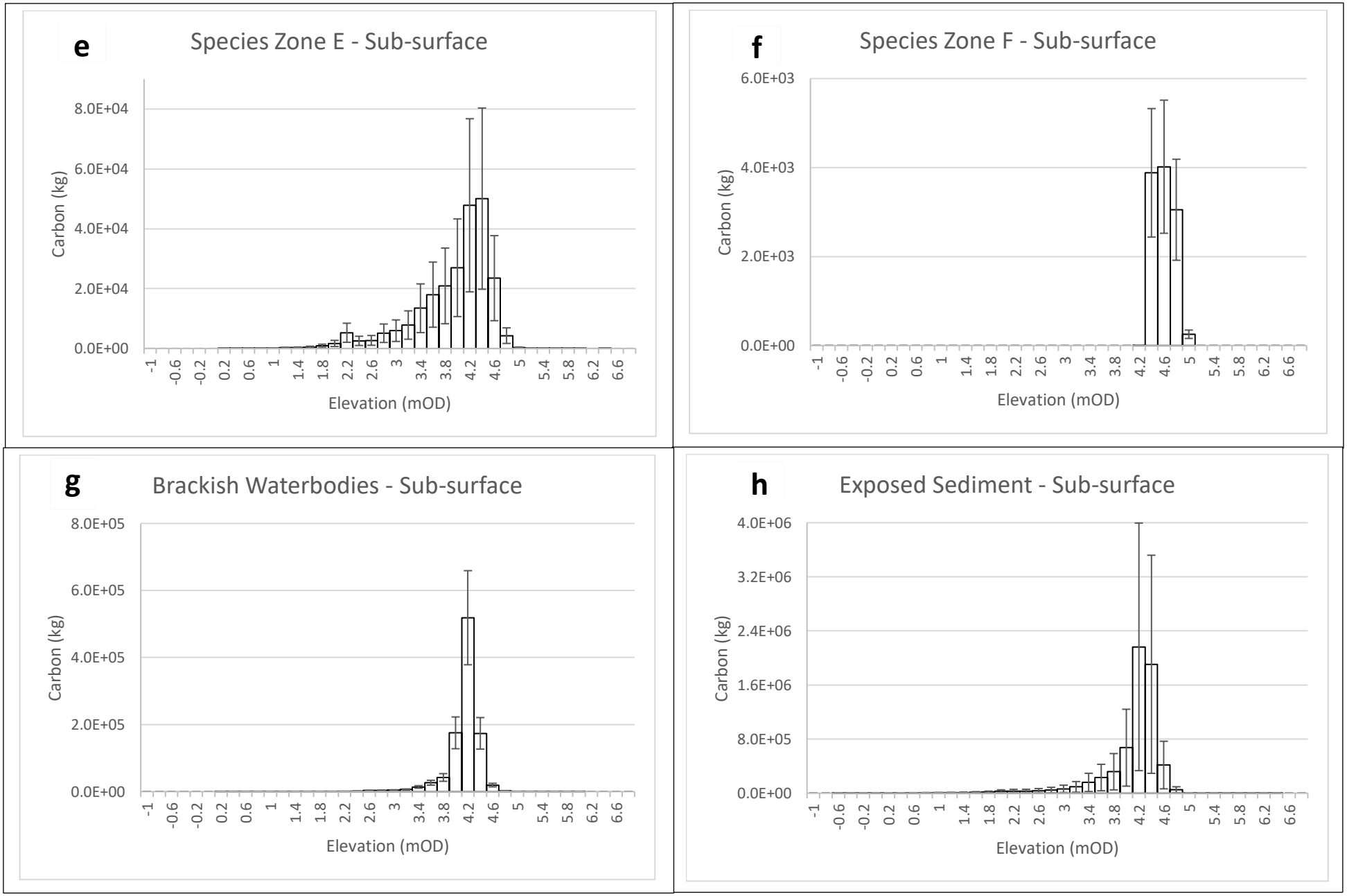

Figure 5.34(e-h). Sub-surface active section carbon variability with elevation within the sub-environments classified as Species Zone E (e), Species Zone F (f), Brackish Waterbodies (g) and Exposed Sediment (h).

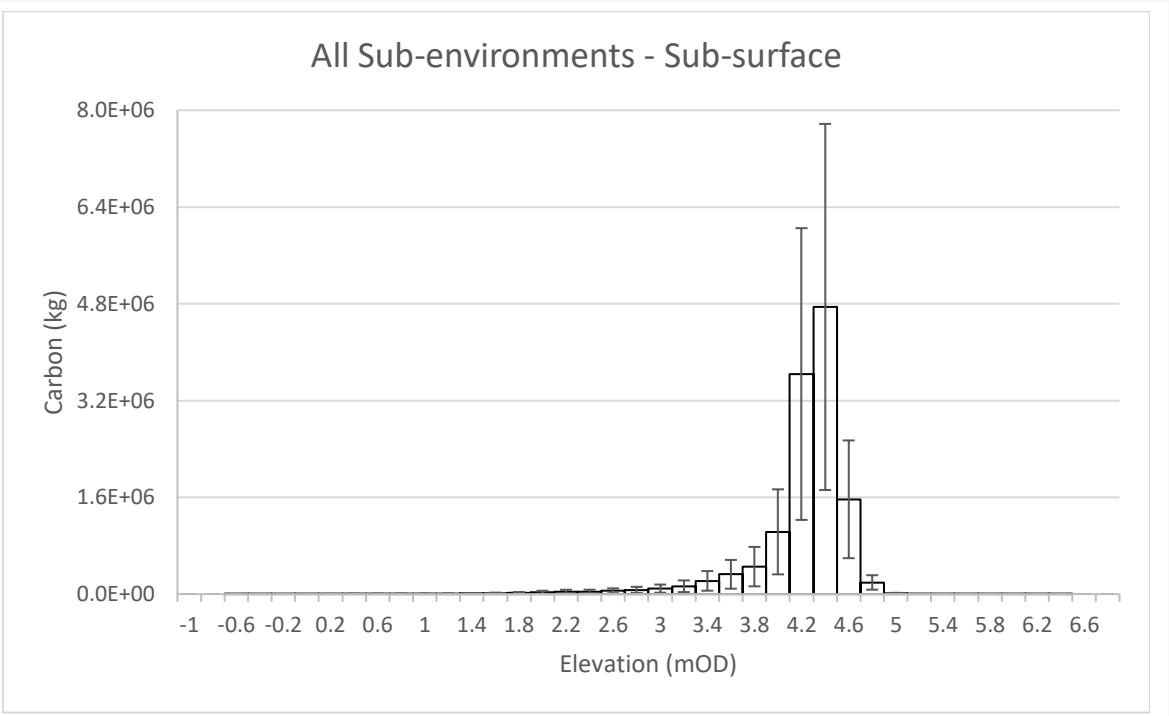

Figure 5.35. Average sub-surface active section carbon variability with elevation across all sub-environments.

5.3.3.3 – Gradient

Above-ground

The majority (1.12 x 10^7 kg or 99.8%) of the carbon stored within the above-ground biomass was found on land with a gradient <4°, whilst 75.7% (9.55 x 10^6 kg) was found at gradients <2° according to the OA projections. Of the area <2°, Species Zones B and C contributed the greatest carbon mass of 3.04 x 10^6 kg (31.8%) and 2.79 x 10^6 kg (29.2%) respectively, whilst the highest proportion of above-ground carbon at <2° was found in Species Zone A (82.9%) and Brackish Waterbodies (81.4%). Alternatively, the above-ground carbon in Species Zone E was found over the largest gradient range, with 14.2% of above-ground carbon store of 3.60 x 10^5 kg being found at a gradient ≥4°. Species Zone F possessed the 2nd least precise distribution (see Figure 5.12), although the total carbon stored within the Species Zone F at gradients ≥4° is < 0.1% of that stored within Species Zone E.

At gradients ≥4°, 53.7% of above-ground carbon was contained within Exposed Sediment as opposed to 9.1% between <2° (see Figure 5.36(h)), highlighting the lack of vegetation biomass on steep slopes surrounding creeks and the marsh perimeter. The large (118.3%) maximal uncertainty surrounding Exposed Sediment and the predominance of the sub-environment in areas >4° resulted in the uncertainty surrounding the overall projections increasing with gradient from 54.3% at <2° to 56.4% between 10-12°. In contrast the maximal upper bound for uncertainty surrounding the projections for Brackish Waterbodies and Species Zone D (Figure 5.36(g)&(d)) were the lowest at 21.2% and 25.6% due to the low areal and OCD uncertainties surrounding the two. However, as the carbon collectively found within Brackish Waterbodies and Species Zone D only comprised 10.7% (original remote area projection) of the total carbon stored within the entire environment, the collective influence on the overall uncertainty is reduced. Instead the influence sub-environments with a higher above-ground biomass such as Species Zone A which are surrounded by greater uncertainty (47.5%) produced the large overall uncertainty range.

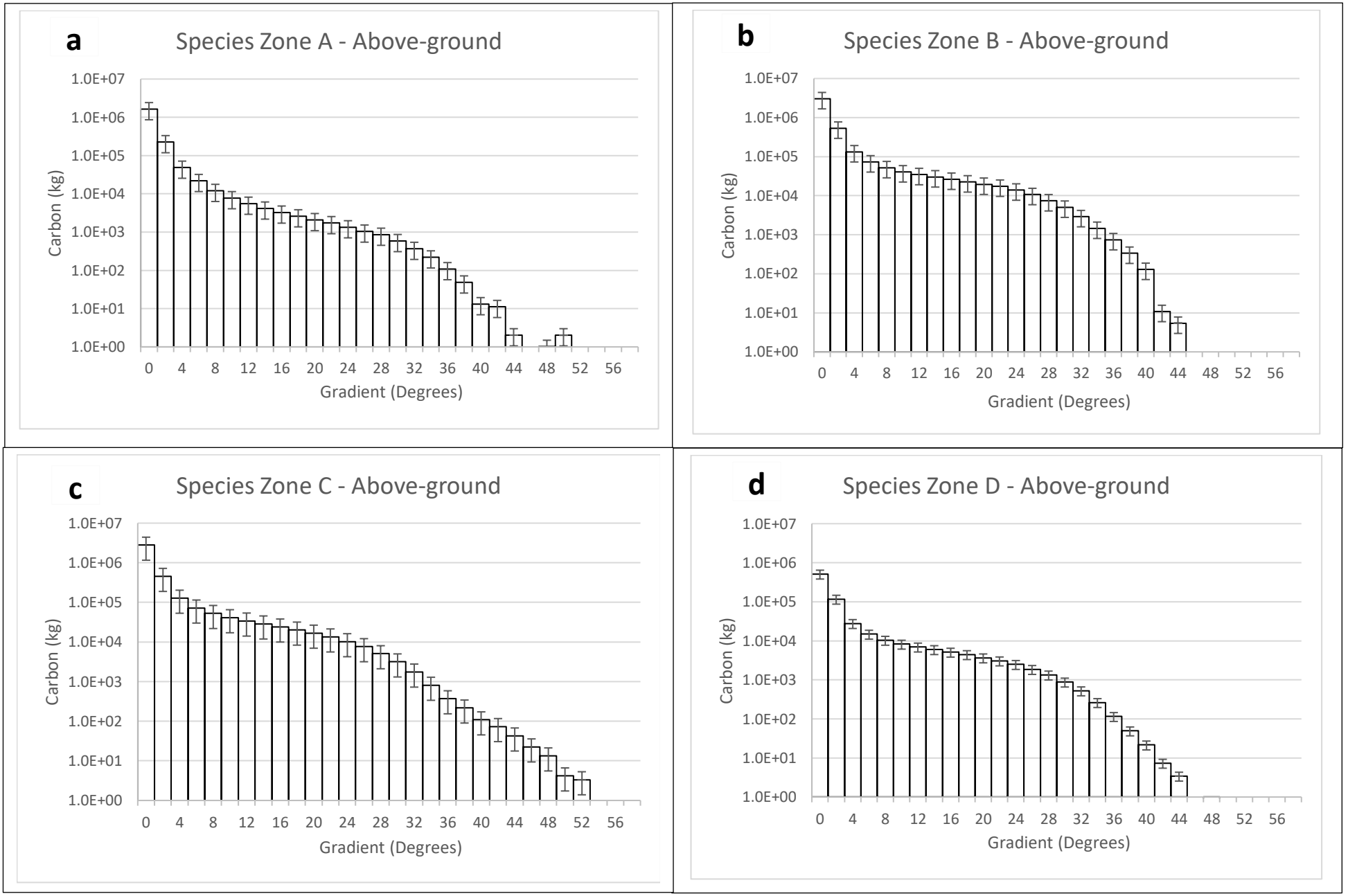

Figure 5.36(a-d). Above-ground biomass carbon variability with gradient within the sub-environments the sub-environments classified as Species Zone A (a), Species Zone B (b), Species Zone C (c) and Species Zone D (d). The error bars represent the maximal error including uncertainities concerning OCD and area.

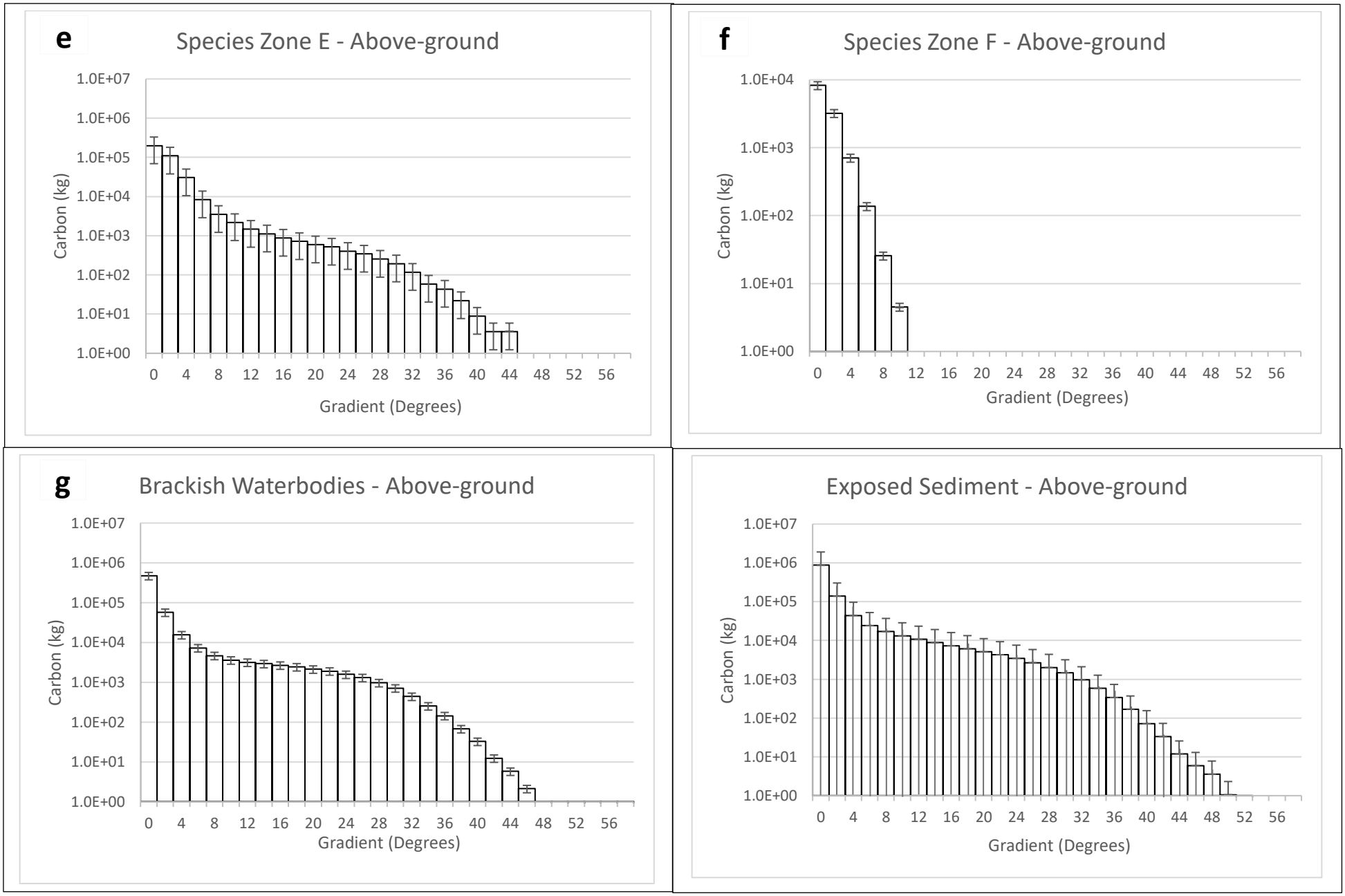

Figure 5.36(e-h). Above-ground biomass carbon variability with elevation within the sub-environments classified as Species Zone E (e), Species Zone F (f), Brackish Waterbodies (g) and Exposed Sediment (h).

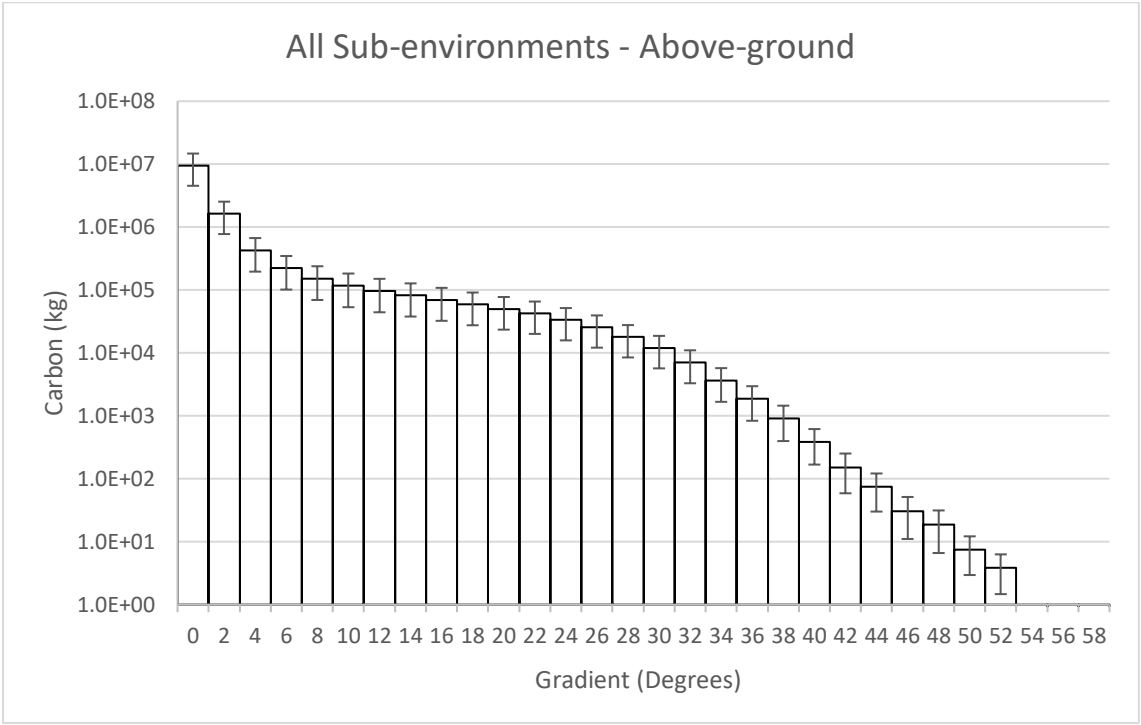

Figure 5.37. Average above-ground biomass carbon variability with gradient across all sub-environments.

Active Layer

The distribution of sub-surface carbon was primarily concentrated on land at gradients <4° with 75.5% (9.62 x 10^6 kg) and 12.5% (1.59 x 10^6 kg) of sub-surface carbon being found at gradients <2° and 2-4° respectively according to the OA x AD projections. The major change in overall distribution compared to above-ground biomass was that 12.0% (1.53 x 10^6 kg) of all sub-surface carbon was stored at gradients >4° compared to 11.3% (1.42 x 10^6 kg) of above-ground biomass. The change in distribution is primarily a result of the increased influence of Exposed Sediment which accounts for 8.26 x 10^5 kg of the 1.53 x 10^6 kg of sub-surface carbon found at a gradient ≥4°. Alternatively, the two sub-environments with the lowest mean gradient values (Species Zone A and Brackish Waterbodies) only collectively comprised 14.6% of the overall sub-surface active section carbon as opposed to 20.4% of above-ground biomass. Likewise, although <86% of the sub-surface carbon within Species Zone E and F was found at gradients <4° their impact on the overall distribution was minor as each only comprised 2.2% and <0.1% of the overall active layer carbon mass respectively. Despite occupying different elevation ranges Species Zone B and C have the most similar gradient distribution with 87.1% and 87.4% of all carbon being found at gradients <4°. However 3.43 x 10^5 kg more carbon is projected to be held within Species Zone C than B which is a result of the higher sub-environment volume and active layer carbon density (0.55 kg m^{-3}) (see Figure 5.38(b) & (c)).

The greater prominence of Exposed Sediment (84.6%) in areas of higher gradient meant the maximum uncertainty for the overall sub-environment increased with gradient. At gradients <2° where Exposed Sediment contributes 49.3% of the overall carbon mass, the overall uncertainty was 65.6% of the OA x AD projection and this increases to 67.2% at 30-32° where Exposed Sediment comprises 56.2% of the area. Asides from Exposed Sediment which is the most influenced by uncertainty both in terms of overall carbon 5.35×10^6 kg (OA x AD) and proportion (84.6%), Species Zone A and E (Figure 5.38(a) & (e)) are the next most proportionally influenced with uncertainty sub-surface uncertainty values of 67.6% and 60.5%. Whilst the influence of Species Zone E is comparably small as it only contributed 2.8% of carbon, if Species Zone A was at the maximal limit of uncertainty the total carbon mass at gradients <2° could change by 5.04×10^5 kg or 7.9% of the total overall total carbon at this gradient interval (OA x AD projection). Alternatively, Species Zones D, F and Brackish Waterbodies were surrounded by the least maximal uncertainty despite the dissimilar gradient distribution between the three sub-environments. Whilst the contribution to Species Zone F remains negligible, if Brackish Waterbodies and Species Zone D were at their minimal or maximal extent the overall carbon mass at gradients <2° would increase by 2.2% in both instances. However, the proportional influence of Brackish Waterbodies and Species Zone D on overall uncertainty decreases as gradient increases primarily due to the increased influence of Exposed Sediment.

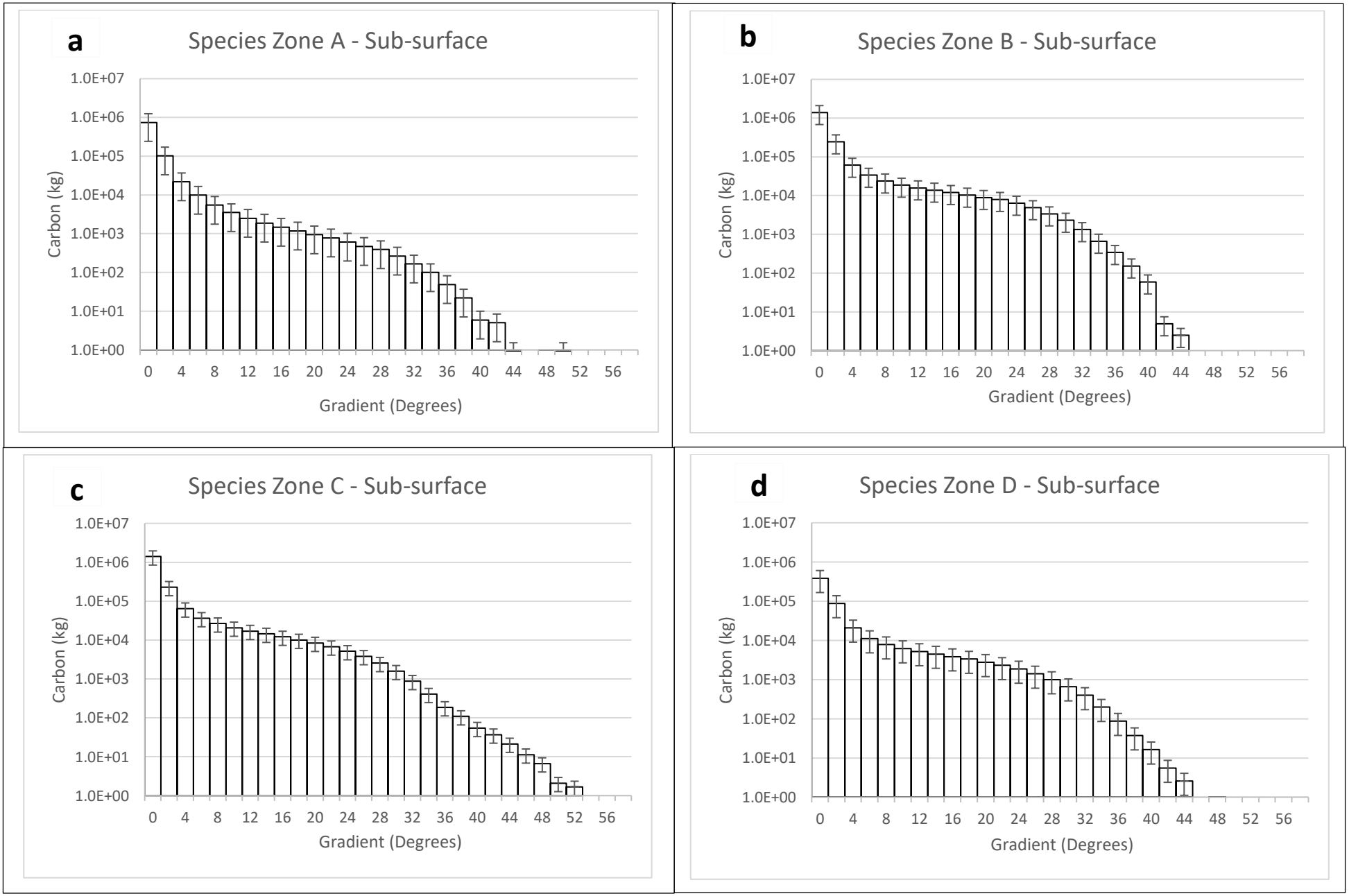

Figure 5.38(a-d). Sub-surface active section carbon variability with gradient within the sub-environments classified as classified as Species Zone A (a), Species Zone B (b), Species Zone C (c) and Species Zone D (d). The error bars represent the maximal error including uncertainities concerning OCD and volume.

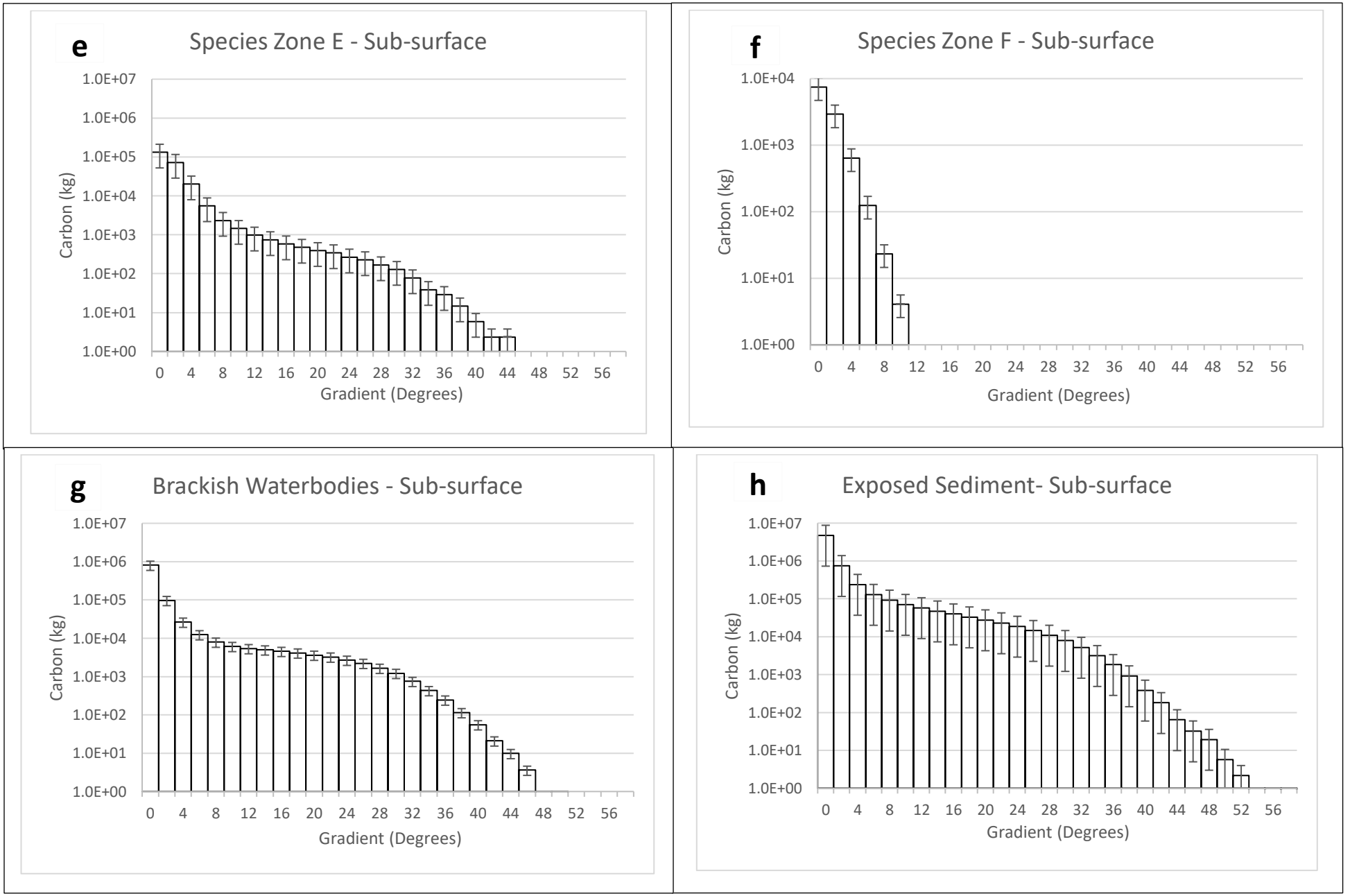

Figure 5.38(e-h). Sub-surface active section carbon variability with gradient within sub-environments classified as Species Zone E (e), Species Zone F (f), Brackish Waterbodies (g) and Exposed Sediment (h).

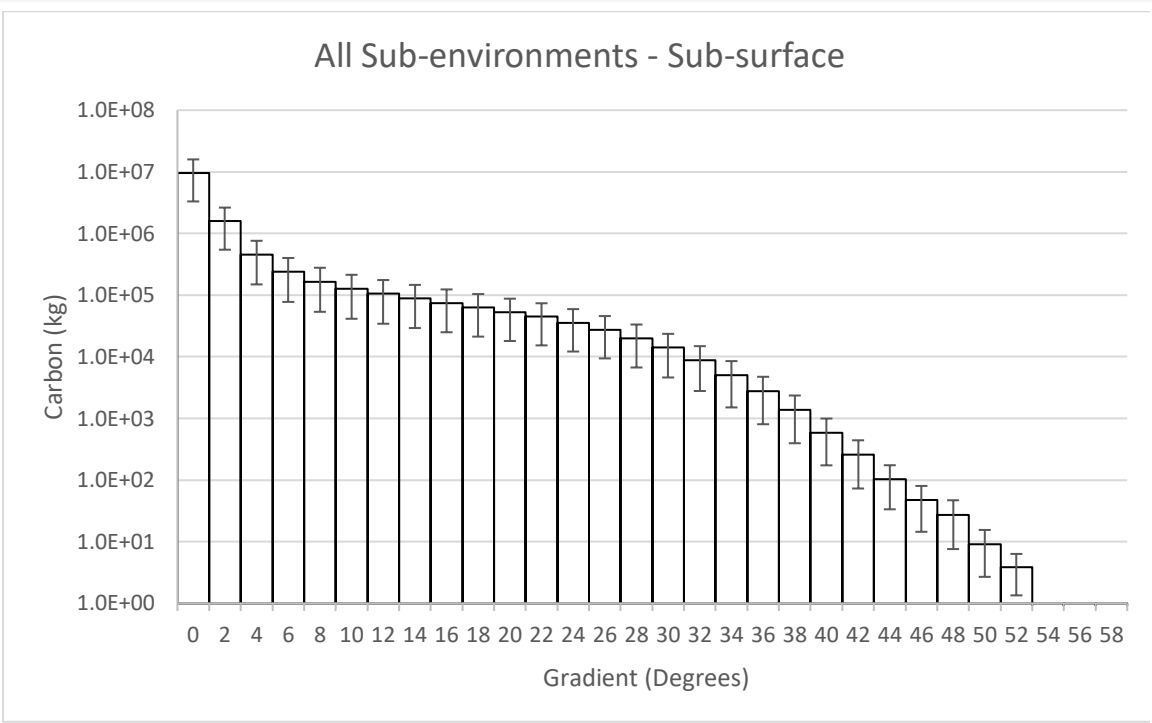

Figure 5.39. Average sub-surface carbon variability with gradient across all sub-environments.

5.3.3.4 – Watercourse Proximity

Above-ground

Of the eight sub-environments, six followed a consistent trend of decreasing above-ground carbon mass with distance from the watercourse, with Species Zones E and F being exceptions to this trend. Therefore, the overall above-ground carbon is throughout the saltmarsh was greatest within <10 m of a watercourse as 34.5% or 4.35 x 10^6 kg was found within this range whilst this decreased to 22.8% (2.87 x 10^6 kg) and 17.0% (2.14 x 10^6 kg) at the respective intervals of 10 – 20 m or 20 – 30 m according to the original remote area projections. At distances <10 m from a watercourse the most above-ground carbon was stored in Species Zone B which stored 1.34 x 10^6 kg or 30.8% of the total carbon (original remote area projection), although there is little disparity between Species Zone B Species Zone C in which 1.34 x 10^6 kg (also 30.8%) is stored. However, between 10 – 20 m from a watercourse the proportional contribution of Species Zone C to the overall above-ground carbon mass was 6.82 x 10^4 kg or 2.4% greater than Species Zone B at 10 – 20 m (see Figure 5.40(b) & (c)). This trend of increasing proportional overall contribution between 10 – 20 m compared to <10 m was also present in Species Zones A and D which increased by 0.9% and 1.3%. Despite the proportional increase, the total above-ground carbon storage in both Species Zones A and D decreased by 30.0% (2.00 x 10^5 kg) and 17.8% (4.17 x 10^4 kg) between the intervals <10 to 10-20 m, highlighting the prominence of carbon at close proximity to watercourses.

The sub-environments associated with watercourses Exposed Sediment and Brackish Waterbodies exhibited the largest proportional decreases of 18.8% (2.19 x 10^5 kg) and 16.0% (9.33 x 10^4 kg) between <10 m and 10-20 m (Figure 5.40(g) & (h)). However, between 10 – 20 m and 20 – 30 m the proportional rate of sub-environment carbon decrease of Species Zone D (7.6%) exceeds that of both Brackish Waterbodies (6.6%) and Exposed Sediment (5.8%). Between a distance of 30 – 40 m and 40 – 50 m the proportional decrease of carbon within each sub-environment remained comparatively consistent compared to intervals at closer distances to watercourses with a range of 7.3% (Species Zone B) to 5.2% (Brackish Waterbodies). At the greatest distances from the watercourses between 260-270 m, Species Zone C, Brackish Waterbodies and Exposed Sediment respectively comprise 44.0%, 1.4% and 54.5% of the above-ground carbon although the mass theoretically collectively totals only 52 kg (original remote area projection).

Species Zone E and F share a comparatively unique distribution as the carbon within the sub-environments does not uniformly decrease with creek proximity. According to the original remote area projections Species Zone E, was comparatively constant over the first three 10 m intervals as above-ground carbon mass totals 6.83 x 10^4 kg, 6.87 x 10^4 kg to 6.86 x 10^4 kg (Figure 5.40(e), before

a rapid decrease of 4.62 x 10^4 kg between the 30 – 40 m and 60 – 70m (78.8% decrease compared to the 30 – 40 m value). Alternatively, Species Zone F exhibits a comparatively anomalous trend when compared to all other sub-environments as the modal above-ground carbon mass of 1880 kg is found between 60 – 70 m from the nearest watercourse.

With regards to the maximal overall above-ground biomass uncertainty, it is theoretically possible that the above-ground biomass could differ by 3.18 x 10^6 kg or 55.4% if the original remote area projection at distances <10 m from a watercourse (Figure 5.41). This is predominantly due to the high level of uncertainty surrounding Species Zone C which comprised 30.7% of the total carbon in this interval and was surrounded by a maximal uncertainty of 58.5%. Moreover, the concentration of Exposed Sediment (10.8% of the original remote area) at distances <10 m also served to increase overall uncertainty compared to the subsequent proximity intervals. Consequently, the overall uncertainty decreases to 54.1% of the original remote area at 10 – 20 m, followed by successive decreases in uncertainty to a minimal value of 51.1% at 70 – 80 m. This trend can be explained by the increased proportional influence of certain predominantly vegetated sub-environments surrounded by lower levels of maximal uncertainty. The influence of the sub-environment with the greatest above-ground carbon mass (original remote area) Species Zone B (maximal uncertainty = 45%) is probably most prominent in this trend as the mass of carbon stored within the sub-environments progressively increased from 29.3% at 10-20 m to a maximum of 48.9% at 70-80 m. Species Zone D (maximal uncertainty = 25.6%) also had a more minor influence as the proportion of the overall above-ground carbon stored within the sub-environment is greater at 10 – 20 m (6.7%) and 20 – 30 m (6.4%). Although the proportional distribution of Species Zone E (maximal uncertainty = 65.4%) does counter this trend as the sub-environment is most prominent between 50 – 60 m, as the sub-environment comprised 2.56 x 10^4 kg at this interval compared to the 1.84 x 10^5 kg in Species Zone B this influence is largely negated. After a distance of 80 m, the proportional uncertainty increases up to 270 m which is a result of the increasing proportional effect of Exposed Sediment which comprises 54.5% of carbon between 260-270 m. This influence on overall above-ground carbon uncertainty is minor however, as the total above-ground carbon stored between 80 – 270 m is only 1.4% of the overall value (see Figure 5.41).

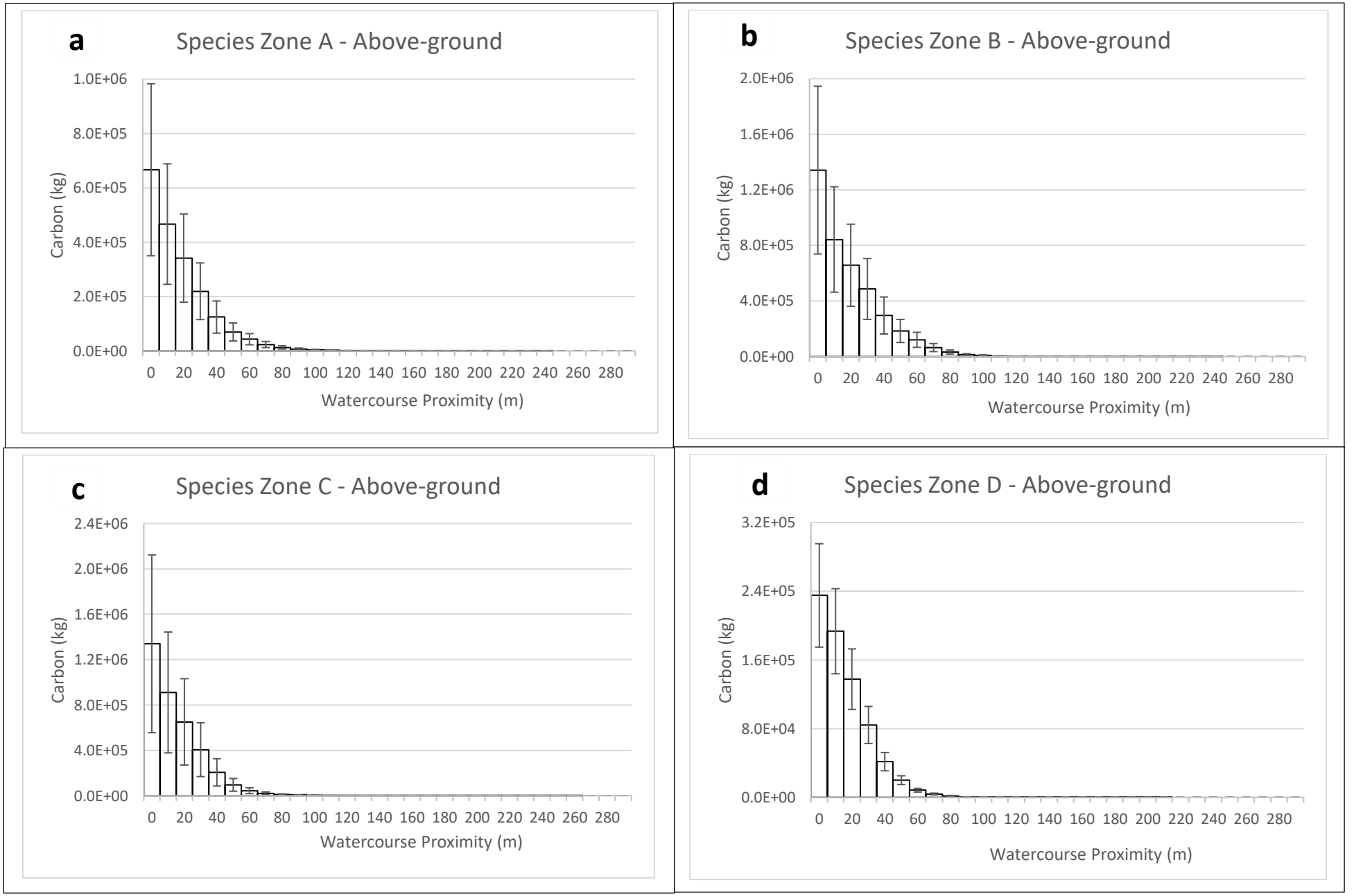

Figure 5.40(a-d). Above-ground biomass carbon variability with watercourse proximity within sub-environments classified as Species Zone A (a), Species Zone B (b), Species Zone C (c) and Species Zone D (d). The error bars represent the maximal error including uncertainities concerning OCD and areal.

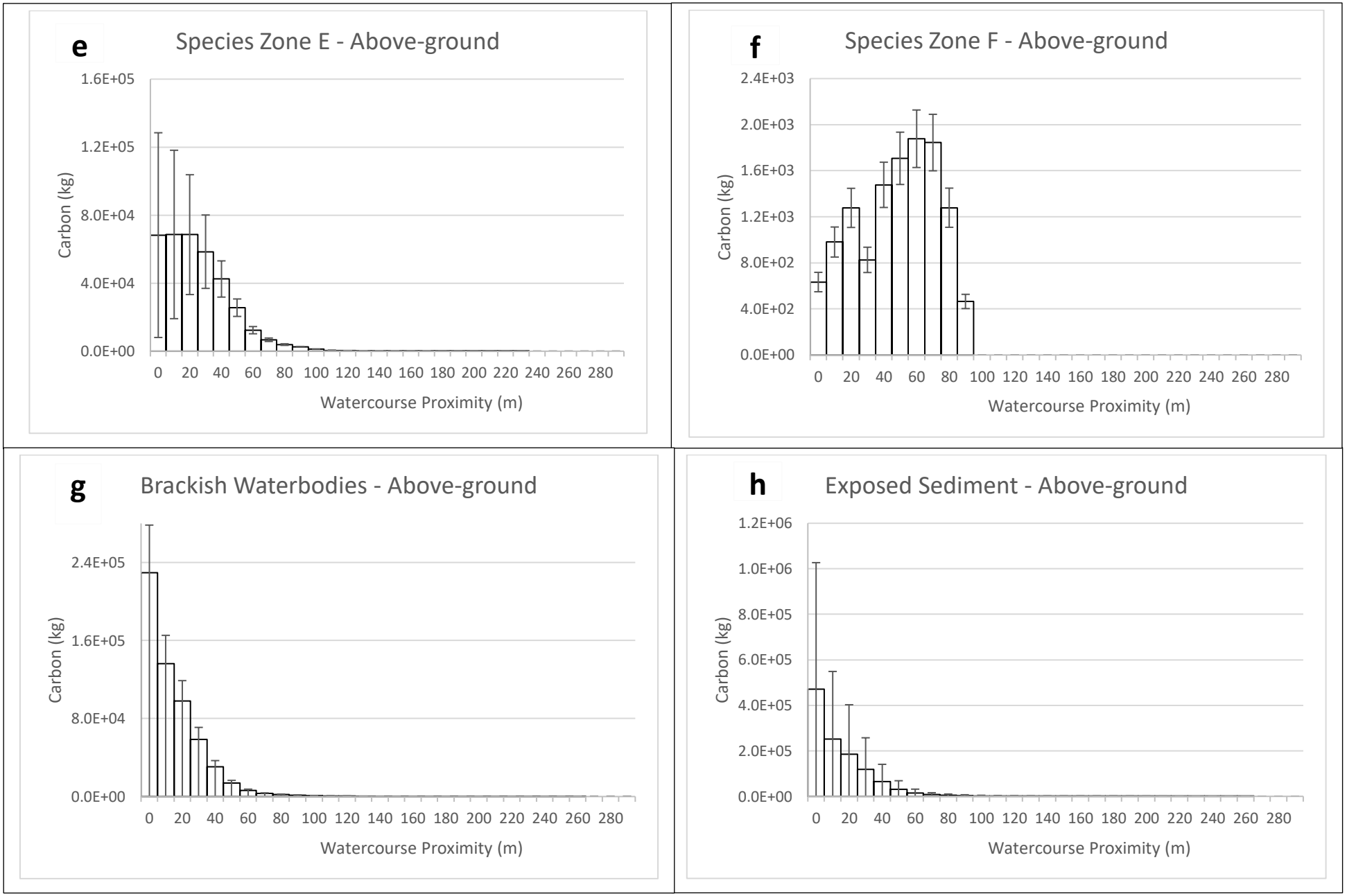

Figure 5.40(e-h). Above-ground biomass carbon variability with watercourse proximity within sub-environments classified as Species Zone E (e), Species Zone F (f), Brackish Waterbodies (g) and Exposed Sediment (h).

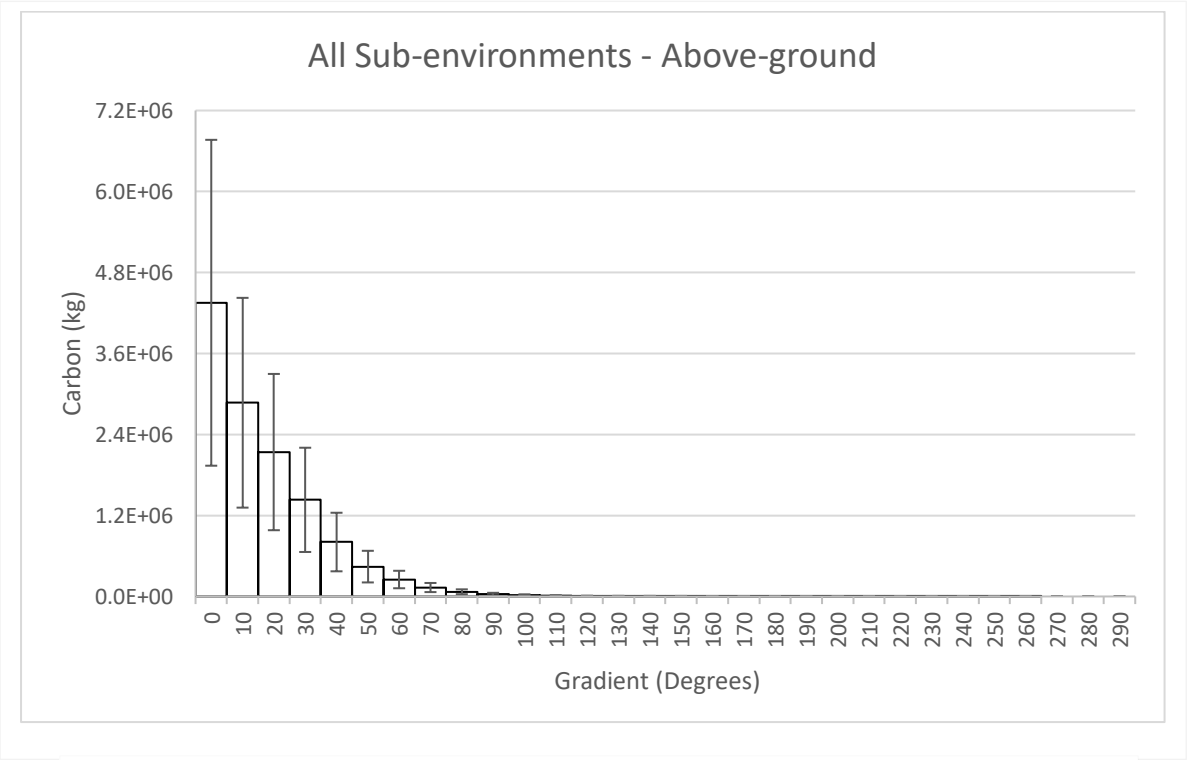

Figure 5.41. Average above-ground biomass carbon variability with watercourse proximity across all sub-environments.

Active Layer

The overall projections for carbon found within the active layer sub-surface sediments across all sub-environments highlighted a concentration of the majority of the overall carbon at close proximity to a watercourse as 37.3% (4.76 x 10^6 kg) and 22.3% (2.84 x 10^6 kg) of all carbon was found within <10 m and 10 – 20 m of a watercourse (OA x AD projections) (Figure 5.43). Of the active layer carbon in the modal watercourse proximity interval of <10 m the sub-environments Exposed Sediment comprised the majority comprising 53.7% (2.56 x 10^6 kg) (Figure 5.42(h)), whilst Species Zone B and C comprised 12.9% (6.15 x 10^5 kg) and 14.1% (6.73 x 10^5 kg) respectively (see Figure 5.42(b) & (c)). The predominance of Exposed Sediment at <10 m can be explained by the spatial clustering of the sub-environment which is associated with creeks (40.4% is found within <10 m) and the large volume (55.3%) of the area according to the OA x AD projections as the mean OCD was only 3.09 kg m^{-3}. Alternatively, the proportional influence of Species Zone B and C was reduced despite having higher OCDs of 3.93 kg m^{-3} and 4.12 kg m^{-3} as well as the fact the latter has the most precise distribution (Figure 5.19) and lowest median creek proximity, as each sub-environment only comprises 12.0% and 14.1% of the volume respectively. The increase in the overall proportion of active layer carbon mass found in Brackish Waterbodies compared to above-ground biomass combined with the association with creeks resulted in 39.3% of all active layer carbon in the sub-environment being found within <10 m of a watercourse. The rate of decrease in carbon storage and the proportional influence of certain sub-environments between <10 m and 10 – 20 m is largest for

Exposed Sediment which contains 1.19 x 10^6 kg less carbon at 10 – 20 m than <10 m. This resulted in the overall sub-environment carbon contribution of Exposed Sediment decreasing from 53.7% at <10 m to 48.0% at 10 – 20m. Alternatively, Species Zone A, B, C, D and E all comprised a greater proportion of sub-surface carbon at 10 – 20 m than <10 m with respective increases of 1.1%, 0.7%, 1.9%, 1.4% and 0.6%. Of the sub-environments that follow the overall trend of decreasing carbon storage Species Zone D decreased by the lowest rate as the carbon mass stored between 10 – 20 m is 17.7% lower than that stored at a proximity <10 m. Species Zones A, B and C exhibited similar rates of decrease between <10 m and 10 – 20 m of 30.0%, 37.2% and 32.0% which results from the similar spatial distributions <20 m from watercourses (see Figure 5.19 (a),(b) & (c)). As with above-ground carbon predominantly vegetated sub-environments contributed the greatest proportion of all active layer carbon at the interval of 70-80 m in which Exposed Sediment comprised a minimum (for the sub-environment) of 37.8% whilst Species Zones B, A and C both comprise 28.2%, 10.2% and 10.1% respectively. The comparatively anomalous spatial distribution of Species Zone F (Figure 5.42(f)) means that it comprised 1.5% and 1.9% of all carbon between 70-80 m and 80-90 m which was a comparatively large contribution considering the sub-environment only occupies 20775 m^2 (<0.1% of any projection). This contribution is relatively negligible compared to the influence of Exposed Sediment which became increasingly more prominent at distances >80 m as the areal cover of predominantly vegetated sub-environment progressively decreased.

The overall proportional uncertainty per proximity interval also corresponded with the abundance of Exposed Sediment as the maximal uncertainty is smallest between 70 – 80 m (63.4% or 6.66 x 10^4 kg) before it increases with watercourse proximity. This increase in overall uncertainty relative to above-ground biomass was because the active layer calculations include depth uncertainty. Uncertainty also increased at a more gradual rate as watercourse proximity decreased and the overall uncertainty value of 66.9% at distances <10 m is principally due to the influence of Exposed Sediment which has a maximal uncertainty value of 84.6% resulting from the OCD uncertainty and the predominance of Exposed Sediment at this distance interval. The reduction in overall uncertainty to 65.1% (1.85 x 10^6 kg) at 10 – 20 m can be attributed to the increasing proportional contribution of sub-environments with lower levels of uncertainty such as Species Zone C (39.7%). However, as the proportional contribution of Brackish Waterbodies, the sub-environment with the lowest level of uncertainty (29.7%), does decline by 0.6% between <10 m to 10-20 m this moderates the decrease in uncertainty.

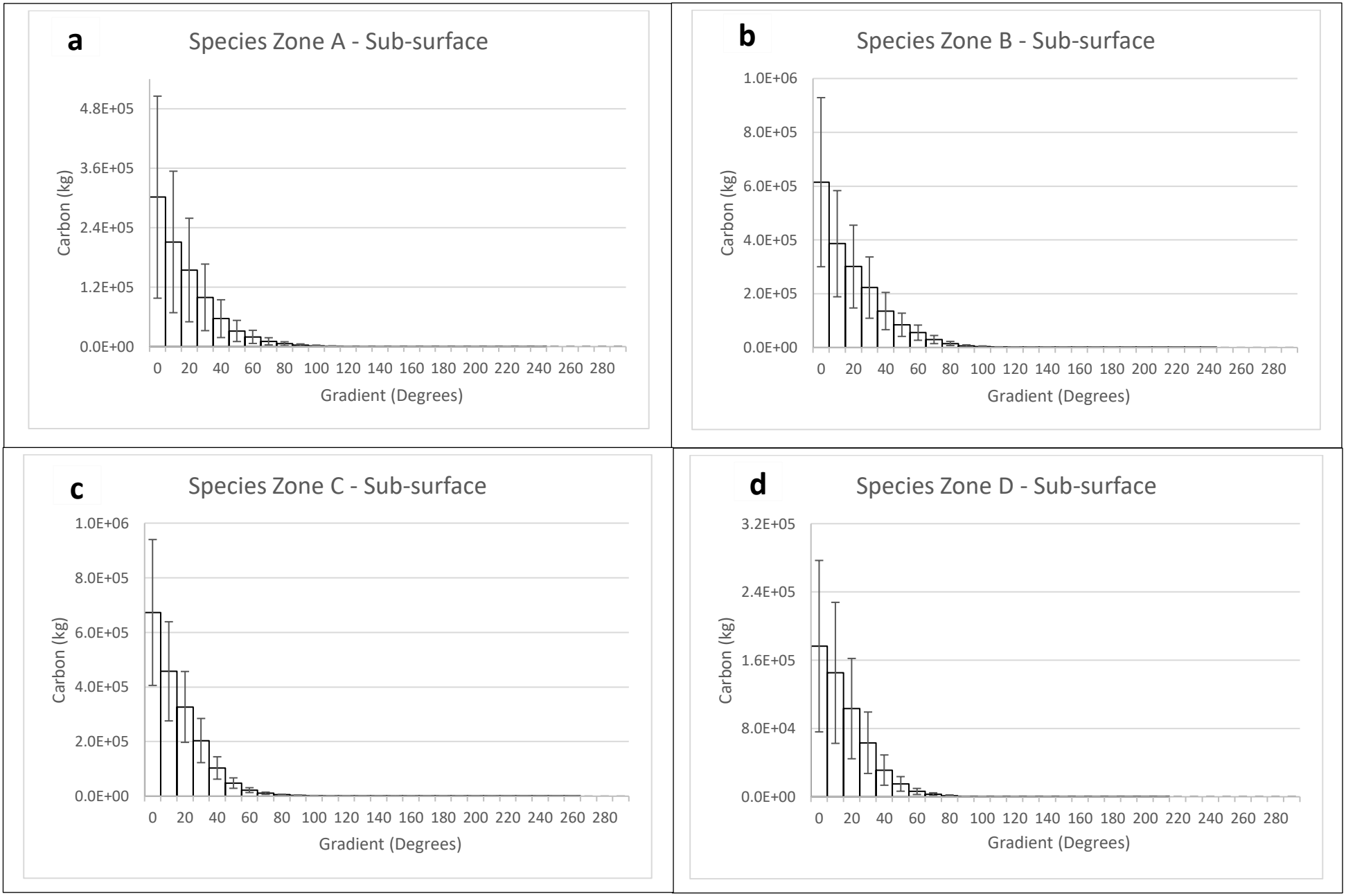

Figure 5.42(a-d). Sub-surface active section carbon variability with watercourse within sub-environments classified as Species Zone A (a), Species Zone B (b), Species Zone C (c) and Species Zone D (d). The error bars represent the maximal error including uncertainities concerning OCD and volume.

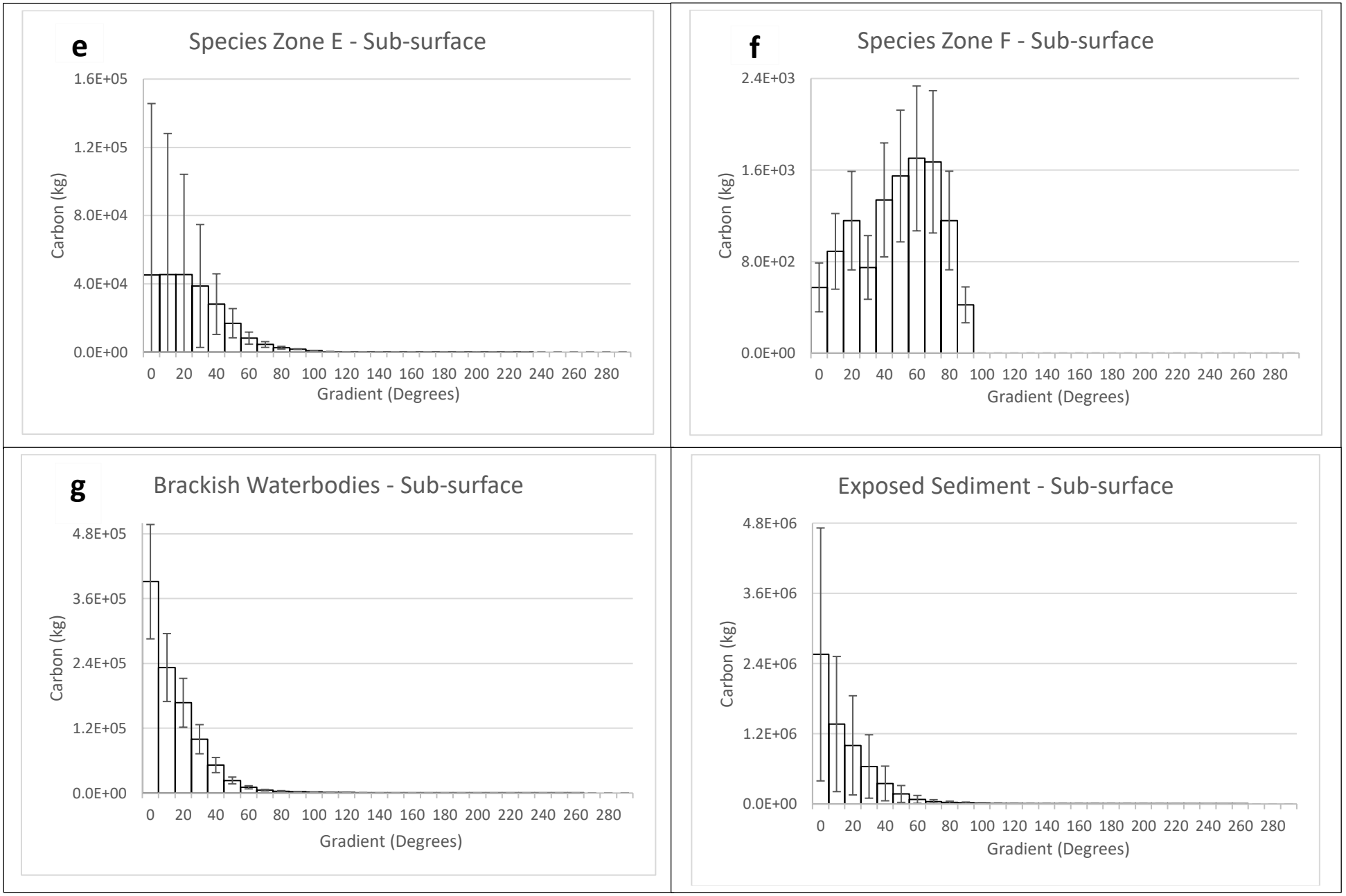

Figure 5.42(e-h). Sub-surface active section carbon variability with gradient within sub-environments classified as Species Zone E (e), Species Zone F (f), Brackish Waterbodies (g) and Exposed Sediment (h).

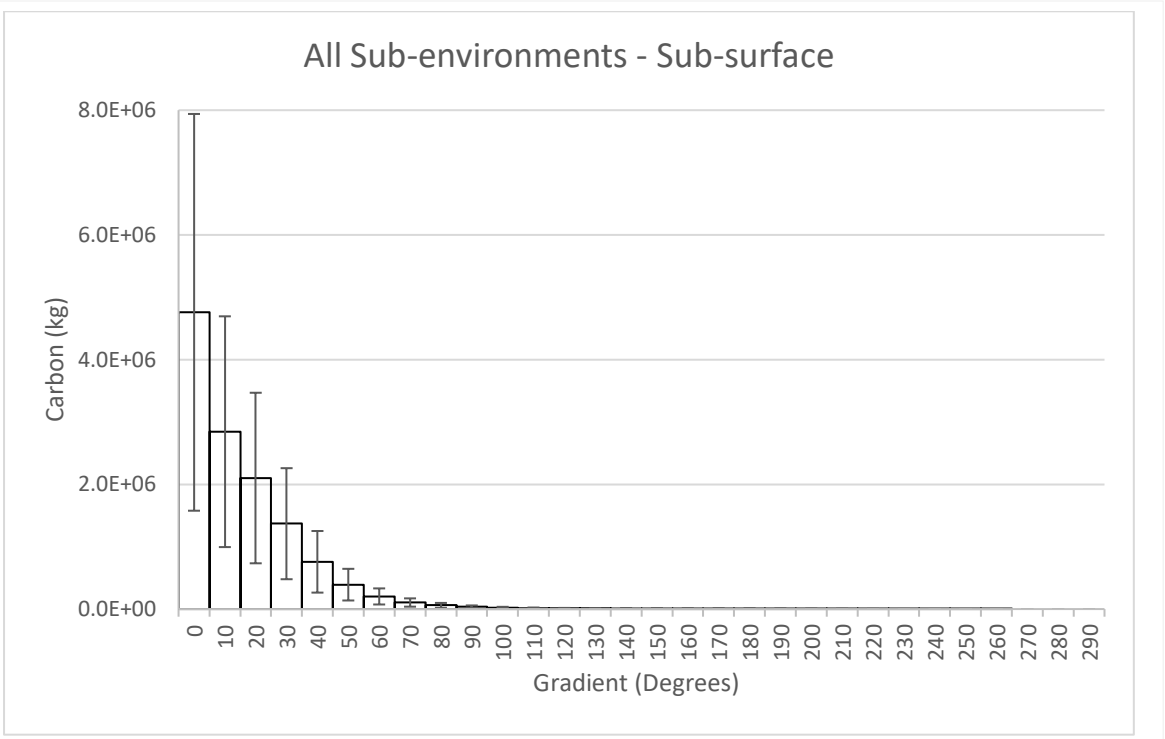

Figure 5.43. Average sub-surface carbon variability with watercourse proximity across all sub-environments.

5.3.4 – Key Controls on Carbon Distribution

5.3.4.1 – Introduction

Whilst the analyses conducted in Section 5.1.5 highlight the variability in sub-environment carbon storage and the respective influences of elevation, gradient and watercourse proximity, the observations and statistics do not completely reveal the contribution of each influence on carbon storage. Whilst standardised beta, T statistic and p value remain equal to those produced in the analysis in 5.1.5, the following results indicate the influence of the three key controls on overall above-ground and active layer carbon storage change as displayed by the unstandardised beta value.

5.3.4.2 – Elevation

Above-ground Biomass

The predictor standardised beta values in Table 5.36 highlighted that the above-ground biomass carbon in the sub-environments Species Zone D (0.268) and Species Zone E (0.263) were most influenced by elevational change, whilst Brackish Waterbodies (0.178) and Species Zone C (0.187) were predicted to be least influenced by elevation. Despite the low standardised values, Species Zone C had an unstandardised value of 3.28×10^4 kg/m and Species Zone B possessed the highest value of 3.82×10^4 kg/m. Species Zones E and F had the lowest unstandardised values of 2390 kg/m and 135 kg/m respectively which was expected from sub-environments with mean above-ground carbon masses of 0.78 kg/m^2 and 0.60 kg/m^2 which cover 2.12% and 0.09% of the marsh respectively. However, the p values for elevation are universally above the alpha value of 0.05 indicating that the influence of elevation is statistically insignificant.

Table 5.36. Multiple regression parameters and the significance of predictor variables concerning elevation and sub-environment above-ground biomass carbon storage (kg).

Sub-environment	Unstandardised Beta (kg per m)	Standardised Beta	T	p
Species Zone A	19944	0.197	1.174	0.249
Species Zone B	38156	0.211	1.257	0.217
Species Zone C	32847	0.197	1.173	0.249
Species Zone D	8986	0.212	1.267	0.213
Species Zone E	2392	0.263	1.592	0.121
Species Zone F	135	0.25	1.506	0.141
Brackish Waterbodies	4639	0.178	1.056	0.298
Exposed Sediment	9005	0.215	1.284	0.208

Active Layer

The standardised beta values, which are equal to those for above-ground biomass, highlight active layer carbon in Species Zone E and F is proportionally influenced the most by elevational change. Alternatively, the standardised values for Species Zone A (0.197) and Brackish Waterbodies (0.0178) indicate the sub-environments were the least influenced. The unstandardised values highlight the increased importance of elevation on controlling the distribution of active layer carbon in the predominantly unvegetated sub-environments of Exposed Sediment (4.89 x 10^4 kg/m) and Brackish Waterbodies (7907 kg/m) when compared to above-ground carbon. Regarding predominantly vegetated sub-environments, a similar trend to that observed in the above-ground biomass is noted with carbon storage increasing by 1.75 x 10^4 kg and 1.65 x 10^4 kg per m for Species Zones B and C respectively. In contrast, Species Zone E and F contribute only 9.1% and 0.6% of the unstandardised value of Species Zone B for every metre of elevation despite the fact Species Zone B has a lower standardised value of 0.211. However the results are again statistically insignificant.

Table 5.37. Multiple regression parameters and the significance of predictor variables concerning elevation and sub-environment active layer carbon storage (kg).

Sub-environment	Unstandardised Beta (kg per m)	Standardised Beta	T	p
Species Zone A	9026	0.197	1.174	0.249
Species Zone B	17483	0.211	1.257	0.217
Species Zone C	16498	0.197	1.173	0.249
Species Zone D	5337	0.212	1.267	0.214
Species Zone E	1584	0.263	1.592	0.121
Species Zone F	122	0.25	1.506	0.141
Brackish Waterbodies	7907	0.178	1.056	0.298
Exposed Sediment	48920	0.215	1.284	0.208

5.3.4.3 – Gradient

Above-ground Biomass

Overall the standardised beta values highlight gradient has the greatest influence on Species Zone E and F with respective values of -0.496 and -0.448, whilst Species Zone A and Brackish Waterbodies are the least influenced by gradient change (-0.384). The two sub-environments with the highest mean above-ground biomass carbon content Species Zone B (1.19 kg/m^2) and Species Zone C (0.97 kg/m^2) have the lowest (most negative) unstandardised beta values of -1.51 x 10^4 kg/m and -1.38 x 10^4 kg/m, whilst Species Zone A had the 3rd lowest unstandardised beta despite the joint highest (closest to zero) standardised value. The p values for gradient are all below the alpha value of 0.05 indicating the relationship is statistically significant.

Table 5.38. Multiple regression parameters and the significance of predictor variables concerning gradient and sub-environment above-ground biomass carbon storage (kg).

Sub-environment	Unstandardised Beta (kg per degree)	Standardised Beta	T	p
Species Zone A	-7673	-0.384	-2.078	0.048
Species Zone B	-15141	-0.41	-2.247	0.034
Species Zone C	-13844	-0.409	-2.239	0.034
Species Zone D	-2696	-0.429	-2.374	0.026
Species Zone E	-1344	-0.496	-2.856	0.009
Species Zone F	-48	-0.448	-2.505	0.019
Brackish Waterbodies	-2207	-0.384	-2.082	0.048
Exposed Sediment	-4333	-0.409	-2.243	0.034

Active Layer

Although the standardised values were lowest (most negative) for Species Zone E and F, both sub-environments contributed little to the overall unstandardised change in kg per degree as the predicted unstandardised figures highlighted a respective change of -890 kg and -43 kg. Exposed Sediment was the most influenced by increasing gradient with an unstandardised change of -2.35 x 10^{-4} kg per degree, whilst Species Zone B and C were predicted to decrease by -6940 kg and -6950 kg per degree respectively. This is a result of Exposed Sediment having the largest volume and therefore overall carbon content as the standardised value for the sub-environment of -0.409 was the joint 2nd highest (closest to zero) with Species Zone C at -0.409. The model predicted active layer carbon in Brackish waterbodies would decrease by -3670 kg per degree, a similar figure to Species Zone A which contributed to a decrease of 3470 kg. This was predictable given the similar respective mean carbon storage of the sub-environments of 3.85 and 3.91 kg m^{-3} and equal (3.s.f) standardised beta values of -0.384.

Table 5.39. Multiple regression parameters and the significance of predictor variables concerning gradient and sub-environment active layer carbon storage (kg).

Sub-environment	Unstandardised Beta (kg per degree)	Standardised Beta	T	p
Species Zone A	-3472	-0.384	-2.078	0.048
Species Zone B	-6938	-0.41	-2.247	0.034
Species Zone C	-6953	-0.409	-2.239	0.034
Species Zone D	-2023	-0.429	-2.374	0.026
Species Zone E	-890	-0.496	-2.856	0.009
Species Zone F	-43	-0.448	-2.505	0.019
Brackish Waterbodies	-3672	-0.384	-2.082	0.048
Exposed Sediment	-23539	-0.409	-2.243	0.034

5.3.4.4 – Watercourse Proximity

Above-ground Biomass

The unstandardised values for above-ground biomass highlighted that Species Zone B and C above-ground biomass carbon would decrease by the greatest net amount per m from a watercourse, despite possessing only the 3rd and 6th lowest standardised values of -0.679 and -0.635. Species Zone E and F had the lowest (most negative) standardised values of any sub-environment and for any significant factor (i.e. lower than gradient), however the two sub-environments contributed to only -232 kg and -6 kg of carbon loss per m. This was a result of low overall carbon storage in Species Zone E (3.60×10^5 kg) and F (1.24×10^4 kg). In contrast, watercourse proximity had a reduced standardised influence on Brackish Waterbodies (-0.617) and Exposed Sediment (-0.614), although the two predominately non-vegetated sub-environments collectively contributed to a change of -1230 kg as they comprised 50.9% of the area (original remote areal assessment). All p values were $\leqslant 0.001$ suggesting it was highly unlikely any relationships occurred by chance.

Table 5.40. Multiple regression parameters and the significance of predictor variables concerning watercourse proximity and sub-environment above-ground biomass carbon storage (kg).

Sub-environment	Unstandardised Beta (kg)	Standardised Beta	T	p
Species Zone A	-1370	-0.661	-4.404	<0.001
Species Zone B	-2761	-0.679	-4.628	<0.001
Species Zone C	-2605	-0.635	-4.108	<0.001
Species Zone D	-510	-0.649	-4.266	<0.001
Species Zone E	-232	-0.757	-5.792	<0.001
Species Zone F	-6	-0.729	-5.325	<0.001
Brackish Waterbodies	-412	-0.617	-3.923	0.001
Exposed Sediment	-814	-0.614	-3.889	0.001

Active Layer

The increased carbon density of the Exposed Sediment in the active layer relative to other sub-environments combined with expansive volume resulted in the sub-environment possessing the greatest unstandardised influence (-4420 kg) on overall carbon storage, despite the high (closest to zero) standardised beta value (-0.614). Alternatively, the influence of Species Zone A (standardised =-0.661) on overall carbon storage was comparatively reduced when compared to both Brackish Waterbodies and Exposed Sediment (larger for above-ground biomass) as the unstandardised beta value for Species Zone A was predicted to be 88.3% and 14.1% of the value for the two respective sub-environments. The unstandardised values of Species Zone E and F were closest to 0 despite

having the lowest (most negative) standardised values. Species Zone D possessed the 3rd highest (closest to zero) unstandardised value of -554 kg despite having the 3rd lowest standardised beta (-0.706). This was a result of the reduced overall active layer carbon storage compared to above-ground biomass in Species Zone D when compared to other sub-environments. All relationships were statistically significant as indicated by p values <0.05.

Table 5.41. Multiple regression parameters and the significance of predictor variables concerning watercourse proximity and sub-environment active layer carbon storage (kg).

Sub-environment	Unstandardised Beta (kg)	Standardised Beta	T	p
Species Zone A	-620	-0.661	-4.404	<0.001
Species Zone B	-1265	-0.679	-4.628	<0.001
Species Zone C	-1308	-0.635	-4.108	<0.001
Species Zone D	-554	-0.706	-4.461	<0.001
Species Zone E	-154	-0.757	-5.792	<0.001
Species Zone F	-6	-0.729	-5.325	<0.001
Brackish Waterbodies	-702	-0.617	-3.923	0.001
Exposed Sediment	-4420	-0.614	-3.889	0.001

5.3.4.5 – Multiple Regression Summary

The multiple regression analyses exhibit that gradient and watercourse proximity have a statistically significant influence on the spatial distribution of sub-environments and the carbon within the above-ground biomass and active layer. Although it is plausible that elevation influences sub-environment carbon distribution, the analyses indicate it has the smallest standardised influence whilst p values ≥0.14 in all sub-environments exhibit the influence is statistically insignificant (alpha level = 0.05). When the statistically significant influences of gradient and watercourse proximity are compared, watercourse proximity has the greatest standardised influence on carbon mass ranging from a decrease in -0.614 (Exposed Sediment) to -0.757 (Species Zone E) standard deviations per increase in one standard deviation of watercourse proximity. Alternatively, the standardised influence of gradient on carbon ranges from -0.384 (Species Zone A and Brackish Waterbodies) to -0.496 (Species Zone E). This exhibits the dual influence of both gradient and watercourse proximity on sub-environment and carbon distribution, although the influence of watercourse proximity is on average 1.6 times greater. Plausible explanations for the disparity between the significant influences, the insignificance of elevation and the variable levels of influence of gradient and watercourse proximity on different sub-environments will be the form the basis of discussion in Sections 6.2 and 6.3.

5.4 – Summary

Overall the results presented in Chapter 5 highlight the Ribble saltmarshes are comprised of a range of different sub-environments with variable carbon storage capacities which are uniquely influenced by elevation, gradient and watercourse proximity. The initial projections highlight that Exposed Sediment covered the largest area of ay sub-environment covering 9.36 km^2 (42.6%) whilst Species Zone C was the most expansive predominantly non-vegetated sub-environment covering 3.81 km^2 (17.3%). The remote and manual uncertainty analyses highlighted that there was the potential an areal uncertainty of 10% and 13.8% (max uncertainty both remote assessment) surrounds the two respective sub-environments, whilst the greatest proportional uncertainty surrounded Species Zone B (20% - manual assessment).

With regards to above-ground ground biomass OCD, Species Zone B and C had the highest mean carbon content of 1.19 kg/m^2 and 0.97 kg/m^2, whilst the predominantly un-vegetated sub-environment of Exposed Sediment had the lowest mean OCD of 0.12 kg/m^2 and was also surrounded by the greatest uncertainty (standard deviation = 108.3% of mean). Species Zone E and C had the highest sub-surface active layer mean OCDs of 4.26 kg m^{-3} and 4.12 kg m^{-3} whilst Exposed Sediment had the lowest 3.09 kg m^{-3}. The greatest active layer carbon uncertainties surrounded Species Zone F (standard deviation = 23.9%) and Species Zone D (standard deviation =19.3%).

The combination of results surrounding area and OCD exhibited that the above-ground biomass was projected to store 1.26 x 10^7 kg with Species Zone B and C contributing the greatest overall proportional of the carbon mass at 32.2% and 29.4% according to the original areal projection. However, it is plausible above-ground carbon could differ by a maximum of 54.5% of the original projection. Alternatively, the active layer sub-surface sediment was projected to contain 1.29 x 10^7 kg according to the original projection with Exposed Sediment and Species Zone C contributing 49.2% and 16.8% respectively. Due to the added uncertainty surrounding depth and the high uncertainty surrounding OCD of the more prominent Exposed Sediment, a theoretical maximal uncertainty of 65.8% surrounds the original active layer projection.

The multiple regression analyses indicated the influences of gradient and watercourse proximity were the only significant influences on all sub-environments. The influence of elevation was insignificant and had the smallest standardised influence on sub-environment and carbon spatial distribution. Watercourse proximity had the greatest standardised influence on spatial distribution and the influence was on average 1.6 times greater than gradient. Above-ground biomass and active layer carbon was concentrated in areas with an elevation between 4.2 - 4.6 m, with a gradient <2° and <10 m from a watercourse.

6 – Discussion

6.1 – Introduction

The distribution of carbon within temperate saltmarshes is controlled by a range of factors which determine the spatial distribution of different sub-environments and the carbon held within them (Sanderson and Uchin, 2002; Zhou et al. 2007; Roner et al. 2016). Whilst multiple factors influence species and carbon distribution: elevation, gradient and watercourse proximity have been exhibited to exert a key influence on this spatial variability (Silvestri et al. 2005; Suchrow and Jensen, 2010; Townend et al. 2011). However, there have been few studies which have attempted to assess the different influence of all three variables on saltmarsh sub-environment and carbon distribution. Consequently, this study has sought to determine sub-environment distribution in the saltmarshes of the Ribble estuary and to quantify the active section carbon storage capacity. The influences of elevation, gradient and watercourse proximity on both sub-environment and carbon distribution are subsequently assessed.

The results presented in Chapter 5 are now discussed and compared with relevant research in temperate saltmarshes. Specifically, the correspondence of the findings with ecological and geomorphological studies in saltmarshes is explored, whilst the influence of sea level rise on saltmarsh dynamics, carbon storage and coastal management is also considered (see Section 6.3).

6.2 – The Spatial Distribution of Sub-environments and Influence of Elevation, Gradient and Watercourse Proximity

6.2.2.1 – Overview

The assessment of landcover variability over the saltmarshes of the Ribble estuary highlights the presence of a variety of halophytes commonly found on UK saltmarshes. Of the predominantly vegetated environments (Species Zones A-F), all comprising species are commonly found on UK saltmarshes (National Biodiversity Atlas, 2018). The areal coverage of the different sub-environments expressed in Table 5.1 highlights that Species Zones A, B and C covered the greatest area covering 9.6%, 15.6% and 17.3% of the total area after Exposed Sediment (42.6%). This widespread presence of species including: *Agrostis stolonifera* (Species Zone A)*, Atriplex portulacoides* (Species Zone A and C), *Festuca rubra* (Species Zone B), *Elymus repens*, (Species Zones B and D) and *Puccinellia maritima* (Species Zone C) in vegetated areas conferred with the findings of other assessments concerning saltmarsh vegetational distribution in North West England (Gray, 1972; National Biodiversity Atlas, 2018).

As exhibited in Section 5.1.1 the areal projections for each sub-environment are surrounded by different levels of uncertainty however. Whilst the overall kappa coefficients for the respective remote and manual uncertainty analyses of 87.6% and 90.0% indicate an overall high level of classification accuracy, this respective 12.4% or 10% discrepancy in sub-environment classification highlights the coverage and spatial distribution of sub-environments could be markedly different than that indicated in Figure 5.1. Therefore a re-run of this study would potentially seek to employ the novel topographic method published by Goodwin *et al.* (2018) after this assessment. Such potential changes in sub-environment coverage would have direct and indirect implications on carbon storage due to the direct gain or loss of above-ground and sub-surface carbon in different sub-environments. Any change would also influence the ecological and geomorphological dynamics both between and in sub-environments and throughout the saltmarsh as a whole (Marani et al. 2006; French, 2019) (see Section 6.3).

According to the original observations, the overall elevation distribution of all saltmarsh sub-environments does not comply with the ramp-salinity hypothesis (e.g. Williams *et al.* 1994; Bao-Shan *et al.* 2011) (see Figure 3.1) as 7.3 % of all predominantly vegetated sub-environments were found between MHWN (2.20 mOD) and MHWS (4.10 mOD). However, 92.2% of all predominantly vegetated were within the elevation range of MHWS and HAT (5.10 mOD) and the interquartile range of all vegetated sub-environments was between 4.18 - 4.46 mOD (see Figure 6.1). This elevation distribution gives support to alternative saltmarsh vegetation distribution theories which suggest the ramp model alone is too simplistic and distribution is instead controlled by a multitude of factors (Zhang *et al.* 2013; D'Alpos and Marini, 2016). The alternative theories state the influence of dendritic creek penetration as well as variable levels of sediment porosity enable saline transportation and deposition in areas above MHWS allowing diverse saltmarsh halophyte colonisation (Silvestri *et al.* 2005; Kim *et al.* 2013; Wilson *et al.* 2014).

Although the ramp model proposed by Williams *et al.* (1994) does not apply to the marsh as a whole Figure 5.5 highlights the rapid decline in area of all sub-environments at an elevation equal to HAT at 5.10 mOD. This could be evidence that the saltmarsh vegetation distribution conforms with the saline stress and competition theory which states that terrestrial vegetation becomes predominant above 5.10 mOD (e.g. Pennings et al. 2005; Colmer and Flowers, 2008). However, it is more likely that this rapid decline exists due to the presence of landward dikes which create an artificial boundary between the saltmarsh and terrestrial environments and are designed to prevent periodic inundation (Townend et al. 2011).

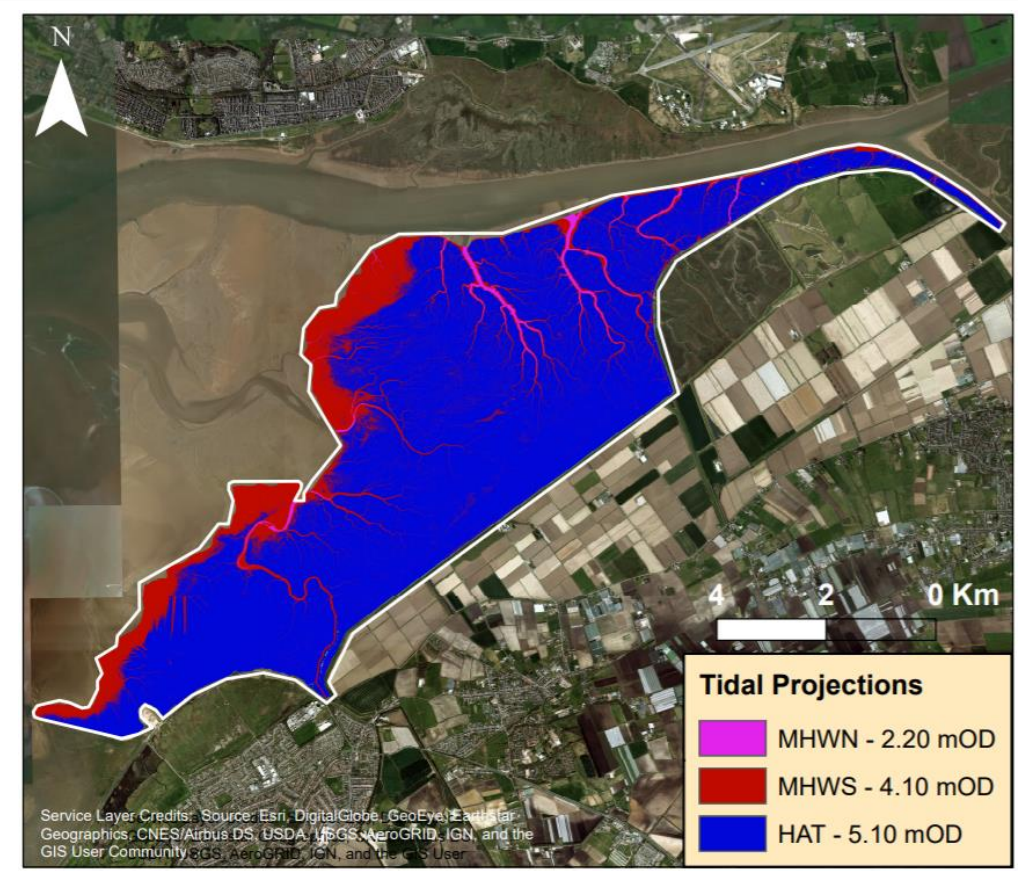

Figure 6.1 - Tidal height projections (2012) relative to land cover on Marsh C.

6.2.2.2 – Species Zone A

Species Zone A is predominantly composed of less tolerant halophytes being found at the highest mean elevation (4.56 mOD) and at the shallowest gradient (1.5°) of all sub-environments. The spatial position and elevation distribution of the environment the reflect previous findings (Olff et al. 1988; Gray, 1992; Skov et al. 2016) as the *Agrostis Stolonifera* dominated sub-environment is found at a higher elevation mean than all sub-environment types expect Species Zone F. This is best shown by Figure 5.7 which highlights the sub-environment occupies >18.9% of the overall area between 4.57 - 5.72 mOD. However, the multiple regression analyses (see Section 5.1.5) indicates that elevation has an insignificant influence on the spatial distribution of all sub-environments and instead gradient and watercourse proximity are the significant influences on Species Zone A distribution. The standardised beta values indicate that watercourse proximity has a greater influence on the distribution of Species Zone A than gradient with a standardised beta value of -0.661 as oppose to -0.384. This suggests the direct proximity of dendritic creeks and fluvial inflows have the greatest relative influence on sub-environment distribution, although the existence of the incised channels also directly affects gradient (Perillo, 2019). Previous research concerning the most populous species *Agrostis stolonifera* largely corresponds with the findings and confirms the predominant location of

the sub-environment in areas of close proximity to fluvial inflows and brackish channels in middle-higher marsh (Gray, 1972; Gehrels and Newman, 2004; Masselink et al. 2017). Moreover, the presence of the second most populous species *Atriplex portulacoides* potentially explains the sub-environment distribution throughout the saltmarsh as the species is commonly observed fringing channels and pools of higher salinity that are flooded at full tide (Redondo-Gomez *et al.* 2007). Likewise the mean watercourse proximity value of 23.3 m (the 3rd closest to watercourses of vegetated sub-environments) exhibits that the sub-environment is not confined to creek margins and is instead widely distributed throughout semi-saturated areas of middle-higher marsh (Bocklemann *et al.* 2002; Hulisz *et al.* 2016).

The other significant influence of gradient is comparatively reduced compared to the influence of gradient on other sub-environments as the Species Zone A has the joint-smallest standardised value of -0.384 (see Table 5.21). When compared to other sub-environments the comparably similar distribution of Species Zone A to Species Zone C is highlighted by the significant F value of 4.9 (Table 5.15). This comparative similarity in distribution may plausible occur because both sub-environments contain *Atriplex portulacoides* and are therefore likely to occupy areas with similar drainage. The 0.9° difference in mean gradient between Species Zone A and C results because the former is not as commonly found in steeper areas surrounding creeks which confers with the salinity tolerances of the respective comprising species (Colmer *et al.* 2008).

The similarity in species composition between Species Zone A and C is also apparent in the remote uncertainty assessment and confusion between sub-environments as 24/25 of the incorrectly classified results fall into the category of Species Zone C. Likewise, 29/35 incorrectly classified remote results for Species Zone C are classified as Species Zone A. Therefore, if the true area was 10.9% larger as indicated by the remote assessment the results would suggest Species Zone A would mostly displace Species Zone C. However the fact the one anomalous reading for the manual assessment was classified as Species Zone B may suggest Species Zone A would jointly displace the two sub-environments. Although the explanation for this one confused manual reading is undetermined, the remote confusion can be explained as Species Zones A and C both contain *Atriplex portulacoides* so therefore possess similar spectral signals. Regarding systematic uncertainty the RMSE of the Environment Agency LiDAR elevation data could potentially influence both elevation and gradient results, however there is no published or clearly anomalous observed evidence to suggest this error would have a disproportion influence on any localised area or sub-environment with certain elevation or gradient characteristics. The influence of this error on the largest significant factor watercourse course proximity is reduced as the difference between the

mean watercourse proximity of the sub-environments is in all cases greater than RMSE. Therefore, the conclusions regarding the proximity of Species Zone A relative to sub-environments remain valid.

The findings concerning Species Zone A (and all sub-environments) add further support to the theory rebuking the ramp model of distribution. The results (particularly the multiple-regression analyses) further support the opposing theory that the penetration of dendritic creeks and fluvial inflows have greater influence on key factors such as on salinity and anoxia which determine saltmarsh vegetation distribution (e.g. Engles *et al.* 2011; Veldhuis *et al.* 2019).

6.2.2.3 – Species Zones B, C and D

The findings indicate that a combination of gradient and watercourse proximity are the main significant influences on the distribution of Species Zones B, C and D, with watercourse proximity having the greatest significant influence. Although the similar IQRs of the three species potentially suggests elevation is a key control on the distribution (see Figure 5.5 and Table 5.11), the multiple regression analysis (Table 5.20) indicates elevation is not a significant influence.

Of the three sub-environments the standardised beta values indicated Species Zone B was most influenced by watercourse proximity (-0.679) with Species Zone C being the least influenced (-0.649). The greatest standardised decrease per metre of Species Zone B can be explained by the fact the sub-environment is predominantly composed of *Festuca rubra* which has lower salinity tolerance when compared to the other temperate marshes species (Kiehl et al. 1997; Suchro and Jensen, 2010). Therefore, a sub-environment with a high abundance of *Festuca rubra* would be expected to be found in areas of low salinity in the higher marsh (mean elevation = 0.38 m above MHWS). As the majority of the watercourses are tidal creeks as opposed to fluvial influences the low negative beta value and the increase in saltmarsh proportional area cover from 14.8% at 5 m from a watercourse to a maximum of 25.0% at 97 m conforms with the sub-environment ecology.

The reduced negative standardised beta value of Species Zone C perhaps reflects the predominance of *Atriplex portulacoides* which is a tolerant halophyte and a physiognomic dominant found widely across well-drained marshes and is less confined to creeks (Cott *et al.* 2013). The standardised beta value of -0.649 for Species Zone D perhaps also reflects the variable distribution of Species Zone D which is found in the higher marsh but also extends into the middle-lower marsh concentrated around the levees and terraces that define tidal creeks. This could be potentially explained the dual influence of *Elymus Repens* and *Puccinellia maritima* in the sub-environment. The presence of the latter plausibly explains the distribution of the species zone in areas where the sediments are

frequently waterlogged and exposed to highly saline conditions (Davy et al. 2011) such as those around the terraces and levees surrounding the tidal creeks networks. This is quantitatively exhibited indicated by the fact the Species Zone D has the lowest mean proximity to watercourses (20.4 m) of all sub-environments expect Brackish Waterbodies (Engels and Jensen, 2010). Alternatively, the presence of *Elymus repens,* would explain also the presence of the Species Zone D in the higher marsh where saline exposure is reduced (Barkowski *et al.* 2009).

Whilst the mean distance of Species Zone C to watercourses is 1.4 m higher than Species Zone D (21.8 m), the value of the 1st quartile of 7.3 m and an IQR 0.7 m wider than Species Zone D (see Figure 5.20 and Table 5.17), perhaps reflects the predominance of *Atriplex portulacoides* in Species Zone C. Moreover, the presence of saline and saturation resistant *Puccinellia maritima* in both Species Zones C and D confers with their spatial gravitation around watercourses and tidal creeks in particular, although Species Zone C on average occupies lower elevations 0.14 m lower than Species Zone D. This discrepancy could be explained by the fact the 3rd and 4th most prominent species in Species Zone C, *Cochlearia officinalis* and *Sueda Maritima*, are also highly tolerant to saline exposure as well as resistant to waterlogging and therefore could tolerate more frequent inundation at lower elevations (Alhdad et al. 2013; de Vos *et al.* 2013). Therefore, it is unsurprising that there is a general concentration of Species Zone C on creek benches and also in the depressions between the levees predominantly occupied by Species Zone D (see Figure 6.2).

Alternatively, the significant influence of gradient had the largest effect on Species Zone D (standardised beta = -0.429) when compared to Species Zone B (-0.41) and C (-0.409). This potentially could have been predicted given the gravitation of *Puccinellia maritima* predominantly on the top of creek levees whilst it was rarely present on the steeper vegetated levee slopes (see Figure 6.2). The disparity of 0.001 in standardised beta values for Species Zones B and C also appears to highlight the similar influence of gradient of the two species zones which have the same mean gradient value of 2.4° despite occupying different areas and being comprised of different species. This is perhaps best indicated by the proportional areal coverage results which highlight the proportion of the saltmarsh covered by each Species Zone B and C consistently ranges from 16-19% from 0-20° (Figure 5.14 and 5.16). The findings combined with fact five sub-environments have a mean gradient value between 2.4 – 2.7° highlights that gradient remains largely constant throughout the marsh and localised areas of high gradient variability do not reflect the marsh as a whole.

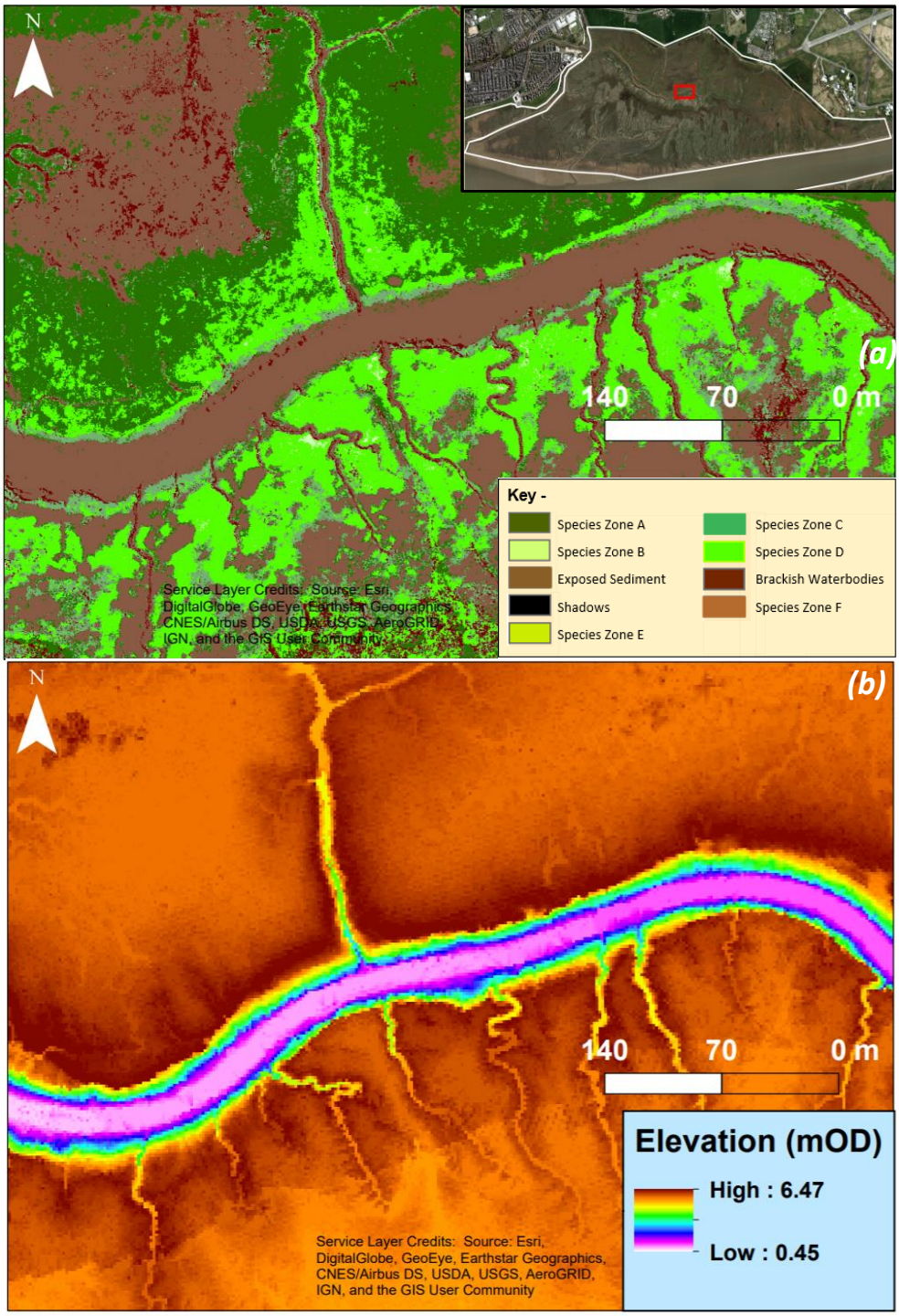

Figure 6.2 (a-b). A comparison of sub-environment distribution and elevation around a major creek in Marsh B

6.2.2.4 – Species Zone E

Species Zone E has the lowest median (4.23 mOD) and mean (4.03 mOD) elevation of all sub-environments. This conforms with the relevant research as *Spartina Anglica* and *Salicornia spp.* have high salinity tolerances and are commonly associated with lower marsh environments (e.g. Armstrong et al. 1985; Williams et al. 1995). The elevation distribution Species Zone E and the fact the sub-environment covers the greatest proportion of the overall saltmarsh at 4.0 mOD (8.2% see Figures 5.7 and 5.9) corresponds with Gray's (1972) region-specific assessment of species elevation distribution of *Spartina Anglica* and *Salicornia spp.* (35 km away) Morecambe Bay (35 km away) (see Figure 6.3).

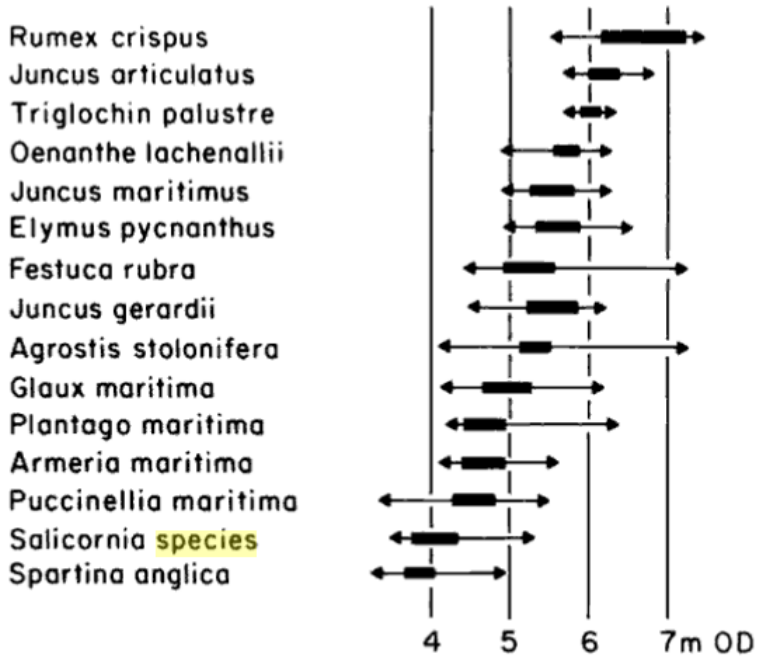

Figure 6.3. Elevation distribution of saltmarsh species in Morecambe Bay. The IQR is indicated by the dark box, whilst the overall range is shown by maximal extent of the arrows. (Source: Gray, 1972)

However, the multiple regression analyses indicated elevation had an insignificant influence (Table 5.20) on the sub-environment distribution. Alternatively, gradient and watercourse proximity had a significant influence on sub-environment distribution although the gradient standardised beta value was 0.261 closer to zero, indicating an increase watercourse proximity resulted in a greater standardised decrease in areal cover. Species Zone E was also the most influenced of all sub-environments by watercourse proximity with a standardised value -0.757 despite the 2nd lowest unstandardised value of 4.32 x 10^{-4} km^2 which was a result of the small area coverage of the sub-environment of 0.46 km^2 (original assessment).

The gravitation of Species Zone E to the lower and pioneer marsh areas in close proximity to watercourses is also partially indicated by the gradient findings which exhibit the sub-environment has the highest first quartile (0.9°), median (1.8°) and third quartile (3.0°). Such findings are indicative of the steep gradients of the lower marsh as marsh topography commonly increases in the exposed pioneer and lower zone, especially if the marsh is situated on a levee of a main estuarine channel (e.g. Sanderson et al. 2000; Silvestri et al. 2003; Hladik and Alber, 2012).

Likewise, the proximity from watercourse statistics (mean proximity = 29.5 m) along with the visual distribution of species (see Figure 5.1) also highlights the spatial clustering of Species Zone E around the largest estuarine channels with highly developed levees. However, there is an absence of Species Zone E around the smaller creeks channels which cover that are characterised by distinctive creek terraces and benches. These findings potentially indicate a link between the significant influences of gradient and watercourse proximity and species distribution as comparatively steep topography of the lower levees theoretically enhances drainage creating suitable conditions for *Spartina Anglica* and to a lesser extent *Salicornia spp.* (Tsuzaki, 2010). However, these species are outcompeted by other tolerant halophytes such as *Puccinellia maritima* in waterlogged environments were gradient is shallow and the drainage poor such as in the depressions between creeks (Cooper, 1982; Davy et al. 2011). This therefore plausibly explains the enhanced presence of Species Zones C and D in developed creeks in the middle-higher marsh and comparative absence of Species Zone E.

Regarding uncertainty, it is plausible that the sub-environment areal coverage could differ by 13.3% according to the remote assessment (Table 5.2). Although this would theoretically only influence 0.06 km^2 of the total area, 16 and 4 of the 22 anomalous classifications are categorised as Exposed Sediment and Brackish Waterbodies. If this area was covered by predominantly un-vegetated sub-environments this would have a direct impact on carbon storage but also substantially influence interconnected ecogeomorphological processes in the lower marsh. This change would potentially enhance saltmarsh degradation as a result of enhanced rates of erosion and a reduction in accretion, as the dissipating impact of *Spartina Anglica* and *Salicornia spp.* would be reduced (Van der Wal and Pye, 2004; Sheehan and Ellison, 2015).

6.2.2.5 – Species Zone F

Whilst the majority of sub-environments exhibit relatively consistent trends throughout the entire saltmarsh, Specie Zone F covers only 20775 m^2 entirely in the western higher marsh of Marsh C. This comparative sparsity of *Eleocharis uniglumis* conforms with a national saltmarsh assessment which indicates that despite being rare nationally, the enhanced rainfall on western British coast enhances

the probability of the appearance of species on in areas the region (Boorman, 2003). The multiple regression analysis indicates watercourse proximity has the largest significant influence with a standardised beta value of -0.729 making the sub-environment the 2nd most influenced by watercourse proximity. The average distance (52.8 m) of Species Zone F from any watercourse in combination with the high mean elevation (4.70 mOD), highlights further similarities with the relevant research which points to the gravitation of the main comprising species *Eleocharis uniglumis* in areas which are seldom inundated with saline water away from watercourses and particularly creeks (Sanchez et al. 1996; Pigott et al. 2000). The high mean elevation and narrow elevation range (4.40 – 5.15 mOD) conforms with the findings of Sanchez *et al.* (1996) who found the species at the had a narrow elevation range and was found at the highest elevation of all species in their study on a temperate European saltmarsh environment. The ANOVA analysis also highlighted the unique elevational distribution of the sub-environment as the significant T-values ranged between 197.4 – 632.3 for all sub-environments expect Exposed Sediment (T-value = 5.0) whilst elevation had an overall insignificant influence on spatial distribution (p=0.208).

The other significant influence of gradient had less influence on sub-environment areal decrease (standardised beta = -0.448) than watercourse proximity although the sub-environment was the 2nd most influenced by gradient increase. This corresponds with the location of Species Zone F in an area of low mean gradient (1.7°) and devoid of creeks as the gradient increase had a large standardised influence on the reduction of sub-environment area. The location of the sub-environment in an area where tidal access has been disturbed by the construction of dykes also shows correspondence with previous research which highlights that tidal restriction enables *Eleocharis uniglumis* to replace more tolerant halophytes in areas of low gradient, prone to the accumulation of stagnant rain water (Dijkema, 1990).

The original remote areal assessment indicates a 13.3% uncertainty surrounds the sub-environment and a two-way confusion correspondence exists with Brackish Waterbodies. This most probably arises due to the similar spectra of the dark brown sub-environments which are located in brackish areas. However, if Species Zone F increased in areal cover by 13.3% displacing 2763 m^2 of Brackish Waterbodies, the influence on above-ground (746 kg more assuming mean OCD disparity) and active layer (1020 kg less assuming mean OCD disparity) carbon storage and ecogeomorphological dynamics would be minor (see Section 6.3).

6.2.2.6 – Exposed Sediment and Brackish Waterbodies

The sub-environment broadly defined as Exposed Sediment was predominantly comprised of exposed silt and sand at the seaward perimeter as well as within creek and saltpans. This spatial distribution at a low mean elevation 0.05 m below MHWS (4.10 mOD) conforms with the theory increased hydroperiods and saline stress at low elevation results in a reduction in vegetation (Bertness *et al.* 1992; Engels and Jensen, 2010; Moffett *et al.* 2010). Moreover, the influence of enhanced erosion by wave action and creek flows also prevents colonisation in regularly inundated areas at close proximity to watercourses leading to the classification as Exposed Sediment (Letzsch and Frey, 1980; Marini et al. 2011; Leonardi et al. 2016). However, the kernel density plot (Figure 5.5) for the sub-environment highlights a wide elevation distribution which is to be expected given the broad definition and it therefore unsurprising elevation is not a significant influence on distribution.

The wide distribution of the sub-environment over the saltmarsh is also reflected by the significant standardised beta scores for gradient (-0.614) which is the joint 5th highest (closet to zero). Given the wide distribution of the Exposed Sediment across all areas of the marsh which is highlighted the sub-environment proportional areal cover compared to watercourse proximity (see Figure 5.21) it is unsurprising the sub-environment has the lowest standardised beta value for watercourse proximity of -0.614. It is also predictable that Brackish Waterbodies has the second-lowest value of -0.627 as it is plausible this could be attributed to the fact this sub-environment also comprises salt pans with no clear outflow or inflow (i.e. watercourse) as they are instead filled with stagnant brackish water from high tides and rainfall (Townend *et al.* 2011). The widespread presence of such salt pans is also indicated by the proportional area cover which highlights the proportion of area defined as Brackish Waterbodies increases to a maximum of 9.1% at 118 m although only 0.3% of total marsh area is found at this distance.

It is possible a confusion anomaly exists between the two sub-environments which are surrounded by a maximal areal uncertainty of 10% (Exposed Sediment – remote) and 14.3% (Brackish Waterbodies – manual). Although the remote assessment indicates confusion for Exposed Sediment is more commonly associated with Species Zone E (35/56) 16 of the anomalous classifications are classified as Brackish Waterbodies (see Table 5.3). Whilst the only anomalous result from the manual classification indicates confusion with Species Zone F, the remote classification for Brackish Waterbodies (uncertainty = 12.6%) identifies Exposed Sediment as being the main source of confusion (13/19). This two-way confusion is unsurprising purely given the gravitation of both

environments to creek channels and the similar spectral signatures produced from semi to fully saturated uncovered sediment. However, if Exposed Sediment hypothetically covered the maximal or minimal extent indicated by the uncertainty assessment, the confusion relationship connecting the sub-environment and Species Zone E would have a more substantial impact on overall saltmarsh carbon storage and ecogeomorphology than the relationship between the two predominantly un-vegetated sub-environments (Kirwan *et al.* 2010; Sheehan and Ellison, 2015).

6.3 - The Distribution of Carbon within the Ribble Estuary

As is shown in Section 5.2 and 5.3 the different sub-environments that comprise the saltmarshes of the Ribble estuary have different active section carbon storage capacities (i.e. the above-ground and active layer). This carbon distribution is influenced by a range of interconnected ecological, hydrological and geomorphological processes which dictate the sub-environment distribution (e.g. Silvestri and Marani, 2004; Belliard et al. 2017 D'Alpaos et al. 2019) (see Section 5.3). However, the sub-environments and the carbon within them does not exist independently as saltmarshes are inherently interconnected ecosystems (Alizad *et al.* 2016; D'Alpaos and Mariani, 2016). The relationships between ecology, geomorphology and carbon storage on the Ribble saltmarshes will form the basis of the discussion in the following section.

6.3.1 – Above-ground Carbon Storage

The above-ground biomass part of active section in this study is directly influenced by the interconnected ecological, hydrological and geomorphological processes (Kim *et al.* 2010; Da Lio *et al.* 2013). As is indicated in Table 5.26 the original remote assessments projected that 1.26 x 10^7 kg of carbon is stored within the above-ground mass of the saltmarshes of the Ribble estuary (see sub-section 5.3.2.1), although this mass was unevenly distributed between sub-environments. The above-ground OCD was on average highest in Species Zone B (1.19 kg/m^2) whilst Species Zone C which has the 2nd mass of carbon mass per m^2 (0.97 kg/m^2) (see Table 5.23) which consequently stored a disproportionally high carbon mass of 32.2% (areal cover 15.6%) and 29.4% (areal cover 17.3%) respectively. The high carbon mass of Species Zone B directly reflects the ecological properties of the comprising species of *Festuca Rubra* and *Triglochin maritima* in particular, which have a high biomass per unit area compared to the majority of other saltmarsh species where there is a plentiful supply of N, P and K (Groenendijk, 1984; Kiehl et al. 1997). This confers with the spatial distribution of 95.7% of Species Zone B on Marsh C in areas of low gradient at close proximity to agricultural land where N, P and K (within artificial fertilisers) is likely to be transported by fluvial drainage channels (Olsen *et al.* 2011). The net result of the expansive cover and high carbon density is that Species Zone B stores the most above-ground carbon of any sub-environment at 4.06 x 10^6 kg, although in theory this mass could differ a maximum of 45% meaning the Species Zone C original projection of 3.71 x 10^6 kg is greater than the Species Zone B lower-bound estimate. Determining why this maximal uncertainty surrounds Species B leads back to the assessment of OCD variability and areal cover, which highlights the areal cover as the largest source of uncertainty due to the 20% uncertainty surrounding the manual assessment (remote 89.6%). As the confusion matrices for both the manual and remote uncertainties highlight that the only anomaly in the manual assessment

(Table 5.6) and 17/27 of anomalies in the remote assessment were classified as Species Zone D, this could mean a greater mass of carbon is concentrated within the latter which only hold 7.28 x 10^5 kg according to the original projections.

The high average above-ground carbon biomass of Species Zones A (0.94 kg/m^2) and Species Zone C (0.97 kg/m^2) also confers to an extent with previous research as both sub-environments contain *Atriplex portulacoides* which has been found to have the highest biomass of any species on Northern-western European saltmarshes (Groenendijk, 1984; Bouchard and Lefeuvre, 2000). Whilst the mean carbon mass of both sub-environments are outside the standard deviation range for *Atriplex portulacoides* stated by Rupprecht et al. (2015) of 0.56 kg/m^2 ± 0.23 kg/m^2, when the standard deviations of ± 0.33 kg/m^2 (Species Zone A) and ± 0.43 kg/m^2 (Species Zone C) along with the influence of the other species and seasonal variability is considered the results are not overly dissimilar and highlight the high carbon density of *Atriplex portulacoides* compared to other in saltmarsh species. The overall influence of the uncertainties is that Species Zones A and C could respectively contain 47.5% and 58.5% more or less carbon than the 1.99 x 10^6 kg and 3.71 x 10^6 kg indicated in the original projections assuming mean OCD. Due to the sub-environment spatial distribution the influences of these uncertainties are largest (absolute mass) at <10m from a watercourse. Therefore, despite the fact gradient and watercourse proximity have smaller standardised beta values than other sub-environments of -0.661 and -0.635, the unstandardised loss per m from a watercourse is the third and second highest for Species Zone A (-1370 kg) and Species Zone C (-2610 kg) respectively due to the high above-ground carbon mass of each sub-environment. (see Figure 6.4(B)). This is also true for the other significant influence of gradient (see Figure 6.4(C)).

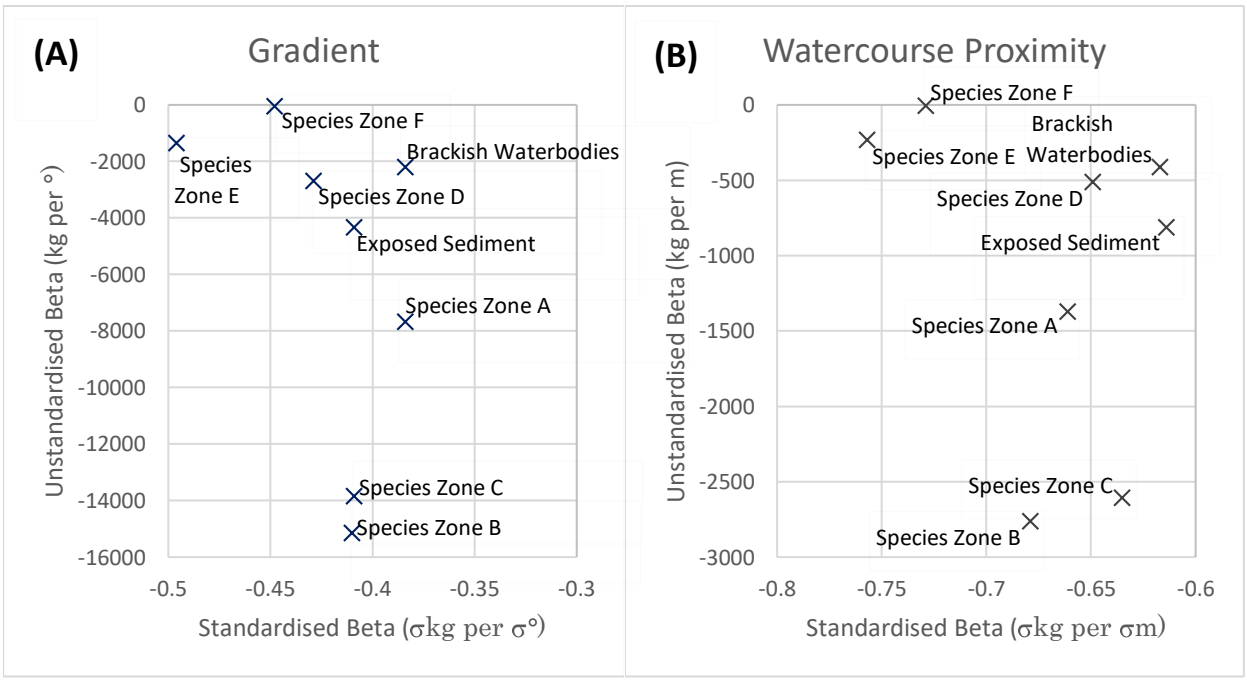

Figure 6.4. A comparison of standardised and unstandardised beta values for the two significant influences on sub-environment and above-ground carbon spatial distribution.

The *Puccinellia maritima* and *Agropyron pungens* dominated Species Zone D had a mean above-ground carbon mass of 0.79 kg/m^2 and contributed the greatest proportion of overall saltmarsh carbon at a distance 10-20 m from a watercourse at 4.7% (Figure 5.23). This distribution combined with fact Species Zone D is only the 5th most influenced (standardised = -0.661) by watercourse proximity highlights that whilst watercourse proximity does influence the sub-environment and carbon distribution, the sub-environment is predominant distributed in the seldom inundated higher marsh and on certain well-developed levee's surrounding mature creek systems. The moderate level of above-ground biomass stored in Species Zone D totalling 7.28 x 10^5 kg (original projection) can potentially be explained by the fact the biomass of *Puccinellia Martimia* has been exhibited to temporally fluctuate more than other common temperate saltmarsh species, as the winter biomass (and so carbon mass) can fall below 50% of the biomass values for late summer and autumn (Rouger, 2014). This peak in biomass productivity corresponds with the timing of increased solar radiation and the occurrence of spring tides which supply nutrients to the higher marsh and levees collectively increasing biological productivity of *Puccinellia maritima* (Oenema and De Laune, 1988; Touchette *et al.* 2019). However, throughout the year the mean biomass of *Puccinellia maritima* has been exhibited to be lower than that of species such as *Atriplex portulacoides* (Species Zones A and C) and *Spartina Anglica* (Species Zone E) (Groenendijk and Vink-Lievaart, 1987; Boorman and Ashton, 1997) which is reflected in the results taken in the winter months.

The lowest above-ground biomass carbon density values were found in sub-environments defined as Brackish Waterbodies (0.33 kg/m^2) and Exposed Sediment (0.12 kg/m^2). This can be explained by the fact both sub-environments are commonly found at low elevations and at close proximity or within waterbodies where a combination of increased salinity stress, waterlogging and erosion from wave action and flow within channels partially inhibits colonisation of these areas (Leonard and Luther, 1995; Townend *et al.* 2011). However, it is plausible that such areas may contain more carbon as according to the maximal estimates Brackish Waterbodies and Exposed Sediment could collectively contribute up to 6.05 x 10^5 kg (13.9%) more above-ground carbon at distances <10m to a watercourse (see Figure 5.40(g) & (h)). Moreover, as watercourse proximity has the largest significant standardised influence on above-ground carbon storage in Brackish Waterbodies and the majority (39.4%) of carbon within the sub-environment is found within <10 of a creek, potential SLR-driven creek expansion (Hughes *et al.* 2009) has the greatest potential to directly influence the areal cover and carbon storage capacity in the sub-environment more than any other (see Section 6.4).

The location of Species Zone E (0.78 kg/m^2) at lower elevations highlighted that lower marsh species such as *Spartina Anglica* and *Spartina spp*. with higher salinity tolerances had the potential to be substantial stores of above-ground carbon (Morris and Jensen, 1998; Cacador et al. 2004). Despite

covering only 2.1% of the overall saltmarsh area, the high proportional coverage of Species Zone E which ranged from 6.7% to 8.2% between 3.2 to 4.0 mOD and the mean above-ground carbon mass of 0.78 kg/m^2 served to reduce the gradient of carbon decrease with elevation from 4.0 mOD to 2.20 mOD (lower boundary for Species Zone E) after which Exposed Sediment predominated (>99.9% areal coverage). The spatial clustering of Species Zone E on the levees surrounding the main estuarine channels was also highlighted by the fact it had the greatest negative standardised beta values for both gradient (-0.496) and watercourse proximity (-0.757). Although the unstandardised decreases of -1340 kg per degree and -232 kg per m were the smallest due to the areal coverage, the distribution in the lower-pioneer marsh and ecogeomorphological importance of *Spartina Anglica* and *Spartina spp*. renders the sub-environments particularly important under a sea level rise scenario where submergence and creek incision is likely (Pont et al. 2002; Sheehan et al. 2014). The potential ecogeomorphological impacts of SLR on the spatial distribution and carbon storage of Species Zone E and the interconnected sub-environments are reviewed in Section 6.4.

6.3.2 – Active Layer Carbon Content

Whilst the carbon stored within the above-ground biomass is a key component of the saltmarsh carbon stocks, the storage potential of the active layer is projected to be 1.03 x 10^5 kg greater (1.29 x 10^7 kg) than the that of the above-ground biomass (1.26 x 10^7 kg) according to the original area and average depth assessment (see section 5.3.2.2). As explained in Section 3.3.2 the surface vegetation and above-ground biomass influences the geomorphological characteristics and the carbon capacity of active layer (sub-surface section of the active section). The results presented in section 5.2.5.4 exhibit that a degree of linear correlation (r^2= 0.44 and p=<0.001) exists between all sub-environments, although the deviation of Species Zone E and Brackish Waterbodies from the linear trend and uncertainty surrounding the overall sub-environment projections suggests this relationship is sub-environment specific (e.g. Kelleway *et al.* 2016; Roner *et al.* 2016).

In order to determine how the carbon stocks of the Ribble compared with other similar environments and analyse the ecological and geomorphological relationships between above-ground biomass carbon and sub-surface content, the results of this study were compared with the input results and projections of the Saltmarsh Carbon Stock Predictor (SCSP) (Skov *et al.* 2016; Ford *et al.* 2019) (see Figure 6.5). The SCSP findings offered a reliable comparison as they consist of four separate models designed to predict the carbon stock (kg m^{-3}) of the first 10 cm of saltmarsh sediment, whilst the average active layer depth for the comparable Species Zones A, C and D which contained the same species featured in SCSP was 12.9 cm.

Moreover, the SCSP data was sourced from 23 saltmarsh sites on the Welsh coast as well as six saltmarshes in Morecambe Bay and the Thames estuary, many of which shared similar ecological and geomorphological characteristics to the Ribble (Halcrow *et al.* 2010c; Halcrow, 2013; Ford *et al.* 2019). Subsequently, comparisons were drawn between relevant findings of this research (see section 5.3.2.2) as well as the contributing data used to form the overall SCSP model projections (see Figures 6.5). The analysis underpinning the SCSP predictions accounted for 37%, 40% and 44% (i.e. r^2 value) of the spatially observed variation in carbon stock for SCSP Models 1, 3 and 4 respectively, whilst SCSP models 3 and 4 take into account the basic sediment composition of the surface layer (i.e. clay, loam or sand).

A comparison of the results exhibits that the mean and standard deviation of carbon within the active layer (samples with a mean OCD >15% than the overall sub-surface sediment which possessed undecomposed organic material) of the relevant species zones predominantly fall within the SD range of the majority of the relevant SCSP findings and projections. This is particularly the case for sub-environments Species Zones C (2^{nd} most abundant species) and Species Zone D (1^{st} most abundant species) which contain *Puccinellia Maritima* (see Figure 6.5(c)), although the value for Species Zone C is 0.32 kg m^{-3} closer than the latter to the SCSP model 4 projections clay/silt dominated sub-environments. As the active layers of Species Zone C and D were predominantly composed of organic silt it could explain why the mean values for Species Zone C are D >0.93 kg m^{-3} than the SCSP Model 3 and 4 projections for sand dominated environments (Figure 6.5(c) - 19 and 21) which are associated with lower levels of organic material and therefore carbon stocks. Whilst the SD surrounding the average Species Zone C active layer carbon stock is only 0.10 kg m^{-3} less than the SD surrounding SCSP Model 4 projections, this disparity increases to 0.69 kg m^{-3} for Species Zone D where the mean carbon content is greater than every finding except the observation at Malltraeth (SD = 1.6 kg m^{-3}).

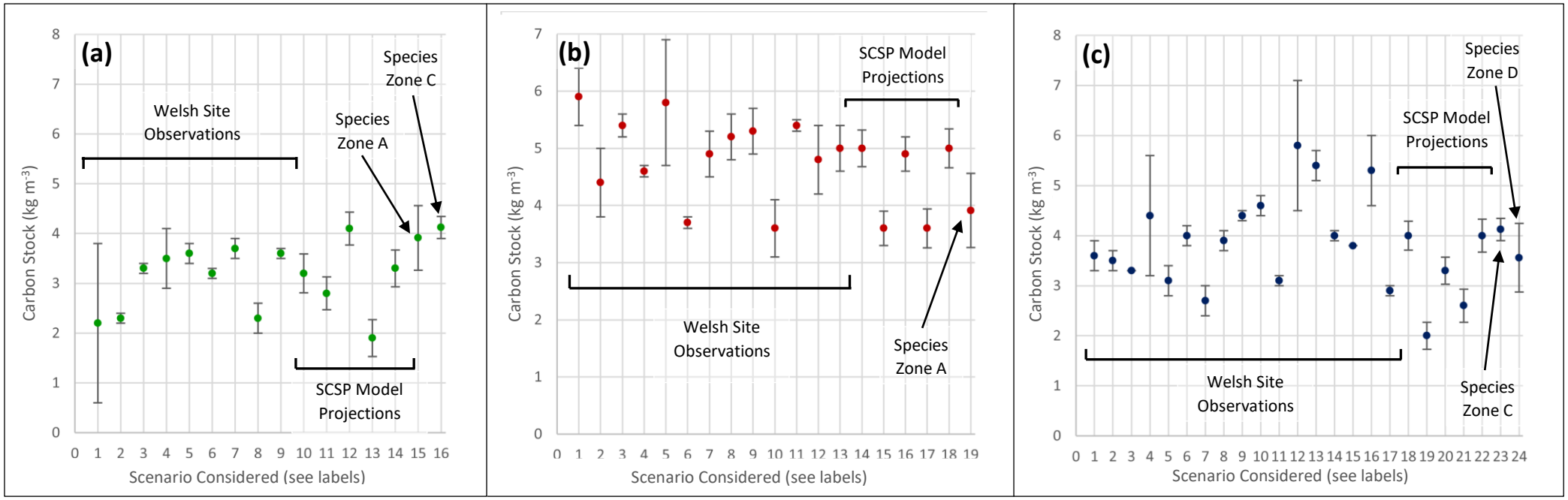

Figure 6.5. Correspondance between the findings of this research and SCSP carbon stock projections (kg m^{-3}) where *Atriplex portulacoides (a), Juncus gerardii (b) and Puccinelia Martima (c)* was the predomiant , 2nd or 3rd most numerous species. Projections are derived from findings in different marshes on the welsh coast where the respective species predominated, the relevant SCSP model projections sourced from this data (Skov *et al.* 2016; Ford *et al.* 2019) and the active layer of relevant sub-environments in this study where either species (a), (b) or (c) was the predominant species or 2nd most numerous. The error bars represent standard deviation.

The findings and projections which correspond with the x-axis value as follows (predominant sediment composition/grain size is also indicated):

(a) : 1= Malltraeth - Sand and Silt loam, 2= Shell Island - Clay loam, 3 = The Gann - Clay loam, 4 = Sandy Haven - Clay loam, 5 = Laugharne Castle – Clay, 6 = Black Scar - Clay loam, 7 = Gwendraeth - Clay loam, 8 = Pembury Burrows - Silt clay with loam, 9 = Salthouse Point - Clay loam, 10 = M1 SCSP, 11 = M3 SCSP Sand, 12 = M3 SCSP Clay/Silt, 13 = M4 SCSP Sand, 14 = M4 SCSP Clay/Silt, 15 = Species Zone A and 16 = Species Zone C.

(b) : 1= Morfa Madryn - Organic Sediment, 2= Malltraeth - Silty Loam, 3 = Four Mile Bridge - Silty clay loam, 4 = Y Foryd - Organic clay loam, 5 = Fairbourne – Loam, 6 = Ynys Hir - Clay loam, 7 = Dyfi West - Silty clay loam, 8 = Black Scar - Organic Loam, 9 = Trefenty - Organic Sediment, 10 = Cor-y-barlys - Organic Sediment, 11 = Gwendraeth- Loam, 12 = Gowerton - Organic Sediment, 13 = Landimore - Clay loam, 14 = M1 SCSP, 15 = M3 SCSP Sand, 16 = M3 SCSP Clay/Silt, 17 = M4 SCSP Sand, 18 = M4 SCSP Clay/Silt and 19 = Species Zone A.

(c) : 1= Morfa Madryn - Organic loam, 2= Four Mile Bridge - Silty clay loam, 3 = Y Foryd - Clay loam, 4 = Morfa Harlech - Clay loam, 5 = Shell Island - Clay loam, 6 = Dyfi North - Clay loam, 7 = Ynys Hir – Loam, 8 = Dyfi West - Silty clay loam, 9 = The Gann - Clay loam, 10 = Sandy Haven - Clay loam, greater clay proportion, 11 = Black Scar - Clay loam, 12 = Trefenty - silty clay with clay loam, 13 = Gwendraeth – Loam, 14 = Pembury Burrows - Clay loam, 15 = Morfa Mawr- Clay loam, 16 = Gowerton – Loam, 17 = Landimore - Silt and loam, 18 = M1 SCSP, 19 = M3 SCSP Sand, 20 = M3 SCSP Clay/Silt, 21 = M4 SCSP Sand, 22 = M4 SCSP Clay/Silt, 23 = Species Zone C, 24 = Species Zone D.

The comparison between the findings concerning *Atriplex portulacoides* (Figure 6.5(a)) highlighted that the mean carbon stock of Species Zones A and C was greater than was found in 8 of the 9 marshes were the species predominated. However, the Model 3 SCSP Clay/silt projections of a mean carbon stock of 4.1 kg m^{-3} was comparable to the mean value for Species Zone C of 4.12 kg m^{-3} which possessed silt dominated active layers. However, the fact Species Zone A was also greater than the majority of field findings and projections could suggest that the other comprising species served to either directly or indirectly increase active layer carbon stock.

The findings concerning *Juncus gerardii* (Figure 6.5(b)) alternatively highlighted that the active layer of Species Zone A on average had a lower carbon density than the marshes surveyed by Skov *et al* (2016) and Ford *et al* (2019). However, although the two sites which had lower average carbon stocks at Ynys Hir (3.7 kg m^{-3}) and Cor-y-barlys (3.6 kg m^{-3}) had a similar organic loam sediment composition to Species Zone A, there was a greater degree of correspondence between the mean projections of the SCSPs models (3 & 4) for sand dominated sediments (3.6 kg m^{-3}) rather than the SCSPs models for clay/silt dominated sediment.

Whilst the findings from this project and the work of Skov *et al.* (2016) and Ford *et al.* (2019) highlight variability in terms of both active/surface layer carbon density, it is also highly plausible that this variability between the results of this project may exist due to the variety of species in each sub-environment and ecogeomorphological localised influences. This particularly applies to the relationship between *Juncus gerardii* and Species Zone A in which it is only the 3rd most prominent species. The difference in species could likely produce a disparity in both the mean and SD between the defined species zones of this project and the species-specific projections and findings of Skov *et al*. (2016) and Ford *et al.* (2019) (Groenendijk and Vink-Lievaart, 1987; Bai et al. 2016; Kelleway et al. 2017). However, none of the findings concerning Species Zone A, C and D and the respective species appear anomalous in Figure 6.5.

With regards to the relationship with carbon and depth there is a consistent difference between the active layer carbon content and the fossil horizons in all sub-environments. This difference in the carbon density between the active layer and sub-surface horizons is lesser in predominantly unvegetated sub-environments such as Brackish Waterbodies when compared to predominantly vegetated areas as the difference between the mean active layer and sub-surface OCD reduces to 17.7% in Brackish Waterbodies compared to the overall mean difference of 43.5% (see Section 5.2.2.3). Moreover, the mean active layer for Exposed Sediment of 3.09 kg m^{-3} is 0.66 kg m-3 (17.6%) less than the overall mean for all sub-environments and 1.17 kg m^{-3} (27.5%) less than the maximal mean active layer OCD in predominately vegetated Species Zone E (4.26 kg m^{-3}). This suggests that

the carbon content of the active layer is likely to be directly influenced by the ecological and geomorphological surface processes in vegetated sub-environments as highlighted in Section 5.2.2.4 and 6.2.1 (Cacador et al. 2004; Kulawardhana et al. 2015). The findings conform with established research in predominately vegetated saltmarsh environments, which highlight an exponential decrease in OCD between the ecogeomorphologically connected organic-rich active surface layers and fossil layers at greater depth (Mishra *et al.* 2009; Bai *et al.* 2016) (see Figure 6.6 for comparison with Bai *et al.* 2016). This disparity arises due to the high levels of surface layer biological productivity which is a result of periodic deposition of nutrients through tidal and fluvial deposition (Zhou *et al.* 2007; Andrews *et al.* 2008; Sousa *et al.* 2010). Alternatively, the progressive decomposition of organic matter over time and reduced biological productivity results in a lower fossil layer OCD and an exponential reduction of OCD with depth (Cacador *et al.* 2004; Mishra *et al.* 2009; Mudd *et al.* 2009).

Despite the low density of the sub-environment defined as Exposed Sediment the combination of the large areal coverage (42.6% original projection), high carbon uncertainty (areal and OCD maximum = 118.3%) and close proximity to watercourses render the sub-environment the largest and potentially most important store of active layer carbon. If the maximal uncertainty for volume and OCDs are assumed it is theoretically possible could contribute 5.35 x 10^6 kg or 84.6% more carbon than indicated in the original projections. Moreover, the association of the sub-environment with watercourses means that the mass of carbon within 10 m of a watercourse could increase by 45.4% of the overall mass indicated in the OA x AD projection, whilst areas with a gradient >10 (i.e. surrounding developed creeks) could increase by 100.4% due to the predominance of Exposed Sediment in such areas. If the maximal uncertainties are correct any potential headward creek expansion or submergence of the lower marsh sub-environments (i.e. Species Zone E) may not lead to as substantial sub-surface carbon loss as predicted assuming mean OCD due to the high active layer volume and carbon content of Exposed Sediment. However the loss of predominantly vegetated sub-environments would have direct impacts on above-ground biomass and a subsequent range of ecogeomorphological consequences that would alter carbon storage dynamics throughout the saltmarsh (e.g. Valentim et al. 2013; Kulawardhana et al. 2015) (see section 6.4).

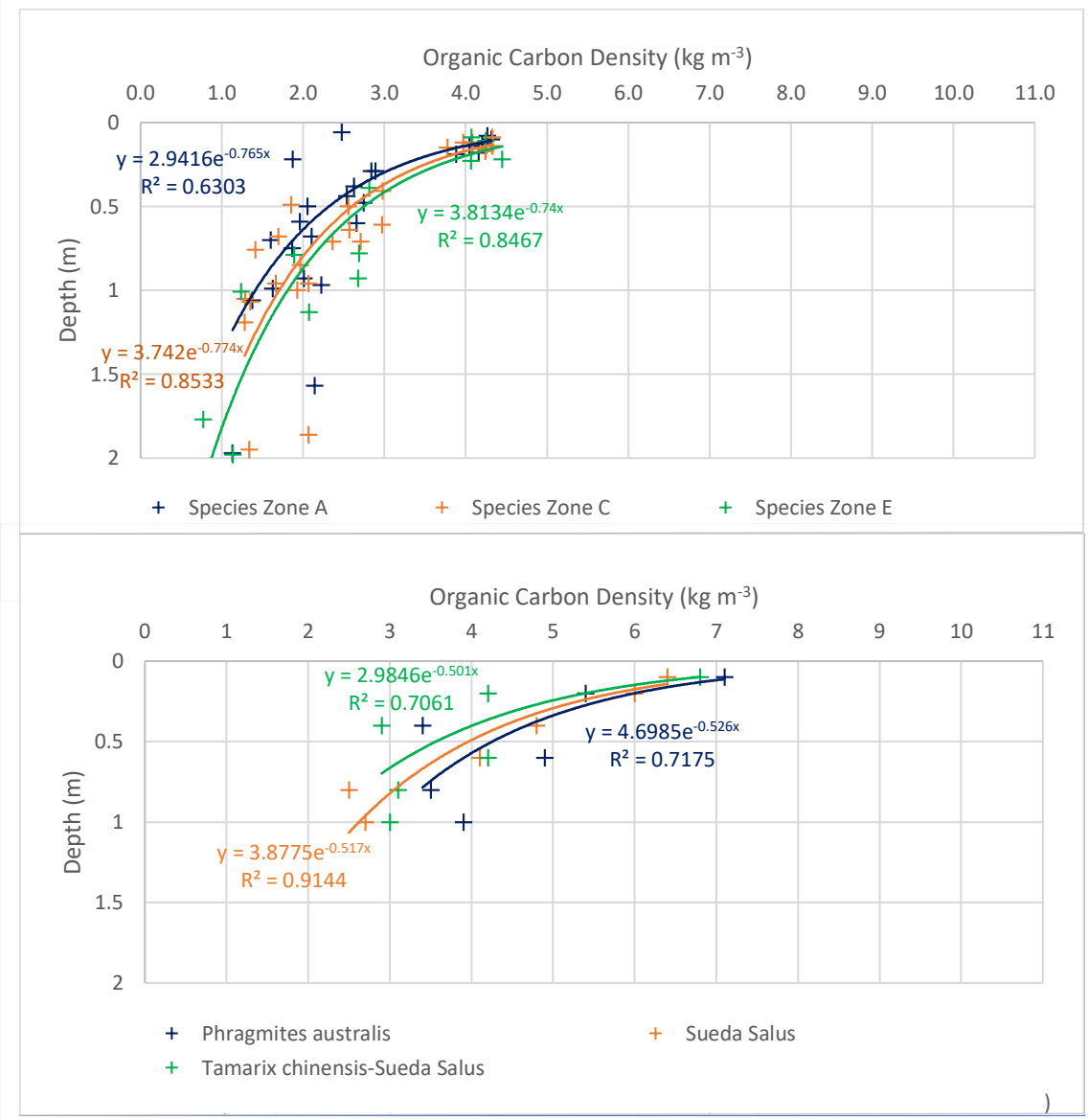

Figure 6.6. Carbon variation with depth comparison highlighting the compartive change in carbon content with depth in this study (a) and in the Yellow River Delta (b) (Bai *et al.* 2016). This figure is an illustration of the exponential decrease in sediment carbon between the surface/active and fossil layers in an active saltmarsh.

6.4 - Sea level rise and Marsh Evolution

As explained in 3.3.2 the active section is the most vulnerable to saltmarsh evolution which could be driven by the predicted regional SLR (Church *et al.* 2013; Palmer *et al.* 2018). Therefore the potential consequences of SLR on saltmarsh: ecology, geomorphology and active section carbon storage in the Ribble estuary will form the basis of the discussion in the following section. Specifically, the direct influence of SLR on elevation and saltmarsh carbon is considered, whilst the plausible consequences of SLR-driven changes on gradient and watercourse proximity are also discussed.

6.4.1 - Potential Scenarios and Consequences

As discussed in section 3.4 the influence of SLR on the future sub-environment and carbon distribution of the saltmarshes of the Ribble estuary will fundamentally depend on the rate of localised SLR and the consequent influences on the geomorphological and ecological dynamics of the estuary. According to the UKCP 18 regional (25 km^2) projections for the area (see Appendix A) the sea level could rise by up to 0.21 m by 2050 and 0.63 m by 2100 under the most extreme IPCC RCP 8.5 scenario (50th percentile), although a rise as high as 1.98 m could occur under the High 1 scenario devised by Pfeffer et al (2008). As indicated by Figure 6.7 (a and b) the projected areal extent of flooding at MHWS is controlled by a combination of the time elapsed, marsh topography and the prevailing sea level rise scenario.

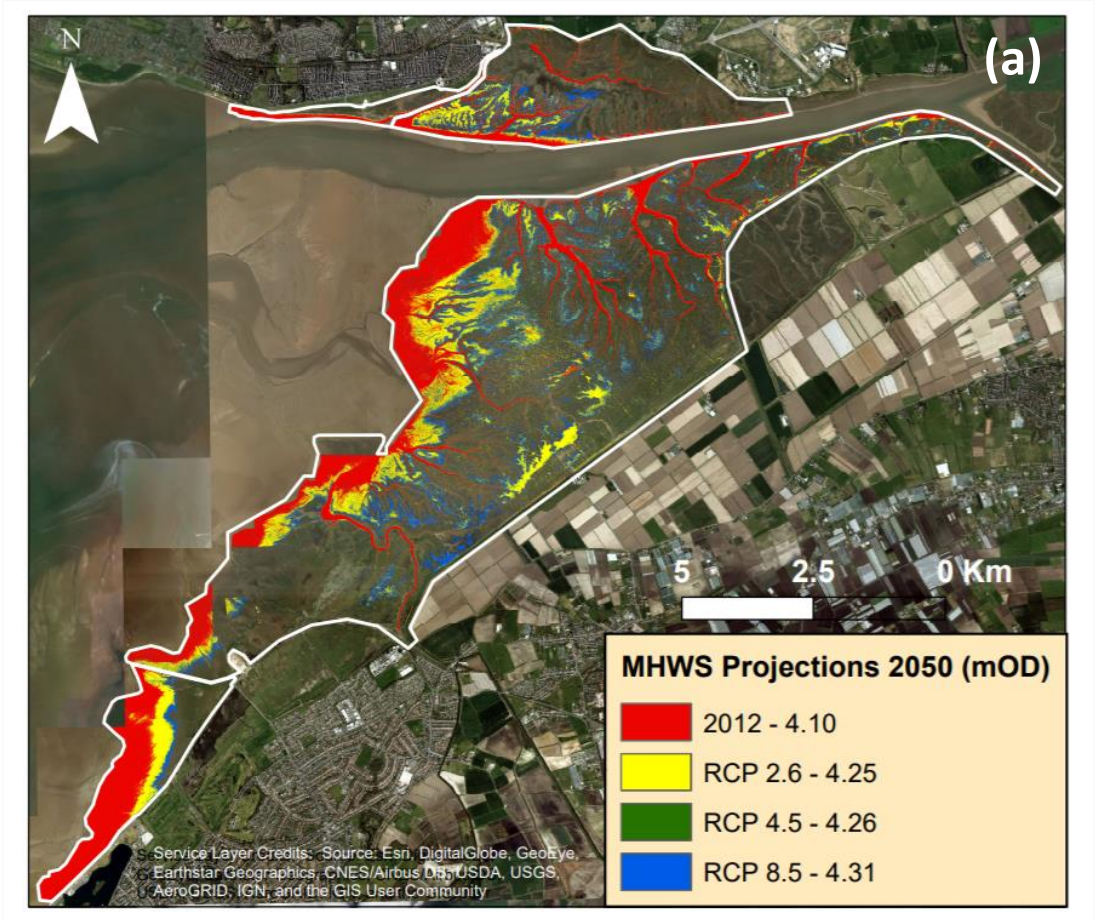

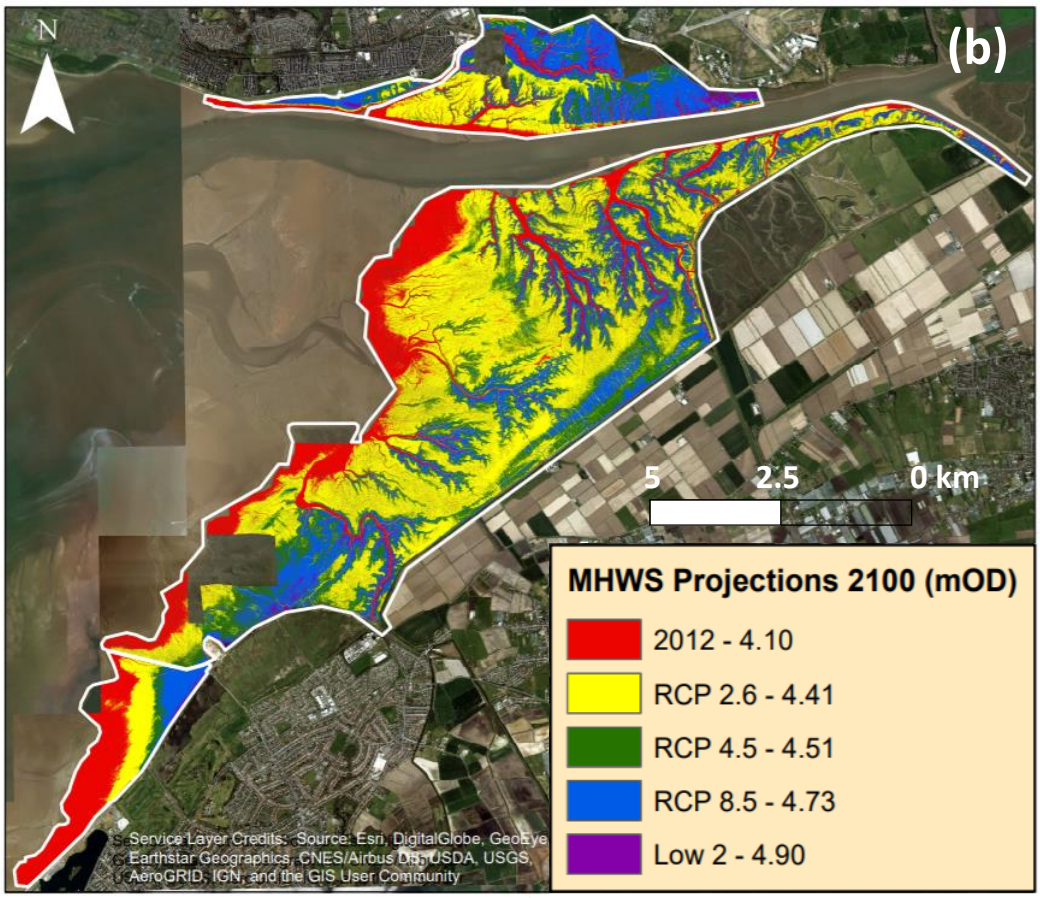

Figure 6.7. Projected heights of MHWS at present in 2050 (a) and 2100 (b) under different sea level rise prediction scenarios assuming no topographic change. The UKCP 18 RCP 50th percentile projections shown are specific to a 25km^2 area encompassing the Ribble estuary, whilst the Low 2 scenario represents Pfeffer et al's (2008) median global sea level rise projection. The data for all SLR projections can be found in Appendix A.

If it is assumed the primary model of coastal squeeze (Doody, 2004; Wolters et al. 2005) (see Section 3.4.1) could be applied to the saltmarsh, SLR could result in submergence prompting the loss of expansive areas of high marsh sub-environments due to the precise distribution of sub-environments between 4.2 - 4.6 mOD (63.1%) and restrictions on landward regression. According to Horton *et al.* (2018) this loss is likely to occur as there is >80% positive tendency of marsh retreat in Liverpool Bay by as early as 2020 under the most extreme RCP 8.5 scenario, suggesting saltmarsh sub-environments and their carbon content are highly vulnerable.

Elevation and Submergence

The calculations of sub-environment and carbon response to SLR suggest it is possible extensive carbon loss is highly likely when the current sub-environment elevation distribution relative to tidal datum is considered (see Figures 6.8 and Appendix A). The calculations, which assume SLR will instigate submergence and coastal squeeze, assume the higher marsh sub-environments comprised of less tolerant halophytes with the highest mean elevations: Species Zone A, B and D will be

collectively converted to Exposed Sediment first, before middle-lower sub-environments comprised of less tolerant halophytes: Species Zone C, Species Zone E and Brackish Waterbodies are subsequently converted in progressive order. The result of this SLR driven conversion is that the observed overall active section carbon storage capacity of the Ribble saltmarshes could decrease by 11.4% of the 2012 capacity by 2050 (2.26×10^7 kg), and 30.7% by 2100 (1.76×10^7 kg) should the RCP 8.5 (50^{th} percentile) scenario or any scenario predicted by Pfeffer *et al* (2008) prevail (2100 only). However even under the RCP 2.6 (50^{th} percentile) scenario, the overall carbon mass is projected to decrease by 23.6% of the 2012 capacity by 2100, whilst a decrease of 30.5% is observed under the RCP 4.5 (50^{th} percentile) scenario (see Figure 6.8 and Appendix Section A Table A(vi)). It should be noted however that these projections represent the 50^{th} percentile and more or less extreme saltmarsh and carbon loss could occur under each RCP scenario according to the 5^{th} or 95^{th} percentile projections.

The standard deviation of error surrounding the carbon projections (considering variation in areal cover, volume and OCD) means it is plausible that 1.58×10^7 kg (38.0% less than the mean for RCP 8.5) of carbon stored in 2012 could decrease to 1.22×10^7 kg (45.8% less than the mean) and 7.14×10^6 kg (59.6% less than the mean) by 2050 and 2100 respectively under the RCP 8.5 projections. Alternatively, it is also possible that 3.52×10^7 kg (38.0% greater than the mean for RCP 2.6) was stored in 2012 and this would decrease to a mass of 3.40×10^7 kg (42.4% greater than the mean) and 2.99×10^7 kg (54.0 % greater than the mean) by 2050 and 2100 under the RCP 2.6 projections. In each scenario uncertainty increases with time and uncertainty increases at a greater rate under more extreme sea level scenarios until the entire marsh is theoretically converted to Exposed Sediment (i.e. after 2070 under the RCP 8.5 scenario). This is due to the faster rate of conversion of predominantly vegetated sub-environments to Exposed Sediment which is surrounded by the greatest overall active section standard deviation of 59.6%. The exponential models fitted to the data which explain a high (≥92.2%) degree of variability highlight that carbon loss could be greater than indicated by the observed reading under the RCP 8.5 scenario by 2100 although losses are less than observed for the RCP 2.6 and 4.5 scenarios. However, all models exhibit that loss will continue with time regardless of the scenario with the progressively increasing rate of SLR (particularly under the RCP 4.5 and 8.5. This exponential loss complies with previous research exhibiting that proportional vegetated saltmarsh areal and carbon loss corresponds with the rate of SLR (Donnelly and Bertness, 2001; Spencer *et al.* 2016; Watson *et al.* 2016). Therefore, although the models predict that the rate of total loss in area and active section carbon storage will decrease after 2070 under all scenarios, the proportional rate of carbon loss which can be lost (i.e. not within Exposed Sediment) is projected to increase due to the increasing rate of SLR.

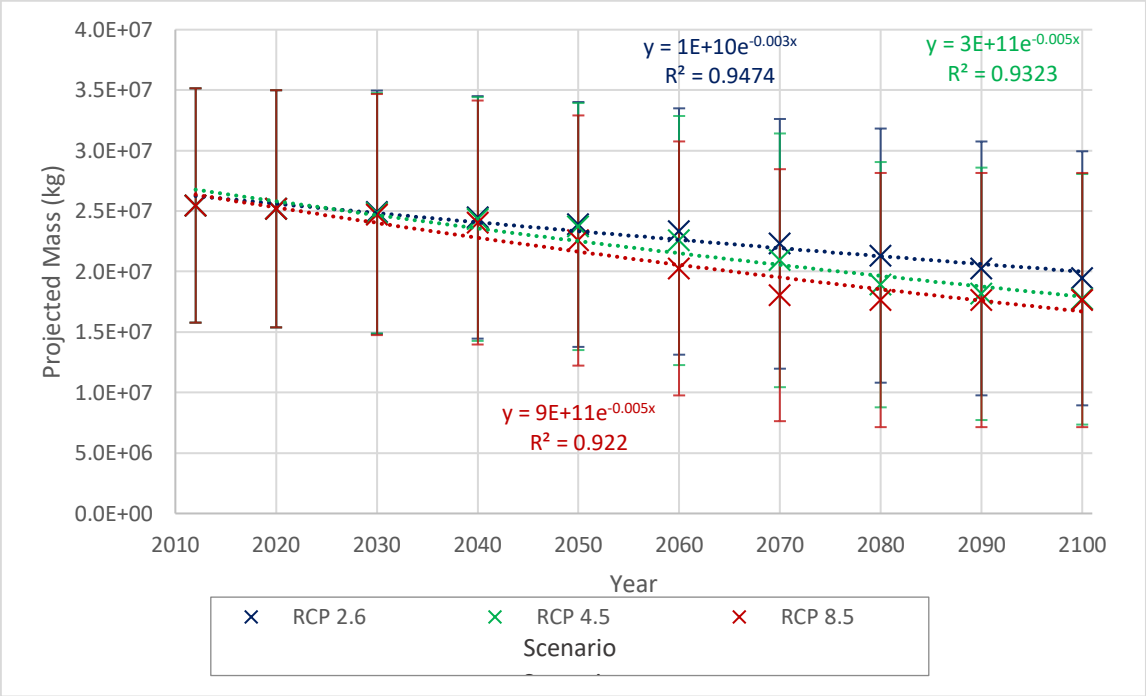

Figure 6.8. Projected change in overall carbon storage during the 21st century under the three differing RCP scenarios featured in the UKCP 2018 report. The plotted graph assumes the mean OCD in all sub-environments as well as the original area projections for above-ground biomass and OA x AD for active layer carbon. Error bars highlight the standard deviation in error surrounding mean projections.

Temporal variability is shown regarding the rate of loss between scenarios with the RCP 8.5 scenario showing the most rapid rate of carbon loss between 2040 and 2070, whilst the RCP 2.6 and 4.5 scenarios exhibit an increase in carbon loss rate with time. This is a result of the greater rate of SLR in RCP 8.5, however when SLR is observed independently (see Figure 6.9) the rate of carbon loss can be seen to vary in relation to the specific elevation intervals of SLR. Specifically, the rate of carbon loss with SLR begins at an average rate of 1.96 x 10^5 kg per cm between 0 – 8 cm before increasing to 4.41 x 10^5 kg per cm between 8 – 21 cm. Once SLR exceeds 21 cm the rate of carbon loss decreases to 8.56 x 10^4 kg per cm between 21 – 27 cm and the observed results show no further carbon loss theoretically occurs between 27 – 38 cm, as all other sub-environments have theoretically been converted to Exposed Sediment. However the model of exponential carbon loss indicates total carbon storage could continue to decrease after a depth of 27 cm, whilst the standard deviation in carbon storage indicates the marsh could contain between 7.14 x 10^6 – 2.82 x 10^7 kg after 38 cm of SLR (see Appendix Tables A (vi) and A(vii)).

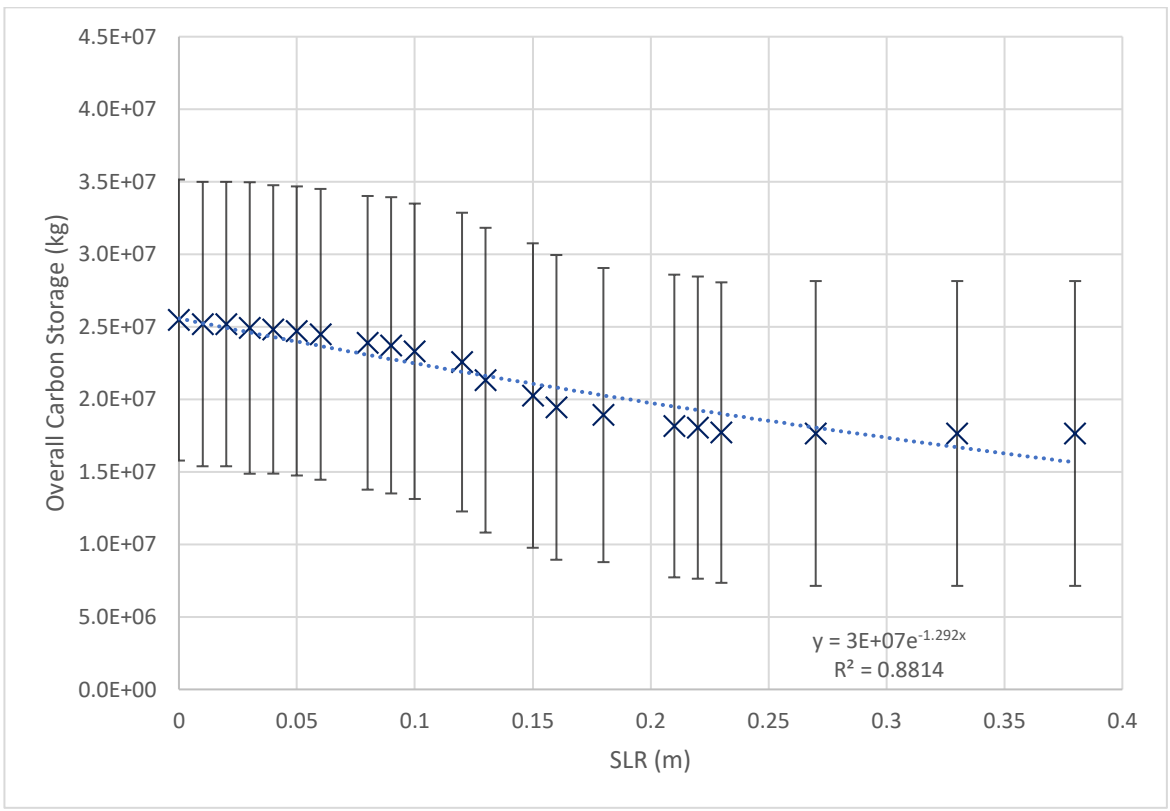

Figure 6.9. Predicted change in overall carbon stocks in accordance with the sea level rise (SLR). Error bars highlight the standard deviation in error surrounding mean projections.

However, despite the low mean carbon density (3.09 kg m^{-3}) of the active layer in sub-environments defined as Exposed Sediment the large mean depth (21.9 cm) and consequently volume of the sub-environment active layer results in an overall increase in active layer carbon with SLR (see Figure 6.10(a)). This increase in active layer carbon is offset by the decrease in carbon stored in above-ground biomass (see Figure 6.9(b)), which decreases by 58.8% and 78.4% of 2012 values by 2100 under the RCP 2.6 and 8.5 scenarios respectively (see Figure 6.10(b)).

Although the exponential models of carbon change associated with carbon stock prediction with SLR in the active layer sediments and above-ground biomass (Figure 6.10) explain a high degree (>88.3%) of the total variation in the three scenarios for above-ground biomass, active layer and overall carbon stocks, the predictions may be underestimates. It is plausible the initial retreat of species in the lower middle marsh may leave carbon-dense sediment which was once occupied by Species Zones C (mean = 4.12 kg m^{-3}) and E (mean = 4.26 kg m^{-3}) in the lower marsh prone to erosion due to the reduction in vegetation sediment stabilisation and wave dissipation (Pethick et al. 1993; Boorman et al. 1998; Schepeers, 2017). This would most likely increase the initial rate of carbon loss with SLR as such ecogeomorphological change could result in complete loss of carbon-dense sediment rather than a progressive conversion to the less carbon-dense sediment found in Exposed

Sediment sub-environments (Craft et al. 2009; Theuerkauf et al. 2015). Moreover, the reduced contribution from decomposed organic matter and sediment interception and deposition would plausibly serve to instigate to long-term organic degradation, producing predominantly non-organic sedimentary layers with reduced active layer sediment carbon density (Mudd et al. 2009; D'Alpaos and Marani, 2016).

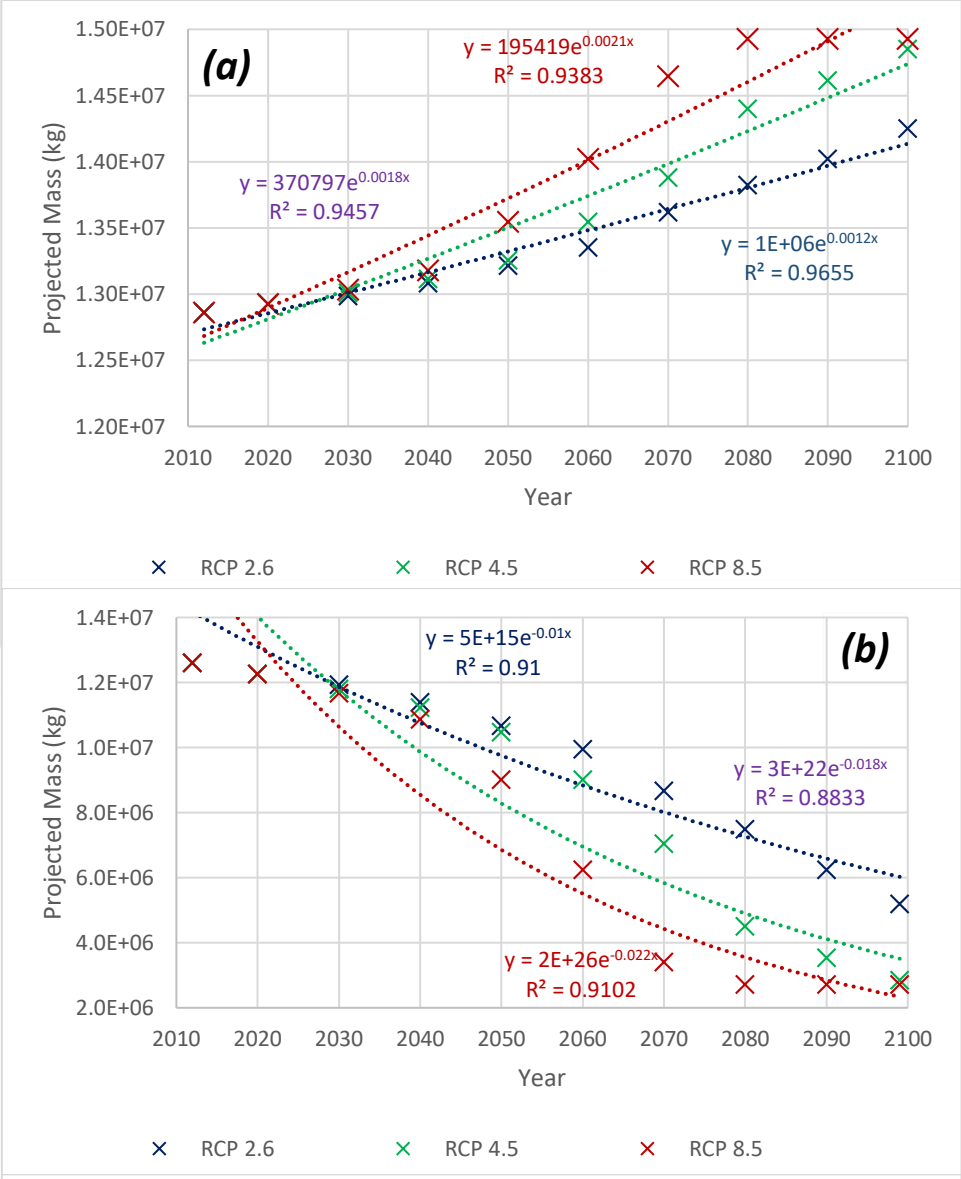

Figure 6.10. Projected change in overall active layer (a) and above-ground biomass (b) carbon storage during the 21st century under the three differing RCP scenarios featured in the UKCP 2018 report.

Alternative research concerning the saltmarsh response to SLR also highlights it is plausible widespread saltmarsh degradation and loss of carbon stock could occur as a result of submergence. Research undertaken by Trivisonno *et al.* (2013) modelling saltmarsh response to SLR in a coastal marsh which was unable to transgress due to embanking indicated widespread saltmarsh loss and

conversion into mudflat areas (i.e. Exposed Sediment) would occur with future SLR. Between 2010-2030 vegetated saltmarsh area cover was projected to decrease by 47.0% and 54.5% under the 'medium' (8 mm y^{-1} or 0.16 m rise) and 'high-end' (11 mm y^{-1} or 0.22 m rise) SLR scenario projections which were respectively based off the IPCC 4th Assessment Report A1B and A1FI scenarios (Bindoff *et al.* 2007). However, the 'high-end' projections also included the impacts of recent warming trends on ice sheet dynamics on SLR in southern Australia (Government of Australia, 2012). In comparison it is predicted the total area excluding exposed sediment will decrease by 7.3% and 8.7% under the equivalent scenarios of RCPs 4.5 and 8.5 between 2012 and 2030 (see Appendices Tables A(xvii) and A((xxii). However the overall UKCP 18 adjusted SLR by 2030 is 0.08 m and 0.09 in the Ribble under the 50th percentile RCPs 4.5 and 8.5 scenarios (see Tables A(i) and A(ii)). Therefore there would be a theoretical decrease in vegetated saltmarsh area of 14.6% and 20.7% between 2012 and 2030 if the rates of SLR were equal to the medium and high-end projections in the work of Trivisonno *et al.* (2013). Regarding carbon, sequestration was predicted to decrease by 36.6% and 44.0% under the 'medium' and 'high-end' SLR scenarios and carbon storage was expected to decrease at a proportional rate.

Theurkauf *et al.* (2015) predicted SLR would reduce the width of a saltmarsh in North Carolina from 314 m in 1996 to 277 m in 2053 (model assumed a 1 m shoreline length). As a result of a combination of carbon storage loss in the top 0.5 m of sediment due to submergence and shoreline erosion, the models indicated the saltmarsh would change from a sink to a source of carbon by 2021 in a moderate sea level rise scenario, although it was plausible this had already occurred in 1996 or would occur as late as 2053. The influence of the model used and the species involved has also been shown to influence retreat as Ge *et al.* (2016) exhibited that the areal covered by *Spartina alterniflora* could change by +8% or -13% under the RCP 8.5 SLR scenario by 2050 according to two different models, whilst the areal cover of the less saline tolerant *Scirpus mariqueter* was projected to change by +35% or -21%. This variability and uncertainty surrounding predictions of saltmarsh response to SLR highlight the need for future research primarily focussed on modelling the influence of SLR on saltmarsh landcover and carbon stock change in the Ribble estuary.

SLR will have highly complex consequences for the saltmarshes and carbon stored within the Ribble, and whilst coastal squeeze may occur it is highly unlikely it will occur at a linear rate (Schile *et al.* 2014; Hunter *et al.* 2017). Although modelling of the impacts of SLR within the CETaSS study (Halcrow, 2010) have indicated a general potential for an increase in flood dominance and the simultaneous amplification of tidal elevations and tidal range in the estuary, SLR may provide a mechanism for import of additional sediment and so accretion of bed levels may negate increased tidal range and elevations (Halcrow, 2010 & 2013). This increase in accretion may allow the

saltmarsh to maintain elevation relative to sea level and could theoretically result in an increase in biological productivity and nutrient deposition, serving to increase the active section carbon stocks particularly if climatic change was favourable to halophyte biological productivity (Day *et al.* 2011; Kirwan *et al.* 2016). Moreover, the impact of the predicted increase in storm surge frequency and magnitude may also have variable consequences on carbon stock and species distribution (Gedan et al. 2011; Moller et al. 2014; Spencer et al. 2016). Whilst increased storminess may potentially increase erosion and removal of carbon from the lower marsh (Wolters et al. 2005; Moller et al. 2014), the increased deposition of transported sediments and nutrients in the middle-higher marsh could serve to potentially increase productivity and subsequent marsh growth (Morris *et al.* 2002; Kirwan and Gutenspergen, 2012). However, accurately predicting future change will require localised modelling of saltmarsh response to SLR rise in the Ribble.

Watercourse Proximity

As watercourse proximity had the largest significance influence on sub-environment spatial and carbon distribution, the impact of SLR on the creeks and watercourses will most likely substantially influence future carbon distribution in the Ribble. This is due to the interconnected influence of creeks evolution on sediment/nutrient supply, saline intrusion, gradient and elevation (Fagherazzi *et al.* 2012; French, 2019). In the most likely scenario in which SLR instigates headward extension and incision of creeks (Hughes *et al.* 2009; Rizzetto and Tosi, 2012) there would be direct effects on the carbon storage capacity of the sub-environments within the creeks themselves, but also on the surrounding levees and depressions. The increase in tidal range forecast by Halcrow *et al.* (2010) (see Section 2.4) could serve to increase creek flow velocity and therefore erosion within the creek systems (Friedrichs and Perry, 2001; Stefanon *et al.* 2012) which would directly influence Species Zone C and D in particular as the two sub-environments are commonly found in close proximity to creek systems. Headward extension of creeks into the higher marsh would in theory result in the propagation of both Species Zones C and D into the higher marsh, replacing sub-environments composed of less tolerant halophytes such as Species Zone A and B which would be unable to withstand the saline stress (Townend et al. 2011; Fagherazzi et al. 2012). Whilst it is not possible to predict the temporal rate of change in watercourse proximity, the results of the multiple regression analyses (Section 5.3.4) highlight that creek extension would variably impact the spatial distribution and carbon storage of different sub-environments.

As the multiple regression analysis indicates carbon mass in all sub-environments decreases with each metre from a watercourse, it could be assumed there would be a linear increase in combined above-ground and sub-surface carbon mass under a scenario of headward dendritic extension, in which all sub-environments became on average closer to a watercourse. However, whilst increasing

mean creek proximity theoretically enhances the overall carbon storage potential of all sub-environments, it should be noted that this does not mean carbon storage will increase. In fact, the replacement of predominantly vegetated sub-environments with more extensive creek systems comprised of the low carbon density sub-environments Brackish Waterbodies and Exposed Sediment would most likely reduce vegetation cover and carbon storage as the sub-environment began a SLR-induced transition into an exposed mudflat environment (Wilson *et al.* 2014; Crosby *et al.* 2016). Moreover, as watercourse proximity was universally indicated to have the greatest significant impact on spatial distribution, sub-environment migration would most likely occur as each sub-environment adjusted to creek expansion in order to maintain ecogeomorphological equilibrium (Phillips *et al.* 2018; D'Alpaos *et al.* 2019). Therefore saltmarsh sub-environment and carbon loss would most likely occur due to the restrictions on transgression in the Ribble. Although this scenario of headward expansion is most likely, unlike progressive SLR, it is not plausible to simulate the influence of SLR on creek hydrogeomorphology without a model adapted for the environment. Therefore, although there is evidence to suggest SLR could potentially result in creek infilling (Stefan *et al.* 2015) which would have direct and indirect impacts on watercourse proximity and gradient, it remains more plausible that creek expansion will occur and catalyse saltmarsh degradation in the long-term given the localised SLR scenarios.

Gradient

The changes in gradient associated with the SLR driven extension of levees and creek benches into the higher marsh would also have consequences on carbon storage. Unlike watercourse proximity which prompts headward expansion of creeks resulting in sub-environments becoming theoretically closer to a creek, the direct influence of headward expansion would be to universally increase the gradient of sub-environments thereby reducing carbon storage. However, like watercourse proximity, the statistically significant influence of gradient on would most plausibly mean sub-environments would re-establish themselves relative to the new saltmarsh gradient. Although the influence of gradient change would likely have only 58.1% (Species Zone A) to 66.6% (Exposed Sediment) of the standardised effect of watercourse proximity, the impact of creek extension on gradient would most likely contribute to the interconnected readjustment of sub-environments re-establishing ecogeomorphological equilibrium following SLR (Fagherrazi *et al*. 2012; Alizad *et al.* 2016).

It is also important to consider that a more expansive network of creeks and the associated influence on drainage and saturation levels (Cahoon and Reed, 1995; Allen, 2000) would produce more partially enclosed basins created between the creek systems. This could potentially result in the creation of salt pans and stagnant brackish waterbodies which could become anoxic areas of low

productivity (Griffin et al. 2011; Kulawardhana et al. 2014) reducing both short and long-term carbon storage capacity in above-ground biomass and the active layer.

Summary

The influence of sea level rise on marsh hydrodynamics and potential creek headward expansion would likely result in ecogeomorphological change in saltmarsh sub-environment distribution and active section carbon storage. This would be driven by SLR-induced changes of the statistically significant influences of watercourse proximity and gradient on saltmarsh distribution which would prompt ecogeomorpholgoical change as the saltmarsh sub-environments adjusted to maintain equilibrium. Therefore, the direct and secondary influences of SLR-driven gradient and watercourse proximity change and the progressive influence of submergence on saltmarsh sub-environment and carbon distribution must be taken in into account when predicting future carbon storage change in the Ribble estuary.

6.4.2 – Implications for Coastal Management and Further Research

Although it is likely the saltmarshes of the Ribble and their carbon stocks will become increasingly vulnerable to SLR-driven marsh evolution and degradation (Cahoon *et al.* 2006; Craft *et al.* 2009; Horton *et al.* 2018), the future shoreline management plan (SLMP) will significantly influence SLR driven saltmarsh response and evolution (Sterr, 2008; Enwright *et al.* 2016; Borchert *et al.* 2018). The current shoreline management plan partially recognises the need to allow transgression to preserve the saltmarshes of the Ribble, however there is both a temporal and spatial variability in the management policies (Halcrow, 2010c – See Figure 6.12) which could consequently result in variability in marsh evolution (Saintilan and Rogers, 2013; Torio and Chmura, 2013).

Most prominently there is a disparity in policy between the North and South banks were hold-the-line and managed realignment (MR) policies are respectively favoured in the long-term. Theoretically, this would potentially enable the marshes C and D to transgress to landward as sea level rises, whilst the evolution of marshes A and B would be restrained as coastal defences are maintained to protect the socio-economic assets on the north bank. Therefore, under a SLR scenario it would be likely that the ecosystem services including carbon stocks provided by the marshes on the northern bank would be more vulnerable than those on the south if the ecogeomorphological response to sea level rise was approximately uniform across the estuary.

When the spatial distribution of sub-environments and carbon is considered, the loss of Species Zone A would most likely be of the greatest concern as 32.1% of the overall sub-environment comprising of 6.37 x 10^5 kg of above-ground biomass carbon (original areal projection) and 2.88 x 10^5 kg (OA x AD projection) of active layer carbon is predominantly found Marsh B (see Appendix section B2). As a hold-the-line policy will be enforced in this area over the next 50-100 years and Species Zone A is more likely to be lost to coastal squeeze due to the location in the higher marsh (mean elevation = 4.56 mOD), a disproportionally high carbon loss could occur from the degradation of Species Zone A in Marsh B due to the inability of the saltmarsh to transgress and maintain ecogeomorphological equilibrium. Whilst the higher marsh sub-environments Species Zone B (average elevation = 4.48 mOD) and D (average elevation = 4.52 mOD) are also likely to be two of the first sub-environments to be impacted upon by coastal squeeze, as 8.4% of the cumulative area of Species Zones B and D is found on Marshes A and B, only a combined 8.4% of above-ground (original areal projection) and 9.1% (OA x AD projection) of sub-surface carbon within the two sub-environments would be at risk.

Although the carbon stocks of Marshes A and B are most at risk to future SLR-driven degradation when future SLMPs are considered, the expansive areal cover of Marsh C over 16.8 km^2 (76.4% of overall) means it represents the most significant concern in terms of overall carbon loss as 9.94 x 10^6 kg (78.8% of overall) of above-ground biomass carbon (original areal projection) and 9.70 x 10^6 kg (76.3% of overall) (OA x AD projection) of active layer carbon is currently stored in the marsh. An area of 3.83 km^2 of Marsh C is classified as Species Zone B and D which cumulatively store 4.33 x 10^6 kg above-ground biomass carbon (original areal projection) and 2.09 x 10^6 kg (OA x AD projection) of active layer carbon which could be vulnerable, particularly if the RCP 4.5 or 8.5 scenarios ensue before the suggested managed alignment policy is implemented between 2060 – 2110 (see Figure 6.11). Although Species Zone F currently contains only 1.24 x 10^4 kg (<0.1% of overall) of above-ground biomass carbon (original areal projection) and 1.12 x 10^4 kg (<0.1% of overall) (OA x AD projection) of active layer carbon, when one considers the rarity of *Eleocharis uniglu*mis in Britain and the national nature conservation designation of the Ribble estuary, there is a stronger argument to bring forward MR in order to preserve species diversity.

The argument to bring forward MR is strengthened when the more complex effects of potential SLR-driven headward creek on watercourse proximity and gradient are considered as well as the progressive influence of submergence. The fact watercourse proximity is the greatest statistically significant influence on sub-environment and carbon distribution is particularly important to consider as sub-environments that are unable to adjust to maintain ecogeomorphological equilibrium relative to creeks will likely be lost if saltmarsh regression and adjustment is prevented.

The same is true but to a reduced extent with the other significant influence of gradient which would theoretically increase on average with creek network expansion. The result of an inability to establish ecogeomorphological relative to gradient and watercourse could be to exacerbate the sub-environment and carbon losses sustained as a result of submergence (Day *et al.* 2008; Wilson et al. 2014). Therefore, when the current research concerning saltmarsh response to SLR, projected SLR in the region and the current ecogeomorphological restrictions on the saltmarsh are collectively considered, a policy of MR should be promptly adopted in the interest of reducing the loss of saltmarsh ecosystem services and carbon storage.

However, the decision to advance such shoreline management strategies must be treated with caution, especially considering the projected increase in regional vulnerability to future high magnitude coastal storms (Halcrow *et al.* 2013; Palmer *et al.* 2018). Whilst MR has already been partially implemented in the estuary to the east of Marsh C (see Figure 6.11), policymakers should be aware of the potential issues of implementing MR through dike breaching. For instance, an attempt to restore former saltmarsh at the Freiston Shore, Norfolk through intentional breaching, substantially enhanced net erosion of the active saltmarsh leading to a 28-fold increase in the annual rate of headward retreat in the 16 months following the 'restoration' attempt compared to the previous 10 years (Symonds and Collins, 2007; Friess *et al.* 2014). This highlights the importance of considering the ecogeomorphological dynamics of a specific saltmarsh before restoration may take place (Townend and Pethick, 2002) in order to ensure the vulnerability of saltmarsh carbon stocks is not further heightened by inadequate management strategies.

However, shoreline management policy is just one of several factors that future research designed to model and predict the influence of saltmarsh carbon stocks must consider. Whilst coastal management is undoubtedly important, this research has emphasised the importance of considering the following:

- The significance of gradient and watercourse proximity on sub-environment distribution.
- The active section carbon density of different sub-environments and the relationship between above-ground biomass and active layer carbon.
- The plausible ecogeomorphological influences of different SLR scenarios on elevation, gradient and watercourse proximity and their direct and secondary influences on carbon storage.

As SLR continues to result in the degradation of UK saltmarshes the loss of carbon from these efficient carbon stores will become an increasingly important factor to consider when assessing the secondary influences of sea level rise on future climatic change (Craft et al. 2009; Chumra, 2013; Horton et al. 2018). Therefore, there is justification for extending the spatial coverage of research of this nature to include other UK saltmarshes and to combine such assessments with models of SLR-driven saltmarsh evolution in order to improve the overall understanding of the potential consequences of future SLR on saltmarsh blue carbon. Such findings could influence and inform coastal management strategies and ultimately reduce the degradation and loss of the key ecosystem services saltmarshes provide.

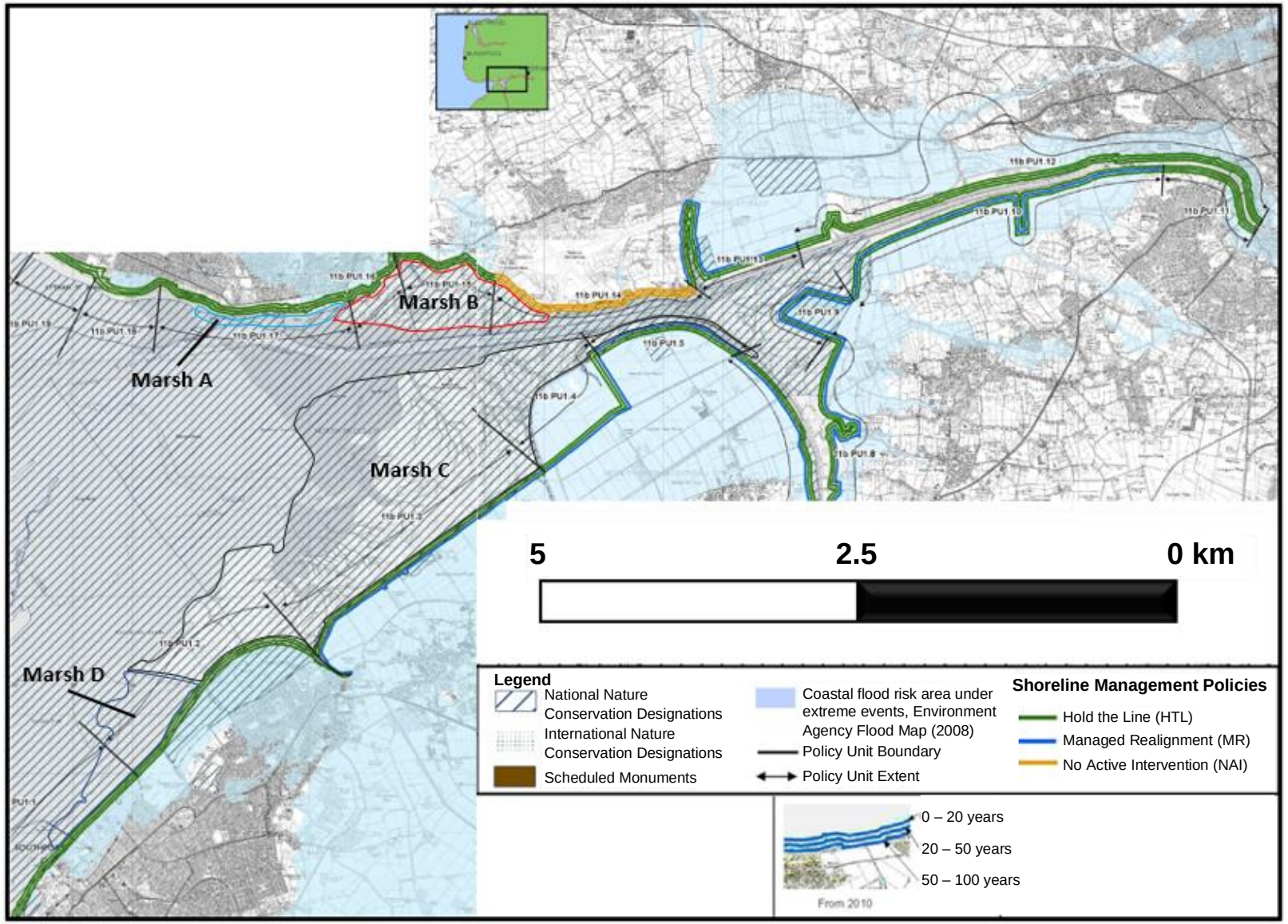

Figure 6.11. Shoreline management plan for the Ribble Estuary from 2010 to 2100.
(Source: Halcrow, 2010c)

7 – Conclusions

This study contributes to improving the overall understanding of the carbon storage potential of temperate saltmarshes and highlights how the distribution of sub-environments and the carbon within them varies throughout an estuarine saltmarsh. Specifically, this research aimed to increase the understanding of the influence of elevation, gradient and watercourse proximity on sub-environment and carbon distribution, whilst also highlighting how future sea level rise could potentially influence the quantified blue carbon stocks of the saltmarshes of the Ribble Estuary. The four main findings of the research are as follows:

1) **Watercourse proximity has the largest statistically significant influence on sub-environment and carbon distribution.**

The results of the remote sensing analysis of sub-environment distribution exhibited that elevation, gradient and watercourse proximity collectively influenced sub-environment distribution, serving to produce the 'mosaic' pattern widely observed throughout temperate saltmarshes (e.g. Silvestri et al. 2005; Zedler et al. 2010; Mudd and Fagherazzi, 2016). Although it is acknowledged that the two assessments of landcover indicate that the true sub-environment distribution could differ from the original findings, the overall kappa accuracy values of the respective remote and manual assessments of 87.6% and 90% exhibit the sub-environment distribution is accurately represented in this study. Of the eight sub-environments, Exposed Sediment and Species Zone C covered the greatest area of 9.36 km^2 (max uncertainty = 10.0%) and 3.81 km^2 (max uncertainty = 13.8%), whilst Species Zone E and F covered the smallest respective areas of 0.46 km^2 and 0.02 km^2 (max uncertainty for both = 13.3%).

Whilst the three influences are inherently connected, the findings indicate that watercourse proximity and gradient have a statistically significant influence on distribution, whilst the influence of elevation is insignificant. Of the statistically significant influences watercourse proximity exerted a greater standardised influence that was between 50.1% (Exposed Sediment) to 72.1% (Species Zone A) greater than the influence of gradient. Of all sub-environments Species Zone E, which was predominantly composed of the lower-middle marsh halophytes *Spartina Anglica* and *Salicornia Spp.,* was most influenced (standardised beta = -0.757) by watercourse proximity whilst the widely distributed Exposed Sediment was the least influenced (standardised beta = -0.614). Regarding the overall influence of watercourse proximity on carbon, Species Zone B had the highest unstandardised above-ground carbon change of -2760 kg per m increase in watercourse proximity, whilst Exposed Sediment had the highest unstandardised active layer value of -4420 kg per m.

Overall the results rebuke the simple elevation ramp model of distribution and therefore support the alternative theories which suggest saltmarsh sub-environment and carbon distribution is controlled by a multitude of factors (Kim et al. 2013; D'Alpaos *et al.* 2019).

2) The exponential decrease in the organic carbon density between the surface sediments and the sediments at greater depth provides evidence of an ecogeomorphologically connected active section and separate fossil layers.

The study principally concerned the carbon storage within the above-ground biomass and the active layer sediments which were collectively termed the active section. There was a persistent difference in the carbon content between the active and fossil layers in all sub-environments. Active layer samples consistently had a mean OCD >15% than in the overall sub-surface sediment and possessed undecomposed organic material whilst an exponential decrease in OCD between the active and fossil layers was observed in all predominately vegetated sub-environments. In predominantly unvegetated sub-environments a smaller disparity existed between active and fossil layers when compared to predominantly vegetated sub-environments, as the difference between the mean active layer and sub-surface OCD reduced to 17.7% in Brackish Waterbodies compared to the overall mean of 43.5%. Moreover, OCD was lower in the predominantly unvegetated sub-environments as the mean active layer for Exposed Sediment of 3.09 kg m^{-3} was 17.6% less than the overall mean for all sub-environments and 27.5% less than the maximal mean active layer OCD in Species Zone E (4.26 kg m^{-3}). The findings suggest that the exponential decrease in OCD with depth in predominately vegetated saltmarsh sub-environments is evidence of an ecogeomorphologically connected organic active section which is found above fossil layers which are not directly influenced by surface processes.

3) The mosaic distribution of saltmarsh sub-environments creates a spatially variable active section carbon distribution produced by the differences in sub-environment ecogeomorphological characteristics.

Overall 1.26 x 10^7 kg and 1.29 x 10^7 kg (3.s.f) of carbon is estimated to be stored within the above-ground biomass and active layer respectively (original area and average depth assessment), although carbon is unevenly distributed between sub-environments. A positive correlation (r^2= 0.44) between above-ground biomass and active layer carbon stock is observed overall, although the high degree of variance from the linear model suggests the existence of unique relationships between above-ground and sub-surface carbon storage in each sub-environment. Regarding above-ground carbon, the highest mean density of 1.19 kg/m^2 and total mass of 4.06 x 10^6 kg (32.2% of overall) was found

in Species Zone B, a middle-higher marsh sub-environment predominantly composed of *Festuca rubra* and *Elymus repens,* although standard deviations in error of 16.3% and 25.0% from the mean surrounded the respective landcover and above-ground biomass carbon density calculations. Alternatively, the largest proportion of active layer carbon (49.6% of overall) was found in sub-environment classified as Exposed Sediment as the projections indicated 6.32 x 10^6 kg was stored in the sub-environment, although standard deviations in error of 50.6 % and 15.5% from the mean surround the respective volume and active layer carbon density estimates. Overall the results highlight the high degree of variability in active layer carbon storage both within and between sub-environments exhibiting the ecogeomorphological heterogeneity of the Ribble saltmarshes.

4) **Future shoreline management plans must take into account the carbon distribution in the saltmarshes of the Ribble in order to minimise the potential loss of carbon storage resulting from sea level rise.**

The current restrictions on saltmarsh migration may result in the saltmarshes of the Ribble experiencing ecogeomorphological disequilibrium as a result of sea level rise rendering the environments vulnerable to future degradation (Robins *et al*. 2016; Horton *et al*. 2018). Assuming coastal squeeze will occur and result in the conversion of the currently vegetated areas to Exposed Sediment, the projections suggest that the overall active section carbon storage capacity of the Ribble saltmarshes could decrease by 23.8%, 30.7% or 30.9% of the 2012 capacity by 2100 under the respective RCP 2.6, 4.5 and 8.5 (50^{th} percentile) scenarios. Whilst the net loss of carbon on Marsh C is likely to the greatest, marshes A and B are likely to suffer the largest proportional losses due to the hold-the-line shoreline management policy in the north of the estuary which prevents saltmarsh regression in response to sea level rise. Moreover, as gradient and watercourse proximity are the statistically significant influences on sub-environment and carbon distribution, the inability of sub-environments to reach equilibrium following potential creek headward expansion could further exacerbate the loss of saltmarsh ecosystem services and active section carbon.

As collective degradation and sub-environment loss could reduce the ability of the Ribble saltmarshes to act as an efficient carbon sink it is essential that appropriate management procedures are implemented that consider saltmarsh adaption and response to SLR. This may require the implementation of managed realignment policies on a wider scale and sooner in time than currently scheduled to ensure the saltmarshes can respond to SLR and can continue to act as a key blue carbon store.

References

Adam, P., 1990. *Saltmarsh Ecology*. Cambridge University Press, pp.461-464.

Adam, P., 2002. Saltmarshes in a time of change. *Environmental conservation*, *29*(1), pp.39-61.

Alber, M., 2002. A conceptual model of estuarine freshwater inflow management. *Estuaries*, *25*(6), pp.1246-1261.

Alhdad, G.M., Seal, C.E., Al-Azzawi, M.J. and Flowers, T.J., 2013. The effect of combined salinity and waterlogging on the halophyte Suaeda maritima: the role of antioxidants. *Environmental and Experimental Botany*, *87*, pp.120-125.

Alizad, K., Hagen, S.C., Morris, J.T., Bacopoulos, P., Bilskie, M.V., Weishampel, J.F. and Medeiros, S.C., 2016. A coupled, two-dimensional hydrodynamic-marsh model with biological feedback. *Ecological Modelling*, *327*, pp.29-43.

Allen, J.R.L. and Fulford, M.G., 1986. The Wentlooge Level: a Romano-British saltmarsh reclamation in southeast Wales. *Britannia*, *17*, pp.91-117.

Allen, J.R.L., 1990. The Severn Estuary in southwest Britain: its retreat under marine transgression, and fine-sediment regime. Sediment. Geol., 66: 13-28.

Allen, J.R.L. and Pye, K., 1992. Coastal saltmarshes: their nature and importance. *Saltmarshes: Morphodynamics, conservation and engineering significance*, pp.1-18.

Allen, J.R.L., 1995. Salt-marsh growth and fluctuating sea level: implications of a simulation model for Flandrian coastal stratigraphy and peat-based sea-level curves. *Sedimentary Geology*, *100*(1-4), pp.21-45.

Allen, J.R.L., 1997. Simulation models of salt-marsh morphodynamics: some implications for high-intertidal sediment couplets related to sea-level change. *Sedimentary Geology*, *113*(3-4), pp.211-223.

Allen, J.R., 2000. Morphodynamics of Holocene saltmarshes: a review sketch from the Atlantic and Southern North Sea coasts of Europe. *Quaternary Science Reviews*, *19*(12), pp.1155-1231.

Andresen, H., Bakker, J.P., Brongers, M., Heydemann, B. and Irmler, U., 1990. Long-term changes of saltmarsh communities by cattle grazing. *Vegetatio*, *89*(2), pp.137-148.

Andrews, J.E., Samways, G., Dennis, P.F. and Maher, B.A., 2000. Origin, abundance and storage of organic carbon and sulphur in the Holocene Humber Estuary: emphasizing human impact on storage changes. *Geological Society, London, Special Publications*, *166*(1), pp.145-170.

Andrews, J.E., Samways, G. and Shimmield, G.B., 2008. Historical storage budgets of organic carbon, nutrient and contaminant elements in saltmarsh sediments: Biogeochemical context for managed realignment, Humber Estuary, UK. *Science of the total environment*, *405*(1-3), pp.1-13.

Ankney, C.D., 1996. An embarrassment of riches: too many geese. *The Journal of wildlife management*, pp.217-223.

ArcGIS., 2018. *How Flow Direction works.* Available: http://pro.arcgis.com/en/pro-app/tool-reference/spatial-analyst/how-flow-direction-works.htm. Last accessed 18 September 2018.

Atkins, R.J., Tidd, M. and Ruffo, G., 2016. Sturgeon Bank, Fraser River delta, BC, Canada: 150 years of human influences on saltmarsh sedimentation. *Journal of Coastal Research*, *75*(sp1), pp.790-794.

Bagstad, K.J., Semmens, D.J., Waage, S. and Winthrop, R., 2013. A comparative assessment of decision-support tools for ecosystem services quantification and valuation. *Ecosystem Services*, *5*, pp.27-39.

Bai, J., Zhang, G., Zhao, Q., Lu, Q., Jia, J., Cui, B. and Liu, X., 2016. Depth-distribution patterns and control of soil organic carbon in coastal saltmarshes with different plant covers. *Scientific reports*, *6*, p.34835.

Bao-Shan, C.U.I., Qiang, H.E. and Yuan, A.N., 2011. Community structure and abiotic determinants of saltmarsh plant zonation vary across topographic gradients. *Estuaries and Coasts*, *34*(3), pp.459-469.

Barnett, R.L., Gehrels, W.R., Charman, D.J., Saher, M.H. and Marshall, W.A., 2015. Late Holocene sea-level change in Arctic Norway. *Quaternary Science Reviews*, *107*, pp.214-230.

Barbier, E.B., Hacker, S.D., Kennedy, C., Koch, E.W., Stier, A.C. and Silliman, B.R., 2011. The value of estuarine and coastal ecosystem services. *Ecological monographs*, *81*(2), pp.169-193.

Barkowski, J.W., Kolditz, K., Brumsack, H. and Freund, H., 2009. The impact of tidal inundation on saltmarsh vegetation after de-embankment on Langeoog Island, Germany—six years time series of permanent plots. *Journal of Coastal Conservation*, *13*(4), p.185.

Bartholdy, J., 2012. Salt Marsh Sedimentation. In: Davis Jr. R., Dalrymple R. (eds) *Principles of Tidal Sedimentology.* Springer, Dordrecht. pp. 151-185.

Bartlett, K.B. and Harriss, R.C., 1993. Review and assessment of methane emissions from wetlands. *Chemosphere*, *26*(1-4), pp.261-320.

Baustian, J.J., Mendelssohn, I.A. and Hester, M.W., 2012. Vegetation's importance in regulating surface elevation in a coastal salt marsh facing elevated rates of sea level rise. *Global Change Biology*, *18*(11), pp.3377-3382.

Beaumont, N.J., Jones, L., Garbutt, A., Hansom, J.D. and Toberman, M., 2014. The value of carbon sequestration and storage in coastal habitats. *Estuarine, Coastal and Shelf Science*, *137*, pp.32-40.

Beeftink, W.G. and Rozema, J., 1993. The nature and functioning of saltmarshes. In *Pollution of the North Sea* (pp. 59-87). Springer, Berlin, Heidelberg.

Belliard, J.P., Temmerman, S. and Toffolon, M., 2017. Ecogeomorphic relations between marsh surface elevation and vegetation properties in a temperate multi-species salt marsh. *Earth Surface Processes and Landforms*, *42*(6), pp.855-865.

Belluco, E., Camuffo, M., Ferrari, S., Modenese, L., Silvestri, S., Marani, A. and Marani, M., 2006. Mapping salt-marsh vegetation by multispectral and hyperspectral remote sensing. *Remote sensing of environment*, *105*(1), pp.54-67.

Berg, G., Esselink, P., Groeneweg, M. and Kiehl, K., 1997. Micropatterns in Festuca rubra-dominated salt-marsh vegetation induced by sheep grazing. *Plant Ecology*, *132*(1), pp.1-14.

Bertness, M.D., Gough, L. and Shumway, S.W., 1992. Salt tolerances and the distribution of fugitive saltmarsh plants. *Ecology*, *73*(5), pp.1842-1851.

Bindoff, N.L., J. Willebrand, V. Artale, A, Cazenave, J. Gregory, S. Gulev, K. Hanawa, C. Le Quéré, S. Levitus, Y. Nojiri, C.K. Shum, L.D. Talley and A. Unnikrishnan., 2007. Observations: Oceanic Climate Change and Sea Level, in Solomon, S., D. Qin, M. Manning, Z. Chen, M. Marquis, K.B. Averyt, M. Tignor and H.L. Miller. (eds.) *Climate Change 2007: The Physical Science Basis. Contribution of Working Group I to the Fourth Assessment Report of the Intergovernmental Panel on Climate Change* Cambridge University Press, Cambridge, United Kingdom and New York, NY, USA.

Bockelmann, A.C., Bakker, J.P., Neuhaus, R. and Lage, J., 2002. The relation between vegetation zonation, elevation and inundation frequency in a Wadden Sea saltmarsh. *Aquatic botany*, *73*(3), pp.211-221.

Boorman, L.A. and Ashton, C., 1997. The productivity of saltmarsh vegetation at Tollesbury, Essex, and Stiffkey, Norfolk, England. *Mangroves and Saltmarshes*, *1*(2), pp.113-126.

Boorman, L.A., Garbutt, A. and Barratt, D., 1998. The role of vegetation in determining patterns of the accretion of saltmarsh sediment. *Geological Society, London, Special Publications*, *139*(1), pp.389-399.

Boorman, L.A., 2003. Saltmarsh review. An overview of coastal saltmarshes, their dynamic and sensitivity characteristics for conservation and management. JNCC Report, 334 pp.6-20.

Borchert, S.M., Osland, M.J., Enwright, N.M. and Griffith, K.T., 2018. Coastal wetland adaptation to sea level rise: Quantifying potential for landward migration and coastal squeeze. *Journal of Applied Ecology*.

Bos, D., Bakker, J.P., de Vries, Y. and van Lieshout, S., 2002. Long-term vegetation changes in experimentally grazed and ungrazed back-barrier marshes in the Wadden Sea. *Applied Vegetation Science*, *5*(1), pp.45-54.

Bouchard, V. and Lefeuvre, J.C., 2000. Primary production and macro-detritus dynamics in a European salt marsh: carbon and nitrogen budgets. *Aquatic Botany*, *67*(1), pp.23-42.

Bouchard, V., Gillon, D., Joffre, R. and Lefeuvre, J.C., 2003. Actual litter decomposition rates in salt marshes measured using near-infrared reflectance spectroscopy. *Journal of Experimental Marine Biology and Ecology*, *290*(2), pp.149-163.

Bradley, P.M. and Morris, J.T., 1990. Physical characteristics of saltmarsh sediments: Ecological implications. *Marine ecology progress series. Oldendorf*, *61*(3), pp.245-252.

Brewer, J.S., Levine, J.M. and Bertness, M.D., 1997. Effects of biomass removal and elevation on species richness in a New England salt marsh. *Oikos*, pp.333-341.

Bridgham, S.D., Megonigal, J.P., Keller, J.K., Bliss, N.B. and Trettin, C., 2006. The carbon balance of North American wetlands. *Wetlands*, *26*(4), pp.889-916.

British Oceanographic Data Centre., 2019. *UK Tide Gauge Network - Download Data.* Available: https://www.bodc.ac.uk/data/hosted_data_systems/sea_level/uk_tide_gauge_network/processed/. Last accessed 15th March 2019.

Browne, J.P., 2017. Long-term erosional trends along channelized salt marsh edges. *Estuaries and Coasts*, *40*(6), pp.1566-1575.

Burden, A., Garbutt, R.A., Evans, C.D., Jones, D.L. and Cooper, D.M., 2013. Carbon sequestration and biogeochemical cycling in a saltmarsh subject to coastal managed realignment. *Estuarine, Coastal and Shelf Science*, *120*, pp.12-20.

Byers, S.E. and Chmura, G.L., 2014. Observations on shallow subsurface hydrology at Bay of Fundy macrotidal saltmarshes. *Journal of Coastal Research*, *30*(5), pp.1006-1016.

Cacador, I., Costa, A.L. and Vale, C., 2004. Carbon storage in Tagus salt marsh sediments. In *Biogeochemical Investigations of Terrestrial, Freshwater, and Wetland Ecosystems across the Globe*. Springer, Dordrecht. pp. 701-714.

Cahoon, D.R., Hensel, P.F., Spencer, T., Reed, D.J., McKee, K.L. and Saintilan, N., 2006. Coastal wetland vulnerability to relative sea-level rise: wetland elevation trends and process controls. In *Wetlands and natural resource management* (pp. 271-292). Springer, Berlin, Heidelberg.

Cahoon, D.R. and Guntenspergen, G.R., 2010. Climate change, sea-level rise, and coastal wetlands. *National Wetlands Newsletter*, *32*(1), pp.8-12.

Cahoon, D.R., 2015. Estimating relative sea-level rise and submergence potential at a coastal wetland. *Estuaries and Coasts*, *38*(3), pp.1077-1084.

Callaway, J.C., Borgnis, E.L., Turner, R.E. and Milan, C.S., 2012. Carbon sequestration and sediment accretion in San Francisco Bay tidal wetlands. *Estuaries and Coasts*, *35*(5), pp.1163-1181.

Cao, Q., Wang, R., Zhang, H., Ge, X. and Liu, J., 2015. Distribution of organic carbon in the sediments of Xinxue River and the Xinxue River constructed wetland, China. *PloS one*, *10*(7), p.e0134713.

Carvalho, L.M., Cacador, I. and Martins-Loução, M., 2001. Temporal and spatial variation of arbuscular mycorrhizas in saltmarsh plants of the Tagus estuary (Portugal). *Mycorrhiza*, *11*(6), pp.303-309.

Cawkwell, F.G., Dwyer, N., Bartlett, D., Ameztoy, I., O'Connor, B., O'Dea, L., Hills, J., Brown, A., Colmer, T.D. and Flowers, T.J., 2008. Flooding tolerance in halophytes. *New Phytologist*, *179*(4), pp.964-974.Cross, N., O'Donnell, M. and Thomas, I., 2007. Saltmarsh habitat classification from satellite imagery.

Colmer, T.D., Pedersen, O., Wetson, A.M. and Flowers, T.J., 2013. Oxygen dynamics in a salt-marsh soil and in Suaeda maritima during tidal submergence. *Environmental and Experimental Botany*, *92*, pp.73-82.

Chapman, V.J., 1960. *Saltmarshes and salt deserts of the world* (No. 581.9095 C43).

Chapman, V.J., 1977. Wet coastal ecosystems: introduction. *Ecosystems of the World*.

Chmura, G.L., Anisfeld, S.C., Cahoon, D.R. and Lynch, J.C., 2003. Global carbon sequestration in tidal, saline wetland soils. *Global biogeochemical cycles*, *17*(4).

Chmura, G.L., 2013. What do we need to assess the sustainability of the tidal salt marsh carbon sink?. *Ocean & Coastal Management*, *83*, pp.25-31.

Church, J.A., P.U. Clark, A. Cazenave, J.M. Gregory, S. Jevrejeva, A. Levermann, M.A. Merrifield, G.A. Milne, R.S. Nerem, P.D. Nunn, A.J. Payne, W.T. Pfeffer, D. Stammer and A.S. Unnikrishnan, 2013: Sea Level Change. In: Climate Change 2013: The Physical Science Basis. Contribution of Working Group I to the Fifth Assessment Report of the Intergovernmental Panel on Climate Change [Stocker, T.F., D. Qin, G.-K. Plattner, M. Tignor, S.K. Allen, J. Boschung, A. Nauels, Y. Xia, V. Bex and P.M. Midgley (eds.)]. Cambridge University Press, Cambridge, United Kingdom and New York, NY, USA.

Clark, C.D., Hughes, A.L., Greenwood, S.L., Jordan, C. and Sejrup, H.P., 2012. Pattern and timing of retreat of the last British-Irish Ice Sheet. *Quaternary Science Reviews*, *44*, pp.112-146.

Collin, A., Lambert, N. and Etienne, S., 2018. Satellite-based saltmarsh elevation, vegetation height, and species composition mapping using the superspectral WorldView-3 imagery. *International Journal of Remote Sensing*, pp.1-19.

Colón-Rivera, R.J., Feagin, R.A., West, J.B. and Yeager, K.M., 2012. Salt marsh connectivity and freshwater versus saltwater inflow: multiple methods including tidal gauges, water isotopes, and LIDAR elevation models. *Canadian Journal of Fisheries and Aquatic Sciences*, *69*(8), pp.1420-1432.

Connor, R.F., Chmura, G.L. and Beecher, C.B., 2001. Carbon accumulation in Bay of Fundy salt marshes: implications for restoration of reclaimed marshes. *Global Biogeochemical Cycles*, *15*(4), pp.943-954.

Cooper, A., 1982. The effects of salinity and waterlogging on the growth and cation uptake of saltmarsh plants. *New phytologist*, *90*(2), pp.263-275.

Costanza, R., d'Arge, R., De Groot, R., Farber, S., Grasso, M., Hannon, B., Limburg, K., Naeem, S., O'neill, R.V., Paruelo, J. and Raskin, R.G., 1997. The value of the world's ecosystem services and natural capital. *nature*, *387*(6630), pp.253-260.

Cott, G.M., Reidy, D.T., Chapman, D.V. and Jansen, M.A., 2013. Waterlogging affects the distribution of the saltmarsh plant Atriplex portulacoides (L.) Aellen. *Flora-Morphology, Distribution, Functional Ecology of Plants*, *208*(5-6), pp.336-342.

Couto, T., Duarte, B., Caçador, I., Baeta, A. and Marques, J.C., 2013. Saltmarsh plants carbon storage in a temperate Atlantic estuary illustrated by a stable isotopic analysis based approach. *Ecological indicators*, *32*, pp.305-311.

Craft, C., Clough, J., Ehman, J., Joye, S., Park, R., Pennings, S., Guo, H. and Machmuller, M., 2009. Forecasting the effects of accelerated sea-level rise on tidal marsh ecosystem services. *Frontiers in Ecology and the Environment*, *7*(2), pp.73-78.

Crosby, S.C., Sax, D.F., Palmer, M.E., Booth, H.S., Deegan, L.A., Bertness, M.D. and Leslie, H.M., 2016. Saltmarsh persistence is threatened by predicted sea-level rise. *Estuarine, Coastal and Shelf Science*, *181*, pp.93-99.

Cundy, A.B., Croudace, I.W., Thomson, J. and Lewis, J.T., 1997. Reliability of saltmarshes as "geochemical recorders" of pollution input: a case study from contrasting estuaries in southern England. *Environmental science & technology*, *31*(4), pp.1093-1101.

Cundy, A.B., Croudace, I.W., Warwick, P.E., Oh, J.S. and Haslett, S.K., 2002. Accumulation of COGEMA-La Hague-derived reprocessing wastes in French saltmarsh sediments. *Environmental science & technology*, *36*(23), pp.4990-4997.

Cundy, A.B., Croudace, I.W., Cearreta, A. and Irabien, M.J., 2003. Reconstructing historical trends in metal input in heavily-disturbed, contaminated estuaries: studies from Bilbao, Southampton Water and Sicily. *Applied Geochemistry*, *18*(2), pp.311-325.

D'Alpaos, A., 2011. The mutual influence of biotic and abiotic components on the long-term ecomorphodynamic evolution of salt-marsh ecosystems. *Geomorphology*, *126*(3-4), pp.269-278.

D'Alpaos, A. and Marani, M., 2016. Reading the signatures of biologic–geomorphic feedbacks in salt-marsh landscapes. *Advances in water resources*, *93*, pp.265-275.

D'Alpaos, A., Lanzoni, S., Rinaldo, A. and Marani, M., 2019. Salt-Marsh Ecogeomorphological Dynamics and Hydrodynamic Circulation. In *Coastal Wetlands* (pp. 189-220). Elsevier.

Da Lio, C., D'Alpaos, A. and Marani, M., 2013. The secret gardener: vegetation and the emergence of biogeomorphic patterns in tidal environments. *Philosophical Transactions of the Royal Society A: Mathematical, Physical and Engineering Sciences*, *371*(2004), p.20120367.

Dalrymple, R.W. and Choi, K., 2007. Morphologic and facies trends through the fluvial–marine transition in tide-dominated depositional systems: a schematic framework for environmental and sequence-stratigraphic interpretation. *Earth-Science Reviews*, *81*(3-4), pp.135-174.

Dankers, N., Binsbergen, M., Zegers, K., Laane, R. and van der Loeff, M.R., 1984. Transportation of water, particulate and dissolved organic and inorganic matter between a salt marsh and the Ems-Dollard estuary, The Netherlands. *Estuarine, Coastal and Shelf Science*, *19*(2), pp.143-165.

Dark, P., Allen, J.R.L., "Seasonal deposition of Holocene banded sediments in the Severn Estuary Levels (southwest Britain): palynological and sedimentological evidence." *Quaternary Science Reviews* 24, no. 1-2 (2005): 11-33.

Davidson, K.E., Fowler, M.S., Skov, M.W., Doerr, S.H., Beaumont, N. and Griffin, J.N., 2017. Livestock grazing alters multiple ecosystem properties and services in saltmarshes: A meta-analysis. *Journal of Applied Ecology*, *54*(5), pp.1395-1405.

Dawson, A.G., Smith, D.E. and Dawson, S., 2001. Potential impacts of climate change on sea levels around Scotland. *SNH Research Survey and Monitoring Report*.

Day, J.W., Christian, R.R., Boesch, D.M., Yáñez-Arancibia, A., Morris, J., Twilley, R.R., Naylor, L. and Schaffner, L., 2008. Consequences of climate change on the ecogeomorphology of coastal wetlands. *Estuaries and Coasts*, *31*(3), pp.477-491.

Day, J.W., Kemp, G.P., Reed, D.J., Cahoon, D.R., Boumans, R.M., Suhayda, J.M. and Gambrell, R., 2011. Vegetation death and rapid loss of surface elevation in two contrasting Mississippi delta saltmarshes: The role of sedimentation, autocompaction and sea-level rise. *Ecological Engineering*, *37*(2), pp.229-240.

de Vos, A.C., Broekman, R., de Almeida Guerra, C.C., van Rijsselberghe, M. and Rozema, J., 2013. Developing and testing new halophyte crops: A case study of salt tolerance of two species of the Brassicaceae, Diplotaxis tenuifolia and Cochlearia officinalis. *Environmental and experimental botany*, *92*, pp.154-164.

de Groot, A.V., Veeneklaas, R.M. and Bakker, J.P., 2011. Sand in the salt marsh: Contribution of high-energy conditions to salt-marsh accretion. *Marine Geology*, *282*(3-4), pp.240-254.

DeLaune, R.D., Nyman, J.A. and Patrick Jr, W.H., 1994. Peat collapse, ponding and wetland loss in a rapidly submerging coastal marsh. *Journal of Coastal Research*, pp.1021-1030.

DeLaune, R.D. and White, J.R., 2012. Will coastal wetlands continue to sequester carbon in response to an increase in global sea level?: a case study of the rapidly subsiding Mississippi river deltaic plain. *Climatic Change*, *110*(1-2), pp.297-314.

Di Bella, C.E., Rodriguez, A.M., Jacobo, E., Golluscio, R.A. and Taboada, M.A., 2015. Impact of cattle grazing on temperate coastal saltmarsh soils. *Soil use and management*, *31*(2), pp.299-307.

Digimap., 2018. *Lidar.* Available: https://digimap.edina.ac.uk/lidar. Last accessed 17 September 2018.

Dijkema, K.S., 1990. Salt and brackish marshes around the Baltic Sea and adjacent parts of the North Sea: their vegetation and management. *Biological Conservation*, *51*(3), pp.191-209.

Doody, J.P., 2004. 'Coastal squeeze'—an historical perspective. *Journal of Coastal Conservation*, *10*(1), pp.129-138.

Doody, J.P., 2007. *Saltmarsh conservation, management and restoration* (Vol. 12). Springer Science & Business Media.

Donnelly, J.P. and Bertness, M.D., 2001. Rapid shoreward encroachment of salt marsh cordgrass in response to accelerated sea-level rise. *Proceedings of the National Academy of Sciences*, *98*(25), pp.14218-14223.

Eggleston, S., Buendia, L. and Miwa, K., 2006. *IPCC Guidelines for National Greenhouse Gas Inventories Agriculture, Forestry and Other Land Use:.Chapter 6*, 4, pp.

Ehlers, J., Nagorny, K., Schmidt, P., Stieve, B. and Zietlow, K., 1993. Storm surge deposits in North Sea saltmarshes dated by 134Cs and 137Cs determination. *Journal of Coastal Research*, *9*(3).

Elgin, B.K., 2012. *Soil organic matter of natural and restored coastal wetland soils in southern California* (Doctoral dissertation, UCLA).

Elschot, K., Bakker, J.P., Temmerman, S., van de Koppel, J. and Bouma, T.J., 2015. Ecosystem engineering by large grazers enhances carbon stocks in a tidal salt marsh. *Marine Ecology Progress Series*, *537*, pp.9-21.

Ember, L.M., Williams, D.F. and Morris, J.T., 1987. Processes that influence carbon isotope variations in saltmarsh sediments. *Marine Ecology Progress Series*, *36*, pp.33-42.

Engels, J.G. and Jensen, K., 2010. Role of biotic interactions and physical factors in determining the distribution of marsh species along an estuarine salinity gradient. *Oikos*, *119*(4), pp.679-685.

Engels, J.G., Rink, F. and Jensen, K., 2011. Stress tolerance and biotic interactions determine plant zonation patterns in estuarine marshes during seedling emergence and early establishment. *Journal of Ecology*, *99*(1), pp.277-287.

Environment Agency., 2018. *Foreshore or intertidal recharge.*Available: http://evidence.environment-agency.gov.uk/FCERM/en/SC060065/MeasuresList/M6/M6T1.aspx?pagenum=2. Last accessed 9 September 2018.

Enwright, N.M., Griffith, K.T. and Osland, M.J., 2016. Barriers to and opportunities for landward migration of coastal wetlands with sea-level rise. *Frontiers in Ecology and the Environment*, *14*(6), pp.307-316.

ESA. (2018). *Overview - Sentinel 2.* Available: https://sentinel.esa.int/web/sentinel/missions/sentinel-2/overview. Last accessed 17 September 2018.

Escapa, M., Perillo, G.M. and Iribarne, O., 2015. Biogeomorphically driven salt pan formation in Sarcocornia-dominated salt-marshes. *Geomorphology*, *228*, pp.147-157.

ESRI., 2018a. *What is lidar data?.* Available: http://desktop.arcgis.com/en/arcmap/10.3/manage-data/las-dataset/what-is-lidar-data-.htm. Accessed 12 September 2018.

ESRI., 2018b. *Image classification using the ArcGIS Spatial Analyst extension*. [ONLINE] Available at: http://desktop.arcgis.com/en/arcmap/latest/extensions/spatial-analyst/image-classification/image-classification-using-spatial-analyst.htm. [Accessed 3 August 2018].

Fagherazzi, S., Hannion, M. and D'Odorico, P., 2008. Geomorphic structure of tidal hydrodynamics in saltmarsh creeks. *Water resources research*, *44*(2).

Fagherazzi, S., Kirwan, M.L., Mudd, S.M., Guntenspergen, G.R., Temmerman, S., D'Alpaos, A., Van De Koppel, J., Rybczyk, J.M., Reyes, E., Craft, C. and Clough, J., 2012. Numerical models of salt marsh evolution: Ecological, geomorphic, and climatic factors. *Reviews of Geophysics*, *50*(1).

Fanjul, E., Grela, M.A. and Iribarne, O., 2007. Effects of the dominant SW Atlantic intertidal burrowing crab Chasmagnathus granulatus on sediment chemistry and nutrient distribution. *Marine Ecology Progress Series*, *341*, pp.177-190.

Feagin, R.A., Martinez, M.L., Mendoza-Gonzalez, G. and Costanza, R., 2010. Saltmarsh zonal migration and ecosystem service change in response to global sea level rise: a case study from an urban region. *Ecology and Society*, *15*(4).

FitzGerald, D.M., Fenster, M.S., Argow, B.A. and Buynevich, I.V., 2008. Coastal impacts due to sea-level rise. *Annual Review of Earth and Planetary Sciences*, *36*.

Foody, G.M., 2002. Status of land cover classification accuracy assessment. *Remote sensing of environment*, *80*(1), pp.185-201.

Ford, H., Garbutt, A., Jones, L. and Jones, D.L., 2012. Methane, carbon dioxide and nitrous oxide fluxes from a temperate saltmarsh: Grazing management does not alter Global Warming Potential. *Estuarine, Coastal and Shelf Science*, *113*, pp.182-191.

Ford, H., Garbutt, A., Duggan-Edwards, M., Harvey, R., Ladd, C. and Skov, M.W., 2019. Large-scale predictions of salt-marsh carbon stock based on simple observations of plant community and soil type. *Biogeosciences*, *16*(2), pp.425-436.

Foster, N.M., Hudson, M.D., Bray, S. and Nicholls, R.J., 2013. Intertidal mudflat and saltmarsh conservation and sustainable use in the UK: A review. *Journal of environmental management*, *126*, pp.96-104.

Friess, D.A., Krauss, K.W., Horstman, E.M., Balke, T., Bouma, T.J., Galli, D. and Webb, E.L., 2012. Are all intertidal wetlands naturally created equal? Bottlenecks, thresholds and knowledge gaps to mangrove and saltmarsh ecosystems. *Biological Reviews*, *87*(2), pp.346-366.

French, J.R. and Stoddart, D.R., 1992. Hydrodynamics of saltmarsh creek systems: Implications for marsh morphological development and material exchange. *Earth surface processes and landforms*, *17*(3), pp.235-252.

French, J.R., 1993. Numerical simulation of vertical marsh growth and adjustment to accelerated sea-level rise, north Norfolk, UK. *Earth Surface Processes and Landforms*, *18*(1), pp.63-81.

French, J., 2006. Tidal marsh sedimentation and resilience to environmental change: exploratory modelling of tidal, sea-level and sediment supply forcing in predominantly allochthonous systems. *Marine Geology*, *235*(1-4), pp.119-136.

French, J.R., 2008. Hydrodynamic modelling of estuarine flood defence realignment as an adaptive management response to sea-level rise. *Journal of Coastal Research*, *24*(sp2), pp.1-12.

French, J., 2019. Tidal Saltmarshes: Sedimentology and Geomorphology. In *Coastal Wetlands*, Elsevier, pp. 479-517.

Frey, R.W. and Basan, P.B., 1978. Coastal saltmarshes. In *Coastal sedimentary environments* (pp. 101-169). Springer, New York, NY.

Friess, D.A., Spencer, T., Smith, G.M., Möller, I., Brooks, S.M. and Thomson, A.G., 2012. Remote sensing of geomorphological and ecological change in response to saltmarsh managed realignment, The Wash, UK. *International Journal of Applied Earth Observation and Geoinformation*, *18*, pp.57-68.

Friess, D.A., Möller, I., Spencer, T., Smith, G.M., Thomson, A.G. and Hill, R.A., 2014. Coastal saltmarsh managed realignment drives rapid breach inlet and external creek evolution, Freiston Shore (UK). *Geomorphology*, *208*, pp.22-33.

García, L.V., Marañón, T., Moreno, A. and Clemente, L., 1993. Above-ground biomass and species richness in a Mediterranean saltmarsh. *Journal of Vegetation Science*, *4*(3), pp.417-424.

Ge, Z.M., Wang, H., Cao, H.B., Zhao, B., Zhou, X., Peltola, H., Cui, L.F., Li, X.Z. and Zhang, L.Q., 2016. Responses of eastern Chinese coastal salt marshes to sea-level rise combined with vegetative and sedimentary processes. *Scientific reports*, *6*, p.28466.

Gedan, K.B., Silliman, B.R. and Bertness, M.D., 2009. Centuries of human-driven change in salt marsh ecosystems. *Annual review of marine science*, *1*, pp.117-141.

Gedan, K.B., Kirwan, M.L., Wolanski, E., Barbier, E.B. and Silliman, B.R., 2011. The present and future role of coastal wetland vegetation in protecting shorelines: answering recent challenges to the paradigm. *Climatic Change*, *106*(1), pp.7-29.

Gehrels, W.R. and Newman, S.W., 2004. Salt-marsh foraminifera in Ho Bugt, western Denmark, and their use as sea-level indicators. *Geografisk Tidsskrift-Danish Journal of Geography*, *104*(1), pp.97-106.

Goman, M., Malamud-Roam, F. and Ingram, B.L., 2008. Holocene environmental history and evolution of a tidal saltmarsh in San Francisco Bay, California. *Journal of Coastal Research*, pp.1126-1137.

Goodwin, G.C., Mudd, S.M. and Clubb, F.J., 2018. Unsupervised detection of saltmarsh platforms: a topographic method. *Earth surface dynamics.*, *6*(1), pp.239-255.

Gosselin, G., Touzi, R. and Cavayas, F., 2014. Polarimetric Radarsat-2 wetland classification using the Touzi decomposition: case of the Lac Saint-Pierre Ramsar wetland. *Canadian Journal of Remote Sensing*, *39*(6), pp.491-506.

Gosselink, J.G., Hatton, R. and Hopkinson, C.S., 1984. Relationship of organic carbon and mineral content to bulk density in Louisiana marsh soils. *Soil Science*, *137*(3), pp.177-180.

Goudie, A., 2013. Characterising the distribution and morphology of creeks and pans on saltmarshes in England and Wales using Google Earth. *Estuarine, Coastal and Shelf Science*, *129*, pp.112-123.

Government of Australia, 2012. *Ozcoasts: Australian online coastal information*. Website: http://www.ozcoasts.gov.au

Gray, A.J., 1972. The ecology of Morecambe Bay. v. The saltmarshes of Morecambe Bay. *Journal of Applied Ecology*, pp.207-220.

Gray, A.J., Parsell, R.J. and Scott, R., 1979. The genetic structure of plant populations in relation to the development of saltmarshes. *Ecological processes in coastal environments*, pp.43-64.

Gray, A.J., Marshall, D.F. and Raybould, A.F., 1991. A century of evolution in Spartina anglica. In *Advances in ecological research* (Vol. 21, pp. 1-62). Academic Press.

Griffin, P.J., Theodose, T. and Dionne, M., 2011. Landscape patterns of forb pannes across a northern New England salt marsh. *Wetlands*, *31*(1), pp.25-33.

Groenendijk, A.M., 1984. Tidal management: Consequences for the salt-marsh vegetation. *Water science and technology*, *16*(1-2), pp.79-86.

Groenendijk, A.M. and Vink-Lievaart, M.A., 1987. Primary production and biomass on a Dutch salt marsh: emphasis on the below-ground component. *Vegetatio*, *70*(1), pp.21-27.

Hacker, S.D. and Bertness, M.D., 1999. Experimental evidence for factors maintaining plant species diversity in a New England saltmarsh. *Ecology*, *80*(6), pp.2064-2073.

Halcrow, 2010a. North West England and North Wales Shoreline Management Plan SMP2. Supporting Studies. Cell Eleven Tide and Sediment transport Study (CETaSS) Phase 2 (ii). Appendix E - Potential Implications of Future Sea Level Rise for Estuarine Sediment Budgets and Morphology in Northwest England and North Wales. Report prepared by K. Pye and S. Blott for Halcrow Group Ltd for the North West and North Wales Coastal Group, October 2009, pp. 102pp + Tables + Figures.

Halcrow, 2010b. North West England and North Wales Shoreline Management Plan SMP2. Supporting Studies. Cell Eleven Tide and Sediment transport Study (CETaSS) Phase 2 (ii). Appendix A - Regional tidal and sediment modelling studies. Report prepared by Halcrow Group Ltd for the North West and North Wales Coastal Group, 2010, pp. 135.

Halcrow, 2010c. North West England and North Wales Shoreline Management Plan SMP2. Annex 1 - Policy Statements – Ribble Estuary. North West and North Wales Coastal Group, February 2011, pp. 4-13.

Halcrow, 2013. North West Estuaries Processes Reports - Ribble Estuary. pp. 4-19

Hewlett, H.W.M., Boorman, L.A. and Bramley, L.A., 1987. *Design of reinforced grass waterways*. Construction Industry Research and Information Association.

Hladik, C. and Alber, M., 2014. Classification of saltmarsh vegetation using edaphic and remote sensing-derived variables. *Estuarine, Coastal and Shelf Science*, *141*, pp.47-57.

Holden, V.J.C., 2008a. Report on the Evolution of the Ribble Estuary, With Particular Reference to the north Sefton Coast. Report to Sefton Council. pp.2-6.

Hopkinson, C.S., Cai, W.J. and Hu, X., 2012. Carbon sequestration in wetland dominated coastal systems—a global sink of rapidly diminishing magnitude. *Current Opinion in Environmental Sustainability*, *4*(2), pp.186-194.

Horton, B.P. and Shennan, I., 2009. Compaction of Holocene strata and the implications for relative sea level change on the east coast of England. *Geology*, *37*(12), pp.1083-1086.

Horton, B.P., Shennan, I., Bradley, S.L., Cahill, N., Kirwan, M., Kopp, R.E. and Shaw, T.A., 2018. Predicting marsh vulnerability to sea-level rise using Holocene relative sea-level data. *Nature communications*, *9*(1), p.2687.

Howe, A.J., Rodríguez, J.F. and Saco, P.M., 2009. Surface evolution and carbon sequestration in disturbed and undisturbed wetland soils of the Hunter estuary, southeast Australia. *Estuarine, coastal and shelf science*, *84*(1), pp.75-83.

Huckle, Jonathan M., Jacqueline A. Potter, and Rob H. Marrs. "Influence of environmental factors on the growth and interactions between saltmarsh plants: effects of salinity, sediment and waterlogging." *Journal of Ecology* 88, no. 3 (2000): 492-505.

Hughes, Z.J., FitzGerald, D.M., Wilson, C.A., Pennings, S.C., Więski, K. and Mahadevan, A., 2009. Rapid headward erosion of marsh creeks in response to relative sea level rise. *Geophysical Research Letters*, *36*(3).

Hunter, E.A., Nibbelink, N.P. and Cooper, R.J., 2017. Divergent forecasts for two saltmarsh specialists in response to sea level rise. *Animal Conservation*, *20*(1), pp.20-28.

Hulisz, P., Piernik, A., Mantilla-Contreras, J. and Elvisto, T., 2016. Main driving factors for seacoast vegetation in the Southern and Eastern Baltic. *Wetlands*, *36*(5), pp.909-919.

Hussey, A. and Long, S.P., 1982. Seasonal changes in weight of above-and below-ground vegetation and dead plant material in a saltmarsh at Colne Point, Essex. *The Journal of Ecology*, pp.757-771.

Isacch, J.P., Costa, C.S.B., Rodríguez-Gallego, L., Conde, D., Escapa, M., Gagliardini, D.A. and Iribarne, O.O., 2006. Distribution of saltmarsh plant communities associated with environmental factors along a latitudinal gradient on the south-west Atlantic coast. *Journal of Biogeography*, *33*(5), pp.888-900.

Isenberg, M., 2018. *LASzip - free and lossless LiDAR compression*. [ONLINE] Available at: https://laszip.org/. [Accessed 14 July 2018].

Jefferies, R.L. and Rockwell, R.F., 2002. Foraging geese, vegetation loss and soil degradation in an Arctic saltmarsh. *Applied Vegetation Science*, *5*(1), pp.7-16.

Jensen, A., 1985. The effect of cattle and sheep grazing on salt-marsh vegetation at Skallingen, Denmark. *Vegetatio*, *60*(1), pp.37-48.

Johnson, R.H. ed., 1985. *The geomorphology of North-west England*. Manchester University Press. Pp. 254-259.

Jones, K.L., Poole, G.C., O'Daniel, S.J., Mertes, L.A. and Stanford, J.A., 2008. Surface hydrology of low-relief landscapes: Assessing surface water flow impedance using LIDAR-derived digital elevation models. *Remote Sensing of Environment*, *112*(11), pp.4148-4158.

Jongepier, I., Wang, C., Missiaen, T., Soens, T. and Temmerman, S., 2015. Intertidal landscape response time to dike breaching and stepwise re-embankment: A combined historical and geomorphological study. *Geomorphology*, *236*, pp.64-78.

Kearney, M.S. and Pendleton, E.C., 1985. Sedimentation and erosion in a Chesapeake Bay brackish marsh system. *Marine Geology*, *67*(3-4), pp.213-235.

Kearney, W.S. and Fagherazzi, S., 2016. Saltmarsh vegetation promotes efficient tidal channel networks. *Nature communications*, *7*(1), pp.1-7.

Kelleway, J.J., Saintilan, N., Macreadie, P.I. and Ralph, P.J., 2016. Sedimentary factors are key predictors of carbon storage in SE Australian saltmarshes. *Ecosystems*, *19*(5), pp.865-880.

Kemp, A.C., Telford, R.J., Horton, B.P., Anisfeld, S.C. and Sommerfield, C.K., 2013. Reconstructing Holocene sea level using salt-marsh foraminifera and transfer functions: lessons from New Jersey, USA. *Journal of Quaternary Science*, *28*(6), pp.617-629.

Kennish, M.J., 2001. Coastal saltmarsh systems in the US: a review of anthropogenic impacts. *Journal of Coastal Research*, pp.731-748.

Kiehl, K., Eischeid, I., Gettner, S. and Walter, J., 1996. Impact of different sheep grazing intensities on saltmarsh vegetation in northern Germany. *Journal of Vegetation Science*, *7*(1), pp.99-106.

Kiehl, K., Esselink, P. and Bakker, J.P., 1997. Nutrient limitation and plant species composition in temperate saltmarshes. *Oecologia*, *111*(3), pp.325-330.

Kim, D., Cairns, D.M. and Bartholdy, J., 2010. Environmental controls on multiscale spatial patterns of saltmarsh vegetation. *Physical Geography*, *31*(1), pp.58-78.

Kim, D., Cairns, D.M., Bartholdy, J. and Morgan, C.L., 2012. Scale-dependent correspondence of floristic and edaphic gradients across salt marsh creeks. *Annals of the Association of American Geographers*, *102*(2), pp.276-294.

Kim, D., Cairns, D.M. and Bartholdy, J., 2013. Tidal creek morphology and sediment type influence spatial trends in saltmarsh vegetation. *The Professional Geographer*, *65*(4), pp.544-560.

Kirwan, M.L., Guntenspergen, G.R., d'Alpaos, A., Morris, J.T., Mudd, S.M. and Temmerman, S., 2010. Limits on the adaptability of coastal marshes to rising sea level. *Geophysical research letters*, *37*(23).

Kirwan, M.L. and Guntenspergen, G.R., 2012. Feedbacks between inundation, root production, and shoot growth in a rapidly submerging brackish marsh. *Journal of Ecology*, *100*(3), pp.764-770.

Kirwan, M.L., Temmerman, S., Skeehan, E.E., Guntenspergen, G.R. and Fagherazzi, S., 2016. Overestimation of marsh vulnerability to sea level rise. *Nature Climate Change*, *6*(3), p.253.

Koch, E.W., Barbier, E.B., Silliman, B.R., Reed, D.J., Perillo, G.M., Hacker, S.D., Granek, E.F., Primavera, J.H., Muthiga, N., Polasky, S. and Halpern, B.S., 2009. Non-linearity in ecosystem services: temporal and spatial variability in coastal protection. *Frontiers in Ecology and the Environment*, *7*(1), pp.29-37.

Kostka, J.E., Gribsholt, B., Petrie, E., Dalton, D., Skelton, H. and Kristensen, E., 2002. The rates and pathways of carbon oxidation in bioturbated saltmarsh sediments. *Limnology and Oceanography*, *47*(1), pp.230-240.

Kulawardhana, R.W., Popescu, S.C. and Feagin, R.A., 2014. Fusion of lidar and multispectral data to quantify saltmarsh carbon stocks. *Remote sensing of environment*, *154*, pp.345-357.

Kumar, L. and Sinha, P., 2014. Mapping salt-marsh land-cover vegetation using high-spatial

Livesley, S.J. and Andrusiak, S.M., 2012. Temperate mangrove and saltmarsh sediments are a small methane and nitrous oxide source but important carbon store. *Estuarine, Coastal and Shelf Science*, *97*, pp.19-27.

Luternauer, J.L., Atkins, R.J., Moody, A.I., Williams, H.E. and Gibson, J.W., 1995. Saltmarshes. In *Developments in Sedimentology* (Vol. 53, pp. 307-332). Elsevier.

Morris, J.T. and Jensen, A., 1998. The carbon balance of grazed and non-grazed Spartina anglica saltmarshes at Skallingen, Denmark. *Journal of Ecology*, *86*(2), pp.229-242.

Morris, J.T., Sundareshwar, P.V., Nietch, C.T., Kjerfve, B. and Cahoon, D.R., 2002. Responses of coastal wetlands to rising sea level. *Ecology*, *83*(10), pp.2869-2877.

National Lacustrine Core Facility., 2013. Loss-on-Ignition Standard Operating Procedure, pp.1-5.

Nolte, S., 2014. *Grazing as a nature-management tool: the effect of different livestock species and stocking densities on salt-marsh vegetation and accretion*.

Langley, A.J., Mozdzer, T.J., Shepard, K.A., Hagerty, S.B. and Patrick Megonigal, J., 2013. Tidal marsh plant responses to elevated CO 2, nitrogen fertilization, and sea level rise. *Global change biology*, *19*(5), pp.1495-1503.

Lawrence, P.J., Smith, G.R., Sullivan, M.J. and Mossman, H.L., 2018. Restored saltmarshes lack the topographic diversity found in natural habitat. *Ecological Engineering*, *115*, pp.58-66.

Leatherman, S.P., 1985. Geomorphic and stratigraphic analysis of Fire Island, New York. *Marine Geology*, *63*(1-4), pp.173-195.

Leonard, L.A. and Luther, M.E., 1995. Flow hydrodynamics in tidal marsh canopies. *Limnology and oceanography*, *40*(8), pp.1474-1484.

Leonardi, N., Carnacina, I., Donatelli, C., Ganju, N.K., Plater, A.J., Schuerch, M. and Temmerman, S., 2017. Dynamic interactions between coastal storms and saltmarshes: A review. *Geomorphology*.

Li, Y.L., Wang, L., Zhang, W.Q., Zhang, S.P., Wang, H.L., Fu, X.H. and Le, Y.Q., 2010. Variability of soil carbon sequestration capability and microbial activity of different types of salt marsh soils at Chongming Dongtan. *Ecological Engineering*, *36*(12), pp.1754-1760.

Long, A.J., Waller, M.P. and Stupples, P., 2006. Driving mechanisms of coastal change: peat compaction and the destruction of late Holocene coastal wetlands. *Marine Geology*, *225*(1-4), pp.63-84.

Luisetti, T., Turner, R.K., Bateman, I.J., Morse-Jones, S., Adams, C. and Fonseca, L., 2011. Coastal and marine ecosystem services valuation for policy and management: Managed realignment case studies in England. *Ocean & Coastal Management*, *54*(3), pp.212-224.

Luisetti, T., Jackson, E.L. and Turner, R.K., 2013. Valuing the European 'coastal blue carbon'storage benefit. *Marine Pollution Bulletin*, *71*(1-2), pp.101-106.

Lytham and District Wildfowling Association. (2018). *Lytham and District Wildfowling Association.* Available: http://www.lythamwildfowlers.co.uk/. Last accessed 12th March 2019.

Maddock, A., 2008. UK Biodiversity Action Plan; Priority Habitat Descriptions. *DEFRA, 5 2pp*.

Magenheimer, J.F., Moore, T.R., Chmura, G.L. and Daoust, R.J., 1996. Methane and carbon dioxide flux from a macrotidal salt marsh, Bay of Fundy, New Brunswick. *Estuaries*, *19*(1), pp.139-145.Marani, M., Belluco, E., Ferrari, S., Silvestri, S., D'Alpaos, A., Lanzoni, S., Feola, A. and Rinaldo, A., 2006. Analysis, synthesis and modelling of high-resolution observations of salt-marsh eco-geomorphological patterns in the Venice lagoon. *Estuarine, Coastal and Shelf Science*, *69*(3-4), pp.414-426.

Marks, T.C. and Truscott, A.J., 1985. Variation in seed production and germination of Spartina anglica within a zoned saltmarsh. *The Journal of Ecology*, pp.695-705.

Mariotti, G., 2018. Marsh channel morphological response to sea level rise and sediment supply. *Estuarine, Coastal and Shelf Science*, *209*, pp.89-101.

Martin, R., Brabyn, L. and Beard, C., 2014. Effects of class granularity and cofactors on the performance of unsupervised classification of wetlands using multi-spectral aerial photography. *Journal of Spatial Science*, *59*(2), pp.269-282.

Masselink, G., Hanley, M.E., Halwyn, A.C., Blake, W., Kingston, K., Newton, T. and Williams, M., 2017. Evaluation of saltmarsh restoration by means of self-regulating tidal gate–Avon estuary, South Devon, UK. *Ecological engineering*, *106*, pp.174-190.

McLaren, J.R., Jefferies, R.L., 2004. Initiation and maintenance of vegetation mosaics in an arctic salt marsh. *Journal of Ecology, 92*, pp.648–660.

Mcleod, E., Chmura, G.L., Bouillon, S., Salm, R., Björk, M., Duarte, C.M., Lovelock, C.E., Schlesinger, W.H. and Silliman, B.R., 2011. A blueprint for blue carbon: toward an improved understanding of the role of vegetated coastal habitats in sequestering CO2. *Frontiers in Ecology and the Environment*, *9*(10), pp.552-560.

Mendelssohn, I.A. and Kuhn, N.L., 2003. Sediment subsidy: effects on soil–plant responses in a rapidly submerging coastal saltmarsh. *Ecological Engineering*, *21*(2-3), pp.115-128.

Metcalfe, S.E., Ellis, S., Horton, B.P., Innes, J.B., McArthur, J., Mitlehner, A., Parkes, A., Pethick, J.S., Rees, J., Ridgway, J. and Rutherford, M.M., 2000. The Holocene evolution of the Humber Estuary: reconstructing change in a dynamic environment. *Geological Society, London, Special Publications*, *166*(1), pp.97-118.

Millington, A.C., Walsh, S.J. and Osborne, P.E. eds., 2013. *GIS and remote sensing applications in biogeography and ecology* (Vol. 626). Springer Science & Business Media.

Mitsch, W.J. and Gosselink, J.G., 2000. The value of wetlands: importance of scale and landscape setting. *Ecological economics*, *35*(1), pp.25-33.

Mitsch, W.J., 2012. What is ecological engineering?. *Ecological Engineering*, *45*, pp.5-12.

Moffett, K.B., Robinson, D.A. and Gorelick, S.M., 2010. Relationship of saltmarsh vegetation zonation to spatial patterns in soil moisture, salinity, and topography. *Ecosystems*, *13*(8), pp.1287-1302.

Moller, I., 2006. Quantifying saltmarsh vegetation and its effect on wave height dissipation: Results from a UK East coast saltmarsh. *Estuarine, Coastal and Shelf Science*, *69*(3-4), pp.337-351.

Möller, I., Kudella, M., Rupprecht, F., Spencer, T., Paul, M., Van Wesenbeeck, B.K., Wolters, G., Jensen, K., Bouma, T.J., Miranda-Lange, M. and Schimmels, S., 2014. Wave attenuation over coastal saltmarshes under storm surge conditions. *Nature Geoscience*, *7*(10), p.727.

Moore, R.D., Wolf, J., Souza, A.J. and Flint, S.S., 2009. Morphological evolution of the Dee Estuary, Eastern Irish Sea, UK: a tidal asymmetry approach. *Geomorphology*, *103*(4), pp.588-596.

Mossman, H.L., Davy, A.J. and Grant, A., 2012. Does managed coastal realignment create saltmarshes with 'equivalent biological characteristics' to natural reference sites?. *Journal of Applied Ecology*, *49*(6), pp.1446-1456.

Mudd, S.M., Howell, S.M. and Morris, J.T., 2009. Impact of dynamic feedbacks between sedimentation, sea-level rise, and biomass production on near-surface marsh stratigraphy and carbon accumulation. *Estuarine, Coastal and Shelf Science*, *82*(3), pp.377-389.

Mudd, S.M., 2011. The life and death of saltmarshes in response to anthropogenic disturbance of sediment supply. *Geology*, *39*(5), pp.511-512.

Mudd, S.M. and Fagherazzi, S., 2016. 12 Saltmarsh Ecosystems: Tidal Flow, Vegetation, and Carbon Dynamics. *A Biogeoscience Approach to Ecosystems*, p.407.

Müller-Navarra, K., Milker, Y. and Schmiedl, G., 2016. Natural and anthropogenic influence on the distribution of saltmarsh foraminifera in the Bay of Tümlau, German North Sea. *The Journal of Foraminiferal Research*, *46*(1), pp.61-74.

National Biodiversity Network Atlas., 2018. *Location.* Available: National Biodiversity Network Atlas. Last accessed 3rd February 2019.

Needles, L.A., Lester, S.E., Ambrose, R., Andren, A., Beyeler, M., Connor, M.S., Eckman, J.E., Costa-Pierce, B.A., Gaines, S.D., Lafferty, K.D. and Lenihan, H.S., 2015. Managing bay and estuarine ecosystems for multiple services. *Estuaries and Coasts*, *38*(1), pp.35-48.

Nicholls, R.J., Klein, R.J. and Tol, R.S., 2007. Managing coastal vulnerability and climate change: a national to global perspective. *Managing Coastal Vulnerability. Oxford, UK: Elsevier*, pp.223-241.

Nixon, S.W., 1980. Between coastal marshes and coastal waters—a review of twenty years of speculation and research on the role of saltmarshes in estuarine productivity and water chemistry. In *Estuarine and wetland processes* (pp. 437-525). Springer, Boston, MA.

Olff, H., Bakker, J.P. and Fresco, L.F.M., 1988. The effect of fluctuations in tidal inundation frequency on a salt-marsh vegetation. *Vegetatio*, *78*(1-2), pp.13-19.

Olsen, Y.S., Dausse, A., Garbutt, A., Ford, H., Thomas, D.N. and Jones, D.L., 2011. Cattle grazing drives nitrogen and carbon cycling in a temperate saltmarsh. *Soil Biology and Biochemistry*, *43*(3), pp.531-541.

Oenema, O. and DeLaune, R.D., 1988. Accretion rates in saltmarshes in the Eastern Scheldt, south-west Netherlands. *Estuarine, Coastal and Shelf Science*, *26*(4), pp.379-394.

Orson, R.A. and Howes, B.L., 1992. Saltmarsh development studies at Waquoit Bay, Massachusetts: Influence of geomorphology on long-term plant community structure. *Estuarine, Coastal and Shelf Science*, *35*(5), pp.453-471.

Orr, M., Crooks, S. and Williams, P.B., 2003. Will restored tidal marshes be sustainable?. *San Francisco Estuary and Watershed Science*, *1*(1).

Osland, M.J., Enwright, N.M., Day, R.H., Gabler, C.A., Stagg, C.L. and Grace, J.B., 2016. Beyond just sea-level rise: considering macroclimatic drivers within coastal wetland vulnerability assessments to climate change. *Global Change Biology*, *22*(1), pp.1-11.

Ozesmi, S.L. and Bauer, M.E., 2002. Satellite remote sensing of wetlands. *Wetlands ecology and management*, *10*(5), pp.381-402.

Otani, S. and Endo, T., 2019. CO 2 flux in tidal flats and salt marshes. In *Blue Carbon in Shallow Coastal Ecosystems* (pp. 223-250). Springer, Singapore.

Owers, C.J., Rogers, K. and Woodroffe, C.D., 2018. Spatial variation of above-ground carbon storage in temperate coastal wetlands. *Estuarine, Coastal and Shelf Science*.

Pack, R.T., Blonquist, K., Carter, B., 2012. Lidar bare-earth modelling of overhanging cliffs – extending 2.5-D Lidar classifiers to handle 3D surface classification problems. *ASPRS 2012 Annual Conference*, pp.1-2.

Palmer, M., Howard, T., Tinker, J., Lowe, J., Bricheno, L., Calvert, D., Edwards, T., Gregory, J., Harris, G., Krijnen, J. and Pickering, M., 2018. UKCP 18 marine report. *Met Office Hadley Centre*: Exeter, UK, pp.10-27.

Pande-Chhetri, R., Abd-Elrahman, A., Liu, T., Morton, J. and Wilhelm, V.L., 2017. Object-based classification of wetland vegetation using very high-resolution unmanned air system imagery. *European Journal of Remote Sensing*, *50*(1), pp.564-576.

Park, R.A., Trehan, M.S., Mausel, P.W. and Howe, R.C., 1989. The effects of sea level rise on US coastal wetlands. *Environmental Protection Agency*.

Passeri, D.L., Hagen, S.C., Medeiros, S.C., Bilskie, M.V., Alizad, K. and Wang, D., 2015. The dynamic effects of sea level rise on low-gradient coastal landscapes: A review. *Earth's Future*, *3*(6), pp.159-181.

Peh, K.S.H., Balmford, A., Bradbury, R.B., Brown., Butchart, S.H.M., Hughes, F.M.R., McDonald, M.A., Stattersfield, A.J., Thomas, D.H.L., Trevelyan, R.J., Walpole, M., and Merriman, J.C., 2017. *Toolkit for Ecosystem Service Site-based Assessment (TESSA) Version 2.0*. *Cambridge*. Available at: http://tessa.tools.

Pendleton, L., Donato, D.C., Murray, B.C., Crooks, S., Jenkins, W.A., Sifleet, S., Craft, C., Fourqurean, J.W., Kauffman, J.B., Marbà, N. and Megonigal, P., 2012. Estimating global "blue carbon" emissions from conversion and degradation of vegetated coastal ecosystems. *PloS one*, *7*(9), p.e43542.

Pennings, S.C. and Callaway, R.M., 1992. Salt marsh plant zonation: the relative importance of competition and physical factors. *Ecology*, *73*(2), pp.681-690.

Pennings, S.C., GRANT, M.B. and Bertness, M.D., 2005. Plant zonation in low-latitude saltmarshes: disentangling the roles of flooding, salinity and competition. *Journal of ecology*, *93*(1), pp.159-167.

Perillo, G.M. and Iribarne, O.O., 2003. Processes of tidal channel development in salt and freshwater marshes. *Earth Surface Processes and Landforms: The Journal of the British Geomorphological Research Group*, *28*(13), pp.1473-1482.

Perillo, G.M., 2019. Geomorphology of Tidal Courses and Depressions. In Wolanski, E., Cahoon, D. R., & Hopkinson, C. S. (Eds.) Coastal Wetlands (pp. 221-261). Elsevier.

Pestrong, R., 1965. The development of drainage patterns on tidal marshes. *Stanford University publications*, *10*(2).

Pethick, J.S., 1974. The distribution of salt pans on tidal saltmarshes. *Journal of Biogeography*, pp.57-62.

Pethick, J.S., 1981. Long-term accretion rates on tidal saltmarshes. *Journal of Sedimentary Research*, *51*(2), pp.571-577.

Pethick, J., 1993. Shoreline adjustments and coastal management: physical and biological processes under accelerated sea-level rise. *Geographical Journal*, pp.162-168.

Pethick, J., 2002. Estuarine and tidal wetland restoration in the United Kingdom: policy versus practice. *Restoration Ecology*, *10*(3), pp.431-437.

Pfeffer, W.T., Harper, J.T. and O'Neel, S., 2008. Kinematic constraints on glacier contributions to 21st-century sea-level rise. *Science*, *321*(5894), pp.1340-1343.

Phillips, J.D., 2018. Environmental gradients and complexity in coastal landscape response to sea level rise. *Catena*, *169*, pp.107-118.

Pigott, C., Ratcliffe, D., Malloch, A., Birks, H., & Proctor., M. 2000. SM20: Eleocharis uniglumis salt-marsh community: Eleocharitetum uniglumis Nordhagen 1923. In J. Rodwell (Ed.), British Plant Communities (British Plant Communities, pp. 92-93). Cambridge: Cambridge University Press. doi:10.1017/CBO9780511541834.024

Pimentel, D., 2014. *Biological invasions: economic and environmental costs of alien plant, animal, and microbe species*. CRC press.

Pomeroy, L.R. and Wiegert, R.G. eds., 2012. *The ecology of a saltmarsh* (Vol. 38). Springer Science & Business Media.

Pont, D., Day, J.W., Hensel, P., Franquet, E., Torre, F., Rioual, P., Ibànez, C. and Coulet, E., 2002. Response scenarios for the deltaic plain of the Rhone in the face of an acceleration in the rate of sea-level rise with special attention toSalicornia-type environments. *Estuaries*, *25*(3), pp.337-358.

Portnoy, J.W. and Giblin, A.E., 1997. Effects of historic tidal restrictions on saltmarsh sediment chemistry. *Biogeochemistry*, *36*(3), pp.275-303.

Rabenhorst, M.C., 1995. Carbon storage in tidal marsh soils. *Soils and Global Change*, *5*, pp.93-103.

Rahman, R. and Plater, A.J., 2014. Particle-size evidence of estuary evolution: A rapid and diagnostic tool for determining the nature of recent saltmarsh accretion. *Geomorphology*, *213*, pp.139-152.

Ramírez-Herrera, M.T., Lagos, M., Hutchinson, I., Kostoglodov, V., Machain, M.L., Caballero, M., Goguitchaichvili, A., Aguilar, B., Chagué-Goff, C., Goff, J. and Ruiz-Fernández, A.C., 2012. Extreme wave deposits on the Pacific coast of Mexico: Tsunamis or storms?—A multi-proxy approach. *Geomorphology*, *139*, pp.360-371.

Reed, D.J., Stoddart, D.R. and Bayliss-Smith, T.P., 1985. Tidal flows and sediment budgets for a salt-marsh system, Essex, England. *Vegetatio*, *62*(1-3), pp.375-380.

Reed, D.J., 1990. The impact of sea-level rise on coastal saltmarshes. *Progress in Physical Geography*, *14*(4), pp.465-481.

Reed, D.J., 1995. The response of coastal marshes to sea-level rise: Survival or submergence?. *Earth Surface Processes and Landforms*, *20*(1), pp.39-48.

Richards, C.L., Pennings, S.C. and Donovan, L.A., 2005. Habitat range and phenotypic variation in saltmarsh plants. *Plant Ecology*, *176*(2), pp.263-273.

Rizzetto, F. and Tosi, L., 2012. Rapid response of tidal channel networks to sea-level variations (Venice Lagoon, Italy). *Global and Planetary Change*, *92*, pp.191-197.

Robins, P.E., Skov, M.W., Lewis, M.J., Gimenez, L., Davies, A.G., Malham, S.K., Neill, S.P., McDonald, J.E., Whitton, T.A., Jackson, S.E. and Jago, C.F., 2016. Impact of climate change on UK estuaries: A review of past trends and potential projections. *Estuarine, Coastal and Shelf Science*, *169*, pp.119-135.

Rogers, K., Saintilan, N. and Copeland, C., 2012. Modelling wetland surface elevation dynamics and its application to forecasting the effects of sea-level rise on estuarine wetlands. *Ecological Modelling*, *244*, pp.148-157.

Roman, C.T. and Daiber, F.C., 1989. Organic carbon flux through a Delaware Bay saltmarsh: Tidal exchange, particle size distribution, and storms. *Marine ecology progress series. Oldendorf*, *54*(1), pp.149-156.

Roman, C.T., 2017. Salt marsh sustainability: challenges during an uncertain future. *Estuaries and coasts*, *40*(3), pp.711-716.

Roner, M., D'Alpaos, A., Ghinassi, M., Marani, M., Silvestri, S., Franceschinis, E. and Realdon, N., 2016. Spatial variation of salt-marsh organic and inorganic deposition and organic carbon accumulation: Inferences from the Venice lagoon, Italy. *Advances in water resources*, *93*, pp.276-287.

Rosenfield, G.H. and Fitzpatrick-Lins, K., 1986. A coefficient of agreement as a measure of thematic classification accuracy. *Photogrammetric engineering and remote sensing*, *52*(2), pp.223-227.

Rouger, R., 2014. Restoration genetics of north-west European saltmarshes: A multi-scale analysis of population genetic structure in Puccinellia maritima and Triglochin maritima.

Rozema, J., Rozema-Dijst, E., Freijsen, A.H.J. and Huber, J.J.L., 1978. Population differentiation within Festuca rubra L. with regard to soil salinity and soil water. *Oecologia*, *34*(3), pp.329-341.

Rupprecht, F., Wanner, A., Stock, M. and Jensen, K., 2015. Succession in saltmarshes–large-scale and long-term patterns after abandonment of grazing and drainage. *Applied Vegetation Science*, *18*(1), pp.86-98.

Sanchez, J.M., Izco, J. and Medrano, M., 1996. Relationships between vegetation zonation and altitude in a salt-marsh system in northwest Spain. *Journal of Vegetation Science*, *7*(5), pp.695-702.

Sanchez-Hernandez, C., Boyd, D.S. and Foody, G.M., 2007. Mapping specific habitats from remotely sensed imagery: support vector machine and support vector data description based classification of coastal saltmarsh habitats. *Ecological informatics*, *2*(2), pp.83-88.

Sanderson, E.W., Ustin, S.L. and Foin, T.C., 2000. The influence of tidal channels on the distribution of saltmarsh plant species in Petaluma Marsh, CA, USA. *Plant Ecology*, *146*(1), pp.29-41.

Saintilan, N. and Rogers, K., 2013. The significance and vulnerability of Australian saltmarshes: implications for management in a changing climate. *Marine and Freshwater Research*, *64*(1), pp.66-79.

Scavia, D., Field, J.C., Boesch, D.F., Buddemeier, R.W., Burkett, V., Cayan, D.R., Fogarty, M., Harwell, M.A., Howarth, R.W., Mason, C. and Reed, D.J., 2002. Climate change impacts on US coastal and marine ecosystems. *Estuaries*, *25*(2), pp.149-164.

Schepers, L., 2017. *Spatial patterns and bio-geomorphological effects of vegetation loss in a submerging coastal marsh*(Doctoral dissertation, University of Antwerp).

Schepers, L., Maris, T., Meire, P. and Temmerman, S., 2018. The Scheldt Estuary: An Overview of the Morphodynamics of Intertidal Areas. In *Landscapes and Landforms of Belgium and Luxembourg* (pp. 281-296). Springer, Cham.

Schile, L.M., Callaway, J.C., Morris, J.T., Stralberg, D., Parker, V.T. and Kelly, M., 2014. Modeling tidal marsh distribution with sea-level rise: Evaluating the role of vegetation, sediment, and upland habitat in marsh resiliency. *PLoS One*, *9*(2), p.e88760.

Schmidt, K.S., 2003. *Hyperspectral remote sensing of vegetation species distribution in a saltmarsh*. Wageningen Universiteit.

Schuerch, M., Dolch, T., Bisgwa, J. and Vafeidis, A.T., 2018. Changing sediment dynamics of a mature backbarrier saltmarsh in response to sea-level rise and storm events. *Frontiers in Marine Science*, *5*.

Shalaby, A. and Tateishi, R., 2007. Remote sensing and GIS for mapping and monitoring land cover and land-use changes in the Northwestern coastal zone of Egypt. *Applied Geography*, *27*(1), pp.28-41.

Sheehan, M.R. and Ellison, J.C., 2014. Intertidal morphology change following Spartina anglica introduction, Tamar Estuary, Tasmania. *Estuarine, Coastal and Shelf Science*, *149*, pp.24-37.

Sheehan, M.R. and Ellison, J.C., 2015. Tidal marsh erosion and accretion trends following invasive species removal, Tamar Estuary, Tasmania. *Estuarine, Coastal and Shelf Science*, *164*, pp.46-55.

Shen, C., Zhang, C., Xin, P., Kong, J. and Li, L., 2018. Salt dynamics in coastal marshes: Formation of hypersaline zones. *Water Resources Research*, *54*(5), pp.3259-3276.

Shennan, I. and Horton, B., 2002. Holocene land-and sea-level changes in Great Britain. *Journal of Quaternary Science: Published for the Quaternary Research Association*, *17*(5-6), pp.511-526.

Shennan, I., Bradley, S.L. and Edwards, R., 2018. Relative sea-level changes and crustal movements in Britain and Ireland since the Last Glacial Maximum. *Quaternary Science Reviews*, *188*, pp.143-159.

Siikamäki, J., Sanchirico, J.N., Jardine, S., McLaughlin, D. and Morris, D., 2013. Blue carbon: coastal ecosystems, their carbon storage, and potential for reducing emissions. *Environment: Science and Policy for Sustainable Development*, *55*(6), pp.14-29.

Silvestri, S., Defina, A. and Marani, M., 2005. Tidal regime, salinity and saltmarsh plant zonation. *Estuarine, coastal and shelf science*, *62*(1-2), pp.119-130.

Silvestri, S., Defina, A. and Marani, M., 2005. Tidal regime, salinity and saltmarsh plant zonation. *Estuarine, coastal and shelf science*, *62*(1-2), pp.119-130.

Simas, T., Nunes, J.P. and Ferreira, J.G., 2001. Effects of global climate change on coastal saltmarshes. *Ecological Modelling*, *139*(1), pp.1-15.

Singh, S.K., Srivastava, P.K., Gupta, M., Thakur, J.K. and Mukherjee, S., 2014. Appraisal of land use/land cover of mangrove forest ecosystem using support vector machine. *Environmental earth sciences*, *71*(5), pp.2245-2255.

Skov, M.W., Ford, H., Webb, J., Kayoueche-Reeve, M., Hockley, N., Paterson, D. and Garbutt, A., 2016. The Saltmarsh Carbon Stock Predictor: a tool for predicting carbon stocks of Welsh and English and salt marshes, UK. *CBESS, Biodiversity and Ecosystem Service Sustainability programme (NERC NE/J015350/1), Bangor University, UK*. pp.5-13.

Slocum, M.G., Mendelssohn, I.A. and Kuhn, N.L., 2005. Effects of sediment slurry enrichment on saltmarsh rehabilitation: plant and soil responses over seven years. *Estuaries*, *28*(4), pp.519-528.

Sousa, A.I., Lillebø, A.I., Pardal, M.A. and Caçador, I., 2010. The influence of Spartina maritima on carbon retention capacity in saltmarshes from warm-temperate estuaries. *Marine pollution bulletin*, *61*(4-6), pp.215-223.

Spencer, T., Schuerch, M., Nicholls, R.J., Hinkel, J., Lincke, D., Vafeidis, A.T., Reef, R., McFadden, L. and Brown, S., 2016. Global coastal wetland change under sea-level rise and related stresses: The DIVA Wetland Change Model. *Global and Planetary Change*, *139*, pp.15-30.

Spencer, K.L. and Harvey, G.L., 2012. Understanding system disturbance and ecosystem services in restored saltmarshes: integrating physical and biogeochemical processes. *Estuarine, Coastal and Shelf Science*, *106*, pp.23-32.

Spencer, T., Möller, I., Rupprecht, F., Bouma, T.J., van Wesenbeeck, B.K., Kudella, M., Paul, M., Jensen, K., Wolters, G., Miranda-Lange, M. and Schimmels, S., 2016. Saltmarsh surface survives true-to-scale simulated storm surges. *Earth Surface Processes and Landforms*, *41*(4), pp.543-552.

Squiers, E.R. and Good, R.E., 1974. Seasonal changes in the productivity, caloric content, and chemical composition of a population of salt-marsh cord-grass (Spartina alterniflora). *Chesapeake Science*, *15*(2), pp.63-71.

Stéphan, P., Goslin, J., Pailler, Y., Manceau, R., Suanez, S., Van Vliet-Lanoë, B., Hénaff, A. and Delacourt, C., 2015. Holocene salt-marsh sedimentary infilling and relative sea-level changes in W est B rittany (F rance) using foraminifera-based transfer functions. *Boreas*, *44*(1), pp.153-177.

Stefanon, L., Carniello, L., D'Alpaos, A. and Rinaldo, A., 2012. Signatures of sea level changes on tidal geomorphology: Experiments on network incision and retreat. *Geophysical Research Letters*, *39*(12).

Sterr, H., 2008. Assessment of vulnerability and adaptation to sea-level rise for the coastal zone of Germany. *Journal of Coastal Research*, pp.380-393.

Stralberg, D., Brennan, M., Callaway, J.C., Wood, J.K., Schile, L.M., Jongsomjit, D., Kelly, M., Parker, V.T. and Crooks, S., 2011. Evaluating tidal marsh sustainability in the face of sea-level rise: a hybrid modeling approach applied to San Francisco Bay. *PloS one*, *6*(11), p.e27388.

STRUCTX., 2018. *Density Ranges for Different Soil Types.* Available: http://structx.com/Soil_Properties_002.html. Last accessed 27th August 2018.

Suchrow, S. and Jensen, K., 2010. Plant species responses to an elevational gradient in German North Sea saltmarshes. *Wetlands*, *30*(4), pp.735-746.

Swindles, G.T., Galloway, J.M., Macumber, A.L., Croudace, I., Emery, A.R., Woulds, C., Bateman, M.D., Parry, L., Jones, J.M., Selby, K. and Rushby, G.T., 2018. Sedimentary records of coastal storm surges: evidence of the 1953 North Sea event. *Marine geology.*, *403*, pp.262-270.

Symonds, A.M. and Collins, M.B., 2005. Sediment dynamics associated with managed realignment; Freiston Shore, The Wash, UK. In *Coastal Engineering 2004: (In 4 Volumes)* (pp. 3173-3185).

Symonds, A.M. and Collins, M.B., 2007. The establishment and degeneration of a temporary creek system in response to managed coastal realignment: The Wash, UK. *Earth Surface Processes and Landforms: The Journal of the British Geomorphological Research Group*, *32*(12), pp.1783-1796.

Teal, J.M., 1962. Energy flow in the saltmarsh ecosystem of Georgia. *Ecology*, *43*(4), pp.614-624.

Temmerman, S., De Vries, M.B. and Bouma, T.J., 2012. Coastal marsh die-off and reduced attenuation of coastal floods: A model analysis. *Global and Planetary Change*, *92*, pp.267-274.

Theuerkauf, E.J., Stephens, J.D., Ridge, J.T., Fodrie, F.J. and Rodriguez, A.B., 2015. Carbon export from fringing saltmarsh shoreline erosion overwhelms carbon storage across a critical width threshold. *Estuarine, Coastal and Shelf Science*, *164*, pp.367-378.

Thomson, A.G., 1998. Supervised versus unsupervised methods for classification of coasts and river corridors from airborne remote sensing. *International Journal of Remote Sensing*, *19*(17), pp.3423-3431.

Thyen, S. and Exo, K.M., 2003. Wadden Sea saltmarshes: Ecological trap or hideaway for breeding Redshanks Tringa totanus?. *BULLETIN-WADER STUDY GROUP*, *100*, pp.43-46.

Tong, C., Jia, R.X., Wang, W.Q. and Zeng, C.S., 2010. Spatial variations of carbon, nitrogen and phosphorous in tidal saltmarsh soils of the Minjiang River estuary [J]. *Geographical Research*, *7*, p.005.

Torio, D.D. and Chmura, G.L., 2013. Assessing coastal squeeze of tidal wetlands. *Journal of Coastal Research*, *29*(5), pp.1049-1061.

Touchette, B.W., Kneppers, M.K. and Eggert, M.C., 2019. Saltmarsh plants: Biological overview and vulnerability to Climate Change. *Halophytes and Climate Change: Adaptive Mechanisms and Potential Uses; Hasanuzzaman, MS, Shabala, S., Fujita, M., Eds*, pp.115-134.

Townend, I. and Pethick, J., 2002. Estuarine flooding and managed retreat. *Philosophical Transactions of the Royal Society of London A: Mathematical, Physical and Engineering Sciences*, *360*(1796), pp.1477-1495.

Townend, I., Fletcher, C., Knappen, M. and Rossington, K., 2011. A review of salt marsh dynamics. *Water and Environment Journal*, *25*(4), pp.477-488.

Trivisonno, F.N., Rodriguez, J.F., Riccardi, G.A. and Saco, P.M., 2013. Modelling soil, carbon and vegetation dynamics in estuarine wetlands experiencing sea-level rise. *Proceedings of 2013 IAHR Congress.* pp. 6-7.

Tröels-Smith, J., 1955. Karakterisaring af Løse jordarter. *Danmarks Geologiska Undersoegelsa IV Reakke Bd*, *3*, pp.1-73.

Tsompanoglou, K., Croudace, I.W., Birch, H. and Collins, M., 2011. Geochemical and radiochronological evidence of North Sea storm surges in salt marsh cores from The Wash embayment (UK). *The Holocene*, *21*(2), pp.225-236.

Turner, R.E., Swenson, E.M. and Milan, C.S., 2002. Organic and inorganic contributions to vertical accretion in saltmarsh sediments. In *Concepts and controversies in tidal marsh ecology* (pp. 583-595). Springer, Dordrecht.

Tsuzaki, T., 2010. *Spartina anglica population and environmental studies within the Solent salt marsh system* (Doctoral dissertation, University of Southampton). pp. 70-84.

Van Der Wal, D., Pye, K. and Neal, A., 2002. Long-term morphological change in the Ribble Estuary, northwest England. *Marine Geology*, *189*(3-4), pp.249-266.

Van Der Wal, D. and Pye, K., 2003. The use of historical bathymetric charts in a GIS to assess morphological change in estuaries. *Geographical Journal*, *169*(1), pp.21-31.

Van der Wal, D. and Pye, K., 2004. Patterns, rates and possible causes of saltmarsh erosion in the Greater Thames area (UK). *Geomorphology*, *61*(3-4), pp.373-391.

Van Eerdt, M.M., 1985. The influence of vegetation on erosion and accretion in saltmarshes of the Oosterschelde, The Netherlands. In *Ecology of coastal vegetation* (pp. 367-373). Springer, Dordrecht.

Van Wijnen, H.J. and Bakker, J.P., 2001. Long-term surface elevation change in salt marshes: a prediction of marsh response to future sea-level rise. *Estuarine, Coastal and Shelf Science*, *52*(3), pp.381-390.

Veldhuis, E.R., Schrama, M., Staal, M. and Elzenga, J.T.M., 2019. Plant stress-tolerance traits predict saltmarsh vegetation patterning. *Frontiers in Marine Science*, *5* (501), pp. 1-11.

Ward, R.D., Burnside, N.G., Joyce, C.B., Sepp, K. and Teasdale, P.A., 2016. Improved modelling of the impacts of sea level rise on coastal wetland plant communities. *Hydrobiologia*, *774*(1), pp.203-216.

Warren, R.S. and Niering, W.A., 1993. Vegetation change on a northeast tidal marsh: Interaction of sea-level rise and marsh accretion. *Ecology*, *74*(1), pp.96-103.

Watson, E.B., Wigand, C., Davey, E.W., Andrews, H.M., Bishop, J. and Raposa, K.B., 2017. Wetland loss patterns and inundation-productivity relationships prognosticate widespread salt marsh loss for southern New England. *Estuaries and Coasts*, *40*(3), pp.662-681.

Wickham, H. and Grolemund, G., 2017. *R for data science: import, tidy, transform, visualize, and model data*. " O'Reilly Media, Inc.".

Wigand, C., Davey, E., Johnson, R., Sundberg, K., Morris, J., Kenny, P., Smith, E. and Holt, M., 2015. Nutrient effects on belowground organic matter in a minerogenic salt marsh, North Inlet, SC. *Estuaries and coasts*, *38*(6), pp.1838-1853.

Williams, T.P., Bubb, J.M. and Lester, J.N., 1994. Metal accumulation within salt marsh environments: a review. *Marine pollution bulletin*, *28*(5), pp.277-290.

Wilson, C.A., Hughes, Z.J., FitzGerald, D.M., Hopkinson, C.S., Valentine, V. and Kolker, A.S., 2014. Saltmarsh pool and tidal creek morphodynamics: Dynamic equilibrium of northern latitude saltmarshes?. *Geomorphology*, *213*, pp.99-115.

Windham, L., 2001. Comparison of biomass production and decomposition between Phragmites australis (common reed) and Spartina patens (salt hay grass) in brackish tidal marshes of New Jersey, USA. *Wetlands*, *21*(2), pp.179-188.

Wolters, M., Garbutt, A. and Bakker, J.P., 2005. Salt-marsh restoration: evaluating the success of de-embankments in north-west Europe. *Biological Conservation*, *123*(2), pp.249-268.

Woodworth, P.L., 1999. High waters at Liverpool since 1768: the UK's longest sea level record. *Geophysical Research Letters*, *26*(11), pp.1589-1592.

Xin, P., Zhou, T., Lu, C., Shen, C., Zhang, C., D'Alpaos, A. and Li, L., 2017. Combined effects of tides, evaporation and rainfall on the soil conditions in an intertidal creek-marsh system. *Advances in water resources*, *103*, pp.1-15.

Yu, O.T. and Chmura, G.L., 2009. Soil carbon may be maintained under grazing in a St Lawrence Estuary tidal marsh. *Environmental Conservation*, *36*(4), pp.312-320.

Zedler, J.B., Winfield, T. and Williams, P., 1980. Saltmarsh productivity with natural and altered tidal circulation. *Oecologia*, *44*(2), pp.236-240.

Zedler, J.B. and Callaway, J.C., 1999. Tracking wetland restoration: do mitigation sites follow desired trajectories?. *Restoration ecology*, *7*(1), pp.69-73.

Zedler, J.B., 2000. Progress in wetland restoration ecology. *Trends in ecology & evolution*, *15*(10), pp.402-407.

Zedler, J.B. and Kercher, S., 2005. Wetland resources: status, trends, ecosystem services, and restorability. *Annu. Rev. Environ. Resour.*, *30*, pp.39-74.

Zhang, C., Zang, S.Y., Jin, Z. and Zhang, Y.H., 2011. Remote sensing classification for Zhalong wetlands based on support vector machine. *Wetland science*, *9*(3), pp.263-269.

Zhang, Z.S., Song, X.L., Lu, X.G. and Xue, Z.S., 2013. Ecological stoichiometry of carbon, nitrogen, and phosphorus in estuarine wetland soils: influences of vegetation coverage, plant communities, geomorphology, and seawalls. *Journal of Soils and Sediments*, *13*(6), pp.1043-1051.

Zhao, Q., Bai, J., Liu, Q., Lu, Q., Gao, Z. and Wang, J., 2016. Spatial and seasonal variations of soil carbon and nitrogen content and stock in a tidal saltmarsh with Tamarix chinensis, China. *Wetlands*, *36*(1), pp.145-152.

Zhou, J., Wu, Y., Kang, Q. and Zhang, J., 2007. Spatial variations of carbon, nitrogen, phosphorous and sulfur in the saltmarsh sediments of the Yangtze Estuary in China. *Estuarine, Coastal and Shelf Science*, *71*(1-2), pp.47-59.

Appendices

Appendix A – Sea Level Rise and Carbon Projections

Table A (i-iii) highlight the variability in elevation of differing tidal levels under various IPCC RCP scenarios from 2020-2100 (Church et al. 2013; Palmer *et al.* 2018). Although relevant, as this report does not specifically assess the influence of SLR inclusion of this data within the main document itself cannot be justified. The calculations utilise specific UKCP 18 future sea level projections which are specific to a 25 km^2 area encompassing the Ribble estuary and account for the effect of glacial isostatic adjustment and regional thermal expansion. As the UKCP 18 projections exhibit the sea-level anomalies from a 1981-2000 baseline and the tidal height projections used in this report are sourced from a 2012 admiralty chart (Halcrow *et al.* 2013) the projections also take into account the 0.03 m of sea-level rise recorded at Heysham (the closest complete tidal gauge) between 1990-2012 (British Oceanographic Data Centre, 2019). It should be noted that the RCP scenario 6.0 is absent from the UKCP 2018 predictions due to the little difference between RCP 4.5 and 6.0 projections (Church et al. 2013).

Table A(iv) exhibits the variability in elevation of differing tidal heights under SLR scenarios predicted by Pfeffer *et al* (2008), takes into account the contribution of extreme global glacial and ice sheet meltwater to global SLR. Although the three projections don't account for localised variability as they drastically differ from the RCP 8.5 projections which inform UKCP 18 predictions, the 0.03 m of sea level rise at Heysham between 2007 and 2012 is accounted for. Whilst considerably more uncertainty surrounds Pfeffer's (2008) projections in the Ribble estuary, they nevertheless approximately indicate an extreme level of SLR that could occur by 2100.

Figure A(v) highlights how overall projected stock will change in accordance with SLR, whilst Tables A(vi) show how total carbon storage will change from 2012-2100 according to the RCP projections 2.6, 4.5 and 8.5. The associated change in error (standard deviation) is exhibited in Table A(vii).

Tables A(viii) – (xxii) exhibit how the area, volume and active section carbon storage potential may plausibly change under the RCP 2.6, 4.5 & 8.5 (50^{th} percentile) SLR featured in the UKCP 18 predictions. The projections assume that submergence and coastal squeeze will occur in accordance with SLR resulting in the conversion of the currently vegetated areas to Exposed Sediment. The calculations assume the carbon-dense higher marsh sub-environments: Species Zone A, B and D will be collectively converted to Exposed Sediment first, before the middle-lower sub-environments: Species Zone C, Species Zone E and Brackish Waterbodies are subsequently converted in progressive order. Projections for the SLR scenarios devised by Pfeffer *et al* (2008) are not exhibited as the

carbon distribution throughout all sub-environments does not change after SLR exceeds 0.27 m as all sub-environments have been converted to Exposed Sediment. Therefore, the carbon projections for the Pfeffer et al (2008) scenarios are identical to the RCP 8.5 projections for the years 2080, 2090 and 2100.

Table A(i). Temporal variability in tidal elevations (mOD) under the IPCC RCP 2.6 scenario

	Time-mean sea level anomaly percentile (m)											
	5th percentile SLR				50th percentile SLR				95th percentile SLR			
Year	SLR post 2012	MHWN 2.2	MHWS 4.1	HAT 5.1	SLR post 2012	MHWN 2.2	MHWS 4.1	HAT 5.1	SLR post 2012	MHWN 2.2	MHWS 4.1	HAT 5.1
2020	0.01	2.21	4.11	5.11	0.04	2.24	4.14	5.14	0.07	2.27	4.17	5.17
2030	0.03	2.23	4.13	5.13	0.07	2.27	4.17	5.17	0.13	2.33	4.23	5.23
2040	0.06	2.26	4.16	5.16	0.11	2.31	4.21	5.21	0.18	2.38	4.28	5.28
2050	0.08	2.28	4.18	5.18	0.15	2.35	4.25	5.25	0.24	2.44	4.34	5.34
2060	0.10	2.30	4.20	5.20	0.18	2.38	4.28	5.28	0.31	2.51	4.41	5.41
2070	0.12	2.32	4.22	5.22	0.22	2.42	4.32	5.32	0.37	2.57	4.47	5.47
2080	0.13	2.33	4.23	5.23	0.25	2.45	4.35	5.35	0.43	2.63	4.53	5.53
2090	0.15	2.35	4.25	5.25	0.28	2.48	4.38	5.38	0.50	2.70	4.60	5.60
2100	0.16	2.36	4.26	5.26	0.31	2.51	4.41	5.41	0.56	2.76	4.66	5.66

Table A(ii). Temporal variability in tidal elevations (mOD) under the IPCC RCP 4.5 scenario.

	Time-mean sea level anomaly percentile (m)											
	5th percentile SLR				50th percentile SLR				95th percentile SLR			
Year	SLR post 2012	MHWN 2.2	MHWS 4.1	HAT 5.1	SLR post 2012	MHWN 2.2	MHWS 4.1	HAT 5.1	SLR post 2012	MHWN 2.2	MHWS 4.1	HAT 5.1
2020	0.01	2.21	4.11	5.11	0.04	2.24	4.14	5.14	0.07	2.27	4.17	5.17
2030	0.04	2.24	4.14	5.14	0.08	2.28	4.18	5.18	0.13	2.33	4.23	5.23
2040	0.06	2.26	4.16	5.16	0.12	2.32	4.22	5.22	0.19	2.39	4.29	5.29
2050	0.09	2.29	4.19	5.19	0.16	2.36	4.26	5.26	0.26	2.46	4.36	5.36
2060	0.12	2.32	4.22	5.22	0.21	2.41	4.31	5.31	0.34	2.54	4.44	5.44
2070	0.15	2.35	4.25	5.25	0.26	2.46	4.36	5.36	0.43	2.63	4.53	5.53
2080	0.18	2.38	4.28	5.28	0.31	2.51	4.41	5.41	0.51	2.71	4.61	5.61
2090	0.21	2.41	4.31	5.31	0.36	2.56	4.46	5.46	0.60	2.80	4.70	5.70
2100	0.23	2.43	4.33	5.33	0.41	2.61	4.51	5.51	0.69	2.89	4.79	5.79

Table A(iii). Temporal variability in tidal elevations (mOD) under the IPCC RCP 8.5 scenario.

	Time-mean sea level anomaly percentile (m)											
	5th percentile SLR				50th percentile SLR				95th percentile SLR			
Year	SLR post 2012	MHWN 2.2	MHWS 4.1	HAT 5.1	SLR post 2012	MHWN 2.2	MHWS 4.1	HAT 5.1	SLR post 2012	MHWN 2.2	MHWS 4.1	HAT 5.1
2020	0.02	2.22	4.12	5.12	0.04	2.24	4.14	5.14	0.07	2.27	4.17	5.17
2030	0.05	2.25	4.15	5.15	0.09	2.29	4.19	5.19	0.14	2.34	4.24	5.24
2040	0.08	2.28	4.18	5.18	0.14	2.34	4.24	5.24	0.21	2.41	4.31	5.31
2050	0.12	2.32	4.22	5.22	0.21	2.41	4.31	5.31	0.31	2.51	4.41	5.41
2060	0.17	2.37	4.27	5.27	0.28	2.48	4.38	5.38	0.42	2.62	4.52	5.52
2070	0.22	2.42	4.32	5.32	0.36	2.56	4.46	5.46	0.55	2.75	4.65	5.65
2080	0.27	2.47	4.37	5.37	0.45	2.65	4.55	5.55	0.68	2.88	4.78	5.78
2090	0.33	2.53	4.43	5.43	0.54	2.74	4.64	5.64	0.84	3.04	4.94	5.94
2100	0.38	2.58	4.48	5.48	0.63	2.83	4.73	5.73	0.98	3.18	5.08	6.08

Table A(iv). Variability in tidal elevations (mOD) for the year 2100 under scenarios devised by Pfeffer et al (2008).

Scenario Type	SLR post 2007	MHWN 2.2	MHWS 4.1	HAT 5.1
Low 1	0.76	2.96	4.86	5.86
Low 2	0.80	3.00	4.90	5.90
High 1	1.98	4.18	6.08	7.08

Table A(v). Projected change in above-ground biomass, active layer and overall carbon storage with SLR in the 21st century according to the IPCC RCP projections. All SLR heights shown are predicted by the RCP projections (hence the absence of certain heights) and the uncertainty indicated in Figure 6.9 is also shown.

SLR (m)	Above-ground Carbon Storage (kg)	Sub-surface Carbon Storage (kg)	Overall Carbon Storage (kg)	Lower Bound Standard Deviation (kg)	Upper Bound Standard Deviation (kg)
0	12604672	12860082	25464754	15776882	35152626
0.01	12265416	12923190	25188606	15384037	34993174
0.02	12265416	12923190	25188606	15384037	34993174
0.03	11932725	12984068	24916793	14869314	34964272
0.04	11811574	13006237	24817811	14875717	34759905
0.05	11682759	13029809	24712568	14747441	34677695
0.06	11398385	13081845	24480230	14454620	34505841
0.08	10681399	13213045	23894443	13770652	34018235
0.09	10470355	13251663	23722018	13508937	33935099
0.1	9959729	13351811	23311541	13128372	33494709
0.12	9021137	13545021	22566158	12268506	32863810
0.13	7499313	13819482	21318795	10812682	31824908
0.15	6242209	14017831	20260041	9765318	30754763
0.16	5193489	14249086	19442575	8938865	29946285
0.18	4516338	14398405	18914743	8775590	29053896
0.21	3546560	14612252	18158811	7723284	28594338
0.22	3404126	14643660	18047786	7631010	28464561
0.23	2856929	14848789	17705718	7347414	28064022
0.27	2719211	14925728	17644940	7137259	28152620
0.33	2719211	14925728	17644940	7137259	28152620
0.38	2719211	14925728	17644940	7137259	28152620

Table A(vi). Projected change overall carbon storage in the 21st century according to the IPCC RCP projections 2.5, 4.5 and 8.5. The values for the predictions made by Pfeffer et al. 2008 are equal to RCP 8.5 2080-2100.

	Overall Carbon Storage (kg)		
Year	RCP 2.6	RCP 4.5	RCP 8.5
2012	25464754	25464754	25464754
2020	25188606	25188606	25188606
2030	24916793	24817812	24712568
2040	24480231	24346389	24055004
2050	23894444	23722018	22566158
2060	23311541	22566158	20260041
2070	22294046	20929149	18047786
2080	21318795	18914743	17644940
2090	20260041	18158812	17644940
2100	19442575	17705718	17644940

Table A(vii). Projected change in the standard deviation of error surrounding carbon storage in the 21st century according to the IPCC RCP projections 2.5, 4.5 and 8.5. The values for the predictions made by Pfeffer et al. 2008 are equal to RCP 8.5 2080-2100.

	Standard Deviation					
	RCP 2.6		RCP 4.5		RCP 8.5	
Year	kg	%	kg	%	kg	%
2012	9687872	0.38	9687872	0.38	9687872	0.38
2020	9804568	0.39	9804568	0.39	9804568	0.39
2030	10047479	0.40	9942094	0.40	9965127	0.40
2040	10025610	0.41	10078638	0.41	10087120	0.42
2050	10123791	0.42	10213081	0.43	10343008	0.46
2060	10183168	0.44	10297652	0.46	10499259	0.52
2070	10322712	0.46	10489834	0.50	10416776	0.58
2080	10506113	0.49	10139153	0.54	10507681	0.60
2090	10494722	0.52	10435527	0.57	10507681	0.60
2100	10503710	0.54	10358304	0.59	10507681	0.60

Table A(viii). Projected change in the active section area (m^2), volume (m^3), above-ground biomass carbon mass (kg) and active layer carbon mass (kg) of Species Zones A and B throughout the 21st century under the RCP 2.5 scenario (50th percentile) assuming coastal squeeze.

	Sub-environment							
	Species Zone A				Species Zone B			
Year	Area	Volume	Above-surface Carbon Content	Active Layer Carbon Content	Area	Volume	Above-surface Carbon Content	Active Layer Carbon Content
2012	2105133	228557	1986706	894290	3423371	445038	4063410	1750632
2020	1988079	215848	1876237	849076	3314368	430868	3934027	1776228
2030	1857021	201619	1752552	793103	3183398	413842	3778572	1706039
2040	1646495	178762	1553870	703191	2973019	386492	3528859	1593293
2050	1363944	148085	1287214	582518	2690672	349787	3193725	1441979
2060	1038280	112727	979870	443433	2365222	307479	2807428	1267564
2070	353155	38342	333287	150827	1680496	218464	1994685	900608
2080	0	0	0	0	835793	108653	992054	447916
2090	0	0	0	0	0	0	0	0
2100	0	0	0	0	0	0	0	0

Table A(ix). Projected change in the active section area (m^2), volume (m^3), above-ground biomass carbon mass (kg) and active layer carbon mass (kg) of Species Zones C and D throughout the 21st century under the RCP 2.5 scenario (50th percentile) assuming coastal squeeze.

	Sub-environment							
	Species Zone C				Species Zone D			
Year	Area	Volume	Above-surface Carbon Content	Active Layer Carbon Content	Area	Volume	Above-surface Carbon Content	Active Layer Carbon Content
2012	3813245	522959	3706886	2155871	917716	128480	728440	457424
2020	3813245	522959	3706886	2155871	793410	111077	629771	472671
2030	3813245	522959	3706886	2155871	662272	92718	525681	394546
2040	3813245	522959	3706886	2155871	451615	63226	358471	269048
2050	3813245	522959	3706886	2155871	168880	23643	134049	100610
2060	3813245	522959	3706886	2155871	0	0	0	0
2070	3813245	522959	3706886	2155871	0	0	0	0
2080	3813245	522959	3706886	2155871	0	0	0	0
2090	3813245	522959	3706886	2155871	0	0	0	0
2100	2150537	294931	2090554	1050032	0	0	0	0

Table A(x). Projected change in the active section area (m^2), volume (m^3), above-ground biomass carbon mass (kg) and active layer carbon mass (kg) of Species Zones E and F throughout the 21st century under the RCP 2.5 scenario (50th percentile) assuming coastal squeeze.

	Sub-environment							
	Species Zone E				Species Zone F			
Year	Area	Volume	Above-surface Carbon Content	Active Layer Carbon Content	Area	Volume	Above-surface Carbon Content	Active Layer Carbon Content
2012	464685	68541	360367	291665	20775	2909	12369	10127
2020	464685	68541	360367	291665	0	0	0	0
2030	464685	68541	360367	291665	0	0	0	0
2040	464685	68541	360367	291665	0	0	0	0
2050	464685	68541	360367	291665	0	0	0	0
2060	464685	68541	360367	291665	0	0	0	0
2070	464685	68541	360367	291665	0	0	0	0
2080	464685	68541	360367	291665	0	0	0	0
2090	464685	68541	360367	291665	0	0	0	0
2100	464685	68541	360367	291665	0	0	0	0

Table A(xi). Projected change in the active section area (m^2), volume (m^3), above-ground biomass carbon mass (kg) and active layer carbon mass (kg) of Brackish Waterbodies and Exposed Sediment throughout the 21st century under the RCP 2.5 scenario (50th percentile) assuming coastal squeeze.

	Sub-environment							
	Brackish Waterbodies				Exposed Sediment			
Year	Area	Volume	Above-surface Carbon Content	Active Layer Carbon Content	Area	Volume	Above-surface Carbon Content	Active Layer Carbon Content
2012	1771562	253924	582914	978623	9362072	2046281	1163580	6321451
2020	1771562	253924	582914	978623	9733210	2153695	1250125	6324146
2030	1771562	253924	582914	978623	10126376	2239918	1299434	6590542
2040	1771562	253924	582914	978623	10757937	2378437	1378661	7018512
2050	1771562	253924	582914	978623	11605570	2564372	1485037	7592987
2060	1771562	253924	582914	978623	12425565	2744298	1588024	8148898
2070	1771562	253924	582914	978623	13795416	3045014	1760286	9078029
2080	1771562	253924	582914	978623	14993274	3308202	1911270	9891232
2090	1771562	253924	582914	978623	15829067	3528839	1639512	10544204
2100	1771562	253924	582914	978623	17491775	3859789	2200822	11887599

Table A(xii). Projected change in the active section area (m^2), volume (m^3), above-ground biomass carbon mass (kg), active layer carbon mass (kg) and overall carbon content (kg) of all areas excluding Exposed Sediment and overall throughout the 21st century under the RCP 2.5 scenario (50th percentile) assuming coastal squeeze.

	Overall excluding Exposed Sediment					Overall				
Year	Area	Volume	Above-surface Carbon Content	Active Layer Carbon Content	Above-ground + Sub-surface carbon content	Area	Volume	Above-surface Carbon Content	Active Layer Carbon Content	Above-ground + Sub-surface carbon content
2012	12516487	1650408	11441091	6538632	7485031	21878559	3696690	12604671	12860082	25464754
2020	12145348	1603217	11090202	6524134	7574271	21878559	3756912	12340327	12848280	25188606
2030	11752183	1553603	10706970	6319847	7889976	21878559	3793521	12006403	12910390	24916793
2040	11120621	1473905	10091366	5991691	8397174	21878559	3852341	11470028	13010203	24480231
2050	10272989	1366940	9265154	5551265	9078024	21878559	3931312	10750191	13144253	23894444
2060	9452994	1265630	8437464	5137155	9736922	21878559	4009928	10025488	13286053	23311541
2070	8083143	1102231	6978138	4477593	10838316	21878559	4147245	8738424	13555622	22294046
2080	6885284	954077	5642220	3874074	11802501	21878559	4262279	7553489	13765306	21318795
2090	6049492	845424	4650166	3426158	12183717	21878559	4374263	6289678	13970363	20260041
2100	4386783	617395	3033834	2320320	14088421	21878559	4477185	5234657	14207918	19442575

Table A(xiii). Projected change in the active section area (m^2), volume (m^3), above-ground biomass carbon mass (kg) and active layer carbon mass (kg) of Species Zones A and B throughout the 21st century under the RCP 4.5 scenario (50th percentile) assuming coastal squeeze.

	Sub-environment							
	Species Zone A				Species Zone B			
Year	Area	Volume	Above-surface Carbon Content	Active Layer Carbon Content	Area	Volume	Above-surface Carbon Content	Active Layer Carbon Content
2012	2105133	228557	1986706	894290	3423371	445038	4063410	1750632
2020	1988079	215848	1876237	849076	3314368	430868	3934027	1776228
2030	1809292	196437	1707508	772719	3135702	407641	3721958	1680478
2040	1581944	171754	1492950	675623	2908514	378107	3452294	1558724
2050	1280761	139054	1208710	546992	2607551	338982	3095064	1397433
2060	536419	58240	506242	229096	1863650	242274	2212081	998763
2070	0	0	0	0	410817	53406	487624	220164
2080	0	0	0	0	0	0	0	0
2090	0	0	0	0	0	0	0	0
2100	0	0	0	0	0	0	0	0

Table A(xiv). Projected change in the active section area (m^2), volume (m^3), above-ground biomass carbon mass (kg) and active layer carbon mass (kg) of Species Zones C and D throughout the 21st century under the RCP 4.5 scenario (50th percentile) assuming coastal squeeze.

	Sub-environment							
	Species Zone C				Species Zone D			
Year	Area	Volume	Above-surface Carbon Content	Active Layer Carbon Content	Area	Volume	Above-surface Carbon Content	Active Layer Carbon Content
2012	3813245	522959	3706886	2155871	917716	128480	728440	457424
2020	3813245	522959	3706886	2155871	793410	111077	629771	472671
2030	3813245	522959	3706886	2155871	614514	86032	487772	366094
2040	3813245	522959	3706886	2155871	387023	54183	307200	230567
2050	3813245	522959	3706886	2155871	85641	11990	67978	51020
2060	3813245	522959	3706886	2155871	0	0	0	0
2070	3813245	522959	3706886	2155871	0	0	0	0
2080	1345807	184568	1308270	657111	0	0	0	0
2090	192704	26428	187329	94090	0	0	0	0
2100	0	0	0	0	0	0	0	0

Table A(xv). Projected change in the active section area (m^2), volume (m^3), above-ground biomass carbon mass (kg) and active layer carbon mass (kg) of Species Zones E and F throughout the 21st century under the RCP 4.5 scenario (50th percentile) assuming coastal squeeze.

	Sub-environment							
	Species Zone E				Species Zone F			
Year	Area	Volume	Above-surface Carbon Content	Active Layer Carbon Content	Area	Volume	Above-surface Carbon Content	Active Layer Carbon Content
2012	464685	68541	360367	291665	20775	2909	12369	10127
2020	464685	68541	360367	291665	0	0	0	0
2030	464685	68541	360367	291665	0	0	0	0
2040	464685	68541	360367	291665	0	0	0	0
2050	464685	68541	360367	291665	0	0	0	0
2060	464685	68541	360367	291665	0	0	0	0
2070	464685	68541	360367	291665	0	0	0	0
2080	464685	68541	360367	291665	0	0	0	0
2090	464685	68541	360367	291665	0	0	0	0
2100	0	0	0	0	0	0	0	0

Table A(xvi). Projected change in the active section area (m^2), volume (m^3), above-ground biomass carbon mass (kg) and active layer carbon mass (kg) of Brackish Waterbodies and Exposed Sediment throughout the 21st century under the RCP 4.5 scenario (50th percentile) assuming coastal squeeze.

	Sub-environment							
	Brackish Waterbodies				Exposed Sediment			
Year	Area	Volume	Above-surface Carbon Content	Active Layer Carbon Content	Area	Volume	Above-surface Carbon Content	Active Layer Carbon Content
2012	1771562	253924	582914	978623	9362072	2046281	1163580	6321451
2020	1771562	253924	582914	978623	9733210	2153695	1250125	6324146
2030	1771562	253924	582914	978623	10269559	2271321	1317393	6687564
2040	1771562	253924	582914	978623	10951586	2420912	1402960	7149747
2050	1771562	253924	582914	978623	11855113	2619118	1516364	7762133
2060	1771562	253924	582914	978623	13428997	2964565	1714190	8829461
2070	1771562	253924	582914	978623	15418249	3401672	1964985	10180051
2080	1771562	253924	582914	978623	18296505	4036709	2301594	12434200
2090	1771562	253924	582914	978623	19449608	4290324	2446068	13217757
2100	678460	97246	223240	380500	21200099	4675392	2658575	14443402

Table A(xvii). Projected change in the active section area (m^2), volume (m^3), above-ground biomass carbon mass (kg), active layer carbon mass (kg) and overall carbon content (kg) of all areas excluding Exposed Sediment and overall throughout the 21st century under the RCP 4.5 scenario (50th percentile) assuming coastal squeeze.

	Overall excluding Exposed Sediment					Overall				
Year	Area	Volume	Above-surface Carbon Content	Active Layer Carbon Content	Above-ground + Sub-surface carbon content	Area	Volume	Above-surface Carbon Content	Active Layer Carbon Content	Overall Carbon Content
2012	12516487	1650408	11441091	6538632	7485031	21878559	3696690	12604671	12860082	25464754
2020	12145348	1603217	11090202	6524134	7574271	21878559	3756912	12340327	12848280	25188606
2030	11609000	1535534	10567404	6245450	8004958	21878559	3806855	11884797	12933014	24817811
2040	10926972	1449468	9902610	5891072	8552706	21878559	3870380	11305570	13040819	24346389
2050	10023446	1335449	9021918	5421604	9278497	21878559	3954568	10538282	13183737	23722018
2060	8449561	1145938	7368490	4654017	10543651	21878559	4110503	9082680	13483478	22566158
2070	6460309	898830	5137790	3646323	12145035	21878559	4300503	7102775	13826373	20929148
2080	3582054	507033	2251550	1927398	14735794	21878559	4543742	4553145	14361598	18914743
2090	2428950	348893	1130609	1364378	15663825	21878559	4639217	3576677	14582135	18158812
2100	678460	97246	223240	380500	17101978	21878559	4772638	2881816	14823903	17705718

Table A(xviii). Projected change in the active section area (m^2), volume (m^3), above-ground biomass carbon mass (kg) and active layer carbon mass (kg) of Species Zones A and B throughout the 21st century under the RCP 8.5 scenario (50th percentile) assuming coastal squeeze.

	Sub-environment							
	Species Zone A				Species Zone B			
Year	Area	Volume	Above-surface Carbon Content	Active Layer Carbon Content	Area	Volume	Above-surface Carbon Content	Active Layer Carbon Content
2012	2105133	228557	1986706	894290	3423371	445038	4063410	1750632
2020	1988079	215848	1876237	849076	3314368	430868	3934027	1776228
2030	1758541	190927	1659612	751044	3084987	401048	3661761	1653299
2040	1441398	156494	1360310	615597	2768068	359849	3285591	1483457
2050	536419	58240	506242	229096	1863650	242274	2212081	998763
2060	0	0	0	0	0	0	0	0
2070	0	0	0	0	0	0	0	0
2080	0	0	0	0	0	0	0	0
2090	0	0	0	0	0	0	0	0
2100	0	0	0	0	0	0	0	0

Table A(xix). Projected change in the active section area (m^2), volume (m^3), above-ground biomass carbon mass (kg) and active layer carbon mass (kg) of Species Zones C and D throughout the 21st century under the RCP 8.5 scenario (50th percentile) assuming coastal squeeze.

	Sub-environment							
	Species Zone C				Species Zone D			
Year	Area	Volume	Above-surface Carbon Content	Active Layer Carbon Content	Area	Volume	Above-surface Carbon Content	Active Layer Carbon Content
2012	3813245	522959	3706886	2155871	917716	128480	728440	457424
2020	3813245	522959	3706886	2155871	793410	111077	629771	472671
2030	3813245	522959	3706886	2155871	563732	78922	447464	335841
2040	3813245	522959	3706886	2155871	246384	34494	195568	146783
2050	3813245	522959	3706886	2155871	0	0	0	0
2060	3396215	465766	3301487	1658254	0	0	0	0
2070	23278	3192	22629	11366	0	0	0	0
2080	0	0	0	0	0	0	0	0
2090	0	0	0	0	0	0	0	0
2100	0	0	0	0	0	0	0	0

Table A(xx). Projected change in the active section area (m^2), volume (m^3), above-ground biomass carbon mass (kg) and active layer carbon mass (kg) of Species Zones E and F throughout the 21st century under the RCP 8.5 scenario (50th percentile) assuming coastal squeeze.

	Sub-environment							
	Species Zone E				Species Zone F			
Year	Area	Volume	Above-surface Carbon Content	Active Layer Carbon Content	Area	Volume	Above-surface Carbon Content	Active Layer Carbon Content
2012	464685	68541	360367	291665	20775	2909	12369	10127
2020	464685	68541	360367	291665	0	0	0	0
2030	464685	68541	360367	291665	0	0	0	0
2040	464685	68541	360367	291665	0	0	0	0
2050	464685	68541	360367	291665	0	0	0	0
2060	464685	68541	360367	291665	0	0	0	0
2070	464685	68541	360367	291665	0	0	0	0
2080	0	0	0	0	0	0	0	0
2090	0	0	0	0	0	0	0	0
2100	0	0	0	0	0	0	0	0

Table A(xxi). Projected change in the active section area (m^2), volume (m^3), above-ground biomass carbon mass (kg) and active layer carbon mass (kg) of Brackish Waterbodies and Exposed Sediment throughout the 21st century under the RCP 8.5 scenario (50th percentile) assuming coastal squeeze.

	Sub-environment							
	Brackish Waterbodies				Exposed Sediment			
Year	Area	Volume	Above-surface Carbon Content	Active Layer Carbon Content	Area	Volume	Above-surface Carbon Content	Active Layer Carbon Content
2012	1771562	253924	582914	978623	9362072	2046281	1163580	6321451
2020	1771562	253924	582914	978623	9733210	2153695	1250125	6324146
2030	1771562	253924	582914	978623	10421807	2304712	1336492	6790731
2040	1771562	253924	582914	978623	11373216	2513400	1455872	7435502
2050	1771562	253924	582914	978623	13428997	2964565	1714190	8829461
2060	1771562	253924	582914	978623	16246097	3586032	2044911	11041822
2070	1771562	253924	582914	978623	19619034	4327599	2467303	13332920
2080	0	0	0	0	21878559	4823828	2742981	14901959
2090	0	0	0	0	21878559	4823828	2742981	14901959
2100	0	0	0	0	21878559	4823828	2742981	14901959

Table A(xxii). Projected change in the active section area (m^2), volume (m^3), above-ground biomass carbon mass (kg), active layer carbon mass (kg) and overall carbon content (kg) of all areas excluding Exposed Sediment and overall throughout the 21st century under the RCP 8.5 scenario (50th percentile) assuming coastal squeeze.

	Overall excluding Exposed Sediment					Overall				
Year	Area	Volume	Above-surface Carbon Content	Active Layer Carbon Content	Above-ground + Sub-surface carbon content	Area	Volume	Above-surface Carbon Content	Active Layer Carbon Content	Above-ground + Sub-surface carbon content
2012	12516487	1650408	11441091	6538632	7485031	21878559	3696690	12604671	12860082	25464754
2020	12145348	1603217	11090202	6524134	17614335	21878559	3756912	12340327	12848280	25188606
2030	11456751	1516322	10419003	6166343	16585345	21878559	3821034	11755494	12957074	24712568
2040	10505342	1396261	9491635	5671995	15163630	21878559	3909661	10947508	13107497	24055004
2050	8449561	1145938	7368490	4654017	12022507	21878559	4110503	9082680	13483478	22566158
2060	5632461	788231	4244768	2928541	7173309	21878559	4374263	6289678	13970363	20260041
2070	2259525	325657	965909	1281653	2247563	21878559	4653256	3433212	14614574	18047786
2080	0	0	0	0	0	21878559	4823828	2742981	14901959	17644940
2090	0	0	0	0	0	21878559	4823828	2742981	14901959	17644940
2100	0	0	0	0	0	21878559	4823828	2742981	14901959	17644940

Appendix B –Spatial Analysis of Land Cover

This section presents the findings concerning the areal extent of the differing sub-environments and the uncertainty surrounding them for each of the four pre-defined marshes in the Ribble. As with the overall analysis, the uncertainty assessments of land cover are divided into the remote and manual assessments and the findings from each marsh are subsequently summarised.

B1 – Marsh A

Table B(i) – Overall area and % composition of each sub-environment determined following the original landcover classification.

Landcover Type	ML Original Area (km²)	% of Overall Area
Brackish Waterbodies	0.010	2.8
Exposed Sediment	0.103	29.6
Shadows	0.001	0.4
Species Zone A	0.026	7.4
Species Zone B	0.033	9.6
Species Zone C	0.071	20.6
Species Zone D	0.027	7.7
Species Zone E	0.076	21.9
Overall	0.35	

Sampling Locations

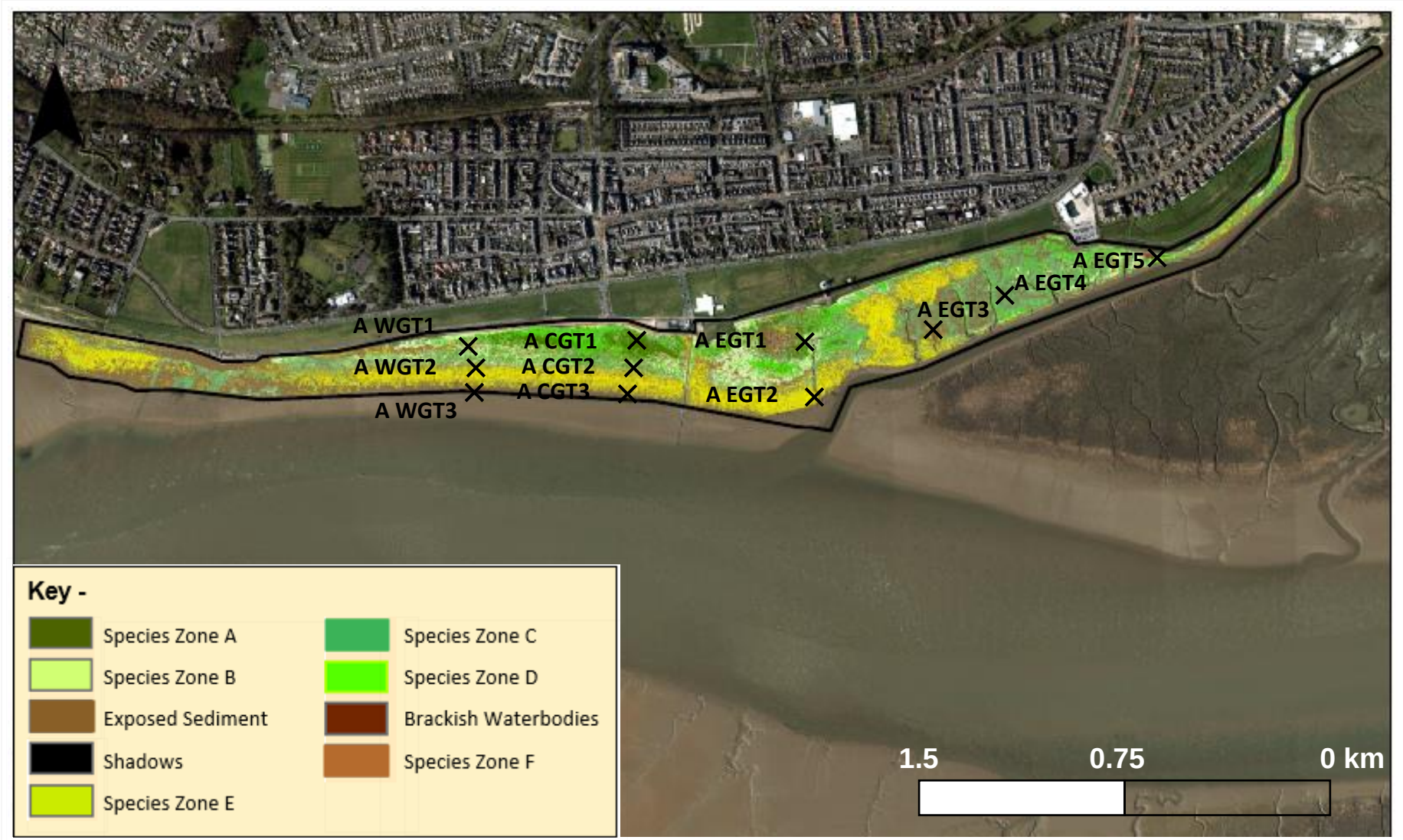

Figure B(i) – ML classification exhibiting the spatial distribution of sub-environments and ground truthing sites on Marsh A.

Remote Uncertainty Analysis –

Table B(ii) – Summary of the remote uncertainity analysis.

Landcover Type	N° Reference Points	Correctly Classified	Accuracy (%)
Brackish Waterbodies	18	15	83.3
Exposed Sediment	38	34	89.5
Shadows	13	13	100.0
Species Zone A	27	23	85.2
Species Zone B	50	44	88.0
Species Zone C	23	20	87.0
Species Zone D	21	18	85.7
Species Zone E	40	34	85.0
Sum	230	201	87.4
		k	85.3

Table B(iii) – Confusion matrix exhibiting the accuracy of the ML classification indicated by the remote uncertainty analysis. The average corresponding value (A) indicates the overall accuracy of the procedure whilst the Kappa coefficent (k) likewise represents the overall accuracy but also takes into account the possibility of the agreement occurring by chance. Anomalous values appear in columns which represent differing species to that of the row. E.g. Of the 18 test polygons for Brackish Waterbodies anomalous readings were recorded as Exposed Sediment (2) and Species Zone E (1).

Landcover Type	Brackish Waterbodies	Exposed Sediment	Shadows	Species Zone A	Species Zone B	Species Zone C	Species Zone D	Species Zone E	Column Total	% of Overall
Brackish Waterbodies	15	2	0	0	0	0	0	1	18	7.8
Exposed Sediment	2	34	0	0	0	0	0	2	38	16.5
Shadows	0	0	13	0	0	0	0	0	13	5.7
Species Zone A	0	0	0	23	0	4	0	0	27	11.7
Species Zone B	0	0	0	2	44	0	4	0	50	21.7
Species Zone C	0	0	0	3	0	20	0	0	23	10.0
Species Zone D	0	0	0	0	3	0	18	0	21	9.1
Species Zone E	2	4	0	0	0	0	0	34	40	17.4
Row Total	19	40	13	28	47	24	22	37	Overall Sum	230
% of Overall Sum	8.3	17.4	5.7	12.2	20.4	10.4	9.6	16.1	A	87.4
									k	85.3

Manual Uncertainty Analysis

Table B(iv) – Summary of the manual, field-based uncertainity analysis (see Figure 5.1. for locations).

Ground Truthing Ref	Pre-fieldwork ML Landcover Type	Post-fieldwork/ Observed Landcover Type	Pre and Post GT correspondence with ML
A EGT1	Dark Green Higher Marsh Vegetation	Species Zone A	Y
A EGT2	Orange-Brown Vegetation	Species Zone E	Y
A EGT3	Exposed Sediment	Exposed Sediment	Y
A EGT4	Mid-Green Lower Terrace Vegetation	Species Zone C	Y
A EGT5	Dark Brown Brackish Waterbodies	Brackish Waterbodies	Y
A CGT1	Dark Green Higher Marsh Vegetation	Species Zone A	Y
A CGT2	Mid-green Lower Creek Terrace Vegetation	Species Zone C	Y
A CGT3	Orange-Brown Vegetation	Species Zone E	Y
A WGT1	Dark Green Higher Marsh Vegetation	Species Zone A	Y
A WGT2	Very Light Green Vegetation	Species Zone B	Y
A WGT3	Exposed Sediment	Exposed Sediment	Y
A WGT4	Mid-Green Lower Terrace Vegetation	Species Zone C	Y
A WGT5	Exposed Sediment	Exposed Brown Sediment	Y
		Accuracy	100%

Summary –

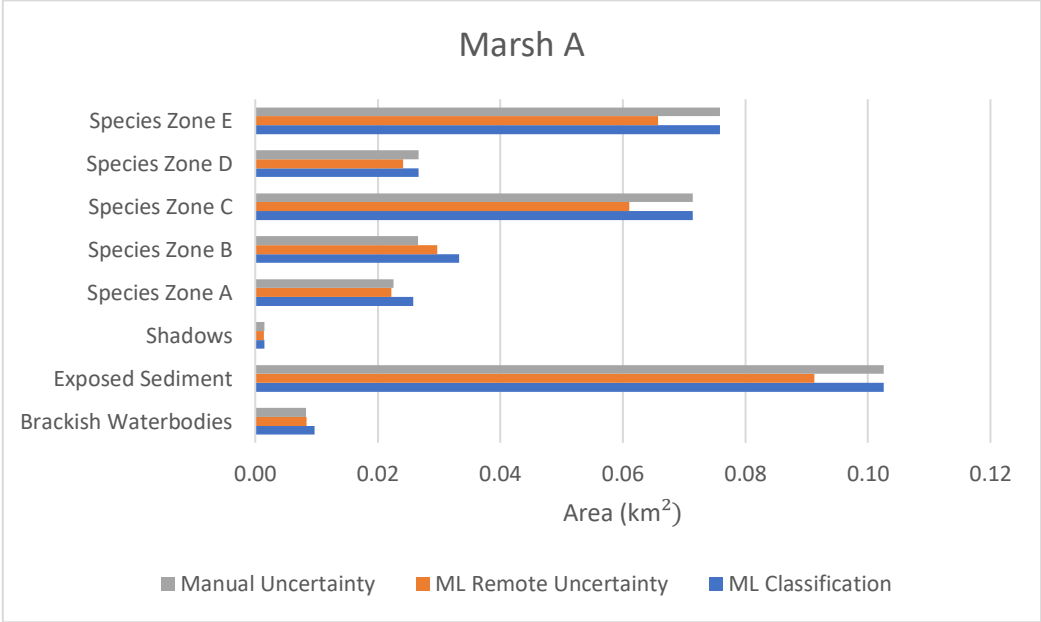

Figure B(ii) – Summary of the landcover area assessments, highlighting variance in projected areas according to the original ML classification and subsequent uncertainity assessments. Both remote and manual uncertainity figures represent the minimal area covered by each sub-environment and utilise overall accuracy figures for all marshes.

Table B(V) – Summary of the landcover area assessments. Both remote and manual uncertainity figures represent the minimal area covered by each sub-environment and utilise overall accuracy figures for all marshes.

Landcover Type	ML Original Area (km²)	% of Overall Area	Overall ML Accuracy (%)	Area - Remote Uncertainty Assessment (km²)	% of Overall Area	Overall Manual Accuracy (%)	Area - Manual Uncertainty Assessment (km²)	% of Overall Area
Brackish Waterbodies	0.010	2.8	86.7	0.008	2.4	85.7	0.008	2.4
Exposed Sediment	0.103	29.6	89.0	0.091	26.3	100.0	0.103	29.6
Shadows	0.001	0.4	96.6	0.001	0.4	N/A	0.001	0.4
Species Zone A	0.026	7.4	86.2	0.022	6.4	87.5	0.023	6.5
Species Zone B	0.033	9.6	89.4	0.030	8.6	80.0	0.027	7.7
Species Zone C	0.071	20.6	85.6	0.061	17.6	100.0	0.071	20.6
Species Zone D	0.027	7.7	90.6	0.024	7.0	100.0	0.027	7.7
Species Zone E	0.076	21.9	86.7	0.066	19.0	100.0	0.076	21.9

B2 – Marsh B

Table B(Vi) – Overall area and % composition of each sub-environment determined following the original landcover classification.

Landcover Type	ML Original Area (km²)	% of Overall Area
Brackish Waterbodies	0.29	8.8
Exposed Sediment	1.36	41.4
Shadows	0.02	0.5
Species Zone A	0.68	20.6
Species Zone B	0.01	0.3
Species Zone C	0.47	14.3
Species Zone D	0.30	9.0
Species Zone E	0.17	5.0
Overall	3.28	

Sampling Location

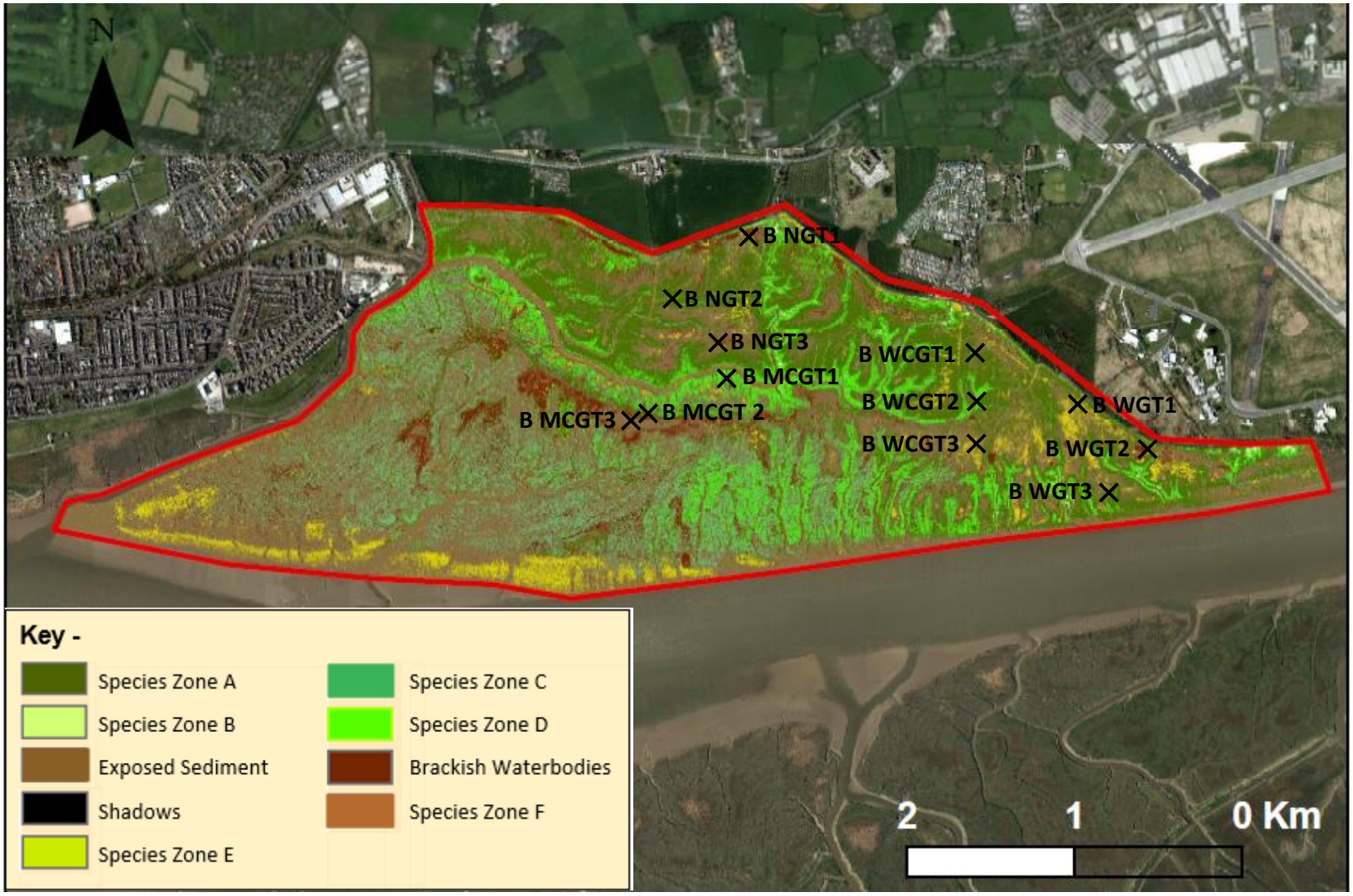

Figure B(iii) – ML classification exhibiting the spatial distribution of sub-environments and ground truthing sites on Marsh B.

Remote Uncertainty Analysis –

Table B(Vii) – Summary of the remote uncertainity analysis.

Landcover Type	No Reference Points	Correctly Classified	Accuracy (%)
Brackish Waterbodies	35	30	85.7
Exposed Sediment	88	77	87.5
Shadows	41	40	97.6
Species Zone A	30	27	90.0
Species Zone B	11	10	90.9
Species Zone C	55	51	92.7
Species Zone D	55	48	87.3
Species Zone E	50	44	88.0
Total	365	327	89.6
		Kappa Coefficient	87.7

Table B(Viii) – Confusion matrix exhibiting the accuracy of the ML classification indicated by the remote uncertainty analysis. The average corresponding value (A) indicates the overall accuracy of the procedure whilst the Kappa coefficent (k) likewise represents the overall accuracy but also takes into account the possibility of the agreement occurring by chance. Anomalous values appear in columns which represent differing species to that of the row.

Landcover Type	Brackish Waterbodies	Exposed Sediment	Shadows	Species Zone A	Species Zone B	Species Zone C	Species Zone D	Species Zone E	Column Total	% of Overall
Brackish Waterbodies	30	4	0	0	0	0	0	1	35	9.6
Exposed Sediment	4	77	0	0	0	0	2	5	88	24.1
Shadows	1	0	40	0	0	0	0	0	41	11.2
Species Zone A	0	0	0	27	0	3	0	0	30	8.2
Species Zone B	0	0	0	0	10	0	1	0	11	3.0
Species Zone C	0	2	0	2	0	51	0	0	55	15.1
Species Zone D	0	0	1	0	6	0	48	0	55	15.1
Species Zone E	0	5	0	0	0	0	1	44	50	13.7
Row Total	35	88	41	29	16	54	52	50	Overall Sum	365
% of Overall Sum	9.6	24.1	11.2	7.9	4.4	14.8	14.2	13.7	A	89.6
									k	87.7

Manual Uncertainty Analysis

Table B(iX) – Summary of the manual, field-based uncertainity analysis.

Ground Truthing Ref	Pre-fieldwork ML Landcover Type	Post-fieldwork/ Observed Landcover Type	Pre and Post GT correspondence with ML
B WGT1	Very light green vegetation	Species Zone B	Y
B WGT2	Brackish Waterbodies	Brackish Water Bodies	Y
B WGT3	Very light green vegetation	Species Zone D	N
B NGT1	Brackish Waterbodies	Brackish Water Bodies	Y
B NGT2	Dark green higher marsh vegetation	Species Zone A	Y
B NGT3	Exposed Sediment	Exposed Sediment	Y
B MCGT1	Light Green Higher Terrace Vegetation	Species Zone D	Y
B MCGT2	Mid-green Lower Terrace Vegetation	Species Zone C	Y
B MCGT3	Exposed Brown Sediment	Exposed Brown Sediment	Y
B WCGT1	Dark green higher marsh vegetation	Species Zone A	Y
B WCGT2	Mid-green Lower Terrace Vegetation	Species Zone C	Y
B WCGT3	Orange-Brown Vegetation	Species Zone E	Y
		Accuracy	91.6 %

Summary –

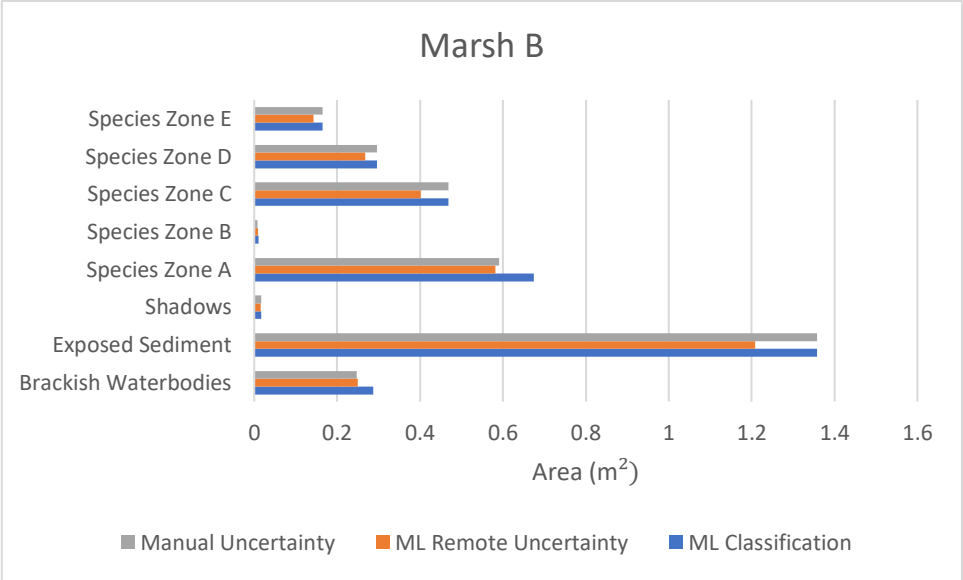

Figure B(iV) – Summary of the landcover area assessments, highlighting variance in projected areas according to the original ML classification and subsequent uncertainity assessments on Marsh B. Both remote and manual uncertainity figures represent the minimal area covered by each sub-environment and utilise overall accuracy figures for all marshes.

Table B(X) – Summary of the landcover area assessments. Both remote and manual uncertainity figures represent the minimal area covered by each sub-environment and utilise overall accuracy figures for all marshes.

Landcover Type	ML Original Area (km²)	% of Overall Area	Overall ML Accuracy (%)	Area - ML Uncertainty Assessment (km²)	% of Overall Area	Overall Manual Accuracy (%)	Area - Manual Uncertainty Assessment (km²)	% of Overall Area
Brackish Waterbodies	0.29	8.8	86.7	0.25	7.6	85.7	0.25	7.5
Exposed Sediment	1.36	41.4	89.0	1.21	36.9	100.0	1.36	41.4
Shadows	0.02	0.5	96.6	0.02	0.5	N/A	0.02	0.5
Species Zone A	0.68	20.6	86.2	0.58	17.8	87.5	0.59	18.0
Species Zone B	0.01	0.3	89.4	0.01	0.3	80.0	0.01	0.2
Species Zone C	0.47	14.3	85.6	0.40	12.2	100.0	0.47	14.3
Species Zone D	0.30	9.0	90.6	0.27	8.2	100.0	0.30	9.0
Species Zone E	0.17	5.0	86.7	0.14	4.4	100.0	0.17	5.0

B3 – Marsh C

Table B(Xi) – Overall area and % composition of each sub-environment determined following the original landcover classification.

Landcover Type	ML Original Area (km²)	% of Overall Area
Brackish Waterbodies	1.43	8.5
Exposed Sediment	6.96	41.4
Shadows	0.10	0.6
Species Zone A	1.35	8.0
Species Zone B	3.28	19.5
Species Zone C	2.93	17.5
Species Zone D	0.56	3.3
Species Zone E	0.17	1.0
Species Zone F	0.02	0.1
Overall	16.79	

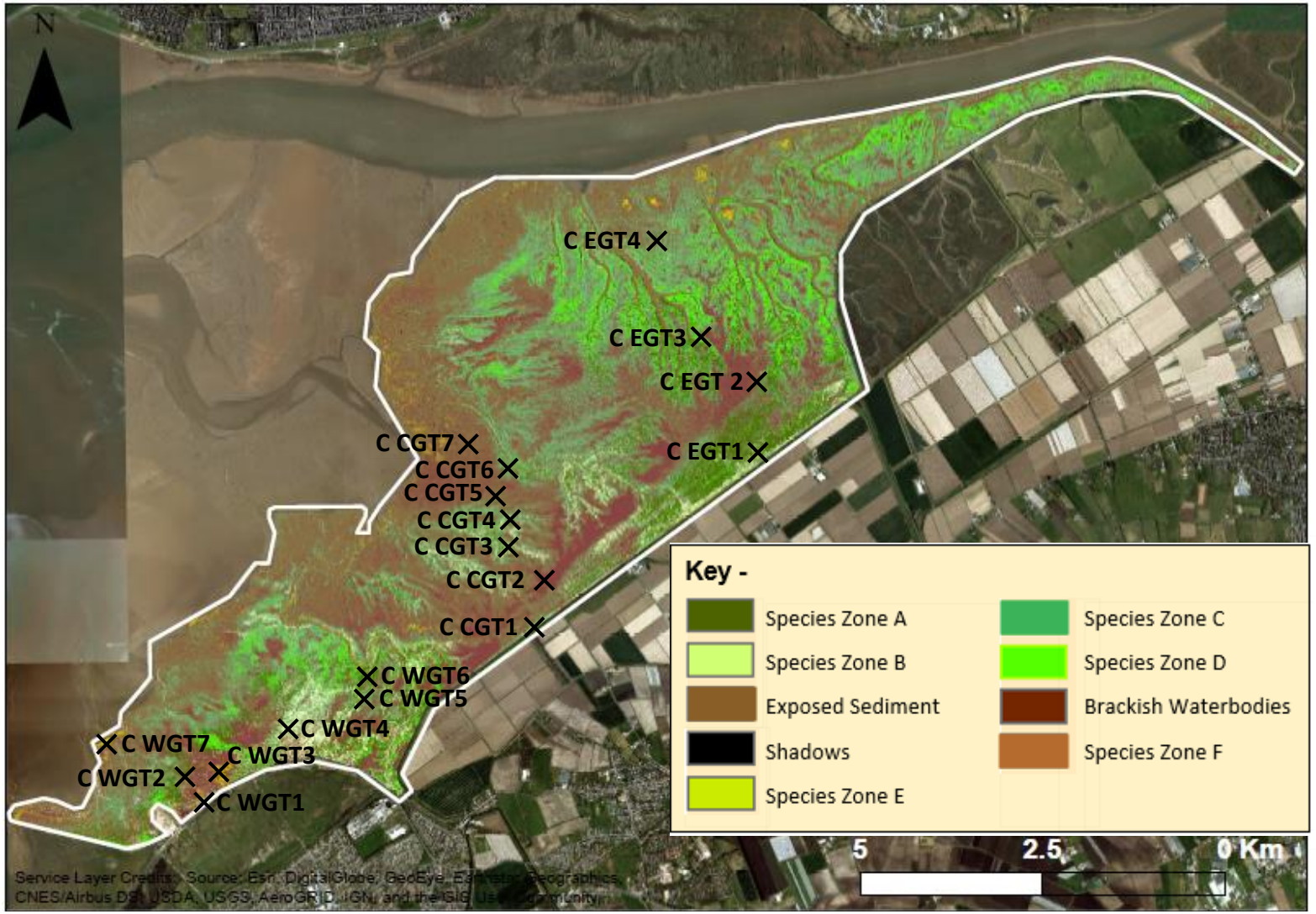

Figure B(V) – ML classification exhibiting the spatial distribution of sub-environments and ground truthing sites on Marsh C.

Remote Uncertainty Analysis –

Table B(Xii). Summary of the remote uncertainity analysis on Marsh C.

Landcover Type	No Reference Points	Correctly Classified	Accuracy (%)
Brackish Waterbodies	80	72	90.0
Exposed Sediment	322	292	90.7
Shadows	56	54	96.4
Species Zone A	112	98	87.5
Species Zone B	164	148	90.2
Species Zone C	126	104	82.5
Species Zone D	142	134	94.4
Species Zone E	60	52	86.7
Species Zone F	30	26	86.7
Sum	1092	980	89.7
		Kappa Coefficient	87.8

Table B(XiV). Confusion matrix exhibiting the accuracy of the ML classification indicated by the remote uncertainty analysis. The average corresponding value (A) indicates the overall accuracy of the procedure whilst the Kappa coefficent (k) likewise represents the overall accuracy but also takes into account the possibility of the agreement occurring by chance. Anomalous values appear in columns which represent differing species to that of the row.

Landcover Type	Brackish Waterbodies	Exposed Sediment	Shadows	Species Zone A	Species Zone B	Species Zone C	Species Zone D	Species Zone E	Species Zone F	Column Total	% of Overall
Brackish Waterbodies	72	4	0	0	0	0	0	1	3	80	7.3
Exposed Sediment	8	292	0	0	0	0	2	20	0	322	29.5
Shadows	2	0	54	0	0	0	0	0	0	56	5.1
Species Zone A	1	0	0	98	0	13	0	0	0	112	10.3
Species Zone B	0	0	0	0	148	7	9	0	0	164	15.0
Species Zone C	0	2	0	20	0	104	0	0	0	126	11.5
Species Zone D	0	0	3	0	5	0	134	0	0	142	13.0
Species Zone E	2	5	0	0	0	0	1	52	0	60	5.5
Species Zone F	4	0	0	0	0	0	0	0	26	30	2.7
Row Total	89	303	57	118	153	124	146	73	29	Overall Sum	1092
% of Overall Sum	8.2	27.7	5.2	10.8	14.0	11.4	13.4	6.7	2.7	A	89.8
										k	87.8

Manual Uncertainty Analysis

Table B(XV). Summary of the manual, field-based uncertainity analysis on Marsh C.

Ground Truthing Ref	Pre-fieldwork ML Landcover Type	Post-fieldwork/ Observed Landcover Type	Pre and Post GT correspondence with ML
C WGT1	Brackish Waterbodies	Species Zone F	N
C WGT2	Dark green higher marsh vegetation	Species Zone A	Y
C WGT3	Orange-Brown Vegetation	Species Zone E	Y
C WGT4	Very light green vegetation	Species Zone B	Y
C WGT5	Mid-green Lower Terrace Vegetation	Species C	Y
C WGT6	Dark green higher marsh vegetation	Species Zone A	Y
C WGT7	Orange-Brown Vegetation	Species Zone E	Y
C CGT1	Very light green vegetation	Species Zone B	Y
C CGT2	Brackish Waterbodies	Brackish Water Bodies	Y
C CGT3	Light Green Higher Terrace Vegetation	Species Zone D	Y
C CGT4	Mid-green Lower Terrace Vegetation	Species Zone C	Y
C CGT5	Exposed Sediment	Exposed Sediment	Y
C CGT6	Light Green Higher Terrace Vegetation	Species Zone D	Y
C CGT7	Exposed Sediment	Exposed Sediment	Y
C EGT1	Light Green Higher Terrace Vegetation	Species Zone D	Y
C EGT2	Exposed Sediment	Exposed Sediment	Y
C EGT3	Mid-green Lower Terrace Vegetation	Species Zone C	Y
C EGT4	Exposed Sediment	Exposed Sediment	Y
		Accuracy	94.7%

Summary –

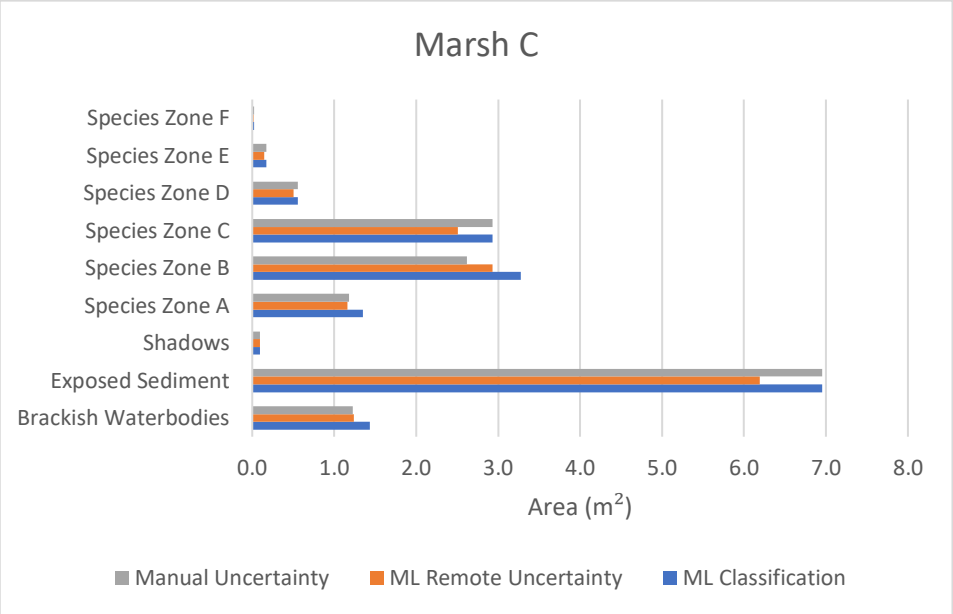

Figure B(Vi) – Summary of the landcover area assessments on Marsh C, exhiting variance in projected areas according to the original ML classification and subsequent uncertainity assessments. Both remote and manual uncertainity figures represent the minimal area covered by each sub-environment and utilise overall accuracy figures for all marshes.

Table B(XVi). Summary of the landcover area assessments. Both remote and manual uncertainity figures represent the minimal area covered by each sub-environment and utilise overall accuracy figures for all marshes.

Landcover Type	ML Original Area (km²)	% of Overall Area	Overall ML Accuracy (%)	Area - ML Uncertainty Assessment (km²)	% of Overall Area	Overall Manual Accuracy (%)	Area - Manual Uncertainty Assessment (km²)	% of Overall Area
Brackish Waterbodies	1.43	8.5	86.7	1.24	7.4	85.7	1.23	7.3
Exposed Sediment	6.96	41.4	89.0	6.19	36.9	100.0	6.96	41.4
Shadows	0.10	0.6	96.6	0.09	0.6	N/A	0.10	0.6
Species Zone A	1.35	8.0	86.2	1.16	6.9	87.5	1.18	7.0
Species Zone B	3.28	19.5	89.4	2.93	17.4	80.0	2.62	15.6
Species Zone C	2.93	17.5	85.6	2.51	14.9	100.0	2.93	17.5
Species Zone D	0.56	3.3	90.6	0.50	3.0	100.0	0.56	3.3
Species Zone E	0.17	1.0	86.7	0.15	0.9	100.0	0.17	1.0
Species Zone F	0.02	0.1	86.7	0.02	0.1	N/A	0.02	0.1

B4 – Marsh D

Table B(XVii). Overall area and % composition of each sub-environment determined following the original landcover classification.

Landcover Type	ML Original Area (km²)	% of Overall Area
Brackish Waterbodies	0.04	2.7
Exposed Sediment	0.95	59.9
Shadows	0.00	0.0
Species Zone A	0.06	3.5
Species Zone B	0.10	6.5
Species Zone C	0.34	21.6
Species Zone D	0.04	2.5
Species Zone E	0.05	3.3
Overall	1.58	

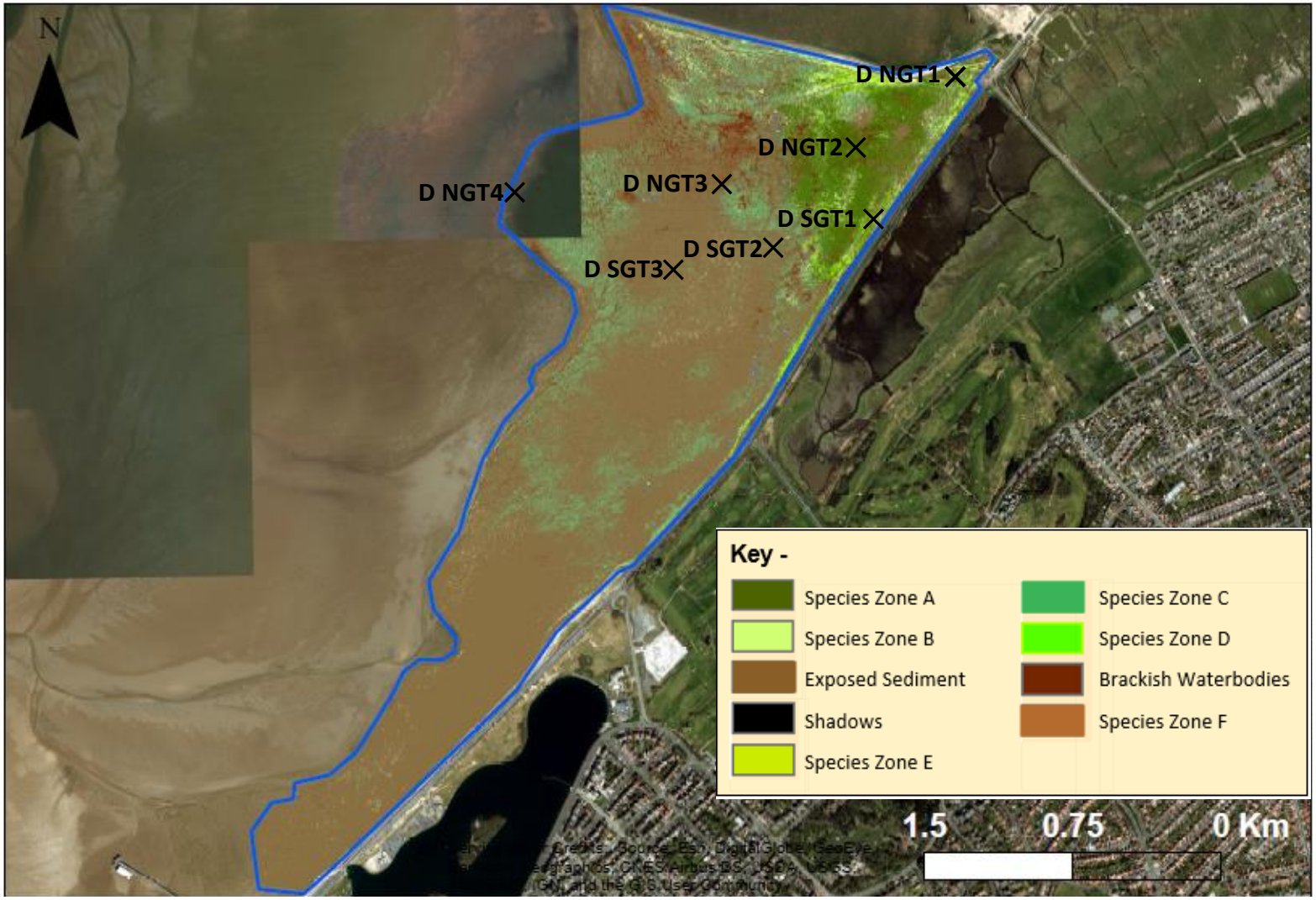

Figure B(Vii) – ML classification exhibiting the spatial distribution of sub-environments and ground truthing sites on Marsh D

Remote Uncertainty Analysis –

Table B(XViii). Summary of the remote uncertainity analysis for Marsh D.

Landcover Type	No Reference Points	Correctly Classified	Accuracy (%)
Brackish Waterbodies	18	15	83.3
Exposed Sediment	112	101	90.2
Shadows	12	11	91.7
Species Zone A	60	56	93.3
Species Zone B	35	31	88.6
Species Zone C	50	44	88.0
Species Zone D	14	12	85.7
Species Zone E	15	13	86.7
Sum	316	283	89.9
		Kappa Coefficient	87.4

Table B(XiiX). Confusion matrix exhibiting the accuracy of the ML classification indicated by the remote uncertainty analysis on Marsh D. The average corresponding value (A) indicates the overall accuracy of the procedure whilst the Kappa coefficent (k) likewise represents the overall accuracy but also takes into account the possibility of the agreement occurring by chance. Anomalous values appear in columns which represent differing species to that of the row.

Landcover Type	Brackish Waterbodies	Exposed Sediment	Shadows	Species Zone A	Species Zone B	Species Zone C	Species Zone D	Species Zone E	Column Total	% of Overall
Brackish Waterbodies	15	3	0	0	0	0	0	0	18	12.7
Exposed Sediment	2	101	0	0	0	0	1	8	112	31.5
Shadows	1	0	11	0	0	0	0	0	12	3.0
Species Zone A	0	0	0	56	0	4	0	0	60	17.3
Species Zone B	0	0	0	1	31	0	3	0	35	10.2
Species Zone C	0	1	1	4	0	44	0	0	50	12.7
Species Zone D	0	0	0	0	2	0	12	0	14	8.6
Species Zone E	0	2	0	0	0	0	0	13	15	4.1
Row Total	18	107	12	61	33	48	16	21	Overall Sum	197
% of Overall Sum	11.7	28.9	3.0	15.2	11.2	13.7	8.1	8.1	A	89.9
									k	87.4

Manual Uncertainty Analysis

Table B(XiX). Summary of the manual, field-based uncertainity analysis on Marsh D.

Ground Truthing Ref	Pre-fieldwork ML Landcover Type	Post-fieldwork/ Observed Landcover Type	Pre and Post GT correspondence with ML
D NGT1	Dark Green Higher Marsh Vegetation	Species Zone A	Y
D NGT2	Very light green vegetation	Species Zone A	N
D NGT3	Mid-green Lower Terrace Vegetation	Species Zone C	Y
D NGT4	Exposed Brown Sediment	Exposed Brown Sediment	Y
D SGT1	Very light green Vegetation	Species Zone B	Y
D SGT2	Mid-green Lower Terrace Vegetation	Species Zone C	Y
D SGT3	Exposed Sediment	Exposed Sediment	Y
		Accuracy	85.7%

Summary

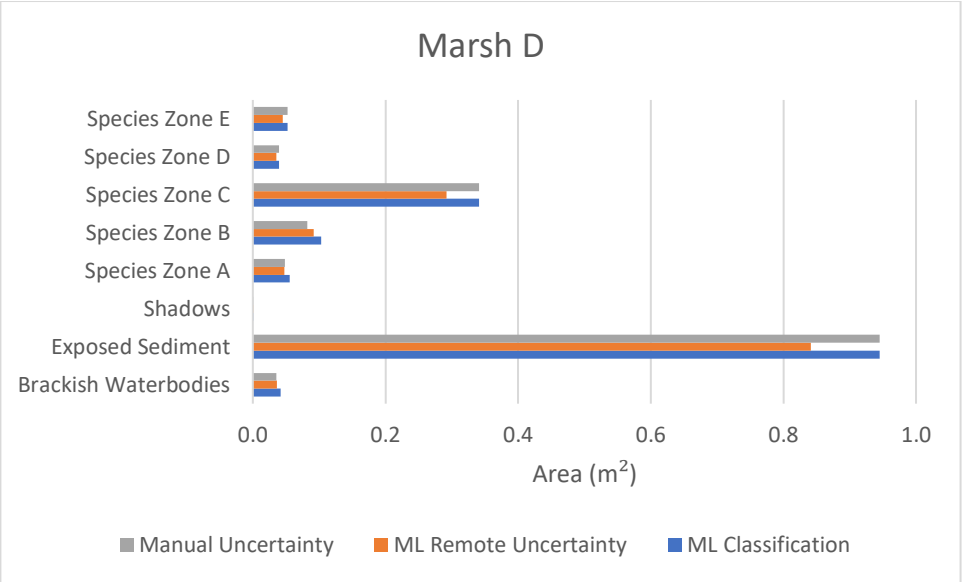

Figure B(Viii) – Summary of the landcover area assessments, highlighting variance in projected areas according to the original ML classification and subsequent uncertainity assessments. Both remote and manual uncertainity figures represent the minimal area covered by each sub-environment and utilise overall accuracy figures for all marshes.

Table B(XX). Summary of the landcover area assessments on Marsh D. Both remote and manual uncertainity figures represent the minimal area covered by each sub-environment and utilise overall accuracy figures for all marshes.

Landcover Type	Area (km^2)	% of Overall Area	Overall ML Accuracy (%)	Area - ML Accuracy (km^2)	% of Overall Area	Overall Manual Accuracy (%)	Area Manual Accuracy (km^2)	% of Overall Area
Brackish			86.7			85.7		
Waterbodies	0.04	2.7		0.04	2.3		0.04	2.3
Exposed Sediment	0.95	59.9	89.0	0.84	53.3	100.0	0.95	59.9
Shadows	0.00	0.0	96.6	0.00	0.0	N/A	0.00	0.0
Species Zone A	0.06	3.5	86.2	0.05	3.0	87.5	0.05	3.1
Species Zone B	0.10	6.5	89.4	0.09	5.8	80.0	0.08	5.2
Species Zone C	0.34	21.6	85.6	0.29	18.5	100.0	0.34	21.6
Species Zone D	0.04	2.5	90.6	0.04	2.3	100.0	0.04	2.5
Species Zone E	0.05	3.3	86.7	0.05	2.9	100.0	0.05	3.3

B5 – Influence on Spatial Distribution

The following section highlights the influence of elevation, gradient and watercourse proximity on the areal coverage of each sub-environment. The results mirror the smoothed kernel density curves shown in Figures 5.5, 5.12 and 5.19 although the areal coverage of each sub-environment at uniform intervals for each influence is quantified in km^2.

B5(i) – Elevation and Sub-environment Areal Coverage

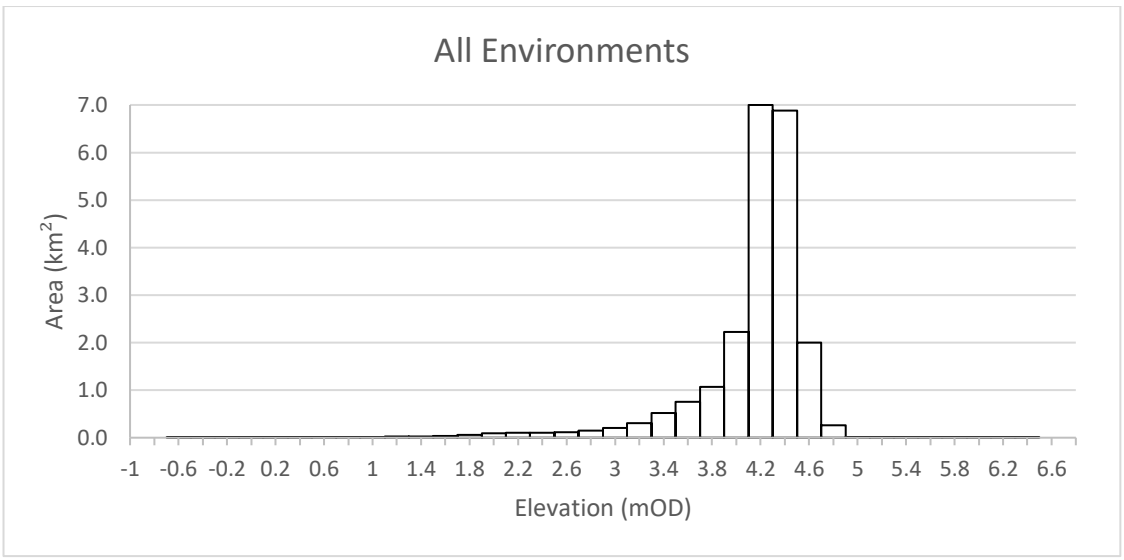

Figure B(iX) – Area of marsh at 0.2m elevation intervals over all sub-environments and marshes. The value on the x axis represents the lower interval of each bin e.g. 4.2 represents the area of land at 4 m - 4.199 m above ordnance datum.

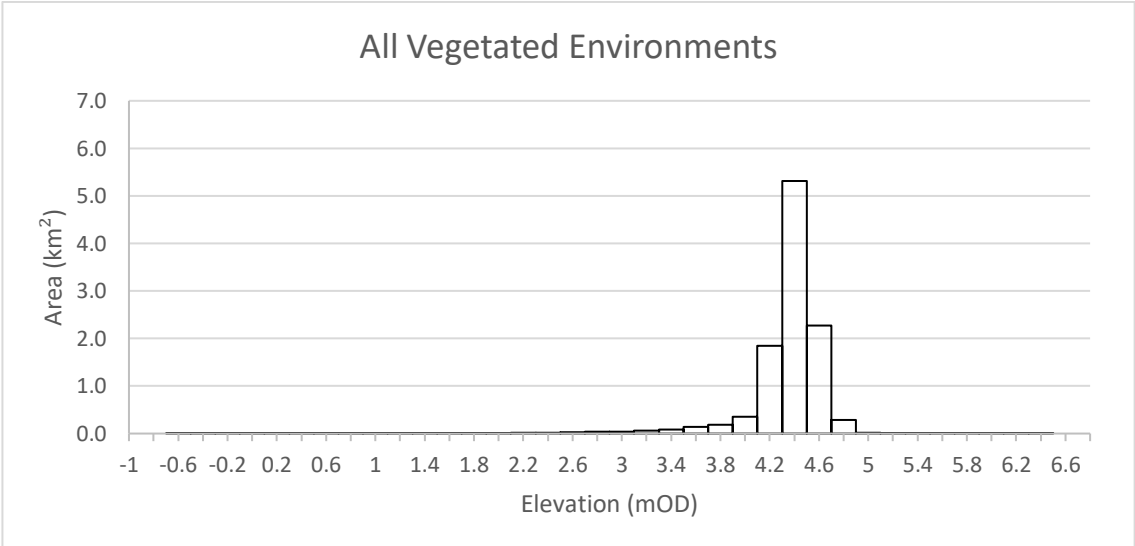

Figure B(X) – Area of marsh at 0.2m elevation intervals over all predominantly vegetated sub-enviornments on all marshes (i.e all environments exluding Exposed Sediment and Brackish Waterbodies).

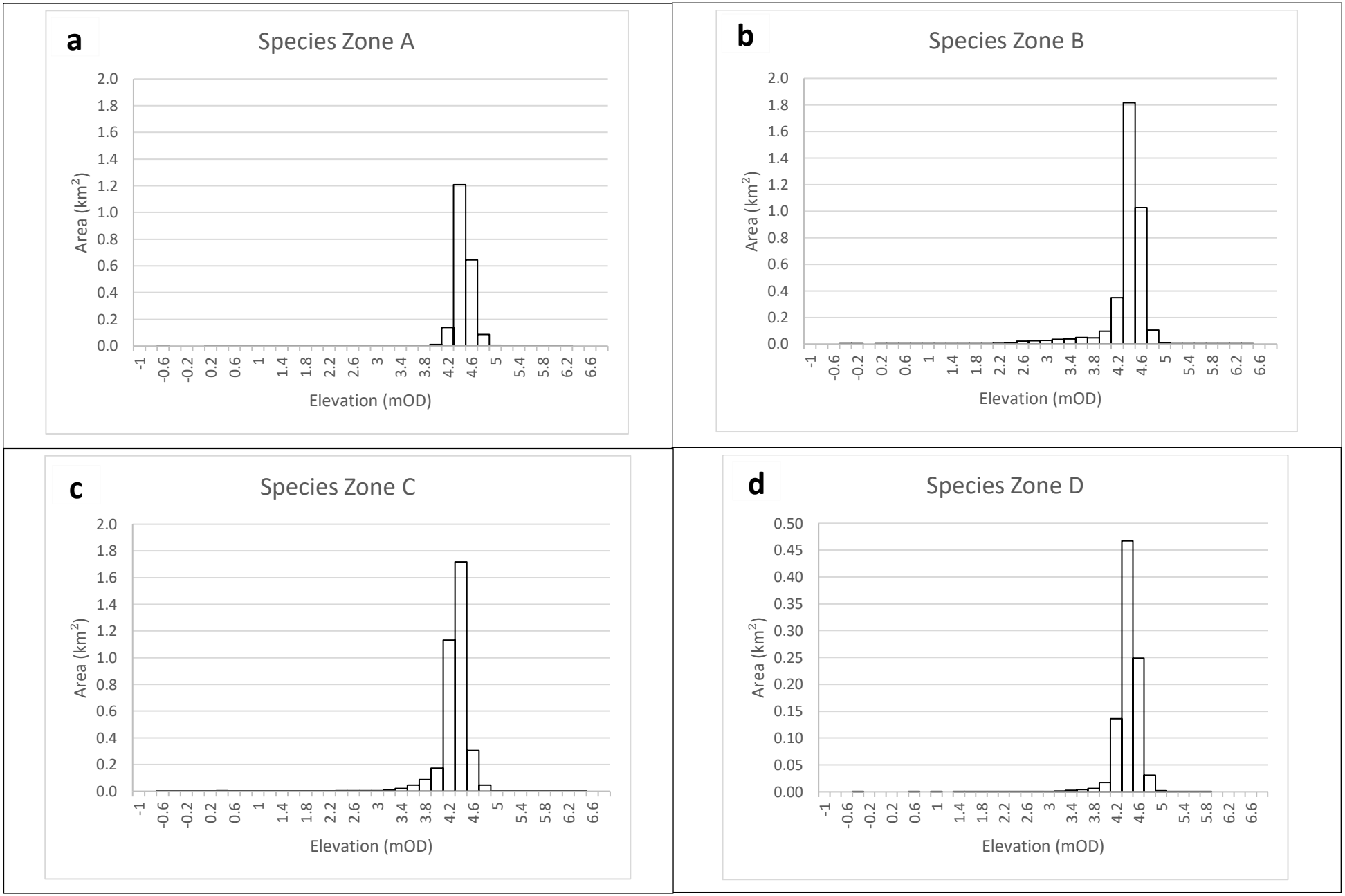

Figure 5.14(Xi) – Area of marsh at 0.2m elevation intervals on the sub-environments classified as Species Zone A (a), Species Zone B (b), Species Zone C (c) and Species Zone D (d).

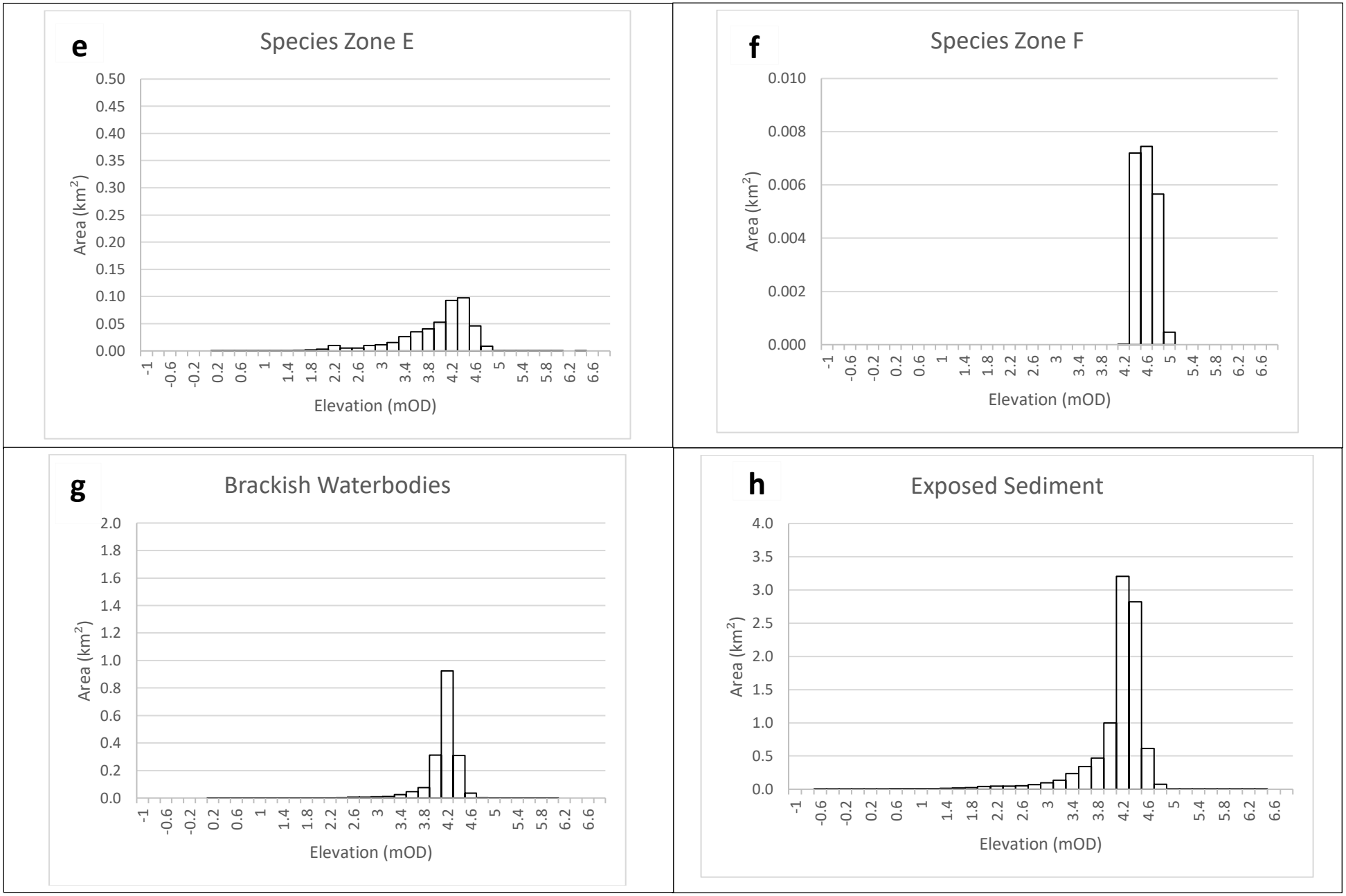

Figure 5.14(Xi) – Area of marsh at 0.2m elevation intervals on the sub-environments classified as Species Zone E (e), Species Zone F (f), Brackish Waterbodies (g) and Exposed Sediment (h).

B5(ii) – Gradient and Sub-environment Areal Coverage

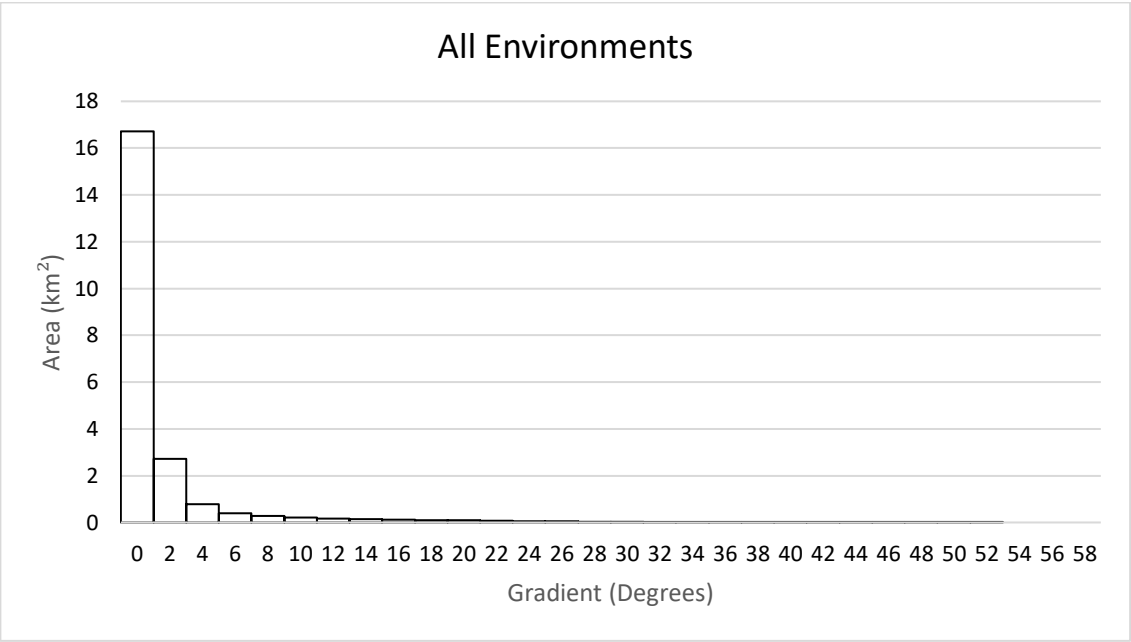

Figure B(Xii) – Area of marsh at 2° gradient intervals over all sub-environments and marshes. The label on the x-axis indicates the lower limit of each 2° bin.

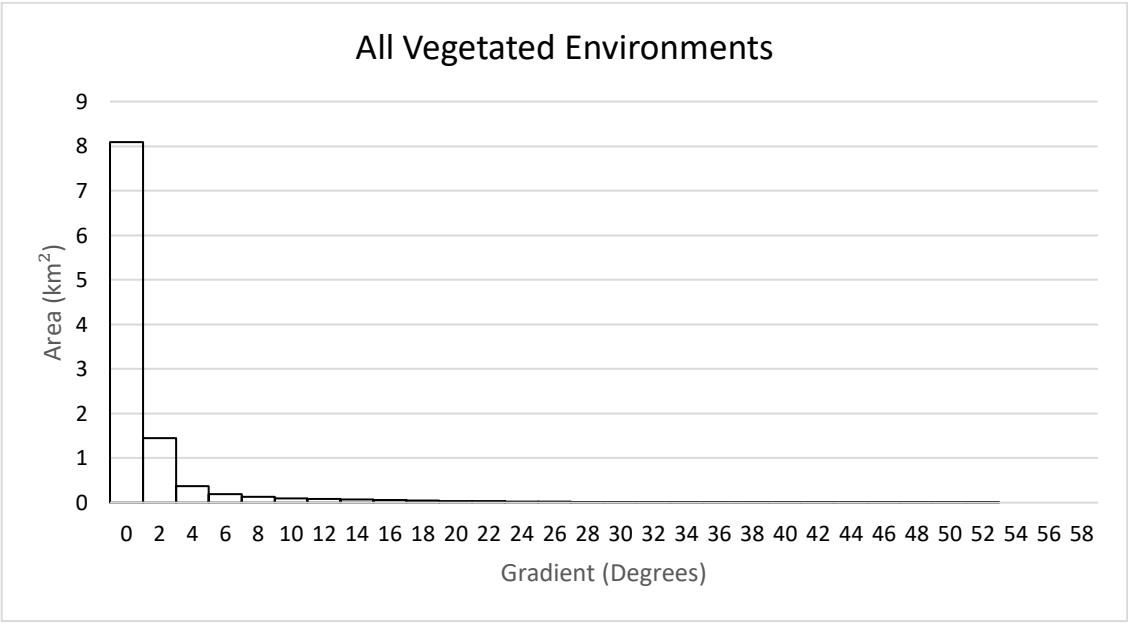

Figure B(Xiii) – Area of marsh at 2° gradient intervals over all predominantly vegetated sub-enviornments on all marshes (i.e all environments exluding Exposed Sediment and Brackish Waterbodies).

Figure B(XiV) – Area of marsh at 2° gradient intervals on the sub-environments classified as Species Zone A (a), Species Zone B (b), Species Zone C (c) and Species Zone D (d).

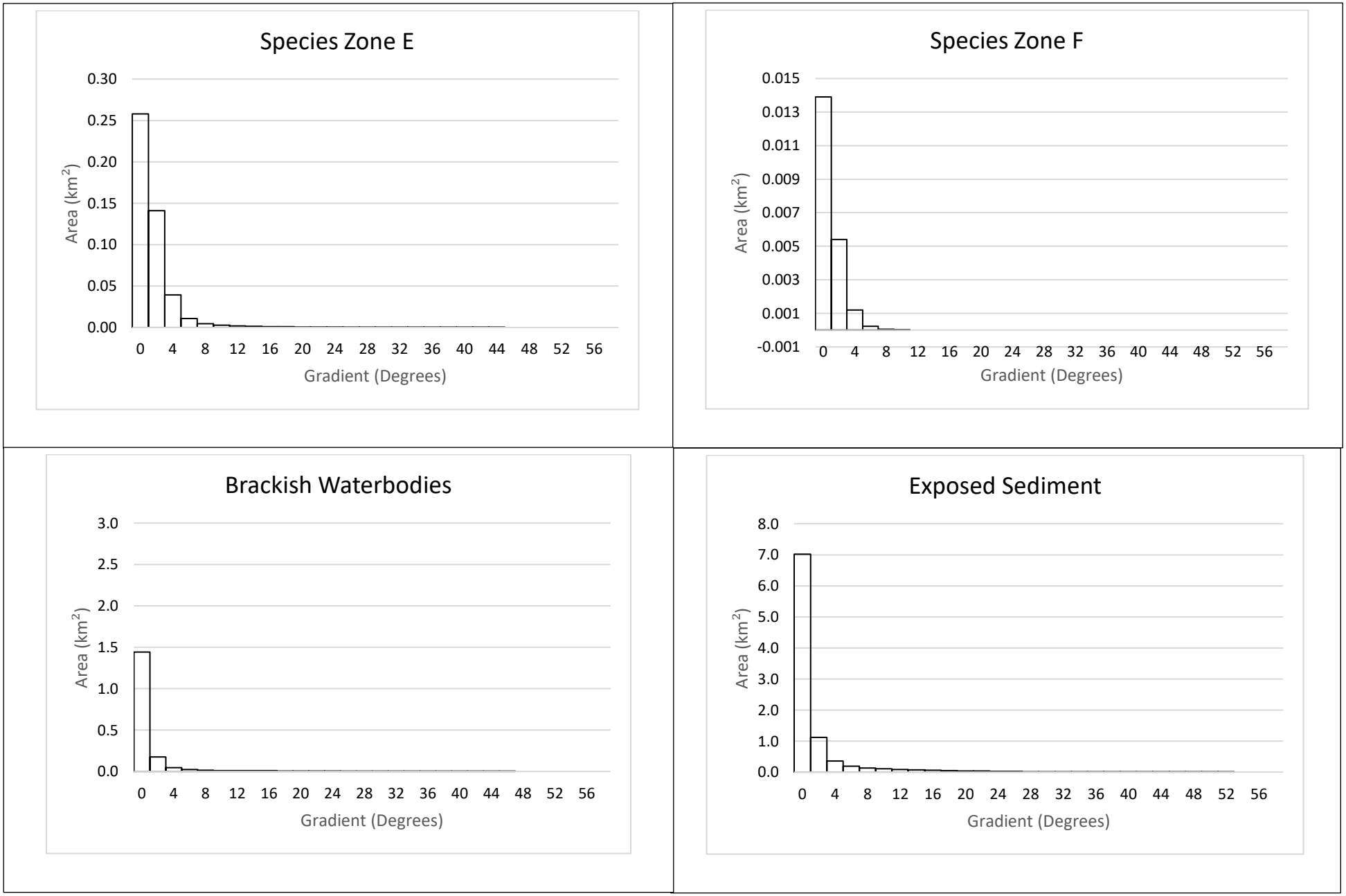

Figure B(XiV) – Area of marsh at 2° gradient intervals on the sub-environments classified as Species Zone E (e), Species Zone F (f), Brackish Waterbodies (g) and Exposed Sediment (h).

B5(iii) – Watercourse Proximity and Sub-environment Areal Coverage

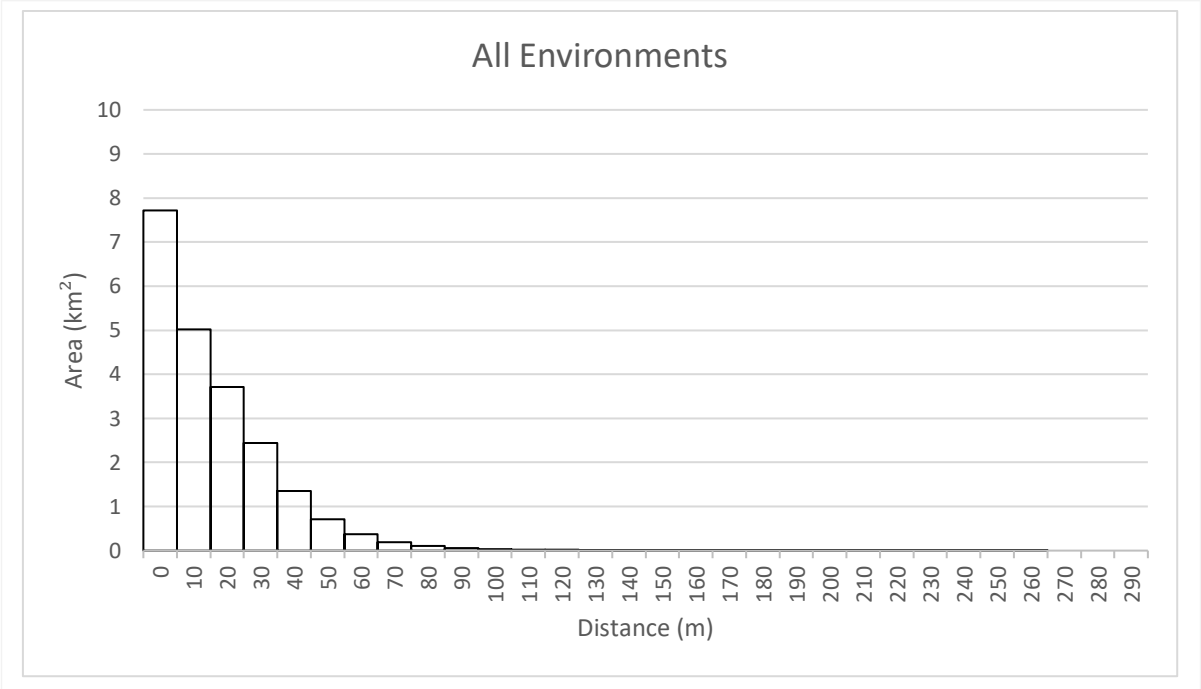

Figure B(XV) – Combined area of all sub-environments at 10m distance intervals from all

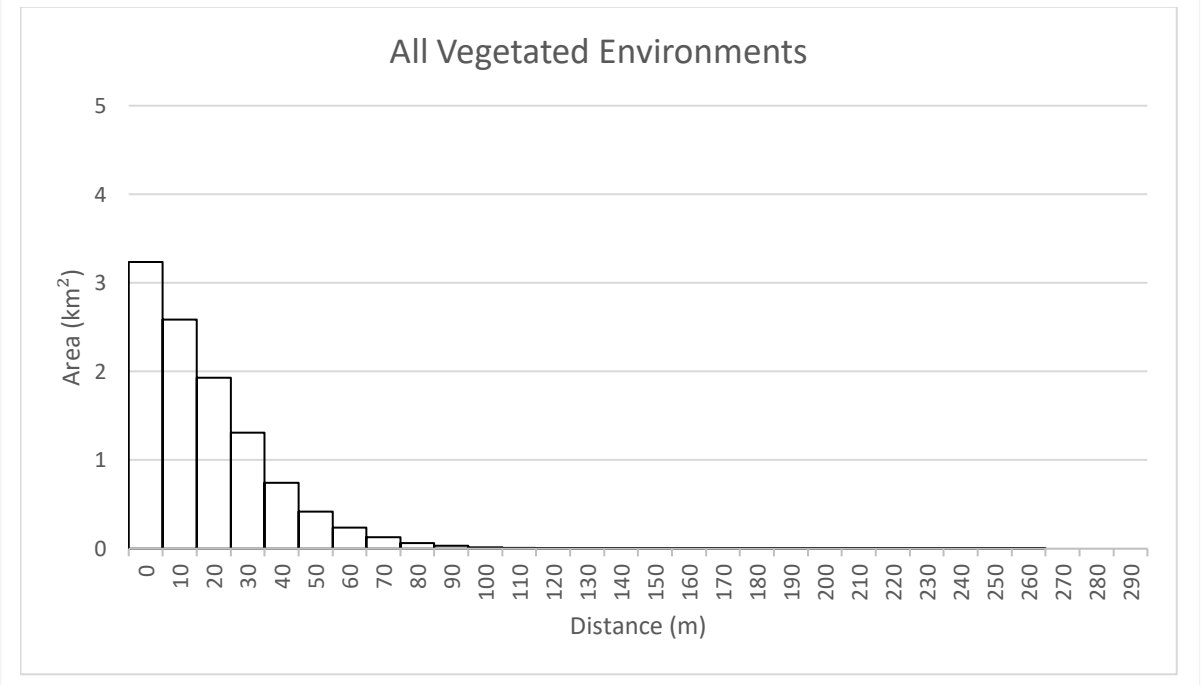

Figure B(XVi) – Combined area of all predominalty vegetated sub-environments at 10m distance intervals from all watercourses.

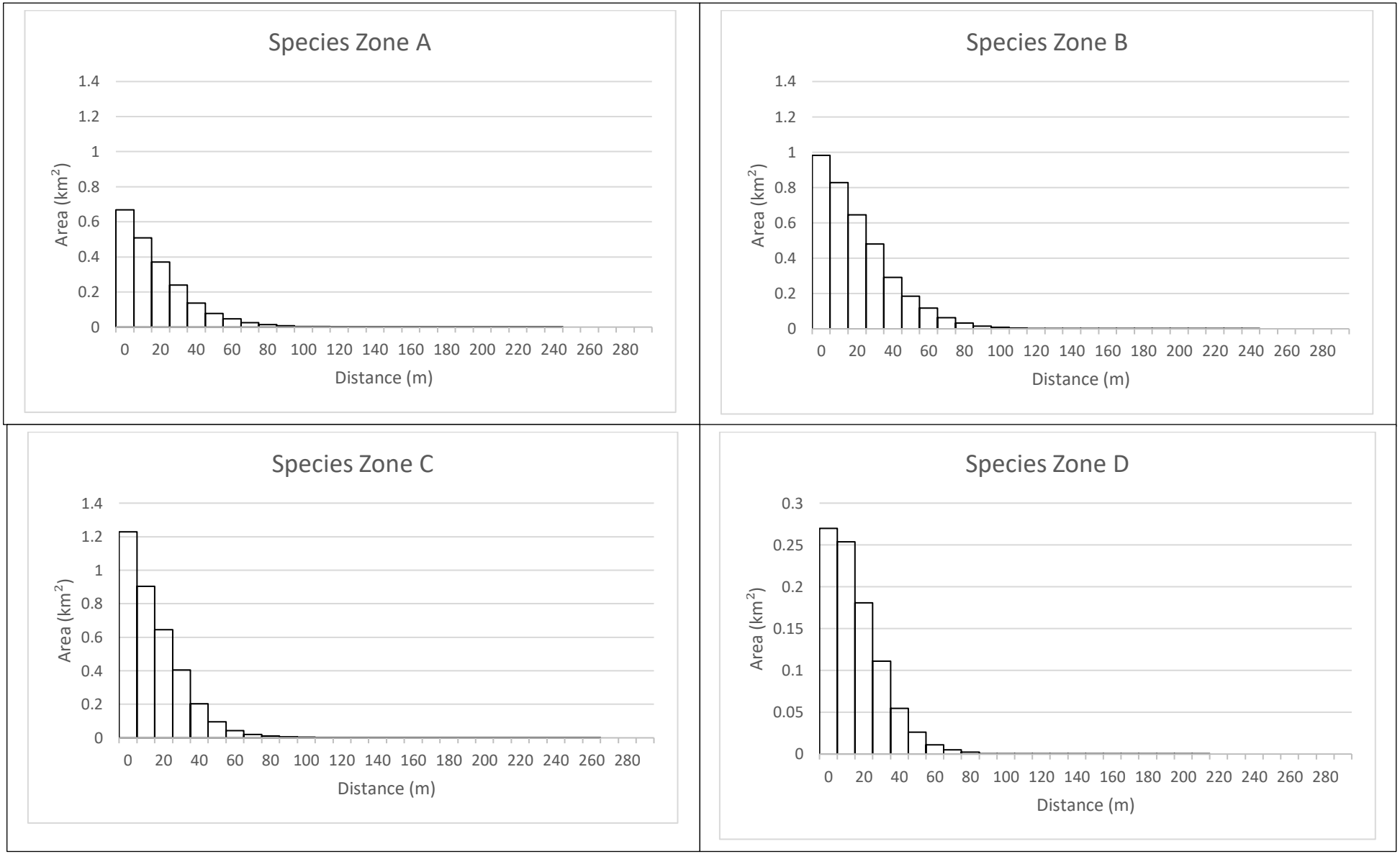

Figure B (XVii) – Area of land at 10m distance intervals from all watercourses for each sub-environment zone over all marshes.

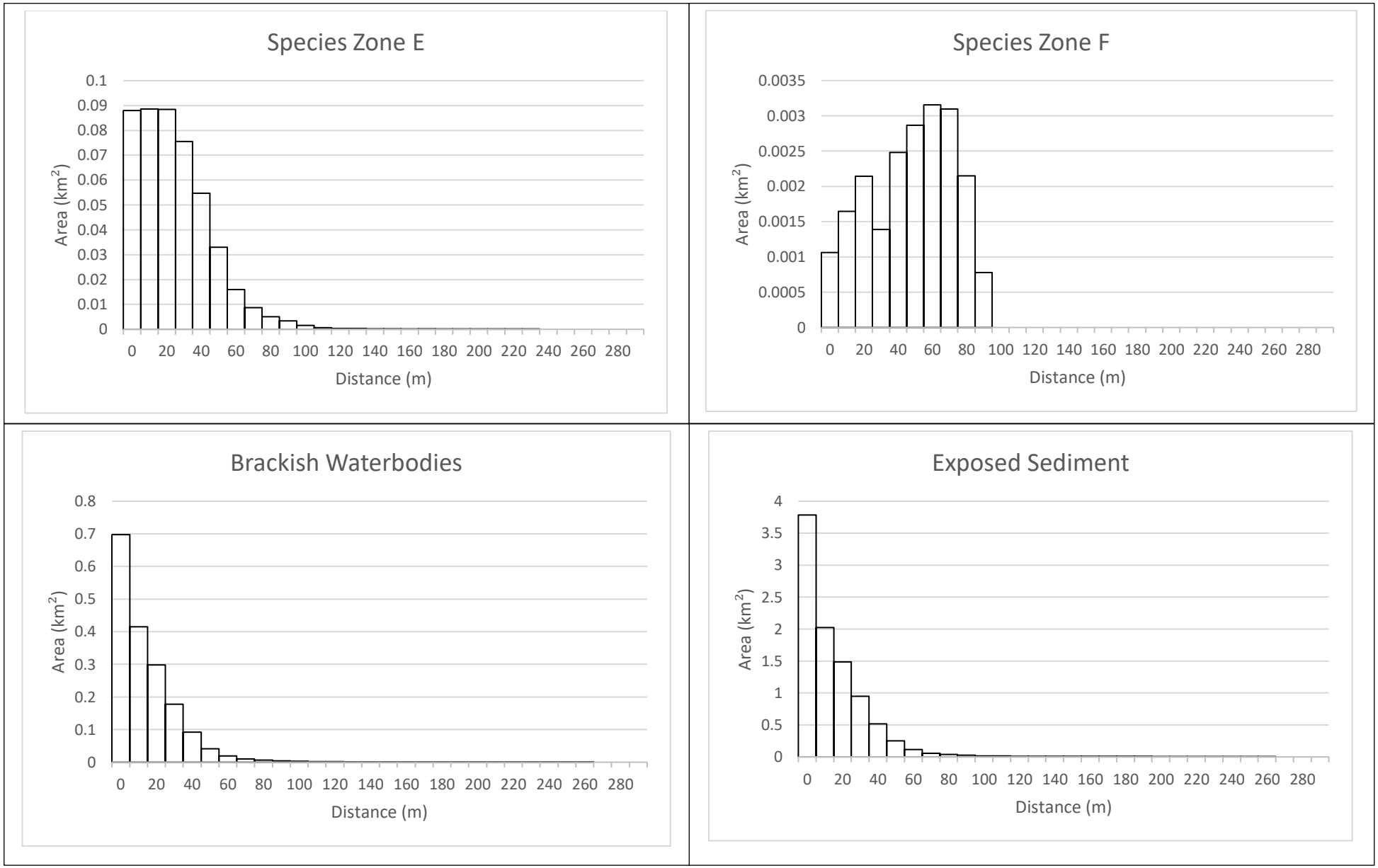

Figure B(XVii) – Area of land at 10m distance intervals from all watercourses for each sub-environment zone over all marshes.

Appendix C - Marsh Specific Geomorphological Findings

The following section presents the findings concerning the geomorphological and carbon assessment of the four marshes of the Ribble estuary which contribute to the overall analysis. The above-ground and sub-surface carbon assessments for each marsh are presented separately whilst the initial observations from the Troels-Smith (1955) assessments at each site are also presented. As with the overall analysis, OCD, BD and depth variability at each site is compared and there is a specific focus on the sedimentological nature and carbon content of the active layer and section.

C1 - Marsh A

C1(i) – Field Findings

The samples taken on Marsh A were highly spatially clustered when compared to the sampling distribution on all other marshes with a maximal distance range between sample sites of 952 m. As with all marshes the sampling design was structured so that it incorporated all the predominant sub-environment zones on the marsh and the number of samples taken from each zone was approximately proportional to the overall area.

Above-ground Biomass

Table C(i). Location of sampling sites and above-ground biomass carbon storage quantification for Marsh A.

Site	Sub-environment Type	OS Grid Reference	Elevation (mOD)	C Mass (kg/m^2)	Uncertainty kg (±)	Uncertainty (%)
W Site A	Species Zone A	SD 36235 26913	5.85	1.257	0.001	0.08
W Site B	Species Zone B	SD 36239 26869	5.6	0.780	0.0005	0.06
W Site C	Exposed Sediment	SD 36242 26816	3.19	0	0	0
C Site A	Species Zone A	SD 36667 26910	5.21	0.999	0.001	0.10
C Site B	Species Zone D	SD 36657 26854	5.37	0.709	0.0005	0.07
C Site C	Species Zone E	SD 36651 26793	3.76	0.647	0.0005	0.08
E Site A	Species Zone D	SD 36963 26901	5.56	1.021	0.001	0.10
E Site B	Species Zone E	SD 37032 26786	3.58	1.316	0.001	0.08

Sampling Locations

Figure C(i). Sampling locations and sub-environment spatial distribution on Marsh A.

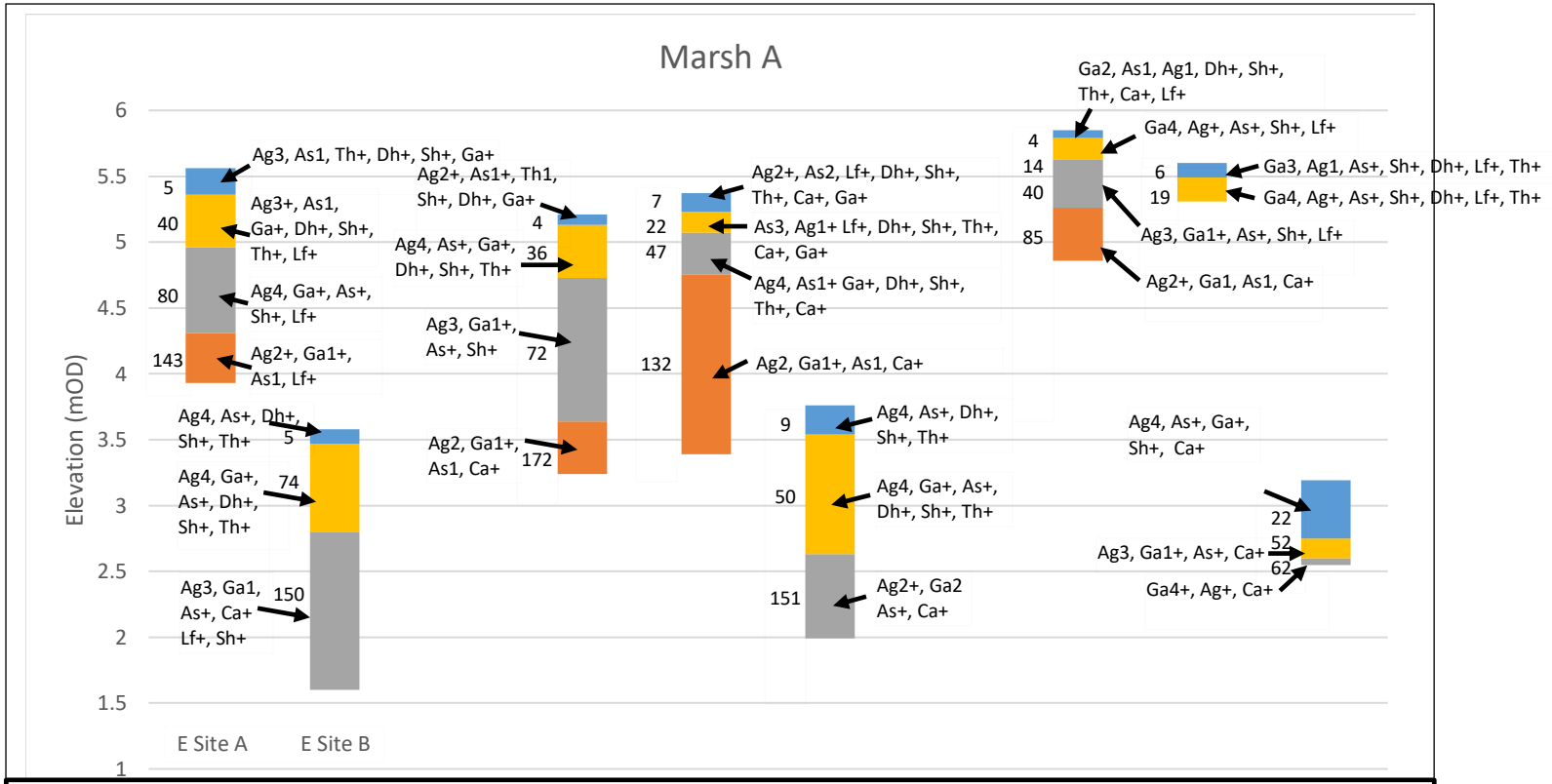

Lithology Key after Troels-Smith (1955)

As = Clay (<0.002mm), **Ag** = Silt (0.002 – 0.06mm), **Ga** = Coarse sand (0.6 – 2mm), **Ca** = Calcareous shell, **Sh** = Humified organics beyond identification, **Th** = Roots, stems and rhizomes of herbaceous plants, **Dh** = Fragments of stems and leaves of herbaceous plants >2mm, **Lf** = Mineral and/or organic iron oxide

Approximate Composition –

4 = 100% 3 = 75% 2 = 50% 1 = 25% + = 12.5% (Trace)

Figure C(ii). Levelled stratigraphy and horizon consistency for all sample sites on Marsh A.

C1(ii) - Sub-Surface Carbon and Bulk Density Variability

Table C(ii). Variation in horizon depth, organic carbon density and bulk density on Marsh A. Horizon 1 in each sample site (highlighted in green) denotes the active layer.

Sub-environment classification	Site Name	Horizon Number	Depth (m)	OCD (kg m^{-3})	BD (kg m^{-3})
Species Zone A	W Site A	1	0.06	2.5	1827
		2	0.22	1.9	2098
		3	0.59	2.0	1866
		4	0.99	1.6	1901
Species Zone D	W Site B	1	0.11	2.4	1978
		2	0.29	2.0	2072
Exposed Sediment		1	0.44	2.2	1777
	W Site C	2	0.59	1.4	1934
		3	0.64	1.3	2103
Species Zone A		1	0.08	4.3	1460
	C Site A	2	0.48	2.7	1729
		3	1.57	2.1	1952
		4	1.97	1.1	2145
Species Zone D		1	0.14	3.8	1403
	C Site B	2	0.3	2.9	1616
		3	0.62	2.1	1892
		4	1.98	1.2	1940
Species Zone E		1	0.22	4.5	1695
	C Site C	2	1.13	2.1	1823
		3	1.77	0.8	2003
Species Zone D		1	0.2	4.2	1510
	E Site A	2	0.6	2.9	1729
		3	1.25	2.1	1989
		4	1.63	0.8	2203
Species Zone E		1	0.11	4.2	1697
	E Site B	2	0.78	2.7	1843
		3	1.98	1.1	2023

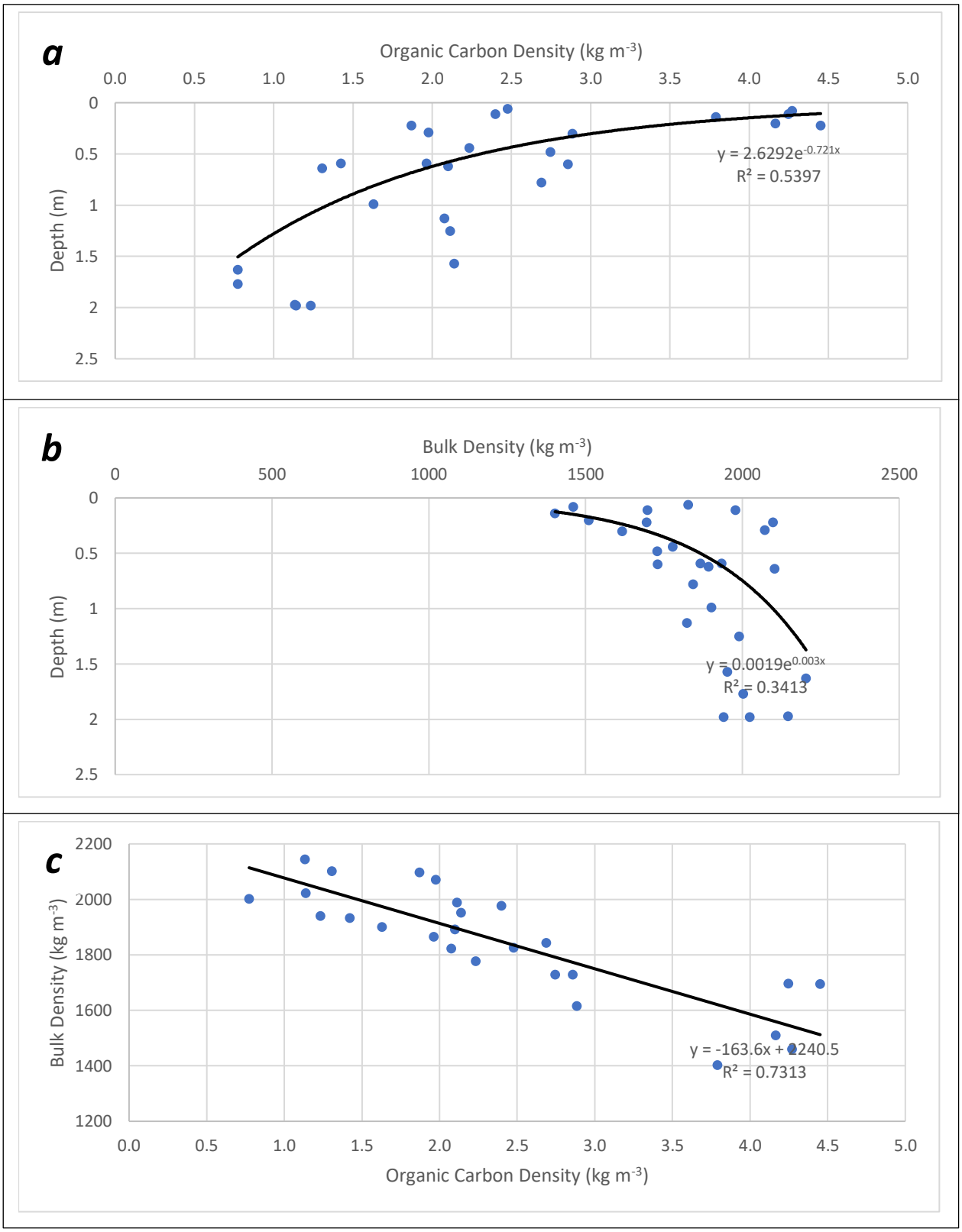

Figure C(iii). Correspondance between the depth, organic carbon density and bulk density in the differing horizons of Marsh A.

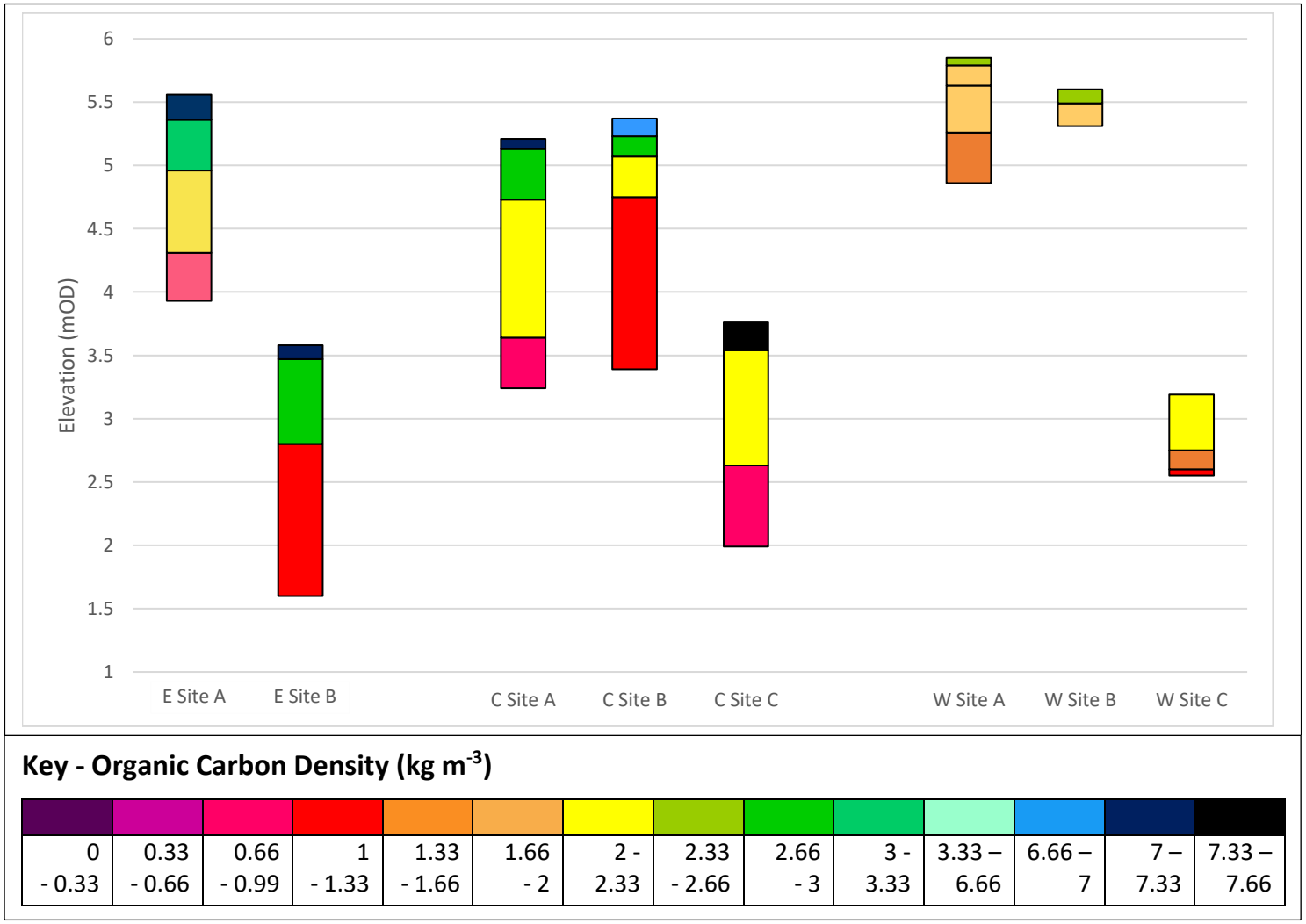

Figure C(iV). Levelled stratigraphy for all sample sites on Marsh A exhibiting organic carbon denisty of each horizon from every sampled core. Resulted were determined derived after a loss on ignition test conducted on all samples following a standardised procedure outlined in the TESSA guidelines.

C1(iii) – Active Layer Characteristics

Table C(iii). Variation in horizon depth, organic carbon density and bulk density in the active layer (i.e. horizon 1) on Marsh A.

				Organic Carbon Density (kg m^{-3})			Bulk Density (kg m^{-3})		
Species Zone	Site Reference	Sub-Horizon Sample Number	Sample Depth	Sample OCD	Average	Standard Deviation	Sample BD	Average	Standard Deviation
SA	W Site A	1	0.01	2.50	2.48	0.02	1819	1827	10
		1b	0.02	2.50			1817		
		1c	0.03	2.48			1828		
		1d	0.04	2.47			1840		
		1e	0.05	2.45			1832		
SD	W Site B	1	0.02	2.43	2.41	0.02	1920	1978	38
		1b	0.04	2.41			1965		
		1c	0.06	2.42			1987		
		1d	0.08	2.39			1997		
		1e	0.1	2.39			2021		
EX	W Site C	1	0.08	2.27	2.24	0.03	1720	1777	80
		1b	0.16	2.24			1699		
		1c	0.24	2.24			1765		
		1d	0.3	2.22			1802		
		1e	0.38	2.20			1901		
SA	C Site A	1	0.01	4.47	4.27	0.18	1302	1460	108
		1b	0.03	4.42			1444		
		1c	0.05	4.21			1498		
		1d	0.06	4.24			1455		
		1e	0.08	4.01			1602		
SC	C Site B	1	0.02	4.04	3.79	0.15	1321	1403	76
		1b	0.05	3.70			1376		
		1c	0.08	3.81			1354		
		1d	0.11	3.72			1462		
		1e	0.14	3.67			1501		
SD	W Site B	1	0.02	2.43	2.41	0.02	1920	1978	38
		1b	0.04	2.41			1965		
		1c	0.06	2.42			1987		
		1d	0.08	2.39			1997		
		1e	0.1	2.39			2021		
SE	C Site C	1	0.02	4.74	4.45	0.19	1592	1695	79
		1b	0.06	4.35			1640		
		1c	0.1	4.24			1711		
		1d	0.14	4.50			1743		
		1e	0.18	4.42			1789		
SD	E Site A	1	0.04	4.23	4.16	0.20	1429	1510	63
		1b	0.08	4.30			1481		
		1c	0.12	3.94			1504		
		1d	0.16	3.97			1537		
		1e	0.2	4.38			1598		
SE	E Site B	1	0.02	4.54	4.25	0.25	1662	1697	51
		1b	0.04	4.30			1657		
		1c	0.06	4.34			1681		
		1d	0.08	4.21			1701		
		1e	0.1	3.85			1782		

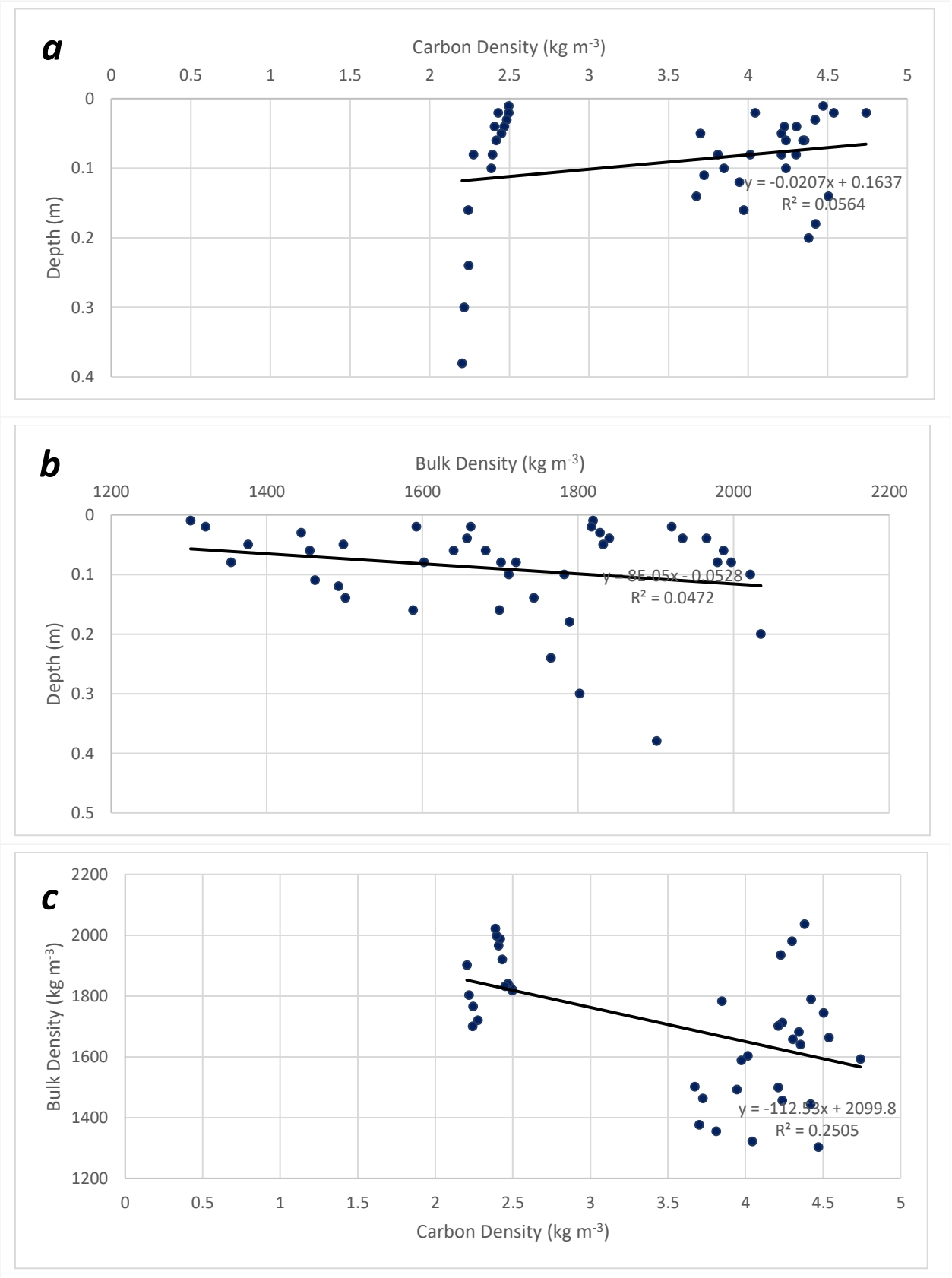
a
Carbon Density (kg m-3)
0
0.5
1
1.5
2
2.5
3
3.5
4
4.5
5
Depth (m)
0
0.1
0.2
0.3
0.4
y = -0.0207x + 0.1637
R² = 0.0564
b
Bulk Density (kg m-3)
1200
1400
1600
1800
2000
2200
Depth (m)
0
0.1
0.2
0.3
0.4
0.5
y = -8E-05x + 0.0528
R² = 0.0472
c
Bulk Density (kg m-3)
2200
2000
1800
1600
1400
1200
0
0.5
1
1.5
2
2.5
3
3.5
4
4.5
5
Carbon Density (kg m-3)
y = -112.53x + 2099.8
R² = 0.2505

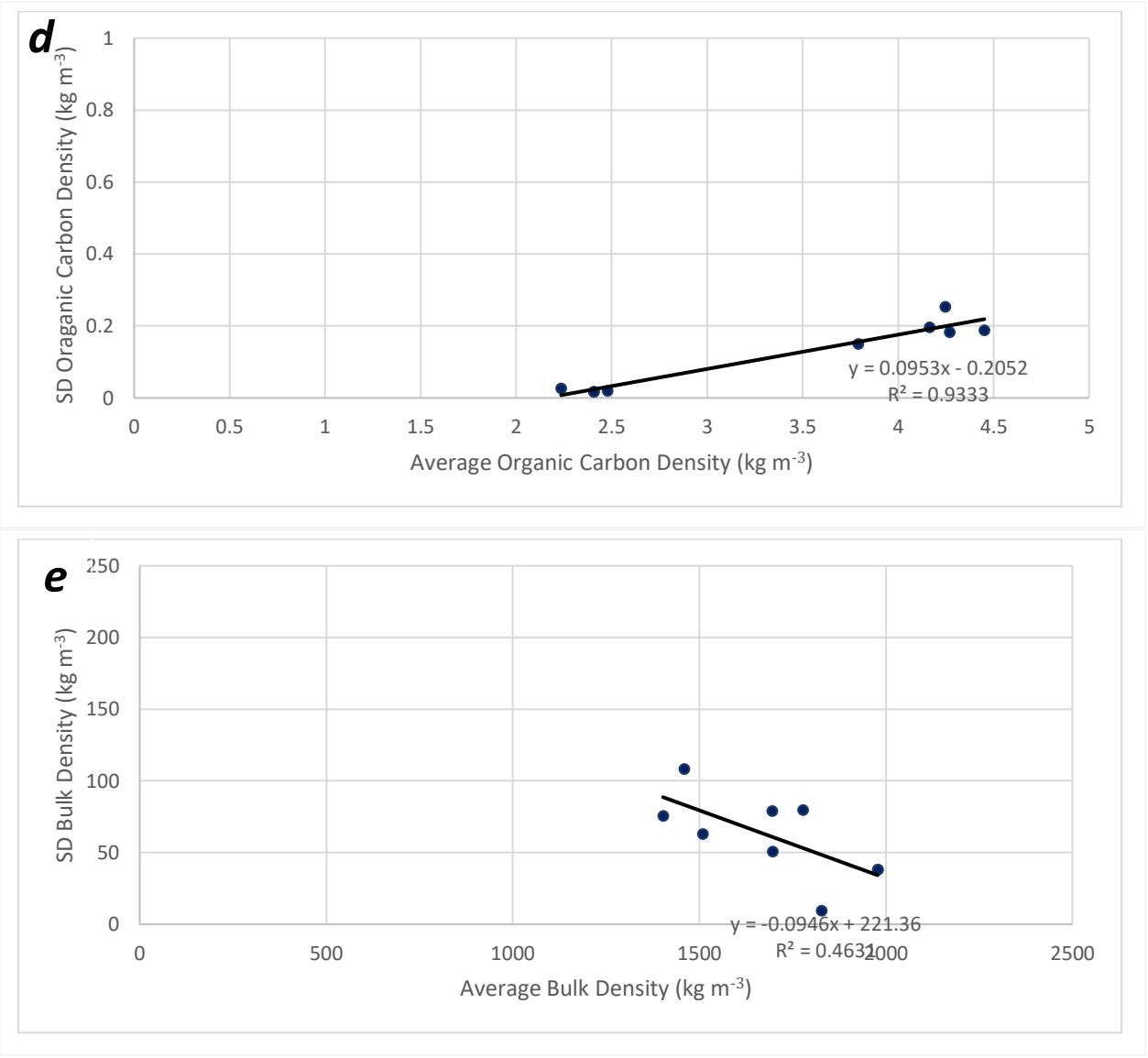

Figure C(V). Correspondance between the depth, organic carbon density and bulk density in the differing active layer horizons of Marsh A.

C2 - Marsh B

C2(i) - Field Findings

The sampling design on Marsh B was structured in order to enable the extraction of cores from the varying sub-environments that characterised the environment which resembled a saltmarsh mosaic discussed in Section 3.2.2. However, it should be noted that accessibility issues and permission restrictions limited sampling in the south-west of the marsh hence the study best represents the sub-environment composition of the marsh given the circumstances.

Above-ground Biomass

Table C(iV). Location of sampling sites and above-ground biomass carbon storage quantification for Marsh B.

Site	Sub-environment Type	OS Grid Reference	Elevation (mOD)	C Mass (kg/m^2)	Uncertainty kg (±)	Uncertainty (%)
W Site A	Species Zone B	SD 40642 27153	5.83	1.326	0.001	0.08
W Site B	Brackish Waterbodies	SD 40895 26936	5.17	0.355	0.0005	0.14
W Site C	Species Zone C	SD 40769 26706	5.62	1.024	0.001	0.10
N Site A	Brackish Waterbodies	SD 39506 27697	5.44	0.312	0.0005	0.16
N Site B	Species Zone B	SD 39190 27458	5.99	1.223	0.001	0.08
N Site C	Exposed Sediment	SD 39470 27296	5.57	0.190	0.0005	0.26
MC Site A	Species Zone D	SD 39471 27222	5.7	0.813	0.0005	0.06
MC Site B	Species Zone C	SD 39228 27058	5.18	1.319	0.001	0.08
MC Site C	Exposed Sediment	SD 39125 27034	4.86	0.017	0.0005	2.97
WC Site A	Species Zone A	SD 40374 27312	5.52	0.903	0.0005	0.06
WC Site B	Species Zone C	SD 40363 27091	4.9	0.897	0.0005	0.06
WC Site C	Species Zone E	SD 40343 26880	5.58	0.789	0.0005	0.06

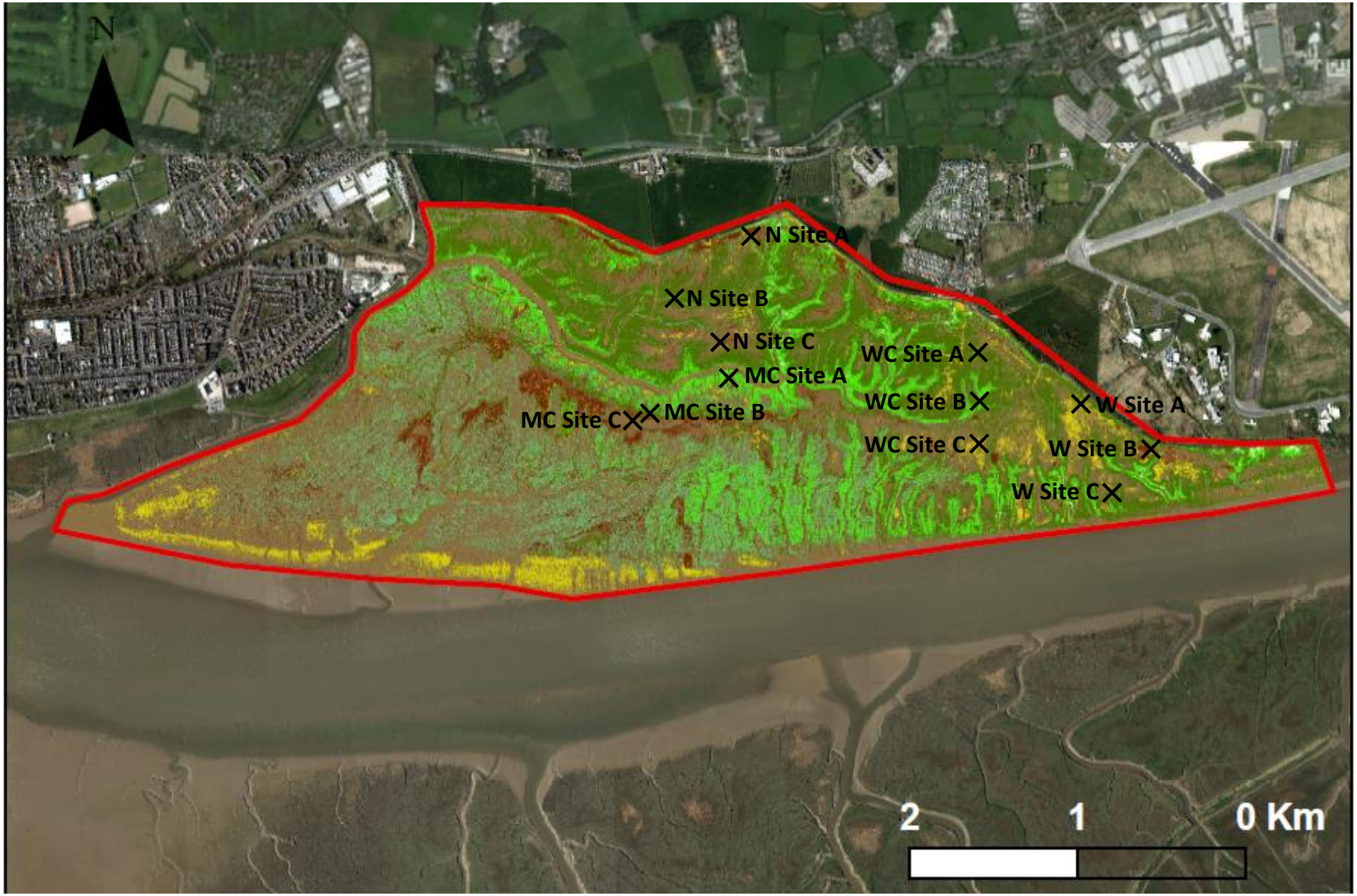

Figure C(Vi). Location of coring sites and post-ground truthing ML sub-enviornment map of Marsh B

Sub-surface

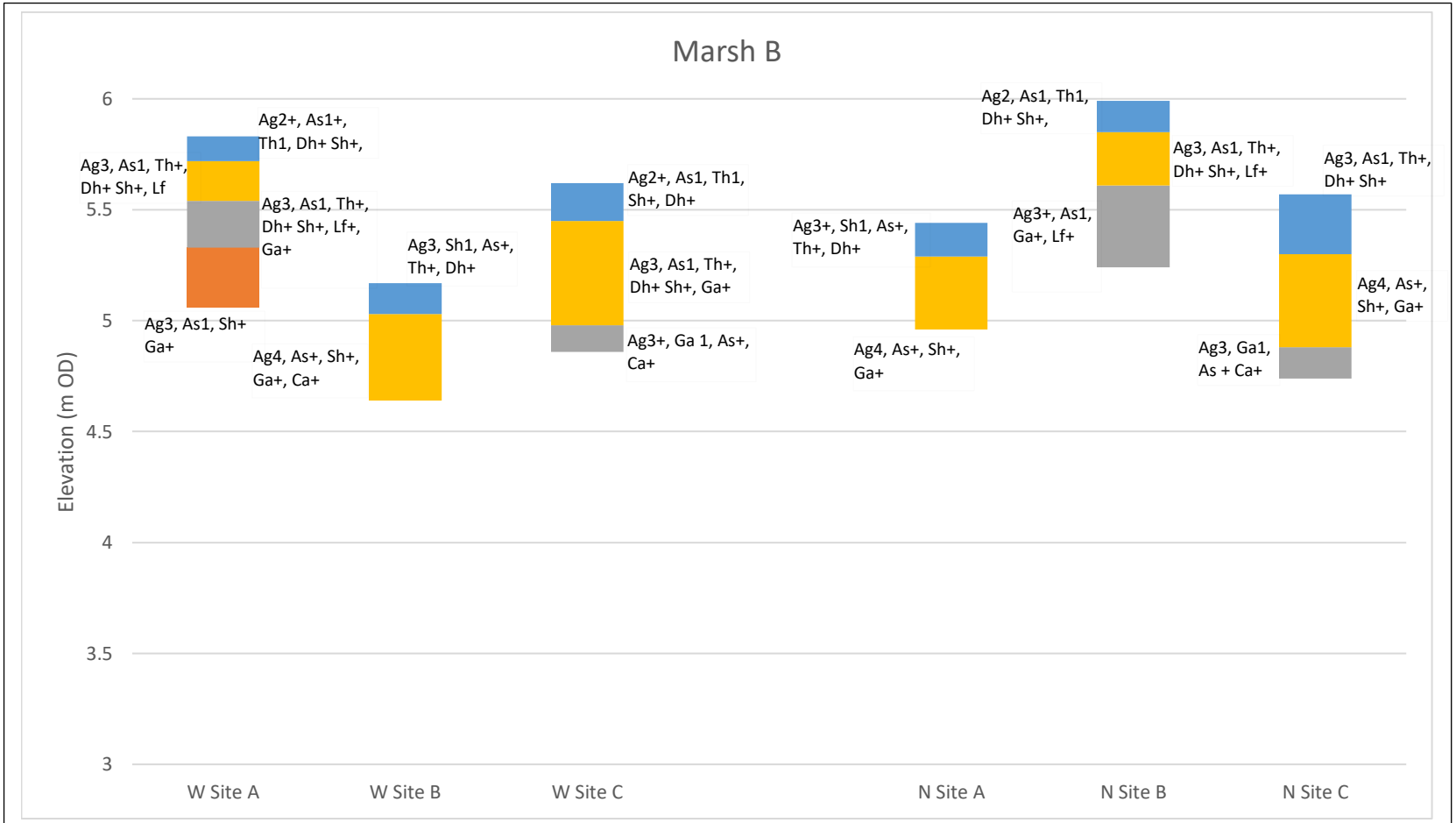

Lithology Key after Troels-Smith (1955)

As = Clay (<0.002mm), **Ag** = Silt (0.002 – 0.06mm), **Ga** = Coarse sand (0.6 – 2mm), **Ca** = Calcareous shell, **Sh** = Humified organics beyond identification, **Th** = Roots, stems and rhizomes of herbaceous plants, **Dh** = Fragments of stems and leaves of herbaceous plants >2mm, **Lf** = Mineral and/or organic iron oxide

Approximate Composition –

4 = 100% 3 = 75% 2 = 50% 1 = 25% + = 12.5% (Trace)

Figure C(Vii). Stratigraphy and composition of cores taken on the western and northern sites of Marsh B.

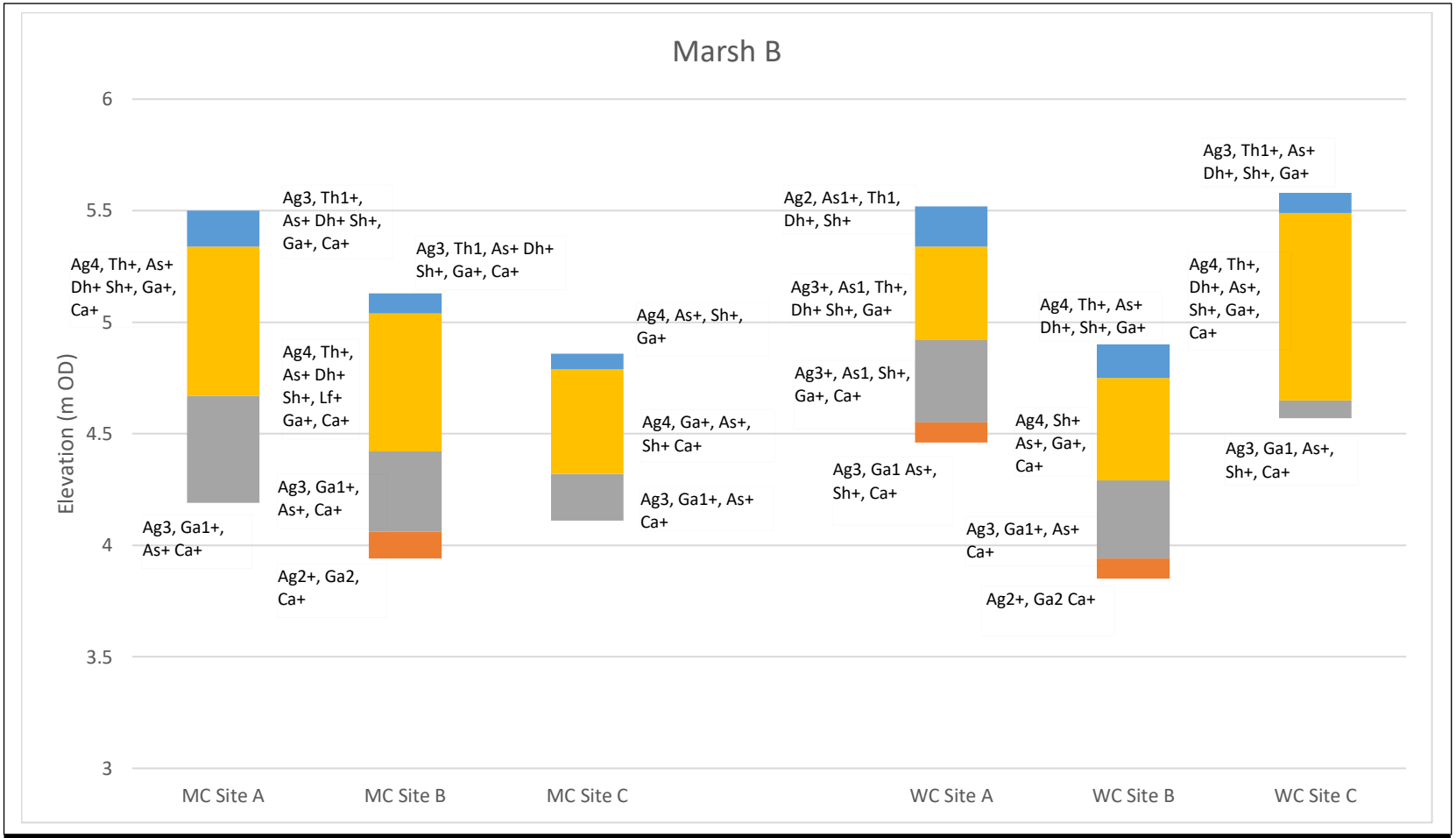

Lithology Key after Troels-Smith (1955)

As = Clay (<0.002mm), **Ag** = Silt (0.002 – 0.06mm), **Ga** = Coarse sand (0.6 – 2mm), **Ca** = Calcareous shell, **Sh** = Humified organics beyond identification, **Th** = Roots, stems and rhizomes of herbaceous plants, **Dh** = Fragments of stems and leaves of herbaceous plants >2mm, **Lf** = Mineral and/or organic iron oxide

Approximate Composition –

4 = 100% 3 = 75% 2 = 50% 1 = 25% + = 12.5% (Trace)

Figure C(Vii). Stratigraphy and composition of cores taken on the main central and west central sites of Marsh B.

C2(ii) - Sub-surface Carbon Content and Bulk Density Variability

Table C(V) Variation in horizon depth, organic carbon density and bulk density on Marsh B.

Sub-environment classification	Site Name	Horizon Number	Depth (m)	OCD (kg m^{-3})	BD (kg m^{-3})
Species Zone D	W Site A	1	0.11	4.19	1468
		2	0.29	2.91	1797
		3	0.5	2.41	1930
		4	0.77	2.14	2123
Brackish Waterbodies	W Site B	1	0.14	3.75	1711
		2	0.53	2.64	1849
Species Zone C	W Site C	1	0.17	4.24	1659
		2	0.64	2.57	1894
		3	0.76	1.41	2045
Brackish Waterbodies	N Site A	1	0.15	4.06	1739
		2	0.48	2.60	1906
Species Zone A	N Site B	1	0.14	4.05	1528
		2	0.38	2.63	1723
		3	0.75	1.86	1980
Exposed Sediment	N Site C	1	0.27	3.57	1832
		2	0.69	2.53	1990
		3	0.83	1.70	2098
Species Zone D	MC Site A	1	0.16	3.65	1626
		2	0.83	2.57	1955
		3	1.31	2.00	2107
Species Zone C	MC Site B	1	0.09	4.33	1543
		2	0.71	2.71	1843
		3	1.07	1.35	1970
		4	1.19	1.28	2089
Exposed Sediment	MC Site C	1	0.07	3.70	1641
		2	0.54	2.50	1795
		3	0.75	1.63	2055
Species Zone A	WC Site A	1	0.18	4.16	1496
		2	0.6	2.66	1760
		3	0.97	2.22	1887
		4	1.06	1.37	2132
Species Zone C	WC Site B	1	0.15	3.77	1582
		2	0.61	2.97	1962
		3	0.96	2.07	2076
		4	1.05	1.29	2190
Species Zone E	WC Site C	1	0.09	4.07	1574
		2	0.93	2.68	1820
		3	1.01	1.24	2093

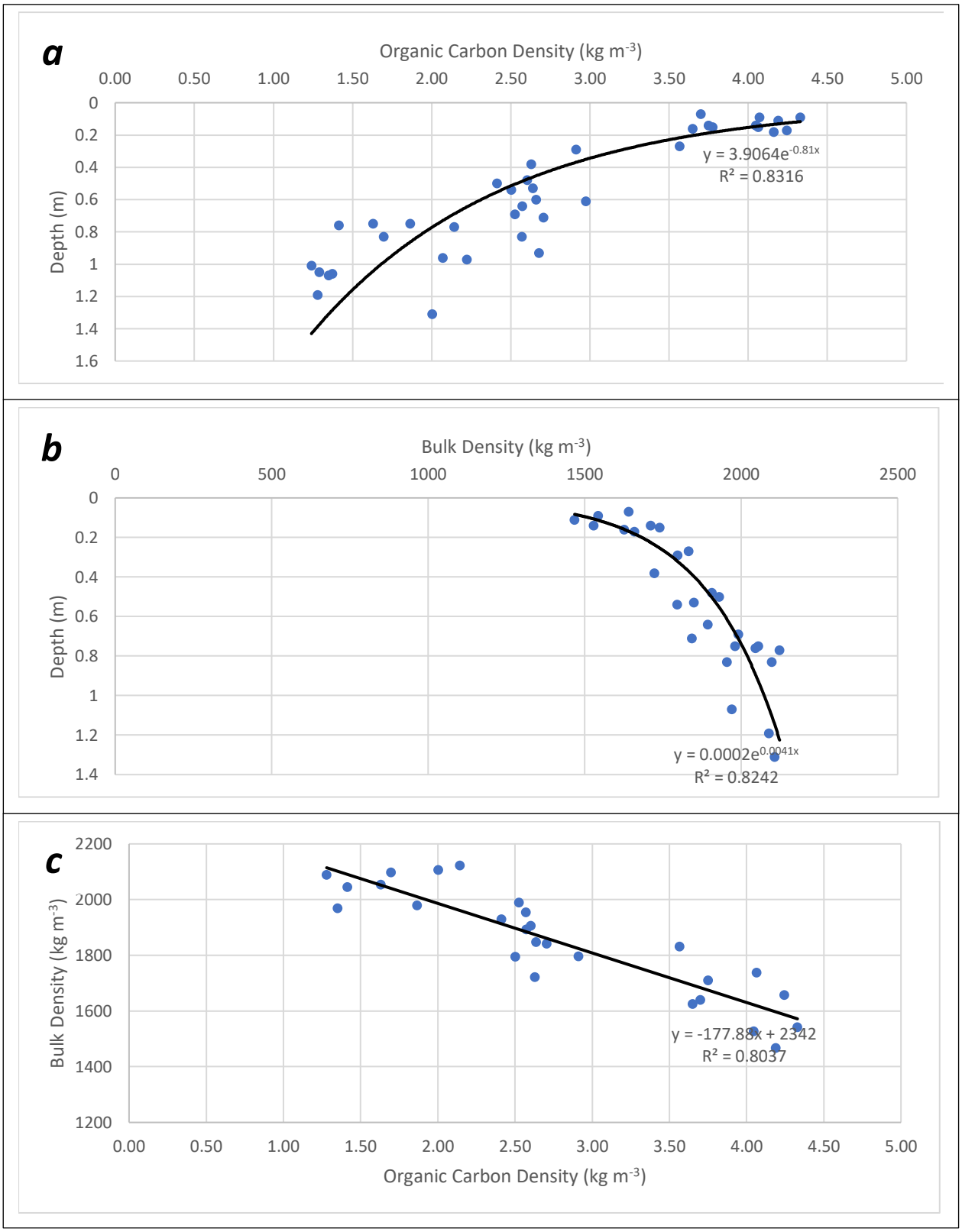

Figure C(Viii). Correspondance between the depth, organic carbon density and bulk density in the differing horizons of Marsh B.

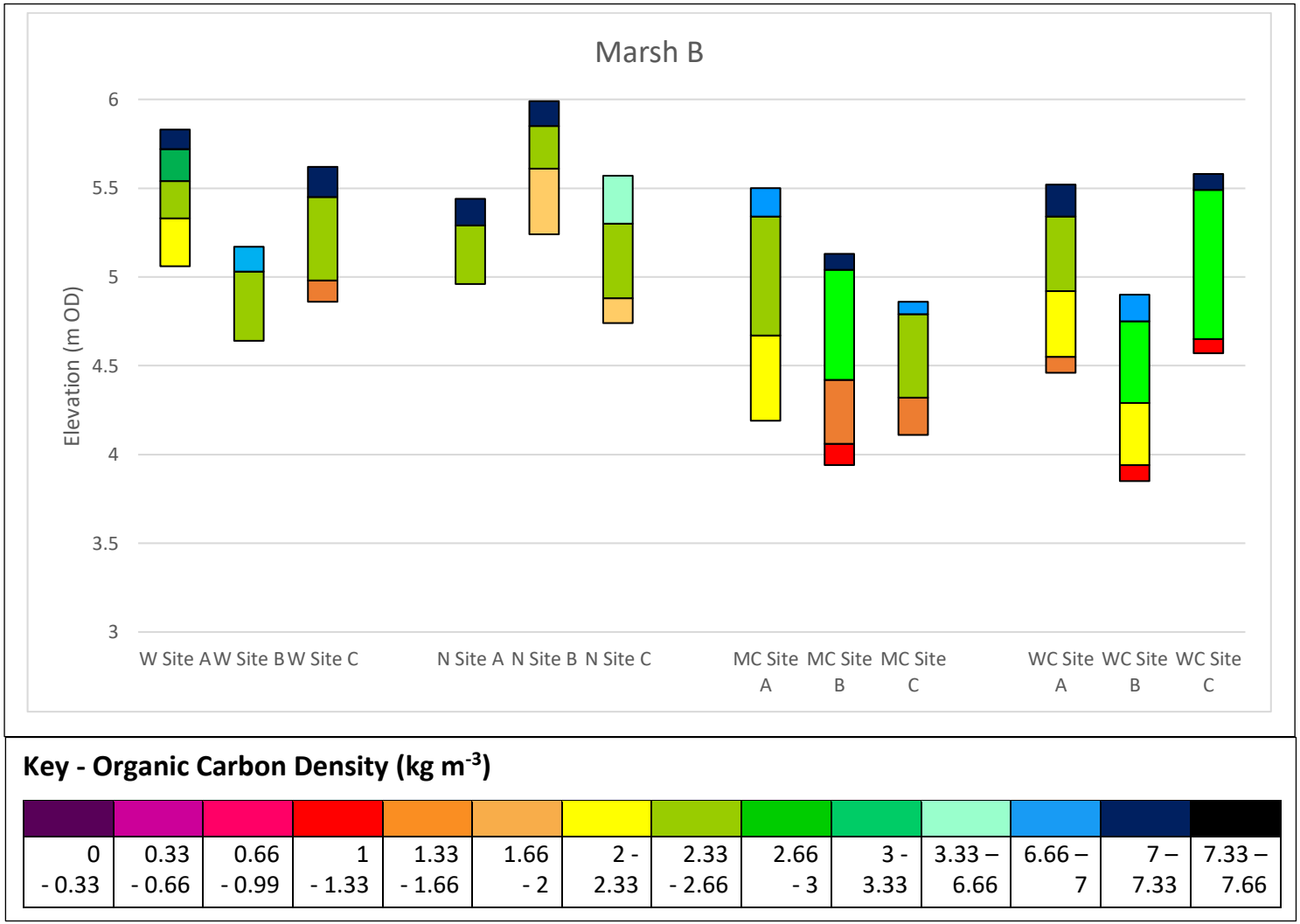

Figure C(iX). Levelled stratigraphy for all sample sites on Marsh B exhibiting organic carbon denisty in each horizon of every sampled core. Resulted were determined derived after a loss on ignition test conducted on all samples following a standardised procedure outlined in the TESSA guidelines. Please see tables 6.2.2.2(a,b,c&d) for estimated organic carbon contents of all horizons.

C2(iii) - Active Layer Characteristics

Table C(Vi) Variation in horizon depth, organic carbon density and bulk density in the active layer (i.e. horizon 1) on Marsh B.

				Organic Carbon Density (kg m^{-3})			Bulk Density (kg m^{-3})		
Species Zone	Site Reference	Sub-horizon Sample Number	Sample Depth (m)	Sample value	Average	Standard Deviation	Sample Value	Average	Standard Deviation
SA	W Site A	1	0.02	4.64	4.19	0.41	1367	1468	87
		1b	0.04	4.01			1423		
		1c	0.06	4.42			1440		
		1d	0.08	4.29			1521		
		1e	0.1	3.58			1589		
BW	W Site B	1	0.03	3.63	3.75	0.12	1602	1711	77
		1b	0.05	3.74			1682		
		1c	0.07	3.93			1720		
		1d	0.1	3.78			1740		
		1e	0.13	3.68			1810		
SC	W Site C	1	0.03	4.36	4.24	0.31	1542	1659	93
		1b	0.07	4.11			1602		
		1c	0.1	4.70			1671		
		1d	0.13	4.17			1788		
		1e	0.17	3.88			1691		
SB	WC Site A	1	0.03	4.33	4.16	0.24	1378	1496	136
		1b	0.07	4.41			1400		
		1c	0.11	4.26			1589		
		1d	0.13	3.93			1423		
		1e	0.17	3.88			1689		
SC	WC Site B	1	0.03	4.00	3.77	0.27	1432	1582	111
		1b	0.06	3.96			1530		
		1c	0.08	3.93			1576		
		1d	0.12	3.60			1650		
		1e	0.15	3.38			1721		
SE	WC Site C	1	0.02	4.11	4.07	0.08	1502	1574	64
		1b	0.04	3.96			1578		
		1c	0.06	4.15			1530		
		1d	0.07	4.04			1589		
		1e	0.09	4.09			1670		
BW	N Site A	1	0.03	4.26	4.06	0.21	1621	1739	71
		1b	0.07	4.30			1730		
		1c	0.1	3.90			1782		
		1d	0.13	4.05			1760		
		1e	0.15	3.82			1802		
SA	N Site B	1	0.03	4.34	4.05	0.28	1401	1528	83
		1b	0.06	4.24			1497		
		1c	0.08	3.82			1543		
		1d	0.11	4.14			1601		
		1e	0.14	3.69			1598		
EX	N Site C	1	0.06	3.74	3.57	0.20	1692	1832	94
		1b	0.11	3.56			1782		
		1c	0.16	3.77			1873		
		1d	0.2	3.45			1890		
		1e	0.25	3.31			1923		

Table C(Vi). Variation in horizon depth, organic carbon density and bulk density in the active layer (i.e. horizon 1) on Marsh B.

				Organic Carbon Density (kg m^{-3})			Bulk Density (kg m^{-3})		
Species Zone	Site Reference	Sub-horizon Sample Number	Sample Depth (m)	Sample value	Average	Standard Deviation	Sample Value	Average	Standard Deviation
SD	MC Site A	1	0.03	4.10	3.65	0.39	1501	1626	85
		1b	0.07	3.98			1593		
		1c	0.1	3.60			1632		
		1d	0.13	3.40			1680		
		1e	0.16	3.16			1723		
SC	MC Site B	1	0.01	4.58	4.33	0.18	1380	1543	173
		1b	0.03	4.40			1421		
		1c	0.05	4.30			1465		
		1d	0.07	4.30			1667		
		1e	0.09	4.08			1780		
EX	MC Site C	1	0.01	4.02	3.70	0.24	1588	1641	40
		1b	0.03	3.79			1624		
		1c	0.05	3.74			1699		
		1d	0.06	3.58			1643		
		1e	0.07	3.37			1650		
SB	WC Site A	1	0.03	4.10	3.65	0.39	1378	1496	136
		1b	0.07	3.98			1400		
		1c	0.11	3.60			1589		
		1d	0.13	3.40			1423		
		1e	0.17	3.16			1689		
SC	WC Site B	1	0.03	4.58	4.33	0.18	1432	1582	111
		1b	0.06	4.40			1530		
		1c	0.08	4.30			1576		
		1d	0.12	4.30			1650		
		1e	0.15	4.08			1721		
SE	WC Site C	1	0.02	4.02	3.70	0.24	1502	1574	64
		1b	0.04	3.79			1578		
		1c	0.06	3.74			1530		
		1d	0.07	3.58			1589		
		1e	0.09	3.37			1670		

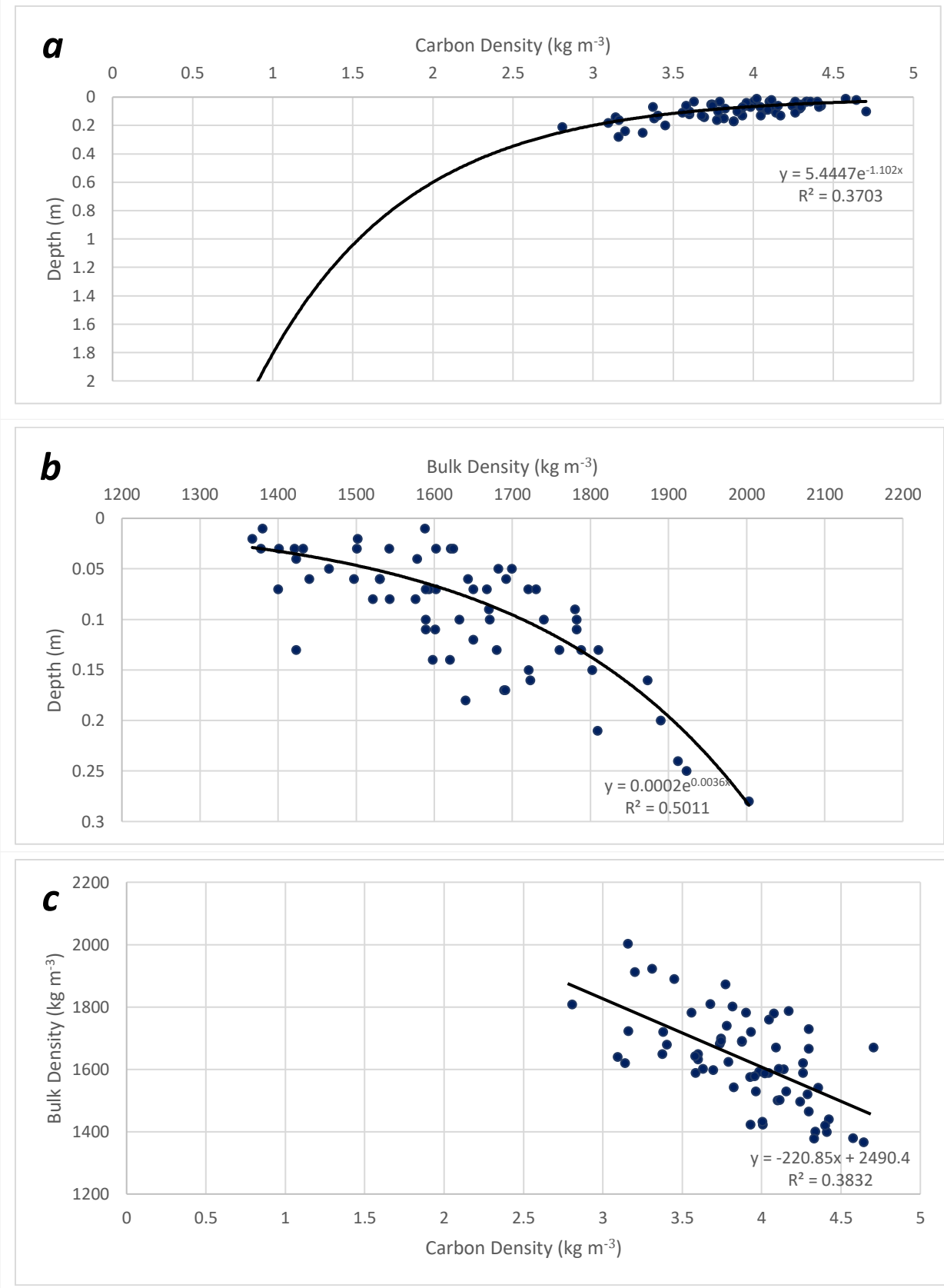
a
Carbon Density (kg m-3)
0 0.5 1 1.5 2 2.5 3 3.5 4 4.5 5
Depth (m)
0 0.2 0.4 0.6 0.8 1 1.2 1.4 1.6 1.8 2
y = 5.4447e-1.102x
R² = 0.3703
b
Bulk Density (kg m-3)
1200 1300 1400 1500 1600 1700 1800 1900 2000 2100 2200
Depth (m)
0 0.05 0.1 0.15 0.2 0.25 0.3
y = 0.0002e0.0036x
R² = 0.5011
c
Bulk Density (kg m-3)
2200 2000 1800 1600 1400 1200
0 0.5 1 1.5 2 2.5 3 3.5 4 4.5 5
Carbon Density (kg m-3)
y = -220.85x + 2490.4
R² = 0.3832

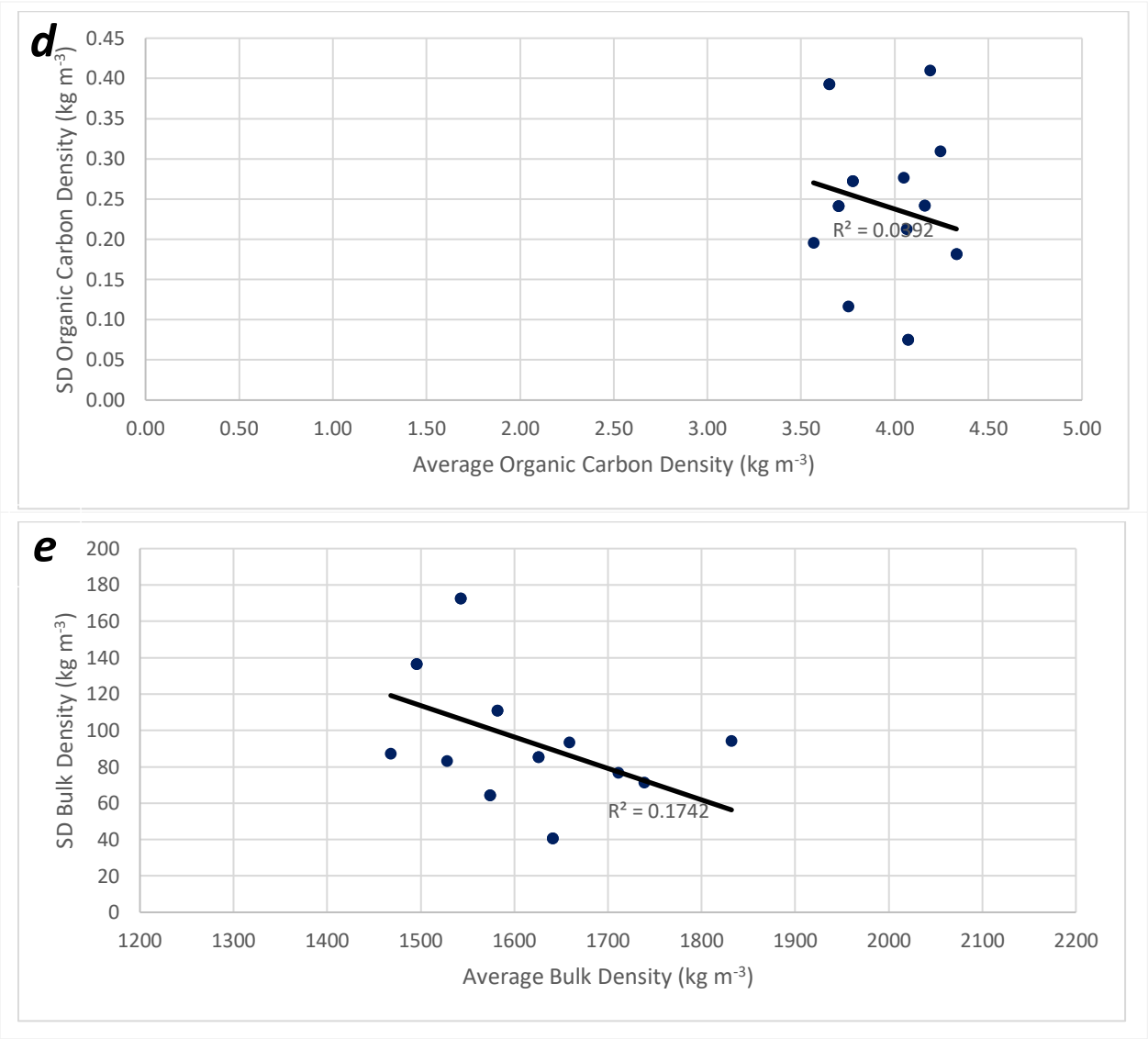

Figure C(X). Correspondance between the depth, organic carbon density and bulk density in the differing active layer horizons of Marsh B.

C3 - Marsh C

C3(i) - Field Findings

The sampling design for Marsh C was structured in order to ensure as many sub-environments as possible were sampled despite logistical and safety restrictions produced as a result of its comparatively large area and the location of major creeks. As can be observed in Figure C (Xiii) the sampling was conducted over the area of Marsh C, enabling an assessment of how carbon storage varied across the accessible marsh.

Above-ground Biomass

Table C(Vii). Location of sampling sites and above-ground biomass carbon storage quantification for Marsh C.

Site	Sub-environment Type	OS Grid Reference	Elevation (mOD)	C Mass (kg/m^2)	Uncertainty kg (±)	Uncertainty (%)
W Site A	Species Zone F	SD 35612 20848	4.93	0.595	0.0005	0.08
W Site B	Species Zone A	SD 35676 20809	5.52	0.459	0.0005	0.11
W Site C	Species Zone E	SD 35587 20954	4.29	0.349	0.0005	0.14
W Site D	Species Zone B	SD 35334 21189	4.58	1.412	0.001	0.07
C Site A	Species Zone A	SD 38401 22373	4.72	1.299	0.001	0.08
C Site B	Brackish Waterbodies	SD 38383 22621	4.39	0.320	0.0005	0.16
C Site C	Species Zone D	SD 37925 22965	4.98	0.734	0.0005	0.07
C Site D	Species Zone C	SD 38014 23066	4.53	0.179	0.0005	0.28
E Site A	Species Zone B	SD 40158 23860	5.21	0.872	0.0005	0.06
E Site B	Exposed Sediment	SD 40164 24235	4.98	0	0	0
E Site C	Species Zone D	SD 39699 24764	5.51	0.692	0.0005	0.07
E Site D	Exposed Sediment	SD 39389 25319	4.82	0.240	0.0005	0.21

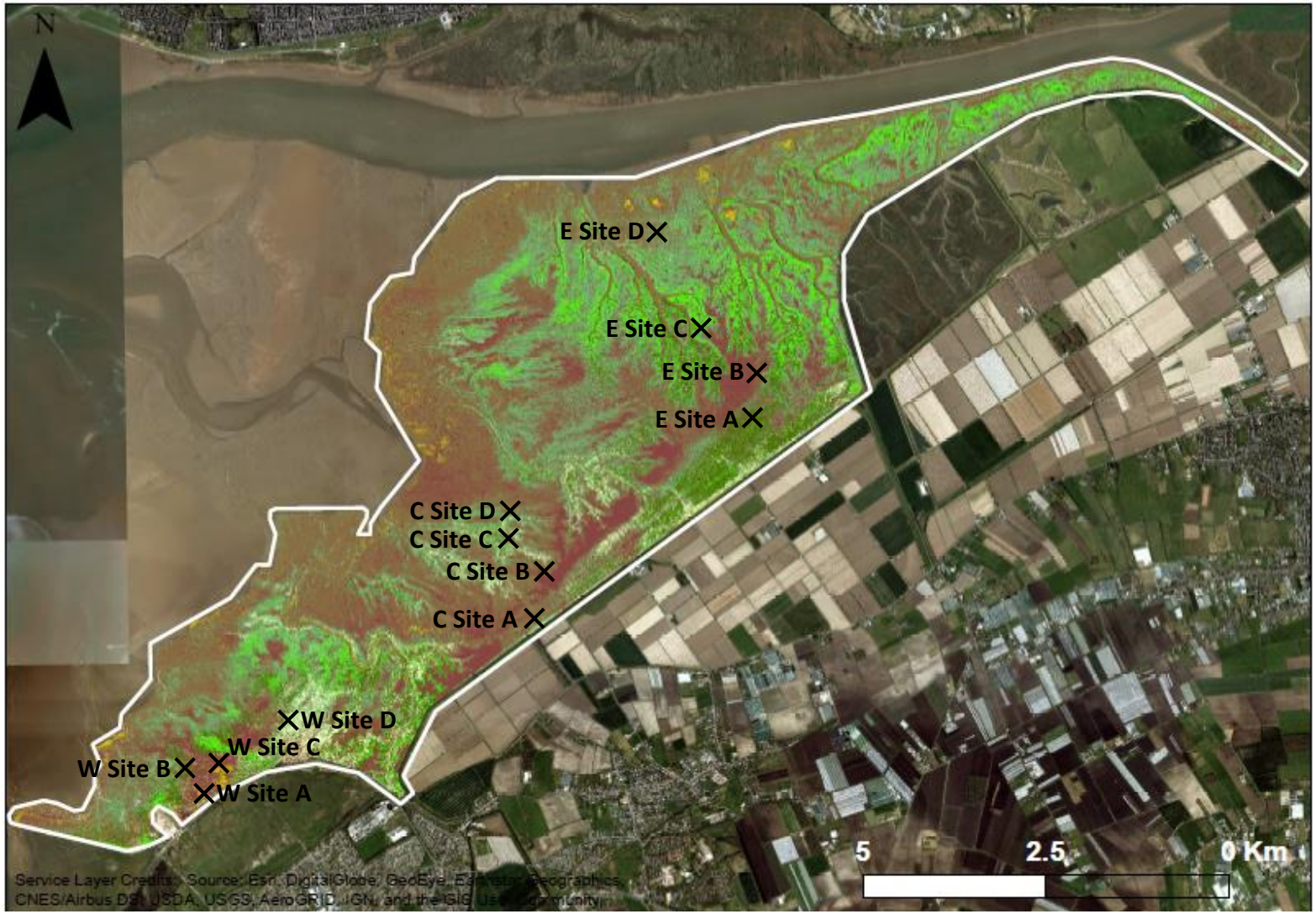

Figure C(Xi). Marsh C sampling locations and landcover distribution.

Sub-surface

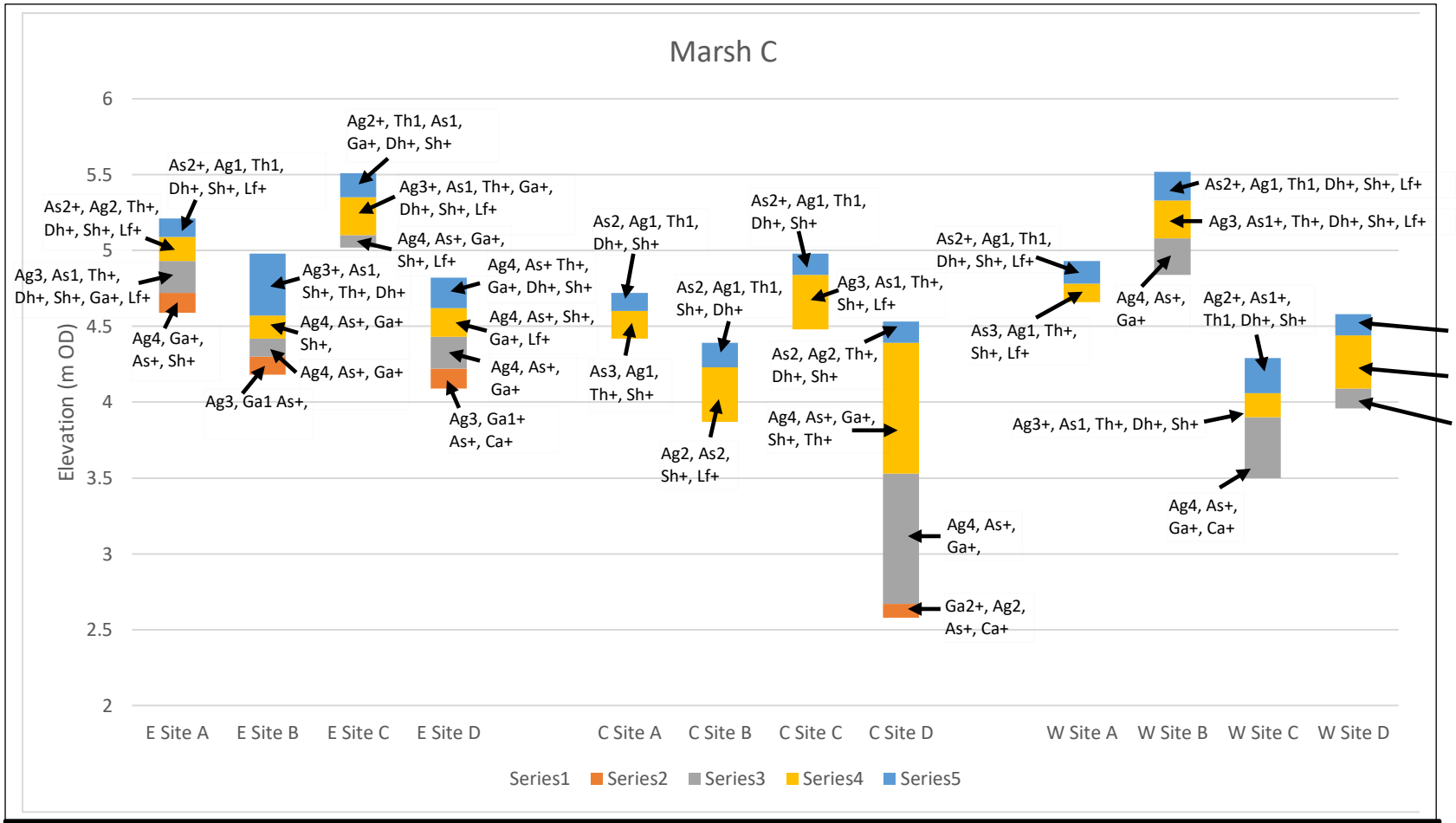

Lithology Key after Troels-Smith (1955)

As = Clay (<0.002mm), **Ag** = Silt (0.002 – 0.06mm), **Ga** = Coarse sand (0.6 – 2mm), **Ca** = Calcareous shell, **Sh** = Humified organics beyond identification, **Th** = Roots, stems and rhizomes of herbaceous plants, **Dh** = Fragments of stems and leaves of herbaceous plants >2mm, **Lf** = Mineral and/or organic iron oxide

Approximate Composition –

4 = 100% 3 = 75% 2 = 50% 1 = 25% + = 12.5% (Trace)

Figure C(Xii). Levelled stratigraphy for all sample sites on Marsh C.

C3(ii) - Sub-surface Carbon Content and Bulk Density Variability

Table C(Viii). Variation in horizon depth, organic carbon density and bulk density on Marsh C.

Sub-environment classification	Site Name	Horizon Number	Depth (m)	OCD (kg m^{-3})	BD (kg m^{-3})
Species Zone F	W Site A	1	0.15	2.89	1502
		2	0.27	1.98	1709
Species Zone A	W Site B	1	0.19	3.88	1498
		2	0.44	2.54	1690
		3	0.68	2.10	1733
Species Zone E	W Site C	1	0.23	4.07	1492
		2	0.39	2.81	1696
		3	0.79	1.89	1773
Species Zone B	W Site D	1	0.14	3.17	1502
		2	0.49	2.23	1692
		3	0.62	1.41	1912
Species Zone B	**C** Site A	1	0.12	4.06	1494
		2	0.3	3.33	1607
Brackish Waterbodies	**C** Site B	1	0.16	3.75	1470
		2	0.52	2.84	1647
Species Zone D	**C** Site C	1	0.14	3.60	1506
		2	0.5	2.08	1612
Species Zone C	**C** Site D	1	0.14	4.33	1523
		2	1	1.93	1743
		3	1.86	2.07	1848
		4	1.95	1.34	2093
Species Zone D	E Site A	1	0.12	3.98	1482
		2	0.28	3.48	1524
		3	0.49	2.40	1600
		4	0.62	1.65	1812
Exposed Sediment	E Site B	1	0.41	3.12	1533
		2	0.56	2.52	1589
		3	0.68	2.15	1721
		4	0.8	1.32	1957
Species Zone C	E Site C	1	0.16	4.25	1473
		2	0.41	2.98	1609
		3	0.49	1.86	1822
Exposed Sediment	E Site D	1	0.2	3.12	1522
		2	0.39	2.33	1690
		3	0.6	2.01	1771
		4	0.73	1.32	1953

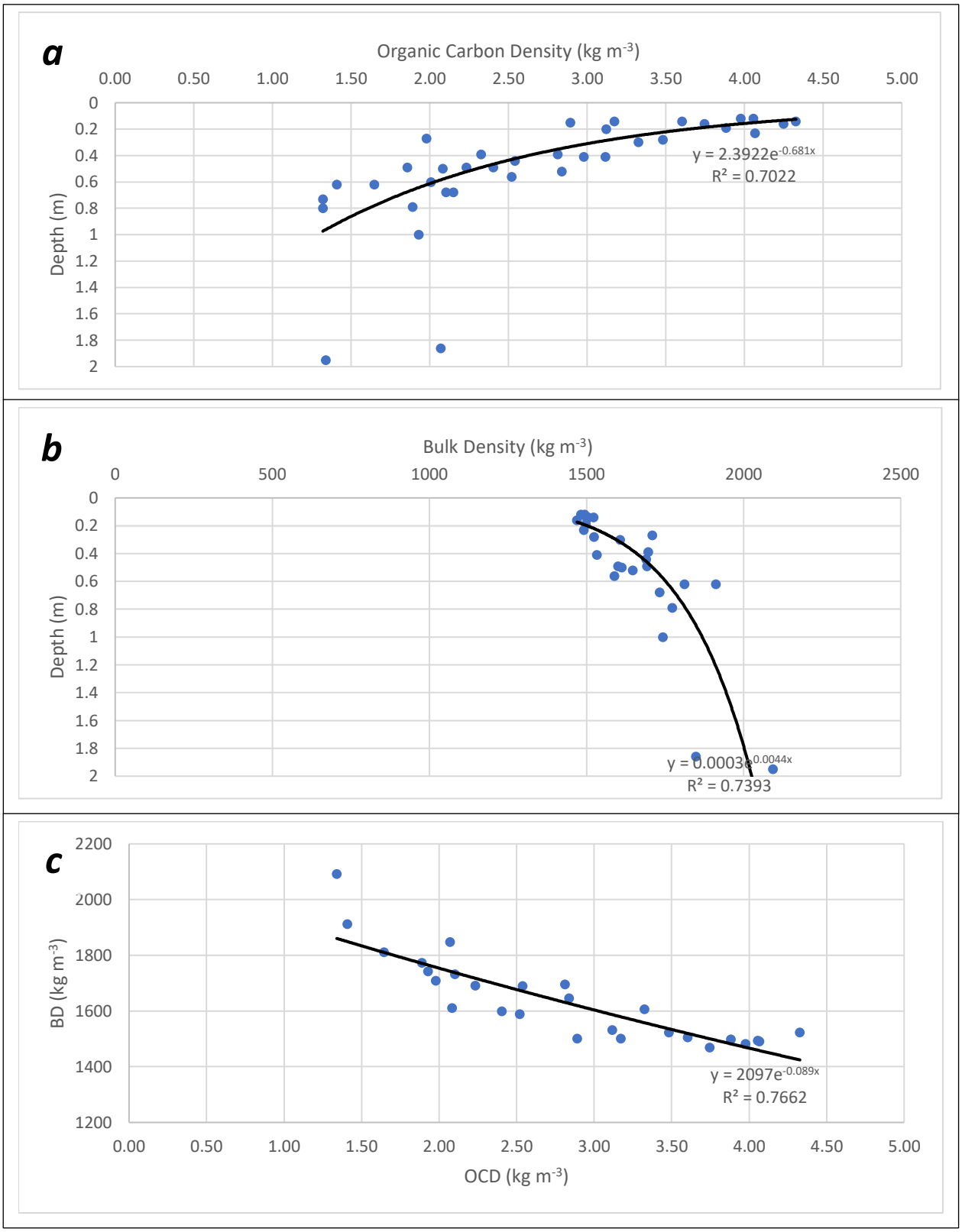

Figure C(Xiii). Correspondance between the depth, organic carbon density and bulk density in the differing horizons of Marsh C.

Marsh C - Carbon Content

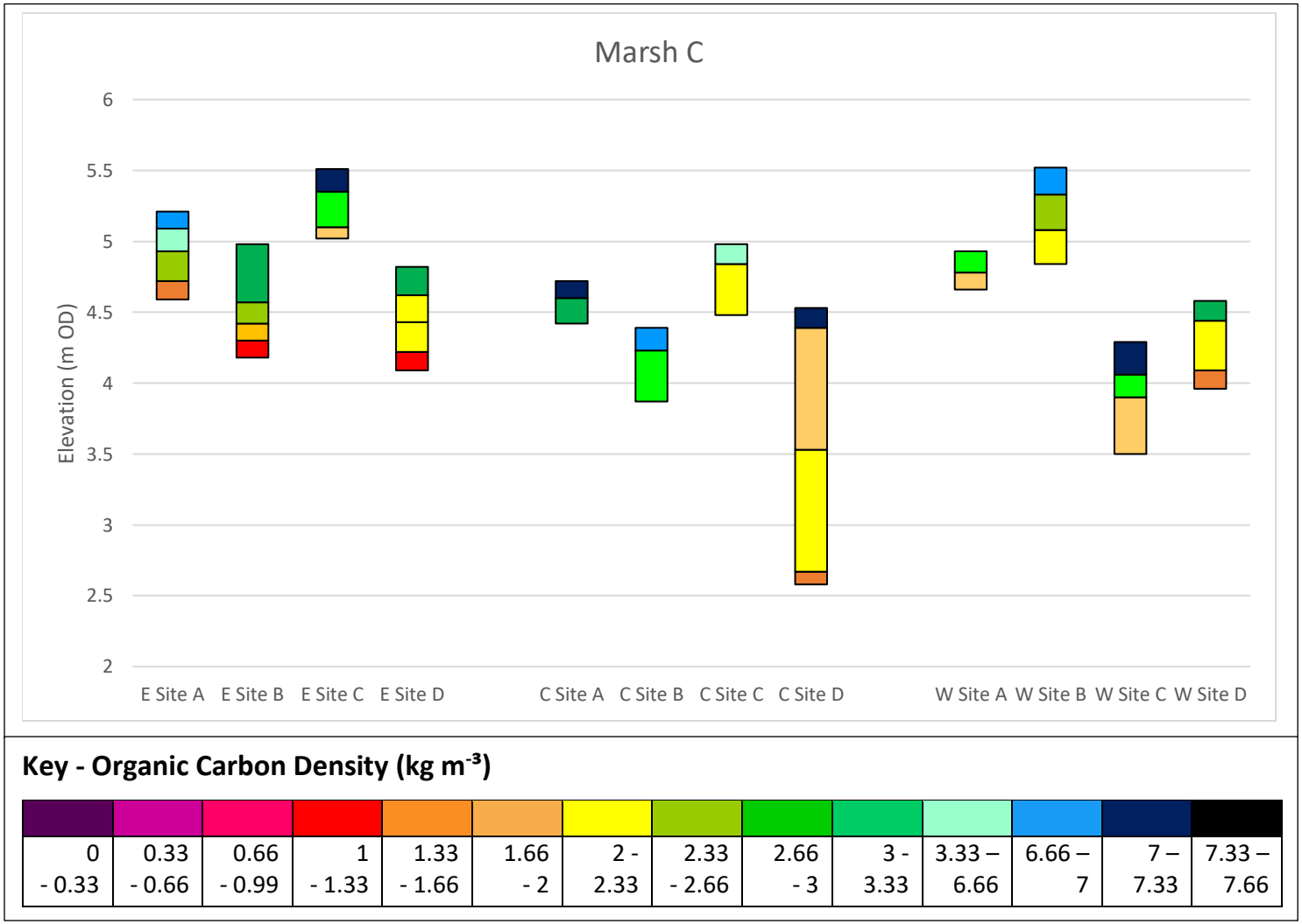

Figure C(XiV). Levelled stratigraphy for all sample sites on Marsh C exhibiting organic carbon denisty in each horizon of every sampled core. Resulted were determined derived after a loss on ignition test conducted on all samples following a standardised procedure outlined in the TESSA guidelines. Please see tables 6.3.2.2(a,b,c&d) for estimated organic carbon contents of all horizons.

C3(iii) - Active Layer Characteristics

Table C(iX). Variation in horizon depth, organic carbon density and bulk density in the active layer (i.e. horizon 1) on Marsh B.

				Organic Carbon Density (kg m^{-3})			Bulk Density (kg m^{-3})		
Species Zone	Site Reference	Sub-horizon Sample Number	Sample Depth (m)	Sample value	Average	Standard Deviation	Sample Value	Average	Standard Deviation
SF	W Site A	1a	0.03	3.14	2.89	0.31	1461	1502	33
		1b	0.06	3.30			1486		
		1c	0.09	2.77			1500		
		1d	0.11	2.66			1513		
		1e	0.14	2.60			1550		
SA	W Site B	1a	0.04	4.27	3.88	0.27	1422	1498	70
		1b	0.07	4.01			1427		
		1c	0.11	3.84			1523		
		1d	0.14	3.72			1544		
		1e	0.18	3.57			1574		
SE	W Site C	1a	0.05	4.34	4.07	0.42	1397	1492	71
		1b	0.09	4.51			1447		
		1c	0.13	4.24			1499		
		1d	0.18	3.71			1545		
		1e	0.22	3.54			1572		
SB	W Site D	1a	0.02	3.14	3.17	0.10	1443	1502	43
		1b	0.05	3.31			1483		
		1c	0.07	3.20			1501		
		1d	0.09	3.04			1527		
		1e	0.12	3.18			1556		
SB	C Site A	1a	0.03	4.36	4.06	0.27	1410	1494	71
		1b	0.05	4.31			1445		
		1c	0.07	3.93			1490		
		1d	0.09	3.95			1536		
		1e	0.11	3.73			1589		
BW	C Site B	1a	0.03	4.07	3.75	0.27	1421	1470	50
		1b	0.06	3.86			1444		
		1c	0.09	3.84			1441		
		1d	0.12	3.59			1502		
		1e	0.15	3.37			1542		
SD	C Site C	1a	0.03	3.96	3.60	0.25	1423	1506	65
		1b	0.05	3.68			1476		
		1c	0.07	3.59			1490		
		1d	0.1	3.51			1552		
		1e	0.13	3.27			1587		
SC	C Site D	1a	0.03	4.64	4.33	0.31	1461	1523	55
		1b	0.05	4.62			1502		
		1c	0.08	4.35			1493		
		1d	0.11	4.07			1568		
		1e	0.14	3.96			1593		

Table C(iX). Variation in horizon depth, organic carbon density and bulk density in the active layer (i.e. horizon 1) on Marsh B.

				Organic Carbon Density (kg m^{-3})			Bulk Density (kg m^{-3})		
Species Zone	Site Reference	Sub-horizon Sample Number	Sample Depth (m)	Sample value	Average	Standard Deviation	Sample Value	Average	Standard Deviation
SD	E Site A	1a	0.02	4.26	3.98	0.21	1464	1482	16
		1b	0.04	4.00			1465		
		1c	0.07	3.96			1486		
		1d	0.08	3.98			1493		
		1e	0.11	3.67			1500		
EX	E Site B	1a	0.08	3.04	3.12	0.26	1510	1553	46
		1b	0.16	3.17			1535		
		1c	0.24	3.29			1520		
		1d	0.31	3.37			1580		
		1e	0.39	2.71			1620		
SC	E Site C	1a	0.03	4.42	4.25	0.13	1385	1447	63
		1b	0.06	4.24			1402		
		1c	0.09	4.25			1429		
		1d	0.13	4.29			1480		
		1e	0.16	4.04			1539		
EX	E Site D	1a	0.03	3.08	3.12	0.19	1484	1522	33
		1b	0.07	2.88			1508		
		1c	0.12	3.24			1509		
		1d	0.16	3.37			1540		
		1e	0.2	3.03			1570		

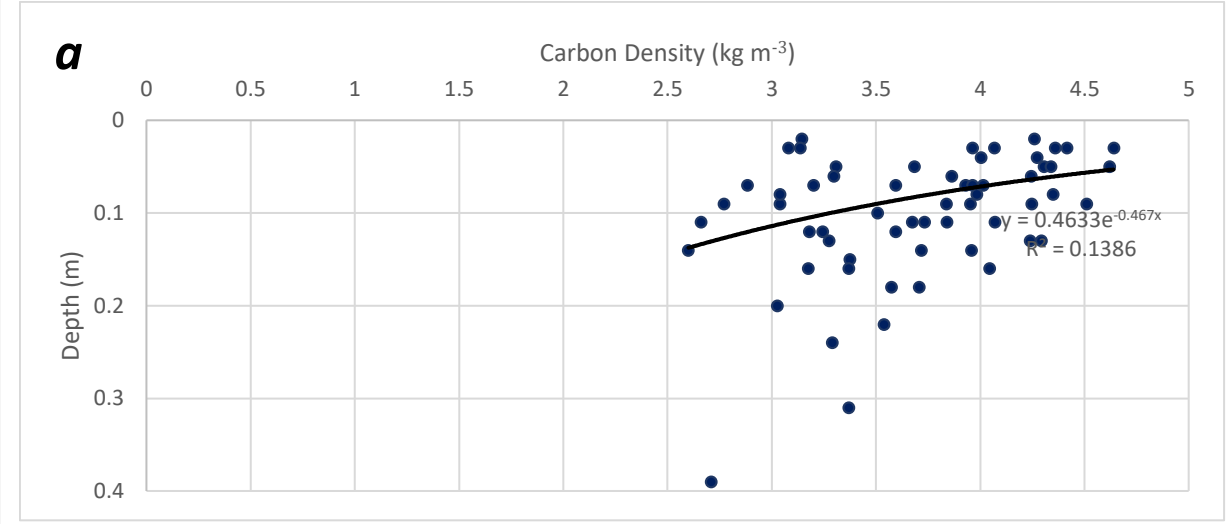
a
Carbon Density (kg m-3)
0
0.5
1
1.5
2
2.5
3
3.5
4
4.5
5
Depth (m)
0
0.1
0.2
0.3
0.4
y = 0.4633e-0.467x
R² = 0.1386

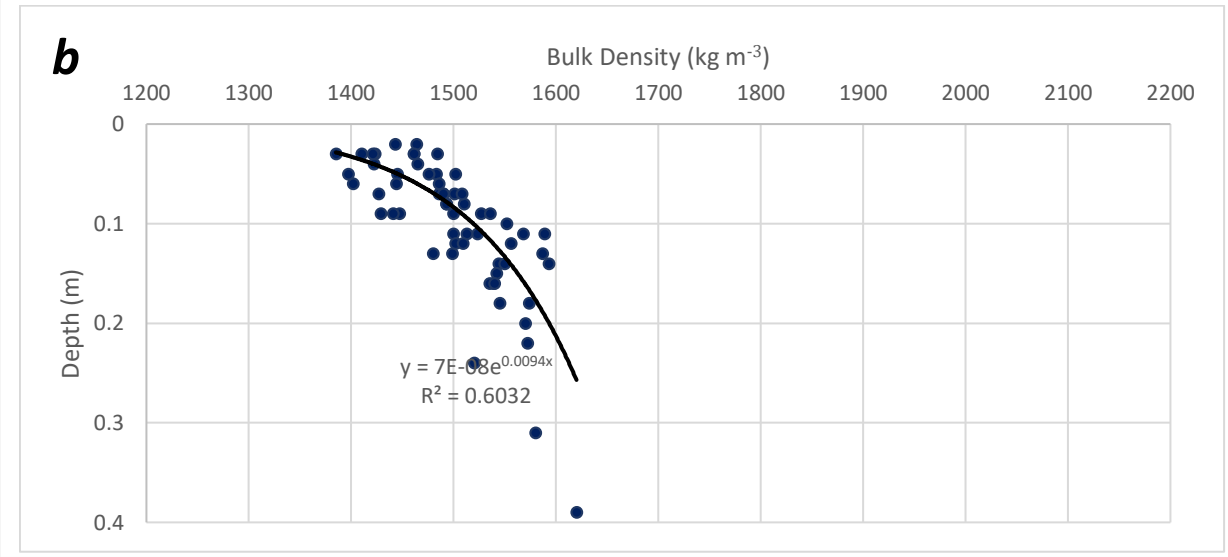
b
Bulk Density (kg m-3)
1200
1300
1400
1500
1600
1700
1800
1900
2000
2100
2200
Depth (m)
0
0.1
0.2
0.3
0.4
y = 7E-08e0.0094x
R² = 0.6032

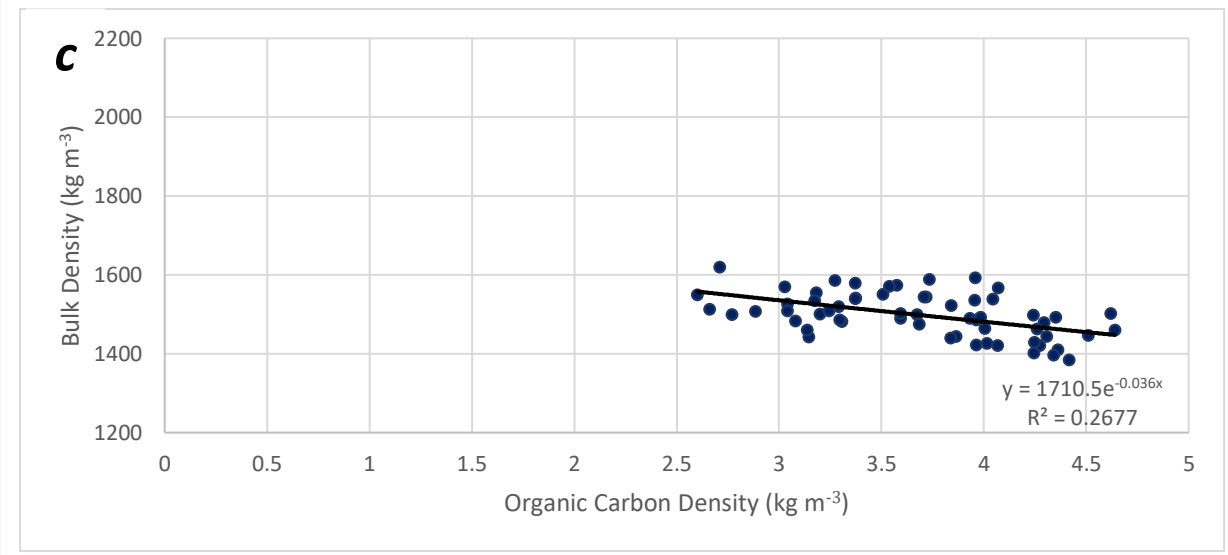
c
Bulk Density (kg m-3)
2200
2000
1800
1600
1400
1200
0
0.5
1
1.5
2
2.5
3
3.5
4
4.5
5
Organic Carbon Density (kg m-3)
y = 1710.5e-0.036x
R² = 0.2677

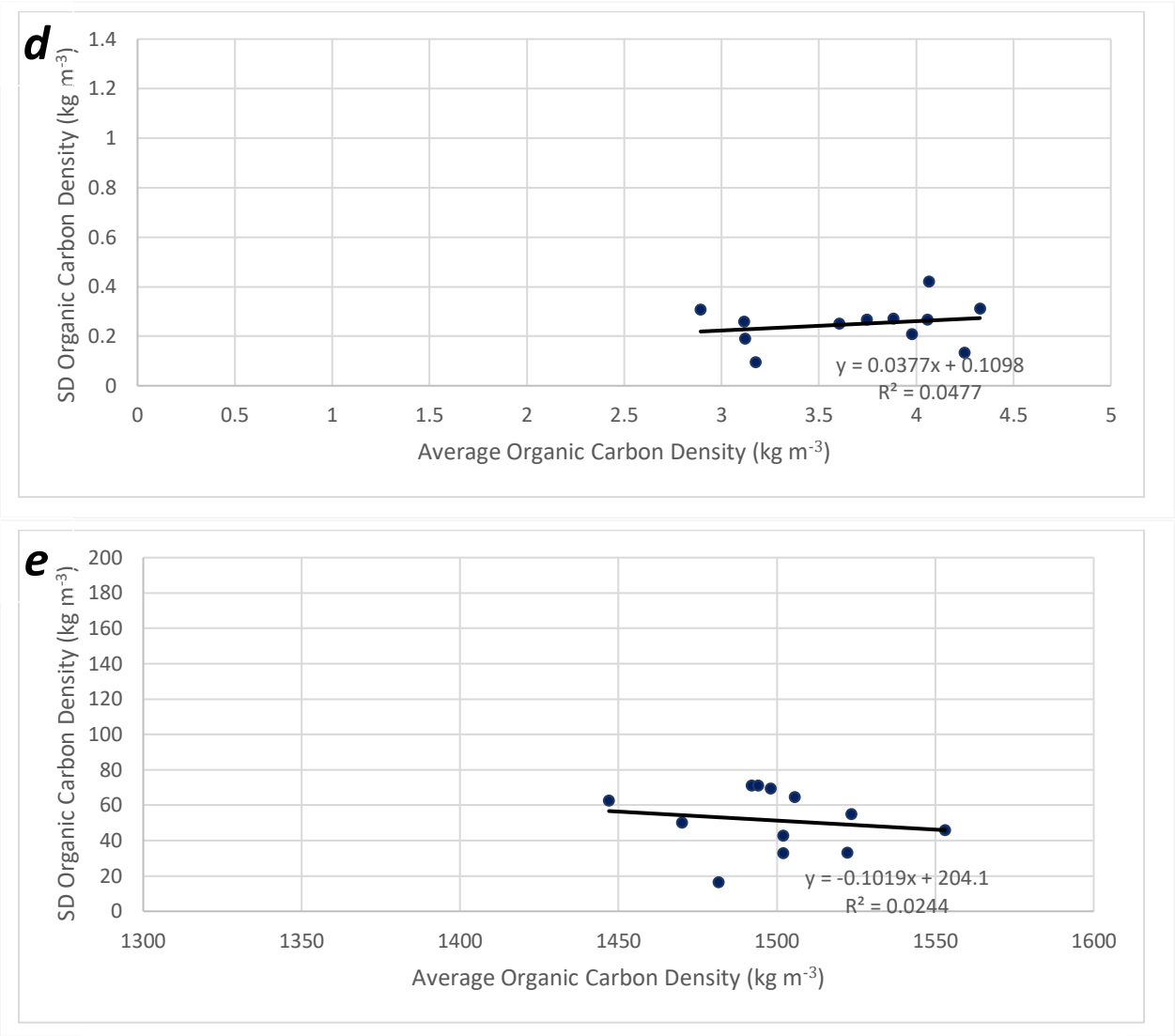

Figure C(XV). Correspondance between the depth, organic carbon density and bulk density in the differing active layer horizons of Marsh C.

C4 - Marsh D

C4(i) - Field Findings

Marsh D represented the furthest western extent of the Ribble saltmarshes at the head of the estuary. Sampling was designed to gauge how the above-ground biomass and sediment characteristics changed between the predominantly vegetated NE and the sparsely vegetated SW.

Above-ground Biomass

Table C(X). Location of sampling sites and above-ground biomass carbon storage quantification for Marsh D.

Site	Sub-environment Type	OS Grid Reference	Elevation (mOD)	C Mass (kg/m^2)	Uncertainty kg (±)	Uncertainty (%)
N Site A	Species Zone A	SD 35169 20432	5.02	1.136	0.001	0.09
N Site B	Species Zone A	SD 34790 20421	4.90	0.553	0.0005	0.09
N Site C	Species Zone C	SD 34479 20302	4.31	1.401	0.001	0.07
N Site D	Exposed Sediment	SD 33902 19723	3.85	0.000	0	0
S Site A	Species Zone B	SD 34602 19772	5.13	1.509	0.001	0.07
S Site B	Species Zone C	SD 34432 19690	4.85	1.012	0.001	0.10
S Site C	Exposed Sediment	SD 34236 19301	4.12	0.299	0.0005	0.17

Figure C(XVi). Marsh D sampling and ground truthing locations.

Sub-surface

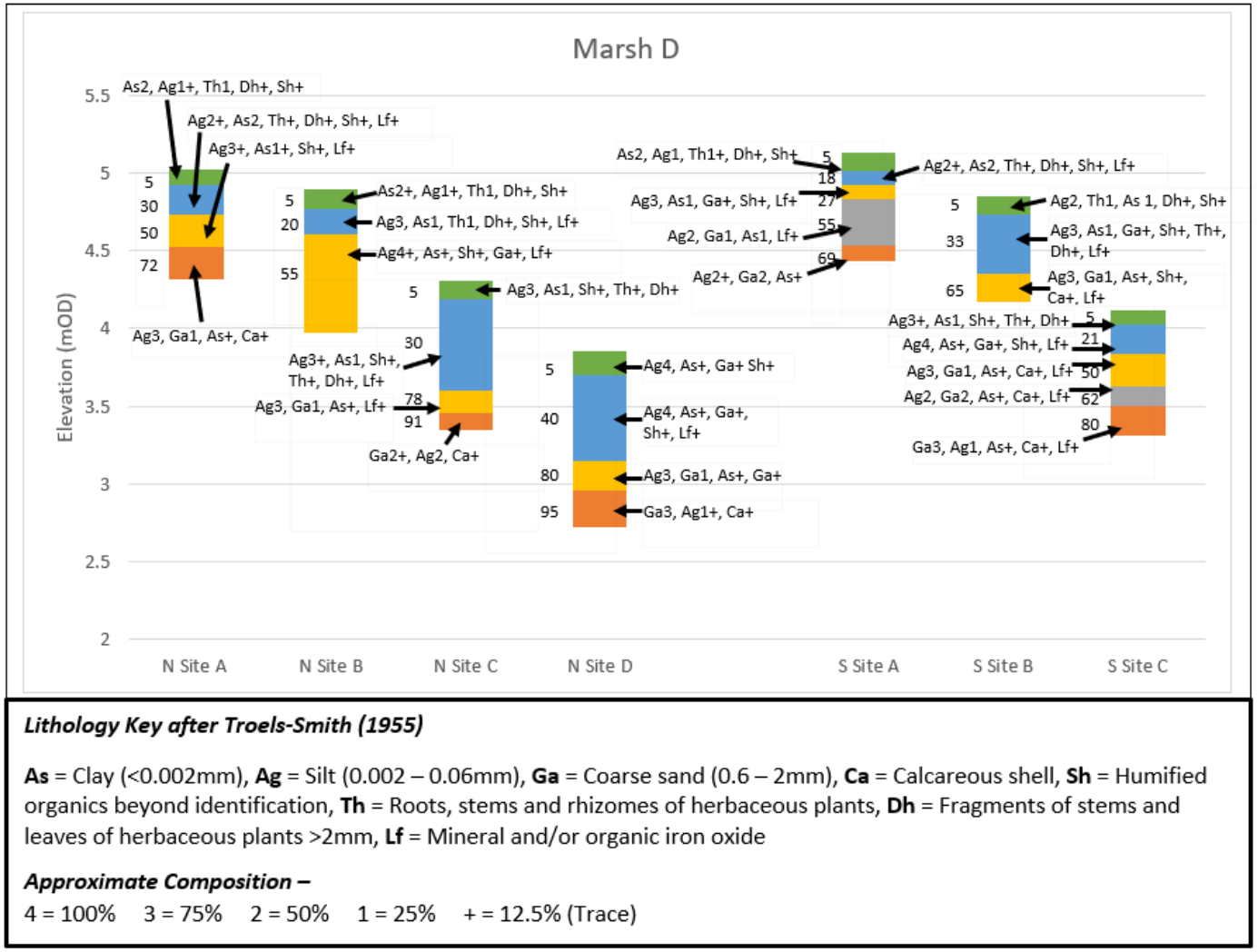

Lithology Key after Troels-Smith (1955)

As = Clay (<0.002mm), **Ag** = Silt (0.002 – 0.06mm), **Ga** = Coarse sand (0.6 – 2mm), **Ca** = Calcareous shell, **Sh** = Humified organics beyond identification, **Th** = Roots, stems and rhizomes of herbaceous plants, **Dh** = Fragments of stems and leaves of herbaceous plants >2mm, **Lf** = Mineral and/or organic iron oxide

Approximate Composition –

4 = 100% 3 = 75% 2 = 50% 1 = 25% + = 12.5% (Trace)

Figure C(XVii). Levelled stratigraphy for all sample sites on Marsh D. N.b. Labels indicate a horizon's physical characteristics determined following a Troels Smith Analysis (see universal key – Figure 1.2.1). Numbers to the left of all horizons indicate the depth at which a sample that was deemed to best represent the entire horizon was taken from. The green layer represents the surface horizon of each core.

C4(ii) - Sub-surface Carbon Content and Bulk Density Variability

Table C(Xi) Variation in horizon depth, organic carbon density and bulk density on Marsh D.

Sub-environment classification	Site Name	Horizon Number	Depth (m)	OCD (kg m^{-3})	(BD kg m^{-3})
Species Zone A	N Site A	1	0.1	4.32	1482
		2	0.29	2.84	1581
		3	0.5	2.06	1723
		4	0.7	1.60	1982
Species Zone A	N Site B	1	0.13	4.20	1469
		2	0.29	2.89	1638
		3	0.93	2.01	1773
Species Zone C	N Site C	1	0.12	3.97	1526
		2	0.71	2.36	1646
		3	0.85	1.97	1953
		4	0.96	1.66	2106
Exposed Sediment	N Site D	1	0.15	2.92	1598
		2	0.7	1.71	1670
		3	0.89	1.62	1821
		4	1.13	1.42	2192
Species Zone B	S Site A	1	0.12	4.18	1442
		2	0.21	2.94	1566
		3	0.3	2.11	1672
		4	0.6	1.95	1865
		5	0.7	1.24	1916
Species Zone C	S Site B	1	0.12	4.09	1382
		2	0.5	2.56	1501
		3	0.68	1.70	1830
Exposed Sediment	S Site C	1	0.09	2.97	1496
		2	0.28	1.97	1631
		3	0.49	1.57	1872
		4	0.62	1.37	1997
		5	0.81	1.30	2178

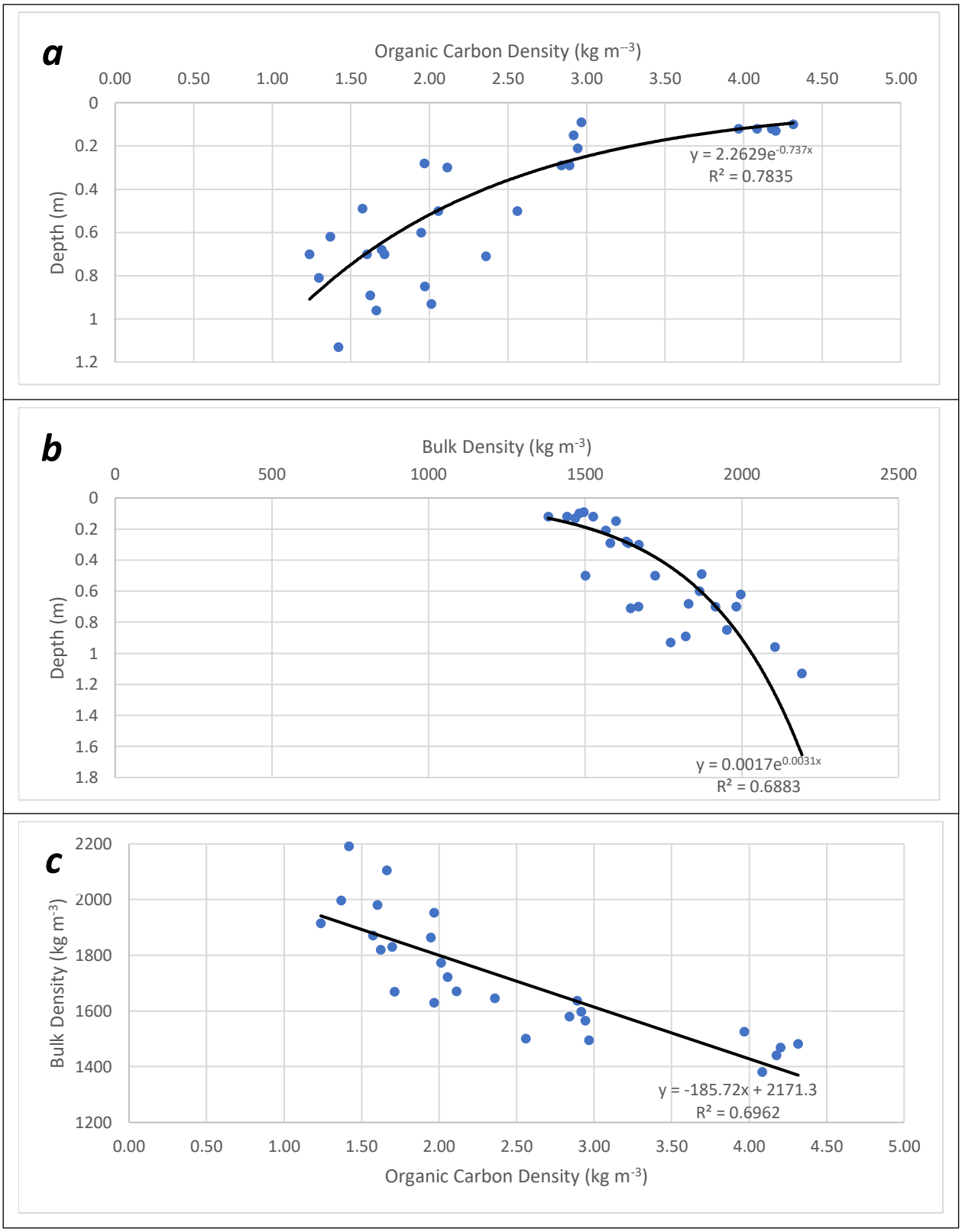

Figure C(XViii). Correspondance between the depth, organic carbon density and bulk density in the differing horizons of Marsh D.

Marsh D - Carbon Content

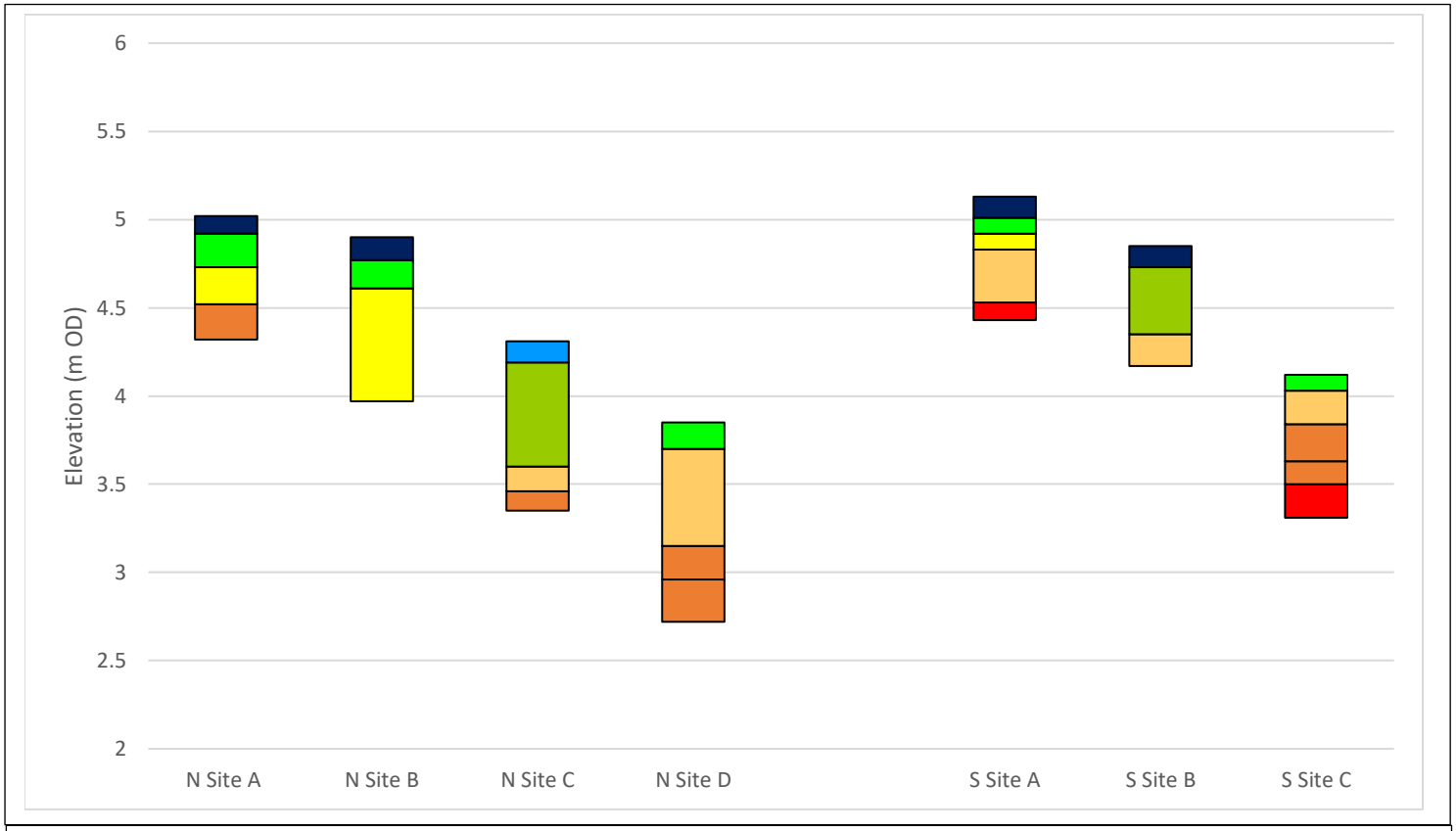

Key - Organic Carbon Density (kg m^{-3})

0 - 0.33	0.33 - 0.66	0.66 - 0.99	1 - 1.33	1.33 - 1.66	1.66 - 2	2 - 2.33	2.33 - 2.66	2.66 - 3	3 - 3.33	3.33 – 6.66	6.66 – 7	7 – 7.33	7.33 – 7.66

Figure C(XiX). Levelled stratigraphy for all sample sites on Marsh D exhibiting organic carbon denisty in each horizon of every sampled core. Resulted were determined derived after a loss on ignition test conducted on all samples following a standardised procedure outlined in the TESSA guidelines. Please see tables 6.3.2.2(a,b,c&d) for estimated organic carbon contents of all horizons.

C4(iii) - Active Layer Characteristics

Table C(Xii). Variation in horizon depth, organic carbon density and bulk density in the active layer (i.e. horizon 1) on Marsh D.

				Organic Carbon Density (kg m^{-3})			Bulk Density (kg m^{-3})		
Species Zone	Site Reference	Sub-horizon Sample Number	Sample Depth (m)	Sample value	Average	Standard Deviation	Sample Value	Average	Standard Deviation
SA	N Site A	1a	0.02	4.60	4.32	0.30	1432	1482	41
		1b	0.04	4.34			1443		
		1c	0.06	4.60			1505		
		1d	0.08	4.13			1521		
		1e	0.1	3.91			1507		
SA	N Site B	1a	0.02	4.09	4.20	0.16	1420	1469	44
		1b	0.04	4.22			1423		
		1c	0.07	4.46			1502		
		1d	0.09	4.17			1489		
		1e	0.11	4.08			1512		
SC	N Site C	1a	0.02	4.17	3.97	0.34	1475	1526	37
		1b	0.04	4.46			1505		
		1c	0.07	3.77			1530		
		1d	0.09	3.83			1552		
		1e	0.11	3.63			1568		
EX	N Site D	1a	0.03	2.98	2.92	0.29	1672	1716	97
		1b	0.06	3.32			1720		
		1c	0.09	2.60			1576		
		1d	0.12	3.01			1802		
		1e	0.15	2.67			1809		
SB	S Site A	1a	0.02	4.41	4.18	0.18	1388	1442	55
		1b	0.04	4.18			1411		
		1c	0.06	4.05			1412		
		1d	0.09	4.30			1489		
		1e	0.12	3.95			1512		
SC	S Site B	1a	0.03	4.34	4.09	0.23	1334	1382	49
		1b	0.05	4.12			1328		
		1c	0.07	4.26			1398		
		1d	0.09	3.77			1410		
		1e	0.11	3.93			1440		
EX	S Site C	1a	0.01	2.94	2.97	0.22	1432	1496	54
		1b	0.03	3.00			1460		
		1c	0.05	3.30			1496		
		1d	0.07	2.67			1521		
		1e	0.09	2.93			1570		

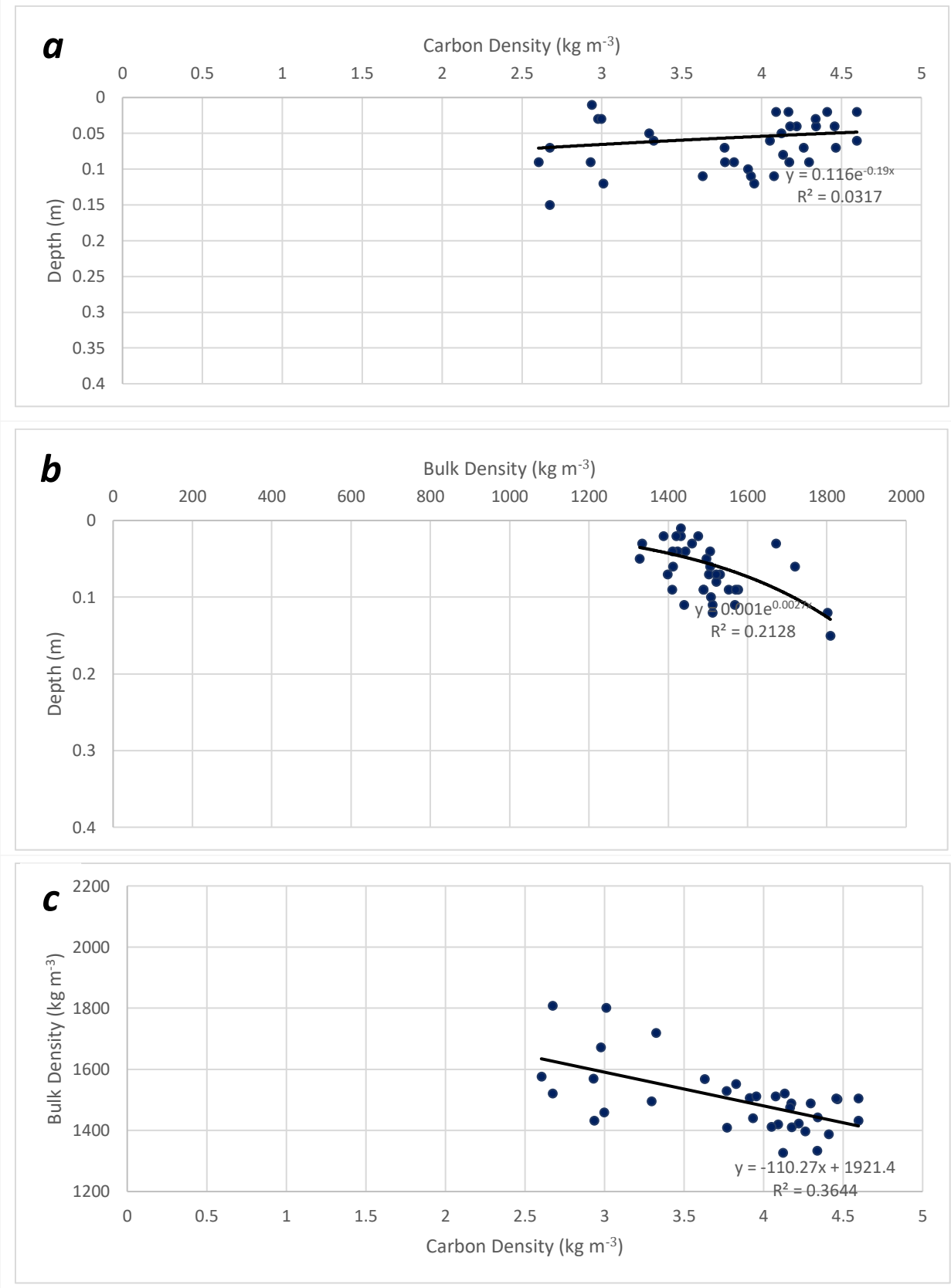
a
Carbon Density (kg m-3)
0
0.5
1
1.5
2
2.5
3
3.5
4
4.5
5
Depth (m)
0
0.05
0.1
0.15
0.2
0.25
0.3
0.35
0.4
y = 0.116e-0.19x
R² = 0.0317
b
Bulk Density (kg m-3)
0
200
400
600
800
1000
1200
1400
1600
1800
2000
Depth (m)
0
0.1
0.2
0.3
0.4
y = 0.001e0.0027x
R² = 0.2128
c
Bulk Density (kg m-3)
2200
2000
1800
1600
1400
1200
0
0.5
1
1.5
2
2.5
3
3.5
4
4.5
5
Carbon Density (kg m-3)
y = -110.27x + 1921.4
R² = 0.3644

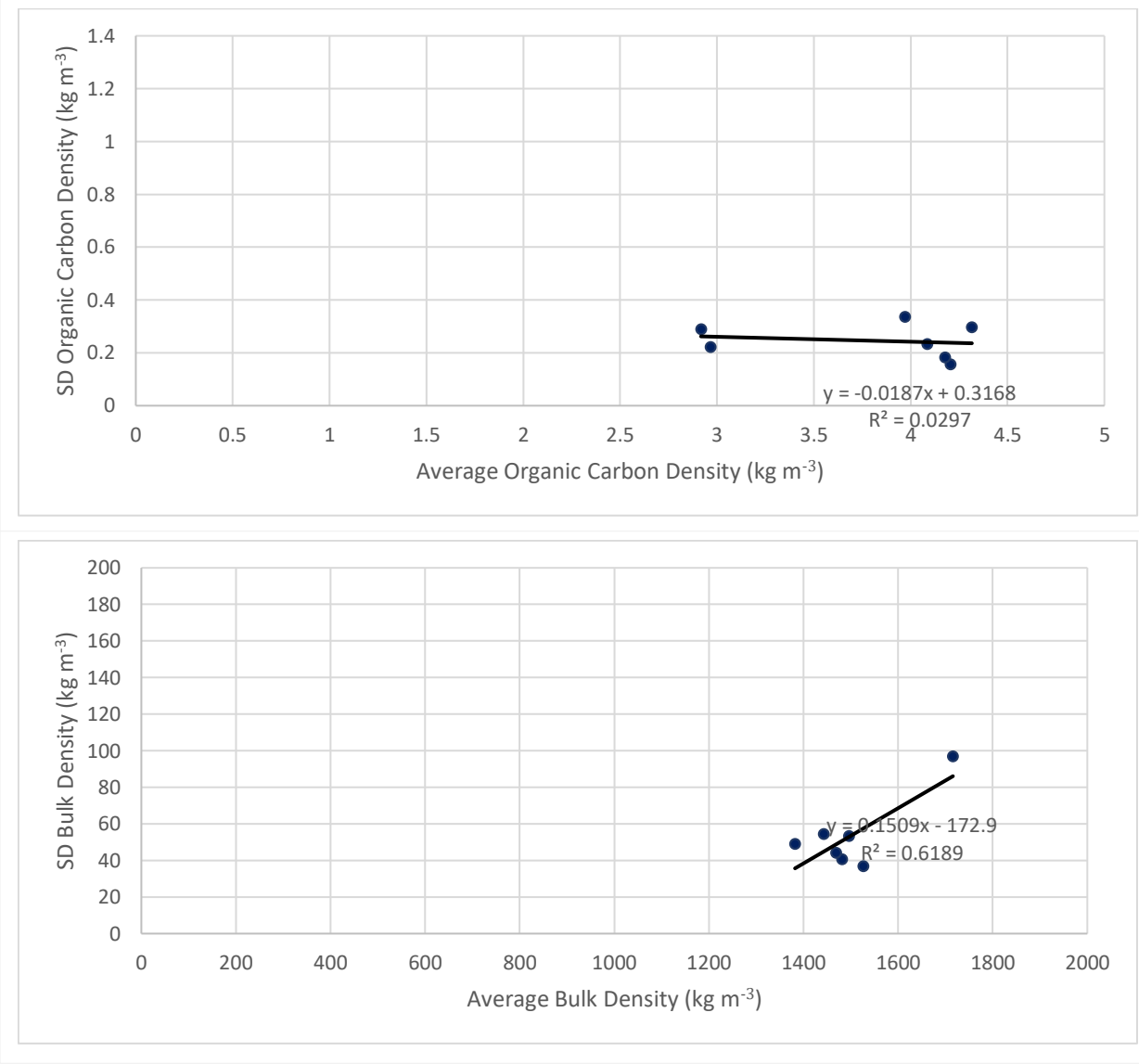

Figure C(XX). Correspondance between the depth, organic carbon density and bulk density in the differing active layer horizons of Marsh D.